TESIS DE LA UNIVERSIDAD DE ZARAGOZA
2021
179

Claudia Puddu

The Sardic Phase in the Ordovician of Southern Sardinia and Eastern Pyrenees: Stratigraphic, Structural and Magmatic Constraints.

Director/es
Casa Tuset, Josep Maria
Alvaro Blasco, José Javier

ISSN 2254-7606

Prensas de la Universidad
Universidad Zaragoza

ISSN 2254-7606

Universidad Zaragoza
1542

Tesis Doctoral

THE SARDIC PHASE IN THE ORDOVICIAN OF SOUTHERN SARDINIA AND EASTERN PYRENEES: STRATIGRAPHIC, STRUCTURAL AND MAGMATIC CONSTRAINTS.

Autor

Claudia Puddu

Director/es

Casa Tuset, Josep Maria
Alvaro Blasco, José Javier

UNIVERSIDAD DE ZARAGOZA
Escuela de Doctorado

2021

The Sardic Phase in the Ordovician of Southern Sardinia and Eastern Pyrenees: Stratigraphic, Structural and Magmatic Constraints

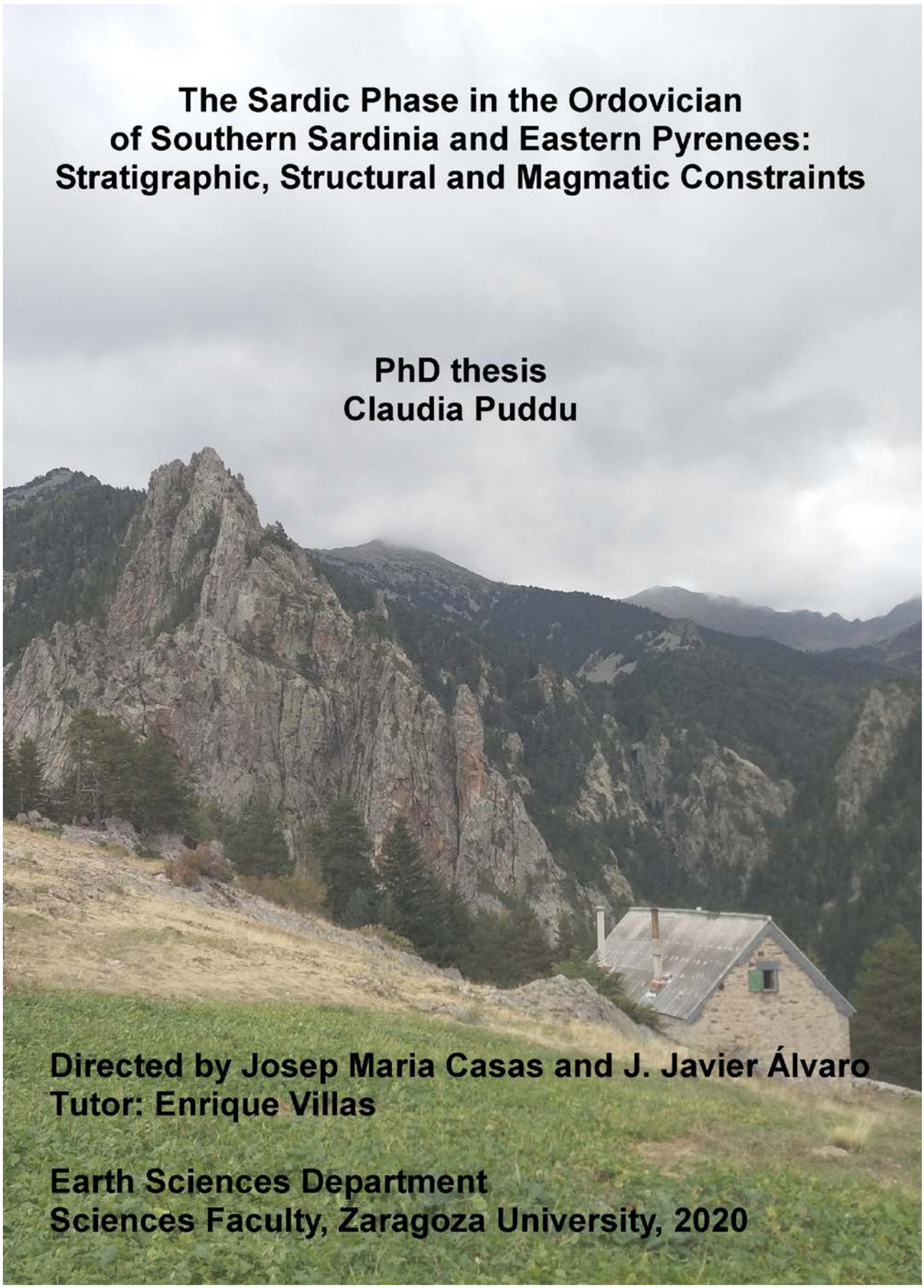

PhD thesis

Claudia Puddu

Directed by Josep Maria Casas and J. Javier Álvaro
Tutor: Enrique Villas

Earth Sciences Department
Sciences Faculty, Zaragoza University, 2020

The Sardic Phase in the Ordovician of Southern Sardinia and Eastern Pyrenees: Stratigraphic, Structural and Magmatic Constraints

PhD thesis

Claudia Puddu

Directed by:

Josep Maria Casas and **J. Javier Álvaro**

Tutor: **Enrique Villas**

Earth Sciences Department
Sciences Faculty
Zaragoza University

2020

This thesis is presented by Claudia Puddu to obtain the degree of Doctor in the University of Zaragoza under the direction of Prof. Josep Maria Casas Tuset (Barcelona University) and Dr. J. Javier Álvaro (Institute of Geosciences, CSIC-UCM, Madrid).

ABSTRACT

This thesis deals with the so-called “Sardic Phase”, a major geodynamic event that caused uplift, widespread emersion and erosion of an inherited Ediacaran-Lower Ordovician basement in the south-western European margin of Gondwana. Its aftermath led to the onlapping of Upper Ordovician sediments capping an inherited and partly eroded palaeorelief. The phase provoked an intra-Ordovician stratigraphic gap, ranging geometrically from paraconformable to angular discordance, named “Sardic unconformity” and subsequently overlain by Upper Ordovician alluvial-fluvial breccias and conglomerates. The Sardic event is associated with neither foliation-related open folds affecting the pre-unconformity succession nor metamorphism. It is also contemporaneous with an important Ordovician magmatic activity whose byproducts point to an important felsic calc-alkaline plutonism intruding within the pre-unconformity sedimentary package.

The first step of this thesis was to characterize the Sardic Phase in its type area, which includes a historical reappraisal of the stratigraphic, sedimentary, structural and magmatic features that successive generations of geologists recognized in SW and SE Sardinia. A revision of the stratigraphic and sedimentary characters of the Sardic unconformity and of the pre- and post-unconformity successions in the type area has been conducted.

The second step is focused on the identification of the Sardic features in two sectors of Eastern Pyrenees. The new data obtained with this research, together to the cartographic, lithostratigraphic, biostratigraphic and geochronologic data present in the literature, led to the individuation of Sardic deformation affecting the Cambrian-Lower Ordovician rocks, and to the definition of Upper Ordovician successions cropping out in Ribes de Freser and La Cerdanya areas. These data contribute to improve the knowledge of the Palaeozoic basement of the Pyrenees, in which the occurrence of an Early-Mid Ordovician episode of uplift and erosion led to the formation of the Sardic unconformity similar to that originally described in Sardinia. Early to Late Ordovician magmatic activity accompanied and followed the uplift, which was pursued by a Late Ordovician extensional pulse that controlled the post-Sardic deposition.

The geological mapping, together to the stratigraphic and facies analysis of the units cropping out in the Alpine Ribes de Freser antiformal stack, led to the definition of the Katian El Baell Formation, which has been revised, formally erected and proposed as a lateral equivalent of the Estana Formation. The geological and structural analysis of the rocks cropping out in the El Baell and Bruguera units led to the definition of two different internal structures, and to the recognizement of a pre-Variscan (Mid Ordovician) deformational episode affecting the pre-Upper Ordovician rocks of the Bruguera unit.

Detailed geological mapping of the La Cerdanya area (Canigó Unit, Eastern Pyrenees) led to the definition of the different structural features exhibited by the pre- (Cambrian-Lower Ordovician) and post-unconformity (Upper Ordovician) successions, allowing the identification of Sardic deformations. The occurrence of Late Ordovician synsedimentary extensional faults affecting the pre-Sardic succession, the Sardic unconformity and the lower part of the post-Sardic succession has been highlighted.

Finally, a comparison between the Toledanian (Furongian-lowemost Ordovician) and Sardic (Ordovician) geochemical byproducts of felsic/acidic affinity, currently interpreted as calc-alkaline and arc-related, seemed necessary to evaluate the different geodynamic interpretations proposed so far for both events. The geochemical character of plutonic and volcanic products from several areas of the aouth-western European margin of Gondwanan suggests a similar melting of metasedimentary rocks associated with the Toledanian and Sardic events, which should help to a better understanding of the geodynamic scenario in which both tectonic phases occurred. In particular, the comparison with the Toledanian event favoured the recognition of a contemporaneity between magmatic events and stratigraphic unconformities, contrasting with the geochemical affinity of the magmatic counterparts, which suggest that the magmatism was likely induced by the underplating of hot magmas in a continental lower crust with partial melting of sediments, triggered by the stepwise opening of the Rheic Ocean.

RESUMEN

Esta tesis versa sobre llamada "Fase Sárdica o Sarda", un importante evento geodinámico que provocó el levantamiento, la emersión generalizada y la erosión de un zócalo heredado del Ediacárico-Ordovícico Inferior en el margen sudoccidental europeo de Gondwana. Sus secuelas coincidieron con el depósito de sedimentos del Ordovícico tardío sobre un palaeorelieve heredado y parcialmente erosionado. La fase provocó un hiato estratigráfico intraordovícica, variable geométricamente desde paraconformidades a discordancias angulares, conocida como la "discordancia sarda", que fue posteriormente refubierta por brechas y conglomerados aluvial-fluviales del Ordovícico superior. El evento Sárdico no se asocia a pliegues con foliación que afecten la sucesión pre-discordancia ni con metamorfismo, pero es contemporáneo con una importante actividad magmática ordovícica que apunta a un importante plutonismo calcoalcalino félsico intercalado en el paquete sedimentario anterior a la discordancia.

En la primera parte de esta tesis se caracteriza la Fase Sarda en su área tipo, incluyedo una reevaluación histórica de las características estratigráficas, sedimentarias, estructurales y magmáticas que sucesivas generaciones de geólogos reconocieron en Cerdeña meridional. La revisión incluye a los caracteres estratigráficos y sedimentarios de la discordancia sarda y de las sucesiones infra y suprayacentes a la discordancia en el área tipo.

La segunda parte se centra en la identificación de los rasgos sárdicos preservados en dos sectores del Pirineo Oriental. Los nuevos datos obtenidos con esta investigación, junto con los datos cartográficos, litoestratigráficos, bioestratigráficos y geocronológicos que ofrecen la literatura especializada, han llevado a la identificación de la deformación sarda que afectó a las rocas del Cambr-Ordovícico Inferior, y a la definición de sucesiones del Ordovícico Superior en los sectores de Ribes de Freser y La Cerdanya, en el Pirineo Oriental. Los primeros datos contribuyen a mejorar el conocimiento del zócalo paleozoico pirenaico, caracterizado por un episodio de levantamiento y erosión del zócalo durante el Ordovícico Temprano-Medio, que condujo a la formación de una discordancia similar a la descrita en Cerdeña meridional. La actividad magmática del Ordovícico temprano a tardío acompañó al levantamiento cortical, que culminó con un pulso extensional que controló la geometría de las cuencuas post-Sardas.

La cartografía geológica, junto con el análisis estratigráfico y de facies de las unidades que afloran en el apilamiento antiformal alpino de Ribes de Freser, permitió la definición de la Formación katiense de El Baell, la cual ha sido formalmente propuesta como equivalente lateral de la Formación de Estana. Además, el análisis geológico y estructural de las rocas que afloran en las unidades El Baell y Bruguera ha permitido definir dos estructuras internas diferentes y reconocer un episodio de deformación pre-varisco (Ordovícico medio) que afecta a las rocas de la unidad Bruguera, anteriores al Ordovícico superior. La cartografía geológica detallada de la zona de La Cerdanya (Unidad del Canigó, Pirineo Oriental) ha permitido distinguir los rasgos estructurales característicos de las sucesiones pre-discordancia (Cambro-Ordovícico Inferior) y post-discordancia (Ordovícico Superior), favoreciendo el reconocimiento de la deformación sarda que afecta la sucesión inferior. Se describe el desarrollo de fallas extensionales sinsedimentarias del Ordovícico tardío que afectan a la sucesión pre-sarda, la discordancia sarda y la parte inferior de la sucesión post-sarda.

Finalmente, se documenta una comparación entre la geoquímica de las rocas magmáticas toledánicas (Furongiense-Ordovícico basal) y Sárdica (Ordovícico), ambas de afinidad félsica/ácida, y actualmente interpretadas como calco-alcalinas y relacionadas con un arco

magmático. Dicha comparación permite evaluar las diferentes interpretaciones geodinámicas propuestas hasta ahora para ambos eventos. El análisis de la afinidad geoquímica de los productos plutónicos y volcánicos de varias áreas del margen soudoccidental europeo de Gondwana sugiere la fusión de rocas metasedimentarias durante el evento Sárdico, lo que podría ayudar a comprender mejor el escenario geodinámico en el que desarrolló esta fase tectónica. En particular, la comparación con el evento toledánico ha favorecido el reconocimiento de la contemporaneidad entre los eventos magmáticos y las discordancias estratigráficas, mientras que las características geoquímicas deducidas indican que el magmatismo podría ser inducido por el *underplating* de magmas calientes en una corteza continental inferior con fusión parcial de sedimentos, relacionados con la apertura del Océano Rheico.

ACKNOWLEDGEMENTS

First of all, I would like to thank my tutor, Enrique Villas, and Zarela for their humanity and availability, and to Marcos Aurell by his support in the Zaragoza University.

I would like to thank my supervisors, Josep Maria Casas and J. Javier Alvaro, for stimulating and supporting me during these last years, and for their trust, opportunities and great patience given to me.

Thanks to all the professors and researchers who helped, listened to and encouraged me: Francesco Leone, Gianluigi Pillola, Carlo Corradini, Antonio Funedda, Alfredo Loi, Raffaello Cioni, Giacomo Oggiano, Bernard Laumonier, Montserrat Liesa, Marina Navidad, Pedro Castiñeiras, Aina Margalef, Pilar Clariana, Cecilio Quesada and Martim Chichorro.

Thanks to all co-authors of the scientific contributions and to all the referees, who cooperated with us improving our works.

Special thanks to my first Sardinian colleagues, Cristina Buttau, Stefania Unida, Guglielmo Caddeo and Maria Corriga, who accompanied me during the first years of research. Thanks to my colleagues from "overseas", Jorge Colmenar and Sofia Pereira, who stimulated me to pick up where I left off.

Thanks to all the technicians and colleagues of the Universities of Zaragoza, Barcelona and Cagliari, for their help and technical support.

Thanks to those who, without knowing it, helped me.

A special thanks to all my family and friends, who believed in me and accompanied me despite my falls, and Giancarlo, who continues to bear with me. Thanks to those who are no longer there, but are always present.

Thanks to those who accompanied me accross the mountains for years, recognizing the Sardic Unconformity with its nose, and looked after me as a parent.

Thank you

INDEX

CHAPTER 1

CHAPTER 1

INTRODUCTION

This thesis is focused on the so-called “Sardic Phase”, a major geodynamic event that caused uplift, widespread emersion and erosion of an inherited Ediacaran-Lower Ordovician basement in the south-western European margin of Gondwana. Its aftermath led to the onlapping of Upper Ordovician sediments capping an inherited and partly eroded palaeorelief. The phase provoked an intra-Ordovician stratigraphic gap, ranging geometrically from paraconformable to angular discordance, named “Sardic unconformity” and subsequently overlain by Upper Ordovician alluvial-fluvial breccias and conglomerates. The Sardic event is associated with neither foliation-related open folds affecting the pre-unconformity succession nor metamorphism. It is also contemporaneous with an important Ordovician magmatic activity whose byproducts point to an important felsic calc-alkaline plutonism intruding within the pre-unconformity sedimentary package.

The term “Sardic Phase” was introduced by Stille (1935, 1939) to account the stratigraphic gap and angular discordance (the “Sardic unconformity”) firstly recognized in SW Sardinia (Zoppi, 1888) separating Cambro-Ordovician and “Silurian” (then including Upper Ordovician) strata. SW Sardinia represents the Variscan Foreland Zone of the island, and the unconformity separates the Cambro-Ordovician Cabitza Formation (Cocozza, 1967a) from the overlying Upper Ordovician Monte Argentu Formation (Laske et al., 1994) marking a stratigraphic gap of almost 18 m.y. (**Fig. 1a**).

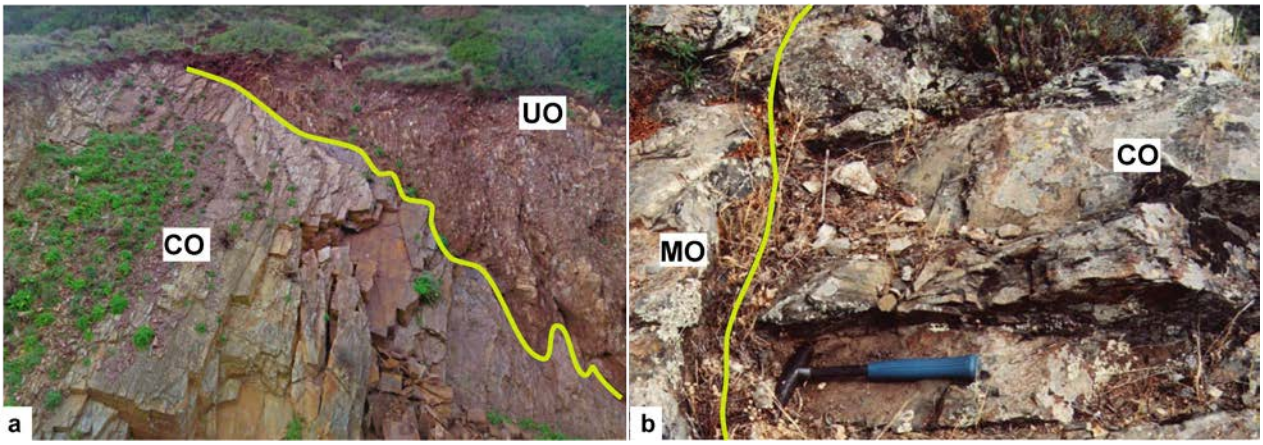

Figure 1 - Sardic unconformity. (**a**) In its type area (road to Nebida, SW Sardinia) between the Cambrian-Lower Ordovician Cabitza Formation (*CO*) and the Upper Ordovician Monte Argentu Formation (*UO*) (Foreland Zone). (**b**) Sarrabese unconformity counterpart in the Sarrabus unit (Su Scoffoni locality, S Muravera) between the Cambrian-Lower Ordovician Arenarie di San Vito Formation (*CO*) and the Middle Ordovician Porfidi Grigi del Sarrabus (*MO*) volcanics. Light green lines highlight the unconformity.

The unconformity was subsequently recognized in SE Sardinia (Calvino, 1959*a*), tectonostratigraphically representing the External Nappe Zone of the Variscan zonation, where the event was is located between the Cambro-Lower Ordovician Arenarie di San Vito Formation (Calvino, 1959*b*) and either the Metaconglomerati di Muravera (Carmignani et al., 2001*a*) or a Middle Ordovician volcanosedimentary complex (**Fig. 1b**), composed of the Monte Santa Vittoria

Formation (Carmignani et al., 2001*a*) and the Porfidi Grigi del Sarrabus (Calvino, 1959*b*), reflecting a gap of about 10 m.y.

Since its definition in the 1930s, the Sardic Phase has become the reference for any Lower Palaeozoic tectonic event punctuating the time span bracketed between the latest Ediacaran-Terreneuvian Cadomian and Late Devonian-Early Permian Variscan orogenies. However, successive chronostratigraphic and radiometric data have offered a new geodynamic scenario in south-western Europe, differentiating two distinct Cambro-Ordovician phases: the Furongian-Ordovician Toledanian and the Ordovician Sardic events. Both phases share common features, such as: (i) uplift and denudation of a subaerial palaeorelief; (ii) contemporaneous emplacement of a massive calc-alkaline magmatism everlastingly interpreted as representative of arc conditions; (iii) development of synsedimentary open folds lacking fold-related cleavage networks; (iv) absence of coeval metamorphic conditions; (v) development of a stratigraphic gap ranging from ca. 10 to 20 m.y.; and (vi) aftermaths characterized by sealing of an inherited palaeorelief by alluvial-to-fluvial deposits.

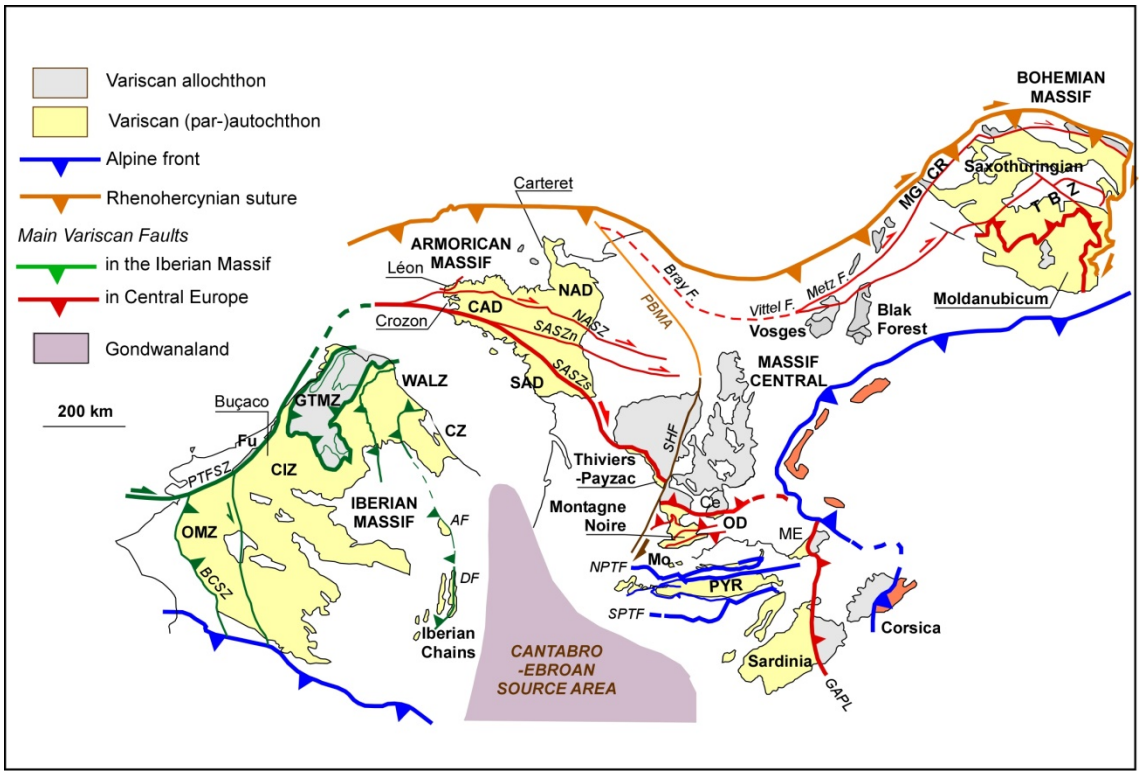

Figure 2 - Tectonostratigraphic zonation of the Variscan Orogen in southwestern Europe with interpolated position of the Gondwana source area for the Iberian Peninsula. Abbreviations: *AF* Anguiano Fault, *BCSZ* Badajoz-Córdoba Shear Zone, *CAD* Central Armorica Domain, *Ce* Cévennes, *CZ* Cantabrian Zone, *CIZ* Central Iberian Zone, *DF* Datos Fault, *F.* fault, *Fu* Finisterra units, *GAPL* Grimaud-Asinara-Posada Line, *GTMZ* Galicia-Trás-os-Montes Zone, *ME* Maures-Estérel massif, *MGCR* Mid-German Crystalline Rise, *Mo* Mouthoumet massif, *NAD* North Armorican Domain, *NASZ* North-Armorican Shear Zone, *NPTF* North Pyrenean Thrust Fault, *OD* Occitan Domain, *OMZ* Ossa-Morena Zone, *PBMA* Paris Basin Magnetic Anomaly, *PTFSZ* Porto-Tomar-Ferreira do Alentejo Shear Zone, *PYR* Pyrenees, *SAD* South Armorican Domain, *SASZN* South-Armorican Shear-Zone northern branch, *SASZS* South-Armorican Shear-Zone southern branch, *SHF* Sillon Houillier Fault, *SISZ* South-Iberian Shear Zone, *SPTF* South Pyrenean Thrust Fault, *TPZ* Teplá-Barrandian Zone, and *WALZ* West Asturian-Leonese Zone; modified from Martínez-Catalán et al. (2007), Ballèvre et al. (2009), Pouclet et al. (2017), Moreira et al. (2019) and Álvaro et al. (in press *a*).

The two unconformities are never found in a same locality. At present, the Toledanian unconformity is restricted to the Anti-Atlas of Morocco (Álvaro & Vizcaïno, 2018), the Iberian Massif (Sánchez-García et al., 2019, and references therein), the North and Central Armorican Domains (there named "lacaune normande"; Le Corré et al., 1991; Robardet et al., 1994) and Bohemia (Hajná et al., 2017, 2018) (**Fig. 2**). A reference to the Sardic Phase in the Cantabrian Zone (Aramburu & García-Ramos, 1988) was correctly re-interpreted as a new geodynamic episode, named the Toledanian Phase (Gutiérrez-Marco et al., 2002). In contrast, the Sardic unconformity occurs in eastern areas, such as the Sardinia-Corsica Block (e.g., Barca et al., 1987*a*; Carmignani et al., 1994), Eastern Pyrenees (Llopis-Lladò, 1965; Santanach Prat, 1972; Ravier et al., 1975; Zwart, 1979; Barrouquère et al., 1983; Muñoz et al., 1983; Muñoz, 1985; Laumonier & Guitard, 1986; Speksnijder, 1987; Laumonier, 1987, 1988; García-Sansegundo & Alonso, 1989; Den Brok, 1989; Kriegsman et al., 1989; Poblet, 1991; Muñoz & Casas, 1996; Gil-Peña et al., 2001, 2004; García-Sansegundo et al., 2004; Laumonier et al., 2004; Casas & Fernández, 2007; Donzeau & Laumonier, 2008; Casas, 2010; Puddu & Casas, 2011; Margalef et al., 2016), the Occitan Domain (including Montagne Noire and Mouthoumet massifs; Von Gaertner, 1937; Gèze, 1949; Durand-Delga & Gèze, 1956; Gonord et al., 1964; Vila, 1965; Ovtracht, 1967; Arthaud et al., 1976; Boulange & Boyer, 1964; Cornet, 1980; Engel et al., 1980-81; Berger, 1982; Cornet, 1980; Bessière & Schulze, 1984; Bessière & Baudelot, 1988; Bessière et al., 1989; Berger et al., 1992, 1993, 1997; Feist & Etchler, 1994; Álvaro et al., 2016) and the Alps (Stampfli et al., 2002; Von Raumer et al., 2002, 2013). Similar Mid Ordovician gaps interpreted as the Sardic Phase have also been suggested for Mid Ordovician gaps in Turkey (central-eastern Taurus and western Pontides Massifs; Dean et al., 2000; Kozlu et al., 2002; Monod et al., 2003; Ghienne et al., 2010), and Nova Scotia (Canada; White et al., 2018). However, as this PhD thesis will document below, the presence of stratigraphic gaps associated with felsic volcanism does not fulfil the real characterization of the Sardic Phase in its type area.

Despite a partial chronological superposition of the Toledanian and Sardic phases, the propagation of their involved geodynamic conditions followed a SW-NE trend along the southwestern European margin of Gondwana (**Fig. 2**). In addition, both phases are related to the formation and evolution of two different continental margins. To the west, the areas affected by the Toledanian unconformity are unanimously agreed to have been located in the Gondwanan margin facing the Rheic Ocean. To the east, the areas afected by the Sardic unconformity were in turn facing the Proto-Tethys (Stampfi et al., 2002) or Ran Ocean (Torsvik & Cocks, 2009), and later on the Palaeo-Tethys Ocean (Torsvik & Cocks, 2004; Von Raumer & Stampfi, 2008). This palaeogeographic difference is key to unravelling the problem, as the ongoing geodynamic scenarios appear to have been radically different from one place to the other during the Late Palaeozoic.

The end of the Cadomian arc in West Gondwana was followed by rifting conditions, which lasted for most of the Cambrian and culminated in the progressive opening of the Rheic Ocean from the late Furongian (Anti-Atlas, Ossa-Morena) to the Tremadocian further along the margin (Sánchez-García et al., 2019, and references therein). The rift-drift or break-up event was associated with a magmatic activity considered responsible for thermal expansion of the area recording the Toledanian unconformity (Álvaro et al., 2018; Sánchez-García et al., 2019). Subsequent thermal collapse after ocean opening caused an important transgression (initiated in continental conditions by the "Purple Series" red-beds underlying the Armorican Quartzite in areas close to the inherited rift axes) and inaugurated a new phase as a passive margin that lasted until the onset of the Variscan orogeny in Early Devonian times (Quesada, 1990, 1991, 2006). Nevertheless, some authors have

claimed for compressive/transpressive events as the cause of the Toledanian gap and unconformity in western parts of the Central-Iberian Zone (Lefort & Ribeiro, 1980; Silva & Ribeiro, 1985; Romão & Ribeiro, 1993; Correia Romão et al., 2005; Amaral et al., 2014). This is the only place where cleavage-bearing, steeply plunging folds afecting Ediacaran-to-Cambrian Series 2 strata beneath the Toledanian unconformity have been documented in Iberia or elsewhere along the margin. This may be related to a local strain regime, causing transient compression and dextral strike-slip conditions along the Central Iberian/Ossa-Morena contact lineament (Correia Romão et al., 2005), within the otherwise generalized extensional (rift) environment. In the Central Iberian Zone, subduction-related processes have been interpreted to account for the arc-like geochemical signatures of the dominantly felsic calc-alkaline rocks (Ollo de Sapo and correlatives) in this zone (Castro et al., 2002; Del Greco et al., 2016, and references therein). However, this geochemical signature can be inherited from the crustal source of the magmas (the Cadomian arc/back-arc system), as postulated by Sánchez-García et al. (2003, 2008, 2019).

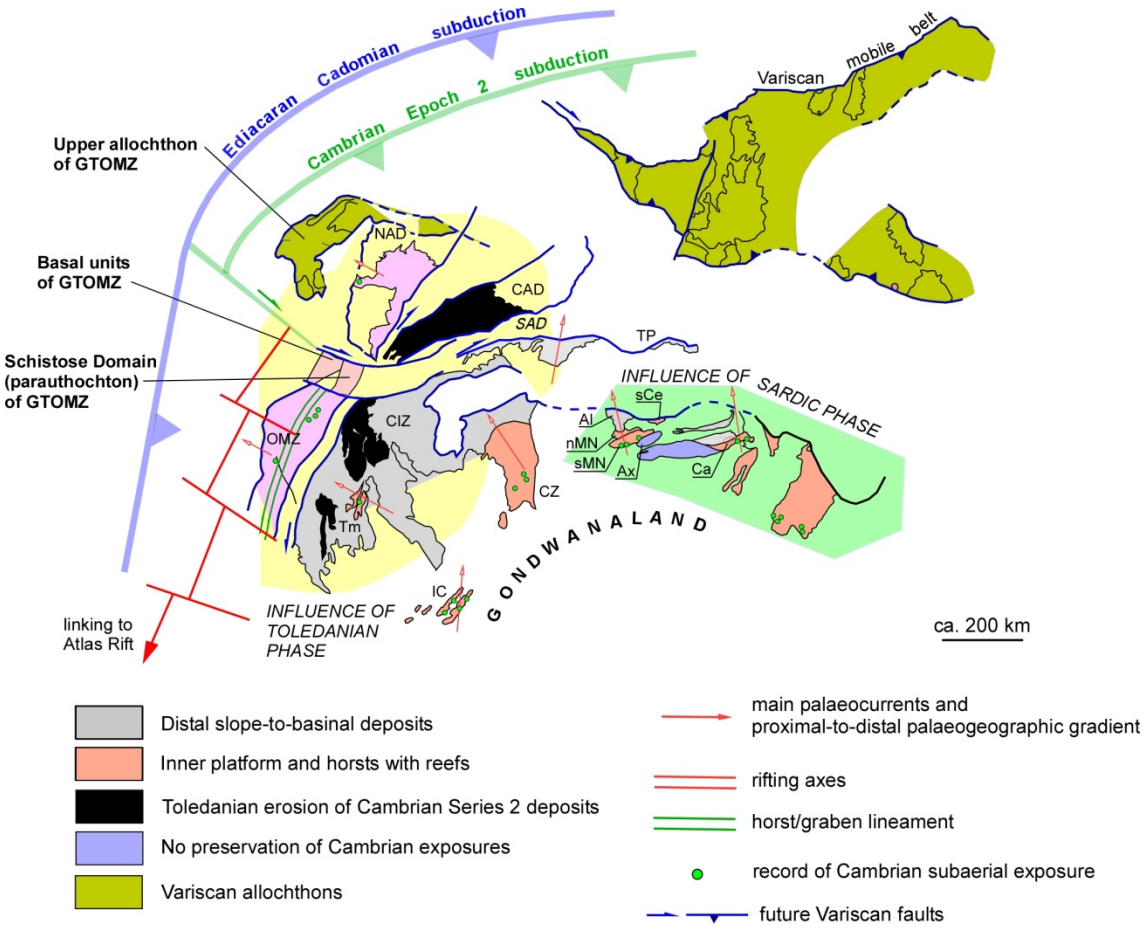

Figure 3 - Palaeogeographic reconstruction of the relative positions of the Variscan tectonostratigraphic units for Cambrian times; modified from Álvaro *et al.* (2003, 2010, in press *a*) and Pouclet *et al.* (2017); abbreviations: *Al* Albigeois mountains, *Ax* Montagne Noire Axial Zone, *Ca* Canigó massif, *CAD* Central Armorican Domain, *CIZ* Central Iberian Zone, *CZ* Cantabrian Zone, *GTOMZ* Galicia-Trás-os-Montes Zone, *IC* Iberian Chains, *NAD* North Armorican Domain, *nMN* northern Montagne Noire, *OMZ* Ossa-Morena Zone, *sCE* southern Cévennes, *sMN* southern Montagne Noire and *Tm* Toledo Mountains.

In eastern areas of the southwestern European margin (Eastern Pyrenees, Occitan Domain, Sardinia/Corsica and Alps), no evidence of the Toledanian Phase is recorded (**Fig. 3**). Their Cambrian sediments are represented by either platformal sediments (Pyrenees, Occitan Domain) or

volcanosedimentary successions belonging to a back-arc/arc/trench system (Memmi et al., 1983) developed in response to subduction of the Proto-Thetys (Von Raumer et al., 2013, 2015) or Ran Ocean (Torsvik & Cocks, 2009). In the Iglesiente-Sulcis region of the Sardic type area, and based on the geochemical features of the Sardic-related volcanics, Carmignani et al. (1982, 1992, 1994, 2001*a*, *b*) suggested that the "Sardic-Sarrabese phase" should be related to the compression of a Cambrian-Ordovician back-arc basin, as a result of which, this tectonostratigraphic area should be originated by the shifting of the Ordovician volcanic arc toward the northwestern Gondwanan margin. However, the geochemical affinities of the calc-alkaline magmatic activity have received several interpretations, such as late-orogenic magmatic-anatectic compressive settings, in an arc-trench system represented by a back-arc basin (Memmi et al., 1983). Other interpretations for the Sardinian-Corsican Massif (**Fig. 3**), including the neighbouring Maures inlier in the French Côte d'Azur (Lancelot et al., 1998; Rossi et al., 2009), point to plutonic emplacement and cleavage-free conditions related to mega-shear conditions and oblique convergence associated with a trantensive-transpressive pull-apart basin (Minzoni, 1985; Cappelli et al., 1992; Carmignani et al., 1994; Funedda & Oggiano, 2009). Whatever the case, it appears that active compressive/transpressive conditions, perhaps reminiscent of the subduction regime that dominated the Ediacaran-Cambrian Epoch 2 evolution of the entire northwestwern Gondwana margin, might have prevailed in this area until post-Sardic times.

In the Alps, the Sardic phase is also interpreted as a result of the collision of this Gondwanan margin with the so-called Qaidam arc, soon followed by the accretion of the Qilian block (Von Raumer & Stampfli, 2008; Von Raumer et al., 2013, 2015). This interpretation is mainly based on the Alpine Briançonnais-Austroalpine basement, where the sections after the Sardic tectonic inversion and folding stage depict a younger arc-arc oblique collision (450 Ma) of the eastern tail of the Hun terrane with the internal Alpine margin, followed by exhumation in a transform margin setting (430 Ma) (Zurbriggen et al., 1997; Franz & Romer, 2007; Von Raumer & Stampfli, 2008; Von Raumer et al., 2013; Zurbriggen, 2015, 2017).

In between the two margins with so diferent geodynamic scenarios during the Ordovician, the Eastern Pyrenees and the Occitan Domain seem to have occupied an intermediate position, closer though to the eastern margin facing the Proto-Tethys, as no indication of the Toledanian event is recognized here. The transition between the areas affected by the Toledanian and Sardic events may have been located close to the Cantabrian Zone (**Figs. 2-3**), considered as the lateral prolongation of the southern Montagne Noire (Álvaro et al., 2010, in press *a*), where the Sardic gap is absent but a Middle Ordovician volcanism associated with minor stratigraphic gaps is present (Aramburu et al., 2004; Álvaro et al., 2007).

Although coeval to the Sardic events in Sardinia and the Alps, no evidence suggests that these intermediate domains (Cantabrian Zone and Pyrenean and Occitan Domains) were reached by compressive deformation at this stage. Instead, normal faulting and bimodal rift-type magmatism characterize the aftermath of the Sardic Phase. The reasons for this difference have not yet been explained (for a discussion, see Álvaro et al., 2018). Widespread collapse of the uplifted Sardic-related regions, associated with transgression and onlapping of inherited palaeoreliefs, led to extensional tectonic events throughout northwerstern Gondwana, in some cases recording the onset of a Late Ordovician tholeiitic-dominant rifting renewal (Caron et al., 1997; García-Sansegundo et al., 2004; Álvaro et al., 2016). A back-arc rifting precursor of the Palaeo-Tethys Ocean, associated with alkaline basalts and the onset of euxinic conditions, is suggested across the Ordovician-Silurian transition in Sardinia (Oggiano & Mameli, 2006; Rossi et al., 2009). All these Late Ordovician events were heralding, and probably related to the subsequent opening of the latter

ocean eastward (Torsvik & Cocks, 2004; Von Raumer & Stampfli 2008). Von Raumer et al. (2013, 2015) suggested a diferent scenario for the far-eastern segment of the margin facing the Iranian-Chinese domain of East Gondwana, where a Cambrian Proto-Rheic or Palaeoasian Ocean would be gradually replaced by the Ordovician Qaidam Ocean.

The palaeogeographic proximity of Sardinia (the type-area of the Sardic Phase) and those "intermediate" areas, represented by the Eastern Pyrenees and the Occitan Domain, offers an opportunity to unravel the lateral propagation of the Sardic Phase in peri-Gondwana areas neighbouring those affected by the Toledanian Phase. This is the main reason why the Sardic Phase of the Eastern Pyrenees was selected as regional target for this multidisciplinary PhD Thesis.

1.1 Aim of the thesis

The above-reported studies of the Sardic unconformity and related phase have pointed to a complex scenario full of contradictory geodynamic interpretations. Some of the latter derived from analysis based on a selection of geological data (e.g., stratigraphic, sedimentary, structural and geochemical features of magmatic activity) that, in some cases, were disparate in different tectonostratigraphic units of Sardinia, Eastern Pyrenees and Montagne Noire. Many works have highlighted the geodynamic complexity of the Sardic Phase (including interpretations ranging from Andean-style arc to extensional conditions; Oggiano et al., 2010; Cruciani et al., 2018) and comparisons with the Toledanian Phase (Álvaro et al., 2018; Sánchez-García et al., 2019; Casas et al., 2019).

The first step of this thesis aims at properly characterizing the Sardic Phase in its type area, which includes a historical reappraisal of the stratigraphic, sedimentary, structural and magmatic features that successive generations of geologists recognized in SW and SE Sardinia (***Chapter 3***). A revision of the stratigraphic and sedimentary characters of the Sardic unconformity and of the pre- and post-unconformity successions in the type area is envisaged in ***Chapter 4***.

The second step is focused on the identification of the Sardic features in two sectors of Eastern Pyrenees (***Chapter 5***) summarizing the state-of-the-art of this topic for the whole Eastern Pyrenees.

(***Section 5.5***) The Ribes de Freser area was selected because it includes two Alpine thrust sheets, the El Baell and Bruguera units (Muñoz, 1985; Puddu et al., 2018). The Upper Ordovician succession of these units differs from that classically described and used as reference for the main part of the Pyrenees. New structural and stratigraphic data from this area improve the Ordovician stratigraphic framework of the Eastern Pyrenees and the recorded effects of Ordovician extensional tectonics. These data may also constrain the future restoration of Variscan and Alpine deformations in this area and refine the geometry of this portion of the Upper Ordovician northern Gondwana margin.

(***Section 5.6***) The Cambro-Ordovician and Upper Ordovician successions of the La Cerdanya area display an interesting structural style, where well-expressed Ordovician deformations took place in the form of extensional faults and folds, the latter affecting only the Cambro-Ordovician succession (Puddu et al., 2019). The interpretation of these pre-Variscan deformation structures should contribute to a better understanding of the origin and meaning of the Sardic Unconformity, and thus to discussion of the geodynamic setting of this fragment of North Gondwana during Ordovician times.

(***Section 5.7***) An updated synthesis of the Sardic Phase in Eastern Pyrenees, combined with its correlation throughout neighbouring areas, such as the Occitan Domain and Sardinia, offers a complete framework of present-dat data, including stratigraphic, sedimentary, structural and magmatic datasets of the study area (Casas et al., 2019).

Finally, a comparison between the Toledanian and Sardic geochemical byproducts of felsic/acidic affinity (***Chapter 6***), currently interpreted as calc-alkaline and arc-related, seemed necessary to evaluate the different geodynamic interpretations proposed so far for both events (Álvaro et al., in press *a*).

1.2 Scientific contributions

The published contributions obtained during the studies carried out during the PhD include five publications (Puddu & Casas, 2011; Belaústegui et al., 2016; Puddu et al., 2018, 2019; Álvaro et al., in press *a*), three book chapters (Casas et al., 2017*a*, *b*, 2019) and four conference abstracts (Casas & Puddu, 2010; Casas et al., 2017; Puddu et al., 2017*a*, *b*):

Publications and book chapters

Puddu, C. & Casas, J.M. 2011. New insights into the stratigraphy and structure of the Upper Ordovician rocks of the la Cerdanya area (Pyrenees). *Cuadernos del Museo Geominero* 14, 441-445.

Belaústegui, Z., **Puddu**, C. & Casas, J.M. 2016. New ichnological data from the lower Paleozoic of the Central Pyrenees: presence of *Arthrophycus brogniartii* (Harlan, 1832) in the Upper Ordovician Cava Formation. *Geo-Temas* 16, 271-274.

Casas, J.M., **Puddu**, C. & Álvaro, J.J. 2017. Upper Ordovician limestones along Ribes-Bruguera road. In: Ordovician Geodynamics: the Sardic Phase in the Pyrenees, Mouthoumet and Montagne Noire massifs (Álvaro, J.J., Casas, J.M. & Clausen, S., eds.). *Géologie de la France* 1 (4), 40-41.

Casas, J.M., **Puddu**, C. & Álvaro, J.J. 2017. Upper Ordovician succession in Talltendre. Ordovician Geodynamics: the Sardic Phase in the Pyrenees, Mouthoumet and Montagne Noire massifs (Álvaro, J.J., Casas, J.M. & Clausen, S., eds.). *Géologie de la France* 1 (4),45-47

Puddu, C., Álvaro, J.J., & Casas, J.M. 2018. The Sardic unconformity and the Upper Ordovician successions of the Ribes de Freser area, Eastern Pyrenees. *Journal of Iberian Geology* 44 (4), 603-617.

Puddu C., Álvaro J.J., Carrera N., & Casas J.M. 2019. Deciphering the Sardic (Ordovician) and Variscan deformations in the Eastern Pyrenees, SW Europe. *Journal of the Geological Society* 176, 1191-1206.

Casas J.M., Álvaro J.J., Clausen S., Padel M., **Puddu** C., Sanz-López J., Sánchez-García T., Navidad M., Castiñeiras P. & Liesa M. 2019. Palaeozoic Basement of the Pyrenees. In: *The Geology of Iberia: a Geodynamic Approach*. Vol. 2: The Variscan Cycle (Quesada, C. & Oliveira J.T., eds.), pp: 229-259.

Álvaro, J.J, Sánchez-García, T., **Puddu**, C., Casas, J.M., Díez-Montes, A., Liesa, M. & Oggiano, G. (in press). Comparative geochemical study on Furongian-earliest Ordovician (Toledanian) and Ordovician (Sardic) felsic magmatic events in south-western Europe: underplating of hot mafic magmas linked to the opening of the Rheic Ocean. *Solid Earth*.

Abstracts (see ***Annexes***)

Casas, J.M. & **Puddu**, C. 2010. Ordovician deformations in the Pyrenees and Sardinia: new insights into the significance of pre-Variscan (“sardic”) tectonics. R. S. T. 25-29/10/2020 Bordeaux, p. 48.

Casas J.M., Sánchez-García T., Álvaro J.J., **Puddu** C. & Liesa M. 2017. Ordovician magmatism in the Pyrenees. In: Ordovician Geodynamics: The Sardic Phase in the Pyrenees, Mouthoumet and Montaigne Noire massifs (Álvaro J.J., Casas J.M. & Clausen S., eds.).). 4-9 September 2017, Figueres, Catalonia. Abstract volume, p. 12.

Puddu C., Casas J.M., & Álvaro J.J. 2017. New knowledge on the Upper Ordovician rocks of El Baell, Ribes de Freser area, eastern Pyrenees. In: Ordovician Geodynamics: The Sardic Phase in the Pyrenees, Mouthoumet and Montaigne Noire massifs (Álvaro J.J., Casas J.M. & Clausen S., eds.).). 4-9 September 2017, Figueres, Catalonia. Abstract volume, pp. 24-27.

Puddu C., Casas J.M., & Álvaro J.J. 2017. On the Upper Ordovician of the La Cerdanya area, Pyrenees. In: Ordovician Geodynamics: The Sardic Phase in the Pyrenees, Mouthoumet and Montaigne Noire massifs (Álvaro J.J., Casas J.M. & Clausen S., eds.).). 4-9 September 2017, Figueres, Catalonia. Abstract volume, pp. 27-29.

CHAPTER 2

CHAPTER 2

MATERIALS AND METHODS

A multidisciplinar methodology based on field mapping has been used, together to aerial photos analysis, rock sampling, thin section analysis, stratigraphic logs and geologic profiles elaboration.

The study of the references allowed choosing the areas to investigate, respectively the Ribes de Freser and La Cerdanya areas (Canigó massif) in the Eastern Pyrenees, and Capo Spartivento in southwestern Sardinia.

Field mapping of the different study areas have been developed between August 2016 and October 2018, throughout 6 field missions (about 115 days) suitable for complete the 1:5.000 geological mapping and the sample collection. The former was addressed to the siliciclastic successions ("Campelles Series" for the Ribes de Freser area; Serdinya, Rabassa, Cava, Ansovell and Bar Formations for the La Cerdanya area) and carbonate successions (El Baell Formation in the Ribes de Freser area, and Estana Formation in La Cerdanya area) in order to collect sedimentary, stratigraphic and structural informations, and finding fossils and microfossils useful as biostratigraphic indicators. Volcanic (Campelles volcanics, Ribes de Freser area) and magmatic bodies (Monte Filau orthogneiss, SW Sardinia) has been sampled, too. Particularly, the Monte Filau orthogneiss has been sampled in order to perform geochronologic datation.

Sample analysis (palynomorphic extraction) has been performed in the Micropalaeontology Laboratory of the Cagliari University (Italy) between December 2016 - April 2017.

2.1 Geological mapping

Field mapping has been used in order to produce geological maps of the studied areas. The methodology chosen is based on the elaboration of a geologic 1:5,000 scale-map in which different data were reported, including lithologies, geologic contacts and boundaries, strata bedding, foliation, intersection lineation, fault and axis folds.

Field mapping was performed using 1:5,000 topographic maps of the Institut Cartogràfic i Geològic de Catalunya as support (sheets: *Cortàs, 279-77, 280-77*; *Éller, 280-76*; Brugu*era, 289-83, 289-84, 290-83, 290-84*) and the relative ortophotos for the Pirenees areas, and the 1:10.000 topographic maps (Carta Tecnica Regionale Numerica 10K) of the Regione Sardegna (sheets: *573-060, 573-070, 573-100, 573-110*) and the ortophotos for Sardinia areas.

The collection of structural data has been useful to deduce the structure and the deformation phases affecting the rocks. The former data were reported in the geologic maps, and used to build geologic profiles. The observation of aerial photos has been useful to do a preliminary analysis of the study areas, especially for the ones not attainable because of the topography or the vegetation.

Stratigraphic log elaboration has been used in order to collect and summarize lithological, stratigraphical, palaeontological and thickness data relative to the studied successions.

The choice of the section has been preceded by geological mapping and structural observations, in order to find an undisturbed succession. Where possible, the stratigraphic log has been measured with the Jacob's bar directly, or deduced indirectly on the basis of the cartographic data.

Together with the collection of structural and geological data, rock sampling was done with the purpose to make different analysis (petrographic preparation for thin sections observation, palynomorphs extraction, geochronologic datation).

2.2 Palynological analysis

Biostratigraphic study focused on the finding of microfossils useful for the determination of the age of the pre-Sardic successions, especially for the Campelles Series (Bruguera unit, Ribes de Freser area, southern Canigó massif), attributed to the Cambrian - Lower Ordovician (Muñoz, 1985) on the basis of lithologic similarities with the Jujols Group cropping out in the Canigó massif.
Eight samples (100 gr each one) of dark fine siltstones with millimetric sandstones interbeds were collected along an undisturbed section selected from the upper part of the Campelles Series (almost 800 m NNW to Bruguera town). The palynomorphs extraction was performed according to the process used at the Utrecht University (NL). All the eight samples treated revealed fossil-barren.

Palynomorphic extraction: the methodology used is the one learned from the Palynology and Palaeobotany Laboratory of the Utrecht University (NL), which provides 7 processing steps:

1) sample cleaning by sediment scraping with knife, water and compressed air;
2) crushing and pulverization of the sample, and weighing of the former one;
3) treatment of the sample powder in a 10% HCl solution;
4) treatment of the residue sample powder in a 40% HF solution;
5) treatment of the residue sample powder in a 30% HCl solution;
6) filtering of the residue with nylon sieves (15 μm);
7) bonding of the residue to the specimen slides.

Siliciclastic samples were prepared by polishing all the surfaces and crushed with a ceramic pestle. After the weighing of the powder, the sample was alternatively treated twice with HCl solution (in order to remove carbonates) and twice with HF solution (in order to remove silicates). Between a proceeding and the following, the sample were left to settle (1 day), deprived of the exceeding liquid and reintegrated alternatively with a HCl and HF solution, centrifugated (2000 rpm for 5 minutes), and agitated mechanically (250 rpm for 2 hours). The residue was filtered with nylon sieves (250 μm and 15 μm), separated in a ultrasound tank, and transferred in tubes with distilled water for the last centrifugation (2000 rpm for 5 minutes). After removing the exceeding liquid and reinstated with distilled water, a sample drop was put in the specimen slide and transferred into a stove in order to remove the water (1 day), before adding some drop of resin in order to fix the palynomorphs between the specimen slide and the cover glass. After 48 hours in the stove, the specimen slide was sealed with transparent nail varnish (in order to prevent air bubbles formation), and was ready for the observation with transmitted light optical microscope.

2.3 Structural analysis

Structural study focused on the characterization of the structures affecting the pre- and post-unconformity successions, in order to verify if Sardic structures occurred and how did they display, and distinguish between them and other deformations.

So, data recovered from the pre- and post-unconformity successions (bedding, unconformity surface, foliation, intersection lineation, fault, axis fold, etc…) have been analized separately (grouped into homogeneous domains if necessary) and processed using equal areal lower hemisphere stereoplot, and finally plotted with *Stereonet 9.8.3* (Allmendinger, 2011-2016).
Furthermore, different geologic profiles were built using the data collected in order to better represent the geometry of the deformations affecting the rocks.

2.4 Geochemical analyses

Carbonates were stained with Alizarin Red S and potassium ferricyanide to distinguish calcite from dolomite and to identify ferroan cements. Mineralogical identification was based on transmitted and reflected light microscopy, X-ray diffraction (XRD in IGEO, Madrid), and scanning electron microscopy (SEM) equipped with an energy-dispersive X-ray analyser (EDX). The chemical composition of selected minerals was determined with a backscattered electron detector (BSE). SEM analysis was made by using a JEOL JSM-6400 fitted with an Oxford Instruments D6679 detector in the Museo Nacional de Ciencias Naturales, Madrid. Back-scattered (BSE) imaging and energy-dispersive X-ray (EDS) analyses were obtained by SEM with the following measurement conditions: accelerating voltage 20 kV, beam current 1–2 nÅ, and a counting interval of 50 s. Analytical results display an error of ± 5–7%.

CHAPTER 3

CHAPTER 3

HISTORICAL REAPPRAISAL OF THE SARDIC PHASE

The aim of this chapter is to understand the original concept of the Sardic phase and its conceptual evolution through time and space. As explained above, the "Sardic Phase" is linked to the occurrence of an angular unconformity punctuating the Variscan basement of SW Sardinia (**Fig. 4**) and separating the Cambro-Ordovician Cabitza Formation (Cocozza, 1967*a*) from the overlying Upper Ordovician Monte Argentu Formation (Laske et al., 1994) (**Fig. 1a**). The "Sardic unconformity" is geometrically recognized as an angular discordance involving a gap that includes part of the Mid-Late Ordovician (Pittau Demelia, 1985; Naud & Pittau Demelia, 1985; Barca et al., 1987*a*, *b*; Ferretti & Serpagli, 1990; Ferretti, 1992; Pillola et al., 1998, 2008).

3.1 Sardic unconformity

Since prehistoric and Roman times, the geological exploration of the Palaeozoic basement in Sardinia has been linked to mineral ore exploitation. The first description of Ordovician rocks in Sardinia (then known as "Lower Silurian") was made by La Marmora (1857) on the basis of Meneghini's palaeontological discoveries. Between 1850 and 1930, mineral ore exploitation in Sardinia generated an increase of geological studies, especially in the south-western area. Several Cambrian fossils were discovered in the succession composed, from bottom to top, of "sandstones" (Nebida Group; Pillola, 1991), "dolostones and limestones" (Gonnesa Group; Pillola, 1991) and "claystones and siltstones" (Cabitza Formation of Iglesias Group; Pillola, 1991). Due to some incorrect taxonomic determinations, such as the trilobite assignation to the genera *Giordanella*, *Olenopsis* and *Paradoxides* (Meneghini, 1888; Bornemann, 1881; Pompeckj, 1901), the stratigraphic succession was misinterpreted: the Palaeozoic stratigraphic succession placed the unit of "claystones and siltstones" at the base and the "limestones" at the top of the regional stratigraphic succession. Both the taxonomic misinterpretation and the compex geological structure induced by the Variscan overprint made unclear the Lower Palaeozoic stratigraphic framework that crops out in south-western Sardinia until the 1950s. Particularly, it was supposed that the Lower Palaeozoic succession had been deposited between the "lower and the middle Cambrian", although Furongian-Early Ordovician fossils had already been signaled by Taricco (1920, 1922). The former reasons led to an ambiguous chronostratigraphic attribution of the Sardic unconformity and the Sardic Phase.

The angular (Sardic) unconformity was already reported by Zoppi (1888), who placed it between the rocks of supposed "mid Cambrian" age (Cabitza Formation: Cocozza, 1967*a*) (**Fig. 1b**) and those of Ordovician age (Monte Argentu Formation: Laske et al., 1994) (**Fig. 1a**) in the Variscan basement of the Iglesiente-Sulcis area in SW Sardinia. The discordance, coined "Sardic unconformity" by Stille (1939), is also known as the "Cambro-Ordovician unconformity" (Cocozza & Valera, 1966). The setting of the discordance and the involved stratigraphic gap was discussed, among others, by Bornemann (1891), Henrotin (1902, 1904), Novarese (1914, 1922), Taricco (1922), Novarese & Taricco (1923), Teichmüller (1931), Minucci (1935) and Cadisch (1938).

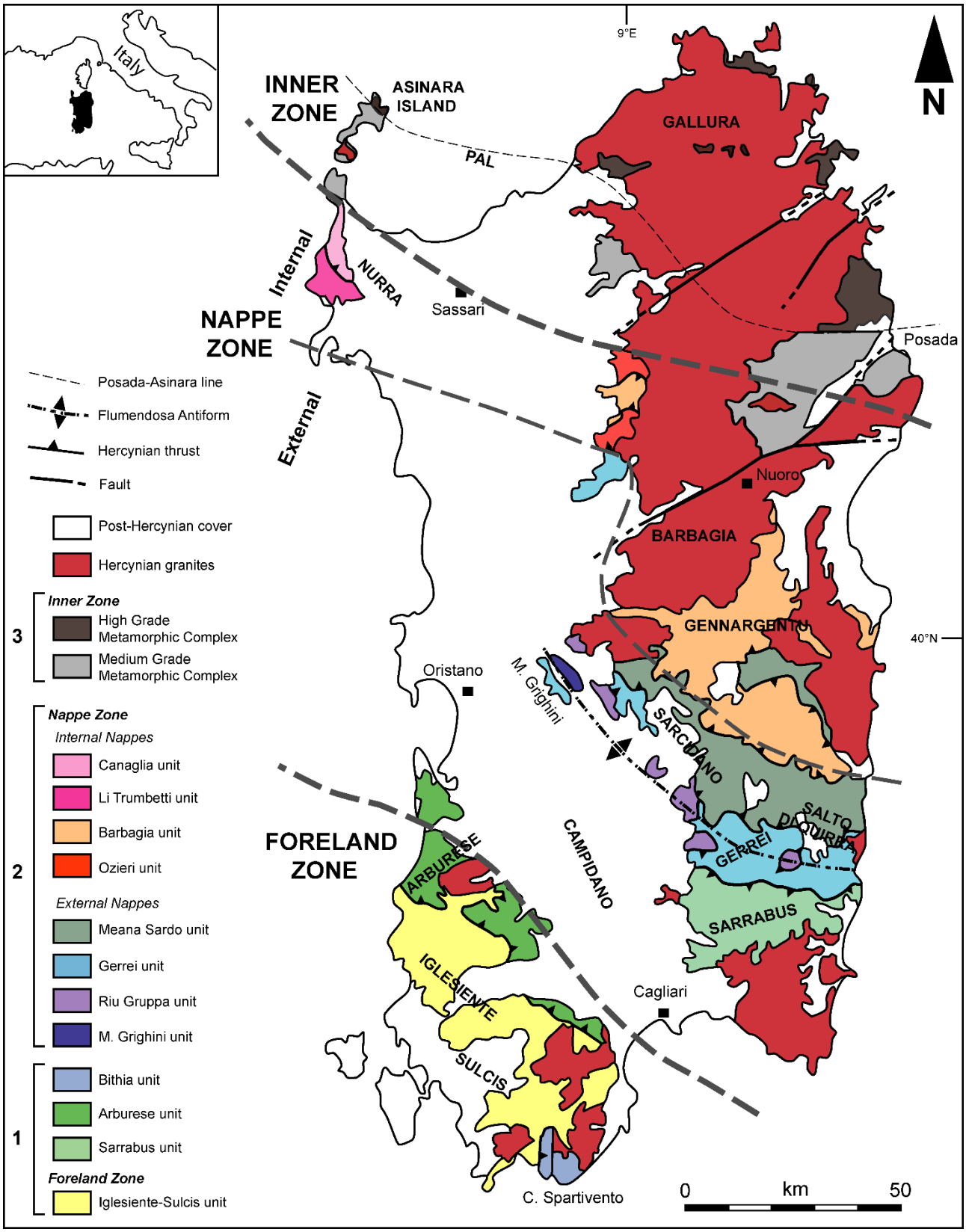

Figure 4 - Geological sketch of the Variscan tectono-metamorphic zones of the Sardinian basement; modified after Cocco et al. (2018): (1) non-metamorphic to low-grade metamorphic rocks; (2) greeschist facies metamorphic rocks; (3) amphibolite to high-grade metamorphic rocks.

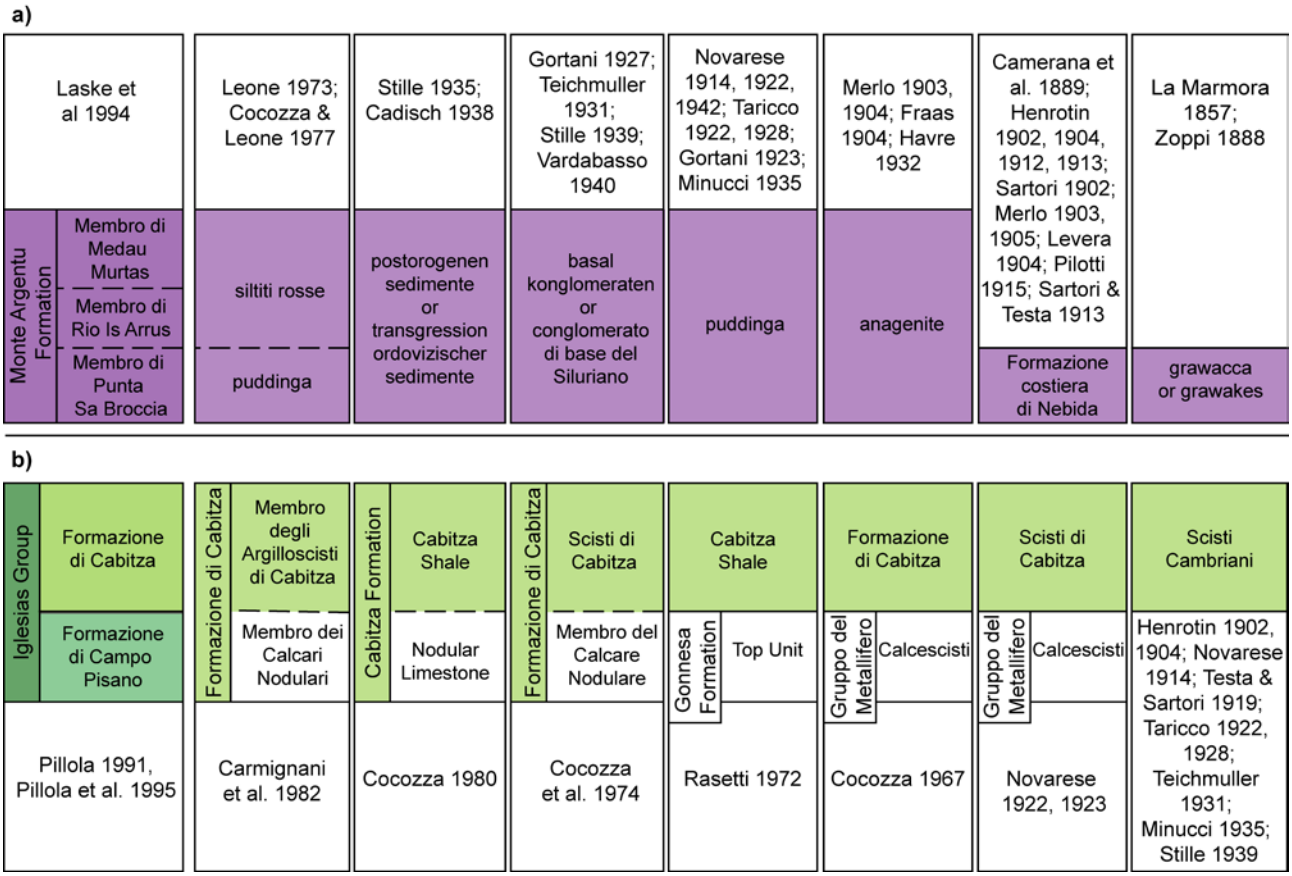

Figure 5 – Chronostratigraphic attributions of lithostratigraphic affected by the Sardic Unconformity (**a**) Overlying the unconformity and including the Monte Argentu Formation. (**b**) Underlying the unconformity and including the Cabitza Formation.

One of the problems related to the identification of the Sardic unconformity is linked to the environmental interpretation of the post-unconformity strata (Monte Argentu Formation; Laske et al., 1994). They were firstly interpreted as "anagenites" or "rocks comprising igneous fragments" (Henrotin, 1904), "crushing breccia" (Fraas, 1904) and broad "transgressive deposits" (Henrotin, 1902; Novarese, 1914, 1942; Taricco, 1922, 1928; Gortani, 1927; Teichmüller, 1931; Minucci, 1935; Vardabasso, 1940). The coarse-grained lag directly capping the unconformity was interpreted as "slope conoid conglomerates" (Del Bono, 1965), "olistostromes and tectonic breccias" (Brower, 1987), "syn-sedimentary tectonics" (Brusca & Dessau, 1968), and "syn-tectonic deposits related to fluvial-lacustrine environments or narrow sea platforms" (Martini et al., 1991). The post-unconformity deposits have been related to a coastaline (Novarese, 1914; Teichmüller, 1931), continental deposits (Cocozza & Valera, 1966; Cocozza, 1967*a*), alluvial (Poll, 1966), deltaic (Cocozza et al., 1974; Oggiano et al., 1986; Laske & Bechstädt, 1987, 1989; Bechstädt & Boni, 1994) and proximal to deep marine settings (Schneider, 1974).

Another question concerned the chronostratigraphic attribution of the post-unconformity strata. Taricco (1922) collected some specimens of supposed "phyllocarids" (in fact, *Taricciocoia arrusensis*; Hammann et al., 1990) from silty levels interbedded in the former deposit, and attributed them to an "Arenig" age. Teichmüller (1931), influenced by the former data, attributed a "Furongian-Ordovician" age to the unconformity. Subsequently, Stille (1935, 1939), coined the term "Sardic

unconformity" to describe the discordance separating the "Cambrian shales" (Cabitza Formation) and the supposed "Arenig puddinga" (Monte Argentu Formation). The stratigraphic gap described by Teichmüller (1931), induced Stille to link the Sardic unconformity with other Furongian-Lower Ordovician gaps recognized throughout western and northern Europe in the Variscan fold belt.

Although the Sardic unconformity is Mid-Late Ordovician in age, and unrelated to Furongian gaps (Stille, 1935, 1939), its name was broadly accepted. From the 1920s to the 1990s, the research focused on the Sardic unconformity led to the recognition of some structures associated with the discordance. Furthermore, from the end of the 1980s, several data allowed a correct dating of the Sardic unconformity: the attribution of *Dictyonema* (former *Rhabdinopora*) *flabelliformis*; Pillola & Gutiérrez-Marco, 1988) and acritarchs (Barca et al., 1987*b*) to the Early Ordovician, sampled in the upper part of the Cabitza Formation, shifted the unconformity to a setting between the Tremadocian and the Sandbian ("Caradoc" of the British chart). Further palaeontological discoveries (e.g., Ferretti & Serpagli, 1990; Ferretti, 1992; Pillola et al., 1998, 2008) permitting the settlement of the unconformity between the Floian and the Sandbian.

3.2 Sardic phase

The connection between the Sardic unconformity and a contemporaneous folding phase was firstly proposed by Zoppi (1888), who distinguished two folding systems affecting the pre-discordance succession.

Novarese (1914) introduced the term "puddinga" (**Fig. 5a**) to describe the "post-tectonic deposit" made up of conglomerates (Monte Argentu Formation; Laske et al., 1994), directly capping the unconformity. On the basis of this interpretation, it was clear that the puddinga was connected to a folding phase chronologically constrained between the pre- and post-unconformity strata. Novarese (1922) and Novarese & Taricco (1923) provided the first tectonic interpretation of this intra-Ordovician deformation phase, which was then considered as Caledonian (developed during the "Silurian", which included the Ordovician in the 1920s) and preceding the Variscan deformation (developed during the Late Carboniferous).

The term "Sardic Phase" was introduced by Stille in 1935 to describe a distinct tectonic event related to the "Sardic" unconformity, which was interpreted as the product of a pre-Arenig (Floian) orogeny (Teichmüller, 1931). The first mention to the Sardic phase appeared in the "Scheme of the Orogenesis phases through Geologic time" made by Stille (1935), where it is tentatively dated at about 480 Ma, predating the Taconic phase of New England (North America) (**Fig. 6**).

Stille (1935) distinguished the Alpine, Variscan and Caledonian orogenies, the latter bracketed between the "Silurian" (including the Ordovician until the 1960s) and the Devonian. In the Caledonian orogeny, he distinguished younger phases that supposedly took place during the Devonian, such as the Ardennes phase and older phases recorded during the Silurian *s.s.*, such as the Taconic phase. On Stille's opinion, the tectonic Sardic phase was an early compressive event of the Caledonian orogeny bracketed between the Upper Cambrian (Furongian) and the Early Ordovician, which caused folding, emersion and erosion of the "Cambrian shales" (Cabitza Formation) unconformably overlain by the "Lower Ordovician". In fact, the occurrence of the puddinga deposit suggested a complete orogeny that led to the uplift of the "Cambrian" succession, the erosion of the former followed by subsidence, and the sedimentation of the transgressive puddinga deposit.

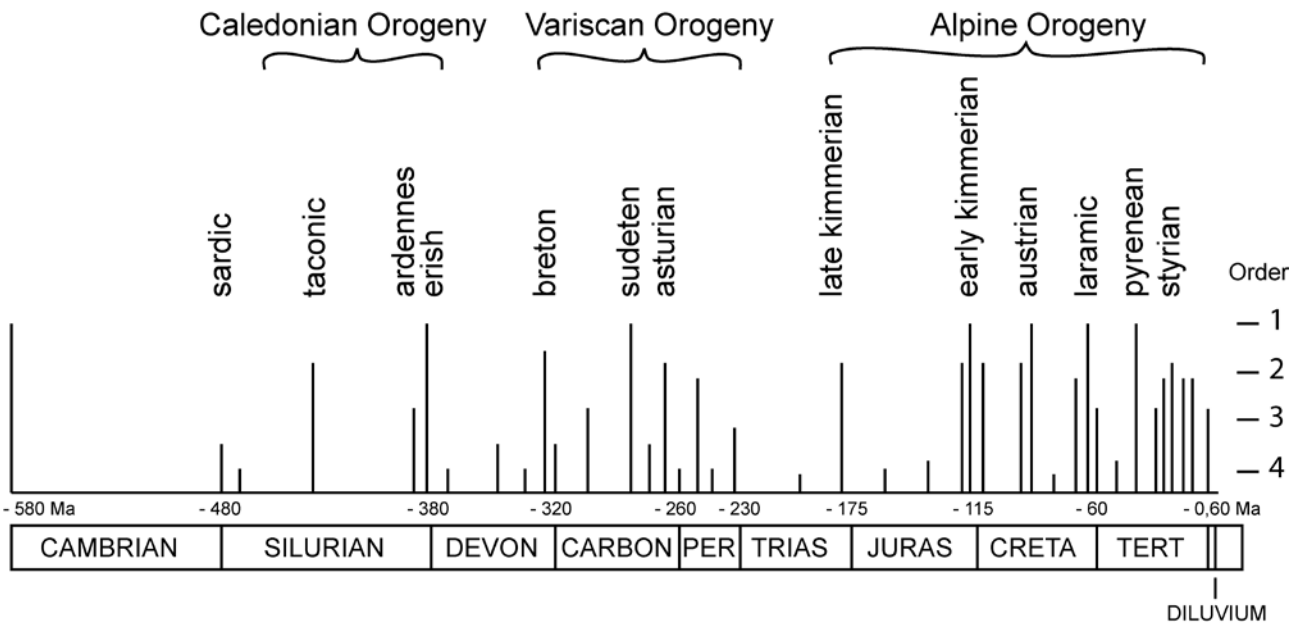

Fig. 6 - Scheme of the "Orogenic phases through time"*;* modified after Stille (1935).

The Sardic phase was largely accepted by the scientific community because it allowed to justify the stratigraphic unconformity and angular discordance recognized by several authors (Zoppi, 1888; Novarese 1914, 1922, 1942; Taricco, 1922, 1928; Teichmüller, 1931), as well as the occurrence of deformations exclusively affecting the pre-unconformity strata (Zoppi, 1888; Novarese, 1923, 1942; Novarese & Taricco, 1923; Gortani, 1923; Teichmüller, 1931; Cadish, 1938; Vardabasso, 1950, 1956; Gèze, 1952; Arthaud, 1963, 1970; Poll & Zwart, 1964; Valera, 1964, 1967; Brusca & Dessau, 1968).

The occurrence of superposed deformation events affecting the Palaeozoic strata cropping out in SW Sardinia, which gave rise to folding interference patterns (firstly recognized by Cadisch, 1938), made difficult to distinguish the Sardic and Variscan deformations. These tectonic structures were described, among others, by Cadisch (1938), Grawlich (1953), Vardabasso (1956), Arthaud (1963, 1970), Poll & Zwart (1964), Valera (1964, 1967), Brouwer (1965), Del Bono (1965), Dunnet (1969), Lüneburg & Lebit (1998) and Carmignani et al. (2001*a*, *b*). Some of them (e.g., Vardabasso, 1956; Arthaud, 1963, 1970; Poll & Zwart, 1964; Dunnet, 1969; Lüneburg & Lebit, 1998; Carmignani et al., 2001*a*) distinguished the occurrence of four folding systems affecting the pre-Sardic succession. In addition, because of the coincidence between the E-W direction of the Sardic and first Variscan deformation phases, several authors considered as distinctly Sardic only those folds cut by the Sardic unconformity and capped by the post-unconformity puddinga deposits (Arthaud, 1963, 1970; Poll & Zwart, 1964; Poll, 1966; Dunnet, 1969) or, recently, cut by the Variscan tectonic foliation (Funedda, 2009).

Although the identification of the unconformity and the deformations affecting the pre-unconformity successions was largely recognized, some authors did not accept the existence of the Sardic phase. Among them, Minucci (1935) recognized the unconformity but not the pre-Ordovician deformation, Grawlich (1953) and Del Bono (1965) did not identify the unconformity because of their interpretations of the puddinga deposit, and Brouwer (1987) rejected the Sardic phase because he considered the conglomerate (Monte Argentu Formation) as a tectonic breccia or mélange and attributed all the deformations to the Variscan orogeny.

CARTA GEOLOGICA SCHEMATICA DEL SARRABUS-GERREI

alla scala 1:100.000

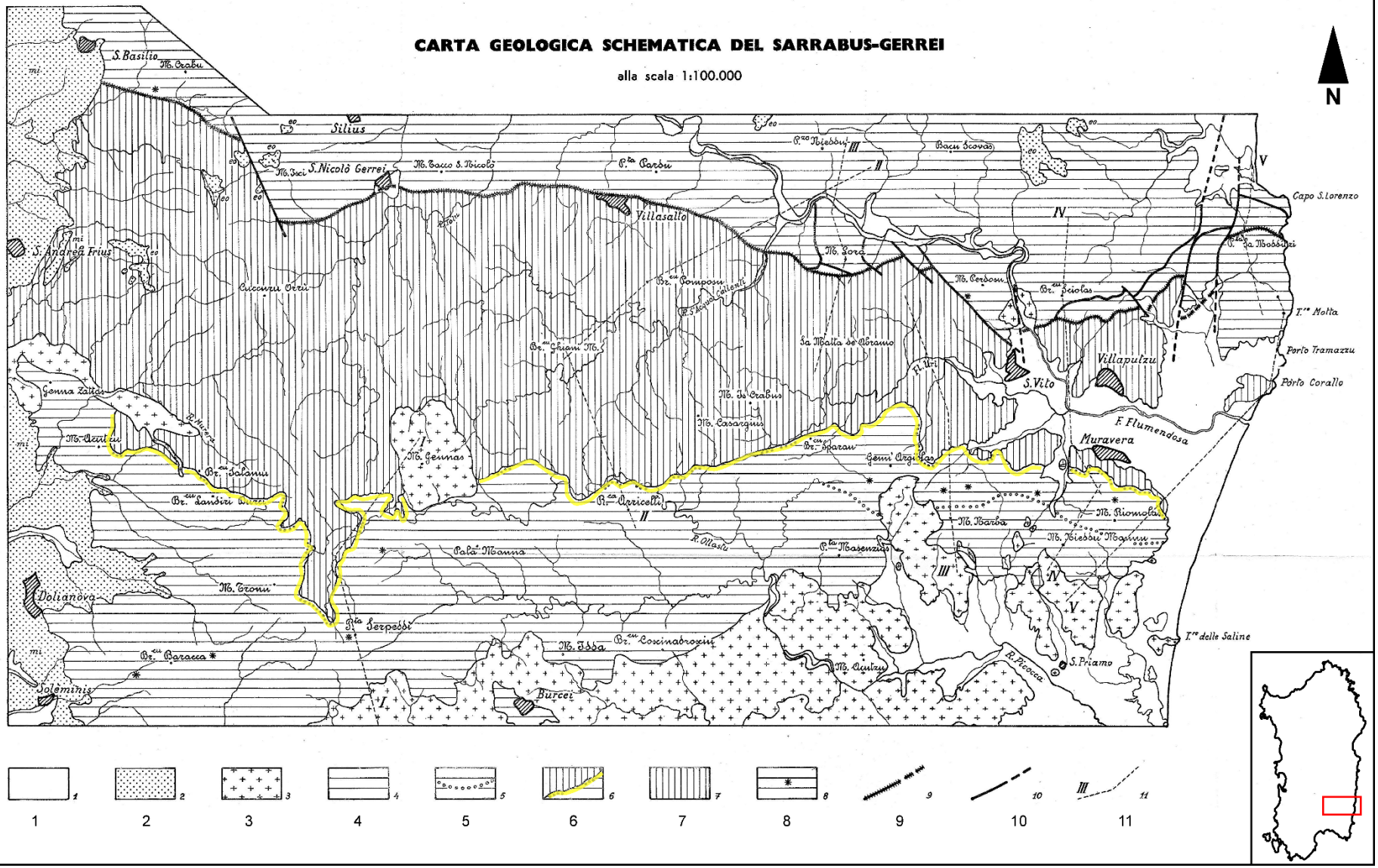

1 2 3 4 5 6 7 8 9 10 11

Figure 7 - Geological map of the Sarrabus area; modified after Calvino (1959*b*), where the yellow line marks the Sardic unconformity: 1) Old and recent alluvial deposits; 2) Sandstones and conglomerates of Miocene and Eocene age; 3) Granites, granodiorites and diorites; 4) Silurian-Devonian series of sandstones, shales, slates, limestone, jasper, basal or embedded volcanites; 5) Monte Narba's transgressive conglomerate; 6) Silurian-Devonian serie's basal conglomerate, placed along the sarrabese unconformity; 7) "Arenarie di San Vito" Formation: sandstone, shales and slates ; 8) Upper and Middle (?) Ordovician fossiliferous localities; 9) Villasalto Fault; 10) Other faults; 11) Geological profiles.

Another question was involved with the metamorphism related to the Sardic phase: a "metamorphic unconformity" was invoked by Eltrudis et al. (1995) and Annino (1995), but most of the authors attributed the low- to very low-metamorphism of some strata to the weak deformations generated by the Sardic phase (Vardabasso, 1966; Conti et al., 1978; Carmignani et al., 1994, 2001*a*). Despite the former reports, the occurrence of a sharp metamorphic change between the pre- and post-Sardic deposits is under discussion. In fact, Franceschelli et al. (2017) have recognized no significant differences between the P-T metamorphic conditions of the Cabitza and Monte Argentu formations.

Another no-man's land throughout the last 50 years has been the interpretation of the Bithia Formation and the Monte Filau Orthogneiss, intruded in the former formation, cropping out in SW Sardinia (**Fig. 4**). The succession cropping out in the Capo Spartivento area, composed of the Bithia and Monte Settiballas formations and the Monte Filau Orthogneiss, has been traditionally interpreted as an autochthonous unit of "Precambrian-early Cambrian" age (Tucci, 1983). The interpretation derived from the geometrical relationship between the lower Cambrian succession (Nebida Group and Bithia Formation), and the Precambrian age attributed to the protolith of the Mt. Filau Orthogneiss (Junker & Schneider, 1983). Subsequent U/Pb zircon and Rb/Sr analyses have revealed an Ordovician age for the Monte Filau Orthogneiss (478 ± 16 Ma from multigrain U/Pb zircon: Delaperrière & Lancelot, 1989; 427 ± 33 Ma from Rb/Sr whole rock: Cocozza et al., 1977), particularly a Mid Ordovician age (458.21 ± 0.32 Ma; Pavanetto et al., 2012), which is coeval with the deposition of the protoliths of the metavolcanic rocks embedded in the Bithia Formation (457.01 ± 0.17 Ma, Pavanetto et al., 2012; 462.1 ± 4.3 Ma, Cruciani et al., 2018).

3.3 Sarrabese unconformity and related phase

The identification of an intra-Ordovician unconformity in the Palaeozoic rocks of central and northern Sardinia has been difficult because of the strong Variscan imprint, which generated a nappe stacking in the central-southeastern zone, and an increasing SW-to-NE tectonic/metamorphic grade along the island. These factors made difficult the recognition and the subsequent correlation between the successions cropping out in the different tectonic units of both the External and Internal nappes in Sardinia. Since the 1970s, different authors signaled the occurrence of significant Variscan deformation associated with kilometric isoclinal folding and regional tectonic thrusts through the Sarrabus and Gerrei units of the External Nappe Zone (Bosellini & Ogniben, 1968; Carmignani & Pertusati, 1977; Naud & Tempier, 1977; Naud, 1979*a*; Barca et al., 1981*a*, *b*; Conti & Patta, 1998), and starting to decipher the complicated puzzle of the Nappe Zone.

Despite the understanding of the nappes' structure and emplacement, the first correlation of the Palaeozoic successions cropping out in the Sarrabus-Gerrei, Barbagia-Sarcidano and Fluminese-Arburese areas of the Nappe Zone (**Fig. 4**) were suggested by La Marmora (1857) on the basis of stratigraphic similarities and palaeontologic record. This correlation, confirmed by Schneider (1974), Barca & Di Gregorio (1979), Barca et al. (1981*a*, 1985), Tongiorgi et al. (1982, 1984), Annino et al. (2000) and Carmignani et al. (2001*a*), was extended throughout the Palaeozoic

succession of the Sulcis-Iglesiente area (Minzoni, 1980; Tongiorgi et al., 1984; Theodoridis, 1989; Barca et al., 1992; Carmignani et al., 2001*a*) of the Foreland Zone. The connection between the tectonostratigraphic units of the Nappe Zone has been strengthened by the correlation of the Ordovician magmatic and volcanic rocks interbedded in the successions below and above the unconformity (Bosellini & Ogniben, 1968; Di Simplicio et al., 1974; Cocozza & Minzoni, 1977; Ferrara et al., 1978; Naud, 1979*b*; Minzoni, 1975, 1980; Carmignani et al., 1981, 2001*a*; Barca & Maxia, 1982; Memmi et al., 1982, 1983; Barca et al., 1985; Borrouilh et al., 1985; Naud & Pittau Demelia, 1985; Minzoni, 1985; Vai & Cocozza, 1986; Theodoridis, 1989; Annino et al., 2000; Pertusati et al., 2002; Palmeri et al., 2004; Garbarino et al., 2005; Giacomini et al., 2005, 2006; Helbing & Tiepolo, 2005; Oggiano & Mameli, 2006; Buzzi et al., 2007*a*, *b*, *c*; Dack, 2009; Rossi et al., 2009; Oggiano et al., 2010; Cruciani et al., 2008, 2013, 2019; Casini et al., 2012, 2015).

The occurrence of a basal transgressive coarse deposit (Metaconglomerato di Muravera; Carmignani et al., 2001*a*) overlying the unconformity in the External Nappe Zone, suggested by Gèze (1952), was firstly confirmed for the Sarrabus unit (Calvino, 1959*a*, *b*), and then for the Gerrei, Arburese, Meana Sardo and Barbagia units (Barca et al., 1985; Naud & Pittau Demelia, 1985; Theodoridis, 1989; Barca et al., 1992; Annino et al., 2000; Funedda, 2000; Carmignani et al., 2001*a*; Pertusati et al., 2002).

After publishing several studies focused on the Palaeozoic of the Sarrabus area (SE Sardinia), Calvino (1956, 1959*a*, *b*) remarked the presence of an angular unconformity separating the Cambrian-Ordovician San Vito Sandstone (Arenarie di San Vito Formation; Calvino, 1959*b*) and the basal conglomerate (Metaconglomerati di Muravera Formation; Carmignani et al., 2001*a*), or directly a volcano-sedimentary complex (firstly named Porfidi Grigi e Bianchi by Calvino (1959*b*), then Volcanites Group by Barca & Maxia (1982), and latter known as the Monte Santa Vittoria and lateral equivalents) of supposed “Caledonian” Mid-Late Ordovician age. This unconformity, which extends through 58 km from W to E (**Fig. 7**), was named “Sarrabese unconformity” and related to a homonymous tectonic event, the “Sarrabese phase” (Calvino, 1959*b*). Although no Cambrian-Ordovician fossils were sampled in the succession below the unconformity, Calvino speculated on a Cambrian age for the San Vito sandstone on the basis of the lithological similarity with some successions of SW Sardinia, and located the Sarrabese phase between the Cambrian and the Ordovician. Calvino (1959*b*, 1967) proposed the correlation between the Sardic and Sarrabese unconformities, and related them to tectonic events. The correlation was subsequently accepted by several authors (Barca et al., 1987*b*) and widely confirmed both for the Sarrabus and the Gerrei units of the External Nappe Zone of Sardinia (Cocozza et al., 1974; Schneider, 1974; Carmignani & Pertusati, 1977; Naud, 1979*a*, *b*, 1981; Barca & Di Gregorio, 1979; Barca et al., 1981*b*, 1985, 1992; Barca & Maxia, 1982; Memmi et al., 1982; Naud & Pittau Demelia, 1985; Carmignani et al., 1992, 2001*a*; Annino et al., 2000; Funedda, 2000; Gnoli & Pillola, 2002; Pertusati et al., 2002).

However, the Sarrabese phase was firstly dated as Lower-Middle Ordovician (Barca et al., 1981*b*), Middle Ordovician (Barca et al., 1988; Gnoli & Pillola, 2002), on the basis of a mid-Furongian and Early Ordovician fauna collected from the Arenarie di San Vito Formation (Barca et al., 1981*a*, *b*, 1984, 1988; Naud & Pittau Denelia, 1985; Gnoli & Pillola, 2002). Several authors signaled that the Cambro-Ordovician rocks of the Nappe Zone had not been surely deformed by the Sardic/Sarrabese phase (Valera, 1967; Carmignani et al., 1978; Barca & Maxia, 1982; Borrouilh et al., 1985; Pertusati et al., 2002). Only recently, Cocco & Funedda (2019) outlined the onset of overturned folds without related foliation affecting the rocks below the unconformity, subsequently randomly cut by the main Variscan foliation, and finally sealed by the post-unconformity succession.

3.4 Geodynamic setting

Due to the record of a distinct angular unconformity, the stratigraphic gap related to the Sardic deformation phase has been generally linked to a major orogeny, ranging from the Caledonian (Novarese, 1922; Novarese & Taricco, 1923; Stille, 1935, 1939; Vardabasso, 1950, 1956, 1966; Gèze, 1952; Valera, 1964; Cocozza et al., 1974; Carmignani & Pertusati, 1977; Cocozza & Minzoni, 1977; Carmignani et al., 1979, 1981, 1982; Cocozza, 1979; Vai, 1982; Barca et al., 1985) to pre-Caledonian (Bederke, 1939; Novarese, 1942; Arthaud, 1963), Cadomian (Schneider, 1974), Taconic (Di Simplicio et al., 1974; Carmignani et al., 1978; Borrouilh et al., 1985), Acadian (Naud, 1979*a*), and Assintic ones (Carmignani et al., 1981), though Schneider (1974), Carmignani & Pertusati (1977), Cocozza (1979) and Theodoridis (1989) regarded the former as a minor tectonic movement developed in the Variscan Europe during Cambro-Ordovician times. Arthaud (1970), while admitting the occurrence of the Sardic unconformity and the related tectonic event which generate it, denied the existence of the Sardic phase outside Sardinia.

The Sardic Phase has been linked to different geodynamic settings. Until the discovery of the Sarrabese unconformity, it was regarded as a compressive event (Novarese & Taricco, 1923; Teichmüller, 1931; Stille, 1935, 1939; Vardabasso, 1950, 1956, 1966; Gèze, 1952; Arthaud, 1963, 1970; Poll & Zwart, 1964; Valera, 1964, 1967; Dunnet, 1969; Cocco & Funedda, 2012, 2019). The tectonic event was also related to rifting (Vai, 1982, 1991; Minzoni, 1985; Vai & Cocozza, 1986; Theodoridis, 1989; Delaperrière & Lancelot, 1989; Hammann, 1992; Helbing & Tiepolo, 2005) and transtensive (Martini et al., 1991) scenarios.

The occurrence of Ordovician magmatic rocks interbedded in the pre- and post-unconformity successions, rhyolitic to andesitic-basaltic composition and with calc-alkaline affinity (Memmi et al., 1983) has been interpreted as late- to post-orogenic or volcanic arc activities (Cappelli et al., 1992; Carmignani et al., 1992, 2001*a*; Garbarino et al., 2005; Helbing & Tiepolo, 2005; Giacomini et al., 2006; Buzzi et al., 2007*a*, *b*, *c*; Boriani, 2008; Cruciani et al., 2008, 2013, 2018, 2019; Oggiano et al., 2010; Gaggero et al., 2012).

Cappelli et al. (1992) and Carmignani et al. (1992, 1994) proposed a collisional geodynamic model to explain the seemingly early compressive-style Sardic deformation and the late “rifting” volcanism. In order to account the simultaneity of structural and magmatic features, extensional-convergent (Andean-type subduction zone; (Rossi et al., 2009; Oggiano et al., 2010; Gaggero et al., 2012; Cruciani et al., 2018) and transpressive margins (Cocco & Funneda, 2019) have been proposed recently.

3.5 Upper Ordovician unconformity in the Eastern Pyrenees

Another intra-Ordovician unconformity has been recognized in the Palaeozoic rocks of the Eastern Pyrenees Axial Zone. It separates a lower inherited palaeorelief, composed of the Cambrian-Lower Ordovician Jujols and the Ediacaran-Terreneuvian Canaveilles groups (Padel et al. 2018*a*) from the overlying Upper Ordovician succession. The unconformity was firstly recognized in Andorra by Llopis Lladó (1965) separating the supposed Cambrian shales and the overlying Upper Ordovician succession that started with conglomerates. The occurrence of this unconformity has been widely confirmed in several tectonic units (Santanach, 1972; Ravier et al., 1975; Zwart, 1979; Muñoz et al., 1983; Barrouquère et al., 1983; Muñoz, 1985; Laumonier & Guitard, 1986; Speksnijder, 1987; Laumonier, 1987, 1988; García-Sansegundo & Alonso, 1989; Den Brok, 1989; Kriegsman et al.,

1989; Poblet, 1991; Muñoz & Casas, 1996; Gil-Peña et al., 2001, 2004; García-Sansegundo et al., 2004; Laumonier et al., 2004; Casas & Fernández, 2007; Donzeau & Laumonier, 2008; Casas, 2010; Puddu & Casas, 2011; Casas & Palacios, 2012; Margalef et al., 2014, 2016; Casas et al., 2015).

Although this intra-Ordovician unconformity has been largely considered as a regional Palaeozoic feature in the Eastern Pyrenees, several authors did not reported it (Dalloni, 1930; Boissevain, 1934; Cavet, 1957, 1969; Brouwer, 1968; Hartevelt, 1970; Speksnijder, 1987), or misinterpretated it (Robert, 1980; **Fig. 8**). Probably, these problems were related to the important thickness variations (0-200 m) exhibited by the conglomeratic post-unconformity lag deposit (Rabassa Conglomerate Formation: Hartevelt, 1970), whose lack made difficult the distinction between the pre- and post-unconformity strata.

The stratigraphic gap involved by the unconformity has been chronologically controlled mainly on the basis of the fossiliferous content yielded by the post-unconformity succession. Some specific levels, such as the Cava and Estana Formations, are fossiliferous allowing its attribution to the Late Ordovician (Faura i Sans, 1913; Dalloni, 1930; Boissevain, 1934; Cavet, 1957, 1960; Llopis-LLadò, 1965; Hartevelt, 1970; Barnolas et al., 1980; Barnolas & García-Sansegundo 1992; Sanz López & Sarmiento, 1995; Sanz López, 2002; Gil-Peña et al., 2004; Roqué Bernal et al., 2017; Štorch et al., 2019). The Estana Formation (Hartevelt, 1970) constitutes a good stratigraphic marker bed, the so-called "schistes troués", "Grauwacke à *Orthis*" and "Caradoc limestones" of French and Dutch geologists, and is easily recognizable by their variegated colours in the Upper Ordovician successions of the Eastern Pyrenees.

The pre-unconformity rocks (Canaveilles and Jujols groups: Padel et al., 2018*a*) were formerly reported as the "Paléozoïque inférieur" (Cavet, 1957) in the Central Pyrenees, and the "Serie de Sant Julià" or "Serie de La Massana" (Llopis-Lladò, 1965) and "Seo Formation" (Hartevelt, 1970) in the Eastern Pyrenees,. This seemingly fossiliferous barren succession has been traditionally attributed to the Cambro-Ordovician on the basis of its stratigraphic position below the Upper Ordovician succession. This attribution has been corroborated by some palaeontological discoveries, such as Cambrian Epoch 2 archaeocyaths in patch-reefs of the Salut thrust-slice unit (Abad, 1988; Perejón et al., 1994) and some Furongian-Early Ordovician acritarchs reported from the upper part of the Jujols Group (Casas & Palacios, 2012) associated with ichnofossils (Gámez et al., 2012).

The radiometric analysis of the volcanic rocks associated with the Sardic Unconformity and the magmatic bodies intruded in the Canaveilles and Jujols groups (Delaperrière & Respaut, 1995; Barbey et al., 2001; Deloule et al., 2002; Castiñeiras et al., 2008, 2011; Denèle et al., 2009; Casas et al., 2010, 2011, 2015; Liesa et al., 2011; Navidad et al., 2010, 2018; Martínez et al., 2011; Martí et al., 2019) allowed a better geochronological constraint of the age of the pre- and post-unconformity succession and a better understanding of the stratigraphic gap bracketed into the unconformity.

The origin of the Upper Ordovician unconformity in the Eastern Pyrenees has been linked to an orogenic event that caused uplift and erosion of a Cambro-Ordovician palaeorelief. Llopis-Lladò (1965) firstly related the pre-"Caradocian" unconformity with the Sardic one and hypotesized the relation with a later Sardic phase. Ravier et al. (1975) proposed a Caledonian, particularly Taconian, orogeny. Ovtracht (1960), recognizing the transgressive character of the Caradocian deposits in the Mouthoumet massif, predicted the existence of two minor tectonic pre-Caradoc phases affecting the pre-unconformity deposits.

Several deformations affecting the pre-unconformity successions have been reported, and some of them have been related to the Sardic phase (Casas, 2010; Casas et al., 2015), albeit they have

been linked either to buckling (Santanach, 1972) or to basement tilting related to a Late Ordovician faulting and erosion (García-Sansegundo et al., 2004; Casas & Fernández, 2007).

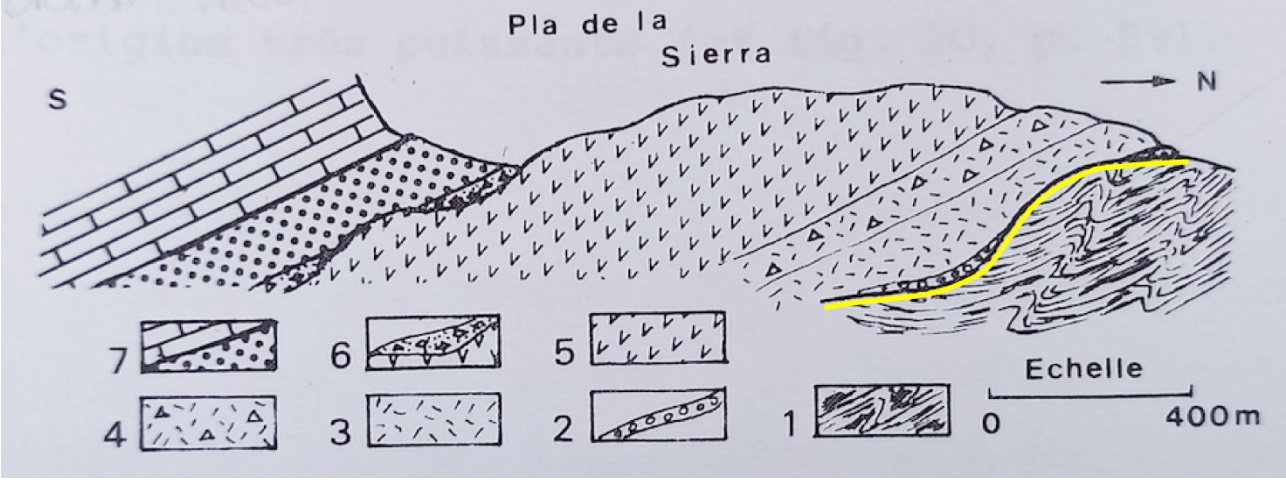

Figure 8 - Geological sketch representing the Palaeozoic succession at Pla de la Sierra (Campellas, Ribes de Freser area) drawn by Robert (1980), in which the yellow line represents the Sardic unconformity between the Cambro-Ordovician strata (1), and the basal conglomerate (2) or directly the lavas (3), volcanic breccias (4) and ignimbritic lavas (5), capped by the Cretaceous (6) and Paleocene (7). Because of the lack of datations, Robert interpreted the volcanics as Permian, although recent radiometric works point to a mid Ordovician age (Martí et al., 2019).

CHAPTER 4

CHAPTER 4

SARDINIA. GEOLOGICAL SETTING AND STRATIGRAPHY

As suggested by lithologic affinities and palaeomagnetic and structural data, the basement of Sardinia and Corsica shared part of their geologic evolution with Provence and Catalonia up to the Oligocene (Cherchi & Montadert, 1982; Cherchi & Trémolières, 1984), when it started to rotate (ca. 20-17 Ma) opening the Gulf of Lion until its present-day position on the western Mediterranean Sea (Edel et al., 1981; Westphal et al., 1986; Vigliotti & Langenheim, 1995).

Although Sardinia has recorded the witnesses of different orogenies ("Sardic", Variscan and Alpine ones), the main structural imprint was induced by the Variscan orogeny. In fact, the Sardinian basement represents a segment of the south-european Variscan chain (**Fig. 2**) that separated from Europe during Early Miocene times. The Variscan orogeny involved rocks of Cambrian-Early Carboniferous age, which display different deformation and metamorphic processes. Rocks of the Variscan cycle are unconformably overlain by Middle-Upper Carboniferous unmetamorphic and undeformed deposits (Cocozza, 1967*b*; Olivieri, 1970; Del Rio, 1973; Vai & Cocozza, 1974; Fondi, 1979; Carmignani et al., 1981, 2001*b*). The main Variscan phases are associated with a plate collision that resulted in the deformation of a Palaeozoic basement, with development of a southward verging stack of allochthonous nappes (Conti et al., 2001), a late extensional episode with normal and transcurrent faults, a late calc-alkaline magmatism, and a Late Carboniferous-Permian continental sedimentation.

Three tectonometamorphic units or zones were recognized in the Sardinian basement (**Fig. 4**), characterized by their own metamorphic grade and deformation (Carmignani et al., 1994): the Foreland Zone in the SW, the Nappe Zone (subdivided into External and Internal zones) in the central part of the island, and the Inner Zone in the northern one. Despite the lack of continuity of Palaeozoic outcrops, due to the onset of large granitoid intrusions and post-Variscan sediments, these three zones can be traced across the entire island following a parallel trending (ca. NW-SE) that follows the axial orientation of the Variscan main phase deformation. Deformation intensity increases northward, from SW to NE, consistent with the regional metamorphic grade: (i) the Foreland Zone restricted to the SW Sardinia (Sulcis and Iglesiente areas) exhibits folding and overthrusts; whereas (ii) the Nappe Zone, which spreads between Sarrabus to Nurra regions, shows intense folding with recumbent folds and important overthrusts; (iii) and the Inner Zone extends along and northward the Posada-Asinara Line (**Fig. 2**), which represents a regional shear zone (Elter et al., 1990; Carosi & Palmeri, 2002; Helbing & Tiepolo, 2005; Giacomini et al., 2006), separating the High-Grade Metamorphic Complex (to the north) and the Low-Medium Grade Metamorphic Complex to the south (Carmignani et al., 2001*b*).

The Variscan collision developed a Barrovian-type metamorphism, whose intensity grows gradually from SW to NE, from a very low-grade in the Foreland Zone (anchizone: Palmerini et al., 1979) to the greenschist facies in the Nappe Zone (amphibolitic zone: Di Simplicio et al., 1974), up to high grade in the Inner Zone. A wide post-collisional plutonic complex emplaced between the Upper Carboniferous and the Lower Permian, mainly made up of calc-alkaline granitoids (Orsini, 1980).

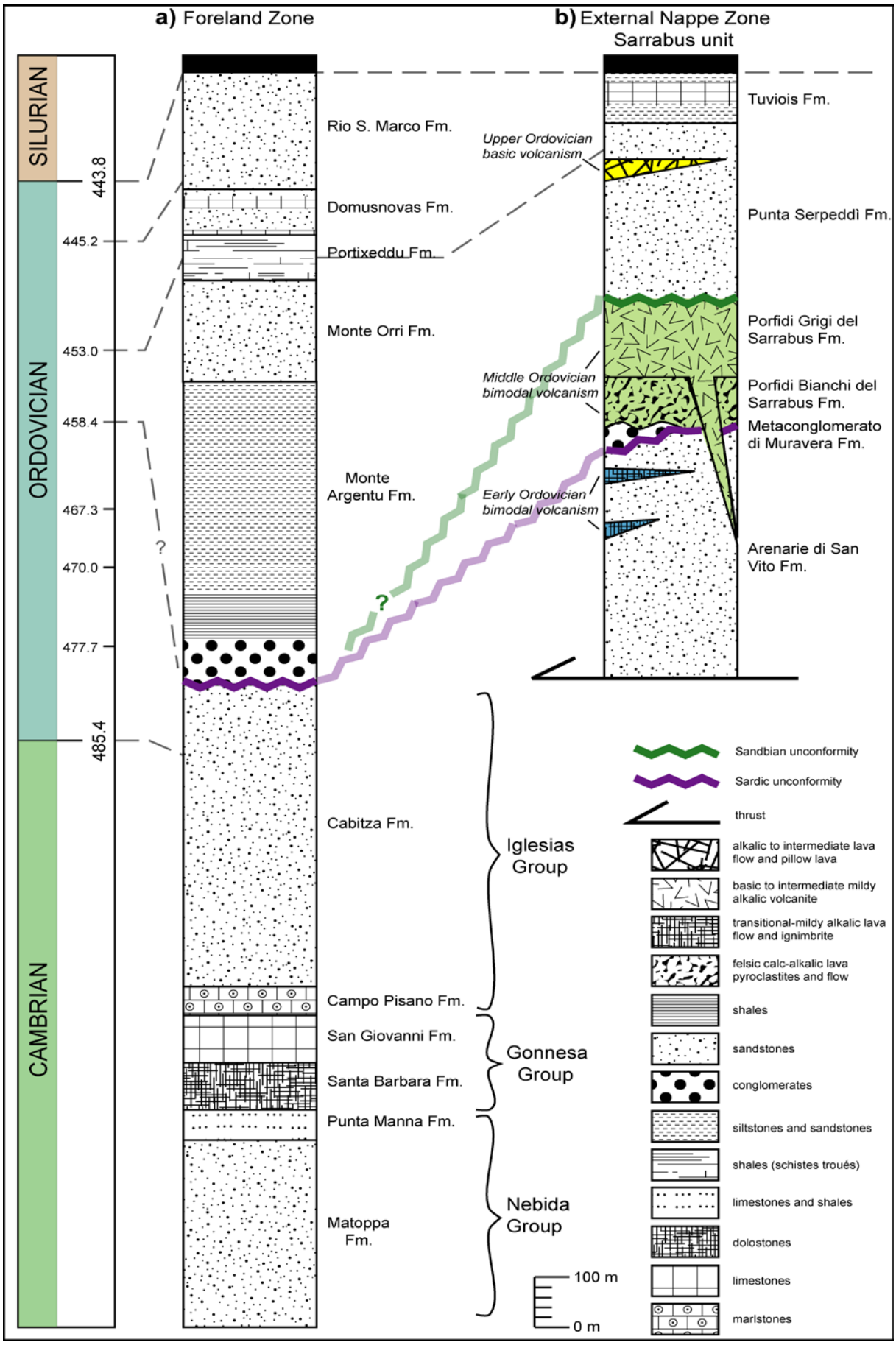

Figure 9 - Stratigraphic pre- and post-Sardic successions (**a**) in the Foreland and (**b**) the Sarrabus unit of the External Nappe Zone.

4.1 Foreland Zone

The Foreland Zone that crops out in SW Sardinia (**Fig. 4**) includes a continuous succession of Palaeozoic rocks interrupted by the Sardic unconformity. The later, firstly recognized in this zone, is an angular discordance that separates "lower Cambrian"-Lower Ordovician strata from a (?)Middle-Upper Ordovician-Lower Carboniferous succession. The pre-unconformity strata are composed of a thick, almost 2000-2500 m, and continuous succession including rocks of "early Cambrian" to Early Ordovician age (**Fig. 9a**). The post-unconformity succession, Late Ordovician in age and at least 1000 m thick, is overlain by Silurian-Lower Devonian deposits (**Fig. 9a**).

The Foreland Zone has been affected by at least three Variscan events involving the whole Cambrian-Lower Carboniferous succession, which suffered a very low-grade metamorphism (T<250°C, Casini et al., 2010). Several deformations are recognisable:

(i) The first Variscan phase, E-W oriented and related to foliation, which tightened the pre-Variscan folds, such as in the Iglesias Syncline.

(ii) The second Variscan phase, characterized by maximum compression with N-S trending folds related to a very penetrative foliation, which provoked overthrusts and folds and the refolding of the former E-W folds axial surfaces.

(iii) The third Variscan phase that generated weak folding with variable directions.

4.1.1 Cambrian-Lower Ordovician succession

The pre-unconformity succession is lithostratigraphically subdivided into three groups (Pillola, 1991; Pillola et al., 1995): a basal terrigenous succession with carbonate interbeds (Nebida Group), a middle portion consisting entirely of carbonate rocks (Gonnesa Group), and a mainly terrigenous upper unit (Iglesias Group) unconformably overlain by Upper Ordovician strata (**Fig. 9a**).

The Nebida Group is made up of a basal siliciclastic succession of sandstones and siltstones with minor microbial-archeocyathan build-ups in the upper part (Matoppa Formation), overlain by alternating siliciclastic and carbonate beds, which include sandstones and shales interbedded with ooidal and oncoidal limestones (Punta Manna Formation). The succession is 320-380 m thick (Galassi & Gandin, 1992), but seems to become thicker (600-1000 m; Pillola et al., 1995) because of deformation. The palaeontological content of the Nebida Group comprises archaeocyaths, microbialites, trilobites, brachiopods and echinoderms, suggesting an "early Cambrian" (Ages 3-to-4, Epoch 2) age (Rasetti, 1972; Pillola & Gross, 1982; Debrenne et al., 1989).

The Gonnesa Group is exclusively composed of carbonates, mainly dolostones at the base (Santa Barbara Formation) and limestones at the top (San Giovanni Formation). The Santa Barbara Formation is known as "Dolomia rigata" because of its banded appearance due to the cyclic alternation of dolostones and limestones with stromatolites and layered carbonated claystones. The San Giovanni Formation, known as "Calcare ceroide", consists of limestones with echinoderms and trilobites, microbial boundstones with archaeocyaths, and vadose pisolites. The thickness of the group ranges from 180 to 480 m (Galassi & Gandin, 1992), and the palaeontological record includes archaeocyaths, microbialites, trilobites and echinoderms, suggesting an "early Cambrian" (Age 4, Epoch 2; or late Botomian to late Toyonian age after the Siberian nomenclature) age (Debrenne & Gandin, 1985).

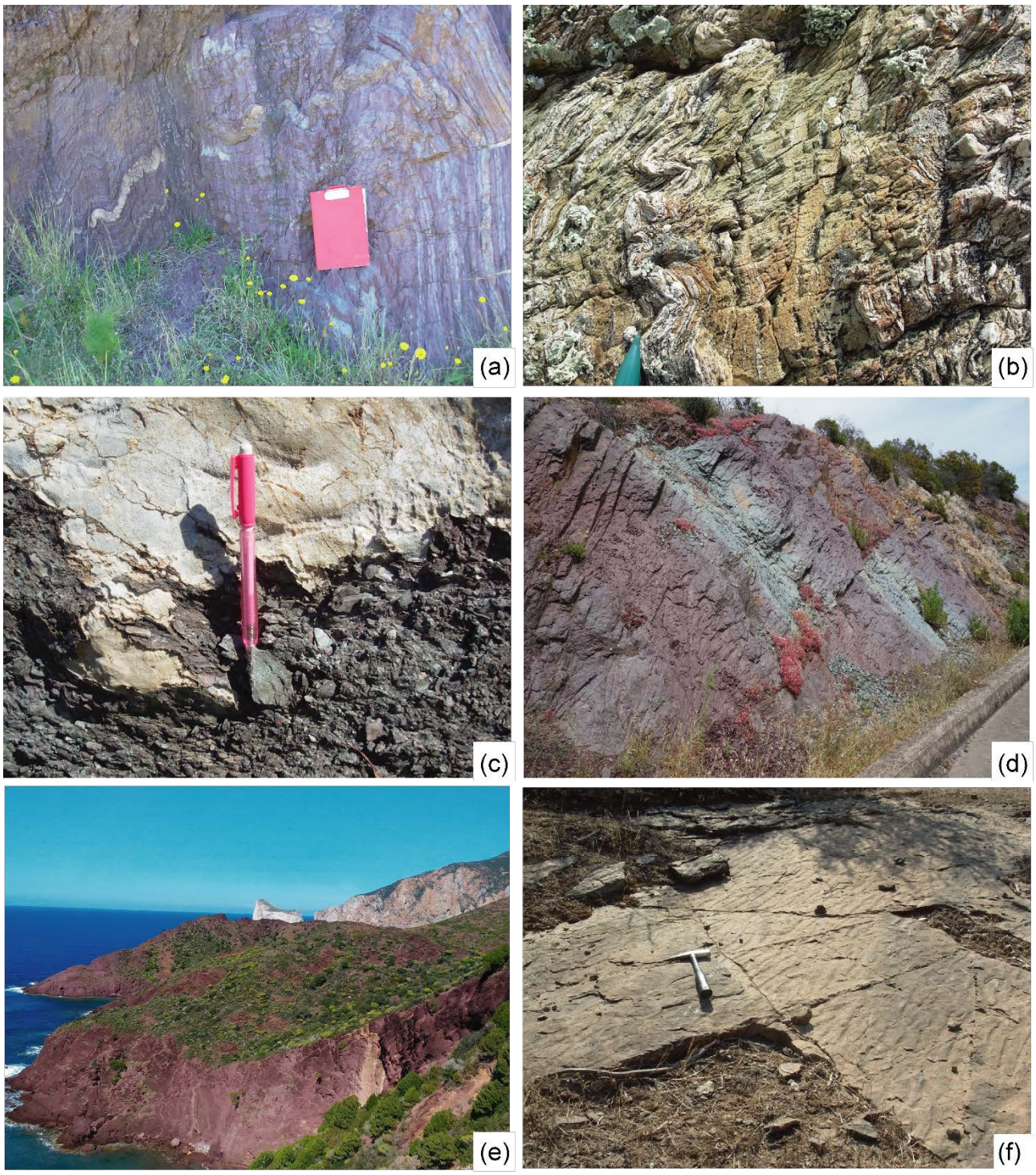

Figure 10 - Pre-Sardic unconformity successions (a-b) and post-Sardic ones (c-f) in the Foreland Zone. (**a)** Red siltstones and (**b)** laminated sandstones of the Cabitza Formation at the homonymous locality, SW Sardinia. (**c)** Basal conglomerate of the Punta Sa Broccia Member, and (**d)** red and green sandstones of the Medau Murtas Member of the Monte Argentu Formation. (**e)** Field aspect of the Monte Argentu Formation along the Nebida-Masua coastline. (**f)** Ripples on the top of sandstones from the Monte Orri Formation (Domusnovas area).

The Iglesias Group is composed of a basal marlstone to nodular limestone (Campo Pisano Formation), known as “Calcari nodulari”, overlain by a siliciclastic-dominant deposit (Cabitza Formation) known as “Scisti cambriani” or “Scisti di Cabitza” (**Fig. 5b**). The Campo Pisano Formation, 20-60 m thick (Galassi & Gandin, 1992), consists of massive to nodular limestone,

calcareous shale and marlstone with terrigenous (clayey to silty fraction) interbeds. A rich fossiliferous content, including echinoderms, trilobites and brachiopods, suggests an age crossing the Cambrian Epoch 2-Miaolingian (former "lower-middle Cambrian") transition.

The overlying Cabitza Formation (Cocozza, 1967*a*) is made up of alternating claystones and siltstones with fine- to coarse-grained sandstones in the basal portion, overlain by variegated shales and fine-grained sandstones in the middle portion of the succession. The upper part consists of red and green laminated sandstones and shales with occasional coarse laminated sandstones (**Fig. 10a**) and fine conglomeratic interbeds. The Cabitza Formation, 400 m (Cocozza, 1979) to 600 m thick (Cocozza & Gandin, 1990), has yielded different faunal assemblages rich in trilobites, brachiopods, echinoderms, graptolites and acritarchs pointing to a "middle Cambrian" or Miaolingian (Pillola et al., 2002) to Early Ordovician age (Tremadoc-Floian?; Pillola et al., 2008). The top of the Cabitza Formation is marked by the Sardic unconformity. So, the younger age of the pre-unconformity rocks is Floian (Lower Ordovician) based on the presence of the graptolites *Rhabdinopora flabelliformis* (Pillola & Gutiérrez-Marco, 1988) and *Anysograptid-Dichograptid murray* (Pillola et al., 2008) found in the upper beds below the Sardic unconformity.

The continuous deposition of the pre-Sardic succession recorded the evolution from a siliciclastic platform (Nebida Group) to a carbonate shelf (Gonnesa Group) across the "lower-middle Cambrian", changing again into a marine terrigenous platform (tidal delta to shoreface and offshore environments) between the "middle Cambrian" (Miaolingian) and the Lower Ordovician (Iglesias Group).

4.1.2 Upper Ordovician succession

In the Foreland Zone, the Cambro-Lower Ordovician strata is unconformably overlain by an Upper Ordovician siliciclastic deposit composed of a basal conglomeratic unit (Monte Argentu Formation) overlain by alternations of medium- to very fine-graine sandstones and dark grey siltstones with pyritic, phosphatic and chloritic nodules (Monte Orri Formation), strongly bioturbated, and topped by alternations of fine sandstones and shales with centimetre-thick carbonate nodules parallel to stratification (Portixeddu Formation). The latter deposits are capped by sandstones with some carbonate interbeds (Domusnovas Formation) and conglomerates bearing volcanic pebbles, epiclastites and siltstones (Rio San Marco Formation). The entire Upper Ordovician succession (**Fig. 9a**), at least 1000 m thick, is overlain by Silurian black shales and limestones.

The Monte Argentu Formation (Laske et al., 1994) is a fining-upward deposit made up of (i) basal heterometric and polygenic conglomerates with a red to purplish hematitic sandy matrix (**Fig. 10c, e**), with clasts ranging in size from 10 to 100 cm and a carbonate breccia interbedded with sandstones and siltstones (Punta Sa Broccia Member, known as "Puddinga"); (ii) an intermediate member formed by grey shales with some sandy interbeds (Rio Is Arrus Member); (iii) followed by a thick succession of red and green siltstones and sandstones (Medau Murtas Member) (**Fig. 10d**). The conglomerate is made up of pebbles derived by the erosion of a pre-Sardic palaeorelilef. It is constituted by shale and sandstone pebbles derived from the Cabitza Formation (**Fig. 10c**), limestone clasts from the San Giovanni Formation (**Fig. 10c**), and dolostone from the Santa Barbara Formation (Gonnesa Group), as well as by vein quartz pebbles. The relative percentage of these components changes in the conglomerate, although the Cabitza-derived pebbles represent the main component of the conglomerate. Limestone and dolostone megabreccia and olistoliths, up to 100 m in size, characterize the base of the Monte Argentu Formation, as a result of syn-sedimentary infill of an inherited palaeorelief (Brusca & Dessau, 1968).

Figure 11 - Post-Sardic succession at Domusnovas. **(a)** Fossiliferous siltstones of the Portixeddu Formation. **(b)** Coarse-graind sandstones of the Maciurru Member. **(c)** Purple fossiliferous siltstones of the Punta s'Argiola Member, Domusnovas Formation. **(a)** Grey laminated sandstones of the Girisi Member, Rio San Marco Formation.

The Monte Argentu Formation, ranging from 200 (Laske et al., 1994) to 600 m (Leone et al., 2002), in thickness, strongly vary in thickness and facies due to the infill of an inherited Sardic-related palaeorelief: e.g., the thickness of the basal member can reach 150 m in the Iglesiente area , but decreases significatively southward (Sulcis area). The basal contact of the Monte Argentu Formation is diachronous: locally, the basal Punta Sa Broccia and the intermediate Rio Is Arrus members are lacking. The upper contact is also diachronous: overlying the Monte Argentu Formation lays either the Monte Orri (Fluminimaggiore, Domusnovas, Monte Orri in the northern Iglesiente area) and Portixeddu (Bacu Abis in the southern Iglesiente area) formations. The age of this formation could not be directly estimated, although its intermediate Rio Is Arrus Member is fossiliferous (*Taricciola arrusensis*; Hammann et al., 1990). The age of the latter is suggested as probably Sandbian on the basis of the younger deposit below the unconformity (Floian, Cabitza Formation) and the older fossiliferous levels yielded by the post-unconformity deposits (Upper Sandbian of the Monte Orri Formation vs. Upper Sandbian-Katian of the Portixeddu Formation; Hammann, 1992).

The Monte Argentu Formation is overlain by the Monte Orri Formation (Laske et al., 1994), made up of alternating greenish-grey to grey medium- to very fine-grained sandstone (**Fig. 10f**) and

dark grey siltstones with pyritic, phosphatic and chloritic nodules and fossils (trilobites, brachiopods, bivalves, cephalopods and hyolithids), characterized by the occurrence of *Skolithos*-style trace fossils. The fossiliferous content of the formation has been attributed to the Sandbian-Upper Sandbian (Caradoc of the British chart: Hammann, 1992; Leone et al., 1991, 1993, 2002). The thickness of the deposit varies significantly from 10 to 200 m, and the member can be eroded. The base and top are both gradual with the underlying Monte Argentu and the overlying Portixeddu formations, respectively.

The Portixeddu Formation (Leone et al., 1991), known as "Scisti ad *Orthis*", consists of 70-90 m of richly fossiliferous dark-grey fine sandstones and shales, sometimes bearing pyritic, phosphatic or siliceous nodules (up to 12 cm in diametrer), more abundant in the upper part. Fossils are generally concentrated in storm-induced layers (**Fig. 11a**), and include brachiopods, bryozoans, cystoids, crinoids, gastropods, bivalves, ostracods, trilobites, cornulitids, conularids and solitary rugose corals. This fossil association indicates a late Sandbian-Katian age (Upper Caradoc-Lower Ashgill of the British chart) (Hammann, 1992; Leone et al., 1991, 1993, 2002).

The overlying Domusnovas Formation (Leone et al., 1991) is made up of 90 m of: (i) a basal whitish sandstone-dominant member (Maciurru Member; **Fig 11b**) consisting of sandy siltstones, quartzitic sandstones, with Mn-bearing carbonates and oxides, and rare lithic fragments and feldspars; and (ii) an upper red to greenish-grey shaly-marly member with some interbedded carbonate levels (Punta s'Argiola Member; **Fig. 11c**). The fossil content, which includes brachiopods, bryozoans, gastropods, conodonts, crinoids, cystoids and trilobites, allows attributing the formation to the early-mid Katian (former Ashgill; Leone et al., 2002; Hammann & Leone, 2007).

The Rio San Marco Formation (Leone et al., 1991) is exclusively made up of siliciclastic deposits including a basal green heterometric conglomerate with mafic volcanic pebbles (Beccaluva et al., 1981), intercalated with epiclastites and black shales (Punta Is Arenas Member), followed by alternations of grey to light grey sandstones and siltstones (Cuccuruneddu Member); dark grey-green fine siltstones showing a fine varve-like lamination, and some sandstones and siltstones layers with parallel lamination and a fossiliferous level (Serra Corroga Member); an upper member (Girisi Member; **Fig. 11d**) consist of dark grey siltstones with interbedded laminated sandstones, and massive micaceous dark claystones and siltstones. The formation, 230 m thick, contains a record with graptolites, bryozoans, brachiopods, crinoids, trilobites and acritarchs of Hirnantian age (Leone et al., 1991; Štorch & Leone, 2003; Hammann & Leone, 2007).

The Silurian succession consists of a 60-70 m thick deposit made up of black shales and black limestones.

The Upper Ordovician succession reflects a change from alluvial fan-delta environments that evolved into a marine platform (Monte Argentu Formation). This transgressive trend is considered syn-to post-tectonic and reflects the sealing of an inherited Sardic-related uplift and denudation (Martini et al., 1991). Although the marine environment lasted up to the end of the Ordovician (Monte Orri, Portixeddu, Domusnovas and Rio San Marco formations), different accommodation space fluctuations have been recorded in the sedimentary record, including regressive (Domusnovas and Rio San Marco formations) and transgressive (Monte Orri Formation) trends, especially during Hirnantian times. The latter fluctuations have been related to glacio-eustatic changes and other factors, such as tectonics, sharp subsidence increase and minor glacio-eustatic pulsations (Leone et al., 2002).

4.1.3. Sardic unconformity and tectonics

The Sardic phase in the Foreland Zone is marked by an angular unconformity (Sardic unconformity), separating the Cambrian-Lower Ordovician and Upper Ordovician packages. The discordance is capped by the continental Monte Argentu Formation. The Sardic unconformity shows angular discordances that grade from low-angle to perpendicular arrangements, showing an irregular surface highlighted with hematite crusts and quartz veining (Salvadori et al., 1982). The age of the Sardic unconformity ranges from Early Ordovician (Floian), based on the presence of graptolites (Pillola & Gutiérrez-Marco, 1988; Pillola et al., 2008) and other Early Ordovician fossils found in the uppermost beds of the Cabitza Formation, to the Late Ordovician (Sandbian) as supported by the older fossils recovered from the Monte Orri Formation (Hammann, 1992; Leone et al., 1991, 1993, 2002; Laske et al., 1994; Hammann & Leone, 2007). This chronostratigraphic control points to a stratigraphic gap of about 18 m.y. The Sardic unconformity is related to the emersion of an inherited palaeorelief, which was partly sealed by the Monte Argentu infill.

The angular unconformity is related to the Sardic phase of Stille (1935, 1939), which affected the pre-unconformity succession and provoked a (present-day) E-W oriented fold network. The Sardic deformation, consisted of km-sized open folds and reverse faults (Pasci et al., 2008), sealed by the unconformity and the Upper Ordovician. This geometrical relationship has been reported in the Gonnesa, Monte San Giovanni, Monte Pertunto, Nuraghe San Pietro, Monte Anna - Monte Pira Roma and Reigraxius valley areas (Iglesiente). The deformations are related to neither metamorphism (Franceschelli et al., 2017) nor foliation, and are in turn cut by the Variscan foliation (Funedda, 2009). Because of the coincidence between the E-W direction of the Sardic and the first Variscan deformation phases, the structures attributable to the Sardic event must be those (i) cut by the Sardic unconformity and overlain by the puddinga deposits, or (ii) cut by the Variscan tectonic foliation.

4.2 Nappe Zone

The rocks of the External Nappe (for location, see **Fig. 4**) have recorded the record of a Variscan polyphase tectonic and metamorphic network of events, with two main deformation and metamorphic events. The first event provoked the emplacement of the nappe plus thrusting and isoclinal folding related to penetrative axial plane foliation. The second one caused a general vertical shortening accommodated by ductile shearing (Casini et al., 2010) and recumbent folds, normal faults and crustal-scale-strike-slip structures (Conti et al., 1999; Casini & Oggiano, 2008).

Figure 12 - **(a)** Pre-Sardic sandstones of the San Vito Formation. **(b)** Post-Sardic basal level of the Metaconglomerato di Muravera Formation. **(c)** Sandstones of the Punta Serpeddì Formation, bearing crinoids (**d**), and capped by the silicified limestones of the Tuviois Formation (**e-f**), cropping out in the Sarrabus Unit, External Nappe Zone.

The Nappe Zone includes several stacked tectonostratigraphic units emplaced with a southward verging stacking, later followed by a large-scale folding producing km-scale antiforms and synforms, such as the NW-SE trending Flumendosa antiform. A change of nappe transport direction occurred during the last stages of the Variscan collisional phase (Conti et al., 2001). Throughout the nappe stack, deformation and metamorphism increased northward toward the Posada-Asinara Line (Carmignani et al., 1994; Franceschelli et al., 2005). Differences in stratigraphic and structural features led to subdivide the Nappe Zone into the external and internal nappes, exposed in SE and western Sardinia, and in central and NW Sardinia, respectively.

The External nappes, cropping out in central-southern Sardinia (**Fig. 4**), consist of a stack of several tectonostratigraphic units organized in an antiformal structure (Flumendosa antiform; Carmignani et al., 1994, 2001*a*, *b*). The distinguished units are, from bottom to top, the Monte Grighini, Riu Gruppa, Gerrei, Meana Sardo and Sarrabus units. They exhibit an increasing degree of metamorphism and deformation intensity from the upper to the lower units (Carmignani et al., 1994; Conti et al., 2001; Funedda et al., 2011, 2015; Meloni et al., 2017). Nappe stacking developed under predominantly greenschist facies conditions (T < 500°C) with increasing metamorphic grade up to the amphibolite facies in the Monte Grighini Unit, representing the deepest tectonic unit of the Nappe Zone.

The Palaeozoic succession cropping out in the tectonostratigraphic units of the External nappes comprise Cambrian-to-Lower Carboniferous rocks. These include a distinctive volcanic with volcanoclastic levels of Mid Ordovician age that evidence a calc-alkaline magmatism (Carmignani et al., 1994). Metavolcanites are calc-alkaline and range in composition from basaltic-andesites and andesites to rhyolites and rhyodacites (Memmi et al., 1983). Most of them correspond to porphyritic lava flows, ignimbrites and tuffs that have been dated as Mid Ordovician on the basis of stratigraphic and palaeontological constraints of sedimentary interbeds. These constraints have been confirmed by zircon U/Pb dates ranging between 465.4 ± 1.4 Ma (on subintrusive dacite, Sarrabus Unit; Oggiano et al., 2010) to 460 ± 1 Ma on a metarhyolite (Giacomini et al., 2005).

The External nappes cropping out in south-western Sardinia allow access to the Bithia (Pavanetto et al., 2012) and Arburese units. Because of lithological affinities, these are correlable with the Gerrei and Sarrabus unit cropping out in SE Sardinia, respectively.

In the Internal nappe zone, because of the metamorphic grade (450-550°C, Casini et al., 2010) and the intensity of deformation (Conti et al., 1998), only some tectonic units have been defined: such as the Barbagia and Ozieri units in central Sardinia, and the Canaglia and Li Trumbetti units in NW Sardinia, in which Ordovician volcanic rocks and Silurian-Devonian limestones are lacking, respectively (Oggiano & Mameli, 2006).

In the whole Nappe Zone, the stratigraphic successions are clearly different from those cropping out in the Foreland Zone (**Fig. 9b**). The Palaeozoic successions from the External nappes, composed of Cambrian-Lower Carboniferous rocks, comprise distinct Middle Ordovician volcanic and volcanoclastic successions encased between two major unconformities: (i) the lower Sardic or Sarrabese unconformity (Calvino, 1959*b*) separating the Cambro-Lower Ordovician succession from the Middle Ordovician volcanic one; and (ii) the upper discordance or “Caradocian” unconformity (Calvino, 1959*b*) that separates the former volcanosedimentary complex from the Upper Ordovician-Lower Carboniferous succession.

The Ordovician magmatic and volcanic rocks interbedded in the successions below and above the Sardic unconformity in the Nappe zone allowed the distinction of three volcanic episodes: a pre-Sardic (~ 490-475 Ma), a Mid-Ordovician (~ 465-455 Ma), and a Late Ordovician-Lower Silurian (~ 447-440 Ma) pulsation.

Figure 13 - Location of the Ordovician volcanic byproducts (**a**) throughout the Foreland, the Nappe (Internal and External) and the Inner Zones of the Hercynian basement. Synoptic schemes representing the regional main age trends of the Ordovician volcanic and magmatic rocks (**b**), and specific age trends for the Ordovician volcanics embedded in the Lower Palaeozoic successions cropping out in the tectonic units stacked in the Nappe Zone (**c**).

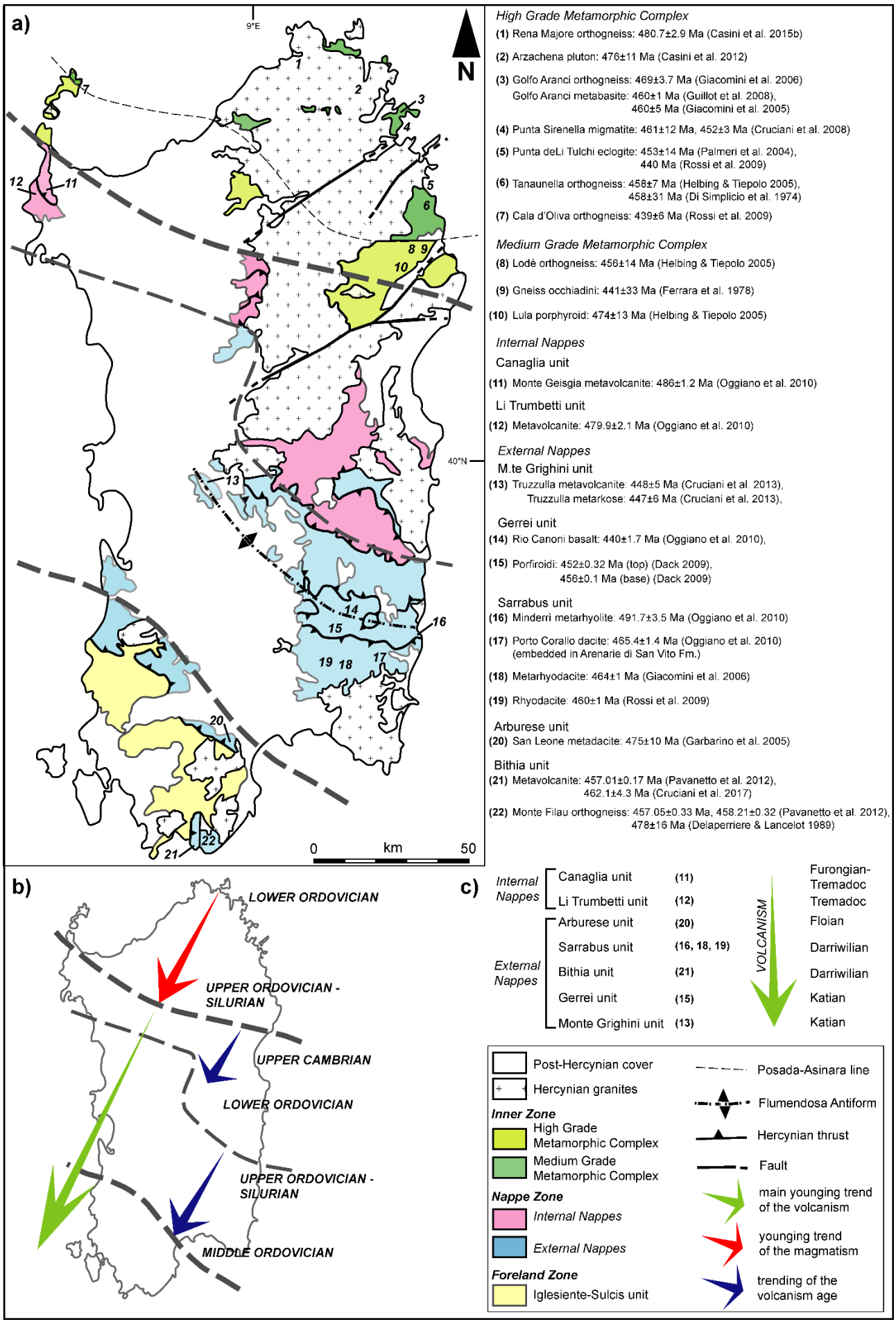

High Grade Metamorphic Complex

(1) Rena Majore orthogneiss: 480.7±2.9 Ma (Casini et al. 2015b)

(2) Arzachena pluton: 476±11 Ma (Casini et al. 2012)

(3) Golfo Aranci orthogneiss: 469±3.7 Ma (Giacomini et al. 2006)
Golfo Aranci metabasite: 460±1 Ma (Guillot et al. 2008), 460±5 Ma (Giacomini et al. 2005)

(4) Punta Sirenella migmatite: 461±12 Ma, 452±3 Ma (Cruciani et al. 2008)

(5) Punta deLi Tulchi eclogite: 453±14 Ma (Palmeri et al. 2004), 440 Ma (Rossi et al. 2009)

(6) Tanaunella orthogneiss: 458±7 Ma (Helbing & Tiepolo 2005), 458±31 Ma (Di Simplicio et al. 1974)

(7) Cala d'Oliva orthogneiss: 439±6 Ma (Rossi et al. 2009)

Medium Grade Metamorphic Complex

(8) Lodè orthogneiss: 456±14 Ma (Helbing & Tiepolo 2005)

(9) Gneiss occhiadini: 441±33 Ma (Ferrara et al. 1978)

(10) Lula porphyroid: 474±13 Ma (Helbing & Tiepolo 2005)

Internal Nappes

Canaglia unit

(11) Monte Geisgia metavolcanite: 486±1.2 Ma (Oggiano et al. 2010)

Li Trumbetti unit

(12) Metavolcanite: 479.9±2.1 Ma (Oggiano et al. 2010)

External Nappes

M.te Grighini unit

(13) Truzzulla metavolcanite: 448±5 Ma (Cruciani et al. 2013), Truzzulla metarkose: 447±6 Ma (Cruciani et al. 2013),

Gerrei unit

(14) Rio Canoni basalt: 440±1.7 Ma (Oggiano et al. 2010),

(15) Porfiroidi: 452±0.32 Ma (top) (Dack 2009), 456±0.1 Ma (base) (Dack 2009)

Sarrabus unit

(16) Minderì metarhyolite: 491.7±3.5 Ma (Oggiano et al. 2010)

(17) Porto Corallo dacite: 465.4±1.4 Ma (Oggiano et al. 2010) (embedded in Arenarie di San Vito Fm.)

(18) Metarhyodacite: 464±1 Ma (Giacomini et al. 2006)

(19) Rhyodacite: 460±1 Ma (Rossi et al. 2009)

Arburese unit

(20) San Leone metadacite: 475±10 Ma (Garbarino et al. 2005)

Bithia unit

(21) Metavolcanite: 457.01±0.17 Ma (Pavanetto et al. 2012), 462.1±4.3 Ma (Cruciani et al. 2017)

(22) Monte Filau orthogneiss: 457.05±0.33 Ma, 458.21±0.32 (Pavanetto et al. 2012), 478±16 Ma (Delaperriere & Lancelot 1989)

4.2.1 Cambrian-Lower Ordovician succession

Like in the Foreland Zone, in the Nappe Zone the Sardic phase is marked by an angular unconformity that separates the Cambrian-Lower Ordovician succession from an Upper Ordovician package (**Fig. 9b**), firstly reported by Calvino (1959*b*). The pre-Sardic succession of the External nappes is represented by dark grey to grey-greenish alternations of quartzites, sandstones and shale with some discontinuous limestone interbeds and dark claystones and conglomerates toward the top of the formation (Arenarie di San Vito Formation; Calvino, 1959*b*). The Arenarie di San Vito Formation (**Fig. 12a**), firstly recognized in the Sarrabus unit, was subsequently reported in all the External nappes, and correlated with the Solanas Formation (Minzoni, 1975) cropping out in Barbagia (Meana Sardo Unit). The top of the San Vito Formation is always erosive and represented by the Sardic or Sarrabese unconformity (**Fig. 7**). The San Vito succession is supposed to be at least 500-600 m thick in the External nappes (Carmignani et al., 1982; Oggiano, 1994), although its base is never exposed because it constitutes the base of the tectonic units.

In the Internal nappes, the pre-Sardic succession comprises siliciclastic deposits metamorphosed in the muscovite + chlorite, biotite up to biotite + garnet zones. It is composed of a thick (ca. 2000 m of apparent thickness for the Filladi del Gennargentu in the Barbagia Unit) succession rich in light grey to greenish or purple alternations of sandstones, quartzites and claystones, which in some localities show lithological similarities with the Arenarie di San Vito Formation. Some fine conglomerates occur close to the top of the formation. A “mid Cambrian”-Early Ordovician age has been attributed to the Arenarie di San Vito Formation because of the presence of: (i) Miaolingian and Tremadocian-Floian acritarchs (Barca et al., 1981*b*, 1988), trilobites and graptolites (Pillola & Leone, 1997), and orthoceratid cephalopods (Floian; Gnoli & Pillola, 2002) in the Sarrabus Unit; (ii) of Miaolingian and Tremadocian-Floian acritarchs in the Gerrei and Meana Sardo units (Tongiorgi et al., 1984; Albani et al., 1985; Naud & Pittau Demelia, 1985); (iii) and because of the occurrence of Furongian volcanic rocks (intermediate to acidic with transitional affinity) interbedded within the latter succession (**Fig. 9b**) in the External (491.7 ± 3.5 Ma rhyolite of the Sarrabus Unit, Oggiano et al., 2010; 475 ± 10 Ma dacite of San Leone in the Arburese Unit; Garbarino et al., 2005) and Internal nappes (479.9 ± 2.1 Ma acidic volcanite in the Li Trumbetti Unit, and 486 ± 1.2 Monte Geisgia rhyolite in the Canaglia Unit; Oggiano et al., 2010) (**Fig. 13a**).

The age of the pre-Sardic succession in the Internal nappes is attributed to the Cambrian-Ordovician due to the lithological similarity with the pre-Sardic succession of the External nappes, despite the lack of fossils and the intense deformation and metamorphism. The pre-Sardic succession cropping out in the Nappe Zone is associated with a distal palaeogeographic scarp flanked by with slope-related fans (Barca & Maxia, 1982), which evolved into a shallow marine deposit in the upper part of the formation.

4.2.2 Middle Ordovician succession

In the External Nappe Zone the pre-Sardic succession is also cut by the Sardic (or Sarrabese) unconformity, which in turn is capped by a volcanosedimentary complex. The latter is a calc-alkaline volcanic suite (Memmi et al., 1982, 1983) ranging in composition from basaltic-andesites and andesites to rhyolites and rhyodacites (Memmi et al., 1983). Most of these volcanic rocks correspond to porphyritic lava flows, ignimbrites and tuffs interbedded in the sedimentary succession, and have been dated as Mid Ordovician on the basis of stratigraphic and paleontological constraints. The succession reflects a sharp change of environments in which the marine settings of

the Arenarie di San Vito Formation are followed by continental deposits (Metaconglomerati di Muravera Formation) succeeded by a volcanosedimentary complex related to subaerial volcanism (Monte Santa Vittoria and Porfidi del Sarrabus or Porfiroidi Formations) of Mid Ordovician age.

Like the Foreland Zone, the Sardic unconformity is marked by the occurrence of a a basal (but not continuous) polygenic and heterometric conglomerate (**Fig. 12b**), which includes quartzites and feldspatic sandstones derived from the underlying succession (Arenarie di San Vito Formation) and rhyolite pebbles, interbedded with sandstones and siltstones (Metaconglomerati di Muravera Formation; Carmignani et al., 2001*a*). This formation, which includes 10-15 cm-sized pebbles embedded in a dark phyllitic or sandy matrix rich in volcanic quartz, crops out in all the External nappe units, except in the Ozieri one: its thickness ranges between 0 to 50 m, and the matrix and pebbles composition is variable depending on the zone. It is attributed to a continental (alluvial) environment contemporaneous to the volcanic activity.

The overlying volcanosedimentary package is made up of grey to greenish andesitic lavas and whitish rhyolitic to rhyodacitic volcanites intercalated with green epiclastites (**Fig. 14a**) (Monte Santa Vittoria Formation; Carmignani et al., 2001*a*; Conti et al., 2001); the rhyolitic member was originally known as "Porfidi Bianchi" in the Sarrabus Unit (**Fig. 14b**) by Calvino (1963). The latter is capped by dark grey rhyolitic and dacitic ignimbrites and lavas in the Sarrabus unit (**Fig. 14b**) (Porfidi Grigi del Sarrabus Formation; Calvino, 1959*b*) and in the Gerrei unit (**Fig. 14c**) (Porfiroidi Formation; Calvino, 1972). In the latter, a 10-30 m thick conglomeratic level (Su Muzzioni Formation *sensu* Funedda, 2000) separates the epiclastites and the overlying Porfiroidi Formation.

The thickness of the volcanosedimentary Complex in the External nappe Zone is strongly variable: 250 m for the Sarrabus unit, 300 m for the Gerrei Unit, and up to 600 m for the Meana Sardo unit. The order of volcanites in the vertical package also varies depending on the tectonic unit: it is generally basic-to-intermediate at the base and acidic toward the top, but it can be inverted, as in the Meana Sardo Unit (felsic at the base and andesitic at the top).

The Mid Ordovician age of the volcanosedimentary complex (**Fig. 13a**) has been confirmed in the Sarrabus unit by zircon U/Pb dates ranging between 465.4 ± 1.4 Ma (on a subintrusive dacite; Oggiano et al., 2010), 464 ± 1 Ma (Giacomini et al., 2006), and 460 ± 1 Ma (rhyolite; Rossi et al., 2009), and between 462.1 ± 4.3 Ma (rhyodacite; Cruciani et al., 2017) and 457.01 ± 0.17 Ma (Pavanetto et al., 2012) in the Bithia Unit. A little bit younger age (Sandbian), ranging between 456 ± 0.1 and 452 ± 0.32 Ma (Dack, 2009), has been obtained for the Porfiroidi Formation cropping out in the volcanosedimentary complex of the Gerrei Unit. Over the effusive volcanites, a granitoid intrusive body has been emplaced in the External nappes: the Monte Filau Orthogneiss (**Fig. 14d**), intruded in the Bithia Formation and cropping out in the homonymous unit, dated as Early Ordovician (478 ± 16 Ma; Delaperrière & Lancelot, 1989) to Mid Ordovician (457.05 ± 0.33 to 458.21 ± 0.32 Ma; Pavanetto et al., 2012) (**Fig. 13a**).

The Internal nappe Zone is characterized by scarcity of Middle Ordovician volcanic rocks, which crop out in the Canaglia and Li Trumbetti units (Nurra region, NW Sardinia). In the latter unit, the supposed Cambro-Ordovician siliciclastic deposit is covered by Middle Ordovician greywackes and volcanites (**Fig. 13a** - acidic volcanites; Oggiano & Mameli, 2006).

Figure 14 - Post-Sardic volcanics cropping out in the External Nappes: Monte Santa Vittoria Formation (**a**) in the Gerrei Unit (Porto Tramatzu area); Porfidi Grigi (on the left) and Porfidi Bianchi (on the right) del Sarrabus (**b**) in the homonymous tectonic unit; Porfiroidi Formation (**c**) of the Gerrei Unit; Monte Filau orthogneiss (**d**) of the Bithia Unit.

4.2.3 Upper Ordovician succession

The Middle Ordovician rocks that crop out in the External nappes are covered by an Upper Ordovician succession. Their contact is erosive and marked by a Sandbian (former "Caradocian") transgression, similar to that observed in the Foreland Zone. The Upper Ordovician succession differs from a nappe to another, but (i) a coarse-grained lag is generally recognizable at its base (Genna Mesa, Punta Serpeddì, and Orroeledu formations, respectively for the Gerrei, Sarrabus and Meana Sardo units), (ii) followed by a Katian fossiliferous level (Rio Canoni Shales, Tuviois and Bruncu Su Pitzu Formations, respectively for the Gerrei, Sarrabus and Meana Sardo units), (iii) finally capped by Silurian strata (Hammann & Leone, 2007).

Several volcanic alkaline products (basic to intermediate) of Katian-to-Silurian age are embedded or cut the Upper Ordovician succession of the External nappes. The thickness of the Upper Ordovician changes from a nappe to another, and shows an important lateral variability, from ca. 80 m in the Gerrei Unit to over 300 m in the Sarrabus Unit. The Upper Ordovician succession reflects a transgression accompanied by the erosion and dismantling of an inherited volcanosedimentary palaeorelief, which recorded the shift from continental (basal member of the Punta Serpeddì and Genna Mesa formations) to marine environments (upper member of the Punta Serpeddì and Tuviois Formations, Rio Canoni Shales Formation).

In the Sarrabus unit (**Fig. 9b**) the Upper Ordovician consists of a basal 250-300 m-thick deposit (**Fig. 12c**) (Punta Serpeddì Formation; Barca & Di Gregorio, 1979) in which three members can be distinguished: (i) the lower, 50-100 m-thick, made up of sandstone and conglomerate with pebbles of volcanic quartz and feldspar; (ii) an intermediate member made up of grey to blackish sandstone and quartzite, (iii) and an upper member (**Fig. 12d**) characterized by light grey sandstone and siltstone bearing brachiopods, crinoids, bryozoans, trilobites and gastropods of Sandbian-Katian age (Calvino, 1959*b*; Barca & Di Gregorio, 1979; Giovannoni & Zanfrà, 1978; Hammann & Leone, 2007).

The Punta Serpeddì Formation is followed by a 100-350 m-thick deposit made up of grey shales and sandstones capped by dark, partly silicified limestones bearing Katian fossils (**Fig. 12e-f**) (Tuviois Formation; Barca & Di Gregorio, 1979), locally interbedded with scattered volcanic tuffs. Further volcanic byproducts are embedded in the Upper Ordovician, mainly composed of epiclastites and lava flows (alkaline basalts) dated at 440 ± 1.7 Ma (Oggiano et al., 2010).

In the Gerrei Unit, the Upper Ordovician succession starts with basal light grey sandstones and conglomerates rich in quartz pebbles, and arkosic and greywacke strata (Genna Mesa Formation; Carmignani et al., 2001*a*), up to 50 m-thick. It is subsequently overlain by a ca. 20 m-thick alternation of calcareous siltstone and shales, green to grey or light brown coloured, bearing limonitized fossils (bryozoans, crinoids, brachiopods, gastropods and trilobites) of late Sandbian-Katian age (Cocozza et al., 1974; Giovannoni & Zanfrà, 1978; Naud, 1979*a*), and reddish to grey encrinitic limestones (Rio Canoni Shales Formation; Naud, 1979*a*).

In the Meana Sardo Unit, the Upper Ordovician, which unconformably overlies a Middle Ordovician volcanosedimentary complex, is composed of a ca. 200 m-thick deposit made up of sandstones, shales and fine conglomerates with quartz and lithic fragments (Orroeledu Formation; Bosellini & Ogniben, 1968) of the underlying deposits, with some encased alkaline pillow lavas (Gattiglio & Oggiano, 1990), and sandstones and siltstones bearing brachiopods, bryozoans and crinoids of Late Ordovician age.

In the Grighini Unit, the Upper Ordovician is represented by a succession of basal felsic volcanites, arkosic sandstones interbedded with shales (448 ± 5 Ma for the acidic volcanism; 447 ± 6 Ma for the arkosic sandstone; Cruciani et al,. 2013), overlain by a metre-thick level of quartzite, and a package of shales with marble interbeds in the upper part.

In the Internal nappe, and based on stratigraphic relationships, a Late Ordovician age has been attributed to a succession made up of greywackes and volcanites (alkaline metabasites; Di Pisa et al., 1992), metapelites bearing ooidal ironstones and diamictites cropping out in the Canaglia Unit, and finally overlain by Silurian black phyllites.

4.2.4. Sardic unconformity and tectonics

In the Internal nappes, the scarcity of Middle Ordovician volcanic rocks, associated with the intense metamorphism and deformation, makes difficult to characterize the Sardic unconformity, whereas the same horizon is well preserved in the External Zone. In the internal nappes, the Sardic unconformity cut the "lower Cambrian"-Lower Ordovician succession at different angles (up to 90°), characterizing a stratigraphic gap of ca. 10 m.y. between the pre-unconformity deposit and the Middle Ordovician volcanosedimentary package. Therefore, the age of the Sardic unconformity ranges between the Floian (Early Ordovician), on the basis of the fossil record recovered in the Arenarie di San Vito Formation (acritarchs, trilobites, graptolites, cephalopods and ichnofossils; Barca et al., 1981*b*, 1988; Tongiorgi et al., 1984; Albani et al., 1985; Naud & Pittau Demelia, 1985; Gnoli & Pillola, 2002) and the Mid Ordovician (U-Pb zircon dating, Porfidi Grigi del Sarrabus Formation: Giacomini et al., 2006; Rossi et al., 2009; Oggiano et al., 2010).

Although the Variscan imprint has affected strongly the rock preservation throughout the Nappe Zone, evidences of pre-Variscan tectonics occurs in the External nappes weakly affected by metamorphism and deformation, especially in the Sarrabus and Gerrei units. Like in the Foreland Zone, in the Nappe Zone the Sardic unconformity is also related to the Sardic phase. The Sardic phase is testified by the occurrence of several byproducts related to a calk-alkaline Mid Ordovician volcanism/plutonism, characterized by the occurrence of a post-unconformity coarse-grained deposit (Metaconglomerati di Muravera Formation), as well as by the deformation that exclusively affects pre-Sardic succession. In the Sarrabus Unit, the Sardic phase provoked the emersion and erosion of an inherited Cambrian-Lower Ordovician palaeorelief. The Sardic deformation is recognizable by the onset of hectometric-sized folds, often overturned, unrelated to foliation. Their fold axes are cut off by the Sardic unconformity (Cocco & Funedda, 2019) and refolded by the Variscan folding. The Sardic folds, which are randomly cut by the main Variscan foliation, are sealed by the Middle Ordovician volcanosedimentary package (Metaconglomerati di Muravera, Monte Santa Vittoria or Porfidi Grigi del Sarrabus formations).

4.3 Inner Zone

On the northern and southern side of the Posada-Asinara Line (**Fig. 4**), the High-Grade Metamorphic Complex and the Medium-Grade Metamorphic Complex of the Inner Zone (**Fig. 13a**), both related to the Variscan orogeny are exposed.

The Medium Grade Metamorphic Complex (MGMC) is a band of mylonitic rocks made up of micaschists, quartzites and paragneisses with a Grt + St + Ky association derived from a primary siliciclastic succession, and orthogneisses derived from granitoids with a gabbro-dioritic composition. Some magmatic and volcanic rocks embedded in the MGMC have been dated and attributed to a pre-Variscan activity (**Fig. 13a**). Middle Ordovician magmatic rocks are mainly represented by calc-alkaline plutonic rocks (Lodè orthogneiss), while volcanic rocks are represented only by the Lula porphyroids. According to Helbing & Tiepolo (2005), U-Pb radiometric data on zircon range between 474 ± 13 Ma (Lula porphyroid) and 456 ± 14 Ma (Lodè orthogneiss).

The High Grade Metamorphic Complex (HGMC) is mainly composed of rocks whose evolution is related to anatectic processes related to plate collision. These rocks (migmatitic orthogneisses, metatexites, diatexites and amphibolites) show different compositions ranging from basalts to trondhjemites (Oggiano et al., 2005). Several protoliths of Ordovician age have been recognized in the HGMC, although the magmatic ones are more common than the volcanics and the sedimentary

ones. Among the plutonic rocks, Furongian-Lower Ordovician magmatic bodies are represented by protholiths of calk-alkaline granitoid from the Arzachena pluton (476 ± 11 Ma; Casini et al., 2012), and from the Rena Majore Orthogneiss (480.7 ± 2.9 Ma; Casini et al., 2015). Middle Ordovician protholiths are represented by the Tanaunella orthogneiss, a calc-alkaline plutonic rock dated as 458 ± 7 Ma (Helbing and Tiepolo; 2005), and by the Golfo Aranci orthogneiss (469 ± 3.7 Ma; Giacomini et al., 2006) and metabasite (460 ±1 Ma; Giacomini et al., 2005). Upper Ordovician protholiths are signified by the Punta Sirenella orthogneiss (ranging from 452 ± 3 to 461 ± 12 Ma; Cruciani et al., 2008) and the Punta de Li Tulchi eclogite that has been dated at 453 ± 14 Ma (Palmeri et al., 2004) and 440 Ma (Rossi et al., 2009). Zircons derived from metabasites with eclogitic facies relics have provide ages of 460-450 Ma for the protolith formation (Cortesogno et al., 2004; Palmeri et al., 2004; Giacomini et al., 2005).

4.3.1 Sardic unconformity and tectonics

Because of the high metamorphic and deformation degree, neither Sardic unconformity nor related deformation has been recognized in the Inner Zone. The witness of pre-Variscan tectonics is represented by the Ordovician magmatic and volcanic rocks cropping out both in the Medium-Grade and High-Grade Metamorphic Complexes. In the Inner Zone, the magmatic/volcanic byproducts could be grouped in an Furongian-Early Ordovician (Casini et al., 2012, 2015), Mid Ordovician one (Helbing & Tiepolo, 2005; Giacomini et al., 2005, 2006), and Late Ordovician-Silurian cycles (Cortesogno et al., 2004; Palmeri et al., 2004; Cruciani et al., 2008; Rossi et al., 2009).

4.4 Remarks and discussion on the Sardic unconformity and related phase and unsolved questions

From the analysis of the regional geologic data described in Sardinia, some peculiar features characterizing the Sardic phase could be highlighted: (i) the occurrence of the Sardic unconformity, (ii) the occurrence of pre-unconformity deformations, and (iii) the emplacement of volcanic and magmatic byproducts with a calc-alkaline affinity. According to previous authors (e.g., Zoppi, 1888; Novarese, 1914; Novarese & Taricco, 1923; Teichmüller, 1931; Stille, 1935, 1939), the Sardic unconformity represent the main distinctive element of the Sardic phase.

In both the Foreland and the Nappe zones it range from angular unconformity to para-conformity, which separates two successions with different structural features, and highlights a stratigraphic gap which ranges between 18 m.y. (Foreland) and 10 m.y. (Nappe Zone).

The Sardic unconformity originated by the emersion/emergence of the Cambrian-Lower Ordovician deposits in response to an uplift (maybe associated to a fall in the eustatic sea-level).
The former uplift caused emersion and erosion of the Cambro-Lower Ordovician deposits in both the pre-Sardic successions of the Foreland and Nappe zones, but with some differences. In the Foreland zone, a widespread emersion and a considerable erosion occurred, considering either (i) the provenience of the conglomerate pebbles (which includes Cabitza, Campo Pisano, San Giovanni and Santa Barbara formations), (ii) the older deposit eroded (Cambrian Series 2), (iii) the thickness of the pre-Sardic succession, (approximatively included between min. 600 and max. 1140 m), and (iiii) the occurrence of pre-Sardic deformation which led to palaeorelief formation. In the Nappe zone, albeit a slight erosion has been described (Cocco & Funedda, 2012, 2019; Cocco et al., 2018), the monotonous character of the pre-Sardic succession and its thickness (included between 200 and

600 m in the External Nappes, and an apparent thickness of ca. 2000 m in the Internal ones), together with the Variscan structure superimposed (nappe stacking), and the San Vito Formation's base lack, do not allow to estimate the real erosion.

The uplift related to the formation of the Sardic unconformity could be related to the occurrence of deformations (folding) affecting the pre-unconformity successions cropping out in the Foreland (Pasci et al., 2008) and Nappe Zones (Cocco & Funedda, 2019), which could be responsible for the different bedding attitudes of the former series, too. The age of the Sardic deformations is included between Early (Floian) and Middle Ordovician (Dapingian). These folding, albeit all sealed by the Sardic unconformity and foliation-free, differs in size and orientation (e.g. E-W trending km-sized folds in the Foreland, and hectometric to decimetric, NNW-SSE or E-trending folds, often overturned, in the Sarrabus unit), making difficult to assign an univocal trend to the former deformations, or understand how the original compression developed.

The data suggest that the Sardic deformation developed under shallow structural levels in a compressive setting in both the Nappe zones, according to Cocco & Funedda (2019), and in the foreland, too. Furthermore, faulting affecting the pre-unconformity succession occurs in the Foreland (Pasci et al., 2008), corroborating the first hypotesis proposed by Brusca & Dessau (1968) and Martini et al. (1991) to account a half-grabens environment in which the post-unconformity deposit (Monte Argentu Formation) developed. The former faults are lacking in the pre-Sardic deposit of the Nappe zone.

Considering the post-Sardic successions cropping out in the Foreland and Nappe Zones, it is possible to distinguish between a free-volcanism domain (Foreland type) (**Fig. 9a**), and a rich-volcanic one (Nappe zone type) (**Fig. 9b**). The former domains share few analogies, but exhibit distinctive features. Both the domains share a pre-Sardic (Furongian-Lower Ordovician) siliciclastic deposits (Cabitza and Arenarie di San Vito formations) related to shallow marine platform (Cocco & Funedda, 2019), which represent the latter deposit below the Sardic unconformity. Below the former deposit, the Foreland's pre-Sardic succession shows important deposits related to carbonate platform (Gonnesa Group), which seems to be absent in the Nappe zone's pre-Sardic succession.

In addition, the domains share similar successions above the Sandbian transgression (former Caradoc), which reflect the establishment of siliciclastic continental (Monte Argentu Formation and lower Punta Serpeddì Formation) to marine shelf deposits (Monte Orri and Portixeddu formations and upper Punta Serpeddì Formation), punctuated by carbonate key levels (Domusnovas and Tuviois formations) of Katian age.

The aforementioned differences between Foreland and Nappe zones could be due on a separation of the two domains during the Lower Palaeozoic, according to Loi & Dabard (1997), Cocco & Funedda (2012, 2019) and Cocco et al. (2018). Differences in the sedimentological influx recorded in the former areas, suggest that the former could be located in two distant parts of the same basin or in two different basins, which were approached by the Variscan tectonics.

The two domains differ also for the occurrence/lacking of magmatic activity. In the former activity, developed between Furongian and Silurian, three main pulses could be distinguished (Oggiano et al., 2010; Cruciani et al., 2018; Cocco et al., 2018): (i) Furongian-Tremadocian, with intermediate to felsic volcanics embedded in the pre-Sardic successions; (ii) Dapingian-Darriwilian, with calc-alkaline byproducts with variable composition, included between the Sardic unconformity and the Sandbian transgression; (iii) Sandbian-Katian, with alkaline epiclastites embedded in the transgressive deposits.

The byproducts of those volcanic/magmatic cycles are not equally spread throughout the Foreland, the Nappe and the Inner zones: (i) in the Foreland, only a volcanoclastic level embedded

in the Hirnantian Rio San Marco Formation (Leone et al., 1991) has been reported and correlated with a widespread Late Ordovician-Silurian volcanic activity linked to a source located in another unit; (ii) in the Nappe zone the volcanic products are widely interbedded into the pre- and post-unconformity successions.

Considering the age of the Ordovician volcanic byproducts (**Fig. 13a**), a main younging trend directed from NE to SW is recognizable (**Fig. 13b**), according to Cruciani et al. (2018). Taking into account the top-to-south direction of the Variscan nappe stacking exposed in the Flumendosa antiform in which the upper units represents the ones located "northward", the uppermost tectonic units in the nappe stack show volcanics older than the ones embedded in the lower nappes (**Fig. 13c**) located deepest in the stacking. So, the age trend exposed in the External Nappes (**Fig. 13b**), showing a southward aging (Mid-to-Late Ordovician) in contrast to the main one (represented by the green arrow) is apparent, and due to the nappe stack.

The diachronic emplacement of the volcanics through the nappes seems to be related to a diachronous development of the Sandbian transgression (Cruciani et al., 2018), which is marked by Sandbian deposits in the Sarrabus unit (similarly to the Foreland), Upper Sandbian-Katian ones in the Gerrei unit, and Katian in the Monte Grighini Unit (Cruciani et al., 2013).

The aforementioned differences between the Foreland and the Nappe zones have been linked to an extensional-convergent margin (Andean-type subduction zone) in which the Foreland represent the back-arc area and the Nappe Zone the volcanic arc (Rossi et al., 2009; Oggiano et al., 2010; Gaggero et al., 2012; Cruciani et al., 2018). This model fits with the volcanic arc migration showed by the diachronous development of the magmatism through the Nappe and Inner zones, and partially with the calc-alkaline affinity and arc-like signature of the products, interpreted as subduction-related (Di Pisa et al., 1992; Carmignani et al., 1994; Tommasini et al., 1995; Oggiano et al., 2010; Del Greco et al., 2016).

However, in other zones (Iberian Massif) the arc-like signature has been interpreted as an inherited character caused by the fast melting of a subduction-related Neoproterozoic crust in a rifting setting (Díez Montes et al. 2010; Navidad et al., 2010), but in Sardinia no unquestionably Neoproterozoic rocks have been recognized up to now.

Regarding the main distinctive characters highlighted (Sardic unconformity, pre-Sardic deformations, felsic to calc-alkaline magmatism) the geodynamic model which fits with the Nappe Zones seems to be linked to subduction-related settings, albeit not completely: it shows differences with either the Andean-type and the Japanese models. The Foreland zone, instead, could be related to collisional settings. The comparison of the Foreland and Nappe series with those cropping out in the Eastern Pyrenees could help to better understand their differences and include them into a univocal geodynamic context.

CHAPTER 5

CHAPTER 5

EASTERN PYRENEES. GEOLOGICAL SETTING AND STRATIGRAPHY

The Pyrenees is a WNW-ESE-trending asymmetrical double-verging belt that includes large outcrops of Mesozoic and Cenozoic rocks deformed by mainly north-directed thrusts in the northern part of the belt, and south-directed thrusts in the southern part. The Ediacaran-Paleozoic rocks of the Axial Zone have been deformed by fold and thrust tectonics derived by the superimposition of the Alpine (Upper Cretaceous-Lower Miocene) and the Variscan (Carboniferous) orogenies. The latter generated a variable regional metamorphism and regional foliation, and is related to the emplacement of important volumes of granitoids in the pre-Variscan successions.

The Pyrenean cordillera formed during the Alpine orogeny due to the collision between the Iberian plate and Euroasia during Early Cretaceous-Early Miocene times. The continental collision (Muñoz, 1992*a*, *b*; Teixell, 1998) generated displacements of about 150-160 km (Muñoz, 1992*b*), so the original Palaeozoic basin should be located northward from present-day arrangement. Pre-Silurian rocks and gneisses derived from Ordovician magmatic rocks crop out in domes (Cocherie et al., 2005; Castiñeiras et al., 2008; Casas et al., 2010; Mezger et al., 2010; Liesa et al., 2011), whereas Silurian and Devonian rocks intruded by Variscan granitoids crop out in synclines.

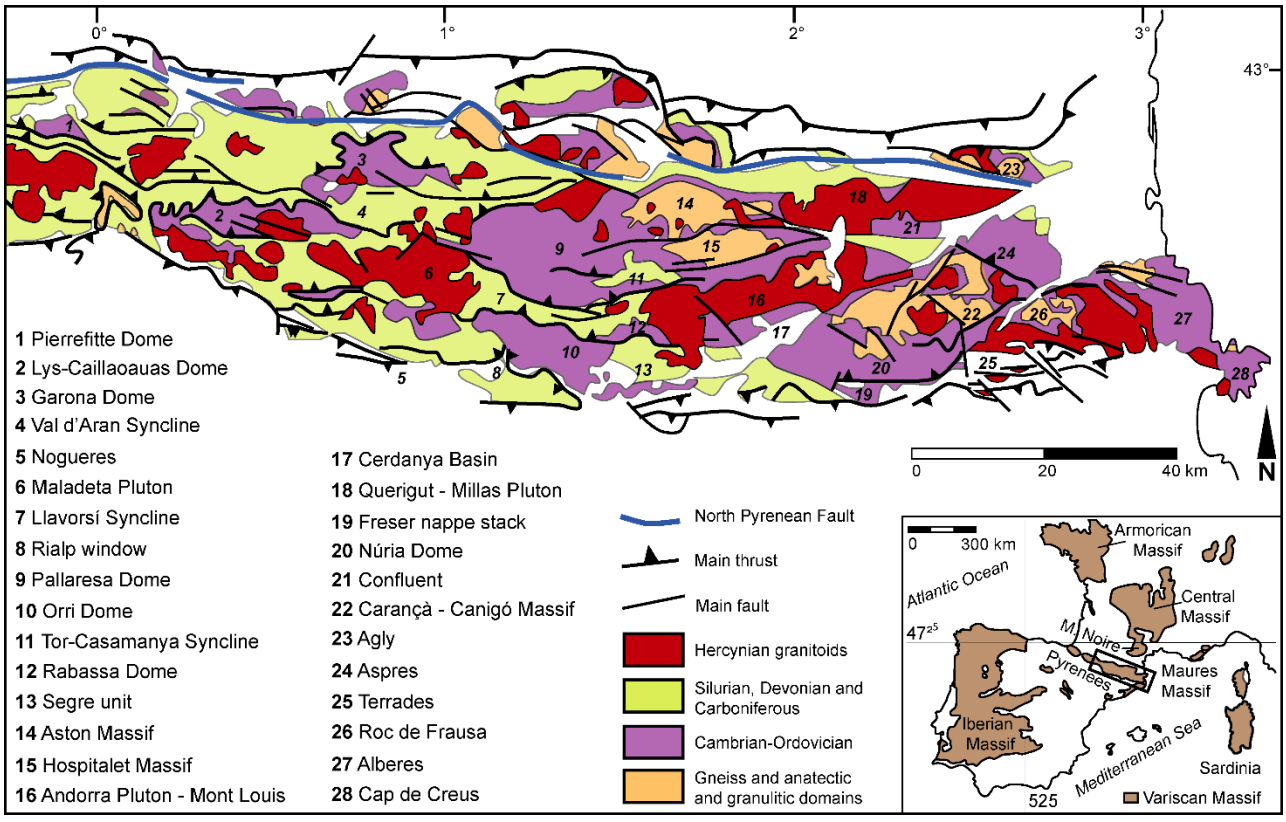

Figure 15 - General geological and geographic map of the Axial Pyrenean Zone; modified after Casas (2010).

The pre-Variscan rocks of the Axial Zone constitute a 3-4 km thick succession forming an elongated strip unconformably overlain by Mesozoic and Cenozoic strata, which lie geographically disconnected from neighbouring outcrops of the Catalan Coastal Range to the south, the

Mouthoumet and Montagne Noire (southern French Central) massifs to the north, and Sardinia to the east. Palaeozoic rocks are involved in three main Alpine thrust sheets, the so-called Lower Structural Units (Muñoz, 1992*b*), named Nogueres, Orri and Rialp thrust sheets. These units form an antiformal stack with their basal thrusts north-dipping or subvertical in the northern side of the chain, sub-horizontal in the central part, and south-dipping in the southern contact with the Mesozoic-Cenozoic cover. The Nogueres and Orri units include a complete pre-Variscan succession, ranging in age from Cambrian to Carboniferous. Exposures of the Rialp unit only occur in a small tectonic window of the central Pyrenees.

Pre-Variscan basement rocks of these Alpine thrust sheets commonly preserve their initial sedimentological and structural characteristics, because the Alpine orogeny is no related to plutonism or metamorphism capable of deleting the previous features induced by previous tectonic events (Muñoz, 1992a), and internal deformation is moderated. As a consequence, the pre-Variscan basement of the Axial Zone preserves evidence of successive Cadomian, Sardic and Variscan magmatic episodes (Cocherie et al., 2005; Castiñeiras et al., 2008; Casas et al., 2010, 2015; Navidad et al., 2010; Pereira et al., 2014; Martínez et al., 2016; Padel et al., 2018*b*), as well as Sardic, Variscan and Alpine deformation events (Guitard, 1970; Zwart, 1979; Muñoz, 1992*b*; Casas, 2010).

In Eastern Pyrenees, the tectonostratigraphic units in which Cambrian-Ordovician rocks crops out, from east to west (**Fig. 15**), are: Cap de Creus, Albera/Albères, Roc de Frausa/France, Terrades, Aspres, Agly, Canigó/Canigou Massif, Conflent, Núria Dome, Freser nappe stack and La Cerdanya units.

The Cap de Creus massif is made up of a thick pre-Upper Ordovician succession made up of greywackes, shales, carbonaceous slates are interbedded with marbles and porphyries, followed by conglomerates and siliciclastic sediments and carbonates. Granitic orthogneiss (ca. 553 Ma, Port gneiss; Castiñeiras et al., 2008) and metabasites crop out, respectively, at the base and the mid part of the succession.

The Albera Massif constitutes a half-dome made up of a pre-Upper Ordovician metasedimentary sequence including acidic metaigneous rocks (ca. 465-472 Ma, Liesa et al., 2011), and an orthogneissic body intruded in the former succession (ca. 470 Ma, Liesa et al., 2011), which in turn is intruded by Variscan plutonic bodies, mainly granitoids.

The Roc de Frausa Massif is made up of a pre-Upper Ordovician thick metasediments (mainly greywackes and shales), punctuated by marbles, volcanics (metabasites and tuffs). Orthogneisses derived from Cadomian granites (ca. 548 Ma Roc de Frausa gneiss; Castiñeiras et al., 2008) and metatuffs (548 Ma; Castiñeiras et al., 2008) occur, respectively, at the base and at the top of the successions.

The Canigó Unit is an Alpine unit which exhibits rocks from Late Neoproterozoic to Carboniferous, and in which several E-W massifs could be distinguished (Roc de Frausa and Canigó massifs, Andorra-Mont Lluis batholith and Rabassa dome). Some of the former massifs crop out in the eastern or in the central Axial Zone, but they exhibit the same metasedimentary sequence, pre-Late Ordovician in age (Cavet, 1957; Guitard, 1970), unconformably capped by an Upper Ordovician one. The Canigó Massif is composed of an Ediacaran-Lower Ordovician thick siliciclastic succession with marbles and volcanites interbeds (Canaveilles and Jujols Groups), unconformably capped by an Upper Ordovician mainly siliciclastic one. The lower succession is intruded by the Upper Ordovician Cadí, Casemí and Canigó protoliths of the granitic orthogneisses (Casas et al. 2010; Martínez et al. 2011; Navidad et al. 2018).

In the Núria Massif, Sandbian conglomerates rest unconformably on Late Proterozoic to Early Ordovician metasedimentary rocks (Julivert & Martínez, 1983; Casas et al., 1986; Martí et al., 1986), which are intruded by several Ordovician granitic bodies (ca. 457 Ma; Martínez et al., 2011) later on transformed on orthogneissic bodies during Variscan tectonics.

The Ribes de Freser area is characterized by an Alpine antiformal stack in which rocks, aged from Cambrian to Mesozoic, crops out in different tectonic units (Robert, 1980; Muñoz, 1985).

The La Salut Unit (Terrades area) is an Alpine thrust sheet in which crops out shales and limestones bearing Cambrian fossils (Abad, 1988; Perejón, 1994).

In the Central Pyrenees, the tectonostratigraphic units in which Cambro-Ordovician rocks crops out, from east to west (**Fig. 15**), are: the Hospitalet, Aston, Segre units, Llavorsí Syncline and Orri, Pallaresa, Garona, Lys-Caillaouas and Pierrefitte domes.

A Cambro-Ordovician succession crops out in the Aston-Hospitalet massif (Cavet, 1957; Hartevelt, 1970; Zwart, 1979). This heterolithic unit is made up of marbles and limestones, shales and sandstones with a fine conglomerate on the top, and is comformably overlain by Silurian slates. The sequence is intruded by a granitic laccolithe (Denèle et al., 2009). On its southwestern side, the Pallaresa dome crops out, with its antiformal structure made up of Cambro-Ordovician succession capped by the Upper Ordovician metasediments, which in turn are capped by the Silurian and Devonian rocks.

The Lys-Caillaouas massif is made up of Cambrian-Ordovician schists and quartzites with marbles intercalations (Kriegsman et al., 1989), capped by metaconglomerates and sandstones, with a marble interbed in its upper part, aged Upper Ordovician (Clin, 1959), and capped by Silurian black slates. The sequence is intruded by Variscan granites.

The Llavorsì Syncline is a NE-SW structure made up of Silurian and Devonian rocks, which separates the Rabassa Dome (on its southern side), from the Massana Anticline (on its northern side), in which crop out the Neoproterozoic to Devonian sequences.

In the Axial Zone, a complete Ediacarian-Lower Ordovician succession is intruded by several Sardic and Variscan plutons (Barbey et al., 2001; Laumonier et al., 2004; Martínez et al., 2011) that led to the imprint of regional and contact metamorphic conditions. The latter, together to the high deformation, partly explains the almost complete lack of confident biostratigraphically significant fossils in the Ediacaran-Lower Ordovician succession of the Pyrenean Axial Zone (Cocchio, 1981, 1982). In fact, the superimposition of these orogeneses generated a complex tectonic structure, in which several tectonostratigraphic units that include major orthogneissic, metagranite intrusions located at the core of the so-called metamorphic domes (Zwart, 1986; Vissers, 1992; Carreras & Capellà, 1994; Denèle et al., 2009; Mezger, 2009; García-Sansegundo et al., 2011; Laumonier et al., 2015).

The Sardic plutons intruded the pre-Upper Ordovician successions during two magmatic pulsations. The first one took place during Early-Middle Ordovician (477-462 Ma) and gave rise to the emplacement of the Albera, Aston, Hospitalet, Canigó, and Roc de Frausa gneisses (**Fig. 15**). The second magmatic pulsation developed during Late Ordovician (457-446 Ma), forming the protoliths of the Cadí, Casemí, Núria and Canigó G-1 type gneisses emplaced in the pre-unconformity strata of the Canigó massif (Casas et al., 2010; Martínez et al., 2011; Navidad et al., 2018), and of the Ribes Granophyre at the base of the Upper Ordovician succession in the Ribes de Freser area (Martínez et al., 2011), in which coeval calc-alkaline volcanic rocks are interbedded (Robert & Thiébaut, 1976; Ayora, 1980; Robert, 1980; Martí et al., 1986, 2019) (**Fig. 12**).

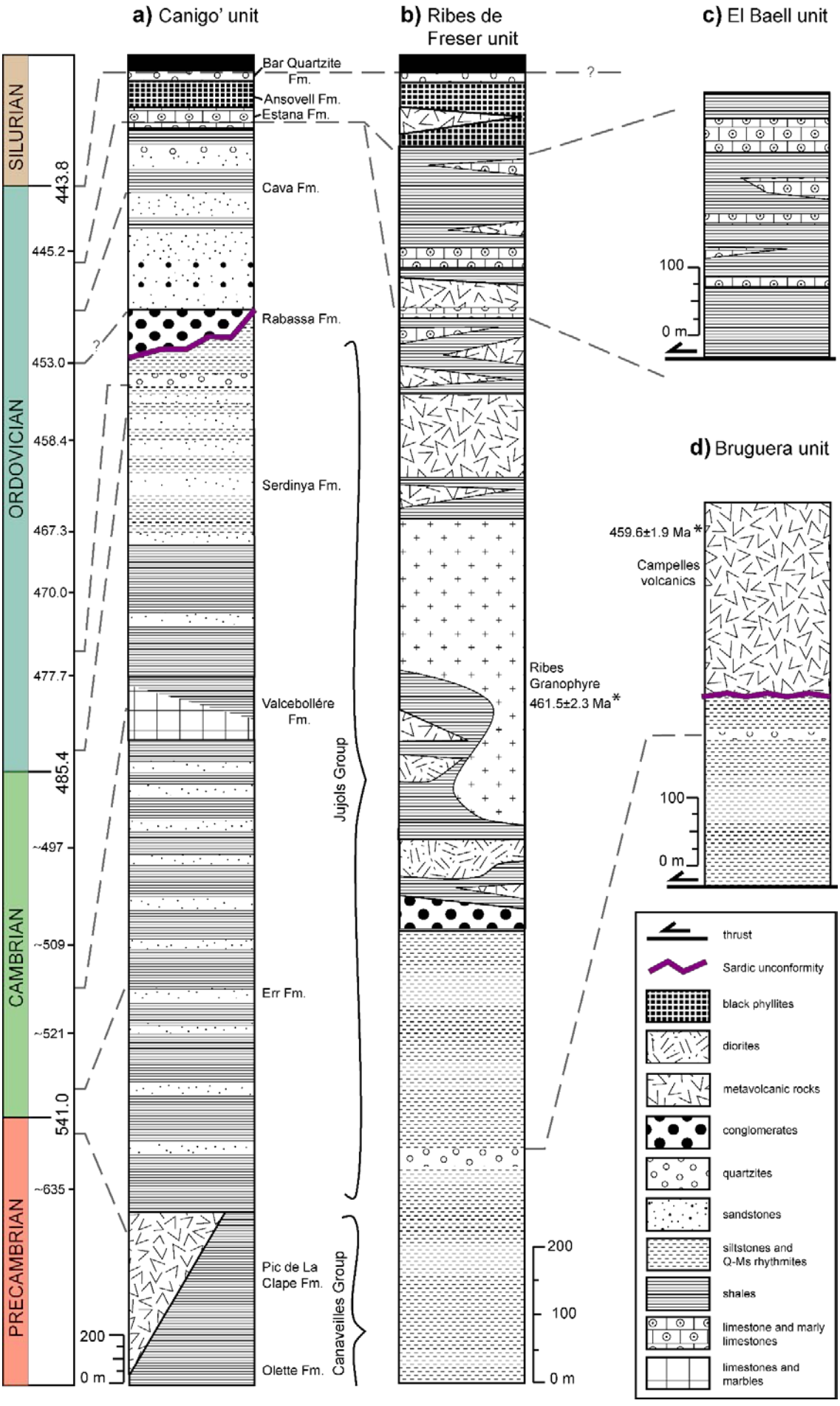
a) Canigo' unit
b) Ribes de Freser unit
c) El Baell unit
d) Bruguera unit
SILURIAN
ORDOVICIAN
CAMBRIAN
PRECAMBRIAN
443.8
445.2
453.0
458.4
467.3
470.0
477.7
485.4
~497
~509
~521
541.0
~635
Bar Quartzite Fm.
Ansovell Fm.
Estana Fm.
Cava Fm.
Rabassa Fm.
Serdinya Fm.
Valcebollére Fm.
Jujols Group
Err Fm.
Pic de La Clape Fm.
Canaveilles Group
Olette Fm.
Ribes Granophyre
461.5±2.3 Ma*
459.6±1.9 Ma*
Campelles volcanics
200
100
0 m
thrust
Sardic unconformity
black phyllites
diorites
metavolcanic rocks
conglomerates
quartzites
sandstones
siltstones and Q-Ms rhythmites
shales
limestone and marly limestones
limestones and marbles

Figure 16 - Pre- and post-Sardic unconformity successions in the Canigó unit (**a**), and Cambrian(?) to Upper Ordovician successions in the Ribes de Freser (**b**), El Baell (**c**) and Bruguera (**d**) units in the Pyrenees (modified after: Casas, 2010; Padel et al., 2018*b*; Martí et al., 2019).

In several pre-Variscan successions, an intra-Ordovician unconformity, separating a lower Cambro-Lower Ordovician succession from another Upper Ordovician has been recognized (**Fig. 16a**).

5.1 Pre-unconformity succession

In the Axial Zone of the Eastern Pyrenees, Cavet (1957) defined two principal Cambro-Ordovician stratigraphic units, the Canaveilles and Jujols Schists Series, which were subsequently considered as lithostratigraphic groups, among others, by Laumonier & Guitard (1986), Laumonier (1988) and Laumonier et al. (1996, 2004, 2015). The Canaveilles Group (former "Canaveilles Schists" by Cavet, 1957) crops out in the Canigó, Roc de Frausa, Albera and Cap de Creus massifs, and in the Guilleries, Montseny (Catalan Coastal Range). The succession is 2-3 km thick and comprises, from bottom to top, the Nyer Formation, the shale-dominant Olette Formation, and the rhyolitic tuffs and volcanosedimentary complexes of the Pic de la Clape Formation (Padel et al., 2018*b*) (**Fig. 17**). The Canaveilles succession crops out throughout the tectonostratigraphic massifs of the Eastern Axial Pyrenees, such as the Albera, Aspres, Canigó, Roc de Frausa and Cap de Creus.

The Nyer Formation *sensu* Padel et al. (2018*b*) is about 2000 m thick and consists of a 2000 m thick succession composed of heterolithic metasedimentary rocks dominated by micaschists but including subsidiary marbles, metasandstones, metabasites and rare metarhyodacites. The Olette Formation (Padel et al., 2018*b*), conformably overlies the Nyer Formation and is made up of 400-500 m of greenish and black shales, schists, greywackes and feldspathic sandstones with an uppermost alternation of black and shale shale interbeds. It is overlain by the Pic de la Clape Formation (Padel et al., 2018*b*), which is a volcanosedimentary complex characterized by alternations of volcanites and carbonates. The age of the Pic de la Clape Formation is considered as latest Ediacaran to Terreneuvian based on new and revised U-Pb dating suggesting a maximum depositional ages of 565 ± 9 to 552 ± 10 Ma (Padel et al., 2018*b*).

The Jujols Group, firstly described by Cavet (1957) as the Jujols Schists, is 3-4 km thick and includes a monotonous succession of shale/sandstone alternations overlying the Canaveilles Series (**Fig. 16a**). The Jujols Group, widely crops out from Vallespir to Cerdanya, in the Albera and Aspres massifs, in the eastern (Confluent, Aspres, Ripolles) and central (Orri, Pallaresa, Garona, Pierrefite and Lys-Caillaouas domes) Axial Zone, and in the North Pyrenean Zone (Agly, Arize, Barousse, etc.). The Group is subdivided, from bottom to top, into the Err, Valcebollère and Serdinya formations (Padel, 2016; Padel et al., 2018*b*). The base of the Jujols Group coincides with the base of the Err Formation, which onlaps the volcanosedimentary palaeorelief formed by the Pic de la Clape Formation to the south of the Canigó massif, or directly overlies the Olette Formation (Canaveilles Group). The top of the Jujols Group is marked by the "Sardic" unconformity, highlighting a Middle-Upper Ordovician gap associated with the Sardic phase. An "early Cambrian"-earliest Ordovician age has been attributed to the entire Jujols Group, on the basis of the radiometric Cambrian age of the Pic de la Clape Formation and the acritarch-based Furongian-Early Ordovician age for the top of the Serdinya Formation (Casas & Palacios, 2012).

Figure 17 - Sardic unconformity (**a, b**) separating the Serdinya Formation (*CO*) from the Rabassa Conglomerate one (OS) in La Bastida (**a**) and Talltendre (**b**) localities (La Cerdanya, Canigó unit); laminated grey siltstones (**c**) and sandstones (**d**) of the pre-Sardic unconformity succession (Serdinya Formation, Jujols Group); post-Sardic conglomerate (**e-f**) lying on the unconformity (Rabassa Conglomerate Formation), made up of Serdinya's clasts in a sandy matrix (**e**) and quartz veins derived clasts (**f**), at La Cerdanya area (Canigó unit).

The Err Formation is a shale-dominant unit, up to about 2000 m thick, consisting of grey, brownish and greenish shales and centimetre- to decimetre-thick, fine-grained sandstones locally punctuated by gravelly sandstones. The sandstone beds, never exceeding 10 m in thickness, can be observed in the Puigmal, Aspres and Conflent areas. The Err Formation is tentatively dated as

Fortunian based on the radiometric constraints of the underlying Pic de la Clape Formation (Padel et al., 2018*b*). The Valcebollère Formation consists of a lower massive-to-bedded limestone-to-marble package (up to 300 m thick), overlain and passing westward to a, shale/carbonate alternation, 15-200 m thick, which changes upsection into green shales bearing carbonate nodules and phosphoritic crusts. The thickness of the formation and its carbonate content diminish northward disappearing to the north of the Canigó massif. Acritarchs from a limestone interbed of the Valcebollère Formation points to a possible "early Cambrian" (Cambrian Epoch 2) age (Laumonier et al., 2015; T. Palacios, pers. com. 2016). The Serdinya Formation (**Fig. 17c**) is a 1500 m-thick rhythmic mm-to-cm alternation of grey to light green or light brown shale rich in sandstone interbeds. Sandstones up to 1 m thick occur at the top of the formation, exhibiting graded bedding, load casts and cross bedding (Fontfrède Member) (**Fig. 17d**). The Serdinya Formation conformably overlies the Valcebollère Formation (in some areas sealing hydrothermally induced karstic features, such as at Roques Blanques) and is capped by the Sardic unconformity (**Fig. 17a-b**).

Acritarchs recovered from the uppermost part of the Serdinya Formation in the southern Canigó massif has yielded a broad Furongian-Early Ordovician microphytoplancton assemblage (Casas & Palacios, 2012). Ichnoassemblages recorded in the La Molina area, although not chronostratigraphically diagnostic, show a low-to-moderate ichnodiversity (Gámez et al., 2012). A maximum depositional age of ca. 475 Ma can be proposed for the quartzites of the Fontfrède Member in the La Rabassa dome, on the basis on the youngest detrital zircon population (Margalef et al., 2016).

Furthermore, the identification of archeocyathans in the Alpine allochthonous La Salut Unit of the Terrades area (Southern Pyrenees), allowed attributing a late Cambrian age 3 (Abad 1988; Perejón et al. 1994; Menéndez et al., 2015) to these rocks.

The scarcity of biostratigraphic data in the Ediacaran-Lower Ordovician succession has been partly compensated by the report of geochronologic U/Pb datings of zircon (Cocherie et al., 2005; Castiñeiras et al., 2008, Casas et al., 2015; Padel et al., 2018*b*). The orthogneisses intruding the Canaveilles Group have been dated as Early (Floian) to Late Ordovician, ranging from ca. 456-446 Ma (Casas et al., 2010) to ca. 475-467 Ma (Deloule et al., 2002; Cocherie et al., 2005) in the Canigó massif; ca. 458 Ma (Martínez et al,. 2001) in the Freser dome; and ca. 477-460 Ma (Castiñeiras et al., 2008; Liesa et al., 2011; Cocherie et al., 2005) in the Roc de Frausa and Albera massifs (orthogneisses and metaporphiric dykes). The Ribes granophyre intruding Upper Ordovician conglomerates have yielded an age of ca. 458 Ma (Martínez et al., 2011).

The siliciclastic sequences cropping out in the Ribes de Freser Alpine stack, which lie below, respectively, the Ribes de Freser volcanoclastic complex in the Ribes de Freser unit, and the Campelles volcanics in the Bruguera one, are considered Cambro-Ordovician in age because of their stratigraphic position and the similarity with the pre-Sardic successions (Canaveilles and Jujols Groups) (Muñoz, 1985). The lack of fossils precludes any age attribution.

5.2 Post-unconformity succession

The Upper Ordovician succession recognized throughout the Axial Zone of the Central and Eastern Pyrenees was firstly described by Cavet (1957) and Hartevelt (1970), who defined five main siliciclastic formations with a carbonate interbed, which can be recognized with some lithologic variations all across most parts of the cordillera. From bottom to top, this broad fining-upward megasequence is composed of the Rabassa Conglomerate, Cava, Estana Ansovell and Bar Formations (**Fig. 16a**). The thickness of the Upper Ordovician varies strongly, from 100 to 1000 m,

decreasing northward, across the Massana anticline and the Aston and Ospitalet domes. In these areas, the basal Rabassa conglomerates are absent, whereas the Estana limestone attains its maximum thickness, about 70 m (Margalef & Casas, 2016).

Figure 18 – Upper Ordovician succession lying on the Rabassa Formation or directly on the pre-Sardic deposit in the Canigó unit: Cava Formation (**a, b, c**) made up of green coarse sandstones, siltstones, and conglomerates (**a**), purple and green siltstones and sandstones (**b**) in the basal part, and sandstones bearing fossils of Katian age (**c**); Estana Formation (**d**), which represents the fossiliferous limestone key level of the Upper Ordovician sequence (late Katian), with its typical "*schistes troués*" feature; dark grey siltstones of the Ansovell Formation (**e**); quartzitic sandstones of the Bar Formation (**f**).

The Rabassa Conglomerate Formation (**Fig. 17e-f**), which unconformably overlies the Serdinya Formation (angular discordance up to 90°), is made up of reddish-purple, unfossiliferous conglomerates showing sharp lateral thickness variations, ranging from 0 to 200 m in thickness. Conglomerates are composed of sub-rounded to well-rounded clasts (**Fig. 17e**) rich in slates and quartzites derived from the underlying deposit (Serdinya Formation, Jujols Group), and vein quartz (**Fig. 17f**). The clasts, up to 50 cm in diameter, are embedded in a green-purple granule-sized matrix. Their massive-to-channelized sets are interpreted as alluvial-to-fluvial deposits (Hartevelt, 1970). Due to its stratigraphic position, the Rabassa conglomerates have been related to a Sandbian-early Katian (former Caradoc) age (Hartevelt, 1970).

The Cava Formation, which either conformably overlies the Rabassa Conglomerate or unconformably overlies the Jujols Group consists of feldspathic conglomerates (**Fig. 18a**) and sandstones in the lower part, grading upward into variegated shales (**Fig. 18b**) and fine-grained sandstones (**Fig. 18c**), with strongly burrowed quartzites in the uppermost part (Belaustegui et al., 2016). A contemporaneous volcanic influence is distinct in the southwestern part of the Canigó massif, where ash levels, andesites and metavolcanic rocks are embedded in the formation (e.g., at Ribes de Freser; Muñoz, 1985). The succession, 100-800 m thick, is dated as Katian (former late Caradoc-early Asghill) due to the presence of brachiopods, bryozoans and echinoderms concentrated in the middle part of the formation.

The Estana Formation (**Fig. 18d**) constitutes a monotonous marlstone-limestone unit, up to 60 m thick, displaying a distinct northward decrease-increase thickness composite trend. The formation disappears between Sant Julià de Lòria and Andorra and between the former and La Massana localities. The formation (para)conformably overlies either the Cava or the Rabassa formations and is unconformably overlain by either the Ansovell or the Bar formations. The unit, which constitutes a key limestone-marlstone interbed (the so-called “schistes troués”, “Grauwacke à *Orthis*” and “Caradoc limestones” of French and Dutch geologists), is rich in brachiopods, bryozoans, cystoids and conodonts dated as late Katian (Gil-Peña et al., 2004).

As stated above, the “Ansovell” Formation (Ansobell *sensu* Hartevelt, 1970) unconformably overlies the Estana limestone. It is made up of blackish shales (**Fig. 18e**) with common contorted, slumped and convoluted layers close to the base, and minor quartzite interlayers in the uppermost part. Where the Estana Formation tapers off, the Ansovell shales directly overlie the Cava sandstones. The Bar Quartzite Formation (**Fig. 18f**), made up of a fining-upward quartzite with dark shale interbeds and fine conglomerates, 5-20 m thick, marks the top of the Upper Ordovician sequence. An Hirnantian age was proposed for the Ansovell and Bar formations by Hartevelt (1970) later on confirmed on the basis of their fossiliferous content (Sanz-López & Sarmiento, 1995; Sanz-López et al., 2002; Roqué Bernal et al., 2017; Štorch et al., 2019). Westward, in the Orri, Pallaresa and Garona domes, Gil-Peña et al. (2000, 2004) reported a calcareous conglomerate, up to 8 m thick, directly capping the erosive unconformity that marks the Estana/Ansovell contact, and attributed to a Hirnantian glacial event.

In several areas of the Pyrenees, from Pierrefitte to the west (Calvet et al., 1988) to Ribes de Freser to the east (Robert & Thiébaut, 1976; Ayora, 1980; Robert, 1980; Martí et al., 2014), some volcanic rocks have been reported interbedded within the Upper Ordovician sediments (**Fig. 13b, d**).

In the Ribes de Freser area (south of the Canigó massif, Eastern Pyrenees), several Alpine structural units are stacked in an antiform bounded to the north by the out-of-sequence Ribes-Camprodon thrust that separates the former ones from the Canigó massif (Puddu et al., 2018) (**Fig. 19**). In this area three Alpine units (named Ribes de Freser, El Baell and Bruguera) contain a

distinct Upper Ordovician succession (Robert, 1980; Muñoz, 1985), topped by the Serra Cavallera unit. The Upper Ordovician succession of the El Baell (**Fig. 16c**) and Bruguera (**Fig. 16d**) units differ from that described by Cavet (1957) and Hartevelt (1970) in the Canigó massif (**Fig. 16a**), and traditionally used as reference for the main part of the Pyrenees.

Restoration of the Alpine deformation (Muñoz, 1985) situates the uppermost Serra Cavallera unit in a pre-Alpine northernmost position, probably north of the Canigó massif, where similar Devonian strata crop out. However, the initial position of the rest of the Upper Ordovician-bearing units cannot be constrained. A preliminary restoration by Muñoz (1985) situates the Bruguera unit in a pre-Alpine northern position, the intermediate El Baell unit in an intermediate setting, and the lowermost Ribes de Freser unit lying originally in a southernmost position.

The Ribes de Freser thrust sheet is the lowermost outcropping unit (Muñoz, 1985). It exhibits a pre-Variscan basement succession comprising a variable thickness, ranging from 600 to 1200 m, mainly composed of Upper Ordovician volcanic, subvolcanic and volcanosedimentary rocks interbedded in Katian sediments (Robert & Thiebaut, 1976; Ayora, 1980; Robert, 1980; Muñoz, 1985; Martí et al., 1986) (**Fig. 17b**). The volcanic activity was mainly explosive and shows a calc-alkaline affinity reflecting crustal melting (Martí et al., 1986). It produced dioritic bodies and volcanosedimentary rocks (**Fig. 20e**) in its lower part, whereas rhyolitic lava flows and ignimbrites predominate in the central part, and ash levels, ignimbrites and volcaniclastic rocks in its upper part. A granitic body with granophyric texture, dated at 458 ± 3 Ma (Martínez et al., 2011), is intruded into the lower part of the succession (**Figs 16b, 20f**) as well as several granitic orthogneissic bodies are emplaced in the lower part of the pre-Variscan succession: the Núria gneiss with a protolith age of 457 ± 4 Ma (Martínez et al., 2011), and the Queralbs gneiss, with a protolith age of 457 ± 5 Ma (Martínez et al., 2011).

The El Baell unit (**Fig. 16c**) is entirely made up of pre-Variscan basement rocks. It comprises a 300 m-thick succession entirely composed of limestones, marly limestones, shales with centimetre-thick, parallel bedding nodules (the so-called “schistes troués” of French literature) (**Fig. 20d**) and shales (Robert, 1980; Muñoz, 1985). There, three limestone-dominant thickening-upward sequences, up to 30 m thick, can be distinguished. Conodonts and echinoderms allowed Robert (1980) to attribute an early Katian (former Caradoc) age to the strata forming this unit. Sánz-López & Sarmiento (1995) dated their conodont faunas a late Katian age (*Amorphognathus ordovicicus* Zone) and correlated them with that described from the Estana Formation. Black shales of probably Hirnantian age unconformably overlie the former Katian beds. Both the base of the Upper Ordovician succession and the contact with Silurian beds are not exposed in this unit.

The Bruguera unit (**Fig. 16d**) lies structurally on the top of the El Baell unit. The former exhibits a 300 m-thick slate-dominant succession, Cambrian to Early Ordovician in age (Muñoz, 1985), subsequently overlain by a volcanosedimentary complex (Fontboté, 1949; Morre-Biot & Robert, 1976; Robert, 1980). The unfossiliferous slate-dominant succession (**Fig. 20a**) is comparable with the Jujols Group cropping out in the Canigó massif, which consists of finely laminated to massive sandstone/slate alternations, with local burrowed beds. Based on this correlation, a broad Cambrian-Ordovician age is assumed for the lower slates (Muñoz, 1985). The overlying volcanosedimentary complex consists of at least 300 m (Muñoz, 1985) of rhyolitic ignimbrites (**Fig. 20b**), variegated in colour and finely banded, and andesitic lava flows. Robert (1980) reported the presence of a basal continental breccia marking the base of the volcanosedimentary complex that has yielded a Carboniferous pollen assemblage. In contrast, recent U-Pb data on these volcanic rocks (Martí et al., 2019) suggest firstly a radiometric age about 455 Ma (Sandbian), and then a Darriwillian age (459.1 ± 5.3, 460.4 ± 2.2 and 459.6 ± 1.9 Ma; Martí et al., 2019) which fits with the age of the

volcanic and subvolcanic rocks cropping out in the Ribes de Freser unit. Finally, the uppermost Serra Cavallera unit is mainly made up of Silurian black shales, Devonian limestones, detrital Carboniferous "Culm" and continental Carboniferous and Permian deposits (Muñoz, 1985).

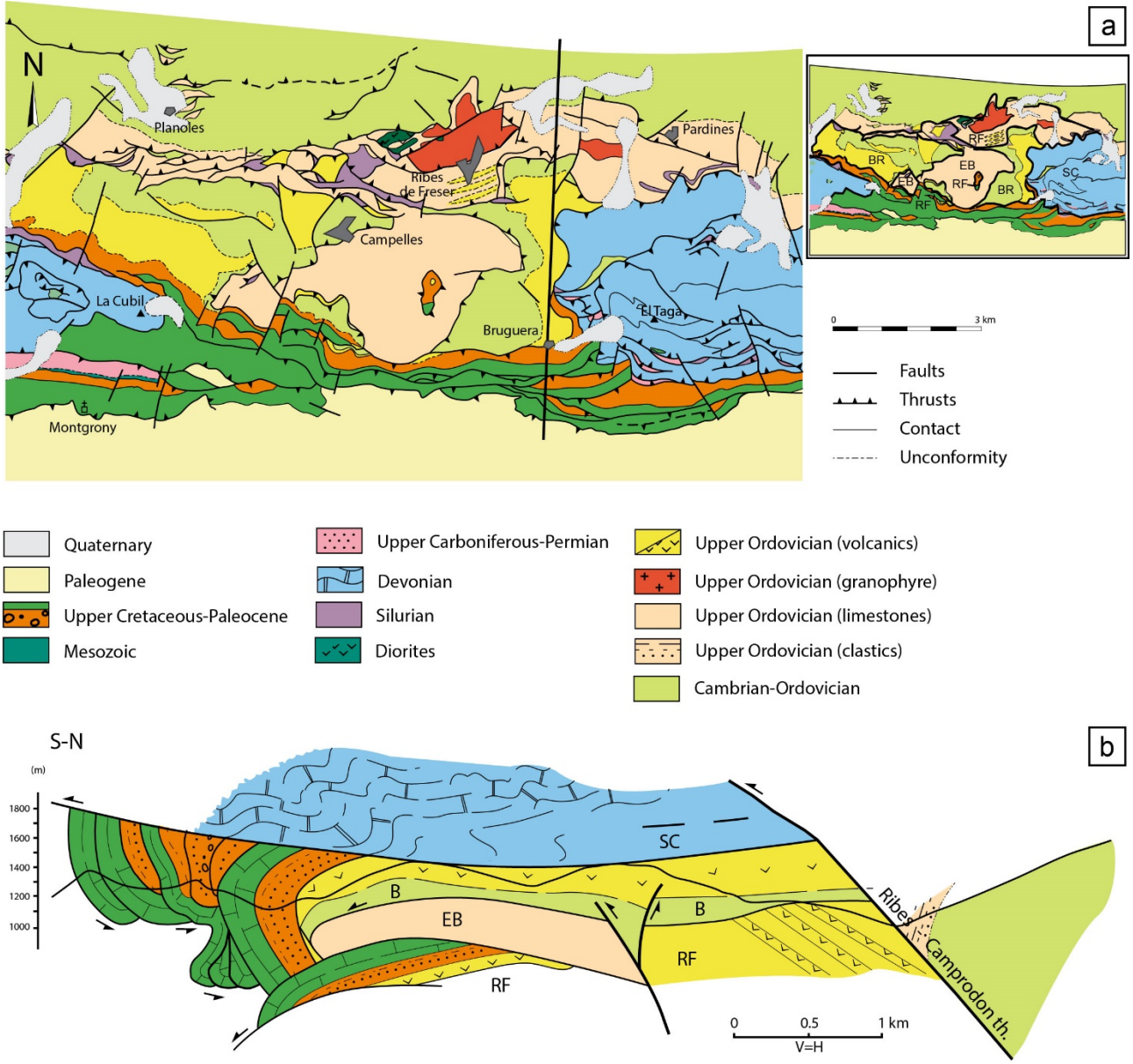

Figure 19 - (figure 2 in Puddu et al., 2018): Geological map of the Ribes de Freser area (**a**). S-N geological cross-section (**b**) (black line in the geological map) of the Freser valley antiformal stack with *RB* Ribes de Freser, *EB* El Baell, *B* Bruguera and *SC* Serra Cavallera units; modified after Muñoz (1985) and Puddu et al. (2018).

5.3 Sardic unconformity and tectonics

The Sardic unconformity (**Fig. 17a-b**), which separates the Serdinya Formation (Jujols Group) from the overlying Upper Ordovician succession, marks a stratigraphic gap that includes part of the Middle Ordovician.

The Sardic unconformity has been recognized in most of the Lower Palaeozoic tectonostratigraphic units cropping out throughout the Axial Zone, from west to east: the Garona

dome, Lys-Caillaoaus dome, Pallaresa dome, Llavorsí Syncline, Rabassa and Orri domes, Segre unit, Conflent, Ribes de Freser, and Canigó massif (Llopis Lladó, 1965; Santanach, 1972; Ravier et al., 1975; Muñoz et al., 1983; Barrouquère et al., 1983; Muñoz, 1985; Casas et al., 1989, 1998, 2012; García-Sansegundo & Alonso, 1989; Den Brok, 1989; Kriegsman et al., 1989; Poblet, 1991; Muñoz & Casas, 1996; Gil-Peña et al., 2001, 2004; García-Sansegundo et al., 2004; Laumonier et al., 2004; Casas & Fernández, 2007; Donzeau & Laumonier, 2008; Casas, 2010; Puddu & Casas, 2011; Casas & Palacios, 2012; Margalef et al., 2016; Puddu et al., 2019). The existence of this stratigraphic gap has been highlighted by Margalef et al. (2014) and Casas et al. (2015), who remarked an interruption between the zircons populations recovered in the pre- (Jujols Group) and post-unconformity (Bar Formation) successions, of about 30 m.y. This gap should be regarded as a maximum estimate, since the Bar Quartzite Formation constitutes the uppermost part of the Upper Ordovician. In the Ribes de Freser area, Upper Ordovician volcanic rocks directly overlying the unconformity have yielded a radiometric age of ca. 460 Ma (Martí et al., 2019). In the neighbouring Catalan Coastal Ranges, a similar age for volcanic rocks overlying the basal Upper Ordovician conglomerates has been obtained in the les Gavarres (455 ± 2 Ma) by Navidad et al. (2010) and in the Les Guilleries (452 ± 4 Ma) by Martínez et al. (2011) areas. These data reduce the time gap span of the unconformity to ~15 m.y. The time span is similar to that found in SW Sardinia (~18 million years) in the type area where the Sardic unconformity was described, where well-dated Upper Ordovician metasediments overlie upper Tremadocian-lower Floian (?) strata (Barca et al., 1987; Pillola et al., 2008).

Several folding episodes have been recognized in the Cambrian-Lower Ordovician rocks below the unconformity in several areas of the Axial Zone, in the Orri dome (Speksnijder, 1987), the Llavorsí Syncline (Laumonier & Guitard, 1986), the Lys-Caillaouas dome (Den Brok, 1989; Kriegsman et al., 1989), the southern Canigó massif (Muñoz & Casas, 1995), the Aspres area of the eastern Canigó massif (Donzeau & Laumonier, 2008), the Segre unit, southern Canigó massif, and Conflent area (Casas, 2010), and La Molina area (Casas et al., 2012) and La Cerdanya area (Casas, 2010; Puddu & Casas, 2011; Puddu et al., 2019) of the Canigó massif, Bruguera unit of the Ribes de Freser area (Puddu et al., 2018). All the deformations recognized and attributed to a pre-Upper Ordovician deformation event are foliation-free, except for the case of the Pallaresa dome, where Clariana et al. (2009) and Clariana & García-Sansegundo (2009) identified a foliation apparently unrelated to folding and only affecting the pre-unconformity succession. Moreover, pre-unconformity deformations have been linked either to buckling (Santanach, 1972) or to basement tilting related to a Late Ordovician faulting and erosion (García-Sansegundo et al., 2004; Casas & Fernández, 2007).

On the other hand, several Ordovician magmatic rocks interbedded in both the pre- and post-unconformity successions have allowed the identification of different volcanic episodes: the Pierrefitte dome (Calvet, 1988); in the vicinity of Ribes de Freser (Morre-Biot & Robert, 1976; Robert, 1980; Robert & Thiebaut, 1976; Muñoz, 1985; Martí et al., 2014, 2019; Martínez et al., 2011), the Canigó massif (Delapèrriere & Soliva, 1992; Delaperriere & Respaut, 1995; Barbey et al., 2001; Deloule et al., 2002; Castiñeiras et al., 2008, 2011; Casas et al., 2010, 2015), Roc de Frausa and Cap de Creus (Castiñeiras et al., 2008; Casas et al., 2015), the Albera massif (Liesa et al., 2011; Castiñeiras et al., 2011), and the Aston and Hospitalet massifs (Denèle et al., 2009). Other magmatic episodes of similar age have been reported southward the Axial Zone, in the Catalonian Coastal Ranges (Barnolas et al., 1980, Barnolas & García-Sansegundo, 1992; Julivert & Martínez, 1980; Julivert & Duran, 1983; Duran et al., 1984; Navidad & Barnolas, 1991; Navidad et al., 2010);

and northward of the Axial Zone, such as in Montagne Noire (Mattauer, 2004; Roger et al., 2004; Cocherie, 2003; Cocherie et al., 2005) and the Mouthoumet Massif (Álvaro et al., 2016).

Figure 20 - Pre- and Post-Sardic sequences cropping out in the Bruguera (**a-b**), El Baell (**c-d**), and Ribes de Freser (**e-f**) units: sandstone beds (**a**) in the slate-dominant succession below the Sardic unconformity, capped by the Sandbian-Katian rhyolitic ignimbrites (**b**) of Campelles-Bruguera area, in the Bruguera unit; fossiliferous limestone (**c**) interbeds in the "schistes troués" (**d**) of the El Baell Formation; Upper Ordovician volcanic and plutonic byproducts cropping out in the Ribes de Freser unit, respectively volcanic breccia (**e**) and Ribes Granophyre (**f**).

5. Summary of main results

The new data obtained with this research, together to the data present in the literature (cartographic, lithostratigraphic, biostratigraphic and geochronologic), led to the individuation of Sardic deformation affecting the Cambrian-Lower Ordovician rocks, and to the definition of Upper Ordovician successions cropping out in some sectors of the Eastern Pyrenees, particularly, Ribes de Freser and La Cerdanya areas.

The former data contribute to improve the knowledge of the Palaeozoic basement of the Pyrenees, in which the occurrence of an Early-Mid Ordovician episode of uplift and erosion led to the formation of the Sardic unconformity similar to the one described in Sardinia. Early to Late Ordovician magmatic activity accompanied and followed the uplift, which was pursued by an extensional pulse (Late Ordovician faulting and hydrothermal activity) that controlled the post-Sardic deposition.

The geological mapping, together to the stratigraphic and facies analysis of the units cropping out in the Alpine Ribes de Freser antiformal stack, led to the definition of the Katian El Baell Formation, which has been revised, formally erected and proposed as a lateral equivalent of the Estana Formation. Furthermore, the geological and structural analysis of the rocks cropping out in the El Baell and Bruguera units led to the definition of two different internal structures, and to the recognizement of a pre-Variscan (Mid Ordovician) deformational episode affecting the pre-Upper Ordovician rocks of the Bruguera unit.

Detailed geological mapping of the La Cerdanya area (Canigó Unit, Eastern Pyrenees) led to the definition of the different structural features exhibited by the Upper Ordovician and the Cambrian - Lower Ordovician successions, allowing us to recognize Sardic deformations affecting the latter serie. Furthermore, the occurrence of Late Ordovician synsedimentary extensional faults associated to hydrothermal activity, which affect the pre-Sardic succession, the Sardic unconformity and the lower part of the post-Sardic succession, has been described.

The analysis of the geochemical character of plutonic and volcanic products from several areas of the north-Gondwanan margin suggests the melting of metasedimentary rocks during the Sardic-event, and could help to a better understanding of the geodynamic scenario in which this tectonic phase occurred. In particular, the comparison with the Toledanian event, led us to define the contemporaneity between the magmatic events and the stratigraphic unconformities, while the geochemical features deduced indicate that the magmatism could be induced by underplating of hot magmas in a continental lower crust with partial melting of sediments, triggered by the opening of the Rheic Ocean.

5.5 The Sardic unconformity and the Upper Ordovician successions of the Ribes de Freser area, Eastern Pyrenees

(*paper 1*)

Journal of Iberian Geology (2018) 44:603–617
https://doi.org/10.1007/s41513-018-0084-0

RESEARCH PAPER

The Sardic unconformity and the Upper Ordovician successions of the Ribes de Freser area, Eastern Pyrenees

Claudia Puddu[1] · **J. Javier Álvaro**[2] · **Josep Maria Casas**[3]

Received: 10 January 2018 / Accepted: 7 September 2018 / Published online: 28 September 2018

Abstract

The Ribes de Freser area of the Eastern Pyrenees is characterized by an Alpine antiformal stack that comprises the so-called El Baell and Bruguera tectonostratigraphic units. This work presents detailed geological mapping and stratigraphic and facies analyses of these units, in order to improve the understanding of the Mid–Late Ordovician paleogeographical features of this sector of the Pyrenean margin of North Gondwana, subsequently affected by the Sardic Phase and the Variscan Orogeny. The Katian El Baell Formation, which crops out in the homonymous unit, is revised, formally erected and proposed as a lateral equivalent of the Estana Formation. The El Baell Formation consists of shale/limestone alternations where the carbonate production was controlled by development of pelmatozoan–bryozoan meadows and mud-mounds with plano-convex geometries and preservation of ramose bryozoans in life position. The thicker limestone levels, marking the top of shallowing-upward sedimentary cycles, contain fissure networks occluded with Pb–Zn–As ore mineralizations, whose clast counterparts occur forming overlying lags. The El Baell/Ansovell contact is marked by karstic clayey byproducts. Both the drastic changes in thickness and facies of the El Baell and Estana formations, and the presence of contemporaneous epithermal and fissuring episodes in the former, point to the onset of Katian (Late Ordovician) extensional tectonics, which may have controlled sharp modifications in accommodation space. Finally, the internal structure of the El Baell and Bruguera units are different, pointing to the record of a pre-Variscan (Mid Ordovician) deformational episode responsible for the dispersion of Variscan mesostructures in pre-Upper Ordovician rocks.

Keywords Carbonate production · Hydrothermalism · Ore mineralization · Mesostructure · North Gondwana

Resumen

El sector de Ribes de Freser, en el Pirineo Oriental, se caracteriza por un apilamento antiformal alpino compuesto por las llamadas unidades tectonostratigráficas de El Baell y Bruguera. El objetivo de este trabajo es profundizar en el conocimiento de estas unidades, a través de la cartografía geológica y el análisis estratigráfico, con el fin de contribuir a la comprensión de la influencia tectónica registrada a lo largo del Ordovícico Medio–Superior. Se revisa y se propone la Formación El Baell, de edad katiense, que aflora en la unidad de El Baell y se considera equivalente lateral de la Formación Estana. La Formación El Baell se compone de alternancias lutítico-calcáreas donde la producción carbonatada se relaciona con el desarrollo de praderas de pelmatozoos-briozoos y montículos micríticos con geometrías plano-convexas y conservación de briozoos ramosos en posición de vida. Los niveles más potentes de caliza, que marcan la parte superior de los ciclos sedimentarios de somerización, contienen redes de fisuras rellenas con mineralizaciones de Pb–Zn–As, cuyos clastos aparecen retrabajados en niveles suprayacentes. Asimismo, el contacto El Baell/Ansovell está marcado por subproductos arcillosos cársticos. Tanto los cambios drásticos de espesor y facies en las formaciones El Baell y Estana, como la presencia de episodios epitermales y de fracturación en el primero, apuntan al registro de una tectónica extensional, de edad katiense (Ordovícico Superior), responsable de cambios importantes en el espacio de acomodación. Por último, la estructura interna de las unidades de El Baell y Bruguera es significativamente diferente, señalando el registro de un episodio de deformación pre-Varisco (Ordovícico Medio) responsable de la dispersión de las mesoestructuras variscas que afectan a las rocas anteriores al Ordovícico Superior.

Extended author information available on the last page of the article

Palabras clave Producción carbonatada · Hidrotermalismo · Yacimientos minerales · Mesoestructura · Gondwana septentrional

1 Introduction

The pre-Variscan basement of the Pyrenees comprises an upper Neoproterozoic–Carboniferous succession, more than 3000 m thick, which provides evidence of Cadomian, Ordovician and Variscan magmatic episodes, associated with Ordovician, Variscan and Alpine deformation events. The knowledge of their stratigraphic, structural and magmatic features is clue to understand the geodynamic evolution of this fragment of North Gondwana after the end of the Cadomian orogeny, the construction of an Early Palaeozoic passive margin and the subsequent Variscan and Alpine deformations.

In the Pyrenees, two Early–Mid and Late Ordovician magmatic events are well documented. The Early–Mid Ordovician magmatism is coeval with an episode of uplift and erosion that led to the formation of the so-called "Sardic" unconformity, whereas the Late Ordovician magmatism is coincident with a subsequent extensional pulse, related to normal faults that controlled the post-Sardic sedimentation and the subsequent infill of palaeorelief depressions (Casas 2010). However, the origin and significance of this Ordovician magmatism is still under debate and a comprehensive model combining geochronological, geochemical and structural data is still lacking.

The aim of this work is to provide new structural and stratigraphic data from the Upper Ordovician rocks involved in two Alpine thrust sheets, the El Baell and Bruguera units, located in the Ribes de Freser area of the Eastern Pyrenees (Fig. 1). The Upper Ordovician succession of these units differs from that classically described and used as reference for the main part of the Pyrenees (Hartevelt 1970). The new data will improve the Ordovician stratigraphic framework of the Eastern Pyrenees and the recorded effects of Ordovician extensional tectonics. These data may also constrain the future restoration of Variscan and Alpine deformations in this area and refine the geometry of this portion of the Upper Ordovician northern Gondwana margin.

2 Geological setting

The Pyrenees is an asymmetrical, double-verging belt consisting of large outcrops of Mesozoic and Cenozoic rocks deformed by mainly north-directed structures in the northern part of the belt, and south-directed structures in the

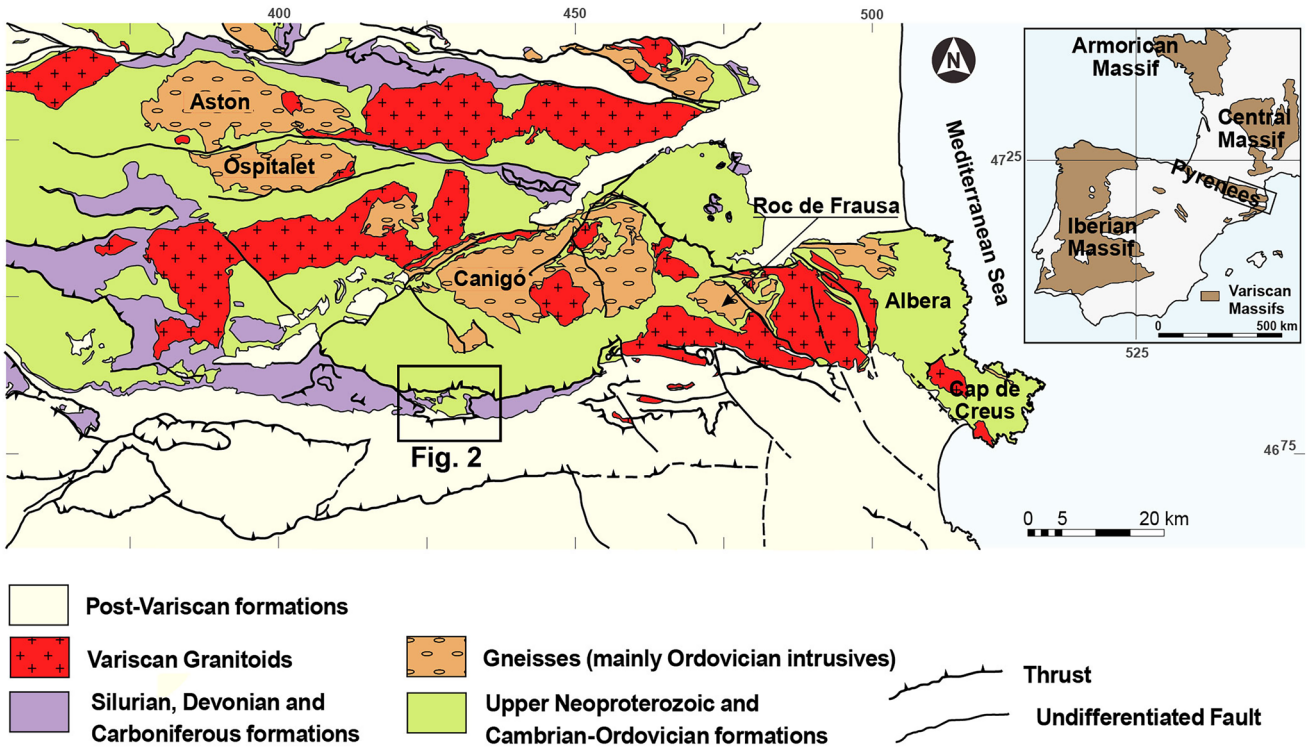

Fig. 1 Geological map of the Axial Zone from the eastern Pyrenees with location of the study area

southern part, separated by a large strip of Neoproterozoic and Palaeozoic rocks in the Axial Zone.

The inner part of the Pyrenean belt comprises pre-Variscan rocks, Ediacaran to Carboniferous in age, incorporated in some Alpine thrust sheets and distributed on E–W-trending elongated domes and synclines (Fig. 1). The pre-Variscan basement rocks of these sheets often preserve their initial sedimentological and structural characteristics.

The study area is located between Ribes de Freser and Bruguera towns, in the Eastern Pyrenees. It was previously studied both by Robert (1980), who informally proposed the El Baell Formation, and by Muñoz (1985), who unraveled the geological structure of the area. In the Ribes de Freser area, an Alpine antiformal stack formed by several units bearing different pre-Variscan stratigraphic successions is recognized (Robert 1980; Muñoz 1985). These are, from bottom to top, the El Baell, Bruguera and Serra Cavallera thrust sheets (Muñoz 1985) (Fig. 2). All these units are bounded to the north by the out-of-sequence Ribes–Camprodon thrust (Muñoz 1985) that separates these units from the Canigó massif (Fig. 2).

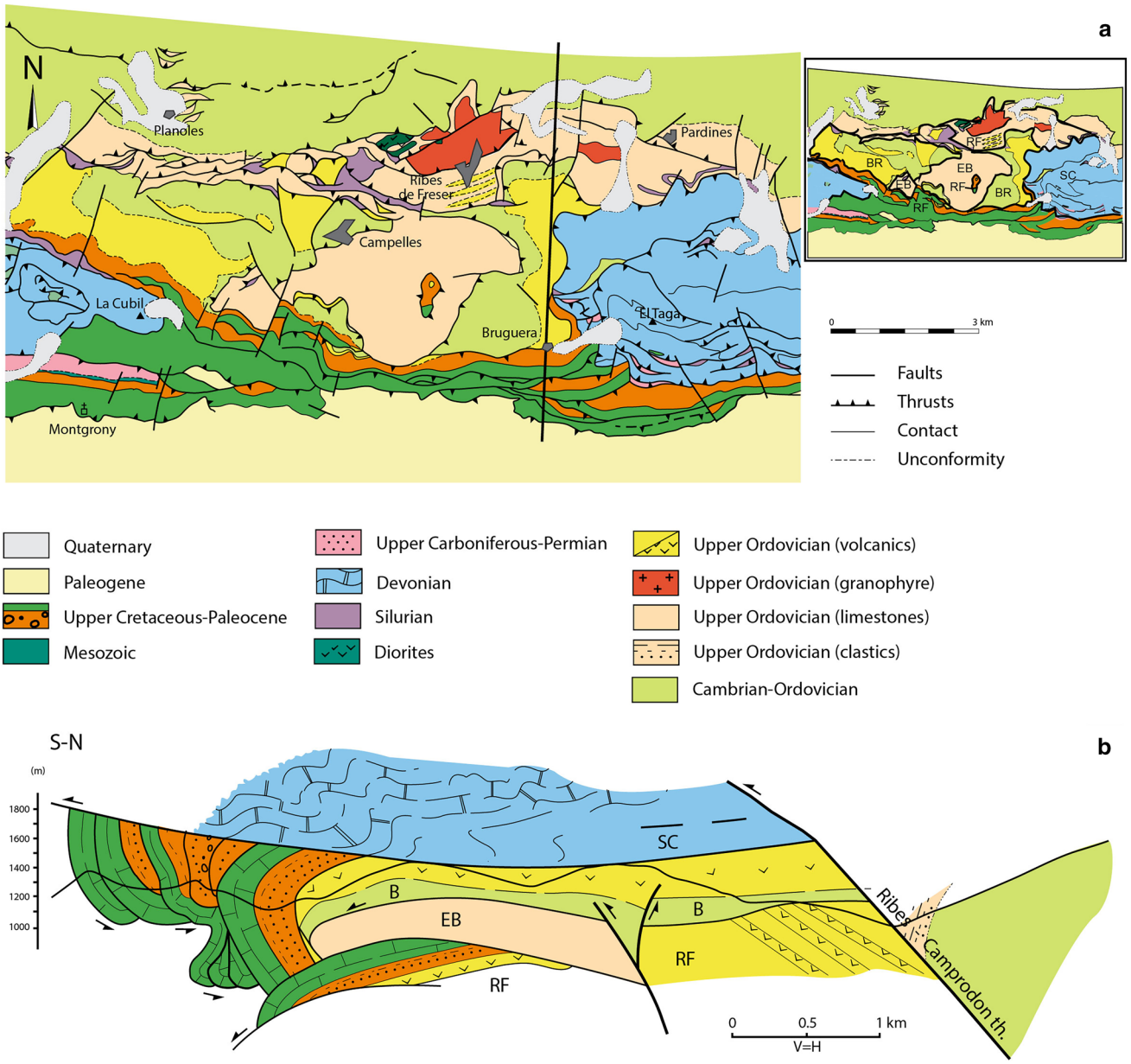

Fig. 2 **a** Geological map of the Ribes de Freser area with the study area. **b** S–N geological cross-section (black line in the geological map) of the Freser valley antiformal stack with the *RB* Ribes de Freser, *EB* El Baell, *B* Bruguera and *SC* Serra Cavallera units; modified after Muñoz (1985); see location on Fig. 1

(1) The Ribes de Freser thrust sheet is the lowermost outcropping unit (Muñoz 1985). It exhibits a 200–600 m-thick pre-Variscan basement succession mainly composed of Upper Ordovician volcanic, subvolcanic and volcanosedimentary rocks interbedded in Katian sediments (Robert and Thiebaut 1976; Ayora 1980; Robert 1980; Muñoz 1985; Martí et al. 1986). The volcanic activity was mainly explosive (Martí et al. 1986). A granitic body with granophyric texture, dated 458 ± 3 Ma (Martínez et al. 2011), is intruded into the lower part of the succession.

(2) The El Baell unit is entirely made up of pre-Variscan basement rocks. It comprises a 500 m-thick succession entirely composed of limestones, marly limestones, shales with centimetre-thick, parallel bedding nodules (the so-called "schistes troués" of French literature) and shales (Robert 1980; Muñoz 1985), in which three limestone-dominated levels can be distinguished. Conodonts and echinoderms allowed Robert (1980) to attribute an early Katian (former Caradoc) age to the strata forming this unit. Sánz-López and Sarmiento (1995) attributed conodont faunas to a late Katian age (*Amorphognathus ordovicicus* Zone) and correlated them with that described from the Estana Formation. Black shales of probably Hirnantian age unconformably cap the former Katian beds. Both the base of the Upper Ordovician succession and the contact with Silurian beds are not exposed in this unit.

(3) The Bruguera unit lies on the top of the El Baell unit and exhibits a 300 m-thick slate-dominant succession, pre-Variscan in age (Cambrian–Lower Ordovician; Muñoz 1985), subsequently overlain by a volcanic complex (Fontboté 1949; Morre-Biot and Robert 1976; Robert 1980). The unfossiliferous slate-dominant succession is comparable with the Jujols Group cropping out in the Canigó massif, which consists of finely laminated to massive sandstone/slate alternations, with local burrowed beds and symmetric ripples. Based on this correlation, a broad Cambro–Ordovician age is assumed for the lower slates. The overlying volcanosedimentary complex consists of at least 300 m (Muñoz 1985) of rhyolitic ignimbrites, variegated in colour and finely banded. Robert (1980) reported the presence of a basal continental breccia marking the base of the volcanosedimentary complex that has yielded a Carboniferous pollen assemblage. In contrast, recent U–Pb data on these volcanic rocks (Martí et al. 2014) suggest a radiometric age about 455 Ma (Sandbian), which fits with the age of the volcanic and subvolcanic rocks cropping out in the Ribes de Freser unit.

(4) Finally, the uppermost Serra Cavallera unit is mainly made up of Silurian black shales, Devonian limestones, detrital Carboniferous "Culm" and continental Carboniferous and Permian deposits (Muñoz 1985).

The Upper Ordovician successions of the El Baell and Bruguera units differ from that described by Cavet (1957) and Hartevelt (1970) in the Canigó massif and traditionally used as reference for the main part of the Pyrenees. The classical Upper Ordovician rocks constitute a 100–1000 m broad fining-upward megasequence, where Hartevelt (1970) defined five main siliciclastic formations with a carbonate interbed unit. From bottom to top, this succession consists of reddish-purple polygenic and heterometric conglomerates, 0–100 m thick (Rabassa Conglomerate Formation), with clasts composed of vein quartz, quartzite and slate derived from underlying rocks. The Cava Formation, 0–850 m thick, consists of conglomerates, sandstones and shales with volcanic interbeds, bearing fossiliferous levels of Katian age (Hartevelt 1970). This formation is overlain by a 5–200 m-thick limestone and marly limestone, named Estana Formation (Hartevelt 1970), rich in brachiopods, bryozoans, cystoids and conodonts aged late Katian (Gil-Peña et al. 2004). The latter is capped by the 20–320 m-thick black–grey shales of the Ansovell sensu Hartevelt (1970), and the 2–20 m thick fining-upward quartzite with dark shale interbeds and fine conglomerates of the Bar Quartzite Formation. Hartevelt (1970) suggested an Hirnantian (former late Ashgill) age, which was confirmed by Roqué Bernal et al. (2017) for the Ansovell and Bar formations.

Restoration of the Alpine deformation (Muñoz 1985) situates the uppermost Serra Cavallera unit in a pre-Alpine northernmost position, probably north of the Canigó massif where similar Devonian succession outcrops (Fig. 1). However, the initial position of the rest of the Upper Ordovician-bearing units cannot be constrained. A preliminary restoration by Muñoz (1985) situates the Bruguera unit in a pre-Alpine northern position, the intermediate El Baell unit in an intermediate setting, and the lowermost Ribes de Freser unit lying originally in a southernmost position.

3 Materials and methods

A detailed (1:5000) geological mapping of the Bruguera and El Baell units was performed and structural data were collected (Fig. 3). A stratigraphic log of the Upper Ordovician was measured along the GIV-5263 road that connects Bruguera and Ribes de Freser, which is considered as the type section for the El Baell unit (Fig. 4).

About 30 limestone samples were prepared for petrographic examination by polishing cut surfaces. Carbonates were stained with Alizarin Red S and potassium ferricyanide to distinguish calcite from dolomite and to identify ferroan cements. Mineralogical identification was based on transmitted and

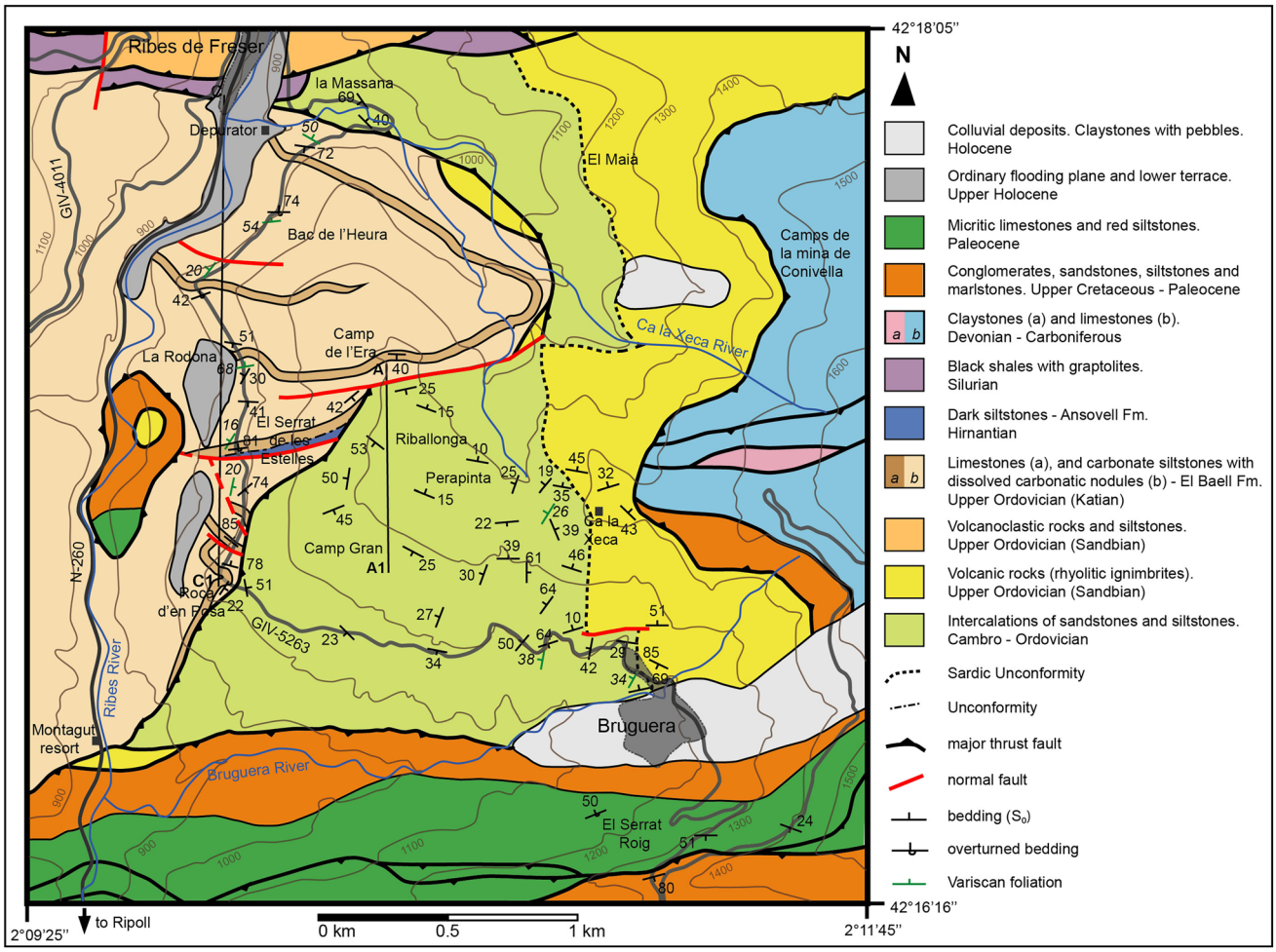

Fig. 3 Detailed geological map of the study area

reflected light microscopy, X-ray diffraction (XRD in IGEO, Madrid), and scanning electron microscopy (SEM) equipped with an energy-dispersive X-ray analyser (EDX). The chemical composition of selected minerals was determined with a back-scattered electron detector (BSE). SEM analysis was made by using a JEOL JSM-6400 fitted with an Oxford Instruments D6679 detector in the Museo Nacional de Ciencias Naturales, Madrid. Back-scattered (BSE) imaging and energy-dispersive X-ray (EDS) analyses were obtained by SEM with the following measurement conditions: accelerating voltage 20 kV, beam current 1–2 nÅ, and a counting interval of 50 s. Analytical results display an error of ±5–7%.

4 Facies and sedimentary features of the El Baell unit

The type section of the Upper Ordovician is selected along the GIV-5263 road, on the left bank of the Freser river. Its lower contact lies at the basal thrust with the Ribes de Freser unit and its upper one is covered by the Bruguera unit. Two formations are distinguished: a lower alternation of shales and limestones (displaying the characteristic "schistes troués" feature of the Estana Formation), unconformably overlain by monotonous grey shales referred by Muñoz (1985) to the Ansovell Formation described by Hartevelt (1970).

Originally, Hartevelt (1970) erected the Estana Formation as a monotonous marlstone–limestone unit, up to 60 m thick, displaying a distinct northward decrease–increase thickness composite trend. The formation disappears between Sant Julià de Lòria and Andorra and between the former and La Massana localities. The formation (para)conformably overlies either the Cava or the Rabassa formations and is unconformably overlain by either the Ansovell or the Bar formations. Hartevelt (1970) pointed out the absence or rare presence ("intercalations of black slate a few cm thick") of shales and slates, which contrasts with the alternations of shales and limestones exposed in the El Baell unit. As a result, on the basis of these new lithologic relationships

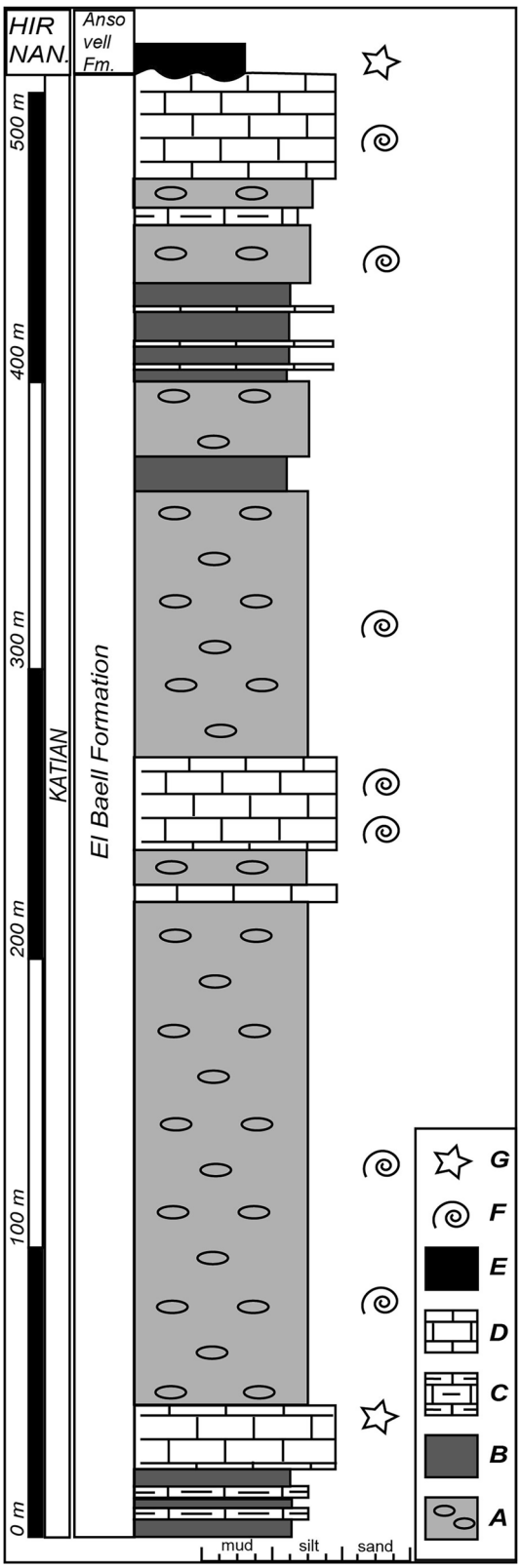

Fig. 4 Stratigraphic log of the Upper Ordovician succession cropping out in the El Baell unit, measured northward along the GIV-5263. The different lithofacies composing the carbonate succession of the El Baell (**A–D**) and Ansovell (**E**) formations are represented. **A** Siltstones with dissolved carbonate nodules, the so called "schistes troués". **B** Siltstones and shales. **C** Marlstones, massive or fossiliferous (containing brachiopods, crinoids, cystoids, bryozoans and gastropods). **D** Limestones. **E** Black shales. Fossils (**F**) indicate a Katian (**A–D**) and Hirnantian age (**E**). Quartz veins are of hydrothermal origin (**G**)

between limestone and shale beds cropping out in the El Baell unit, we propose a formal definition of the El Baell Formation. This formation was informally proposed by Robert (1980), albeit without following the rules of the Stratigraphic Guide of the International Commission on Stratigraphy (Salvador 1994: article 3B.4a), and used by Sanz-López and Sarmiento (1995), who correlated it with the Estana Formation based on their content in conodonts.

The El Baell Formation (base of stratotype at N42°17′51.29″, E2°10′16.34″) consists of shale/limestone alternations, about 490 m (visible) thick (Fig. 4). The exposed succession comprises three shallowing-upward sedimentary cycles, 200–230 m thick, each one composed of basal greenish massive-to-bedded shales that increase upsection the content in carbonate nodules parallel to stratification ("schistes troués") and centimetre-thick limestone interbeds, until the final disappearance of shale interbeds. The uppermost cycle ends with a plano-convex limestone, up to 5 m thick, onlapped by centimetre-thick beds (Fig. 5). The top of the formation is marked by a karstic surface, overlain by a silty dolostone, up to 30 cm, and the subsequent onlap of the Ansovell blackish shales rich in slumping levels.

The bedded limestones consist of floatstones rich in bryozoans, pelmatozoans and subsidiary brachiopods, gastropods, nautiloid orthoceratids and trilobites (Figs. 5b–f, 6a–e), finely interrupted by erosively based, centimetre-thick pelmatozoan packstone interlaminae. Vertically, the erosive bases (in some cases irregularly scoured) are paved with abraded shell layers that pass into partly articulated skeletal elements, such as pelmatozoan columns. The thicker limestone strata and lenses exhibit numerous delicate and robust branched bryozoans, preserved in life position, and embedded in a pseudosparry matrix. The latter is dominant and can reach up to 60% in volume. The uppermost plano-convex lens is onlapped by packstone–floatstone flank beds.

The three sedimentary cycles reflect shallowing-upward conditions, from clayey to carbonate shelly substrates. Shelly carbonate production became repeatedly more continuous in time leading to the establishment of echinoderm-bryozoan meadows episodically affected by storms. Partly articulated echinoderms reflect calm episodes interrupted by storm influence on an open-sea platform. Similar cycles were reported from the Iberian Chains and Hesperian massifs of NE Spain (Vennin et al. 1998; Álvaro and Van Vliet-Lanoë 2009), where their facies allowed distinction between the shale-dominant Ocino Member and the storm-induced shelly

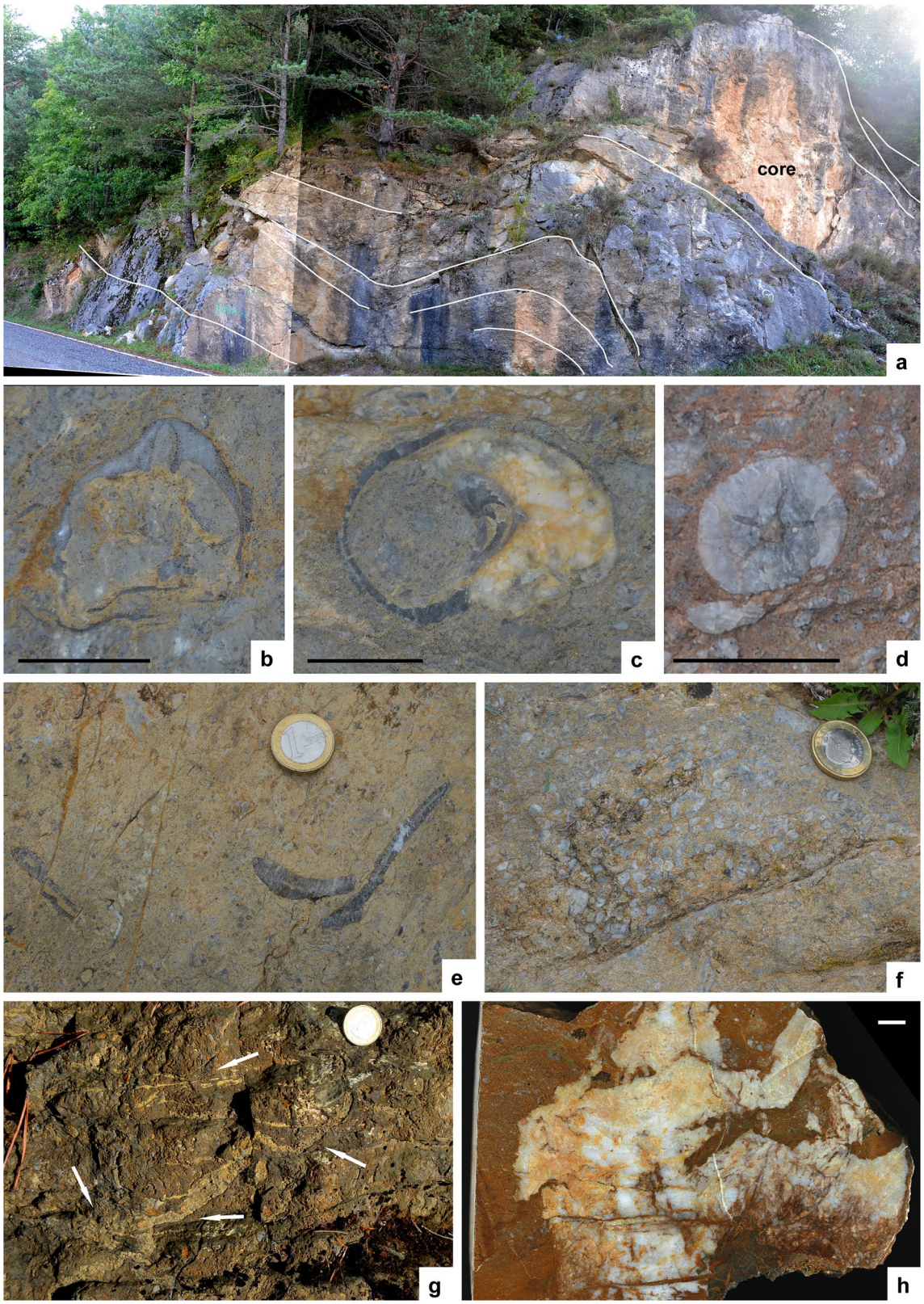

Fig. 5 Field aspect of the El Baell stratotype outcrops and macrofacies. **a** Top of the El Baell Formation showing folded strata and lenticular core (right). **b** Section of the rhynconelliformean brachiopod; scale = 2 cm. **c** Section of a gastropod with a mosaic of sparry calcite occluding primary porosity; scale = 2 cm. **d** Section of a cystoid ossicle; scale = 1 cm. **e** Partly articulated pelmatozoan columns. **f** Disarticulated column and cystoid ossicles. **g** Fissuring network (arrowed) with a yellowish staining. **h** Polished slab of a reworked angular extraclast sourced from an hydrothermal quartz vein, top of the El Baell Formation; scale = 1 cm

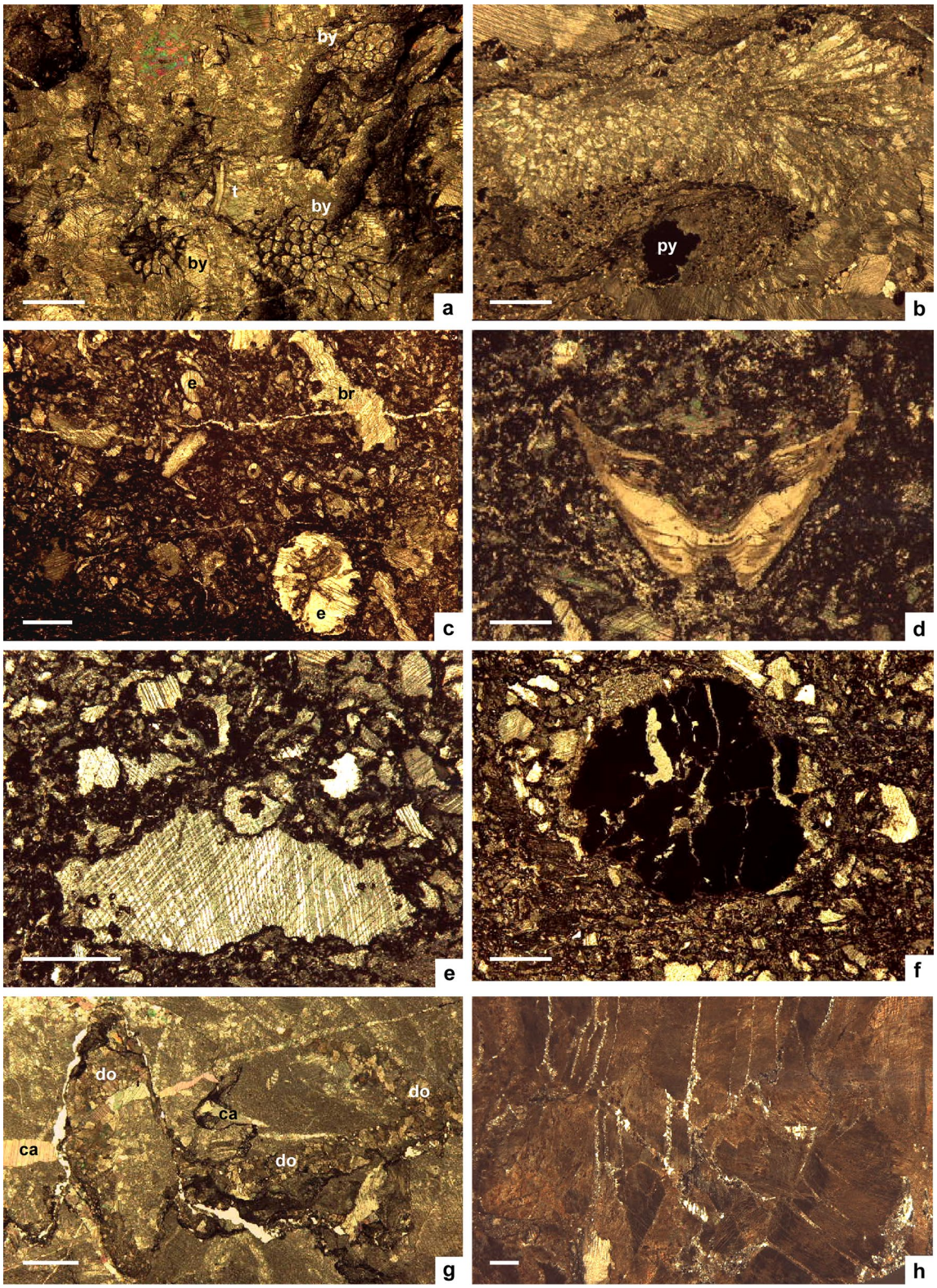

pavements of the Rebosilla and la Peña Members sensu Hammann (1992).

Despite intense neomorphism into pseudosparite, it is possible to recognize the presence of ramose and encrusting bryozoans preserved in life position embedded in a pseudosparry mass that can reach up to 60% in volume. These features point to the possible development of bafflestone (frame-building) facies in successive pelmatozoan–bryozoan

◂**Fig. 6** Photomicrographs of carbonate microfacies from the El Baell Formation. **a** Floatstone rich in ferruginized bryozoan fragments and trilobite sclerites embedded in a pseudosparry matrix. **b** Bryozoan fragment with intraparticle porosity, occluded with sparry mosaics of calcite, and pyritic aggregates. **c** Storm-induced packstone rich in echinoderm ossicles, brachiopod valves and bryozoan fragments embedded in a ferruginized microsparitic matrix. **d** Longitudinal section of the apical piece from a nautiloid orthoceratid. **e** Ossicle fragments affected by stylolites in a microsparitic matrix rich in hematite cements. **f** Rounded pyritic extraclast, surrounded by a shaly (illitic) aureole, encased in an echinoderm-rich packstone. **g** Stylolite crosscutting (so postdating) a veining network infilled with calcite and dolomite. **h** Fissure network affecting a dolomitized host-rock occluded with mosaics of micro-to-macroquartz; scales = 1 mm; abbreviations: *br* brachiopod valves, *by* bryozoans, *ca* calcite, *do* dolomite, *e* echinoderm ossicles, *py* pyrite, *t* trilobite sclerite

meadows (preserved as strata), finally capped by a single mud-mound (similar to the Rebollarejo Member sensu Hammann 1992) overlain by bedded packstone-rich flanks. Unfortunately, the strong recrystallization of the matrix and skeletons precludes a distinct identification of the core microfacies. Although a detailed palaeontological study has not been performed in the El Baell Formation, the presence of the brachiopod *Nicolella* sp. in the "schistes troués" (Robert 1980; Casas et al. 2017) points to a Katian age similar to that yielded by the laterally equivalent Estana Formation (Hartevelt 1970).

In addition, it is remarkable the presence of two hydrothermally influenced episodes, marking the top of the second and third sedimentary cycles:

(a) The top of the second sedimentary cycle contains a network of fissures infilled with calcite, dolomite and quartz mosaics, illite and angular host-rock carbonate clasts (Figs. 5g; 6g, h). The latter represent cataclastic rocks lining the fissure-related deformed zones. Sulfide minerals, such as galena, sphalerite, pyrite and orpiment-to-realgar, occur as authigenic crystals infilling the fissure porosity and as subrounded clasts embedded in the matrix and the lag that cover the limestone bed (so reflecting their synsedimentary character) (Figs. 6f, 7a–d). Some calcite veins are crosscut by dolomite veins (Fig. 6g), and both ones crosscut by quartz-rich epithermal veins of quartz, allowing a chronological order of veining events. Some sulfides show oxidized aureoles reflecting Eh modifications during precipitation. Other mineralizations are TiO_2-bearing quartz and apatite.

(b) The upper hydrothermally influenced marly dolostone, up to 30 cm thick, marks the El Baell/Ansovell contact. This breccia level contains angular and subangular clasts, up to 10 cm size, of limestone, dolostone, shale and hydrothermal quartz floating in a marly matrix (Fig. 5h). Hydrothermal TiO_2-rich quartz occurs as scattered angular clasts, up to 30 cm sized associated with subsidiary Pb–Zn sulfide mineralizations. XRD analysis allows identification of a matrix composed of calcite, quartz, illite, muscovite and palygorskite (Fig. 8), pointing to karstic influence (Draidia et al. 2016).

In summary, during Katian times, the marine platform preserved in the El Baell unit recorded shallowing-upward trends accompanied by distinct episodes of shelly carbonate productivity. These were marked by the development of pelmatozoan–bryozoan meadows and a possible mud-mound directly affected by the karstic contact with the Hirnantian Ansovell Formation. The presence of, at least, two fissuring processes marking the end of shallowing-upward sedimentary cycles reflects sharp perturbations in the marine platform associated with fissuring and emplacement or Pb–Zn–As ore mineralizations.

5 Structure

The study area involves rocks cropping out in two of the units that form the Alpine Freser antiformal stack: (1) the Ribes de Freser and Bruguera thrust sheets, which comprehend both Palaeozoic basement rocks and Upper Cretaceous-Lower Paleocene deposits, and (2) the El Baell thrust sheet, only made by Upper Ordovician rocks (Figs. 2 and 9). The Alpine Freser antiformal stack crops out in a kilometric scale culmination at both sides of the Freser valley. It is roughly constituted by an antiform, cut to the north by the Ribes–Camprodon out of sequence thrust (Muñoz 1985) (Fig. 2), and developed as a piggy-back thrusting sequence. Alpine thrusts climb up southward from Variscan basement to Cenozoic cover rocks. Thrusts exhibit an antiform structure, dipping northward on the northern limb of the antiform, and southward on the southern limb of the antiform, except for the ones that are overturned (Figs. 2 and 9). The axis of this antiform is subhorizontal and E–W trending, as evidenced by the bedding planes of Garumnian strata (Fig. 10). Apart from the thrusts and the kilometer-scale fold, pervasive pressure–solution cleavage is the most extensive Alpine mesostructure preserved in the Garumnian marlstones and marly limestones. This cleavage forms an almost right angle to the bedding irrespective of the bedding attitude (Casas and Muñoz 1987). In the detrital layers and massive limestones, cleavage is weakly developed, whereas small-scale thrusts structures, such as pop-ups and triangle zones, are well preserved (Casas and Muñoz 1987). The former ones are especially well developed in the second-order antiformal stack and duplex formed by the Garumnian beds near the leading part of the antiform, to the south of the study area (Fig. 2). Alpine mesostructures are not recognized in the

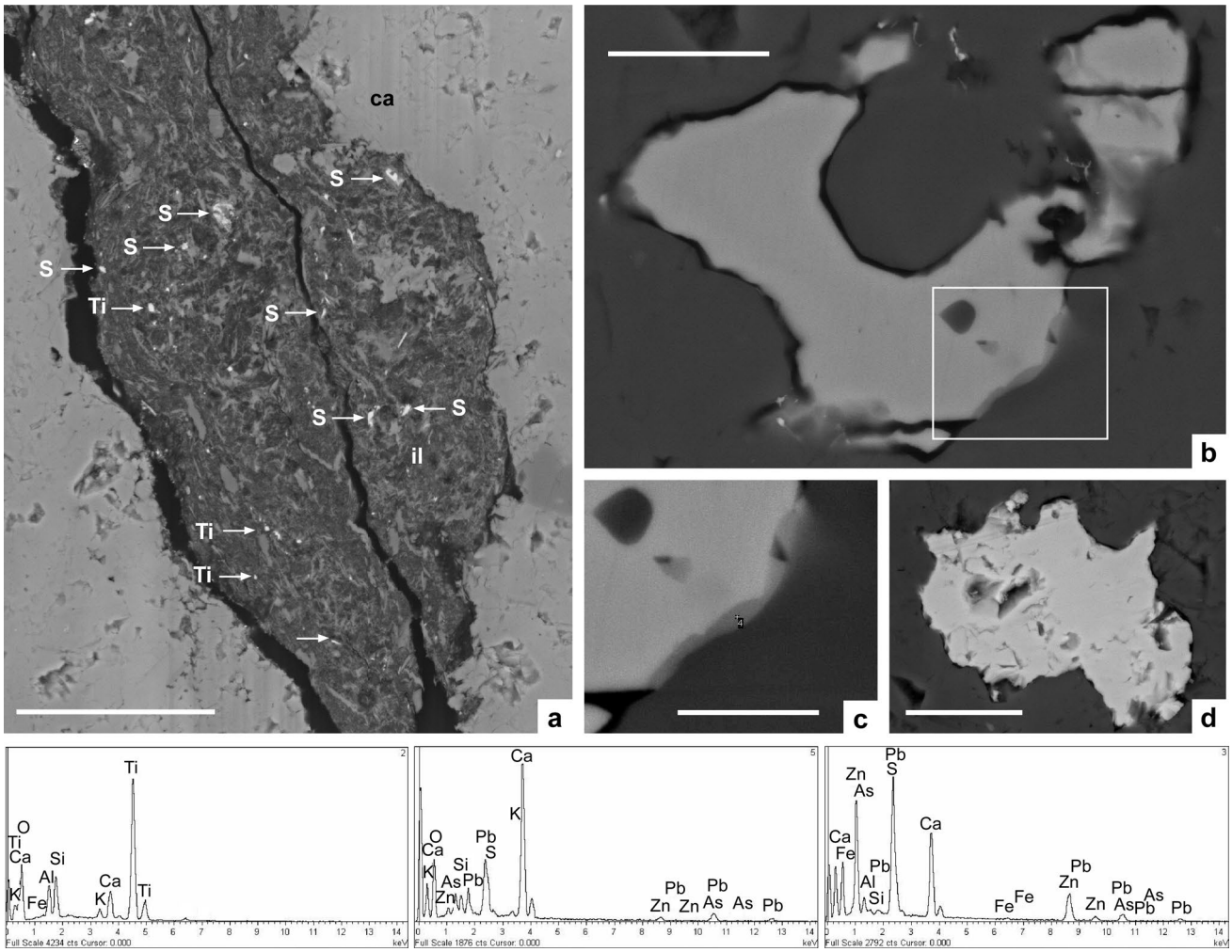

Fig. 7 BSE–SEM photomicrographs of hydrothermal mineralizations from the fissure network affecting the limestone top of the first sedimentary cycles in the El Baell Formation stratotype. **a** Fissure-related porosity occluded with illite (il), TiO_2 (Ti) and sulfides (S); scale = 50 μm. **b** Galena crystal embedded in calcite; scale = 10 μm. **c** Detail of previous boxed area with sphaleritic aureole; scale = 5 μm. **d** Sphalerite crystal embedded in calcite; scale = 10 μm. Bottom: three EDS spectra at pointed locations showing TiO_2 and Pb–Zn–As sulfide compositions

pre-Variscan basement rocks of the El Baell and Bruguera units, which, in turn, exhibit different internal structures.

5.1 Bruguera unit

The rocks cropping out in the Bruguera unit comprises a slate-dominant Jujols-style succession unconformably overlain by a volcanosedimentary complex, which exhibits different mesostructural features. The slate-dominant succession is weakly deformed; the most visible mesostructures are the bedding surfaces that display a marked dispersion (Figs. 3, 10a). This wide dispersion, with axes dipping alternatively to opposite directions, results from the presence of two main fold systems with axes oriented E–W and N–S (Fig. 10d). The E–W fold system produced decametre- to metre-sized S-verging open folds with sub-horizontal axes, N-dipping axial surfaces and a poorly developed related cleavage. The N–S trending folds produced decametric to metric open folds, with sub-horizontal axes and sub-vertical axial surfaces, as well as local development of a cleavage-related fold. It should be noted that fold superposition is not evidenced by interference patterns at outcrop scale, so their relative chronology has not been established. It is assumed that they are pre-Alpine in age because earlier Upper Cretaceous-Palaeocene rocks cropping out in neighbouring units are not affected by these deformations. Alpine E–W folding is recognizable in the the basal thrust between the Bruguera and El Baell units (Fig. 9), which is north-dipping on the northern side of the study area, near the Ribes de Freser depurator, and south-dipping on the southern side, near Bruguera (Roca d'en Posa locality).

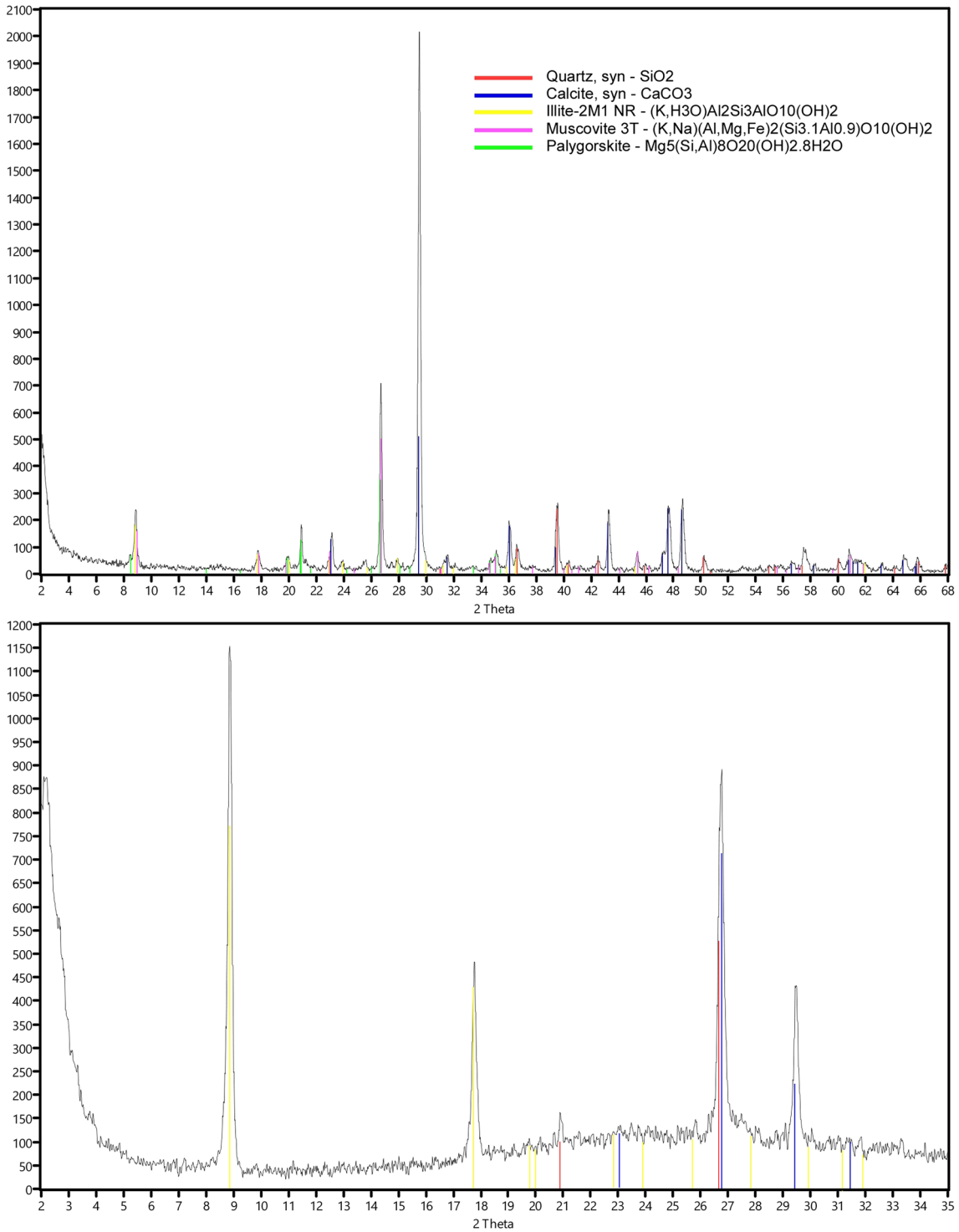

Fig. 8 Diffraction data from a marly fraction marking the top of the El Baell Formation stratotype, including identified shifts

The Upper Ordovician volcanic rocks in this area display a well-developed flow structure that is used as surface reference. This mesostructure is affected by a kilometric E–W trending fold (Fig. 10b) that can be either correlated to the E–W folds affecting the underlying slate-dominant

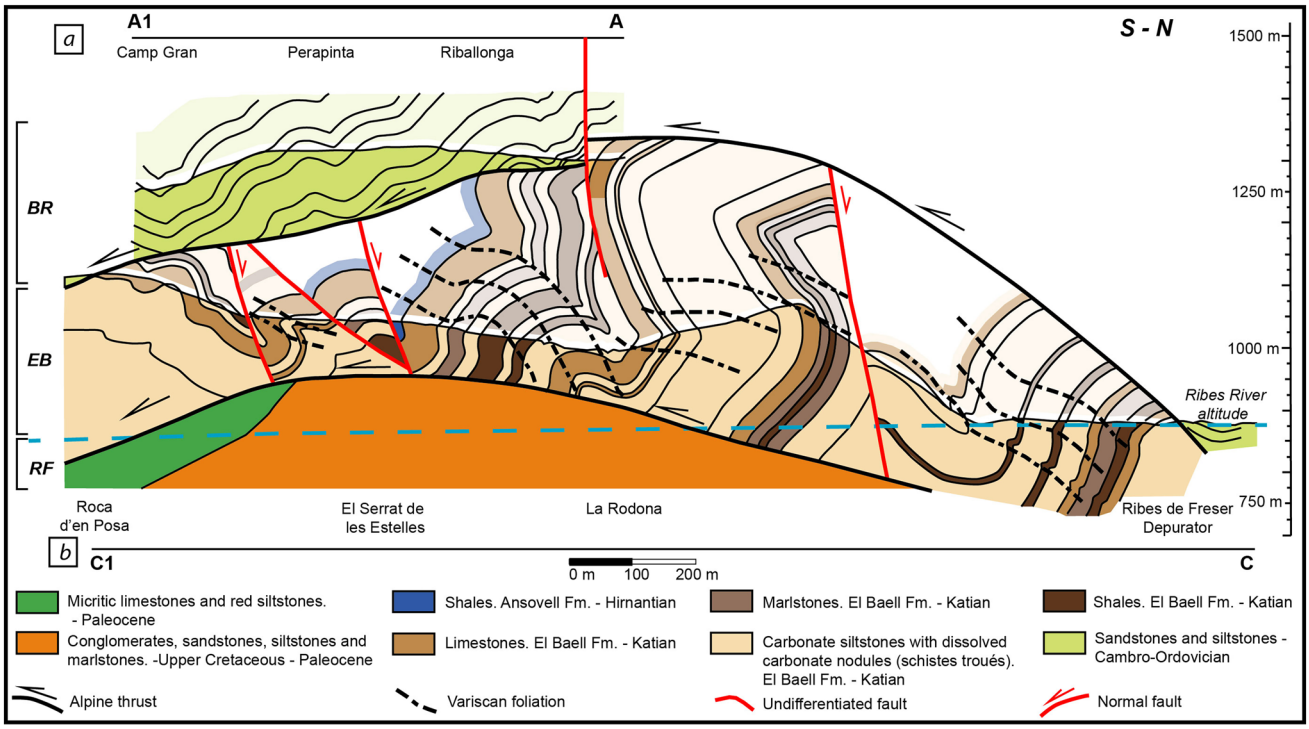

Fig. 9 **a** Composite cross-section of **a** Bruguera (A–A1) and **b** El Baell (C–C1) units (see Fig. 3 for location). From bottom to top, three tectonic units delimited by thrusts (black bold lines) occur: *RB* Ribes de Freser, *EB* El Baell and *BR* Bruguera units. The Ribes de Freser unit (RB) crops out in a tectonic window along the Freser riverand is overlain by the El Baell unit (**b**), which in turn is overlain by the Bruguera unit (**a**)

succession or to the Alpine E–W fold linked to antiformal stack development.

5.2 El Baell unit

The rocks that form the El Baell unit are affected by an E–W oriented fold system (Fig. 10c). The wavelength of these folds varies from a few to several metres and they are asymmetrical with gently north-dipping limbs and south or north dipping overturned limbs (Fig. 9). In profile, these E–W folds are open to tight and south-verging, with axial surfaces dipping 15°–30° toward the N. Associated with these folds, a well-expressed axial plane cleavage is developed. Cleavage is sub-horizontal or gently dipping to the north, with a general antiformal attitude (Fig. 9). These folds should be Variscan in age, because they do not affect the Alpine thrust that bounded these units or the Upper Cretaceous-Paleocene rocks of the adjoining tectonic units. The E–W folds of the El Baell unit can be correlated with the E–W folds of the Bruguera unit. The antiformal cleavage attitude may reflect the effect of an E–W trending Alpine fold that also affect both, the top thrust contact with the overlying Bruguera unit and the basal one with Ribes de Freser unit.

6 Discussion

The pre-Variscan rocks cropping out in Bruguera and El Baell units exhibit different folding systems. The N–S folds recognized in the slate-dominant succession of the Bruguera unit have been recognized neither in the Upper Ordovician volcanic rocks of the Bruguera unit nor in the shale/limestone alternations of the El Baell unit. Based on this, two possibilities arise: (1) the N–S folds recognized in the Bruguera unit are pre-Late Ordovician in age and thus developed only in the pre-Upper Ordovician succession; or (2) N–S and E–W folds may be synchronous, both Variscan in age, being their variation in orientation controlled by some pre-existing pre-Variscan folds, only developed in the slate-dominant succession underneath the Upper Ordovician volcanic rocks of the Bruguera unit. In any case, both possibilities require the existence of a deformational event predating the sedimentation of Upper Ordovician strata in the Bruguera and El Baell units. Considering a ca. 455 Ma as the age for the volcanic rocks that cap the unconformity in the Bruguera unit (Martí et al. 2014), and a broad Cambro–Ordovician age for the slate-dominant Jujols style succession, the age of this N–S folding event or the pre-Variscan folding event controlling the orientation of both fold systems should be late Early Ordovician to Mid Ordovician.

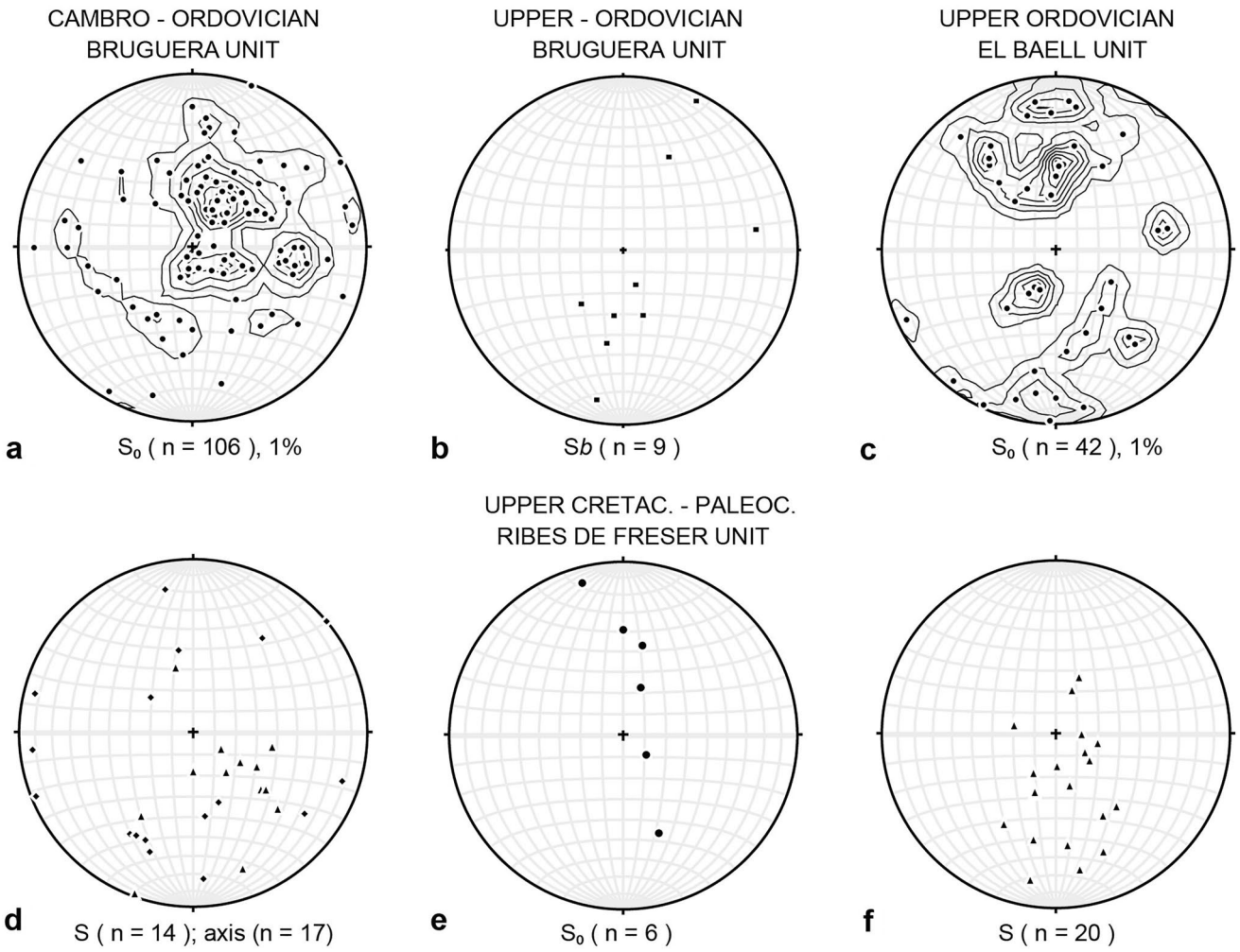

Fig. 10 Equal area stereoplots of the data collected (*n* indicates the number of measurements) in the Ribes de Freser area included in Fig. 3. **a** Poles to bedding (S_0) from the Cambro–Ordovician succession of the Bruguera unit. **b** Poles to banded surfaces (S_b) recognized in the Upper Ordovician ignimbrite of the Bruguera unit. **c** Poles to bedding (S_0) from the Upper Ordovician succession in the El Baell unit. **d** Poles to main Variscan foliation (S—black triangles) and Variscan fold axes (black diamonds), from the Cambro-Ordovician succession of the Bruguera unit. **e** Poles to bedding (S_0) from the Upper Cretaceous-Paleocene succession in the Ribes de Freser unit. **f** Poles to main Variscan foliation (S) from the Upper Ordovician of the El Baell unit

As a result, the unconformity that separates the Upper Ordovician volcanic complex and the underlying Cambro–Ordovician slate-dominant succession should be assumed as the Sardic unconformity. Unfortunately, the stratigraphic gap between both successions cannot be evaluated here due to the lack of biostratigraphically significant fossils in the slates underlying the unconformity.

The El Baell formation is assumed to be Katian in age because of the occurrence of the brachiopod *Nicolella* sp. in the "schistes troués" (Robert 1980; Casas et al. 2017). Based on this preliminary context and lithological similarities, it is considered as a lateral equivalent of the Estana Formation. The record in the El Baell Formation of distinct sedimentary shallowing-upward cycles associated with progressive increases in carbonate context, punctuated by sharp modifications in facies and thickness related to fissuring and hydrothermal activity at the top of the sedimentary cycles, suggest changes in accommodation space associated with platform instability.

By comparison with laterally equivalent units of the Eastern Pyrenees, the occurrence of shallowing-upward sedimentary cycles ranging from clayey to shelly carbonate substrates and the contemporaneous fracturing and fissuring activity point to sharp modifications in accommodation space, nucleated by a graben depocentre in the El Baell unit. The boundaries of this depocentre may have played a distinct role in the Alpine thrusting that led to the onset of the Ribes de Freser antiformal stack.

7 Conclusions

A new geological map at 1/5000 scale of the Ribes de Freser Alpine antiformal stack of the Eastern Pyrenees has yielded a new stratigraphic, sedimentological and structural framework for this sector of the Pyrenean margin in North Gondwana. The presence of shale/limestone alternations has allowed the formal erection of the Katian El Baell Formation, informally defined previously and proposed as a lateral equivalent of the monotonous (marlstone/limestone-dominant) Estana Formation. In its stratotype, the El Baell Formation displays three shallowing-upward sedimentary cycles, 200–230 m thick, related to changing conditions from clayey to carbonate substrates, controlled by episodes of shelly carbonate productivity derived from pelmatozoan–bryozoan meadows. A mud-mound is suggested forming the top of the formation as a result of plano-convex geometries, displaying preservation of ramose bryozoans in life position, capped by shelly bedded flanks. The thicker limestone levels, marking the top of the sedimentary cycles, contain fissure networks occluded with Pb–Zn–As ore mineralizations, whose clast counterparts occur forming lags of reworked extraclasts on the overlying beds, so pointing to synsedimentary conditions. The El Baell/Ansovell contact is marked by karstic clayey byproducts. Both the drastic changes in thickness and facies of the El Baell and Estana formations, and the presence of linked epithermal and fissuring episodes in the former, point to the onset of extensional tectonic pulsations, which may have controlled sharp modifications in accommodation space and development of (half-) grabens with hydrothermally mineralized bounding faults.

In addition, a pre-Variscan (Mid Ordovician?) deformation event may have controlled the wide dispersion of the folding axes of the main Variscan phase in the pre-Upper Ordovician succession preserved in the Bruguera unit. A better understanding of the pre-Variscan deformations (Mid Ordovician? folding event and Late Ordovician extensional tectonics) should help us to unravel the geometry of the main Variscan deformations in the Pyrenees.

Acknowledgements We thank the constructive criticism made by two anonymous reviewers. C.P. thanks Prof. C. Corradini for allowing the use of laboratories in the Cagliari University (Department of Earth Sciences), and S. Unida who provided the techniques for unsuccessful palynological preparations. M. Sánchez-Román (VU, Amsterdam) and J. Ibáñez (ICTJA, Barcelona) are thanked for XRD interpretation. Financial support for this work was provided by CGL2015-66335-C2-1-R and CGL2017-87631-P projects from Spanish MINECO.

References

Álvaro, J.J., & Van Vliet-Lanoë, B. (2009). Late Ordovician carbonate productivity and glaciomarine record under quiescent and active extensional tectonics in NE Spain. In: Bassett, M.G. (Ed.), *Early Palaeozoic Peri-Gondwana Terranes: New Insights from Tectonics and Biogeography*. Geological Society, London, Special Publications, *325*, 117–139.

Ayora, C. (1980) Les concentrationes metàl·liques de la Vall de Ribes. PhD, Univ. Barcelona.

Casas, J. M. (2010). Ordovician deformations in the Pyrenees: new insights into the significance of pre-Variscan ("sardic") tectonics. *Geological Magazine, 147,* 647–689.

Casas, J. M., & Muñoz, J. A. (1987). Sequences of mesostructures related to the development of Alpine thrusts in the Eastern Pyrenees. *Tectonophysics, 135,* 65–75.

Casas, J. M., Puddu, C., & Álvaro, J. J. (2017). Upper Ordovician limestones along the Ribes-Bruguera road. In: Álvaro, J.J., Casas, J.M., Clausen, S. (Eds.), Ordovician Geodynamics: the Sardic Phase in the Pyrenees, Mouthoumet and Montagne Noire massifs. *Géologie de la France, 1*(4), 40–41.

Cavet, P. (1957). Le Paléozoïque de la zone axiale des Pyrénées orientales françaises entre le Roussillon et l'Andorre (étude stratigraphique et paléontologique). *Bulletin du Service de la Carte géologique de France, 254,* 303–518.

Draidia, S., El Ouahabi, M., Daoudi, L., Harvenith, H. B., & Fagel, N. (2016). Occurrences and genesis of palygorskite/sepiolite and associated minerals in the Barzaman formation, United Arab Emirates. *Clay Minerals, 51,* 763–779.

Fontboté, J. M. (1949). Nuevos datos geológicos sobre la cuenca alta del Ter. *Anales del Instituto de Estudios Gerundenses, 4,* 1–57.

Gil-Peña, I., Barnolas, A., Villas, E., & Sanz-López, J. (2004). El Ordovícico Superior de la Zona Axial. In J. A. Vera (Ed.), *Geología de España* (pp. 247–249). Madrid: SGE-IGME.

Hammann, W. (1992). The Ordovician trilobites from the Iberian Chains in the province of Aragón, NE Spain. I. The trilobites of the Cystoid Limestone (Ashgill Series). *Beringeria, 6,* 1–219.

Hartevelt, J. J. A. (1970). Geology of the upper Segre and Valira valleys, central Pyrenees, Andorra/Spain. *Leidse Geologische Mededelingen, 45,* 167–236.

Martí, J., Casas, J.M., Guillén, N., Muñoz, J. A., & Aguirre, G. (2014). Structural and geodynamic constraints of Upper Ordovician volcanism of the Catalan Pyrenees. *Gondwana 15 Abstracts book*, 104.

Martí, J., Muñoz, J. A., & Vaquer, R. (1986). Les roches volcaniques de l'Ordovicien supérieur de la région de Ribes de Freser-Rocabruna (Pyrénées Catalanes): caractères et signification. *Comptes Rendus de l'Académie des Sciences, Paris, 302*(20), 1237–1242.

Martínez, F. J., Iriondo, A., Dietsch, C., Aleinikoff, J. N., Peucat, J. J., Cirès, J., et al. (2011). U-Pb SHRIMP-RG zircon ages and Nd signature of lower Paleozoic rifting-related magmatism in the Variscan basement of the Eastern Pyrenees. *Lithos, 127,* 10–23.

Morre-Biot, N., & Robert, J. F. (1976). Sur la découverte d'un complexe ignimbritique stéphanien dans la région de Ribes de Freser (Province de Gérone, Espagne). *Comptes Rendus de l'Académie des Sciences, Paris, 282,* 1933–1935.

Muñoz, J.A. (1985). Estructura alpina i herciniana a la vora sud de la Zona Axial del Pirineu oriental. PhD, Univ. Barcelona. *Monografies núm. 1. Publicació del Servei Geològic de Catalunya*. Generalitat de Catalunya, Departament de Política Territorial i Obres Públiques, Servei Geologic de Catalunya, Barcelona, 227 pp.

Robert, J.F. (1980). Étude géologique et métallogenique du val de Ribes sur le versant espagnol des Pyrénées Catalanes. PhD, Univ. Franche-Compté.

Robert, J. F., & Thiebaut, J. (1976). Découverte d'un volcanisme acide dans le Caradoc de la région de Ribes de Freser (province de Gérone). *Comptes Rendus de l'Académie des Sciences, Paris, 282,* 2049–2050.

Roqué Bernal, J., Štorch, P., & Gutiérrez-Marco, J. C. (2017). Bioestratigrafía (graptolitos) del límite Ordovícico-Silúrico en los Pirineos orientales (curso alto del río Segre, Lleida). *Geogaceta, 61,* 27–30.

Salvador A. (ed.) (1994). International stratigraphic guide, 2nd ed. Geological Society of America, 214 p. Boulder.

Sánz-López, J., & Sarmiento, G. N. (1995). *Asociaciones de conodontos del Ashgill y Llandovery en horizontes carbonatados del Valle del Freser (Girona)* (pp. 157–160). Tremp: XI Jornadas de Paleontología.

Vennin, E., Álvaro, J. J., & Villas, E. (1998). High-latitude pelmatozoan–bryozoan mud-mounds from the late Ordovician northern Gondwana platform. *Geological Journal, 33,* 121–140.

Affiliations

Claudia Puddu[1] · J. Javier Álvaro[2] · Josep Maria Casas[3]

✉ Claudia Puddu
732168@unizar.es

J. Javier Álvaro
jj.alvaro@csic.es

Josep Maria Casas
casas@ub.edu

[1] Dpto Ciencias de la Tierra, Universidad de Zaragoza, 50009 Zaragoza, Spain

[2] Instituto de Geociencias (CSIC-UCM), Dr. Severo Ochoa 7, 28040 Madrid, Spain

[3] Dpto de Dinàmica de la Terra i de l'Oceà, Universitat de Barcelona-Institut de recerca GEOMODELS, Martí Franquès s/n, 08028 Barcelona, Spain

5.6 Deciphering the Sardic (Ordovician) and Variscan deformations in the Eastern Pyrenees

(*paper 2*)

Research article

JGS
Journal of the Geological Society

Published online July 30, 2019

https://doi.org/10.1144/jgs2019-057 | Vol. 176 | 2019 | pp. 1191–1206

Deciphering the Sardic (Ordovician) and Variscan deformations in the Eastern Pyrenees, SW Europe

Claudia Puddu[1], J. Javier Álvaro[2], Núria Carrera[3] & Josep Maria Casas[3]*

[1] Dpto. Ciencias de la Tierra, Universidad de Zaragoza, Pedro Cerbuna 12, 50009 Zaragoza, Spain
[2] Instituto de Geociencias (CSIC-UCM), Dr. Severo Ochoa 7, 28040 Madrid, Spain
[3] Dpt. de Dinàmica de la Terra i de l'Oceà, Universitat de Barcelona–Institut de Recerca GEOMODELS, Martí Franquès s/n, 08028 Barcelona, Spain

CP, 0000-0001-5137-7519; JJA, 0000-0001-6294-1998; NC, 0000-0001-6931-7821; JMC, 0000-0001-7760-7028

* Correspondence: casas@ub.edu

Abstract: Detailed geological mapping of the La Cerdanya area (Canigó unit, Eastern Pyrenees) provides new data characterizing the different structural styles exhibited by Cambrian–Lower Ordovician (Jujols Group) and Upper Ordovician successions. Their unconformable contact, related to the Sardic Phase, ranges from 0° (paraconformity) to 90° (angular discordance). The Jujols Group rocks topped by the unconformity are affected by Sardic foliation-free open folds. The pre-Sardic succession, the Sardic Unconformity and the lower part of the post-Sardic succession (Rabassa Conglomerate and Cava formations) are cut and offset by several Late Ordovician NNE–SSW-trending synsedimentary extensional faults associated with hydrothermal activity, which dramatically affected the thickness of the lower part of the Upper Ordovician succession. We relate (1) the Mid-Ordovician Sardic uplift and erosion, and (2) a Mid- to Late-Ordovician upward propagating extensional fault system bounding the outline of half-grabens, subsequently infilled by alluvial deposits, to a thermal doming event (about 475–450 Ma) that led to the uplift and stretching of the Ordovician lithosphere. Thermal doming may be caused by mafic magma underplating and responsible for the coeval calc-alkaline magmatic activity broadly developed in the Eastern Pyrenees. We discuss the similarities between the Mid-Ordovician Sardic Unconformity and other Early Paleozoic unconformities described in neighbouring areas. Finally, we suggest a geodynamic scenario in which a regional-scale thermal event was related to the opening of the Rheic Ocean that led to the drift of Avalonia from the SW European margin of Gondwana.

Received 2 April 2019; **revised** 13 June 2019; **accepted** 14 June 2019

The Pyrenees are a WNW–ESE-trending Alpine fold and thrust belt that contains pre-Variscan basement rocks of late Neoproterozoic to Carboniferous age (Fig. 1). The pre-Variscan basement forms a large strip in the core of the cordillera and provides evidence of Cadomian, Sardic and Variscan magmatic episodes (Cocherie *et al.* 2005; Castiñeiras *et al.* 2008; Casas *et al.* 2010, 2015; Navidad *et al.* 2010; Pereira *et al.* 2014; Martínez *et al.* 2016; Padel *et al.* 2018*a*), and Variscan and Alpine deformation events (Guitard 1970; Zwart 1979; Muñoz 1992). The onset and significance of the Ordovician deformation has been matter of debate since the pioneer work of Llopis Lladó (1965). After Santanach (1972), it is widely accepted that the Upper Ordovician succession unconformably overlies either the Cambrian–Lower Ordovician Jujols Group or the Ediacaran–Terreneuvian Canaveilles Group (Den Brok 1989; García-Sansegundo & Alonso 1989; Kriegsman *et al.* 1989; Poblet 1991; Muñoz & Casas 1996; García-Sansegundo *et al.* 2004; Casas & Fernández 2007). However, the origin of this unconformity has been the subject of several interpretations. Santanach (1972) in the Canigó massif and García-Sansegundo *et al.* (2004) in the Garona dome attributed the unconformity to basement tilting, related to a Late Ordovician faulting episode and subsequent erosion. In the Lys–Caillaouas massif, Den Brok (1989) and Kriegsman *et al.* (1989) proposed the existence of a pre-Variscan deformation event. A pre-Late Ordovician folding episode has been also suggested as related to the unconformity on the southern Canigó massif (Casas 2010; Casas *et al.* 2012). However, the geodynamic significance of this deformation episode is not yet well established: it is not related to metamorphism or cleavage development, although it seems to be related to uplift, widespread emersion and considerable erosion before the onset of Late Ordovician deposition (Casas 2010). As a result, the Upper Ordovician rocks onlap a palaeorelief formed by different pre-Upper Ordovician formations, ranging from the upper Neoproterozoic to the Lower Ordovician in the Central and Eastern Pyrenees (Santanach 1972; Laumonier & Guitard 1986; Cirés *et al.* 1994). This intra-Ordovician unconformity may be interpreted as equivalent to the 'Sardic Phase' described in Sardinia (Teichmüller 1931; Stille 1939), which separates the Cambrian–Ordovician from the Upper Ordovician successions (Pillola *et al.* 2008).

In this paper we present new data on the structural style exhibited by the Cambrian–Ordovician and Upper Ordovician successions of the La Cerdanya area, in the Eastern Pyrenees. The data provide clear evidence of well-expressed Ordovician deformations in the form of extensional faults and folds, the latter affecting only the Cambrian–Ordovician succession. The interpretation of these pre-Variscan deformation structures should contribute to a better understanding of the origin and meaning of the Sardic Unconformity, and thus to discussion of the geodynamic setting of this fragment of North Gondwana during Ordovician times, bracketed between the Cadomian and Variscan orogenies.

Geological setting

The study area crops out in the southern flank of the Canigó Unit, which represents an antiformal Alpine structure with exposures ranging in age from Late Neoproterozoic to Carboniferous (Fig. 1). The Alpine floor thrust of this unit is the Orri thrust (Muñoz 1992).

In the study area (Fig. 2), the Cambrian–Lower Ordovician succession consists of a thick package (*c.* 1500 m) of grey to greenish shales alternating with subsidiary centimetre-scale sandstone interbeds. This succession represents the Serdinya Formation

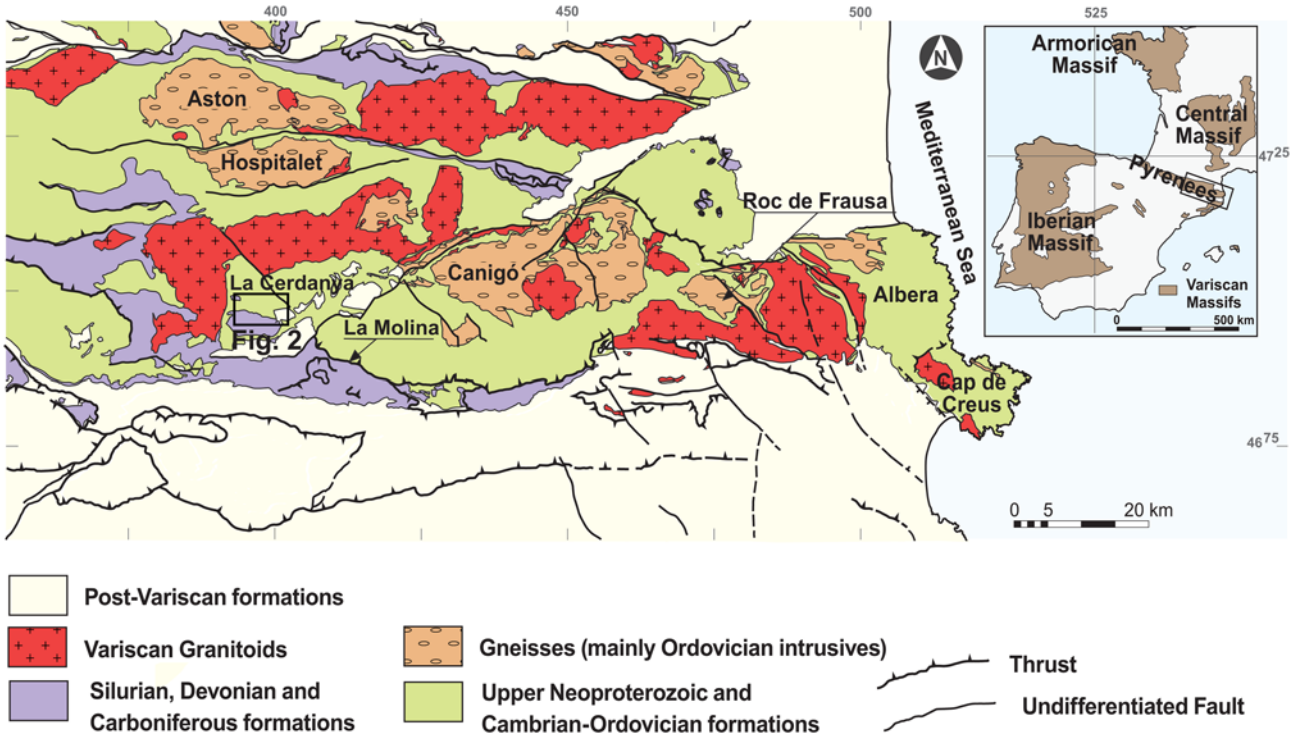

Fig. 1. Geological sketch of the Eastern Pyrenees with the location of the study area.

(Padel *et al.* 2018*b*) of the Jujols Group (Laumonier 1988). Acritarchs recovered from the uppermost part of this succession, close to the Sardic Unconformity at La Molina locality (Fig. 1) (southern slope of the Canigó massif), indicate a Furongian–earliest Ordovician age (Casas & Palacios 2012). This age is coincident with a maximum depositional age of *c.* 475 Ma for the uppermost part of the Jujols Group in the La Rabassa dome, on the basis of the youngest detrital zircon population (Margalef *et al.* 2016). To the

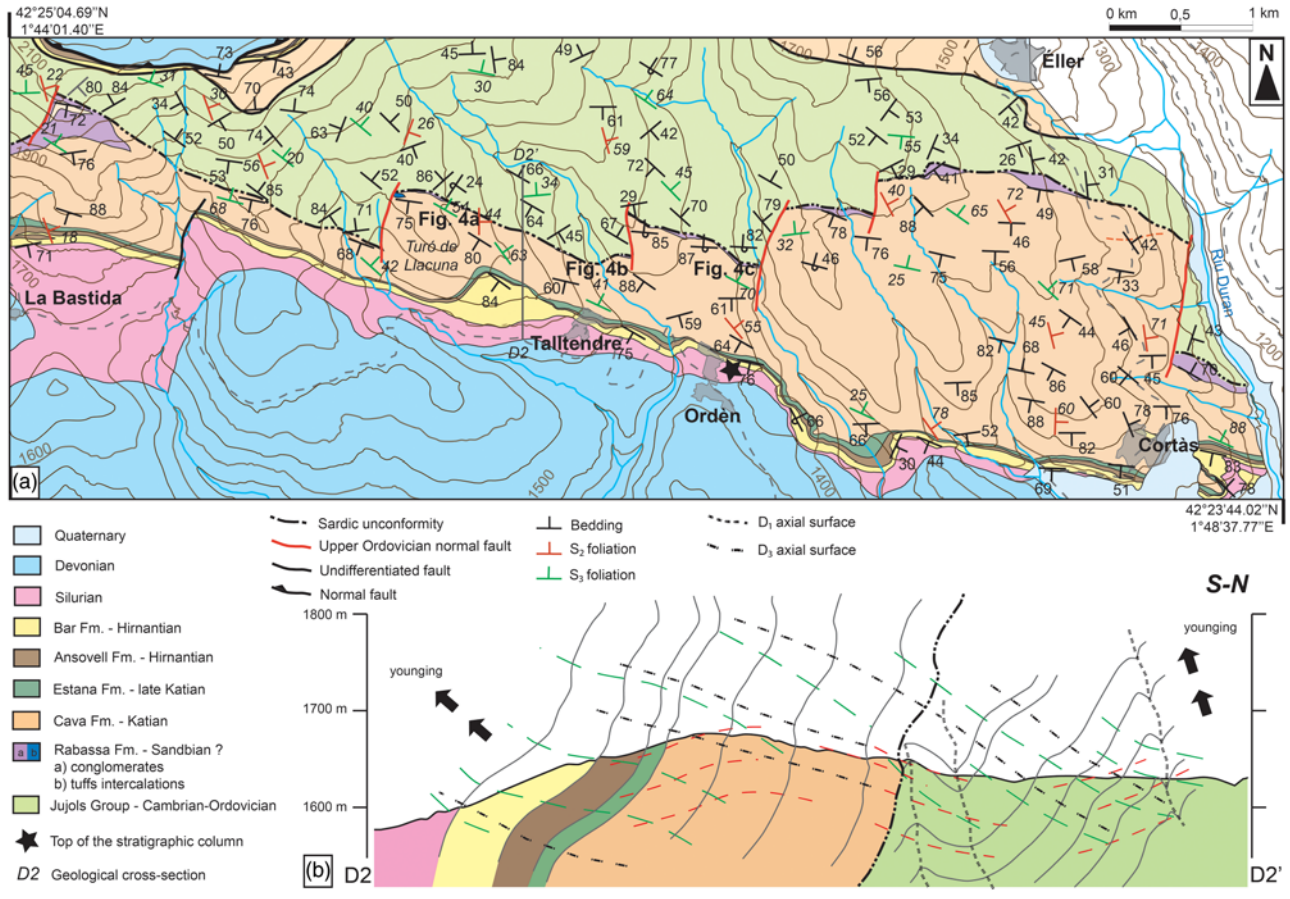

Fig. 2. (**a**) Detailed geological map of the study area. (**b**) Geological cross-section of the study area. Location shown in Figure 1.

east, in the Albera massif, metapelites and metapsammites from the uppermost part of a metasedimentary succession that can be correlated with the Jujols Group are crosscut by acidic subvolcanic dykes, which constrain its minimum depositional age to 465–472 Ma (Liesa *et al*. 2011). All these data suggest a depositional age for the uppermost part of the Jujols Group at *c*. 475 Ma. On the other hand, a *c*. 455 Ma U–Pb age for the Upper Ordovician volcanic rocks directly overlying the Sardic Unconformity has been proposed in the Eastern Pyrenees (Martí *et al*. 2014), in the Les Gavarres (455 ± 1.8 Ma, Navidad *et al*. 2010) and Les Guilleries (452 ± 4 Ma, Martínez *et al*. 2011) areas. This suggests a time gap of about 20 myr for the Sardic Phase in the Pyrenees, similar to the gap found in SW Sardinia, the type area where the original unconformity was described; there, the unconformity separates the Cambrian–Ordovician from the Upper Ordovician successions, marking a stratigraphic gap of *c*. 18 myr that includes part of the Floian (Pillola *et al*. 2008), the entire Dapingian and Darriwilian, and part of the Sandbian (Hammann 1992; Leone *et al*. 2002).

In the Eastern Pyrenees, the overlying Upper Ordovician succession (Cavet 1957; Hartevelt 1970) forms a broad fining-upward siliciclastic package that comprises some limestone key levels and displays significant thickness variations, ranging from 100 to 1000 m (Fig. 3). This succession was originally described by Hartevelt (1970), who distinguished five formations: from base to top, the Rabassa Conglomerate, Cava, Estana, Ansobell and Bar Quartzite formations. The Rabassa Conglomerate Formation, up to 100 m thick, consists of reddish-purple, polygenetic conglomerates with heterometric clasts composed of quartzite and slate derived from underlying rocks and vein quartz. The overlying Cava Formation, 0–850 m thick, is made up of conglomerates, sandstones and shales with volcanic intercalations; one coquina punctuating the shale interbeds has yielded brachiopods (*Svobodaina havliceki*, *Rostricellula* sp. and *Rafinesquina* sp.) and bryozoans, suggesting a Katian (former late Caradoc–early Ashgill) age (Hartevelt 1970; Gil-Peña *et al*. 2004; Puddu & Casas 2011). The Estana Formation, 5–200 m thick, is composed of limestone and marly limestone rich in brachiopods, bryozoans, echinoderms and conodonts of late Katian age (Gil-Peña *et al*. 2004). The top of the carbonate succession is unconformably capped by the black–grey shales of the Hirnantian Ansobell Formation, 20–320 m thick, which in turn is overlain by the Bar Quartzite, 2–20 m thick and dated as Hirnantian on the basis of its fossiliferous content (Sanz-López & Sarmiento 1995; Sanz-López *et al*. 2002; Roqué Bernal *et al*. 2017; Štorch *et al*. 2018).

In several areas of the Pyrenees, from Pierrefite to the west (Calvet *et al*. 1988) to the Ribes de Freser area to the east (Robert & Thiébaut 1976; Ayora 1980; Robert 1980; Martí *et al*. 2014) volcanic rocks have been reported interbedded with the Upper Ordovician sediments. These volcanic rocks consist of pyroclastic deposits with subsidiary lavas and subvolcanic intrusive rocks (Martí *et al*. 1986, 2019). They include andesite, rhyodacite and rhyolite, which make up a small fraction of the corresponding Ordovician succession. Additionally, the Ribes area includes a subvolcanic granitic body, the Ribes granophyre, emplaced in the lower part of the Sandbian–lower Katian succession and dated at 458 ± 3 Ma by Martínez *et al*. (2011), and several granitic orthogneissic bodies emplaced in the lower part of the pre-Variscan succession (the Núria gneiss with a protolith age of 457 ± 4 Ma, Martínez *et al*. 2011; and the Queralbs gneiss, with a protolith age of 457 ± 5 Ma, Martínez *et al*. 2011).

All these pre-Variscan rocks display a polyphase deformation linked to the Variscan deformation and a low-pressure–high-temperature metamorphism (Guitard 1970; Zwart 1979). A pervasive foliation is the main deformational structure in the medium- to high-grade metasediments and the gneissic bodies derived from Ordovician and Cadomian granitoids. This foliation ($S_{1–2}$) is a composite

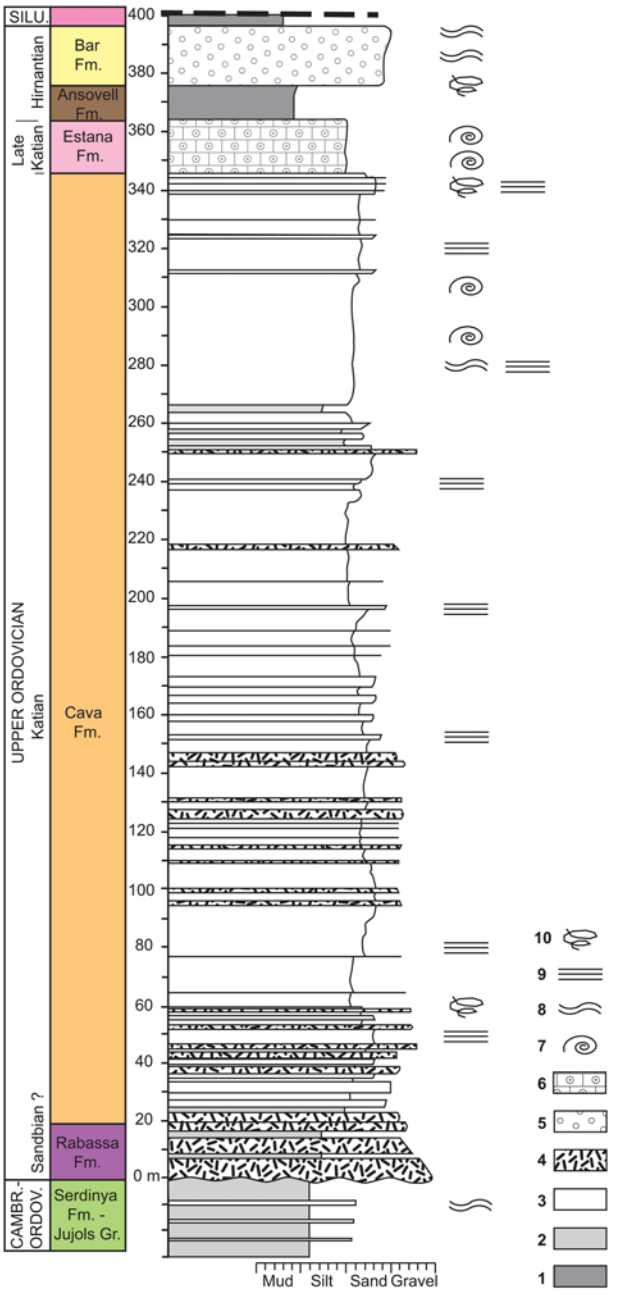

Fig. 3. Cambrian–Ordovician and Upper Ordovician stratigraphic log measured near Ordén. Location shown in Figure 2. 1, shales; 2, siltstones; 3, sandstones; 4, conglomerates; 5, quartzites; 6, marlstones; 7, fossils; 8, ripples; 9, plane lamination; 10, bioturbation.

fabric developed prior to or coeval with the Variscan regional metamorphism, being associated with an east–west- to NE–SW-oriented stretching lineation. $S_{1–2}$ is folded by later east–west to NW–SE upright folds, forming the mesostructure that depicts the Aston–Hospitalet, Canigó, Roc de Frausa and Albera gneissic domes along the backbone of the chain. According to Clariana & García-Sansegundo (2009) and García-Sansegundo *et al*. (2011), in the Garona dome and the Pallaresa massif, S_1 is a slaty cleavage developed only in the Cambro-Ordovician succession and not related to folds, and S_2 is associated with north-verging recumbent folds formed at Carboniferous time. In the eastern part of Pallaresa massif (central Pyrenees), south of Aston massif and north of the Tor–Casamanya syncline, Clariana & García-Sansegundo (2009) and Clariana *et al*. (2009) described a subvertical S_3 crenulation cleavage, axial plane of east–west-trending upright folds, deforming $S_{1–2}$. This S_3 becomes the main cleavage in the Pallaresa

massif, the Tor–Casamanya and Llavorsí synclines, and the Rabassa and Orri domes (Speksnijder 1986; Poblet 1991; Clariana & García-Sansegundo 2009; Margalef & Casas 2016). S_3 exhibits a fan-like attitude close to the southern contact with the post-Variscan rocks owing to the Alpine rotations linked to thrust sheet stacking (Muñoz 1992) The Devonian and the Carboniferous Culm rocks of the study area exhibit a well-developed cleavage that can be correlated with this S_3 mesostructure (Martín-Closas *et al*. 2018). Additionally, to the south of the study area, several thrust sheets involving Devonian and Carboniferous rocks can be observed (Hartevelt 1970; Domingo *et al*. 1988; Casas *et al*. 1989; Martín-Closas *et al*. 2018). Their basal detachment is located at the base of the Silurian black shales; although most of the thrusts are south-directed, some north-directed thrusts can be observed. In the southern limb of the D_3 megastructures, such as the Rabassa dome, thrusts and the lower detachment dip to the south. In turn, thrusts cut the fold-related cleavage. Thus, thrust development in the post-Silurian rocks must have been broadly coeval with the onset of D_3 folds in the low-grade pre-Silurian rocks (Martín-Closas *et al*. 2018). In the Eastern and Central Pyrenees this deformation episode occurred at 330–319 Ma, according to the age of synorogenic Carboniferous Culm deposits (decribed as latest Visean to Serpukhovian by Sanz-López *et al*. 2006; Namurian by Delvolvé 1981; Delvolvé & Perret 1989; Delvolvé *et al*. 1993; Martín-Closas *et al*. 2018). This age is coincident with the maximum deposition ages of 336 ± 2 and 356 ± 9 Ma obtained from U–Pb dating on detrital zircon from Carboniferous rocks (Martínez *et al*. 2016). A minimum age, in turn, is provided by the age of the crosscutting Andorra–Montlluís granodiorite, dated as 305 ± 3 Ma by Romer & Soler (1995), 305 ± 5 Ma by Maurel *et al*. (2004) and 301.5 ± 1.9 Ma by Pereira *et al*. (2014).

Structure

We made a detailed (1:5000 scale) geological map of the Talltendre area and measured a stratigraphic log of the Upper Ordovician succession cropping out along the road near Ordén village (Fig. 2). This study area constitutes the WNW–ESE-oriented vertical to subvertical southern flank of the Canigó antiform that joins southwards with a synformal megastructure, where Silurian, Devonian and pre-Variscan Carboniferous successions are extensively exposed (Fig. 1). Together with this subvertical arrangement, excellent outcrop conditions allow the recognition of the Sardic Unconformity, a system of extensional faults and several deformation mesostructures chronologically subdivided into three episodes. To better visualize and reconstruct the fault geometry, cartographic data were integrated into a 3D environment (MOVE software), which also facilitated the geometric analysis of the Sardic Unconformity.

Sardic Unconformity

The Cambrian–Lower Ordovician outcrops are onlapped, at angles ranging from a few degrees to 90°, by both the Rabassa Conglomerate and the Cava formations (Figs 2–4). The angular discordance separates the Upper Ordovician succession on its southern side from underlying Cambrian–Ordovician strata on its northern side. This contact shows a planar to weakly undulated, locally irregular surface capping the Cambrian–Ordovician strata, and can be considered as an unconformity laterally ranging from a paraconformity to an angular discordance. The unconformity exhibits a roughly WNW–ESE trend (194/75), although locally the orientation ranges from east–west to NW–SE (Fig. 5a and b).

The Upper Ordovician succession shows a NW–SE trend of vertical to subvertical strata. Upper Ordovician beds may be either overturned or strongly dipping northwards or dip eastwards in the eastern part of the study area (Fig. 6). In contrast, Cambrian–Ordovician bedding surfaces exhibit a wide range of orientations (see below).

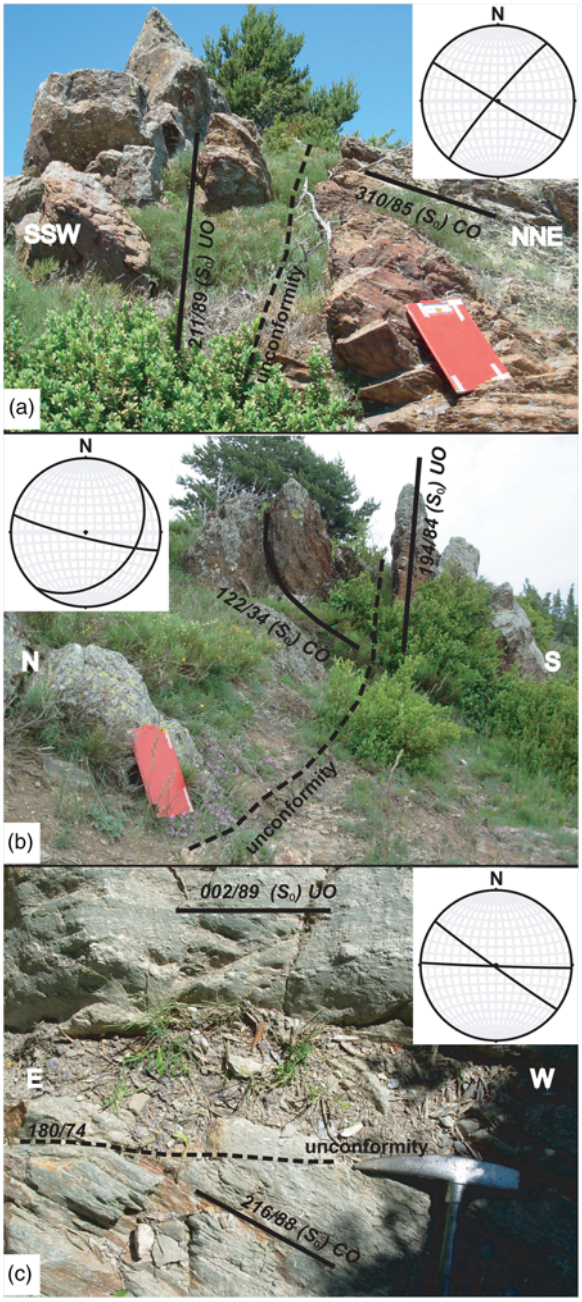

Fig. 4. Examples of the Upper Ordovician unconformity in the study area. UO, Upper Ordovician; CO, Cambrian–Ordovician. Angular unconformity is 78° (**a**), 69° (**b**) and 34° (**c**), respectively. Location shown in Figure 2.

Polyphase folding

The most visible mesostructures of the Cambrian–Ordovician and Upper Ordovician rocks are bedding surfaces. Field data show that bedding surfaces exhibit different orientations (Fig. 7). Orientation of the Cambrian–Ordovician succession presents a marked dispersion and dip values ranging from subvertical to subhorizontal (Fig. 7a). In contrast, the Upper Ordovician bedding poles exhibit a more regular NW–SE trend (Fig. 7b). As we will discuss below, the marked dispersion of the bedding poles in Cambrian–Ordovician strata suggests the superposition of several fold systems. In the

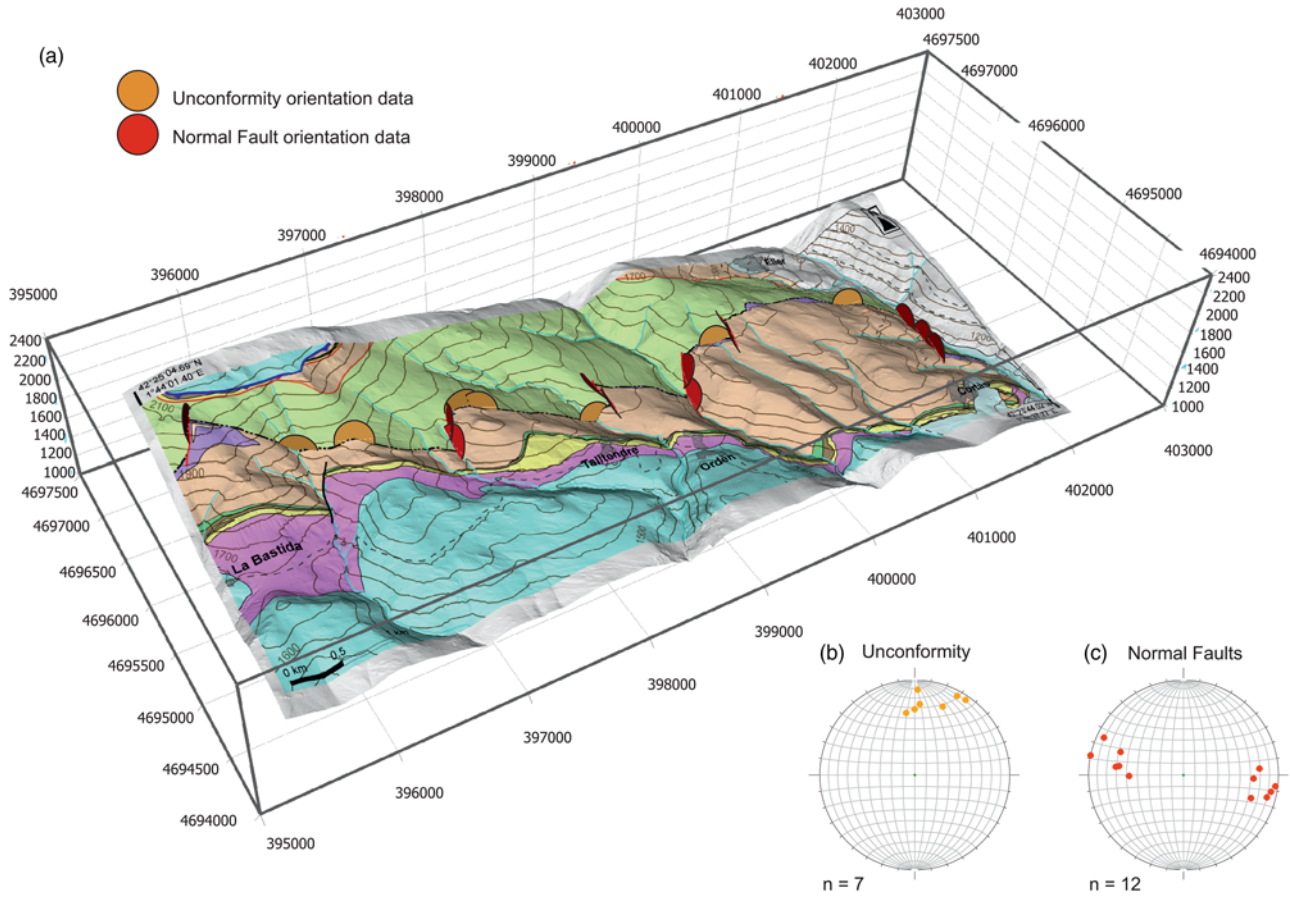

Fig. 5. (**a**) A 3D representation of the study area with estimation of the orientation of the unconformity surface and the extensional faults; (**b**) equal area lower hemisphere stereoplot of the unconformity; (**c**) equal area lower hemisphere stereoplot of extensional faults from cartographic data using MOVE software.

description that follows, L_1 and L_3 refer to different fold axes, and L_{0-2} and L_{0-3} to bedding–cleavage intersection lineations.

D_1 structures

The existence of D_1 folds can be inferred from the arrangement of bedding surfaces at outcrop and different map scales, and from the pattern displayed by D_3 linear elements, intersection lineations and fold axes in the Cambrian–Ordovician sequence. That is, D_3 folds developed over initially non-horizontal surfaces and D_1 folds control the geometry of D_3 mesoscale folds (e.g. Turner & Weiss 1963, p. 130; Mey 1967, p. 194; Ramsay 1967, p. 539). The existence of previous D_1 folds may also explain the distribution of D_2 mesostructures in the Cambrian–Ordovician rocks. Concerning the initial orientation of D_1 fold axes, the map analysis suggests the following: (1) despite dispersion, Cambrian–Ordovician bedding exhibits two maxima in orientations at WNW–ESE and NE–SW (Fig. 7a); (2) WNW–ESE orientations predominate over NE–SW ones; (3) especially interesting are the outcrops in which the Cambrian–Ordovician beds are NE–SW oriented, and are both vertical and normal to the unconformity horizon (Fig. 8a). In such a situation, after unfolding the Upper Ordovician sequence using a WNW–ESE horizontal rotational axis parallel to the Upper Ordovician unconformity, the NE–SW vertical Cambrian–Ordovician beds still remain vertical and with a similar NE–SW orientation (Fig. 8b). This observation suggests that D_1 fold axes presented an initial subhorizontal NE–SW orientation, with a short limb oriented NE–SW subvertical or strongly dipping, and a long limb subhorizontal or gently dipping towards the SE or NW. However, the effect of superimposed D_3 folds precludes assessment of whether D_1 folds have a NW or SE vergence. Analysis of the areas where subvertical WNW–ESE and NE–SW orientations coexist allows the estimation of 10–100 m scale dimensions of D_1 folds (Fig. 9). It should be noted that there is no evidence of an axial planar cleavage development or other mesostructures related to D_1 fold formation.

D_2 structures

A not very pervasive cleavage (S_2) is observable at outcrop scale in the Cambrian–Ordovician rocks, whereas S_2 is well developed in the fine fraction of the Upper Ordovician, being deflected by coarser deposits (such as conglomerates and sandstones), where it develops irregularly. S_2 surfaces generally dip 20–80° towards the east or ENE (Fig. 7c and d) and are commonly deformed by D_3 folds. In the Upper Ordovician rocks, S_2 exhibits dispersion along a north–south-oriented girdle (Fig. 7d). Neither folds nor other mesostructures related to this event have been clearly identified in the field. As for D_3 linear mesostructures, L_{0-2} exhibits a wider dispersion in the pre- than in the post-unconformity rocks (Fig. 7c and d).

D_3 structures

A north-dipping S_3 cleavage is the dominant deformation structure recognizable in the exposures of the study area. S_3 cleavage is observable from outcrop down to microscopic scale, and is correlated with the dominant cleavage observed in the Silurian and Devonian rocks cropping out to the south of the area. S_3 is oriented NW–SE with variable dips towards the NE. In the eastern area, it is subvertical or strongly dipping, whereas in the western sector it dips gently to moderately towards the NE (Fig. 2).

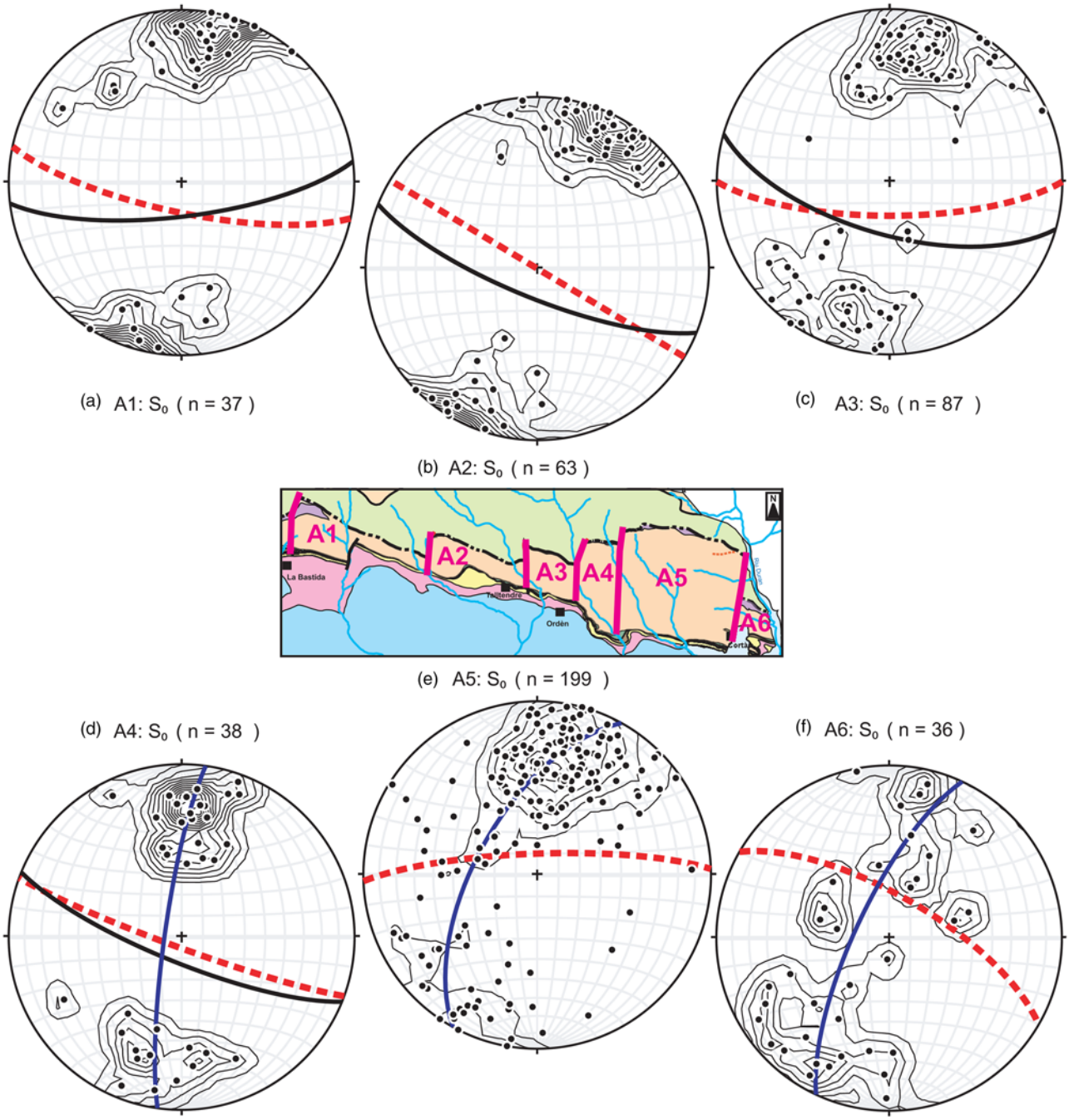

Fig. 6. (**a**–**f**) Equal area lower hemisphere stereoplots of the disposition of the Upper Ordovician bedding surfaces in the six domains (A1, A2, A3, A4, A5 and A6) defined from west to east between the extensional faults. The Upper Ordovician unconformity surface is shown (red dashed line) in the stereoplots together with the average bedding planes (black lines) in (**a**) to (**d**), or the best-fit girdle (blue line) in (**e**) and (**f**). *n* indicates the number of measurements.

S_3 is related to D_3 folds affecting both the pre- and post-unconformity rocks. As for the S_3 surfaces, the D_3 fold axial surfaces are generally gently dipping (10–45°) towards the north or NE in the western part of the study area, whereas to the east they have the same orientation, although steeply dipping or subvertical. D_3 folds are SW vergent, open to tight and generally 1–100 m in scale with centimetre-scale minor folds (second- or third-order folds) on the limbs of the main folds. D_3 folds show mildly curved hinges that generally developed harmonic folding, especially in the Upper Ordovician rocks. D_3 fold axes exhibit different orientations in the pre- and post-unconformity rocks (Fig. 7e and f). In the Upper Ordovician succession, L_3 axes and $L_{0–3}$ intersection lineations are grouped forming a maximum with a moderate plunge to the WNW or ESE (Fig. 7f). The bedding–cleavage relationship indicates that the study area constitutes the southern flank of a south-facing first-order D_3 fold oriented WNW–ESE (Fig. 2b).

In contrast, the minor L_3 axes and $L_{0–3}$ intersection lineations of the Cambro-Ordovician rocks display a wide range of orientations. $L_{0–3}$ plunge ranges from subhorizontal to 45° (Fig. 7e), and no simple distribution pattern may be deduced from map analysis (Fig. 2). If $L_{0–3}$ and L_3 are plotted together, they are mainly distributed along a great circle coincident with the S_3 average plane, although two maxima. oriented *c.* 20°–40°/000 and 25°/115, can be envisaged with predominance of low plunge values (Fig. 7e).

Extensional faults and tectonically induced sedimentation

At the map scale, several extensional faults affecting the Cambrian–Ordovician strata, the Sardic Unconformity and the lowermost part

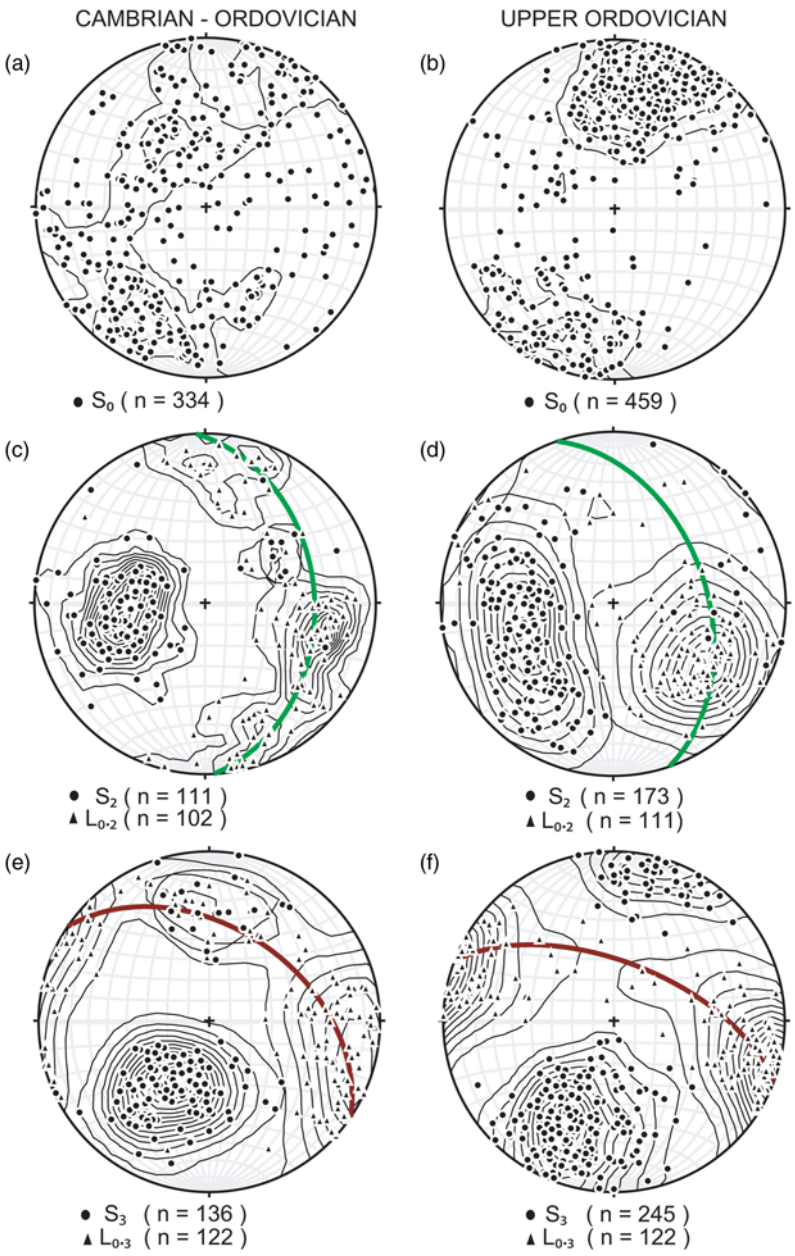

Fig. 7. Equal area lower hemisphere stereoplots of bedding (S_0), D_2-related mesostructures (S_2 cleavage and L_{0-2} intersection lineation), and D_3-related mesostructures (S_3 cleavage and L_{0-3} intersection lineation) from the Cambrian–Ordovician (**a**, **c**, **e**) and Upper Ordovician successions (**b**, **d**, **f**) in the study area. In (**c**) and (**d**), the L_{0-2} intersection lineations are distributed along a great circle that is coincident with the S_2 average plane (in green), and in (**e**) and (**f**) the L_{0-3} intersection lineations are distributed along a great circle that is coincident with the S_3 average plane (in red). *n* indicates the number of measurements.

of the Upper Ordovician succession can be recognized (Figs 2–5) (Casas & Fernández 2007; Casas 2010). At present, the faults trend broadly north–south to NNE–SSW, and their hanging wall generally appears to be the eastern block, despite the presence of some antithetic faults (Fig. 2). The faults are steep, domino-style and their surface dips range from 48 to 90° towards the WNW and ESE. This variation in orientation together with the changes in strike along a fault plane detected in 3D analysis suggest that the faults are slightly folded around a subhorizontal NNE–SSW axis (189/00) (Fig. 5c). Maximum throws vary between 200 and 750 m. The NNE–SSW fault orientation could have prevented the inversion of the faults during the Variscan and Alpine deformation events, but the orientation did not prevent their rotation following horizontal east–west axes during the former events. The faults are associated with synsedimentary hydrothermal activity, represented by dense networks of quartz veins encased in the uppermost part of the Jujols Group and subparallel to the trace of the extensional faults. These served as the source for huge amounts of vein quartz clasts that form the Rabassa Conglomerate (Fig. 10a and b).

The displacement of some of these faults diminishes progressively up-section and vanishes in the upper part of the Upper Ordovician rocks, especially in the lower part of the Cava Formation, indicating that the faults became inactive before deposition of the overlying Estana strata (Fig. 2). Thus, the Rabassa Conglomerate and the lower part of the Cava Formation are syntectonic sediments, whereas the upper part of the Cava Formation and the overlying Estana, Ansobell and Bar formations are post-tectonic sediments. As a result, the whole Upper Ordovician succession shows sharp changes in total thickness ranging between 190 and 900 m, with a general increase from west to east. Perpendicular to these faults, the Rabassa Conglomerate Formation displays sharp changes in thickness (from 0 to 100 m) and facies associations. Deposits of the Rabassa Conglomerate Formation neighbouring the extensional faults consist of chaotic breccias ranging both laterally and vertically to matrix- to clast-supported conglomerates (Fig. 11d and e). These include massive to weakly stratified, unsorted, pebble-dominated deposits of sandstone, shale, vein quartz and mafic phenocrysts (Fig. 11a and b). Contacts are commonly scoured and grading is both normal and inverse. Breccias and matrix-supported conglomerates show either chaotic or amalgamated patterns; they interfinger laterally with packages of clast-supported conglomerates and pebbly sandstones that pinch out or change abruptly, both laterally and vertically, into sandstone–shale alternations (Cava Formation). Clast-supported conglomerates show massive to weakly imbricated pebbles and cobbles (Fig. 11f), which

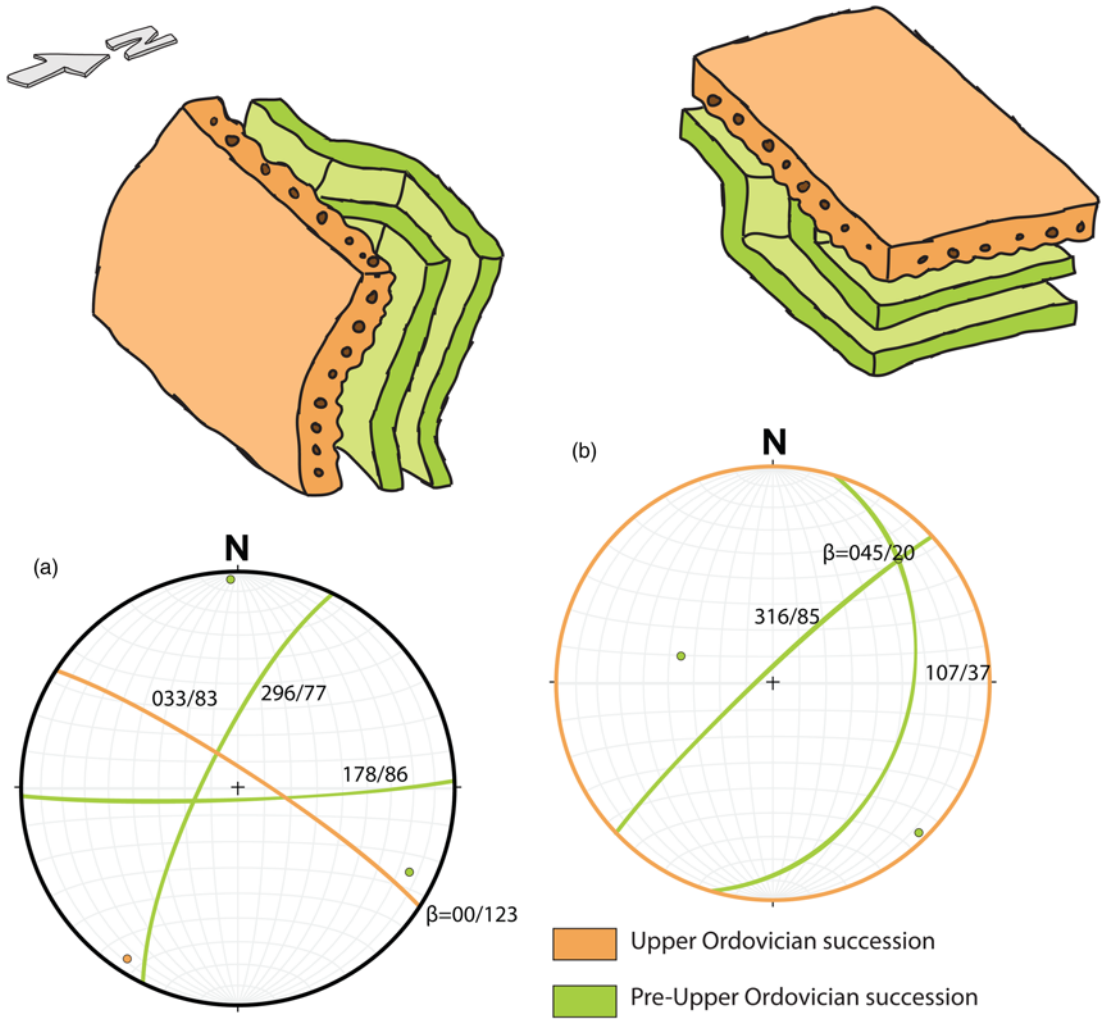

Fig. 8. (**a**) Sketch and equal area lower hemisphere stereoplot of the Upper Ordovician unconformity (033/83) overlying Cambrian–Ordovician subvertical beds (296/77 and 178/86); (**b**) disposition of the Cambrian–Ordovician beds after a *c.* 90° rotation about a horizontal axis parallel to the unconformity (00/123).

are subrounded, moderately sorted and grade upsection and laterally into litharenites; the latter display centimetre- to decimetre-scale trough and low-angle cross-stratified sets alternating with shales (Fig. 11g), which are irregularly burrowed. Lithostratigraphically, the occurrence of shale interbeds marks the base of the Cava Formation. Three facies associations can be recognized, as follows.

(1) Breccias and matrix-supported conglomerates are interpreted as having undergone different types of downslope transport by basal sliding of plastic to semi-rigid sediment masses that included contemporaneous hydrothermal dykes of quartz (Fig. 11e). Amalgamation of debris-flow deposits indicates the presence of neighbouring slopes close to synsedimentary extensional faults.
(2) Packages of clast-supported conglomerates and pebbly sandstones represent in-channel gravel bars that graded into straight to sinuous crested bedforms in shallow, braided systems. During high-discharge events, sediments were reworked and accumulated as channelized conglomerates.
(3) Finally, sandstone–shale alternations reflect the influence of marine shoreface-to-offshore conditions with local development of burrowing by soft-bodied metazoans.

It should be noted that as the Upper Ordovician unconformity is cut by these normal faults, significant pre-Upper Ordovician erosive processes took place preceding the normal faulting event.

Synsedimentary faults are planar, either non-rotational or with small amounts of rotation affecting the beds in the hanging wall. The geographical distribution of these normal faults allows subdivision of the Upper Ordovician succession into six domains (Fig. 6). In the four western domains (A_1–A_4), the Upper Ordovician bedding planes exhibit an east–west- or NW–SE-trending orientation, ranging from N100E to N120E with subvertical or strongly dipping attitude. In domain A_5, the Upper Ordovician bedding planes exhibit a wider range of dipping values, with bedding poles distributed in a NE–SW girdle, as a result of a 119/28-oriented fold axis (Fig. 6). In the easternmost domain A_6, the Upper Ordovician bedding planes show a roughly NW–SE trend with variable dip as a result of a 115/16-oriented fold axis. The divergence between the beds next to the hanging wall varies between a minimum value of 10° (A_5) and a maximum of 24° (A_4), with a main value of 18° (A_2) and 20° (A_3), which allows us to infer a *c.* 20° fault rotation.

It is difficult to identify the faults and to recognize an eventual detachment horizon in the Cambrian–Ordovician rocks. This and the steep arrangement of the fault surfaces preclude an estimate of the amount of extension linked to fault movements. In any case, the small amount of bed rotation in the hanging wall of the faults, *c.* 20°, indicates a small amount of east–west extension.

Discussion

Structure: age and significance of folds D_1, D_2 and D_3

D_1 folds affecting the Cambrian–Ordovician succession are sealed by Upper Ordovician strata. Thus, it is assumed that the episode D_1 is earlier than the successions deposited above. An Early–Mid-

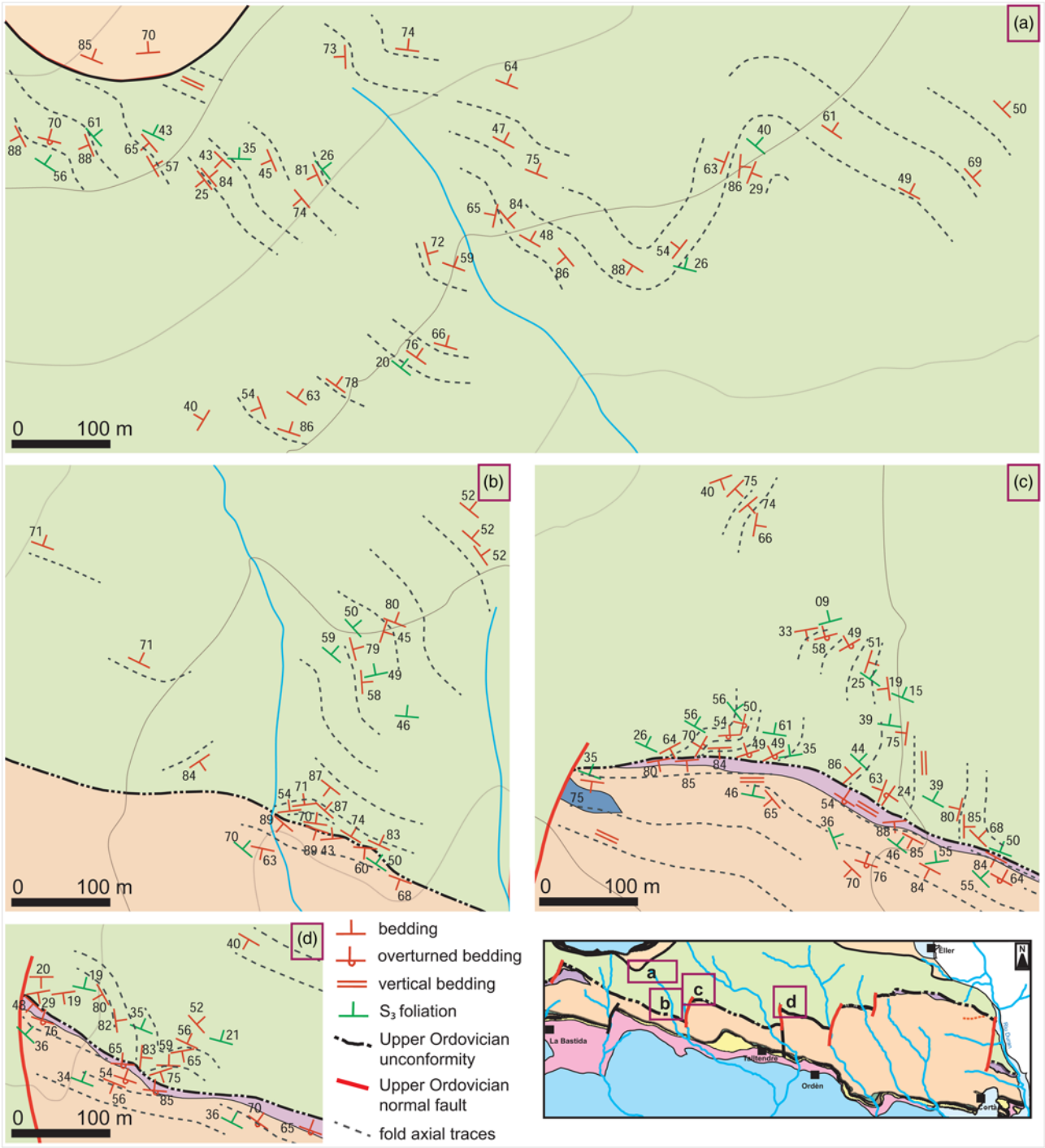

Fig. 9. (**a**–**d**) Detailed sketches showing the disposition of S_0 bedding planes in the Cambrian–Ordovician rocks. Inset map shows location of the different zones.

Ordovician age can be proposed for this folding event. Moreover, D_1 fold axes are parallel to subparallel to the direction of the Late Ordovician extensional faults. We noted the absence of microscale D_1 folds and the lack of either associated cleavage or metamorphism. We interpret that D_1 folds can form at the hanging-wall blocks of extensional faults. Folds related to extensional faults have been extensively described, caused by slip on nonplanar normal faults (Xiao & Suppe 1992), on faults with ramp–flat–ramp fault geometry (Rotevatn & Jackson 2014), on a localized zone of shortening between two fault trends (Abu Sharib *et al*. 2017) or as fault-propagation folds (Sharp *et al*. 2000). From these possibilities, we favour that D_1 folds formed as fault-propagation folds of upward-propagating normal faults. In this situation, vertical or steeply dipping pre-Sardic beds in the hanging wall near the fault surface are common as propagation of the fault tip to the surface results in breaching of a previous fold (Sharp *et al*. 2000). Therefore, two possibilities can be envisaged: either the fold formation is linked to pre-Sardic (Early–Mid-Ordovician) movements of the mapped extensional faults, or they resulted from the movement of other extensional faults, not detected in the area because of the monotonous character of the Cambrian–Ordovician succession and the lack of cartographic marker beds. According to the first possibility, post-Sardic (Late Ordovician) upward fault propagation should lead to normal faults cutting previous folds, the topographic surface and the unconformity, and post-Sardic sediments filling the hanging walls thinning away from fault surfaces (Fig. 2). According

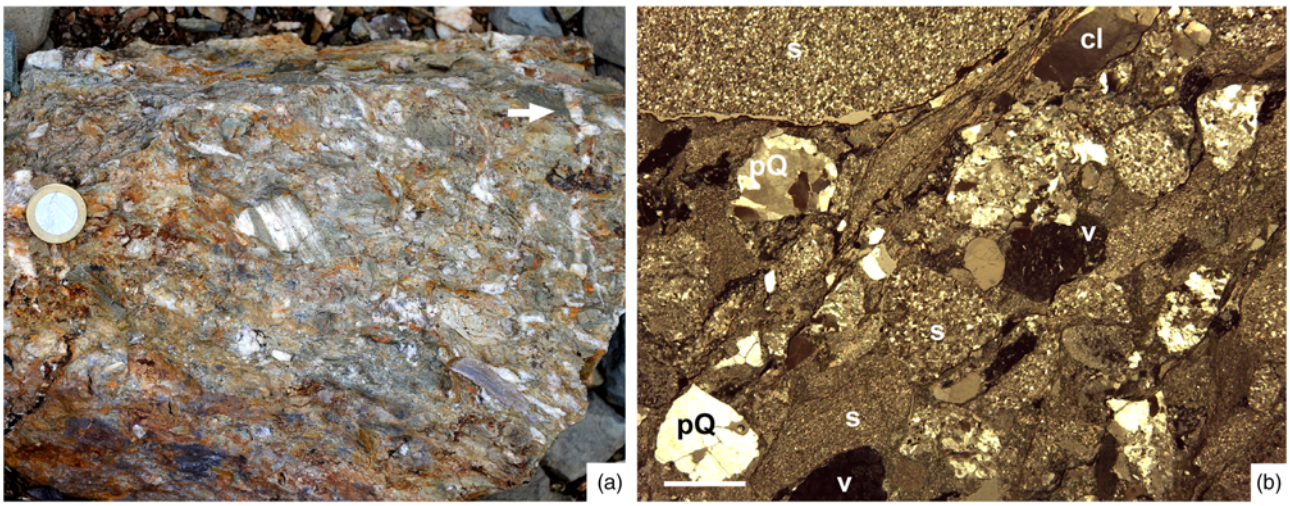

Fig. 10. Breccia levels of the Rabassa Conglomerate Formation neighbouring synsedimentary normal faults at La Molina. (**a**) Clast-supported angular cobbles of sandstone and shale (derived from the underlying Jujols Group) mixed with hydrothermal quartz clasts sourced from synsedimentary veins (arrowed). (**b**) Thin-section photomicrograph of previous sample showing reworked hydrothermal polycrystalline quartz (pQ), siltstone (s), claystone (cl) and mafic phenocryst (v) clasts embedded in an unsorted sandy-to-clayey matrix; scale represents 1 mm.

to the second option, the faults would not reach the topographic surface, and normal faults would remain as blind faults in the pre-Sardic sequence. In any case, the Upper Ordovician unconformity changes from a paraconformity in the long limb of the D_1 folds or in the footwall of the faults, to an angular unconformity in the hinge zone or in the vertical limbs of the D_1 folds in the hanging wall of the faults (Fig. 9). As stated before, the outcrop conditions, together with the monotonous character and the lack of cartographic key levels in the pre-Sardic sequence, make it difficult to identify these blind faults as well as the continuation in the pre-unconformity sequence of the normal faults cutting the unconformity. The situation described above argues against a contractional origin for the Ordovician (Sardic) folds in the Eastern Pyrenees as previously proposed by Casas (2010) and Casas *et al*. (2012).

Equivalent D_1 pre-main cleavage folds were described by Casas (2010) to the north of the Canigó unit, in the El Conflent area, and further to the east, in the La Molina area. The former exhibit a similar north–south direction with axes strongly dipping to the north, whereas in the La Molina area, pre-main cleavage folds are mainly oriented NNW–SSE. As in the study area, the combination of pre-main cleavage folds and syn-foliation folds with variable orientations gives rise to a complex disposition of bedding planes (Casas 2010).

The interpretation of the deformation episode D_2 is more difficult owing to the lack of related mesostructures. It could be correlated with the S_2 cleavage associated with north-verging recumbent folds described in the Garona and Pallaresa domes by Clariana & García-Sansegundo (2009) and Clariana *et al*. (2009). However, the lack of related folds in the study area makes this correlation speculative. In any case, the age of this deformation should be post-Ordovician (Variscan) because it affects both the pre- and post-unconformity deposits.

The main foliation (S_3) recognized in the study area can be correlated with the pervasive axial plane crenulation cleavage (S_3) of east–west-trending upright folds, which represents the main cleavage preserved in the Pallaresa massif, the Tor–Casamanya and Llavorsí synclines, and the Rabassa and Orri domes (Speksnijder 1986; Poblet 1991; Clariana & García-Sansegundo 2009; Margalef & Casas 2016). It should be noted that the Cambrian–Ordovician succession of these Pyrenean massifs shares a common structural arrangement: a regional crenulation cleavage, regularly oriented and dipping to the north, associated with intersection lineations and minor fold axes displaying a significant dispersion. This arrangement, described, for example, in the Rabassa dome (Poblet 1991; Capellà & Bou 1997), the Massana anticline (Hartevelt 1970; Poblet 1991; Casas *et al*. 1998), the Orri dome (Hartevelt 1970; Speksnijder 1986; Poblet 1991) and the Lys–Caillaouas massif (Den Brok 1989), among others, has been attributed to the presence of pre-foliation (pre-D_3) deformations.

Origin of the Sardic Unconformity, extensional faults and D_1 folds

The angular unconformity described above represents the prolongation of those described westwards by Casas & Fernández (2007), and in the La Molina area by Santanach (1972) and Casas (2010). The unconformity can be attributed to the doming, tilting and erosion of a pre-Sardic succession, which preceded the deposition of the Upper Ordovician conglomerates and sandstones (Santanach 1972; García-Sansegundo *et al*. 2004). Doming, tilting and truncation of Cambrian–Ordovician strata suggest relative uplift, perhaps associated with a fall in the eustatic sea-level.

The Sardic Unconformity was affected by a Late Ordovician extensional pulsation, which was responsible for the movement of the NNE–SSW-oriented normal faults that led to the contemporaneous opening of grabens and half-grabens. These were infilled with the alluvial, fluvial and volcano-sedimentary deposits of the Upper Ordovician Rabassa Conglomerate and Cava formations, which also reflected a significant and stepwise hydrothermal activity. Simultaneously, a Late Ordovician magmatic pulse yielded a varied suite of magmatic rocks: small granitic bodies are emplaced in the pre-unconformity strata of the Canigó massif and form the protoliths of the Cadí, Casemí, Núria and Canigó G-1 type gneisses (*c.* 457–446 Ma, Casas *et al*. 2010; Martínez *et al*. 2011; Navidad *et al*. 2018), together with metre-scale thick bodies of metadiorite (*c.* 453 Ma, Casas *et al*. 2010). Coeval calc-alkaline volcanic rocks (ignimbrites, andesites and volcaniclastic rocks) are interbedded in the Upper Ordovician succession of the Ribes de Freser area (Robert & Thiébaut 1976; Ayora 1980; Robert 1980; Martí *et al*. 1986, 2019); a granitic body at Ribes with granophyric texture, dated at *c.* 458 Ma by Martínez *et al*. (2011), intrudes at the base of the Upper Ordovician succession. Metre-scale rhyodacitic to dacitic subvolcanic sills intercalated within the pre-unconformity succession close to the base of the Upper Ordovician have also yielded Late Ordovician ages in the La Pallaresa dome (*c.* 453 Ma, Clariana *et al*. 2018).

Previously, a Floian–Dapingian magmatic pulse, coeval with the uplift and subsequent extensional activity related to D_1 fold

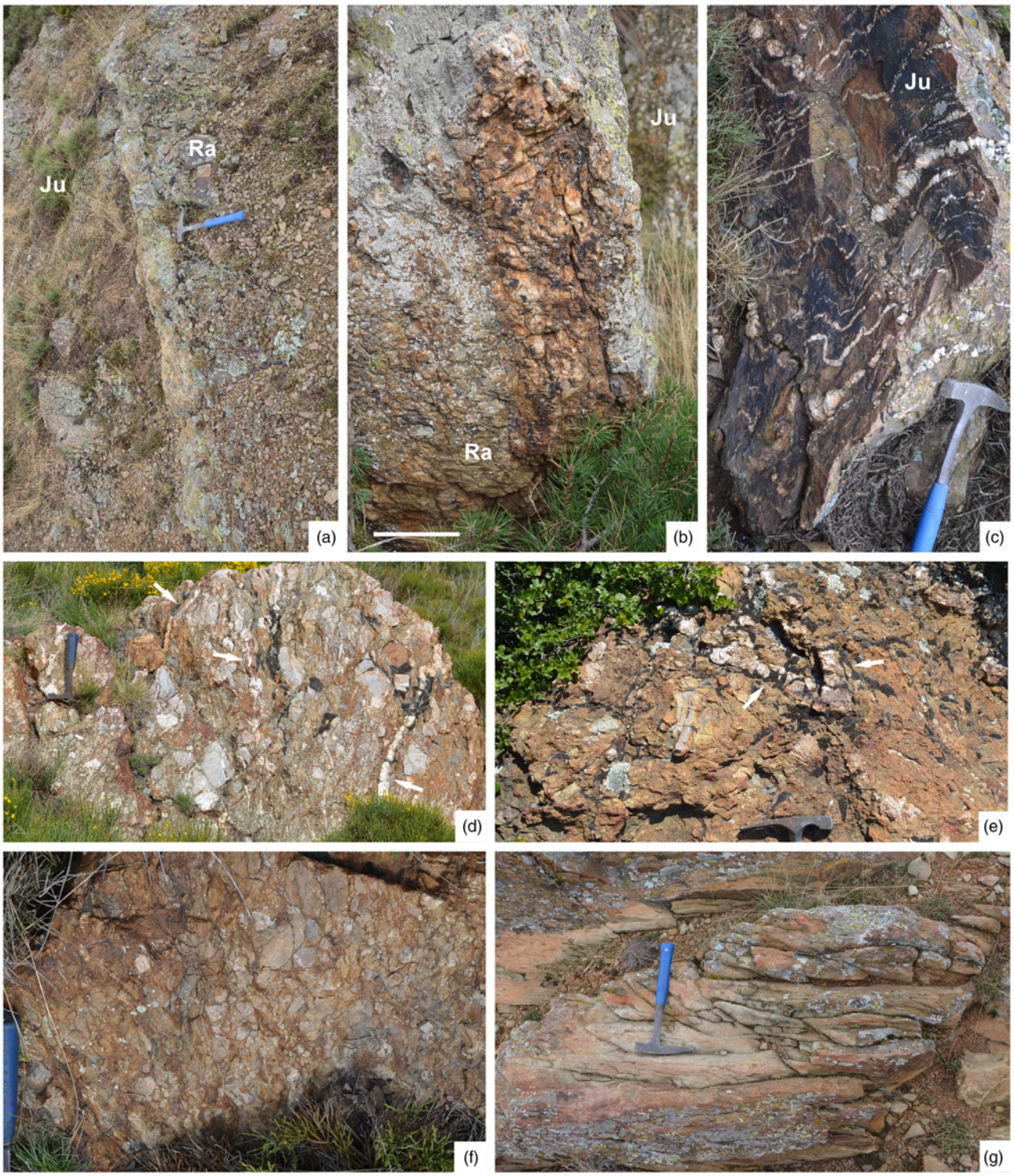

Fig. 11. (**a**) Sardic angular discordance separating the Jujols shales (Ju; left) from the Rabassa breccia deposits (Ra; right) at Talltendre. (**b**) Subvertical dyke of hydrothermal quartz representing a synsedimentary fault marking the Jujols–Rabassa contact at La Molina; scale represents 10 cm. (**c**) Folded dykes of hydrothermal quartz encased in the Jujols shale neighbouring a synsedimentary normal fault that separates it from the Rabassa Formation at Talltendre. (**d**) Basal part of the Rabassa Formation close to the unconformity of (**a**), showing a breccia of clast-supported polymictic blocks rich in shales and sandstones of the underlying Jujols Group and hydrothermal quartz clasts sourced from the dykes (arrowed) that crosscut the outcrop at Talltendre. (**e**) Matrix-supported breccia of the Rabassa Formation with folded dykes of hydrothermal quartz (arrowed) at Talltendre. (**f**) Typical clast-supported polymictic conglomerate of the Rabassa Formation at La Molina. (**g**) Amalgamated trough cross-stratified sets of a lenticular sandstone package, up to 2.2 m thick and with 8 m of lateral continuity, embedded in shales; lower part of Cava Formation at Talltendre.

formation, took place. This pulse gave rise to the intrusion of voluminous peraluminous granites, about 500–3000 m thick and emplaced into the pre-unconformity strata. They form the protoliths of the large laccolith-shaped, orthogneissic bodies that punctuate the backbone of the Pyrenees, from west to east, the Aston (*c.* 470–467 Ma, Denèle *et al*. 2009; Mezger & Gerdes 2016), Hospitalet (*c.* 472 Ma, Denèle *et al*. 2009), Canigó (*c.* 472–462 Ma, Cocherie *et al*. 2005; Navidad *et al*. 2018), Roc de Frausa (*c.* 477–476 Ma, Cocherie *et al*. 2005; Castiñeiras *et al*. 2008) and Albera (*c.* 470 Ma, Liesa *et al*. 2011) massifs. As a whole, the Ordovician magmatism

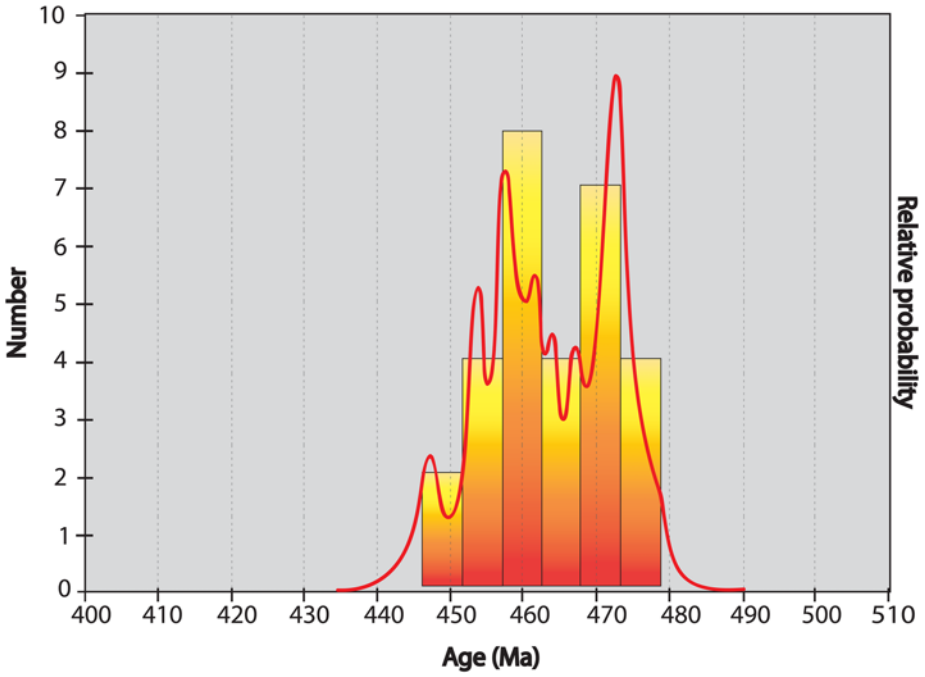

Fig. 12. Relative probability plot of the geochronological ages (U–Pb on zircon) of the Ordovician magmatism of the Pyrenees. Data after Deloule *et al.* (2002), Cocherie *et al.* (2005), Castiñeiras *et al.* (2008), Denèle *et al.* (2009), Casas *et al.* (2010), Liesa *et al.* (2011), Martínez *et al.* (2011), Mezger & Gerdes (2016), Navidad *et al.* (2018) and Liesa *et al.* (unpublished data); $n = 25$.

in the Pyrenees lasted about 30 myr, from *c.* 477 to 446 Ma, a time span contemporaneous with the Ordovician deformations described above (Fig. 12).

Taken altogether, uplift, denudation, extensional tectonics and magmatic activity may be related to a thermal doming caused by the underplating of hot mafic magmas (Fig. 13). This scenario has been

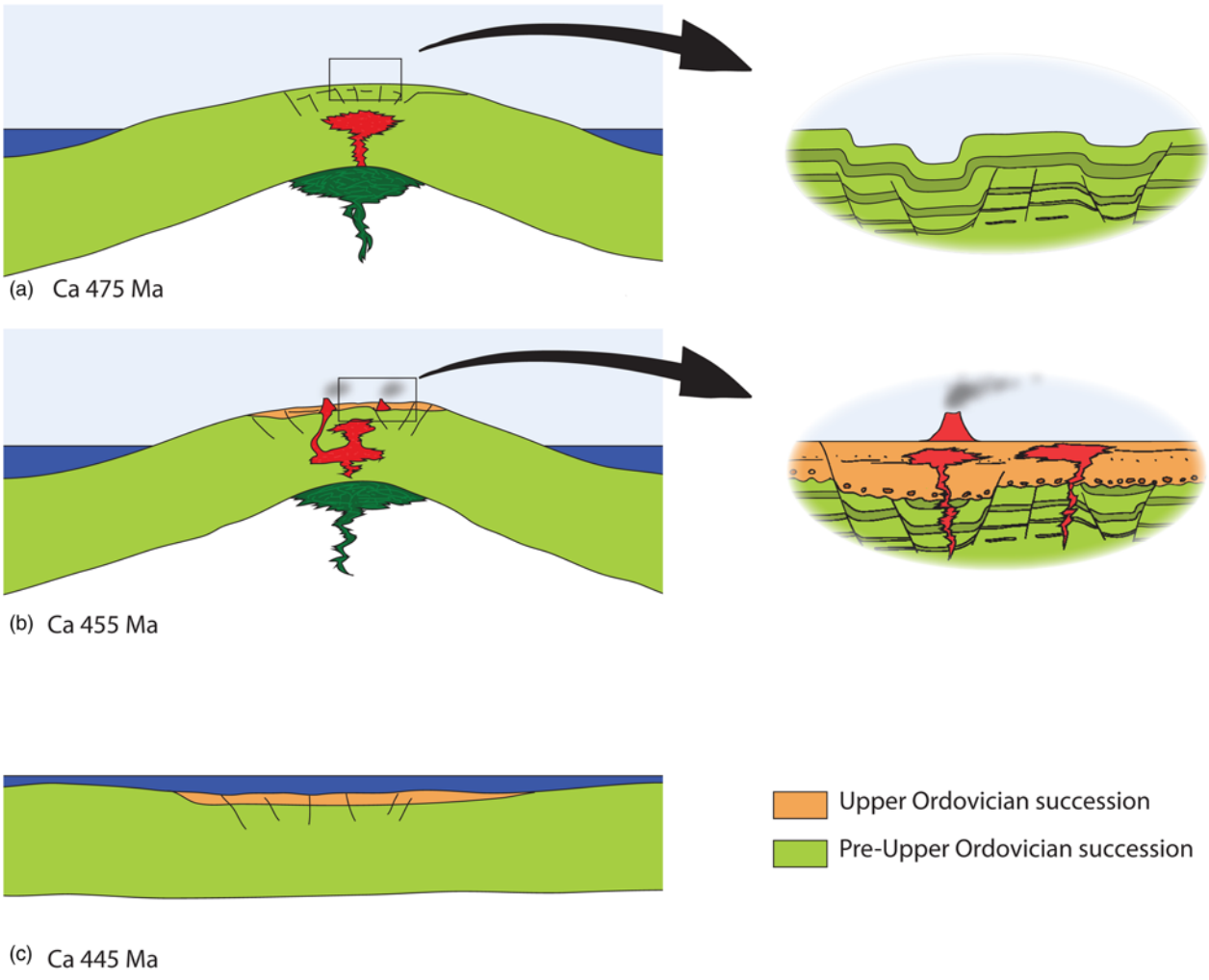

Fig. 13. Sketch showing the geodynamic evolution described in the text (not to scale).

invoked as the origin of the Furongian–Early Ordovician magmatism in the Central Iberian Zone of the Iberian Massif related to the so-called Toledanian Phase (Bea *et al*. 2007; Montero *et al*. 2009; Díez Montes *et al*. 2010). The latter is characterized by a Furongian gap associated with the onset of a remarkable magmatic activity of calc-alkaline affinity, giving rise to the Ollo de Sapo and Urra formations, *c.* 495–470 Ma (see summaries by Álvaro *et al*. 2007; Casas & Murphy 2018; García-Arias *et al*. 2018; Sánchez-García *et al*., in press). In the Pyrenees, doming started at *c.* 475 Ma, causing regional uplift and emersion responsible for the end of the marine Jujols Group sedimentation, its erosion and the emplacement of a widespread calc-alkaline granitic magmatism (Fig. 13). Subsequent extensional episodes were related to the opening of half-grabens and their infill with the Rabassa Conglomerate Formation and the lower part of the Cava Formation. The latter sedimentation was coeval with magmatic activity until *c.* 450 Ma, when thermal relaxation led to marine transgression and sedimentation (middle part of the Cava Formation) that onlapped an inherited Sardic-related palaeorelief. After a glaciogenic transgression represented by the blanketing of the basin by the Ansobell Formation, isostatic rebound at *c.* 445 Ma may be signalled by the progradation of the Bar Quartzite Formation, coincident with the end of the magmatic activity and with the final sealing of inherited Sardic palaeotopographies in Silurian times. Later, the Variscan deformation overprinted all these rocks and structures in Mid-Carboniferous times.

Comparison with neighbouring areas

In Sardinia, the Sardic Unconformity is associated with an intra-Ordovician stratigraphic gap in the autochthonous Paleozoic basement of the Iglesiente–Sulcis area (southwestern Sardinia), which corresponds to the External Zone of the South European Variscan Chain. Similar gaps (named the Sarrabese Unconformity) are found in the External nappe Zone, associated with coeval igneous activities in the Sarrabus–Gerrei area (*c.* 465 Ma: Buzzi *et al*. 2007*a*, 2007*b*; Oggiano *et al*. 2010). The post-unconformity succession is related to Late Ordovician magmatism in SW Sardinia (*c.* 457 Ma: Pavanetto *et al*. 2012) and central–northern Sardinia (*c.* 469 Ma to *c.* 456 Ma: Helbing & Tiepolo 2005; Giacomini *et al*. 2006; Boriani 2008). Indeed, in Sardinia, the pre-Sardic sequence is affected by different east–west-striking structures with neither regional metamorphism nor cleavage, displaying 1–100 m scale folds without cleavage and faults, subsequently sealed by Upper Ordovician strata (Pasci *et al*. 2008; Cocco & Funedda 2012, 2019; Cocco *et al*. 2018). We recall, for instance, the structure of the Su Scoffoni area in southeastern Sardinia, where Cocco & Funedda (2019) described the Sardic Unconformity sealing folds affecting only the pre-Upper Ordovician succession. As a result, the Upper Ordovician succession in SE Sardinia overlies Cambrian–Ordovician beds with different attitudes, in a similar way to that described above for the Eastern Pyrenees. The occurrence of faults and an environment of half-grabens have been supposed by Brusca & Dessau (1968) and Martini *et al*. (1991), who associated them with a post-unconformity deposit (Monte Argentu Formation) in SW Sardinia.

In the Occitan Domain (Mouthoumet and Montagne Noire massifs) of southern France, the Ordovician is punctuated by two major gaps: a Sardic Unconformity (ranging from paraconformable to angular discordant contacts) and a diachronous Silurian erosive unconformity that represents blanketing of an inherited glaciogenic palaeorelief (Álvaro *et al*. 2016). As in the case for the Eastern Pyrenees and Sardinia, the Montagne Noire includes emplacement of massive (Sardic-related) Middle Ordovician granitic bodies. The migmatitic Somail Orthogneiss of the southern Axial Zone was derived from an Ordovician metagranite that was emplaced at 471 ± 4 Ma and 450 ± 6 Ma (U–Pb zircon ages; Roger *et al*. 2004; Cocherie *et al*. 2005). Recent geochronological dating of these augen orthogneisses has updated the story of various generations of granitoids that form the core of the Axial Zone (e.g. Cocherie 2003; Faure *et al*. 2004; Roger *et al*. 2004; Bé Mézème 2005; Charles *et al*. 2009). A post-Sardic rifting reactivation is recorded in the Mouthoumet massif and the Cabrières klippes (southern Montagne Noire), where Late Ordovician fault-controlled subsidence and the record of rift-related continental tholeiitic lavas were coeval, in some areas, with the onset of the Hirnantian glaciation (Álvaro *et al*. 2016, 2018). Reopening of rifting branches was followed by onlapping patterns and final sealing of Sardic palaeotopographies during Silurian and Early Devonian times. It led to fault-controlled subsidence and the generation of structurally controlled depocentres, at least in the Cabrières sector of the Montagne Noire and the Mouthoumet area. It was accompanied by marine transgression and extensional pulses that gradually led to flooding and onlapping on the shoulders of the rifting branches, which were finally sealed during Early Devonian times.

As a result, the Sardic Phase is shared by the Occitan Domain, the Eastern Pyrenees and Sardinia, all of them located along the eastern branch of the Variscan Ibero-Armorican Arc. According to some researchers (e.g. Stampfli *et al*. 2002), this margin of Gondwana faced the Proto-Tethys, also called Ran Ocean (Torsvik & Cocks 2009), and later the Paleo-Tethys Ocean (Torsvik & Cocks 2004; Von Raumer & Stampfli 2008). This geodynamic setting is different from that faced by the Iberian Massif, which is located along the western branch of the Ibero-Armorican Arc. In the Central Iberian and Ossa–Morena zones of the Iberian Massif, a similar but earlier unconformity, the Toledanian Unconformity, is represented by an angular discordance that separates variably tilted Ediacaran–Cambrian Series 2 rift-related successions from an overlying Tremadocian–Floian passive-margin succession. The gap involved (at least *c.* 22 myr) includes, at least, most of the Furongian and basal Ordovician, although the erosion can incise into the entire Cambrian and the upper Ediacaran Cadomian basement (Gutiérrez-Marco *et al*. 2002). The Toledanian Phase has been recently interpreted (Sánchez-García *et al*. in press) as representing the rift–drift transition that led to the opening of the Rheic Ocean (Díez Montes *et al*. 2010; Nance *et al*. 2010; Thompson *et al*. 2010; Álvaro *et al*. 2014, 2018; Casas *et al*. in press). Neither metamorphism nor penetrative deformation related to this unconformity has been described, except in the Marão Anticline and the Amêndoa–Carvoeiro Synform of the Central Iberian Zone. In these areas, cleavage-bearing folds with steep axial planes at high angles to Variscan structures have been described and related to transient compression and dextral strike-slip features along the Central Iberian-Ossa–Morena contact lineament (Romão & Ribeiro 1993; Correira Romão, *et al*. 2005; Romão *et al*. 2013; Amaral *et al*. 2014). A similar volcanic-free 'Furongian gap' related to a break-up unconformity has been reported in the central Anti-Atlas of Morocco, and related to the above-reported Toledanian Phase (Álvaro & Vizcaïno 2018).

The magmatism associated with the Toledanian and Sardic phases is dominantly felsic and calc-alkaline, and exhibits an arc-like signature that some researchers have interpreted as linked to subduction conditions (Castro *et al*. 2002; Del Greco *et al*. 2016). However, others have interpreted this signature as an inherited character caused by the fast melting of a subduction-related Neoproterozoic crust (Díez Montes *et al*. 2010; Navidad *et al*. 2010; Sánchez-García *et al*. in press). This fast melting may also explain the great amount of inherited zircons, the highly porphyritic character and the virtual absence of mafic bodies in these magmas. These may have resulted from the partial melting of granitoids or sediments in the continental lower crust caused by the underplating or intrusion of hot mafic magmas that produced a great heat input

during an extensional event (Bea *et al*. 2007; Montero *et al*. 2009; Díez Montes *et al*. 2010).

Conclusions

In the Eastern Pyrenees, the Sardic Unconformity separates two successions with different structural features. The Cambrian–Lower Ordovician and the Upper Ordovician successions are affected by Late Ordovician extensional tectonics and by two Variscan deformation events. Moreover, the Cambrian–Lower Ordovician succession is also affected by an Early–Mid-Ordovician fold system that we relate to extensional faults. Upward propagation of some of these extensional faults during Sandbian–Katian times caused the faults to affect the Sardic Unconformity and the lowermost part of the Upper Ordovician succession.

We relate the extensional fault formation to a thermal doming that developed between 475 and 450 Ma. The doming should have produced stretching of the Ordovician lithosphere, together with emersion, uplift and erosion of the Cambrian–Ordovician sequence giving rise to the formation of the Sardic Unconformity. Thermal doming may also be responsible for coeval magmatic activity that is well developed in the same area and caused by hot mafic magma underplating. We compare the Mid-Ordovician Sardic Unconformity in the Pyrenees with contemporaneous gaps recognized in Sardinia and the Occitan Domain, and also discuss the similarities with the Furongian Toledanian gap described in the neighbouring Iberian Massif, which may have originated in similar scenarios.

We suggest a regional-scale thermal event ranging in age from Early–Mid- to Late Ordovician, which affected several areas of the Northern Gondwana margin. Its role in the geodynamic scenario that led to other significant Early Paleozoic events, such as the opening of the Rheic Ocean and the drift of Avalonia (*sensu lato*) from the western part of North Gondwana, requires investigation.

Acknowledgements We acknowledge the use of MOVE (Midland Valley) and Stereonet (R. W. Allmendinger) software packages. Detailed reviews by R. Vissers and an anonymous referee greatly improved the first version of the paper.

Funding Financial support was provided by Spanish MINECO projects CGL2015-66335-C2-1-R and CGL2017-87631-P.

Author contributions J.M.C.: investigation (equal); C.P.: investigation (equal); J.J.Á.: investigation (equal); N.C.: visualization (equal).

Scientific editing by Stuart Jones

References

Abu Sharib, A.S.A.A., Abdel-Fattah, M.M., Salama, Y.F. & Abdel-Gawad, G.I. 2017. Extension-related buttress-like folds, the western side of the Gulf of Suez rift, Egypt. *International Journal of Earth Sciences*, **106**, 2527–2547, https://doi.org/10.1007/s00531-017-1445-1

Álvaro, J.J. & Vizcaïno, D. 2018. The Furongian break-up (rift–drift) transition in the Anti-Atlas, Morocco. *Journal of Iberian Geology*, **44**, 567–587, https://doi.org/10.1007/s41513-018-0066-2

Álvaro, J.J., Ferretti, F., González-Gómez, C., Serpagli, E., Tortello, M.F., Vecoli, M. & Vizcaïno, D. 2007. A review of the Late Cambrian (Furongian) palaeogeography in the western Mediterranean region, NW Gondwana. *Earth-Science Reviews*, **85**, 47–81, https://doi.org/10.1016/j.earscirev.2007.06.006

Álvaro, J.J., Bellido, F., Gasquet, D., Pereira, F., Quesada, C. & Sánchez-García, T. 2014. Diachronism in the late Neoproterozoic–Cambrian arc–rift transition of North Gondwana: A comparison of Morocco and the Iberian Ossa–Morena Zone. *Journal of African Earth Sciences*, **98**, 113–132, https://doi.org/10.1016/j.jafrearsci.2014.03.024

Álvaro, J.J., Colmenar, J., Monceret, E., Pouclet, A. & Vizcaïno, D. 2016. Late Ordovician (post-Sardic) rifting branches in the North-Gondwanan Montagne Noire and Mouthoumet massifs of southern France. *Tectonophysics*, **681**, 111–123, https://doi.org/10.1016/j.tecto.2015.11.031

Álvaro, J.J., Casas, J.M., Clausen, S. & Quesada, C. 2018. Early Palaeozoic geodynamics in NW Gondwana. *Journal of Iberian Geology*, **44**, 551–565, https://doi.org/10.1007/s41513-018-0079-x

Amaral, A., Dias, R., Coke, C., Romão, J. & Ribeiro, A. 2014. Fase de deformação sarda na Zona Centro-Ibérica. *Comunicações Geológicas*, **101**, 239–242.

Ayora, C. 1980. *Les concentrationes metàlliques de la Vall de Ribes*. PhD thesis, Barcelona University.

Bea, F., Montero, P., González Lodeiro, F. & Talavera, C. 2007. Zircon inheritance reveals exceptionally fast crustal magma generation processes in Central Iberia during the Cambro–Ordovician. *Journal of Petrology*, **48**, 2327–2339, https://doi.org/10.1093/petrology/egm061

Bé Mézème, E. 2005. *Contribution de la géochronologie U–Th–Pb sur monazite à la compréhension de la fusion crustale dans la chaîne Hercynienne française et implication géodynamique*. PhD thesis, Orléans University.

Boriani, A. 2008. Age and origins of the Italian continental crust: data and interpretations. *Rendiconti online della Società Geologica Italiana, Abstracts*, **3**, 124.

Brusca, C. & Dessau, G. 1968. I giacimenti piombo-zinciferi di S. Giovanni (Iglesias) nel quadro della geologia del Cambrico sardo. *L'Industria Mineraria*, **19**, 533–556.

Buzzi, L., Funedda, A., Gaggero, L. & Oggiano, G. 2007*a*. Sr–Nd isotope, trace and REE element geochemistry of the Ordovician volcanism in the southern realms of the Variscan belt. EGU General Assembly 2007, Wien, 15–20 April 2007, *Geophysical Research Abstracts*, **9**, EGU General Assembly 2007.

Buzzi, L., Gaggero, L., Funedda, A., Oggiano, G. & Tiepolo, M. 2007*b*. Zircon geochronology and Sr/Nd study of the Ordovician magmatic events in the southern Variscides (Sardinia). *Géologie de la France*, **2**, 73.

Calvet, P., Lapierre, H. & Charvet, J. 1988. Diversité du volcanisme ordovicien dans la région de Pierrefitte (Hautes-Pyrénées): rhyolites calco-alcalines et basaltes alcalins. *Comptes Rendus de l'Académie des Sciences, Série 2*, **307**, 805–812.

Capellà, I. & Bou, O. 1997. La estructura del domo de la Rabassa y del sector oriental del sinclinal de Llavorsi (Pirineo central). *Estudios Geológicos*, **53**, 121–133, https://doi.org/10.3989/egeol.97533-4237

Casas, J.M. 2010. Ordovician deformations in the Pyrenees: new insights into the significance of pre-Variscan ('sardic') tectonics. *Geological Magazine*, **147**, 674–689, https://doi.org/10.1017/S0016756809990756

Casas, J.M. & Fernández, O. 2007. On the Upper Ordovician unconformity in the Pyrenees: New evidence from the La Cerdanya area. *Geologica Acta*, **5**, 193–198.

Casas, J.M. & Murphy, B. 2018. Unfolding the arc: The use of pre-orogenic constraints to assess the evolution of the Variscan belt in Western Europe. *Tectonophysics*, **736**, 47–61, https://doi.org/10.1016/j.tecto.2018.04.012

Casas, J.M. & Palacios, T. 2012. First biostratigraphical constraints on the pre-Upper Ordovician sequences of the Pyrenees based on organic-walled microfossils. *Comptes Rendus Géoscience*, **344**, 50–56, https://doi.org/10.1016/j.crte.2011.12.003

Casas, J.M., Domingo, F., Poblet, J. & Soler, A. 1989. On the role of the Hercynian and Alpine thrusts in the Upper Paleozoic rocks of the Central and Eastern Pyrenees. *Geodinamica Acta*, **3**, 135–147, https://doi.org/10.1080/09853111.1989.11105181

Casas, J.M., Parés, J.M. & Megías, L. 1998. La fábrica magnética de los materiales cambro-ordovícicos del Anticlinal de la Massana (Andorra, Pirineo Central). *Revista de la Sociedad Geológica de España*, **11**, 317–329.

Casas, J.M., Castiñeiras, P., Navidad, M., Liesa, M. & Carreras, J. 2010. New insights into the Late Ordovician magmatism in the Eastern Pyrenees: U–Pb SHRIMP zircon data from the Canigó massif. *Gondwana Research*, **17**, 317–324, https://doi.org/10.1016/j.gr.2009.10.006

Casas, J.M., Queralt, P., Mencos, J. & Gratacós, O. 2012. Distribution of linear mesostructures in oblique folded surfaces: Unravelling superposed Ordovician and Variscan folds in the Pyrenees. *Journal of Structural Geology*, **44**, 141–150, https://doi.org/10.1016/j.jsg.2012.08.013

Casas, J.M., Navidad, M. *et al.* 2015. The Late Neoproterozoic magmatism in the Ediacaran series of the Eastern Pyrenees: new ages and isotope geochemistry. *International Journal of Earth Sciences*, **104**, 909–925, https://doi.org/10.1007/s00531-014-1127-1

Casas, J.M., Álvaro, J.J. *et al.* in press. Palaeozoic basement of the Pyrenees. *In*: Quesada, C. & Oliveira, J.T. (eds) *The Geology of Iberia: a Geodynamic Approach, Volume 2: The Variscan Cycle*, Regional Geology Reviews Series. Springer, Berlin, https://www.springer.com/gp/book/9783030105181

Castiñeiras, P., Navidad, M., Liesa, M., Carreras, J. & Casas, J.M. 2008. U–Pb zircon ages (SHRIMP) for Cadomian and Lower Ordovician magmatism in the Eastern Pyrenees: new insights in the pre-Variscan evolution of the northern Gondwana margin. *Tectonophysics*, **46**, 228–239, https://doi.org/10.1016/j.tecto.2008.04.005

Castro, A., Corretgé, G. *et al.* 2002. Palaeozoic magmatism. *In*: Gibbons, W. & Moreno, T. (eds) *The Geology of Spain*. Geological Society, London, 117–153.

Cavet, P. 1957. Le Paléozoïque de la zone axiale des Pyrénées orientales françaises entre le Roussillon et l'Andorre. *Bulletin du Service de la Carte géologique de France*, **55**, 303–518.

Charles, N., Faure, M. & Chen, Y. 2009. The Montagne Noire migmatitic dome emplacement (French Massif Central): new insights from petrofabric and AMS studies. *Journal of Structural Geology*, **31**, 1423–1440, https://doi.org/10.1016/j.jsg.2009.08.007

Cirés, J., Casas, J.M., Muñoz, J.A., Fleta, J. & Barbera, M. 1994. *Mapa geológico de España a escala 1:50.000, hoja de Molló (no. 218)*. ITGE, Madrid.

Clariana, P. & García-Sansegundo, J. 2009. Variscan structure in the eastern part of the Pallaresa massif, Axial Zone of the Pyrenees (NW Andorra). Tectonic implications. *Bulletin de la Société géologique de France*, **180**, 501–511, https://doi.org/10.2113/gssgfbull.180.6.501

Clariana, P., García-Sansegundo, J. & Gavaldà, J. 2009. The structure in the Bagneres de Luchon and Andorra cross sections (Axial Zone of the central Pyrenees). *Trabajos de Geología, Universidad de Oviedo*, **29**, 175–181.

Clariana, P., Valverde-Vaquero, P., Rubio-Ordóñez, A., Beranoaguirre, A. & García-Sansegundo, J. 2018. Pre-Variscan tectonic events and Late Ordovician magmatism in the Central Pyrenees: U–Pb age and Hf in zircon isotopic signature from subvolcanic sills in the Pallaresa massif. *Journal of Iberian geology*, **44**, 589–601, https://doi.org/10.1007/s41513-018-0076-0

Cocco, F. & Funedda, A. 2012. The Variscan basement of the Riu Ollastu area (Sarrabus, SE Sardinia, Italy). *Géologie de la France*, **1**, 89–90.

Cocco, F. & Funedda, A. 2019. The Sardic phase: field evidence of Ordovician tectonics in SE Sardinia, Italy. *Geological Magazine*, **156**, 25–38, https://doi.org/10.1017/S0016756817000723

Cocco, F., Oggiano, G., Funedda, A., Loi, A. & Casini, L. 2018. Stratigraphic, magmatic and structural features of Ordovician tectonics in Sardinia (Italy): a review. *Journal of Iberian Geology*, **44**, 619–639, https://doi.org/10.1007/s41513-018-0075-1

Cocherie, A. 2003. *Datation avec le SHRIMP II du métagranite oeillé du Somail–Montagne Noire*. Compte Rendu Technique ANA-ISO/NT. BRGM, Orléans.

Cocherie, A., Baudin, T., Guerrot, C., Autran, A., Fanning, M.C. & Laumonier, B. 2005. U–Pb zircon (ID-TIMS and SHRIMP) evidence for the early Ordovician intrusion of metagranites in the late Proterozoic Canaveilles Group of the Pyrenees and the Montagne Noire (France). *Bulletin de la Société géologique de France*, **176**, 269–282, https://doi.org/10.2113/176.3.269

Correira Romão, J.M., Coke, C., Dias, R. & Ribeiro, A. 2005. Transient inversion during the opening stage of the Wilson cycle 'Sardic phase' in the Iberian Variscides – Stratigraphic and tectonic record. *Geodinamica Acta*, **18**, 115–129, https://doi.org/10.3166/ga.18.115-129

Del Greco, K., Johnston, S.T. & Shaw, J. 2016. Tectonic setting of the North Gondwana margin during the Early Ordovician: a comparison of the Ollo de Sapo and Famatina magmatic events. *Tectonophysics*, **681**, 73–84, https://doi.org/10.1016/j.tecto.2016.02.034

Deloule, E., Alexandrov, P., Cheilletz, A., Laumonier, B. & Barbey, P. 2002. *In-situ* U–Pb zircon ages for Early Ordovician magmatism in the eastern Pyrenees, France: the Canigou orthogneisses. *International Journal of Earth Sciences*, **91**, 398–405, https://doi.org/10.1007/s00531-001-0232-0

Delvolvé, J.J. 1981. Arguments en faveur de l'âge namurien du Culm des Pyrénées Centrales françaises. *Comptes Rendus de l'Académie des Sciences*, **293**, 219–222.

Delvolvé, J.J. & Perret, M.F. 1989. Variations de l'âge des sédiments calcaires et 'Culm' carbonifère dans la chaîne varisque du Sud de la France: migration de l'orogenèse varisque. *Geodinamica Acta*, **3**, 117–126, https://doi.org/10.1080/09853111.1989.11105179

Delvolvé, J.J., Souquet, P., Vachard, D., Perret, M.F. & Aguirre, P. 1993. Caractérisation d'un bassin d'avant-pays dans le Carbonifère des Pyrénées: faciès, chronologie de la tectonique synsédimentaire. *Comptes Rendus de l'Académie des Sciences, Série 2*, **316**, 959–966.

Den Brok, S.W.J. 1989. Evidence for pre-Variscan deformation in the Lys Caillaouas area, Central Pyrenees, France. *Geologie en Mijnbouw*, **68**, 377–380.

Denèle, Y., Barbey, P., Deloule, E., Pelleter, E., Olivier, P. & Gleizes, G. 2009. Middle Ordovician U–Pb age of the Aston and Hospitalet orthogneissic laccoliths: their role in the Variscan evolution of the Pyrenees. *Bulletin de la Société géologique de France*, **180**, 209–221, https://doi.org/10.2113/gssgfbull.180.3.209

Díez Montes, A., Martínez Catalán, J.R. & Bellido Mulas, F. 2010. Role of the Ollo de Sapo massive felsic volcanism of NW Iberia in the Early Ordovician dynamics of northern Gondwana. *Gondwana Research*, **17**, 363–376, https://doi.org/10.1016/j.gr.2009.09.001

Domingo, F., Muñoz, J.A. & Santanach, P. 1988. Estructures d'encavalcament en les materials del sòcol hercinia del massís de la Tossa d'Alp, Pirineu oriental. *Acta Geológica Hispánica*, **23**, 141–153.

Faure, M., Ledru, P., Lardeaux, J.M. & Matte, P. 2004. Paleozoic orogenies in the French Massif Central. A cross section from Béziers to Lyon. *In*: *32nd International Geological Congress. Field-trip Guide Book, Florence (Italy)*, APAT: Italian Agency for the Environmental Protection and Technical Services, Roma, Italy, 1–40.

García-Arias, M., Díez-Montes, A., Villaseca, C. & Blanco-Quintero, I.F. 2018. The Cambro-Ordovician Ollo de Sapo magmatism in the Iberian Massif and its Variscan evolution: A review. *Earth-Science Reviews*, **176**, 345–372, https://doi.org/10.1016/j.earscirev.2017.11.004

García-Sansegundo, J. & Alonso, J.L. 1989. Stratigraphy and structure of the southeastern Garona Dome. *Geodinamica Acta*, **3**, 127–134, https://doi.org/10.1080/09853111.1989.11105180

García-Sansegundo, J., Gavaldà, J. & Alonso, J.L. 2004. Preuves de la discordance de l'Ordovicien supérieur dans la zone axiale des Pyrénées: exemple de dôme de la Garonne (Espagne, France). *Comptes Rendus Géoscience*, **336**, 1035–1040, https://doi.org/10.1016/j.crte.2004.03.009

García-Sansegundo, J., Poblet, J., Alonso, J.L. & Clariana, P. 2011. Hinterland–foreland zonation of the Variscan orogen in the Central Pyrenees: comparison with the northern part of the Iberian Variscan Massif. *In*: Poblet, J. & Lisle, R.J. (eds) *Kinematic Evolution and Structural Styles of Fold-and-Thrust Belts*. Geological Society, London, Special Publications, **349**, 169–184, https://doi.org/10.1144/SP349.9

Giacomini, F., Bomparola, R.M., Ghezzo, C. & Guldbransen, H. 2006. The geodynamic evolution of the Southern European Variscides: constraints from the U/Pb geochronology and geochemistry of the lower Palaeozoic magmatic–sedimentary sequences of Sardinia (Italy). *Contributions to Mineralogy and Petrology*, **152**, 19–42, https://doi.org/10.1007/s00410-006-0092-5

Gil-Peña, I., Barnolas, A., Villas, E. & Sanz-López, J. 2004. El Ordovícico Superior de la Zona Axial. *In*: Vera, J.A. (ed.) *Geología de España*. SGE-IGME, Madrid, 247–249.

Guitard, G. 1970. *Le métamorphisme hercynien mésozonal et les gneiss œillés du massif du Canigou (Pyrénées orientales)*. Mémoires du BRGM, **63**.

Gutiérrez-Marco, J.C., Robardet, M., Rábano, I., Sarmiento, G.N., San José-Lancha, M.A., Herranz Araújo, P. & Pieren Pidal, A.P. 2002. Ordovician. *In*: Gibbons, W. & Moreno, T. (eds) *The Geology of Spain*. Geological Society, London, 31–49.

Hammann, W. 1992. The Ordovician trilobites from the Iberian Chains in the province of Aragón, NE Spain. The trilobites of the Cystoid Limestone (Ashgill Series). *Beringeria*, **6**, 1–219.

Hartevelt, J.J.A. 1970. Geology of the upper Segre and Valira valleys, central Pyrenees, Andorra/Spain. *Leidse Geologische Mededelingen*, **45**, 167–236.

Helbing, H. & Tiepolo, M. 2005. Age determination of Ordovician magmatism in NE Sardinia and its bearing on Variscan basement evolution. *Journal of the Geological Society, London*, **162**, 689–700, https://doi.org/10.1144/0016-764904-103

Kriegsman, L.M., Aerden, D.G.A.M., Bakker, R.J., den Brok, S.W.J. & Schutjens, P.M.T.M. 1989. Variscan tectonometamorphic evolution of the eastern Lys–Caillaouas massif, Central Pyrenees – evidence for late orogenic extension prior to peak metamorphism. *Geologie en Mijnbouw*, **68**, 323–333.

Laumonier, B. 1988. Les groupes de Canaveilles et de Jujols ('Paléozoïque inférieur') des Pyrénées orientales – arguments en faveur de l'âge essentiellement Cambrien de ces séries. *Hercynica*, **4**, 25–38.

Laumonier, B. & Guitard, G. 1986. Le Paléozoïque inférieur de la moitié orientale de la Zone Axiale des Pyrénées. Essai de synthèse. *Comptes Rendus de l'Académie des Sciences*, **302**, 473–478.

Leone, F., Ferretti, A., Hammann, W., Loi, A., Pillola, G.L. & Serpagli, E. 2002. A general view on the post-Sardic Ordovician sequence from SW Sardinia. *Rendiconti della Società Paleontologica Italiana*, **1**, 51–68.

Liesa, M., Carreras, J., Castiñeiras, P., Casas, J.M., Navidad, M. & Vilà, M. 2011. U–Pb zircon age of Ordovician magmatism in the Albera Massif (Eastern Pyrenees). *Geologica Acta*, **9**, 1–9, https://doi.org/10.1344/105.000001651

Llopis Lladó, N. 1965. Sur le Paléozoïque inférieur de l'Andorre. *Bulletin de la Société géologique de France*, **7**, 652–659.

Margalef, A. & Casas, J.M. 2016. Corte geológico compensado del sur de Andorra: aportaciones a la estructura varisca del Pirineo central. *Geo-Temas*, **16**, 61–63.

Margalef, A., Castiñeiras, P. *et al.* 2016. Detrital zircons from the Ordovician rocks of the Pyrenees: Geochronological constraints and provenance. *Tectonophysics*, **681**, 124–134, https://doi.org/10.1016/j.tecto.2016.03.015

Martí, J., Muñoz, J.A. & Vaquer, R. 1986. Les roches volcaniques de l'Ordovicien supérieur de la région de Ribes de Freser–Rocabruna (Pyrénées catalanes): caractères et signification. *Comptes Rendus de l'Académie des Sciences*, **302**, 1237–1242.

Martí, J., Casas, J.M., Guillén, N., Muñoz, J.A. & Aguirre, G. 2014. Structural and geodynamic constraints of Upper Ordovician volcanism of the Catalan Pyrenees. *In*: *Gondwana 15 Abstracts Book*, 104, Instituto Geológico y Minero de España, Madrid.

Martí, J., Solari, L., Casas, J.M. & Chichorro, M. 2019. New geochronological data on the Upper Ordovician volcanism in the Eastern Pyrenees (NE Iberia): Stratigraphic and geodynamic implications. *Geological Magazine*, https://doi.org/10.1017/S0016756819000116

Martín-Closas, C., Trias, S. & Casas, J.M. 2018. New palaeobotanical data from Carboniferous Culm deposits constrain the age of the Variscan deformation in the Eastern Pyrenees. *Geologica Acta*, **16**, 107–123, https://doi.org/10.1344/GeologicaActa2018.16.2.1

Martínez, F., Iriondo, A. *et al.* 2011. U–Pb SHRIMP-RG zircon ages and Nd signature of lower Paleozoic rifting-related magmatism in the Variscan basement of the Eastern Pyrenees. *Lithos*, **127**, 10–23, https://doi.org/10.1016/j.lithos.2011.08.004

Martínez, F.J., Dietsch, C., Aleinikoff, J., Cirés, J., Arboleya, M.L., Reche, J. & Gómez-Gras, D. 2016. Provenance, age, and tectonic evolution of Variscan flysch, southeastern France and northeastern Spain, based on zircon geochronology. *Geological Society of America Bulletin*, **128**, 842–859, https://doi.org/10.1130/B31316.1

Martini, I.P., Tongiorgi, M., Oggiano, G. & Cocozza, T. 1991. Ordovician alluvial fan to marine shelf transition in SW Sardinia, Western Mediterranean Sea: tectonically ('Sardic phase') influenced clastic sedimentation. *Sedimentary Geology*, **72**, 97–115, https://doi.org/10.1016/0037-0738(91)90125-W

Maurel, O., Respaut, J.P., Monié, P., Arnaud, N. & Brunel, M. 2004. U–Pb emplacement and $^{40}Ar/^{39}Ar$ cooling ages of the eastern Mont-Louis granite massif (Eastern Pyrenees, France). *Comptes Rendus Géoscience*, **336**, 1091–1098, https://doi.org/10.1016/j.crte.2004.04.005

Mey, P.H.W. 1967. The geology of the Upper Ribagorzana and Baliera valleys, Central Pyrenees, Spain. *Leidse Geologische Mededelingen*, **41**, 153–220.

Mezger, J. & Gerdes, A. 2016. Early Variscan (Visean) granites in the core of central Pyrenean gneiss domes: implications from laser ablation U–Pb and Th–Pb studies. *Gondwana Research*, **29**, 181–198, https://doi.org/10.1016/j.gr.2014.11.010

Montero, P., Talavera, C., Bea, F., Lodeiro, F.G. & Whitehouse, M.J. 2009. Zircon geochronology of the Ollo de Sapo Formation and the age of the Cambro-Ordovician rifting in Iberia. *Journal of Geology*, **117**, 174–191, https://doi.org/10.1086/595017

Muñoz, J.A. 1992. Evolution of a continental collision belt: ECORS-Pyrenees crustal balanced cross-section. *In*: Clay, K.R.M. (ed.) *Thrust Tectonics*. Chapman & Hall, London, 235–246.

Muñoz, J.A. & Casas, J.M. 1996. Tectonique préhercynienne. *In*: Barnolas, A. & Chiron, J.C. (eds) *Synthèse Géologique et Géophysique des Pyrénées*. BRGM–ITGE, Orléans–Madrid, 587–589.

Nance, R.D., Gutiérrez-Alonso, G. *et al.* 2010. Evolution of the Rheic Ocean. *Gondwana Research*, **17**, 194–222, https://doi.org/10.1016/j.gr.2009.08.001

Navidad, M., Castiñeiras, P. *et al.* 2010. Geochemical characterization and isotopic ages of Caradocian magmatism in the northeastern Iberia: insights into the Late Ordovician evolution of the northern Gondwana margin. *Gondwana Research*, **17**, 325–333, https://doi.org/10.1016/j.gr.2009.11.013

Navidad, M., Castiñeiras, P., Casas, J.M., Liesa, M., Belousova, E., Proenza, J. & Aiglsperger, T. 2018. Ordovician magmatism in the Eastern Pyrenees: Implications for the geodynamic evolution of northern Gondwana. *Lithos*, **314–315**, 479–496, https://doi.org/10.1016/j.lithos.2018.06.019

Oggiano, G., Gaggero, L., Funedda, A., Buzzi, L. & Tiepolo, M. 2010. Multiple early Paleozoic volcanic events at the northern Gondwana margin: U–Pb age evidence from the Southern Variscan branch (Sardinia, Italy). *Gondwana Research*, **17**, 44–58, https://doi.org/10.1016/j.gr.2009.06.001

Padel, M., Álvaro, J.J., Casas, J.M., Clausen, S., Poujol, M. & Sánchez-García, T. 2018*a*. Cadomian volcanosedimentary complexes across the Ediacaran–Cambrian transition of the eastern Pyrenees, France and Spain. *International Journal of Earth Sciences*, **107**, 1579–1601, https://doi.org/10.1007/s00531-017-1559-5

Padel, M., Clausen, S., Álvaro, J.J. & Casas, J.M. 2018*b*. Review of the Ediacaran–Lower Ordovician (pre-Sardic) stratigraphic framework of the Eastern Pyrenees, southwestern Europe. *Geologica Acta*, **16**, 339–355, https://doi.org/10.1344/GeologicaActa2018.16.4.1

Pasci, S., Pertusati, P.C., Salvadori, I. & Murtas, A. 2008. I rilevamenti CARG del Foglio geologico 555 'Iglesias' e le nuove implicazioni strutturali sulla tettonica della 'Fase Sarda'. *Rendiconti online della Società Geologica Italiana, Abstracts*, **3**, 614–615.

Pavanetto, P., Funedda, A., Northrup, C.J., Schmitz, M., Crowley, J. & Loi, A. 2012. Structure and U–Pb zircon geochronology in the Variscan foreland of SW Sardinia, Italy. *Geological Journal*, **47**, 426–445, https://doi.org/10.1002/gj.1350

Pereira, M.F., Castro, A., Chichorro, M., Fernández, C., Díaz-Alvarado, J., Martí, J. & Rodríguez, C. 2014. Chronological link between deep-seated processes in magma chambers and eruptions: Permo-Carboniferous magmatism in the core of Pangaea (Southern Pyrenees). *Gondwana Research*, **25**, 290–308, https://doi.org/10.1016/j.gr.2013.03.009

Pillola, G.L., Piras, S. & Serpagli, E. 2008. Upper Tremadoc–Lower Arenig? Anisograptid–Dichograptid fauna from the Cabitza Formation (Lower Ordovician, SW Sardinia, Italy). *Revue de Micropaléontologie*, **51**, 167–181, https://doi.org/10.1016/j.revmic.2007.08.002

Poblet, J. 1991. *Estructura herciniana i alpina del versant sud de la zona axial del Pirineu central*. PhD, University of Barcelona.

Puddu, C. & Casas, J.M. 2011. New insights into the stratigraphy and structure of the Upper Ordovician rocks of the la Cerdanya area (Pyrenees). *In*: Gutiérrez-Marco, J.C., Rábano, I. & García-Bellido, D. (eds) *Ordovician of the World*. Cuadernos del Museo Geominero, **14**, 441–445.

Ramsay, J.G. 1967. *Folding and Fracturing of Rocks*. McGraw–Hill, New York.

Robert, J.F. 1980. *Étude géologique et métallogénique du val de Ribas sur le versant espagnol des Pyrénées catalanes*. PhD thesis, Franche-Comté University, Besançon.

Robert, J.F. & Thiébaut, J. 1976. Découverte d'un volcanisme acide dans le Caradoc de la région de Ribes de Freser (Prov. de Gérone). *Comptes Rendus de l'Académie des Sciences*, **282**, 2050–2079.

Roger, F., Respaut, J.P., Brunel, M., Matte, P. & Paquette, J.L. 2004. Première datation U–Pb des orthogneiss oeillés de la zone axiale de la Montagne Noire (Sud du Massif central): nouveaux témoins du magmatisme ordovicien dans la chaîne Varisque. *Comptes Rendus Géoscience*, **336**, 19–28, https://doi.org/10.1016/j.crte.2003.10.014

Romão, J. & Ribeiro, A. 1993. Thrust tectonics of Sardic age in the Rosmaninhal area (Beira Baixa, Central Portugal). *Comunicações dos Serviços Geológicos de Portugal*, **78**, 87–95.

Romão, J., Metodiev, D., Dias, R. & Ribeiro, A. 2013. Evolução geodinâmica dos sectores meridionais da Zona Centro-Ibérica. *In*: Dias, R., Araújo, A., Terrinha, P. & Kullberg, J.C. (eds) *Geologia do Portugal*, **1**. Escolar Editora, Lisbon, 206–257.

Romer, R.L. & Soler, A. 1995. U–Pb age and lead isotopic characterization of Au-bearing skarn related to the Andorra granite. *Mineralium Deposita*, **30**, 374–383, https://doi.org/10.1007/BF00202280

Roqué Bernal, J., Štorch, P. & Gutiérrez-Marco, J.C. 2017. Bioestratigrafía (graptolitos) del límite Ordovícico–Silúrico en los Pirineos orientales (curso alto del río Segre, Lleida). *Geogaceta*, **61**, 27–30.

Rotevatn, A. & Jackson, C.A.L. 2014. 3D structure and evolution of folds during normal fault dip linkage. *Journal of the Geological Society, London*, **171**, 821–829, https://doi.org/10.1144/jgs2014-045

Sánchez-García, T., Chichorro, M., *et al*. in press. Rifting stage. *In*: Quesada, C. & Oliveira, J.T. (eds) *The Geology of Iberia: a Geodynamic Approach, Volume 2: The Variscan Cycle*. Regional Geology Reviews Series. Springer, Berlin, https://www.springer.com/gp/book/9783030105181

Santanach, P. 1972. Sobre una discordancia en el Paleozoico inferior de los Pirineos orientales. *Acta Geológica Hispánica*, **7**, 129–132.

Sanz-López, J. & Sarmiento, G.N. 1995. Asociaciones de conodontos del Ashgill y Llandovery en horizontes carbonatados del Valle del Freser (Girona). *In*: López, G., Obrador, A. & Vicens, E. (eds.) *XI Jornadas de Paleontología*, Tremp. Comunicaciones, 157–160.

Sanz-López, J., Gil-Peña, I. & Valenzuela-Ríos, J.I. 2002. Lower Palaeozoic rocks from the Pyrenees: A synthesis. *In*: García-López, S. & Bastida, F. (eds) *Palaeozoic Conodonts from Northern Spain, 8th International Conodont Symposium held in Europe*. Serie Cuadernos del Museo Geominero (IGME), **1**, 349–365.

Sanz-López, J., Perret, M.F. & Vachard, D. 2006. Silurian to Mississippian series of the eastern Catalan Pyrenees (Spain), updated by conodonts, foraminifers and algae. *Geobios*, **39**, 709–725, https://doi.org/10.1016/j.geobios.2005.06.003

Sharp, I.R., Gawthorpe, R.L., Underhill, J.R. & Gupta, S. 2000. Fault-propagation folding in extensional settings: Examples of structural style and synrift sedimentary response from the Suez rift, Sinai, Egypt. *Geological Society of America Bulletin*, **112**, 1877–1899, https://doi.org/10.1130/0016-7606(2000)112<1877:FPFIES>2.0.CO;2

Speksnijder, A. 1986. Geological analysis of Paleozoic large-scale faulting in the south–central Pyrenees. *Geologica Ultraiectina*, **43**, 1–211.

Stampfli, G.M., von Raumer, J.F. & Borel, G.D. 2002. Paleozoic evolution of pre-Variscan terranes: from Gondwana to the Variscan collision. *In*: Martínez Catalán, J.R., Hatcher, R.D., Arenas, R. & García, F.D. (eds) *Variscan–Appalachian Dynamics: the Building of the Late Paleozoic Basement*. Geological Society of America, Boulder, CO, 263–280.

Stille, H. 1939. Bemerkungen betreffend die 'Sardische' Faultung und den Ausdruck 'Ophiolitisch'. *Zeitschrift der Deutschen Gessellschaft für Geowissenschaften*, **91**, 771–773.

Štorch, P., Roqué Bernal, J. & Gutiérrez-Marco, J.C. 2018. A graptolite-rich Ordovician–Silurian boundary section in the south–central Pyrenees, Spain: stratigraphical and palaeobiogeographical significance. *Geological Magazine*, https://doi.org/10.1017/S001675681800047X

Teichmüller, R. 1931. Zur Geologie des Thyrrhenisgebietes. Teil 1: Alte und junge Krustenbewegungen im südlichen Sardinien. *Abhandlungen von der Gesellschaft der Wissenschaften zu Göttingen, Mathematisch-Physikalische Klasse*, **3**, 857–950.

Thompson, M.D., Grunow, A.M. & Ramezani, J. 2010. Cambro-Ordovician paleogeography of the Southeastern New England Avalon Zone: Implications for Gondwana breakup. *Geological Society of America Bulletin*, **122**, 76–88, https://doi.org/10.1130/B26581.1

Torsvik, T.H. & Cocks, L.R.M. 2004. Earth geography from 400 to 250 Ma: a palaeomagnetic, faunal and facies review. *Journal of the Geological Society, London*, **161**, 555–572, https://doi.org/10.1144/0016-764903-098

Torsvik, T.H. & Cocks, L.R.M. 2009. The Lower Palaeozoic palaeogeographical evolution of the northeastern and eastern peri-Gondwanan margin from Turkey to New Zealand. *In*: Basset, M.G. (ed.) *Early Palaeozoic Peri-Gondwana Terranes: New Insights from Tectonics to Biogeography*. Geological Society, London, Special Publications, **325**, 3–21, https://doi.org/10.1144/SP325.2

Turner, F.J. & Weiss, L.E. 1963. *Structural Analysis of Metamorphic Tectonites*. McGraw–Hill, New Cork.

Von Raumer, J.F. & Stampfli, G.M. 2008. The birth of the Rheic Ocean – early Palaeozoic subsidence patterns and tectonic plate scenarios. *Tectonophysics*, **461**, 9–20, https://doi.org/10.1016/j.tecto.2008.04.012

Xiao, H. & Suppe, J. 1992. Origin of rollover. *AAPG Geologists Bulletin*, **76**, 509–529.

Zwart, H.J. 1979. The geology of the Central Pyrenees. *Leidse Geologische Mededelingen*, **50**, 1–74.

5.7 Palaeozoic basement of the Pyrenees

(*paper 3*)

Palaeozoic Basement of the Pyrenees

8

J. M. Casas, J. J. Álvaro, S. Clausen, M. Padel, C. Puddu, J. Sanz-López, T. Sánchez-García, M. Navidad, P. Castiñeiras, and M. Liesa

Abstract

In the Pyrenees, the Cambrian-Lower Ordovician strata represent a quiescent time span with no remarkable tectonic activity, followed by a late Early-Mid Ordovician episode of uplift and erosion that led to the formation of the Sardic unconformity. Silurian sedimentation was widespread and transgressive followed by a Devonian succession characterized by a complex mosaic of sedimentary facies. Carboniferous pre-Variscan sediments (Tournaisian-Viséan cherts and limestones) precede the arrival of the synorogenic siliciclastic supplies of the Culm flysch at the Late Serpukhovian. All this succession was subsequently affected by the Serpukhovian-Bashkirian (Variscan) collision, as a result of which, the Palaeozoic rocks were incorporated into the northeastern branch of the Ibero-Armorican Arc.

8.1 Introduction

J. M. Casas, J. J. Álvaro

In the Pyrenees, the aftermath of the late Ediacaran-early Terreneuvian magmatism, related to the Cadomian subduction, records the transition to passive-margin conditions. Cambrian-Lower Ordovician strata represent a quiescent time span with no remarkable tectonic activity, followed by a late Early-Mid Ordovician episode of uplift and erosion that led to the formation of the Sardic unconformity. Uplift was accompanied by magmatic activity that pursuit until the Late Ordovician, the latter coinciding with an extensional pulse that developed normal faults and controlled the record of post-Sardic sediments infilling palaeorelief depressions (the significance of this magmatism and tectonic activity is still

Coordinators: J. M. Casas, J. J. Álvaro.

J. M. Casas (✉)
Departamento de Dinàmica de la Terra i de l'Oceà-Institut de Recerca Geomodels, Universitat de Barcelona, Martí Franquès s/n, 08028 Barcelona, Spain
e-mail: casas@ub.edu

J. J. Álvaro
Instituto de Geociencias (CSIC-UCM), Dr. Severo Ochoa 7, 28040 Madrid, Spain
e-mail: jj.alvaro@csic.es

S. Clausen
UMR 8198 EEP CNRS, Université de Lille 1, Bâtiment SN5, Avenue Paul Langevin, 59655 Villeneuve d'Ascq Cedex, France
e-mail: sebastien.clausen@univ-lille1.fr

M. Padel
BRGM, 3 Avenue Claude Guillemin, 45100 Orléans, France
e-mail: m.padel@brgm.fr

C. Puddu
Departamento de Ciencias de la Tierra, Universidad de Zaragoza, Pedro Cerbuna 12, 50009 Zaragoza, Spain
e-mail: claudiapuddugeo@gmail.com

J. Sanz-López
Dpto. de Geologia, Universidad de Oviedo, Jesus Arias de Velasco s/n, 33005 Oviedo, Spain
e-mail: jasanz@geol.uniovi.es

T. Sánchez-García
Departamento Investigación Recursos Geológicos, Área Recursos Minerales y Geoquímica, Instituto Geológico y Minero de España, Ríos Rosas 23, 28003 Madrid, Spain
e-mail: t.sanchez@igme.es

M. Navidad · P. Castiñeiras
Departamento de Petrología y Geoquímica, Universidad Complutense de Madrid, Novais 12, 28040 Madrid, Spain
e-mail: navidad@geo.ucm.es

P. Castiñeiras
e-mail: castigar@ucm.es

M. Liesa
Departament de Mineralogia, Petrologia i Geologia aplicada, Universitat de Barcelona, Martí Franquès s/n, 08028 Barcelona, Spain
e-mail: mliesa@ub.edu

C. Quesada and J. T. Oliveira (eds.), *The Geology of Iberia: A Geodynamic Approach*, Regional Geology Reviews,
https://doi.org/10.1007/978-3-030-10519-8_8

under debate; see Sect. 8.3). Silurian sedimentation was widespread and transgressive, sealing the Sardic uplift palaeorelief and Late Ordovician rifting pulsation, followed by a Devonian succession characterized by a complex mosaic of sedimentary facies. Tournaisian-Viséan cherts and limestones represent the Carboniferous pre-Variscan sediments, preceding the arrival of the synorogenic siliciclastic supplies of the Culm flysch at the Late Serpukhovian. All this succession was subsequently affected by the Serpukhovian-Bashkirian (Variscan) collision, as a result of which, the Palaeozoic rocks were incorporated into the northeastern branch of the Ibero-Armorican Arc. In this chapter, we update data and interpretations from these Palaeozoic rocks of the Pyrenees, with a new proposal for the lower Cambrian-Ordovician stratigraphy and an update of the Upper Ordovician, Silurian, Devonian and pre-Variscan Carboniferous stratigraphy. Exposed data emphasize the affinity of the Pyrenean basement rocks with that of the neighbouring Sardinia, Mouthoumet and Montagne Noire-French Central Massif domains, as well as its differences with the Palaeozoic evolution of the Iberian Massif.

In the Pyrenees, the pre-Variscan Palaeozoic rocks constitute a 3–4 km-thick succession that crops out in the backbone of the cordillera (Fig. 8.1). These rocks form an elongated strip unconformably overlain by Mesozoic and Cenozoic rocks, which lie geographically disconnected from neighbouring outcrops of the Catalan Coastal Range to the south, the Mouthoumet and Montagne Noire (southern French Central) massifs to the north, and Sardinia to the east. Palaeozoic rocks are involved in three main Alpine thrust sheets, the so-called Lower Structural Units (Muñoz 1992) named Nogueres, Orri and Rialp thrust sheets. These units form an antiformal stack with their basal thrusts north-dipping or subvertical in the northern side of the chain, subhorizontal in the central part, and south-dipping in the southern contact with the Mesozoic-Cenozoic cover. In the description that follows, we will focus on the Palaeozoic rocks of the Nogueres and Orri units, which constitute a complete pre-Variscan succession, ranging in age from Cambrian to Carboniferous. Exposures of the Rialp unit only occur in a small tectonic window of the central Pyrenees.

Transverse (N-S-trending) displacement related to the Alpine deformation is about 150–160 km (Muñoz 1992), so the original Palaeozoic basin should be located northward from present-day arrangement. Moreover, the Alpine deformation gave rise to important horizontal axes rotation related to antiformal stack development. In contrast, Alpine metamorphism is absent and internal deformation is moderated. As a result, the original characteristics of the Palaeozoic rocks may be confidently reconstructed in the Pyrenees. As discussed below, other pre-Alpine movements may be also envisaged in order to obtain a reliable original Early Palaeozoic palaeoposition of the Pyrenenan domain and to establish its geodynamic relationship with the neighbouring Variscan Sardinia, Mouthoumet and Montagne Noire-French Central Massif domains.

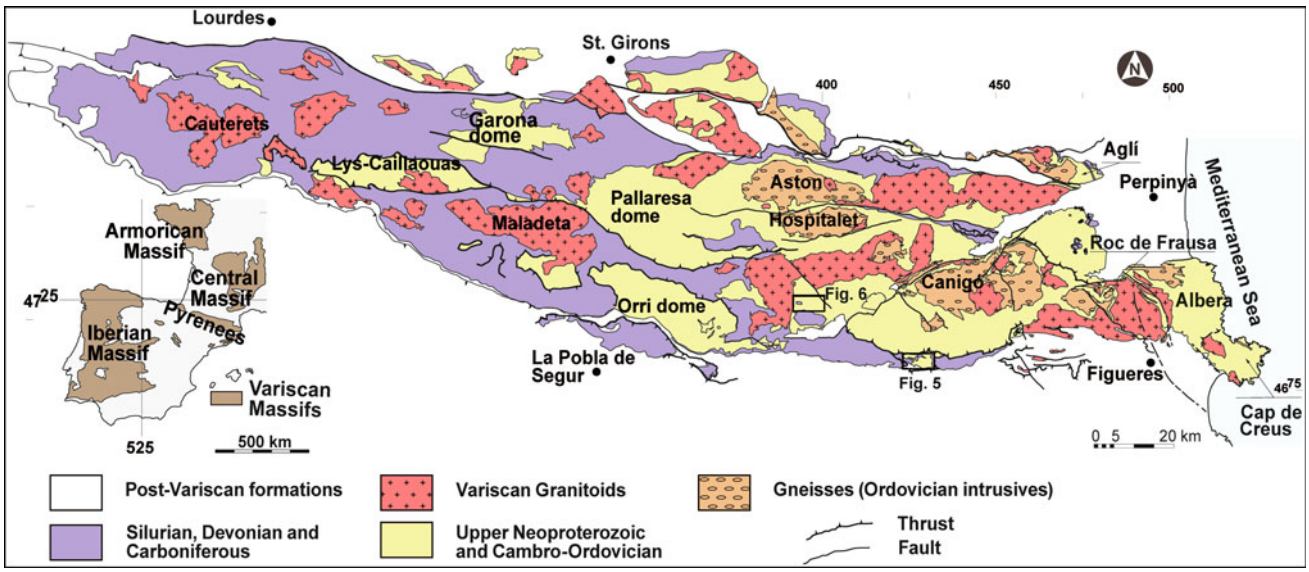

Fig. 8.1 Simplified geological map of the Pyrenees with the location of the massifs mentioned in the text

8.2 Cambro-Ordovician (pre-Sardic) Stratigraphy: Jujols Group

J. J. Álvaro, J. M. Casas, S. Clausen, M. Padel

The Jujols Group (Fig. 8.2) was firstly described by Cavet (1957) as the Jujols Schists, comprising a monotonous succession of alternating shale and sandstone overlying the Canaveilles Series in the northern Canigó massif. Cavet (1957) attributed an Ordovician age to the Jujols Schists, which then included what is now considered as Upper Ordovician conglomerates and volcanic deposits. These are underlain by a significant erosive unconformity and angular discordance representative of the Sardic Phase, and therefore excluded from the Jujols Group (Laumonier 1988). According to Cavet (1957), the base of the Jujols Schists was characterized by the presence of grey shales with carbonate nodules and quartzite interbeds. As reported in Chap. 2, the Jujols Group overlies the Cadomian volcanic activity reported in the Canaveilles Group.

In this contribution, we follow Padel (2016) and Padel et al. (2018) updating revision of the Jujols Group in the Eastern Pyrenees based on new stratigraphic data and geometric relationships (Fig. 8.2). These authors propose a subdivision of the Jujols Group into the Err, Valcebollère and Serdinya formations. The base of the Jujols Group coincides with the base of the Err Formation (Fig. 8.2), which onlaps an inherited palaeorelief formed by the Pic de la Clape Formation to the south of the Canigó massif (see Chap. 2). Where the Pic de la Clape volcanosedimentary complexes are absent, the Err Formation conformably overlies the Olette Formation. The top of the Jujols Group is highlighted by the Middle-Upper (*pars*) Ordovician hiatus associated with the Sardic Phase. The thickness of the group can be estimated at about 3–4 km.

The Err Formation (Fig. 8.2) is a relatively monotonous shale-dominated unit, up to about 2000 m thick. It consists of grey, brownish and greenish shales and centimetre-to-decimetre thick, fine-grained sandstones locally punctuated by gravelly sandstones. The latter never exceed 10 m in thickness and can be observed in the Puigmal area, near the summit of the Puigmal d'Err and at the Pic de la Clapa, where they overlie the Puig Sec Member. These sandstones are also well developed in the Aspres and Conflent areas.

The Valcebollère Formation (Fig. 8.3) consists of a lower massive-to-bedded limestone-to-marble package (up to 300 m thick), overlain and passing westward to a 15–200 m thick, shale/carbonate alternation that changes upsection into green shales bearing carbonate nodules. The thickness of the formation and its carbonate content diminish northward disappearing to the north of the Canigó massif. Despite the absence of archaeocyaths, several outcrops exhibit typical plano-convex exposures and microbial framebuilding textures (e.g., Gorges de la Fou in the Vallespir-Roc de Frausa area, and isolated bioherms close to Valcebollère village; Fig. 8.3 a–d) characteristic of reefal complexes. In the Aspres area, the Courbis Limestone of the Valcebollère Formation has yielded the acritarch *Archaeodiscina* cf. *umbonulata* Volkova, 1968. *A. umbonulata* is a cosmopolitan species ranging approximately from Cambrian Age 3 to early Cambrian Age 4 (Laumonier et al. 2015; T. Palacios, pers.com. 2016). Associated with the Courbis Limestone, some centimetric layers of grainy phosphorites have been identified, for the first time, marking the topmost part of the Valcebollère Formation.

The Serdinya Formation consists of a roughly 1500 m thick rhythmic alternation of shale and sandstone beds. Layers are 1 mm to several cm thick, change in colour from grey to characteristic light green or light brown grey to greenish, and exhibit sedimentary structures representative of tidal-to-storm influence (Fig. 8.4a). Sandstones up to 1 m thick occur at the top of the formation, exhibiting graded bedding, load casts and cross bedding (Fontfrède Member) (Fig. 8.4b). The Serdinya Formation conformably overlies the Valcebollère Formation (in some areas sealing hydrothermally induced karstic features, such as in the Roques Blanques section along the road N260; Fig. 8.3e–g) and is topped by the Sardic unconformity (Fig. 8.4c). Acritarchs recovered from the uppermost part of the Serdinya Formation in the southern Canigó massif has yielded a broad Furongian-Early Ordovician microphytoplancton assemblage (Casas and Palacios 2012). Ichnoassemblages recorded in the La Molina area, although not chronostratigraphically diagnostic, show a low-to-moderate ichnodiversity (Gámez et al. 2012). A maximum depositional age of ca. 475 Ma can be proposed for the quartzites of the Fonfrède Member in the La Rabassa dome, on the basis on the youngest detrital zircon population (Margalef et al. 2016).

Considering a Cambrian Fortunian age for the base of the Err Fomation, and a Furongian-Early Ordovician age for the top of the Serdinya Formation (Fig. 8.2), a broad Cambrian-earliest Ordovician age can be envisaged for the entire Jujols Group. As discussed below, it should be noted that Middle Ordovician sedimentary rocks have not yet been described in the Pyrenees.

8.3 Upper Ordovician Succession

J. J. Álvaro, J. M. Casas, C. Puddu

The Upper Ordovician succession of the Central and Eastern Pyrenees, well known after the works of Cavet (1957) and Hartevelt (1970), constitutes a broad fining-upward megasequence bearing a key limestone-marlstone interbed

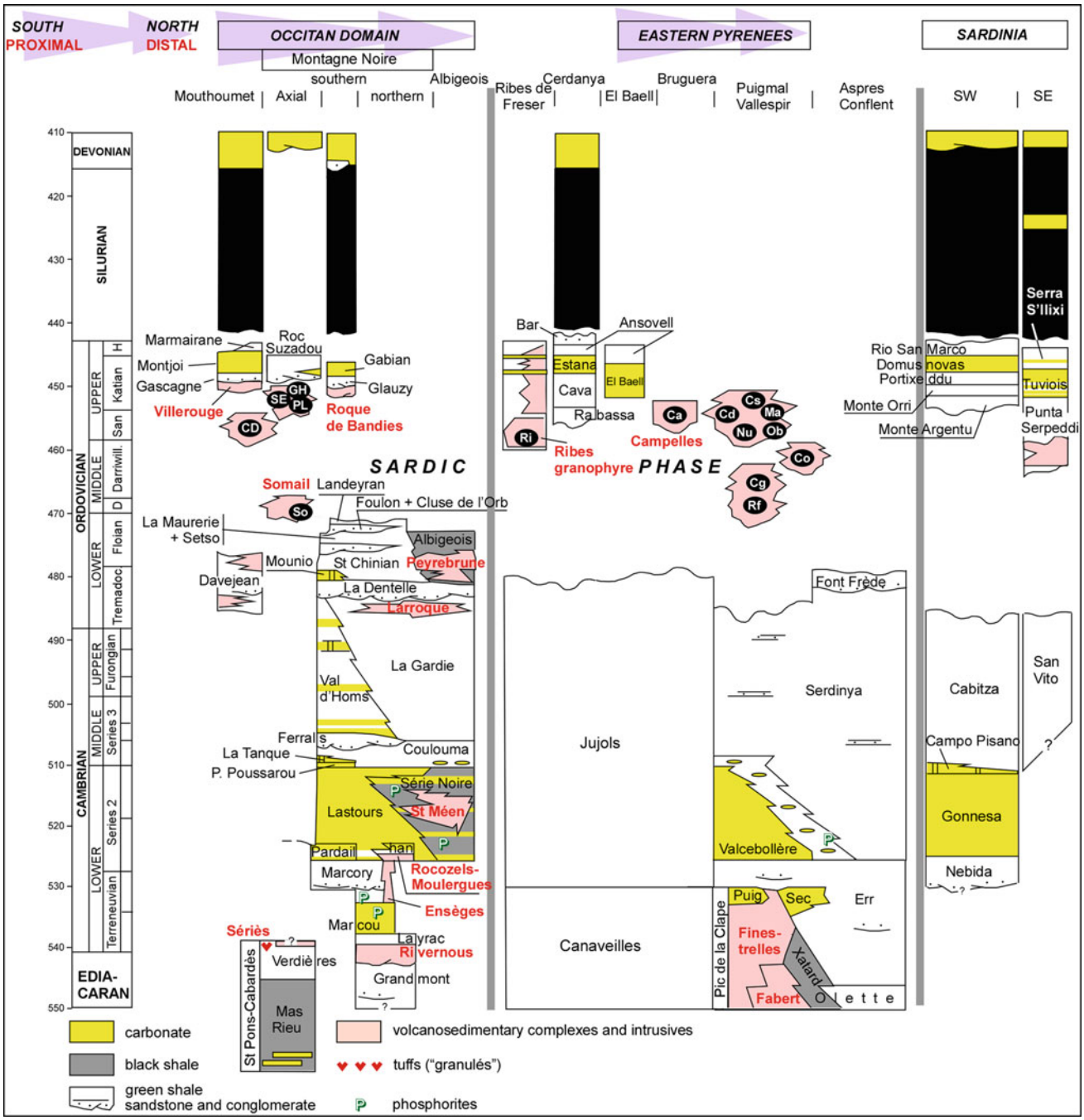

Fig. 8.2 Stratigraphic comparison of the Cambro-Ordovician successions from the Occitan Domain (Montagne Noire and Mouthoumet), Eastern Pyrenees and Sardinia. So: Somail orthogneiss (471 ± 4 Ma, Cocherie et al. 2005); SE: Saint Eutrope gneiss (455 ± 2 Ma, Pitra et al. 2012); GH: Gorges d'Heric orthogneiss (450 ± 6 Ma, Roger et al. 2004); Pl: Pont de Larn orthogneiss (456 ± 3 Ma, Roger et al. 2004); Ri: Ribes granophyre (458 ± 3 Ma, Martínez et al. 2011); Ca: Campelles ignimbrites (ca. 455 Ma, Martí et al. 2014); Cs: Casemí gneiss (446 ± 5, 452 ± 5 Ma, Casas et al. 2010); Cd: Cadí gneiss (456 ± 5 Ma, Casas et al. 2010); Ma: Marialles microdiorite (453 ± 4 Ma, Casas et al. 2010); Nu: Núria gneiss (457 ± 4 Ma, Martínez et al. 2011); Qb: Queralbs gneiss (457 ± 5 Ma, Martínez et al. 2011); Co: Cortalets metabasite (460 ± 3 Ma, Navidad et al. submitted); Cg: Canigó gneiss (472–462 Ma, Cocherie et al. 2005, Navidad et al. 2018); Rf: Roc de Frausa gneiss (477 ± 4, 476 ± 5 Ma, Cocherie et al. 2005; Castiñeiras et al. 2008)

and marked thickness variations, ranging between 100 and 1000 m. Hartevelt (1970) defined five formations, which can be recognized with some lithologic variations all across most part of the cordillera (Fig. 8.2). Furthermore, various volcanic and volcanosedimentary complexes crop out in different areas (Robert and Thiébaut 1976), although

Fig. 8.3 **a** Field aspect of a hectometre-size, microbial bioherm of the Valcebollère Formation cropping out in the vicinity of the homonymous village; *co*: core, *f*: flank. **b** Detail of boxed area in **a** showing the intertonguing contact (arrowed) of the core (white) and flank (grey). **c** Detail of boxed area in **a** illustrating the distant core/flank contact. **d** Biohermal flank composed of elongated marble clasts embedded in a silty (brownish) matrix; scale = 4 cm. **e** Contact (arrowed) of massive marbles (Valcebollère Fm) and bedded sandy shales (Serdinya Fm) marked by ferrigenous crusts. **f** Photomicrograph of the contact marked in **e** showing a fissure network of hydrothermal veins infilled with hematite, goethite and ankerite sealed (top) by a clean sparry mosaic of calcite (marble); scale = 2 mm. **g** Valcebollère/Serdinya transition characterized by the presence of unselected marble nodules "floating" in a shaly matrix (facies named "schistes troués" in France and "facies rizada" in Spain)

◀ **Fig. 8.4** **a** Convoluted alternations of centimetre-thick sandstones and shales showing amalgamation of migrating bars and storm-induced processes; Serdinya Formation at La Molina. **b** Burrowing surfaces of soft-bodied metazoan suspensivores marking low-sedimentation events; Font Frède Member at Camporells. **c** Angular discordance separating the Serdinya Formation (left) and the Rabassa conglomerates (right) at Talltendre. **d** Alluvial-to-fluvial trough cross-stratified conglomerates and sandstones of the Rabassa Formation at Talltendre. **e**, **f** Hydrothermal dykes infilled with quartz marking the outlines of the half-grabens infilled with the Rabassa conglomerates at La Molina. **g** Field aspect of the Rabassa conglomerate rich in subangular hydrothermal quartz clasts; La Molina. **h** Top of the Katian El Baell Formation at its stratotype unconformably overlain by the Hirnantian Ansovell Formation. **i** Detail of the El Baell limestones showing echinoderm-rich packstones with scattered, partially articulated columns

radiometric ages are necessary to distinguish between Sardic-related and post-Sardic (Upper Ordovician) volcanogenic events.

Unconformably overlying the Sardic-related palaeotopography, the Rabassa Conglomerate Formation is made up of reddish-purple, unfossiliferous conglomerates with sharp lateral thickness variations, from zero to 200 m. Conglomerates are composed of subrounded to well-rounded clasts rich in slates, quartzites and vein quartz, up to 50 cm in diameter, embedded in a green-purple granule-sized matrix (Fig. 8.4d). Their massive-to-channelized sets are interpreted as alluvial-to-fluvial deposits (Hartevelt 1970). Due to its stratigraphic position, this author attributed the Rabassa conglomerates to the Sandbian-Early Katian (former Caradoc).

The overlying Cava Formation, 100–800 m thick, which either cover the Sardic unconformity or the Rabassa Conglomerate Formation, is made up of feldspathic conglomerates and sandstones in the lower part, grading upwards into variegated shales and fine-grained sandstones, with strongly burrowed quartzites in the uppermost part (Belaustegui et al. 2016). A contemporaneous volcanic influence is distinct in the southwestern part of the Canigó massif, where ash levels, andesites and metavolcanic rocks are embedded (e.g., in Ribes de Freser; Muñoz 1985). Brachiopods, bryozoans and echinoderms are locally abundant, concentrated in fine-grained sandstones of the middle part of the formation, based on which, Gil-Peña et al. (2004) attributed a Katian (former late Caradoc-early Asghill) age to this formation.

The Estana Formation, which lies above the Cava Formation, consists of limestones and marly limestones, up to 10 m thick. The unit constitutes a good stratigraphic marker bed, the so-called "schistes troués", "Grauwacke à *Orthis*" and "Caradoc limestones" of French and Dutch geologists. Conodonts, brachiopods, bryozoans and echinoderms are abundant, yielding a Katian (former mid Ashgill; Gil-Peña et al. 2004) age for the development of echinoderm-bryozoan meadows on shelly, offshore-dominated substrates.

The "Ansovell" Formation (Ansobell sensu Hartevelt 1970) unconformably overlies the Estana limestone and consists of blackish shales with common slumping and convoluted layers close to the base and minor quartzite interlayers in the uppermost part. Where the Estana Formation tapers off, the Ansovell shales directly overlie the Cava sandstones. Finally, the Bar Quartzite Formation marks the top of the Upper Ordovician as a quartzitic layer, 5–10 m thick. An Hirnantian age (former late Ashgill) was proposed for the Ansovell and Bar formations by Hartevelt (1970), and confirmed by Roqué et al. (2017). Westward, in the Orri, Pallaresa and Garona domes, Gil-Peña et al. (2000, 2004) reported a calcareous conglomerate, up to 8 m thick, directly capping the erosive unconformity that marks the Estana/Ansovell contact, and attributed it to a Hirnantian glacial event.

Thickness of the Upper Ordovician succession diminishes northward, across the Massana anticline and the Aston and Ospitalet domes. In these areas, the Rabassa conglomerates are absent, whereas the Estana limestone attains its maximum thickness, about 70 m (Margalef 2015).

In the Ribes de Freser area (south of the Canigó massif, Eastern Pyrenees), an Upper Ordovician succession, different from the above-mentioned one, is located. There, several Alpine structural units form an antiformal stack bounded to the north by the out-of-sequence Ribes-Camprodon thrust. In this antiformal stack, three Alpine units (named Ribes de Freser, El Baell and Bruguera) exhibit a characteristic Upper Ordovician succession (Fig. 8.5). Restoration of the Alpine deformation allows us to situate the Bruguera unit in a pre-Alpine northernmost position, the El Baell unit in an intermediate setting, and the Ribes de Freser unit would lie originally in a southernmost one.

The Ribes de Freser unit is predominantly made up of volcanic and volcanosedimentary rocks (Fig. 8.5) (Robert and Thiébaut 1976; Ayora 1980; Robert 1980; Muñoz 1985; Martí et al. 1986), with a variable thickness ranging from 600 to 1200 m. Its lower part consists of dioritic bodies and volcanosedimentary rocks, whereas rhyolitic lava flows and ignimbrites predominate in the central part, and ash levels, ignimbrites and volcaniclastic rocks form its upper part. A granophyric body, dated as 458 ± 3 Ma (Martínez et al. 2011), intruded into the lower part of the succession. The volcanic activity was mainly explosive and had a calc-alkaline affinity reflecting crustal melting (Martí et al. 1986).

The El Baell unit, in turn, comprises a 300 m-thick succession entirely composed of limestones, marly limestones ("schistes troués") and shales (Robert 1980; Muñoz 1985). Three limestone-dominated thickening-upward sequences, up to 30 m thick, can be distinguished. Conodonts and crinoids allowed Robert (1980) to attribute an early Katian (former Caradoc) age to the beds forming this unit (Fig. 8.4h, i).

The Bruguera unit lies on the top of the El Baell unit and is composed of a 200 m-thick undated slate-dominated

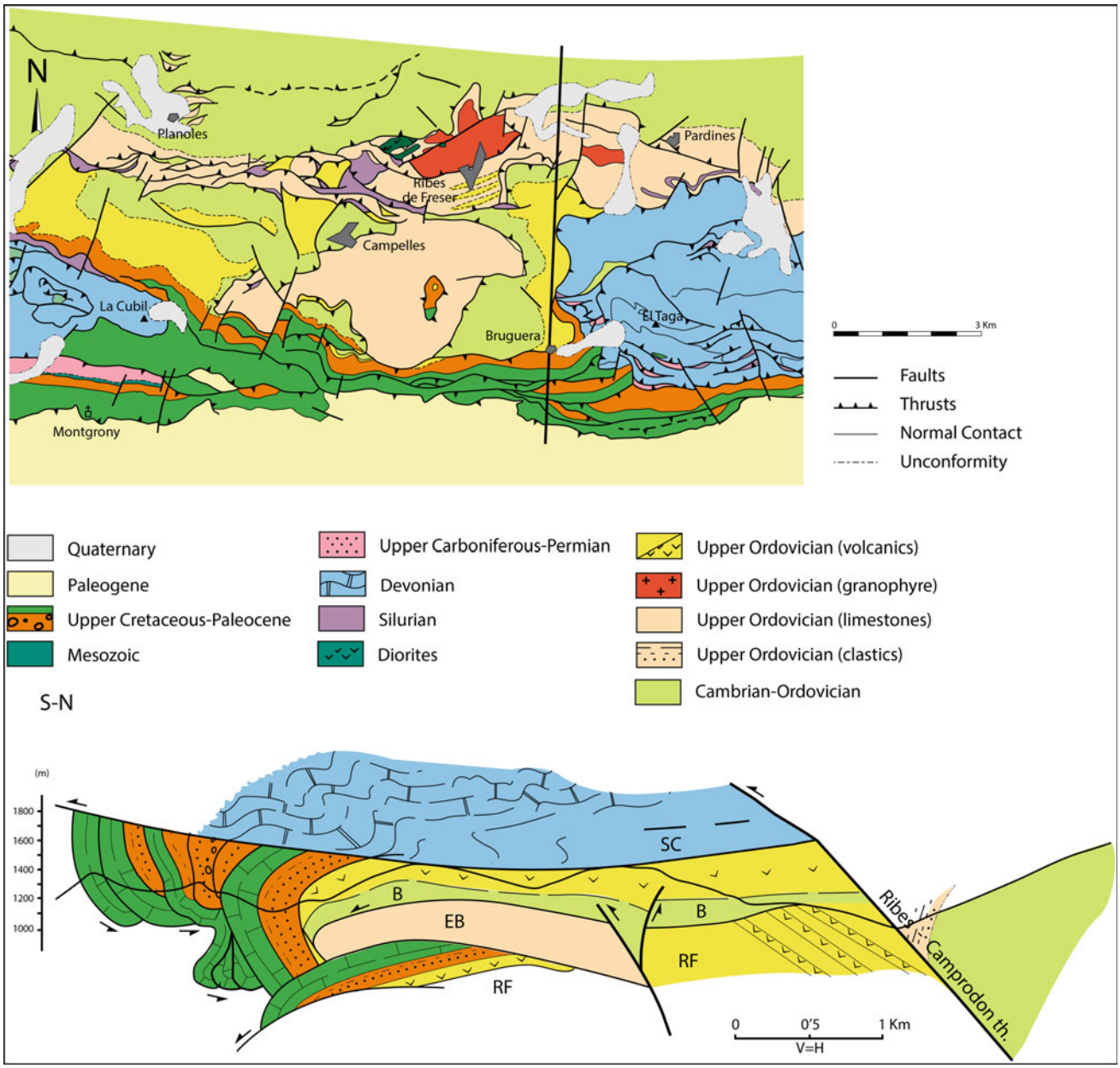

Fig. 8.5 Cross-section of the Freser river antiformal stack with the Ribes de Freser (RF), El Baell (EB) and Bruguera (B) units. After Muñoz (1985) modified. See location on Fig. 8.1

succession, pre-Variscan (Cambrian-Ordovician?) in age, overlain by a volcanic complex (Muñoz 1985). The latter consists of rhyolitic ignimbrites and andesitic lava flows, recently dated at ca. 455 Ma (Martí et al. 2014), an age similar to that of the Ribes granophyre cropping out in the Ribes de Freser unit.

After Santanach's (1972a) work, it is widely accepted that the Upper Ordovician succession lies unconformably over either the Jujols or Canaveilles groups (García-Sansegundo and Alonso 1989; Den Brok 1989; Kriegsman et al. 1989; Poblet 1991; Muñoz and Casas 1996; García-Sansegundo et al. 2004; Casas and Fernández 2007). However, the origin of this unconformity has been object of several interpretations. Santanach (1972a) in the Canigó massif and García-Sansegundo et al. (2004) in the Garona dome attributed the Sardic unconformity to basement tilting, related to of a Late Ordovician faulting episode and subsequent erosion. In the Lys-Caillaouas massif, Den Brok (1989) and Kriegsman et al. (1989) proposed the existence of a pre-Variscan deformation event. A pre-Upper Ordovician folding episode has been also suggested as related to the unconformity on the southern Canigó massif (Casas 2010; Casas et al. 2012).

However, the meaning of this deformation episode is unclear: it is related neither to metamorphism nor cleavage development, although it seems related to uplift, widespread emersion and considerable erosion before the onset of Upper Ordovician deposition. As a result, the Upper Ordovician rocks directly onlap different formations of the pre-Sardic succession, ranging from the upper Neoproterozoic to the Lower Ordovician in the Central and Eastern Pyrenees (Santanach 1972a; Laumonier and Guitard 1986; Cirés et al. 1994).

Based on the above-reported maximum depositional age of the Jujols Group (ca. 475 Ma) and the ca. 455 Ma U–Pb age for the Upper Ordovician volcanic rocks directly overlying the Sardic unconformity in the Bruguera unit (Martí et al. 2014), a time gap of about 20 m.y. can be estimated for the Sardic Phase. Similar gaps are found in SW Sardinia (ca. 18 m.y.), the type area where the original unconformity was described, where the discontinuity is constrained by well-dated Upper Ordovician metasediments overlying upper Tremadoc-lower Floian(?) strata (Barca et al. 1987; Pillola et al. 2008).

The Sardic uplift (whatever its origin) was necessarily followed by a succession of Late Ordovician extensional pulsations, which preceded and were contemporaneous with the opening of grabens and half-grabens infilled with the alluvial-to-fluvial Rabassa Conglomerate Formation. At outcrop scale, a synsedimentary hydrothermal activity is associated with the onset of decametre-sized normal faults lined with quartz veins and dykes, which subsequently feed the Rabassa conglomerates as vein quartz pebbles (Fig. 8.4 e–g). At cartographic scale, a detailed geological map of the La Cerdanya area reveals a set of normal faults sharply affecting the thickness of the Rabassa and Cava formations (Fig. 8.6) (Casas and Fernández 2007; Casas 2010; Puddu and Casas 2011). The faults are steep and currently exhibit broad N-S to NNE-SSW trending. In most cases, their hangingwall is the eastern block despite the presence of some antithetic faults; maximum throws of about 0.2–0.9 km can be recognized. Displacement progressively diminishes upward and fades out in the Cava rocks (Fig. 8.6). Based on these orientations, an E-W extension (in present day coordinates) can be proposed. The original orientation of the faults cannot be pinpointed owing to subsequent deformation events, although an original N-S orientation can be proposed. This orientation probably prevented the faults from being inverted during subsequent Variscan and Alpine deformation events, although the faults probably suffered rotations on horizontal E-W axes during these deformation episodes. On the other hand, sharp variations in the thickness of the Upper Ordovician succession have been reported by several authors (Llopis Lladó 1965; Hartevelt 1970; Speksnijder 1986). Hartevelt (1970) documented variations from 200 to more than 850 m in the thickness of the Cava Formation: e.g., eastward from La Seu d'Urgell, the thickness of the Rabassa and Cava formations attain more than 800 m before sharply diminishing to some tens of metres within a few kilometres (Casas and Fernández 2007). There, the maximum observed thickness occurs associated with the maximum grain size of the conglomerates (pebbles exceeding 50 cm in diameter are common). Variations in thickness and grain size can be attributed to palaeorelief formation controlled by fault activity and subsequent erosion of uplifted palaeotopographies, with subsequent infill controlled by alluvial fan and fluvial deposition.

A set of roughly E-W oriented normal faults originally limited the Ribes de Freser, El Baell and Bruguera units, nucleated the contemporaneous active volcanism reported in the Ribes de Freser and Bruguera units, and the high patterns

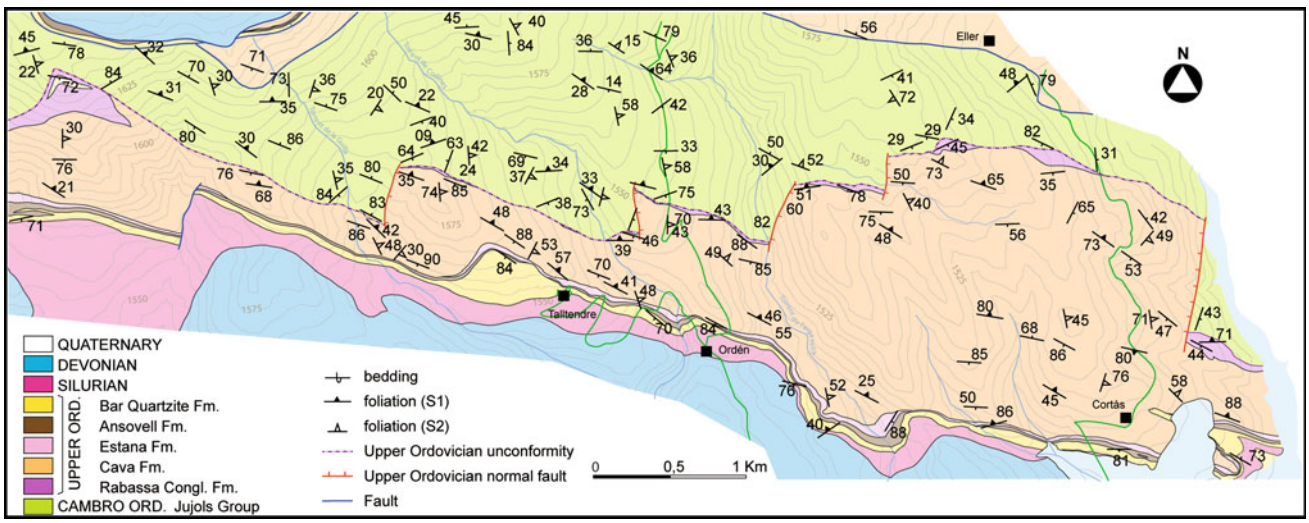

Fig. 8.6 Geological map of the Talltendre area, north of Bellver de Cerdanya; modified from Puddu and Casas (2011). See location on Fig. 8.1

of Katian carbonate productivity on an unstable epeiric platform, now preserved in the El Baell unit. These E-W oriented faults seemingly coexisted with the aforementioned N-S normal faults. The former faults were probably inverted during subsequent Variscan and Alpine tectonics, whereas the latter ones, because of their unfavourable orientation, are preserved and currently recognizable.

8.4 Ordovician Magmatism

J. J. Álvaro, J. M. Casas, C. Puddu, T. Sánchez-García, M. Navidad, P. Castiñeiras, M. Liesa

Successive Ordovician magmatic pulsations are well documented in the pre-Variscan basement of the Pyrenees (Fig. 8.1). According to radiometric data, magmatism lasted about 30 m.y., from ca. 477 to 446 Ma. Although the magmatic activity seems to be continuous, two peaks can be distinguished at 473–472 Ma and 457 Ma (Fig. 8.7). Based on geochronological and geochemical data, two different magmatic complexes can be distinguished: latest Early-Mid Ordovician and Late Ordovician in age.

(i) *Latest Early and Mid Ordovician magmatism*

During Early to Mid Ordovician times, the magmatic activity gave rise to the intrusion of voluminous aluminous granites, about 500–3000 m in size and emplaced into the Canaveilles and Jujols strata. They constitute the protoliths of the large laccolithe-shaped, orthogneissic bodies that crop out at the core of the domal massifs that punctuate the backbone of the Pyrenees. These are, from west to east, the Aston (470 ± 6 Ma, Denèle et al. 2009; 467 ±2 Ma, Mezger and Gerdes 2016), Hospitalet (472 ± 2 Ma, Denèle et al. 2009), Canigó (472 ± 6 to 467 ± 7 Ma, Cocherie et al. 2005), Roc de Frausa (477 ± 4 Ma, Cocherie et al. 2005; 476 ± 5 Ma, Castiñeiras et al. 2008) and Albera (470 ± 3 Ma, Liesa et al. 2011) massifs (Fig. 8.8), which exhibit a dominant Floian-Dapingian age. It should be noted that only a minor representation of basic coeval magmatic rocks are exposed (e.g., Cortalet metabasite). The acidic volcanic equivalents have been reported in the Albera massif, where subvolcanic rhyolitic porphyroid rocks yielded similar ages than those of the main gneissic bodies: 465 ± 4, 472 ± 3, 473 ± 2 and 474 ± 3 Ma (Liesa et al. 2011; Liesa unpubl.). Other acidic products are represented by the rhyolitic sills of Pierrefite (Calvet et al. 1988) (Fig. 8.8). Granites are medium to coarse grained and exhibit porphyritic textures with rapakiwi K-feldspars.

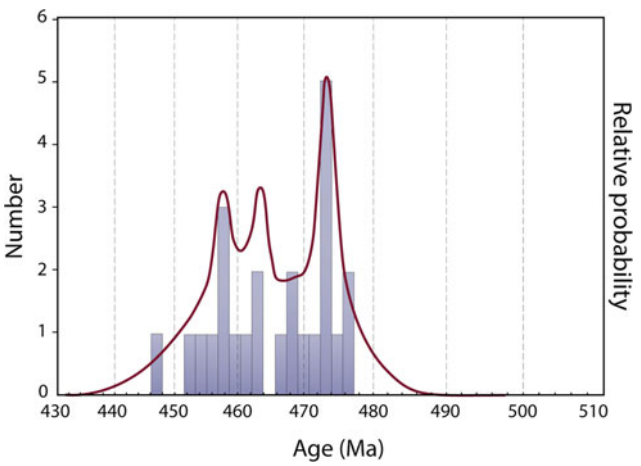

Fig. 8.7 Relative probability plot of the geochronological ages of the Ordovician magmatism of the Pyrenees. Data after Deloule et al. (2002); Cocherie et al. (2005); Castiñeiras et al. (2008); Denèle et al. (2009); Casas et al. (2010); Liesa et al. (2011); Martínez et al. (2011); Mezger and Gerdes (2016); Navidad et al. (2018) and Liesa et al. (unpublsh.). n = 25

The rocks selected for geochemical analysis have suffered from variable degrees of metamorphism and hydrothermalism, so only the most inmobiles elements have been taken into account. We have differentiated three geochemical assemblages: the Cortalets metabasite, the Volcanic Assemblage A and the Gneissic Assemblage A. Some of the differentiated assemblages are based on very few samples and further sampling could modify the geochemical signature documented below.

The Cortalets metabasite (Metabas A in Fig. 8.9) shows low silica content (43.22%) and high FeO_t (10.05), MgO (9.43%) and CaO (12.16%) values. It is metaluminous (A/CNK = 0.64) and subalkaline in the Pearce's diagram (1996) (Fig. 8.9a). REE patterns present slightly more fractionated values for LREE (La_n/Sm_n = 1.54) than HREE (Gd_n/Yb_n = 1.19), without Eu anomalies and an almost flat arrangement for HREE (Fig. 8.10a). This suggests the lack of plagioclase fractionation and garnet in the melt. Nb, Sr and Ti positive anomalies are distinct in the spider-diagram of Palme and O'Neil (2004) (Fig. 8.10b) reflecting the possible influence of mantle-derived magmas lacking plagioclase and magnetite in the melt. The metabasite exhibits average values of La/Nb, (average = 0.54), Th/Nb (0.06), Th/La (0.12), Nb/Y (0.60), Zr/Nb (5.89) and Nb/Yb (5.81) close to the Lower Continental Crust parameters of Rudnick and Gao (2004), and Th/Yb (average = 0.37) values close to the Ocean Island Basalt of Sun and McDonough (1989) (Fig. 8.11a). In the Wood's (1980) tectonic discrimination diagram, the analysis plots in the arc-basalt domain (Fig. 8.12a), while the Pearce's (2008) diagram informs about crustal contamination (Fig. 8.12b). The TiO_2/Yb versus Nb/Yb diagram (Fig. 8.12c) shows E-MORB character. All geochemical characteres may reflect primitive mantle-derived melts with crustal contamination at their origin. Further samples are necessary to confirm this interpretation.

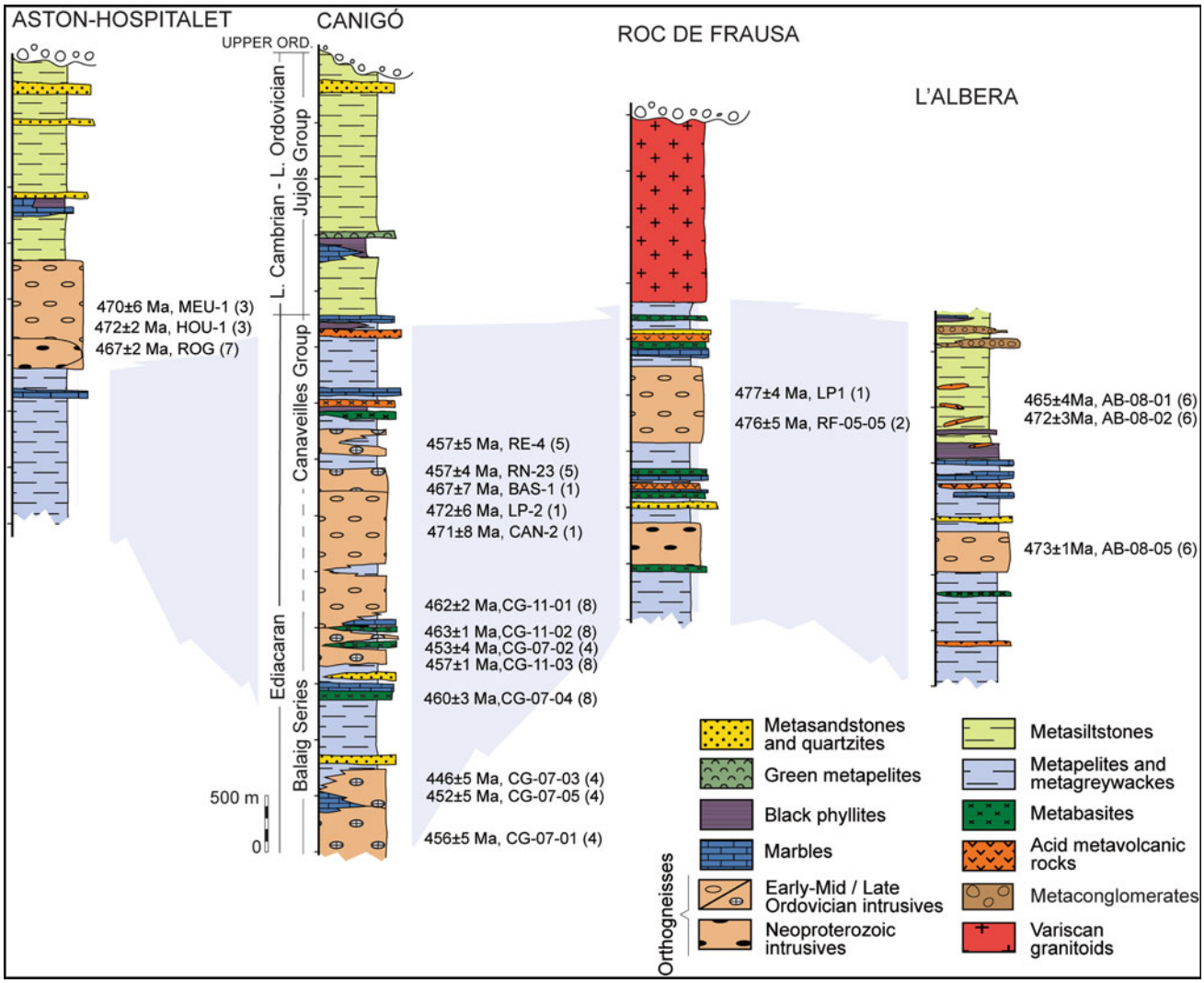

Fig. 8.8 Synthetic stratigraphic logs of the pre-Upper Ordovician rocks from the Aston-Hospitalet, Canigó, Roc de Frausa and Albera massifs with the location of the geochronological data of the protoliths of the Ordovician gneisses: (1) Cocherie et al. (2005); (2) Castiñeiras et al. (2008); (3) Denèle et al. (2009); (4) Casas et al. (2010); (5) Martínez et al. (2011); (6) Liesa et al. (2011); (7) Mezger and Gerdes (2016) and (8) Navidad et al. (2018). Stratigraphic data from Guitard (1970), Santanach (1972b), Ayora and Casas (1986), Liesa and Carreras (1989) and Liesa et al. (2011)

The Volcanic Assemblage A includes 6 samples from the Albera (Liesa et al. 2011) and Pierrefite (Calvet et al. 1988) massifs. They show a narrow range of SiO_2 content ($70.09 < SiO_2 < 74.87$) and peraluminous (A/CNK = 2.03 − 1.12) and subalkaline features, with an average content of Nb/Y = 0.32 (Fig. 8.9a). REE patterns present more fractionated values for LREE ($La_n/Sm_n = 2.63$) than HREE ($Gd_n/Yb_n = 1.32$) being $(La/Yb)_n = 5.88$. The average Eu anomalies show moderate negative values (0.68) reflecting plagioclase crystallization (Fig. 8.10c). It should be noted that this assemblage presents two subsets, one with a distinct enrichment in HREE and a flat slope, and another with a moderate slope in HREE. This suggests different magmatic sources for both subsets. In the spider-diagram of Palme and O'Neil (2004), they show negative anomalies of Nb, Sr and Ti (Fig. 8.10d). The overall chondrite-normalized pattern is close to the values of the Upper Continental Crust of Rudnick and Gao (2004), and display slight enrichments in Th/Nb (average = 1.13) and Th/La (average = 0.56), and depletion in La/Nb (average = 2.43), Th/Yb (average = 3.50) and Nb/Yb (average = 3.06) ratios close to EMORB values (3.5 values of Sun and McDonough 1989) (Fig. 8.11b). In the tectonic diagram of Pearce et al. (1984), the samples plot in the volcanic arc-I type field (Fig. 8.13a). In the Zr versus TiO_2 diagram of Syme (1998), they plot in the arc association (Fig. 8.13b). No εNd values are yet available for this

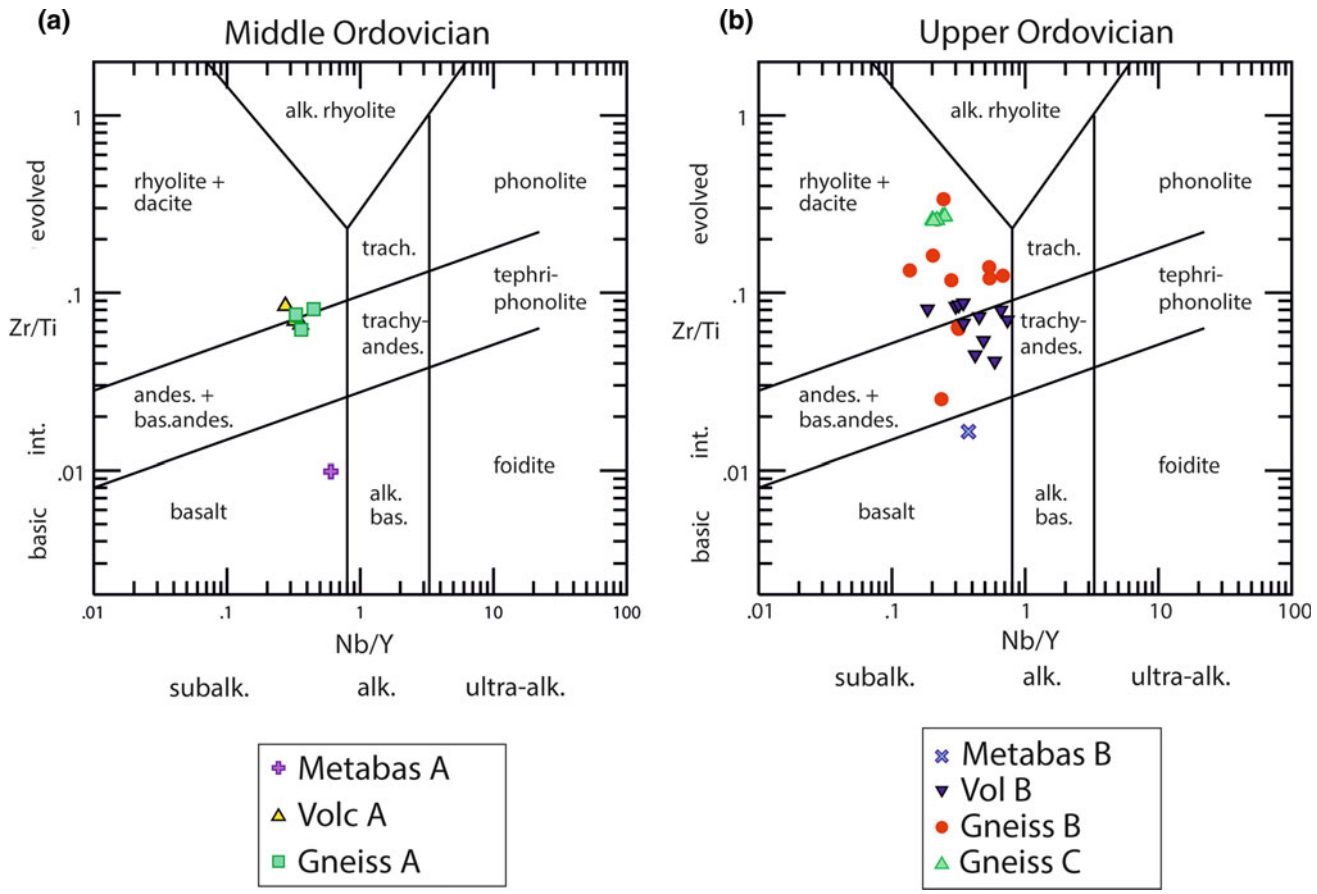

Fig. 8.9 Zr/Ti versus Nb/Y diagram (Pearce 1996). **a** Uppermost Lower-Middle Ordovician rocks; **b** Upper Ordovician rocks (data after Robert and Thiébaut 1976; Calvet et al. 1988; Castiñeiras et al. 2008; Navidad et al. 2010; Liesa et al. 2011; Navidad et al. 2018)

assemblage. All these geochemical data suggest a calc-alkaline magmatic source from active margin environments related to the first stages of extension, as pointed out by Calvet et al. (1988).

The Gneissic Assemblage A includes 4 samples of the Roc de Frausa (Castiñeiras et al. 2008), Albera (Liesa et al. 2011) and Canigó (Navidad et al. 2018) massifs. They show SiO_2 contents ranging between 67.17 and 73.62%. They are peraluminous (A/CNK = 1.20 − 1.10) and subalkaline, with an average content of Nb/Y = 0.37 (Fig. 8.9a). REE patterns present more fractionated values for LREE (La_n/Sm_n = 3.13) than for HREE (Gd_n/Yb_n = 1.43) being $(La/Yb)_n$ = 6.52. The average Eu anomalies show moderate negative values (0.39) reflecting plagioclase crystallization (Fig. 8.10c). In the spider-diagram of Palme and O'Neil (2004), they show negative anomalies of Nb reflecting crustal magmas, Sr and Ti (Fig. 8.10d) suggesting fractionation of plagioclase and Fe–Ti oxides, respectively. The overall chondrite-normalized pattern is close to the values of the Upper Continental Crust of Rudnick and Gao (2004), with slight enrichment in the Th/Nb (average = 1.13) and Th/La (average = 0.56) ratios, and depletion in the La/Nb (average = 2.43), Th/Yb (average = 3.50) and Nb/Yb (average = 3.06) ratios close to EMORB values (3.5 values of Sun and McDonough 1989) (Fig. 8.11b). In the tectonic diagram of Pearce et al. (1984), the samples plot in the volcanic arc-I type field (Fig. 8.13a), whereas in the Zr versus TiO_2 diagram of Syme (1998) they plot in the arc association (Fig. 8.13b). No εNd values are available for this assemblage. All the geochemical characters outlined above indicate that they are similar to the above-reported volcanic assemblage, so these rocks were mainly derived from a continental crustal source. Navidad et al. (2010) suggested that crustal recycling would account for the volcanic arc signature of these samples. This signature was probably inherited by melting of a pre-existing Neoproterozoic-Lower Palaeozoic calc-alkaline crust.

(ii) *Late Ordovician magmatism*

A Late Ordovician magmatic pulse yielded a varied suite of magmatic rocks. Small granitic bodies are emplaced in the Canaveilles and Jujols strata of the Canigó massif and constitute the protoliths of the Cadí, Casemí and Núria

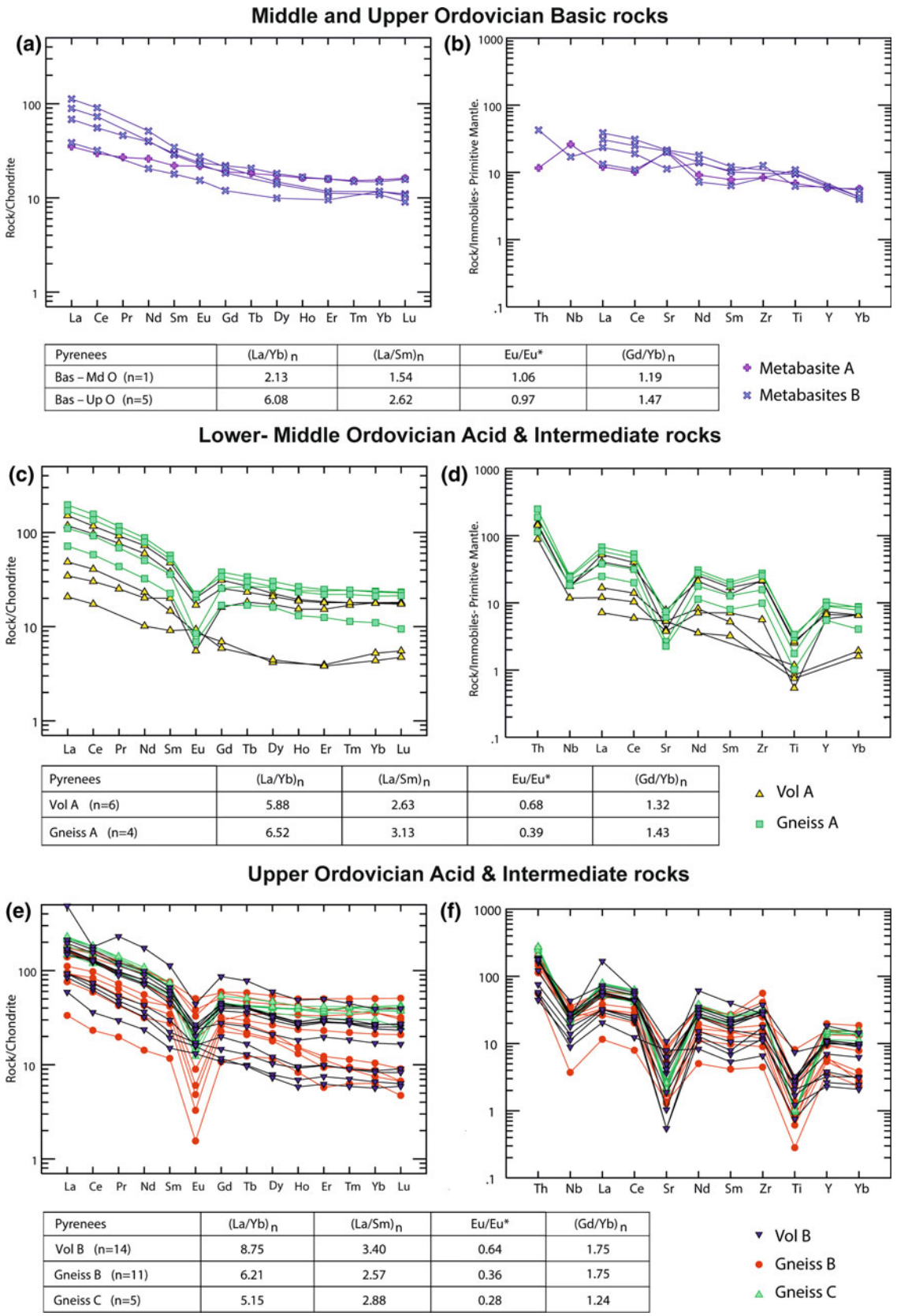

Pyrenees	$(La/Yb)_n$	$(La/Sm)_n$	Eu/Eu*	$(Gd/Yb)_n$
Bas – Md O (n=1)	2.13	1.54	1.06	1.19
Bas – Up O (n=5)	6.08	2.62	0.97	1.47

Pyrenees	$(La/Yb)_n$	$(La/Sm)_n$	Eu/Eu*	$(Gd/Yb)_n$
Vol A (n=6)	5.88	2.63	0.68	1.32
Gneiss A (n=4)	6.52	3.13	0.39	1.43

Pyrenees	$(La/Yb)_n$	$(La/Sm)_n$	Eu/Eu*	$(Gd/Yb)_n$
Vol B (n=14)	8.75	3.40	0.64	1.75
Gneiss B (n=11)	6.21	2.57	0.36	1.75
Gneiss C (n=5)	5.15	2.88	0.28	1.24

Fig. 8.10 Geochemical features; **a** chondrite-normalized REE patterns for basic Middle and Upper Ordovician rocks; **b** spider-diagram for basic Middle and Upper Ordovician rocks; **c** chondrite-normalized REE patterns for acid and intermediate Middle Ordovician rocks; **d** spider-diagram for acid and intermediate Middle Ordovician rocks **e** chondrite-normalized REE patterns for acid and intermediate Upper Ordovician rocks; **f** spider-diagram for acid and intermediate Upper Ordovician rocks. (Chondrite normalizing values of Sun and McDonough 1989 and Primitive Mantle normalizing values of Palme and O'Neil 2004)

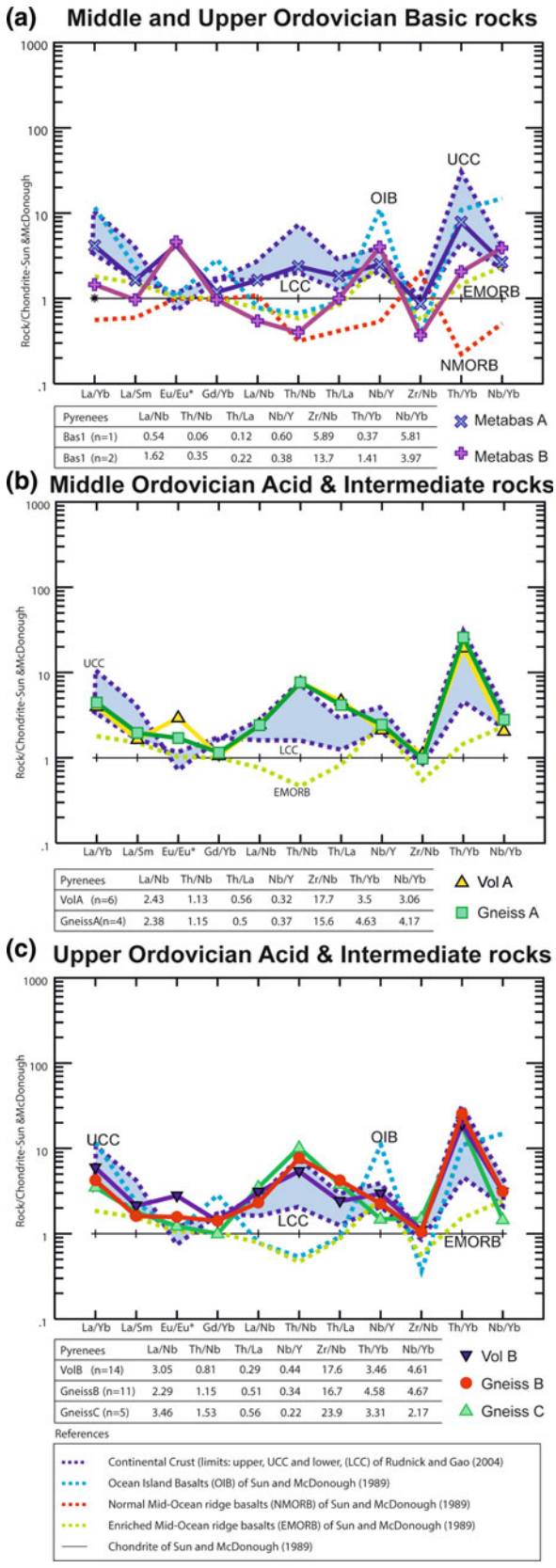

Fig. 8.11 Chondrite-normalized isotope ratios patterns (Sun and McDonough 1989). **a** mafic Middle and Upper Ordovician rocks; **b** acid and intermediate Middle Ordovician rocks; **c** acid and intermediate Upper Ordovician rocks. Blue area: Continental crust values of Rudnick and Gao (2004)

gneisses. The Cadí gneiss (Guitard 1970), dated at 456 ± 5 Ma by Casas et al. (2010), is an aluminous metagranite body with petrographic characteristics similar to those of the Canigó gneiss; it represents the lowest structural unit recognized in the Canigó massif (Fig. 8.8). The Casemí gneiss (Guitard 1970) is a tabular body up to 1000 m thick mainly made up of fine-grained biotitic and amphibolic granitic gneisses. Geochronological data indicate a Late Ordovician age for the protolith of this orthogneiss (446 ± 5 and 452 ± 5 Ma Ma, SHRIMP U–Pb in zircon, Casas et al. 2010). In the southern Canigó massif, the protoliths of the Núria granitic gneiss and the homonymous augen gneiss (Santanach 1972b) also yield Late Ordovician ages (457 ± 4 and 457 ± 5 Ma, respectively, Martínez et al. 2011). Moreover, metre-scale thick bodies of metadiorite are interlayered in the micaschists of the Balaig series, which has also yielded a Late Ordovician age for the formation of its protolith (453 ± 4 Ma, SHRIMP U–Pb in zircon, Casas et al. 2010) (Fig. 8.8).

Coeval calc-alkaline volcanic rocks (ignimbrites, andesites and volcaniclastic rocks) are interbedded in the Upper Ordovician of the Ribes de Freser and Bruguera units. The lower part of the Ribes de Freser unit is made up of dioritic bodies and volcaniclastic rocks, whereas rhyolitic lava flows and ignimbrites predominate in the central part, and ash levels, ignimbrites and volcaniclastic rocks constitute its upper part. The Ribes granophyric body, dated at 458 ± 3 Ma by Martínez et al. (2011), crops out at the base of the Upper Ordovician. On the other hand, the rhyolitic ignimbrites and andesitic lavas of the Bruguera unit have been recently dated at ca. 455 Ma by Martí et al. (2014). This volcanism was mainly explosive and displays a calc-alkaline affinity (Martí et al. 1986). Based on their geochemical data, we have differentiated four Upper-Ordovician magmatic assemblages: the metabasites B, the Volcanic Assemblage B and the Gneissic Assemblages B and C.

The metabasites B include 5 samples of the Marialles diorite (Navidad et al. 2010) and the alkali-pillow basalts of the Pierrefite massif (Calvet et al. 1988). They are undersaturated with SiO_2, whose content ranges from 47.3 to 52.4 wt%. Most of them are metaluminous (average A/CNK ratio = 0.98), although a sample (25-1) from the Pierrefite massif presents a value of 1.47. In the Pearce's diagram (1996), the assemblage plots in the subalkaline field (Fig. 8.9b), whereas the Pierrefite samples are alkaline in the Shervais (1982) diagram with Ti/V values = 100 to 50. The REE patterns present more fractionated values for LREE (La_n/Sm_n = 2.62) than HREE (Gd_n/Yb_n = 1.47), without Eu anomalies and higher slopes that the Cortalets metabasites (Fig. 8.10e) suggesting little plagioclase fractionation. Most of them show Nb, Sr and Ti negative anomalies in the spider diagram of Palme and O'Neil (2004) (Fig. 8.10b). This

assemblage displays a different behaviour in the La/Nb, Th/Nb, Th/La, Zr/Nb (depleted) and Nb/Y (enriched) ratios that the Cortalet metabasite. The Th/La, Zr/Nb and Th/Yb values are close to the Ocean Island basalts of Sun and McDonough (1989), while the Nb/Y value is close to the Upper Continental Crust of Rudnick and Gao (2004), and the Th/Nb ratio is close to the NMORB values of Sun and McDonough (1989) (Fig. 8.11a). In the tectonic discrimination diagram of Wood (1980), this assemblage plots in the Ocean Island Basalts domain (Fig. 8.12a), in the Pearce's (2008) diagram in the MORB array (Fig. 8.12b), and in the TiO_2/Yb versus Nb/Yb diagram (Fig. 8.12c) the dataset shows a distinct E-MORB character. The Sm–Nd isotopic data obtained from the Marialles sample are given in Table 8.1 and plotted in Fig. 8.14. The reference age considered for the emplacement of the Marialles diorite is 453 Ma (Navidad et al. 2010). The analysed sample shows a $^{147}Sm/^{144}Nd$ ratio of 0.1474, slightly negative εNd values (−0.8) and a TDM age of 1.18 Ga. This value could indicate that their protoliths were derived from mantle melts with heterogeneous crustal contamination (Navidad et al. 2010). In summary, the geochemical data discussed above could reflect a more primitive origin mantle-derived but with crustal contamination at their origin.

The Volcanic Assemblage B includes 14 samples from the Els Metges volcanic tuffs, Les Gavarres epiclastic ash (Navidad et al. 2010) and the Ribes de Freser rhyolitic lavas (Robert and Thiébaut 1976). Although no geochemical data are available, we suggest including in this assemblage the Bruguera volcanic rocks due to their similar field characteristics. This assemblage shows a SiO_2 content ranging between 86.06 and 62.98%. They are peraluminous (A/CNK = 3.63 − 1.04) and subalkaline, with an average content of Nb/Y = 0.44 (Fig. 8.9b). REE patterns present more fractionated values for LREE (La_n/Sm_n = 3.40) than HREE (Gd_n/Yb_n = 1.75) being $(La/Yb)_n$ = 8.75. The average Eu anomalies show negative values (0.64) reflecting plagioclase crystallization (Fig. 8.10e). In the spider-diagram of Palme and O'Neil (2004), they show negative anomalies of Nb, Sr and Ti (Fig. 8.10f). Overall chondrite-normalized pattern are close to the values of the Upper Continental Crust of Rudnick and Gao (2004), with slight enrichment in the La/Nb (average = 3.05) and Zr/Nb (average = 17.6) ratios, and depletion in the Th/Nb (average = 0.81), Th/La (average = 0.29), Nb/Y (average = 0.44), Th/Yb (average = 3.46) and Nb/Yb (average = 4.61) ratios (Fig. 8.11c). In the tectonic diagram of Pearce et al. (1984), most of samples plot in the volcanic arc-I type field and the anomalous rift field (Fig. 8.13c). In the Zr versus TiO_2 diagram of Syme (1998), most of samples plot in the arc association (Fig. 8.13d). The volcanic tuffs of Les Gavarres show an $^{147}Sm/^{144}Nd$ isotope ratio ranging between 0.1410 and 0.1372 and εNd between −5.1 and −4.8, indicating a crustal origin (Navidad et al. 2010). Similar isotopic values have been obtained by Martínez et al. (2011) for the Ribes granophyre (εNd −2.6) indicating also a crustal origin.

The Gneissic Assemblage B includes 11 samples from the Canigó and Cadí gneisses, (Canigó massif, Navidad et al. 2010; Navidad et al. 2018). Although no geochemical data are available, we suggest including here the Núria gneisses. The assemblage shows a SiO_2 content between 76.42 and 56.47%. The samples are peraluminous (A/CNK = 1.24 − 0.64) and subalkaline, with an average content of Nb/Y = 0.34 (Fig. 8.9b). REE patterns present more fractionated values for LREE (La_n/Sm_n = 3.13) than HREE (Gd_n/Yb_n = 1.43) being $(La/Yb)_n$ = 6.38. The average Eu anomalies show moderate negative values (0.36) reflecting plagioclase crystallization (Fig. 8.10e). In this assemblage, two subsets can be distinguished, one with flat slope and another with negative slope. This could indicate two different magmatic sources. In the spider-diagram of Palme and O'Neil (2004), they show negative anomalies of Nb, Sr and Ti (Fig. 8.10f). The overall chondrite-normalized pattern is close to the values of the Upper Continental Crust of Rudnick and Gao (2004), with a slight enrichment in the Th/Nb (average = 1.15), Th/La (average = 0.51) and Zr/Nb (average = 16.7) ratios and depletion in the La/Nb (average = 2.29) and Th/Yb (average = 4.58) values. The Nb/Y (average = 0.34) value is close to the Lower Continental Crust of Rudnick and Gao (2004) (Fig. 8.11c). In the tectonic diagram of Pearce et al. (1984), the samples plot in the volcanic arc-I type field and the anomalous rift field (Fig. 8.13c). In the Zr versus TiO_2 diagram of Syme (1998), the samples plot both in the arc association (Fig. 8.13d) and the extensional field. The Cadí orthogneisses show a Nd isotope ratio (0.5118) similar to the most differentiated assemblage (Casemí, Gneissic Assemblage C; see below) and a higher negative isotopic signature with εNd negative values (−4.2 to −5.2) (Fig. 8.14) than these gneisses (Gneissic Assemblage C) suggesting a crustal origin (Navidad et al. 2010). Similar isotopic values have been obtained by Martínez et al. (2011) for the Núria gneisses (εNd between −3.0 and −4.7). All the geochemical characters outlined above indicate that this assemblage was mainly derived from different magmas of continental crustal source.

The Gneissic Assemblage C includes 5 samples from the Casemí and Canigó gneisses (Canigó massif, Navidad et al. 2010). They present more silica and alkalis and less Al, Fe and Mg than the Gnesissic Assemblage B. They show a narrow range of composition (73.62% < SiO_2 < 75.02%) and are peraluminous (A/CNK = 1.24 − 0.64) and subalkaline, with an average content of Nb/Y = 0.22 (Fig. 8.9b). The REE pattern is similar to the subset with flat slope of HREE in the Gneissic Assemblage B, with more fractionated

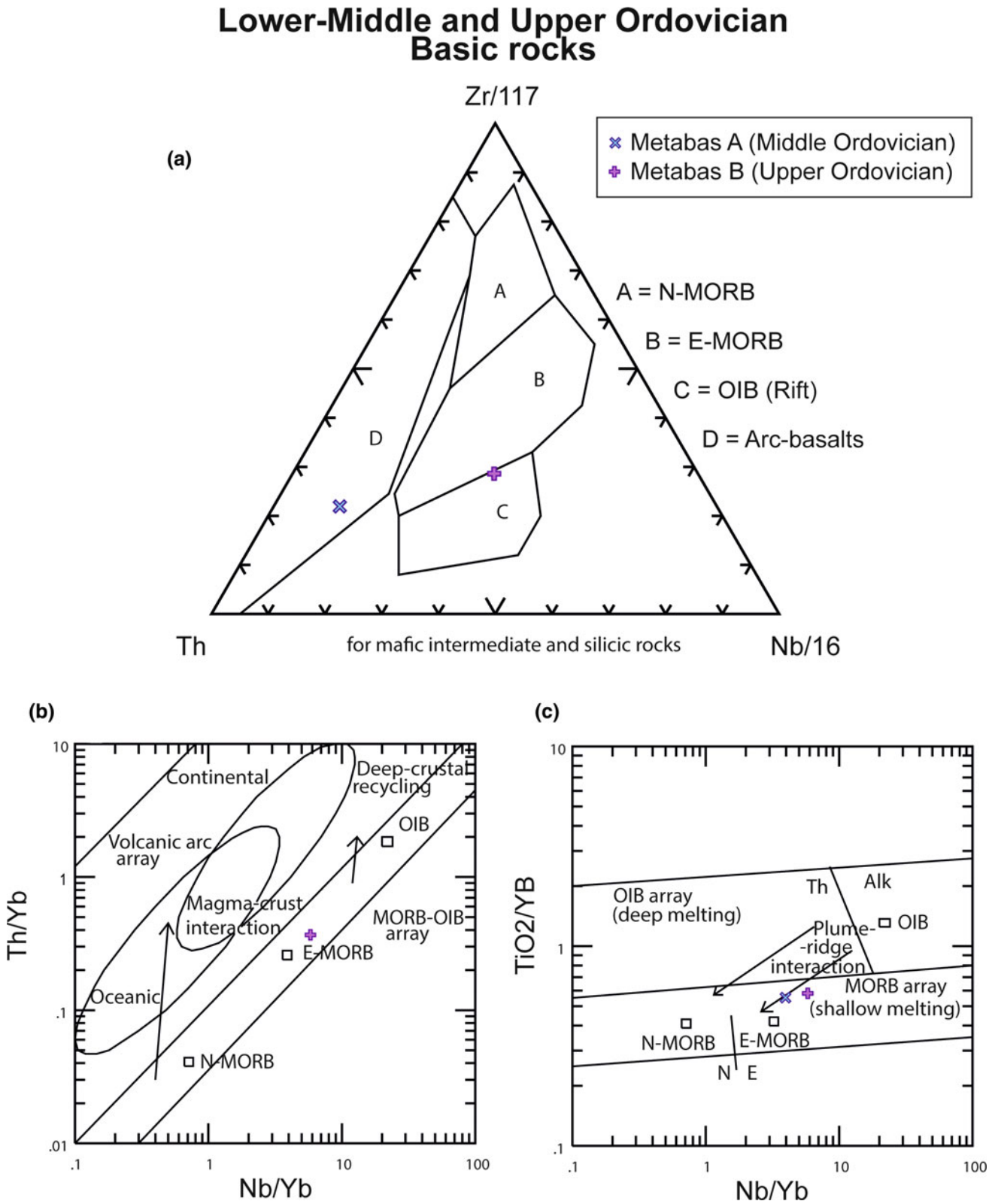

Fig. 8.12 Tectonic discriminating diagram of basic rocks. **a** Wood (1980); **b** Th/Yb versus Nb/Yb of Pearce (2008); **c** TiO_2/ Yb versus Nb/Yb of Pearce (2008)

Table 8.1 Sr–Nd isotopic data of the Upper Ordovician magmatic rocks of the Pyrenees (data after Navidad et al. 2010 and Martínez et al. 2011). (Bas B: Metabasites B; Gneiss B: Gneisssic Assemblage B; Gneiss C: Gneisssic Assemblage C; Vol B: Volcanic assemblage B)

Sample	Unit rock	Litology	Sm	Nd	$^{147}Sm/^{144}Nd$	$^{143}Nd/^{144}Nd$	$^{143}Nd/^{144}Nd_{age}$	eNd_0	eNd_{age}	Age (Ma)	Tdm (Ga)	$(^{87}Sr/^{86}Sr)_0$	$(^{87}Sr/^{86}Sr)_{age}$	Author
CG-07-02a	Marialles (Bas B)	Diorite	4.51	18	0.1508	0.51246	0.512014	−3.5	−0.6	453	1.18	0.736385	0.731345	2
C96767aQ2	Canigó (Gneiss B)	Bt orthogneiss	10.45	47	0.1338	0.5123	0.511909	−6.6	−3	445.9	1.41	0.770513	0.660161	2
CG-07-01a	Cadí (Gneiss B)	Orthogneiss	7.3	34	0.1292	0.51223	0.511841	−8	−4.2	456.1	1.47	0.736385	0.708542	2
100768	Canigó (Gneiss B)	Amph. orthogneiss	11.3	48	0.1417	0.51236	0.511941	−5.5	−2.3	445.9	1.45	0.720992	0.707661	2
100786	Canigó (Gneiss B)	Bt orthogneiss	6.41	22	0.1754	0.51239	0.511878	−4.8	−3.5	445.9	2.63	0.817270	0.690857	2
C-96940F	Canigó (Gneiss B)	Amph. orthogneiss	11.57	47	0.1482	0.51238	0.51195	−5	−2.2	445.9	1.53	0.720939	0.708524	2
C-770288	Canigó (Gneiss B)	Amph. orthogneiss	11.46	43	0.1604	0.51233	0.51186	−6	−4	445.9	2.04	0.718292	0.709528	2
RE-2	Núria (Gneiss B)	Augen gneiss	7.07	35.1	0.1217	0.51226	0.511901	−7.4	−3	450	1.47	–	–	1
RE-10	Núria (Gneiss B)	Augen gneiss	2.4	9.9	0.1468	0.51231	0.51188	−6.3	−3.5	450	1.9	–	–	1
RN-16	Núria (Gneiss B)	Two-mica gneiss	2.74	10.14	0.1634	0.51234	0.511855	−5.9	−4	450	2.45	–	–	1
RN-26	Núria (Gneiss B)	Two-mica gneiss	6.18	27.13	0.1377	0.51227	0.511865	−7.2	−3.8	450	1.76	–	–	1
RN-27	Núria (Gneiss B)	Two-mica gneiss	0.86	1.88	0.2765	0.51264	0.511825	0	−4.7	450	–	–	–	1
GRF-05-1A	Ribes (Gneiss B)	Granophyre	8.51	37.09	0.1381	0.51233	0.511927	−5.9	−2.6	450	1.66	–	–	1
CG-07-05a	Casemí (Gneiss C)	Bt orthogneiss	11.29	50	0.1359	0.51239	0.511991	−4.8	−1.2	451.6	1.27	0.745438	0.696910	2
CG-07-03a	Casemí (Gneiss C)	Bt orthogneiss	8.36	34	0.148	0.5124	0.511969	−4.6	−1.7	445.9	1.48	0.742716	0.702258	2
100766	Canigó (Gneiss C)	Bt orthogneiss	10.3	44	0.1409	0.51241	0.511998	−4.5	−1.4	445.9	1.32	0.754248	0.706702	2
NF-29a	Les Gavarres (Vol B)	Volcanic tuff	8.67	37	0.141	0.51223	0.511806	−8	−4.8	455.2	1.71	0.733067	0.703181	2
NF-32	Les Gavarres (Vol B)	Volcanic tuff	7.75	34	0.1372	0.51221	0.511802	−8.3	−4.9	455.2	1.65	0.726113	0.707025	2
NF-63	Les Gavarres (Vol B)	Volcanic tuff	8.57	37	0.1394	0.51221	0.511789	−8.4	−5.1	455.2	1.71	0.729263	0.705315	2

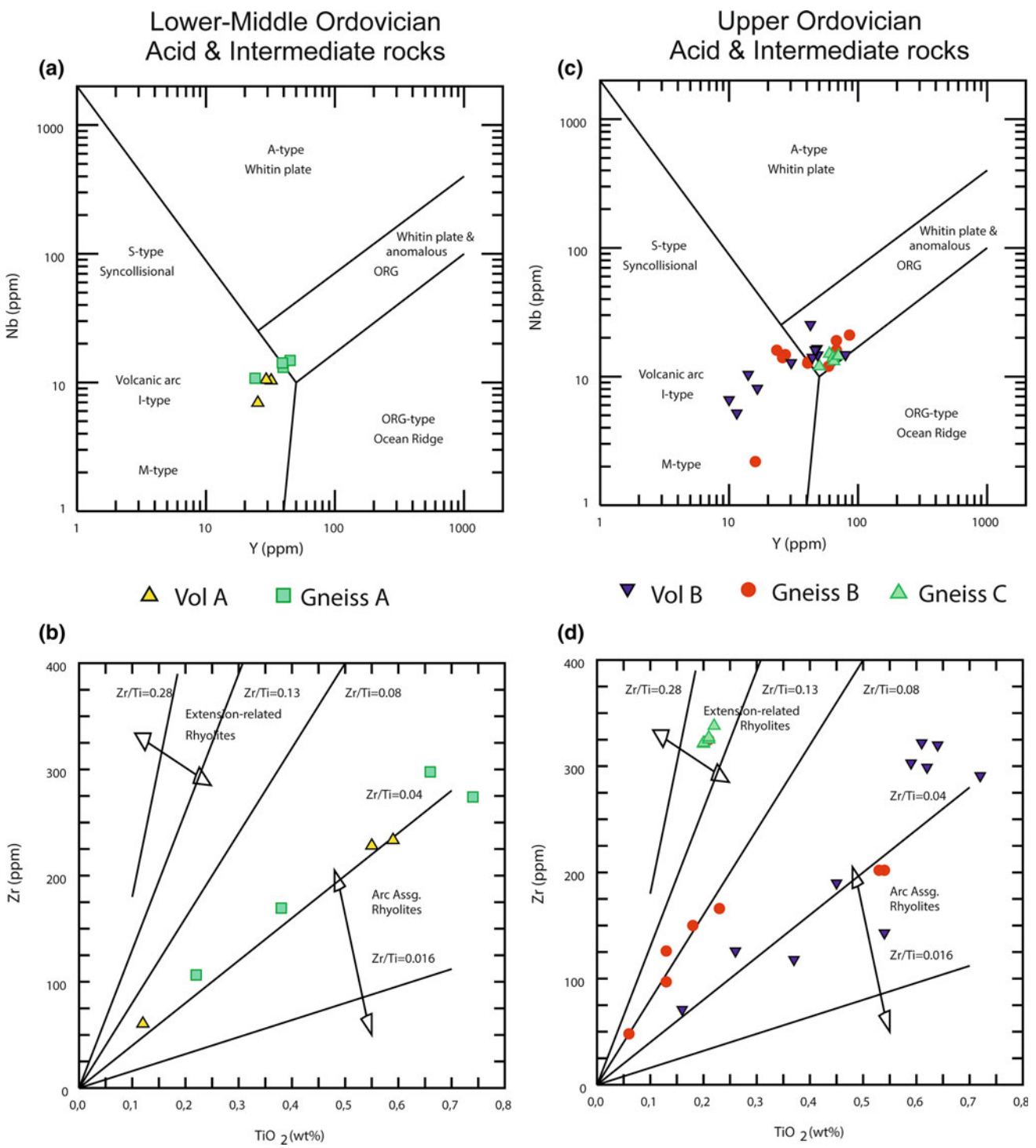

Fig. 8.13 Tectonic discriminating diagram of acid and intermediate rocks. **a** and **c** Y versus Nb diagram (Pearce et al. 1984); **b** and **d** Zr versus TiO_2 diagram (Syme 1998)

values for LREE (La_n/Sm_n = 3.13) than HREE (Gd_n/Yb_n = 1.43), being $(La/Yb)_n$ = 6.38. The average Eu anomalies show moderate negative values (0.36) reflecting plagioclase crystallization (Fig. 8.10e). In the spider-diagram of Palme and O'Neil (2004), they show negative anomalies of Nb, Sr and Ti (Fig. 8.10f). Overall chondrite-normalized pattern close to the values of the Upper Continental Crust of Rudnick and Gao (2004) values with slight enrichment in the Th/Nb (average = 1.15), Th/La (average = 0.51) and Zr/Nb (average = 16.7) and depletion in the

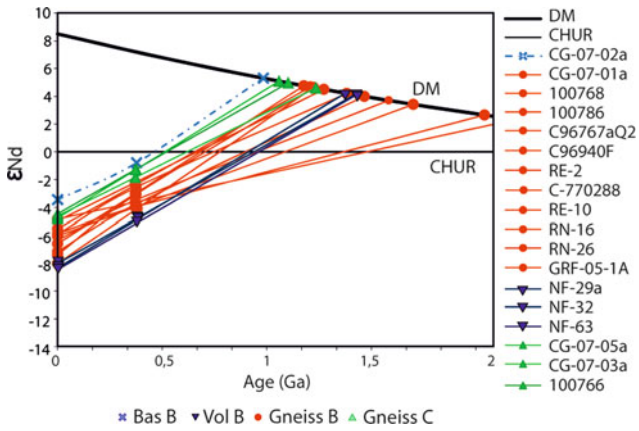

Fig. 8.14 εNd versus age diagram (DePaolo and Wasserburg 1976; DePaolo 1981) for the Upper Ordovician magmatic rocks of the Pyrenees (data after Navidad et al. 2010; Martínez et al. 2011). Depleted mantle evolution calculated according to DePaolo (1981)

La/Nb (average = 2.29) and Th/Yb (average = 4.58) ratios. The Nb/Y (average = 0.34) value is close to the Lower Continental Crust of Rudnick and Gao (2004) (Fig. 8.11c). This suggests a certain degree of crustal contamination and recycling of materials. In the tectonic diagram of Pearce et al. (1984), the samples plot in the volcanic arc-I type field and the anomalous rift (Fig. 8.13c). In the Zr versus TiO_2 diagram of Syme (1998), the data plot in the extensional field (Fig. 8.13d). The initial Nd isotope ratio of the Casemí gneiss ($^{147}Sm/^{144}Nd$ between 0.1480 and 0.1359 and εNd between −1.9 and −1.3) indicates that their protoliths were derived from mantle melts with heterogeneous crustal contamination (Navidad et al. 2010). Castiñeiras et al. (2011) reached similar conclusions on the basis of zircon composition. Despite their different age, the zircons from the Cadí orthogneiss and the Albera gneiss exhibit similar characteristics. The zircon composition suggests that this mineral grew in a melt formed by anatexis of continental crust. In contrast, zircons from the Casemí gneiss and the metadiorite point out that the mantle was involved in the origin of these rocks. Extrapolations of εNd data back to the depleted mantle curve yield TDM values varying between 1.3 and 1.5 Ga (Navidad et al. 2010; Martínez et al. 2011; Fig. 8.14, Table 8.1). The absence of inherited zircons from these ages led the authors to interpret these values as the result of the melting of a Neoproterozoic source mixed with Palaeoproterozoic components.

All geochemical characteristics broadly suggest crustal sources in their parental magmas. According to Navidad et al. (2010), the whole-rock geochemistry shows that the Upper Ordovician orthogneiss of the Canigó massif are compositionally uniform. As fractionation processes cannot be recognized, crustal contamination of mantle melts is the most probable process accounting for the formation of the various geochemical datasets (Casemí biotite and amphibole orthogneisses, and metadiorite).

It should be noted that the latest Early-Mid Ordovician magmatism is coincident with the pre-Late Ordovician episode of uplift and erosion that led to the formation of the Sardic unconformity. Uplift was followed by an extensional pulse that developed normal faults, directly affecting the onset of the basal unconformity and controlling deposition of the (post-Sardic) Upper Ordovician strata and coeval Late Ordovician magmatic activity.

Early and Late Ordovician ages have also been obtained in magmatic bodies from the French Massif Central, such as in the Axial Zone of the Montagne Noire (Somail orthogneiss: 471 ± 4 Ma, Cocherie et al. 2005; Pont de Larn and Gorges d'Heric orthogneisses: 456 ± 3 Ma and 450 ± 6 Ma, Roger et al. 2004; Saint Eutrope gneiss: 455 ± 2 Ma, Pitra et al. 2012). As in the Pyrenees, the emplacement of Late Ordovician felsic granitic bodies is coeval in the Montagne Noire with a tholeiitic volcanic activity originated by melting of mantle and crustal lithosphere and infilling of rifting branches preserved on the southern Montagne Noire (Álvaro et al. 2016). These authors also describe a similar Late Ordovician volcanism in the Mouthoumet massif and relate it to the end of the Sardic Phase and the opening of rift branches linked to those developed on the southern Montagne Noire.

8.5 Correlation with Surrounding Areas and Other Northern Gondwanan Domains

J. J. Álvaro, J. M. Casas, S. Clausen, M. Padel, C. Puddu

To the west of the Canigó massif, the Jujols Group extends as far as the Noguera Pallaresa and Ribagorçana rivers, where the Serdinya Formation may be correlated with the Seo Formation defined by Hartevelt (1970) in the Orri Dome. In the La Pallaresa dome, the La Massana antiform and the western slopes of the Aston and Hospitalet domes, a siliciclastic-dominated succession, more than 4000 m thick, was subdivided into three formations by Laumonier et al. (1996), from bottom to top: the Alós d'Isil, Lleret-Bayau and Alins formations. The Alós d'Isil and Alins formations are dominated by shales, locally alternating with thin- to medium-grained sandstones, and are separated by the metasandstones and marbles of the Lleret-Bayau Formation. Despite the lack of any geochronologic or biostratigraphic control, we suggest that the Pallaressa succession should be correlated with the Jujols Group, being the Alós d'Isil, Lleret-Bayau and Alins triad equivalent to the Err, Valcebollère and Serdinya formations, respectively (Fig. 8.9). In the same way, the Jujols Group may be correlated with

the pre-Sardic rocks of the Garona Dome, which have been subdivided into three terms by García-Sansegundo and Alonso (1989), from bottom to top: the Urets beds, the Bantaillou limestone and the Orlà beds. Again, these terms may be equivalent to the Err, Valcebollère and Serdinya formations, respectively.

In contrast, the Jujols Group cannot be easily recognized in the easternmost Cap de Creus, where some geochronological ages of Cadomian magmatic rocks constrain the depositional ages of the pre-Sardic succession from ca. 570 to 542 Ma. In the Albera massif, alternating layers of metapelites and metapsamites form the uppermost part of a metasedimentary succession that is crosscut by a network of acidic subvolcanic porphyritic dykes, which constrain its minimum depositional age to 465–472 Ma (Liesa et al. 2011). This uppermost part can be tentatively correlated with the Jujols Group, although coarse-grained terms (sandstone and conglomerate) are locally abundant in the Albera massif.

The only Cambrian shelly fossils reported until present in the Pyrenees occur in an Alpine thrust sheet of the Terrades area. Abad (1988) described the presence of archaeocyathan patch reefs, alternating with green to brownish shales in an up to 50 m thick succession, and assigned the sponges to the Cambrian Age 3. A complete taxonomic study by Perejón et al. (1994) confirmed a late Cambrian Age 3. The detailed preservation of pristine microfacies and microbial textures in these limestone strata, contrasting with the traditional marble aspect of any carbonate bed of Cambrian age, is in accordance with the allochthonous provenance of this Alpine thrust slice: the Cambrian limestones of the Salut slice thrust Eocene strata and are, in turn, unconformably overlain by Eocene strata (Pujadas et al. 1989). Biogeographic affinities of the archaeocyaths point to strong similarities with similar assemblages from SW Sardinia (Matoppa Formation of the Nebida Group) (Perejón et al. 1994). A pre-Alpine northward setting, in a lateral prolongation of the archaeocyath-bearing carbonates cropping now in SW Sardinia and southern Montagne Noire, may be envisaged.

Since the pioneer work of Cavet (1957), the Ediacaran-Lower Ordovician succession of the Pyrenees has been traditionally compared to fossiliferous successions from the neighbouring southern Montagne Noire. These lithostratigraphic correlations between both Variscan massifs have remained, up to recently, the main way to interpolate the age of the Canaveilles and Jujols groups (Cavet 1957; Laumonier et al. 1996, 2004). The stratigraphic framework of the Montagne Noire has recently been updated (Álvaro et al. 1998, 2014) and better constrained based on recent chronostratigraphic (Devaere et al. 2013, 2014) and geochronologic studies (Roger et al. 2004; Pitra et al. 2012; Padel et al. 2017). As a result, the Valcebollère Formation and, as suggested above, the Lleret Bayau Formation and the Bentaillou limestone from the Central Pyrenees, can be confidently considered as representative of the characteristic Cambrian Age 3–4 episode of subtropical carbonate production highlighted by the Pardailhan and Lastours formations in the Montagne Noire (Álvaro et al. 2010; Devaere et al. 2014) (Fig. 8.2). The upper part of the Valcebollère Formation (limestone/shale alternations and monotonous shales bearing carbonate centimetre-thick nodules) is lithologically equivalent to the La Tanque-Coulouma transition. A distinct lithological difference between the Eastern Pyrenees and the Montagne Noire is marked by the absence, in the former, of the Guzhangian (regional Languedocian) regression represented by the onset of the Ferrals Formation (Álvaro et al. 2007). This sandstone-dominated formation, representative of prograding shoal complexes, is absent in the Eastern Pyrenees (Fig. 8.2). The regression recorded by the input of sandstones marking the uppermost part of the Serdinya Formation (Font Frède Member) may represent the onset of the early Tremadocian regression marked, in the Montagne Noire, by the La Dentelle Formation.

In SW Sardinia, the 1500–3000 m thick Cambrian-Lower Ordovician succession is subdivided into the Nebida, Gonnesa and Iglesias groups (Pillola 1990). The lower siliciclastic deposits of the Sa Tuvara Member (Matoppa Formation, Nebida Group) should represent a lateral equivalent of the Err (Eastern Pyrenees) and Marcory (Montagne Noire) formations (Fig. 8.2). The upper carbonate and siltstone alternations of the Matoppa Formation have yielded a Cambrian Age 3–4 fauna (Pillola 1990) which was correlated with the Pardailhan Formation of Montagne Noire (Álvaro et al. 2010). The Matoppa Formation is conformably overlain by the Punta Manna Formation, the uppermost heterolithic unit of the Nebida Group. The following Gonnesa Group, mainly composed of massive archaeocyathan-bearing carbonates, is correlatable with the Pardailhan and Lastours formations (Álvaro et al. 2010). The upper part of the Matoppa Formation, the Punta Manna Formation and the Gonnesa Group were deposited during the Cambrian Epoch 2 and are interpreted as lateral equivalents of the Valcebollère Formation and the La Salut thrust slice (Fig. 8.2). The carbonate sequence of the Gonnesa Group is overlain by the Iglesias Group, which begins with the carbonate-shale alternations and/or nodular limestones of the Campo Pisano Formation that can be considered as a lateral equivalent of the Coulouma Formation (Álvaro et al. 2010) and the upper part of the Valcebollère Formation. The Campo Pisano Formation (Cambrian Series 2–3 transition; Pillola 1990) is conformably overlain by the terrigenous rocks of the Cambrian Series 3-Lower Ordovician Cabitza Formation, correlated herein with the Serdinya Formation.

In SW Sardinia, according to Loi et al. (1995), a regressive trend culminating with local coarse-grained sandstones, is recognized in the middle member of the Cabitza Formation (sensu Gandin and Pillola 1985; Pillola

1989), biostratigraphically represented by the so-called CAB-4 fossil assemblage, correlatable with the late Languedocian. This sandy-dominant level might represent the Ferrals regression, but somewhat delayed in time. The Acerocare Regressive Event is proposed close to the Cambrian-Ordovician boundary, which lies at the so-called Cabitza "tubi" part and is directly overlain by the first occurrence of Tremadocian graptolites (CAB-6; Loi et al. 1995). Therefore, the lack of the Guzhangian Ferrals Formation regression in the Eastern Pyrennes, present in the Iberian Peninsula, the Montagne Noire and somewhat diachronous in SW Sardinia, might be related to peneplanation of source areas, unable to yield coarse-grained sediments.

The Sardic unconformity recognized in Sardinia and the Pyrenees could be considered as a correlation element for both areas. Such as the Sardic unconformity, the Upper Ordovician successions that follow this unconformity are broadly comparable. In Sardinia, two post-Sardic sequences have been recognized, reported at the SW and SE of the island. The SW Sardinian sequence starts with a conglomerate-to-sandstone, fining-upward package, followed by a sandy-siltstone succession characterized by two late Katian key-levels: the fossiliferous Portixeddu Formation and the carbonate-dominated Domusnovas Formation. The SE Sardinian sequence starts with conglomeratic deposits and volcanic products of Mid Ordovician age, topped by a terrigenous and volcanoclastic complex characterized by a fossiliferous lower Katian level (Punta Serpeddì Formation), and an upper-Katian key carbonate level, the Tuviois Formation (Fig. 8.2). Based on their lithology, fossil record and age, the SW Sardinian sequence is comparable to the Hartevelt's (1970) sequence of the Eastern Pyrenees, where the Rabassa Conglomerate Formation is the corresponding of the Monte Argentu Formation (Sandbian), the Cava Formation (Katian) represents the Monte Orri (Early Katian) and Portixeddu formations (Late Katian), while the Estana Formation (Late Katian) is the lateral equivalent of the Domusnovas Formation (Late Katian). The Ansovell and Bar formations broadly represent the Rio San Marco counterpart (Hirnantian).

The SE Sardinian sequence could be comparable to that cropping out in the Ribes de Freser area. In the Bruguera unit, the Upper Ordovician volcanites that overlie the Sardic unconformity are similar to the volcanic products that overlie the Sardic unconformity in the SE Sardinian sequence. The basal tuffs of the Ribes de Freser unit may correspond to the volcanites of SE Sardinia that overlie the Sardic unconformity, while the Katian sediments that cover the former tuffs represent the Punta Serpeddì Formation (lower Katian) followed by limestones comparable to the Tuviois Formation. The thickness, facies and fossil record of the limestones in the El Baell unit are different from the two above-reported Sardinian sequences. These limestones could be comparable only in age with the Estana Formation (Eastern Pyrenees), the Domusnovas Formation (SW Sardinia) or the Tuviois Formation (SE Sardinia) (Fig. 8.2).

The south-north, proximal-distal palaeogeographic trend recorded in the Lower Palaeozoic of the eastern Pyrenees is repeated across the Mouthoumet and Axial Zone-southern-northern (proximal-to-distal) Montagne Noire transect. Moreover, the biogeographic affinity displayed by the archaeocyaths of the Alpine Salut thrust sheet, and the comparative analysis of zircon provenance (Padel 2016) point to closer palaeogeographic affinities between the Pyrenees and Sardinia than between the Pyrenees and the Montagne Noire. As a result, in addition to the estimated 150–160 km accumulated in a south-north Alpine displacement of the Pyrenean thrust sheets, other pre-Alpine movements may be envisaged to solve the present-day relationship between the Pyrenees and the Occitan Domain (sensu Álvaro et al. 2016). Dextral shearing along the southern branch of the South Armorican Shear Zone, between 315 and 305 Ma (Martínez Catalán 2012 and references therein), may account for an original westernmost position of the Montagne Noire and the French Central Massif in pre-Variscan, Early Palaeozoic times.

The inner peri-Gondwanan massifs that form the eastern branch of the Variscan Ibero-Armorican Arc (Southern Armorican, Pyrenean and Occitan Domains and lateral prolongation into Corsica and Sardinia) offer a common geodynamic framework during Early Palaeozoic times. They differ from the Iberian Massif (western branch of the same arc) by the absence of Cadomian deformation, the record of Cadomian felsic-dominated volcanic activity crossing the Ediacaran-Cambrian boundary interval, a significant episode of carbonate productivity capping the top of palaeohorsts and volcanosedimentary edifices during Terreneuvian times, the lack of the Toledanian phase (marking the rift/drift transition in parts of the Iberian Peninsula) and the common record of the Sardic phase. The latter is characterized by intrusion of granites in the Pyrenees and the Axial Zone of the Montagne Noire, contemporaneously with the opening of Katian rifting branches and the record of a basaltic-dominated, tholeiitic magmatism in the Mouthoumet and Cabrières klippes (southern Montagne Noire). The palaeorelief generated as a result of the Sardic uplift was succeeded by extensional pulses, tilting, discontinuous erosion of the pre-Sardic basement, and infill of the new palaeorelief with alluvial-to-fluvial deposits, volcanosedimentary complexes and final sealing of the whole palaeotopography during Silurian to Early Devonian times.

The interpretation of the Sardic phase as (i) the onset of a Mid Ordovician arc that developed in North Gondwana as a consequence of subduction of oceanic crust under continental crust (Andean-type convergence; see Di Pisa et al. 1992; Carmignani et al. 2001; Stampfli et al. 2002; Buzzi et al. 2007;

Funedda and Oggiano 2009), (ii) a change from symmetric to asymmetric opening conditions of the Rheic Ocean leading to local crustal fusion, or (iii) the onset of a rift/drift unconformity similar to the Toledanian one recorded in the Iberian massif, is still open to future discussion.

8.6 Silurian, Devonian and pre-Variscan Carboniferous

J. Sanz-López

The Pyrenean successions show a great spatial variation on the distribution of sedimentary facies, particularly during the Devonian, where a plethora of local lithostratigraphic units have been differentiated (Fig. 8.15). Consequently, detailed description and reference to the original studies are here avoided, since it overpasses the subject of this synthesis. It may be found in extended and recent publications (Dégardin 1988; Sanz-López 1995, 2002a, b, 2004; Dégardin et al. 1996; Delvolvé et al. 1996; García-López et al. 1996; Majesté-Menjoulas et al. 1996; García-Alcalde et al. 2002). Sanz-López (2002a, 2004) described several sedimentary domains modifying the previous Devonian facies-area defined in the Pyrenean Axial zone (Mirouse 1966; Mey 1967, 1968; Boersma 1973; Zwart 1979) and the Basque massifs (Heddebaut 1975) (Fig. 8.16). The western margin of the preserved basin is characterized by the occurrence of a sedimentary hiatus between the Ordovician and Upper Devonian rocks (Basque Cinco Villas domain, CVd; Fig. 8.15). The southern margin is interpreted since shallow-water carbonate platforms are located in a southern belt (Fig. 8.16), and siliciclastic systems were fed from the current south (the Cantabro-Ebroan massif after Mey 1967; Llopis Lladó et al. 1968; Requadt 1974; Carls 1988). An intra-Devonian, or Devonian-late Tournaisian hiatus, is usually recognized in the southernmost successions (Mirouse 1966). Subsidence rates were decreasing and, in parallel, deep-water conditions were increasing along the marginal southern belt from west to east; from the southern Alduides-Mendibeltza to the Sallent, Baliera, Sierra Negra and el Comte domains (AMd, Sd, Bd, SNd and ECd; Fig. 8.16). The norhern belt represents a deep-water epicontinental basin where a condensed carbonate sedimentation prevailed (Northern and Eastern domains, Nd and Ed), although shallow-water facies with sedimentary hiatus also occur in the westernmost part (Ferrières domain, Fd). Among the southern and northern belts, an asymmetric central trough (Central domain, Cd) differentiated from the Eifelian to the Tournaisian (Fig. 8.15). The highest subsidence was located at the southern margin probably in relation to fault activity, mainly in the early Frasnian, when the occurrence of extensional listric faults bounding some blocks was interpreted (Majesté-Menjoulas et al. 1991). The siliciclastic supplies filling this trough came from the west highly subsiding area (AMd). Siliciclastic input piled up in the southern part of the trough and disappeared toward the east and the north.

The Silurian sedimentation was onlapping and transgressive, covering the Late Ordovician rifting basins throughout the Pyrenees. Deposition of black carbonaceous shales (Lower Graptolitic Shales after Schmidt 1931 in Fig. 8.15; 70–180 m thick) on a poorly oxygenated bottom sea characterized the Pyrenees as other Variscan areas of southern Europe and northern Africa (García-López et al. 1996). Late Rhuddanian to Aeronian (Llandovery) graptolites are traditionally the lowermost described in black shales of many Pyrenean sections (Dégardin 1988). Late Hirnantian (latest Ordovician) and basal Llandovery graptolites are known in a single locality (Roqué Bernal et al. 2017). The early Llandovery may be recorded by sandy shales without graptolites or by shallow-water deltaic sandstones of the Bar Formation in the southern part of the Central and Eastern Pyrenees. The drowning of this sandy platform seems to have been diachronous, because Aeronian-Telychian graptolites and Llandovery conodonts were described from the transition interval (Llopis Lladó 1969; Sanz-López and Sarmiento 1995). Furthermore, black shales are usually a common detachment horizon.

Condensed carbonate and/or reworking beds with mainly mollusks recorded occasional oxygenation events in the deep basin (Orthoceras Limestone after Dalloni 1913). It may constitute a composite horizon, 5–15 m thick, with Gorstian-Lutfordian (Ludlow) conodonts, although upper Wenlock to lower Prídolí beds are also known (García-López et al. 1996; Sanz-López et al. 2002c). Locally, condensed crinoidal limestones with corals were interpreted as an early Wenlock sedimentary high in the central Pyrenees (Marxant Limestone after Sanz-López and Palau 2000). In the southern, central Pyrenees, ochre condensed and bioturbated carbonates of type Ockerkalk replaced to the Orthoceras Limestone between the early Ludlow and the latest Prídoli (Llessui Formation and Toloriu Limestone; see Sanz-López et al. 2002c). This Ockerkalk facies was deposited on swells or ridges areas and could be in the subsurface of the Ebro basin, because it crops out in the Catalan Coastal Range and is known in the External Nappe zone of Sardinia.

The carbonate deposition and oxygenation of the sea-bottom in the Axial zone coincided with the arrival of distal siliciclastic deposits from the Ludlow in the higher subsiding Basque AMd (Arnéguy Formation; Requadt 1974). There, a shoaling interval is recognized trough Prídolí and early Lockhovian shallow-water faunas (Heddebaut 1975; Requadt 1974). At this time, it corresponds with the east extension of the distal siliciclastic sedimentation

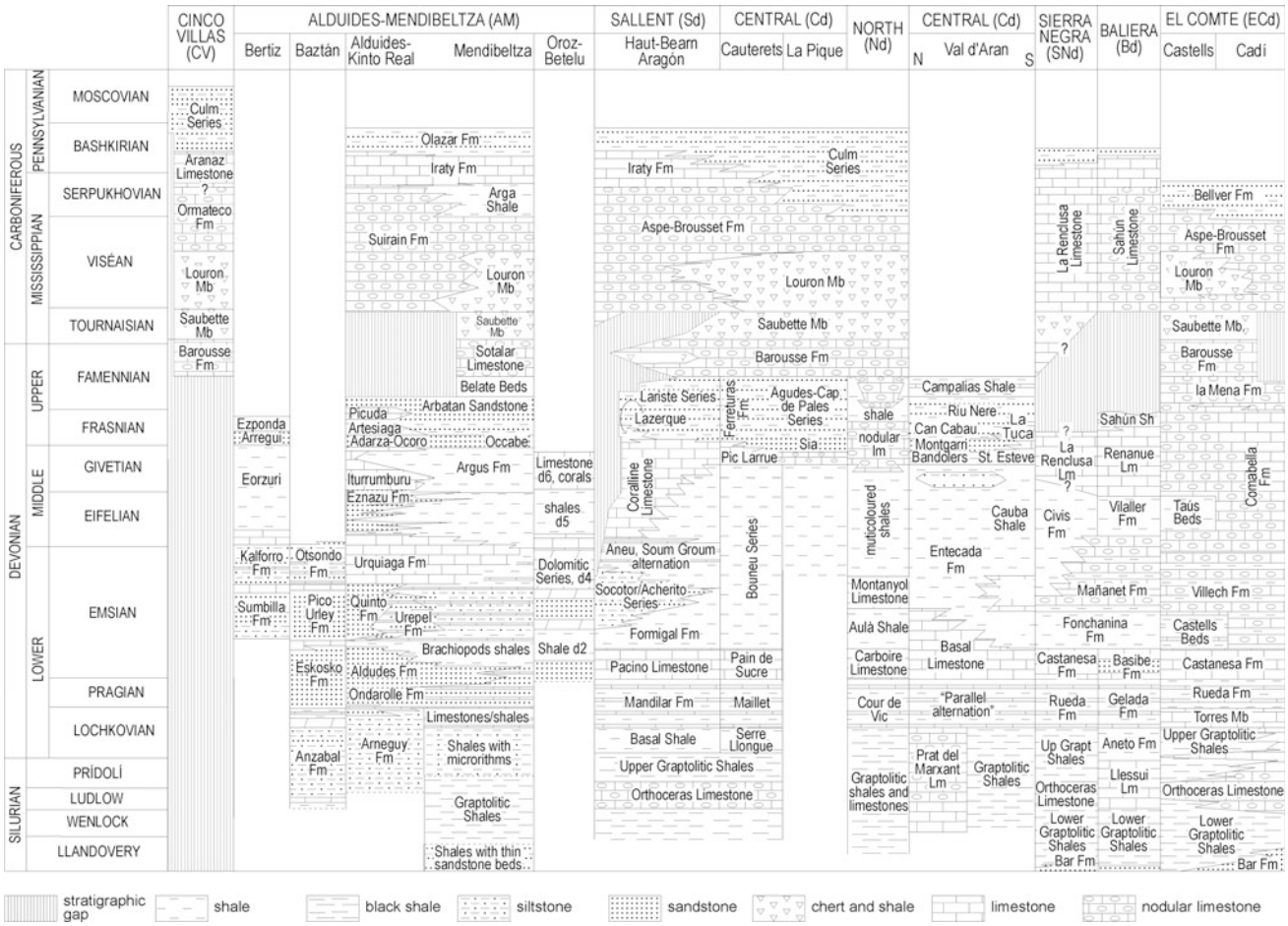

Fig. 8.15 Correlation chart among the Silurian to Middle Pennsylvanian lithostratigraphic units described in the different sedimentary domains. Explanation of units is in the text

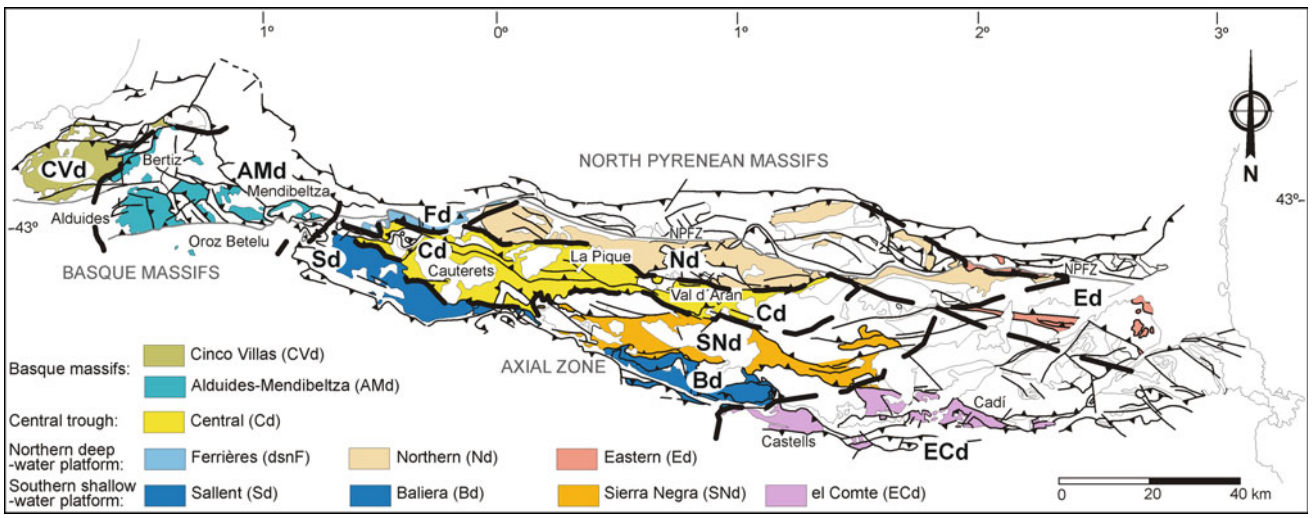

Fig. 8.16 Geological sketch of the Paleozoic rocks in the Pyrenees (Basque massifs, Axial zone and North Pyrenean massifs-north of the North Pyrenean Fault zone, NPFZ) showing the sedimentary domains differentiated for the Silurian to Middle Pennsylvanian rocks

eastward in the Axial zone (Serre Llongue Shale in the Sd, Aneto Formation in the Bd; 40–80 m thick), although black shale and limestone (Upper Graptolitic Shales; 20–40 m) were restricted to the oxygen depleted basin (Sd, SNd and ECd) and condensed crinoidal limestone deposited on sedimentary highs (ECd). Prídolí to early Lochkovian conodonts, graptolites, chitinozoans and a varied of invertebrate fauna are known (Dégardin 1988; Sanz-López et al. 1999).

A highstand sea-level interval ended the prevalent stratified water and black shale deposition in the Pyrenean Basin. It is recorded in the Torres Member of the ECd (Rueda Formation; 10–20 m thick) or the equivalent units locally described in the Bd, Nd and Ed. It consists of condensed carbonate hemipelagic sedimentation with bioturbated sea-bottom and occasional hardground development. A high resolution conodont zonation spans the mid to late Lochkovian (Valenzuela-Ríos et al. 2015). In the western part of the basin (AMd), shallow water sedimentation corresponds to crinoidal limestones and shales with brachiopods (200 m thick; Klarr 1974).

Siliciclastic input and high subsidence occurred in the AMd during the Pragian (200–700 m of sandstones, shales and quartzites of the Ondarelle and Aldudes formations) in coincidence with a change from extremely hot Lochkovian to hot and humid Pragian climate conditions according to Slavík et al. (2016), and a worldwide sea level lowering (Johnson et al. 1985). A well-oxygenated basin recorded the development of a vast extended Pragian ramp with a distal siliciclastic component (limestones and shales of the Mandilar, Gelada and Rueda formations, 50–120 m thick).

The Aldudes siliciclastic system was retrograding during the late Pragian-early Emsian in the western AMd, and was replaced by 100–200 m of "Brachiopod Shale" (Klarr 1974). In most parts of the Pyrenees, a carbonate ramp with moderate subsidence was onset (Basibé, Castanesa and Pacino formations; 30–60 m thick). In the Central Pyrenees, a late Pragian siliciclastic wedge prograded northward (San Silvestre Member of the Basibé Formation in the Bd). The carbonate platform shows early Emsian local coralline growth developed on sedimentary highs (ECd; Sanz-López 1995).

An important deepening of the sedimentation occurred during the early Emsian, but it was subdivided into several pulses (from the Middle *P. excavatus* to the Upper *P. nothorperbonus* conodont Zones; Sanz-López 2002a, b; Martínez-Pérez and Valenzuela-Ríos 2014). Shallow-water mixed siliciclastic-carbonate sedimentation was located in the AMd (Quinto and Urepel formations, 500–600 m thick), while shaly input extended in the Central Pyrenees (Formigal Formation in the Sd, Fonchanina Formation in the Bd and SNd, Aulà Shales in the Nd; Fig. 8.15). Shale sedimentation was replaced by condensed limestone with dacrioconarids in the ECd (less than 30 m thick of the Castells Beds). In the late Emsian, a prevailing carbonate sedimentation with reefal development occurred in the AMd (Urquiaga Formation; 500 m). The reduction of mud supply into the southern Pyrenees is related to hemipelagic carbonate sedimentation with deep-water dacrioconarids, ostracods and ammonoids in the Bd and SNd (Mañanet Formation; 280 m thick; García-López et al. 1990). More condensed and carbonate deposition is recorded by the Villech Formation in the distal Eastern Pyrenees (ECd; 35–70 m thick). Local changes among successions were related to the location in the basin and slopes of sedimentary highs where limestone with coral biostromes may occur (Dalloni 1930; Cavet 1957). A drowning event was recognized at the top of the Villech Fomation (upper Emsian) and followed by the progradation of resedimented carbonate of the Comabella Formation in the ECd (Sanz-López 1995; Montesinos and Sanz López 1999). Late Emsian to basal Eifelian distal siliciclastic wedges arrived to the Western Pyrenees (Socotor and Acherito Beds in the Sd and Fd) and limestone beds yielded brachiopods from the Emsian-Eifelian interval (Requadt 1974; Juch and Schafer 1974; García-Alcalde et al. 2002). Distal siliciclastic deposits were sedimented in the deepest and subsiding areas of the Central Pyrenees (Vilaller Formation in the Bd and SNd; Boneu and Entecada formations in the Cd).

The early Eifelian corresponds to a new episode of siliciclastic progradation characterized by sandstones rich in iron oxides in the southern part of AMd (Eznazu Formation, about 200 m in thickness). Thick successions of shales extended along the Central Pyrenees (Vilaller, Boneu and Entecada formations) as a wedge of condensed shales and marls with abundant dacriconarids in the deep-water nodular limestones of the Comabella Formation deposited in the Ed and the ECd (Taús Beds in Montesinos and Sanz López 1999).

High subsidence and growth of shallow-water reefal limestone is recorded during the latest Eifelian to early Givetian in the Sd and Fd, the Coral Limestone (150–500 m thick; Mirouse 1966; Joseph and Tsien 1975; Joseph et al. 1980, 1984). It seems to be equivalent to the Iturrumburu Limestone in the southernmost part of the AMd (Chesterikoff 1964; Wirth 1967). The prograding of outer carbonate platform above shales is also recorded from the latest Eifelian in the Bd (Renanué Formation in the central Pyrenees). Slope-apron carbonate bodies were prograding above hemipelagic carbonates derived from reefal biostromes in the ECd.

The mid-Givetian to early Frasnian interval corresponds to the decreasing in the distal siliciclastic sources and highstand sea level. Reefal growth extended to the southern margin of the Cd (Sant Esteve Limestone) and deep-water carbonate sedimentation (dacrioconarid limestone) occurred in the central trough, the Northern and Eastern Pyrenees

(Bandolers, Gabiedou and Pic de Larrue limestones; Perret et al. 1972; Bodin 1988; Palau and Sanz 1989; García-López et al. 1991). The shale sedimentation was confined to the western highly subsiding margin of the basin in the AMd (Argus Shale, 800–1000 m thick).

Differential subsidence increased probably in relation with extensional tectonics and an early Frasnian compartmented palaeogeography has been suggested (Raymond 1987; Sanz-López 1995). The proximal siliciclastic deep sea-fan deposits occurred in the southern margin of the high subsiding trough in the Cd (Les Bordes Sandstone; Kleinsmiede 1960). The input should be located at the west, concretely in the AMd, where early Frasnian 800–1500 m of shallow-water sandstones and shales deposited as deltaic systems (Irurita Group; de Boer et al. 1974). The trough is not recognizable eastwards, in the Tor–Casamanya syncline, where Givetian to Frasnian nodular limestones and shales were recently described (Clariana 2015). The siliciclastic supplies decreased in the middle Frasnian, but high subsidence continued as shale deposition in the AMd (500 m thick of the Artesiaga Shale). In this line, the Givetian coralline reefal development in the southern belt was retrograding southwards from the Middle-Middle *M. asymmetricus* conodont zones (Sd, Bd and southern ECd), may be in relation to the tilting of the southern basin margin. Siliciclastic facies and carbonates resedimented beds deposited in the outer platform (Lazerque and Lariste series, Ferreturas Formation, Sahún Shale) and arrived to the southern part of the Cd (La Tuca Shale and limestone), whereas distal deep sea fans deposits filled the central and northern parts of the central trough (Riu Nere Sandstone and shale, Tourmalet unit). Condensed and deep-water hemipelagic limestone deposited laterally in the epicontinental basin of the Nd, Ed and ECd. Frasnian intraformational breccias, slope deposits and local reefal growth suggest the occurrence of swollen areas probably bounded by faults in the ECd (Sanz-López 1995, 2002b). Shallow-water sandstones and bioclastic limestones with brachiopods and corals (Arbartán and Picuda formations; 60–120 m thick) suggest a late Frasnian shoaling in the AMd.

The uppermost Frasnian deepening pulse is characterized by poorly oxygenated shale sedimentation, which included tempestite limestone beds in the lower Famennian of the AMd (Belate Beds, 30 m thick). It is not differentiated in the outer platform deposits of the Sd and in the distal siliciclastic turbidites of the Cd. A deepening horizon corresponding to shales with carbonate nodules and ammonoids was described in the hemipelagic north and east carbonate sedimentation, and deep-water nodular limestone buried coralline limestone in successions of the Comabella Formation (ECd; Sanz-López 2002b).

The Frasnian/Famennian boundary was correlated with a condensed shale horizon in the Comabella Formation, where a sharp change in the conodont and ostracod faunas occurred in relation to the global Kellwasser Event (Sánchez de Posada et al. 2008). In the Cadí nappe, the Frasnian/Famennian boundary is located at the base of the La Mena Formation, red limestone with brachiopod shoals and derived tempestistes deposited on sedimentary highs (Sanz-López 2002b). The succession shows a lower–middle Famennian deepening sequence, where cephalopod "Griotte" limestone deposited on the slope and basin. The La Mena Formation is a condensed, reddish, nodular limestone with cephalopods (12–30 m thick) deposited in the basinal area of the ECd, Ed and part of the Nd (Bouquet and Stoppel 1975; Cygan 1979). At time, anoxic deep-water black shale sedimentation with resedimented limestone beds deposited in the central trough (Campalias Shale) and in the AMd (Belate Beds), whereas siliciclastic beds of the Ferreturas Formation seems to be the lateral equivalent in the southern Pyrenean belt.

The Barousse Formation consists of nodular cephalopod-bearing limestones (25–70 m thick) deposited during the mid Famennian to the early Tournaisian. It formed a deep-water, starved, carbonate ramp extending along mostly of the Pyrenees, including the CVd (where it is above Ordovician rocks). This formation marks the beginning of the onlap on the Cantabro-Ebroian block and predated its burial in the upper Tournaisian. The Barousse Formation lacks or is locally preserved, as bioclastic or crinoidal limestone, in the southern part of the Sd. The upper part of the Barousse Formation includes ash and cherts beds in the Sd and AMd (Soques Chert after Perret 1993). At the top, the Boyer et al. (1974)'s horizon B is a continuous shale less than 1 m in thickness (2 m in the deep basin of the Cd) and equivalent to the Rhenish Hangenberg Shale. It is associated with the latest Famennian, global, cooling event and the life extinction crisis (Walliser 1996). The base of the Boyer et al. (1974)'s limestone C of the Barousse Formation (about 2 m thick) corresponds to a worldwide eustatic rise post-glacial horizon close to the lower boundary of the Carboniferous according to conodont faunas (Boyer et al. 1974; Sanz-López 1995, 2002c; Kaiser et al. 2008). The top of this limestone provided mid Tournaisian conodonts (*Siphonodella cooperi* or *S. crenulata* zones).

Above, the Saubette Chert consists of black radiolarian cherts and shales with horizons of phosphatic nodules (Perret 1993). A mid to late Tournaisian age is derived from radiolarians, crustaceans and ammonoids in coincidence with the conodonts obtained in the limestone above and below the chert unit (Delépine 1935; Goumerlon 1987). These poorly oxygenated sediments extended throughout the Pyrenees in coincidence with the worldwide Lower Alum Shale event or Mid-Tournaisian event described by Walliser (1996). It lacks on the southern marginal area and on the sedimentary highs in relation to the tilting of the southern Devonian platform and to extensional tectonics in the Sd and Fd. These areas

were drowned by condensed sandy transgressive bioclastic limestones (lowest part of the Aspe-Brousset Formation) with late Tournaisian and reworked Devonian conodonts (Perret 1993; Perret and Weyant 1994). Consequently, the onlap of the marginal area was contemporaneous with the deposition of the upper part of the Saubette Chert in the basin. Tournaisian cherts or limestones are directly overlying different Cambrian to Upper Devonian rocks in the adjacent Palaeozoic outcrops of the current western Mediterranean Sea (Aiguafreda Formation of the Catalonian Coastal Range, cherts and siliceous shales in the Minorque Island and the lower member of the Falcoña Formation in the Betic Chains) indicating a subdivided basin maybe in relation to extensional faults (Raymond and Lethiers 1990). An intra-Tournaisian hiatus and erosion has also been recognized in the Cantabrian zone (Sanz-López and Blanco-Ferrera 2012). The mid–late Tournaisian starved basins recorded episodic high planktonic productivity and poorly oxygenated bottom-sea, far of siliciclastic supplies and locally related to submarine volcanism. In the southern Catalonian Coastal Range, lava flows derived from alkali basalts solidified in shallow-waters marine setting in an intraplate extensional context (Melgarejo and Martí 1989; Melgarejo 1992).

Complete deep-water sedimentation above sedimentary highs had a maximum flooding event at the late Tournaisian (*Scaliognathus anchoralis* Conodont Zone). Sedimentation of condensed, nodular to massive, cephalopod limestones (Aspe-Brousset Formation; 25–30 m thick) recorded an increase in the oxygen content of the sea-bottom respect to the mid Tournaisian (Perret 1976; Sanz-López 2002b). A similar episode is known in the Cabrières klippes (Montagne Noire), the Valls unit (Catalonian Coastal Range) and the Cantabrian Mountains, and corresponds to the Avins Event in the Dinant Basin (Poty 2007). Sedimentation of cherts and siliceous shales with inter-bedded graded tuff layers (Louron Member) deposited above the Saubette Chert in the deep part of the Pyrenean basin, including the CVd, eastern AMd, Cd and locally the Nd and ECd (Krylatov 1963; Crilat 1983; Sanz-López 1995). The lower-middle Viséan cherts are replaced by condensed cephalopod limestone on the swollen areas in a similar line to the described in the Cantabrian Mountains and the Montagne Noire (cherts of the Lavandera Member in the Alba Formation; Colonnes Formation, respectively). The basinal, starved, Tournaisian to lower Viséan chert sedimentation in known in other adjacent Palaeozoic outcrops of the current western Mediterranean Sea—region (Catalonian Coastal Range, Minorque Island, Betic Chains and the Palentine nappes of the Cantabrian Mountains). In all these areas, centimetre-thick fine-grained tuffaceous clayey horizons occurred and suggest volcanism in relation with a faulted, subdivided basin.

Condensed nodular carbonate sedimentation of the Aspe-Brousset Formation extended in the Pyrenees and the western Mediterranean area from the mid to late Viséan (*G. praebilineatus* to *G. bilineatus* conodont zones). A deeper sedimentation corresponds to the limestone and siliceous shales (Larbont facies of Clin 1959) in the northeastern part of the Pyrenees (ECd, Cd and Nd). There, the top of the Aspe-Brousset Formation provided conodonts and ammonoid considered late Viséan or early Serpukhovian. This limestone-shale sedimentation was described in the Catalonian Coastal Range (el Papiol Formation; 10–12 m thick) and in Minorque (Bourrouilh 1983; Martínez Chacón et al. 2003). Rich endemic trilobite, brachiopods and coral faunas adapted to quiet water conditions in soft, muddy sea bottom muddy bottoms are known (Martínez Chacón et al. 2003; Plusquellec et al. 2007; Gandl et al. 2015). Shallow-water carbonate shelves grew up north of the Pyrenees during the Viséan and the Serpukhovian. It is preserved in the Mouthoumet massif ("Calcaires à algues et foraminifers" Formation in Bessière and Schulze 1984) and as deposits derived as calciturbidites and debris flows in the Montagne Noire (Colonnes Formation and Puech Capel Formation in Korn and Feist 2007). The arrival of synorogenic siliciclastic supplies of the Culm flysch ended the carbonate sedimentation. It occurred in the late Serpukhovian drowning episode recorded at the top of the Aspe-Brousset Formation in the southern central and western Pyrenees (Sd, Bd and AMd). Late Viséan to late Serpukhovian clasts and olistoliths from shallow-water carbonate platforms were reworked in the synorogenic flysch deposits of the Montagne Noire and Pyrenees (Delvolvé et al. 1996; Vachard et al. 2016).

References

Abad A (1988) El Cámbrico inferior de Terrades (Gerona). Estratigrafía, facies y paleontología. Batallería 2:47–56.

Álvaro JJ, Courjault-Radé P, Chauvel JJ, Dabard MP, Debrenne F, Feist R, Pillola GL, Vennin E, Vizcaïno D (1998) Nouveau découpage stratigraphique des séries cambriennes des nappes de Pardailhan et du Minervois (versant sud de la Montagne Noire, France). Géol Fr 1998 (2):3–12.

Álvaro JJ, Ferretti F, González-Gómez C, Serpagli E, Tortello MF, Vecoli, M, Vizcaïno D (2007) A review of the Late Cambrian (Furongian) palaeogeography in the western Mediterranean region, NW Gondwana. Earth-Sci Rev 85:47–81.

Álvaro JJ, Monceret E, Monceret S, Verraes G, Vizcaïno D (2010) Stratigraphic record and palaeogeographic context of the Cambrian Epoch 2 subtropical carbonate platforms and their basinal counterparts in SW Europe, West Gondwana. Bull Geosci 85:573–584.

Álvaro JJ, Bauluz B, Clausen S, Devaere L, Imaz AG, Monceret E, Vizcaïno D (2014) Stratigraphy of the Cambrian–Lower Ordovician volcanosedimentary complexes, northern Montagne Noire, France. Stratigraphy 11:83–96.

Álvaro JJ, Colmenar J, Monceret E, Pouclet A, Vizcaïno D (2016) Late Ordovician (post-Sardic) rifting branches in the North Gondwanan Montagne Noire and Mouthoumet massifs of southern France. Tectonophysics 681:111–123.

Ayora C (1980) Les concentrationes metàl·liques de la Vall de Ribes. PhD, Univ. Barcelona.

Ayora C, Casas JM (1986) Strabound As-Au mineralization in pre-Caradocian rocks from the Vall de Ribes, Eastern Pyrenees, Spain. Mineralium Deposita 21:278–287.

Barca S, Carmignani L, Cocozza T, Franceschelli M, Ghezzo C, Memmi I, Minzoni N, Pertusati PC, Ricci CA (1987) The Caledonian events in Sardinia. In The Caledonian Orogen-Scandinavian and related areas. In: Gee DG, Sturt BA (eds) John Wiley ans Sons Ltd, p 1195–1199.

Belaustegui Z, Puddu C, Casas JM (2016) New ichnological data from the lower Paleozoic pf the Central Pyrenees: presence of *Artrophycus brogniartii* (Harlam, 1832) in the Upper Ordovician Cava Formation. Geo-Temas 16:271–274.

Bessière G, Schulze H (1984) Le Massif de Mouthoumet (Aude, France): nouvelle définition des unités structurales et essai d'une reconstruction paléogéographique. Bull Soc géol Fr 26:885–894.

Bodin J (1988) Le Dévonien inférieur et moyen des Pyrénées ariégeoises et centrales. Biostratigraphie, séries hétéropiques et mise en évidence de nappes hercyniennes précoces. Doc BRGM 153:1–255.

Boer HU de, Krausse MF, Mohr K, Pilger A, Requadt H (1974) La région de magnésite d'Eugui dans les Pyrénées Occidentales espagnoles: Une explication de la carte géologique. Pirineos 111:21–39.

Boersma KT (1973) Devonian and Lower Carboniferous biostratigraphy, Spanish Central Pyrénées. Leidse Geol Meded 49:303–377.

Bouquet C, Stoppel D (1975) Contribution à l'étude du Paléozoïque des Pyrénées centrales (Hautes vallées de la Garonne et d'Aure). Bull BRGM (sec 1) 1:7–61.

Bourrouilh R (1983) Estratigrafía, sedimentología y tectónica de la isla de Menorca y del noreste de Mallorca (Baleares). La terminación nororiental de las Cordilleras béticas en el Mediterráneo occidental. Mem IGME 99, Madrid.

Boyer F, Krylatov S, Stoppel D (1974) Sur le problème de l'existence d'une lacune sous les lydiennes à nodules phosphatés du Dinantien des Pyrénées et de la Montagne Noire (France, Espagne). Geol J (B) 9:1–60.

Buzzi L, Funedda A, Gaggero L, Oggiano G (2007) Sr-Nd isotope, trace and REE element geochemistry of the Ordovician volcanism in the southern realms of the Variscan belt. EGU General Assembly 2007, Wien, 15–20 April 2007, Abstract.

Calvet Ph, Lapierre E, Charvet J (1988) Diversité du volcanisme ordovicien dans la région de Pierrefitte (Hautes Pyrénées): rhyolites calco-alcalines et basalts alcalins. C R Acad Sci Paris 3078: 805–812.

Carls P (1988) The Devonian of Celtiberia (Spain) and Devonian paleogeography of SW Europe. Can Soc Petrol Geol Mem 14: 421–464.

Carmignani L, Oggiano G, Barca S, Conti P, Salvadori I, Eltrudis A, Funedda A, Pasci S (2001) Geologia della Sardegna. Note illustrative della Carta Geologica della Sardegna a scala 1:200.000. Memorie Descrittive della Carta Geologica d'Italia, Servizio Geologico 60:1–283. Instituto Poligrafico e Zecca dello Stato, Roma.

Casas JM (2010) Ordovician deformations in the Pyrenees: new insights into the significance of pre-Variscan ('sardic') tectonics. Geol Mag 147: 674–689.

Casas JM, Fernández O (2007) On the Upper Ordovician unconformity in the Pyrenees: New evidence from the La Cerdanya area. Geol Acta 5:193–198.

Casas JM, Palacios T (2012) First biostratigraphical constraints on the pre-Upper Ordovician sequences of the Pyrenees based on organic-walled microfossils. C R Géosci 344:50–56.

Casas JM, Castiñeiras P, Navidad M, Liesa M, Carreras J (2010) New insights into the Late Ordovician magmatism in the Eastern Pyrenees: U-Pb SHRIMP zircon data from the Canigó massif. Gondwana Res 17:317–324.

Casas JM, Queralt P, Mencos J, Gratacós O (2012) Distribution of linear mesostructures in oblique folded surfaces: Unravelling superposed Ordovician and Variscan folds in the Pyrenees. J Struct Geol 44:141–150.

Castiñeiras P, Navidad M, Liesa M, Carreras J, Casas JM (2008) U-Pb zircon ages (SHRIMP) for Cadomian and Lower Ordovician magmatism in the Eastern Pyrenees: new insights in the pre-Variscan evolution of the northern Gondwana margin. Tectonophysics 46:228–239.

Castiñeiras P, Navidad M, Casas JM, Liesa M, Carreras J (2011) Petrogenesis of Ordovician magmatism in the Pyrenees (Albera and Canigó Massifs) determined on the basis of zircon minor and trace element composition). J Geol 119:521–534.

Cavet P (1957) Le Paléozoïque de la zone axiale des Pyrénées orientales françaises entre le Roussillon et l'Andorre. Bull Serv Carte géol Fr 55:303–518.

Chesterikoff A 1964 Note sur l'existence d'un palédôme dans la région de Burguete-Arive-Arrieta (Pyrénées basques espagnoles) et ses relations métallogéniques avec les mineralizations périphériques. Bull Soc géol Fr (6) 8:225–232.

Cirés J, Casas JM, Muñoz JA, Fleta J, Barbera M (1994) Memoria explicativa del mapa geológico de España a escala 1:50.000, hoja de Molló (n°218). ITGE, Madrid.

Clariana P (2015) Estratigrafía, estructura y su relación con el metamorfismo de la Zona Axial pirenaica en la transversal del Noroeste de Andorra y comarcas del Pallars Sobirá y el Alt Urgell (Lleida). Dissertation, University of Oviedo.

Clin M (1959) Etude géologique de la haute chaine des Pyrénées Centrales entre le cirque de Troumouse et le cirque du Lys. Dissertation, University of Nancy.

Cocherie A, Baudin Th, Autran A, Guerrot C, Fanning C.M, Laumonier B (2005) U-Pb zircon (ID-TIMS and SHRIMP) evidence for the early Ordovician intrusion of metagranites in the late Proterozoic Canaveilles Group of the Pyrenees and the Montagne Noire (France). Bull Soc géol Fr 176:269–282.

Crilat S (1983) Le Devonien supérieur et le Carbonifère inférieur des Pyrénées et de la Montagne Noire (Frasnien, Famennien, Tournaisien). Newsl IGCP 5:231–254.

Cygan C (1979) Etude de conodontes dévoniens des Pyrénées et du massif de Mouthoumet. Dissertation, University of Toulouse.

Dalloni M (1913) Stratigraphie et tectonique de la région des Nogueras (Pyrénées centrales). Bull Soc géol Fr (sér 4) 1:243–263.

Dalloni M (1930) Etude géologique des Pyrénées Catalanes. An Fac Sci Marseille 26, 3:1–373.

Dégardin JM (1988) Le Silurien des Pyrénées. Biostratigraphie. Paléogéographie. Bull Soc géol Nord 15:1–355.

Dégardin JM (coord) et al (1996) Ordovicien supérieur-Silurien. In: Barnolas A, Chiron JC, Guérangué B (eds) Synthèse géologique et géophysique des Pyrénées vol 1. Editons BRGM-ITGE, Orléans, Madrid, pp 211–233.

Delépine G (1935) Contribution a l'étude de la faune du Dinantien des Pyrénées Deuxième partie: la faune de Mondette. Bull Soc géol Fr (sér 5) 5:171–189.

Deloule E, Alexandrov P, Cheilletz A, Laumonier B, Barbey P (2002) In-situ U-Pb zircon ages for Early Ordovician magmatism in the eastern Pyrenees, France: the Canigou orthogneisses. Int J Earth Sci 91:398–405.

Delvolvé JJ et al (1996) Carbonifère à faciès Culm In Barnolas A, Chiron JC (eds) Synthèse géologique et géophysique des Pyrénées vol 1. Editions BRGM-ITGE, Orléans, Madrid, pp 303–338.

Den Brok SWJ (1989) Evidence for pre-Variscan deformation in the Lys Caillaouas area, Central Pyrenees, France. Geol Mijnbouw 68:377–380.

Denèle Y, Barbey P, Deloule E, Pelleter E, Olivier Ph, Gleizes G (2009) Middle Ordovician U-Pb age of the Aston and Hospitalet orthogneissic laccoliths: their role in the Variscan evolution of the Pyrenees. Bull Soc géol Fr 180:209–221.

DePaolo DJ (1981) Neodymiun isotopes in the Colorado Front range and crust-mantle evolution in the Proterozoic. Nature 291:193–196.

DePaolo DJ, Wasserburg GJ (1976) Nd isotopic variations and petrogenetic models. Geophys Res Lett 3 (5):249–252.

Devaere L, Clausen S, Steiner M, Álvaro JJ, Vachard D (2013) Chronostratigraphic and palaeogeographic significance of an early Cambrian microfauna from the Heraultia Limestone, northern Montagne Noire, France. Palaeonto Electr 16(2), 17A:1–91.

Devaere L, Clausen S, Monceret E, Vizcaïno D, Vachard D, Genge MC (2014) The tommotiid *Kelanella* and associated fauna from the early Cambrian of southern Montagne Noire (France): implications for Camenellan phylogeny. Palaeontology 57:979–1002.

Di Pisa A, Gattiglio M, Oggiano G (1992) Pre–Hercynian magmatic activity in the nappe zone (internal and external) of Sardinia: evidence of two within plate basaltic cycles. In Carmingnani L, Sassi F P (eds) Contributions to the Geology of Italy with Special Regard to the Paleozoic Basements. Newsletter IGCP no. 276:107–116.

Funedda A, Oggiano G (2009) Outline of the Variscan basement of Sardinia. In: Corradini C, Ferretti A, Štorch P (eds) The Silurian of Sardinia. Volume in Honour of Enrico Serpagli. Rendicontti della Società Paleontologica Italiana 3:23–35.

Gámez Vintaned JA, de Gibert JM, Casas JM (2012) First ichnological data from the pre-Upper Ordovician rocks of the Pyrenees. Geo-Temas 13.

Gandin A, Pillola GL (1985) Biostratigrafia e sedimentologia della Formazione di Cabitza nell'Iglesiente. In: Gruppi di lavoro del CNR: "Paleozoico" e "Evoluzione magmatica e matemorfica della costra fanerozoica". Riunione Scientifica Siena, 13–14 Decembre 1985, 30–31.

Gandl J, Ferrer E, Magrans J, Sanz-López J (2015) Trilobiten aus dem Unter-Karbon des Katalonischen Küstengebirges (NE-Spanien). Abh Senckenberg Ges Naturforsch 571, Schweizerbart and Borntraeger Science Publishers, Stuttgart.

García-Alcalde JL, Carls P, Pardo-Alonso MV, Sanz-López J, Soto FM, Truyols-Massoni M, Valenzuela-Ríos JI (2002) Devonian. In: Gibbons W, Moreno MT (eds) The Geology of Spain. Geol Soc London, pp 67–91.

García-López S, García-Sansegundo J, Arbizu M (1990) Datos estratigráficos y paleontológicos de la sucesión devónica del área del río Baliera (Zona Axial, Pirineos centrales españoles). Geogaceta 7:33–35.

García-López S, García-Sansegundo J, Arbizu M (1991) Devonian of the Aran Valley Synclinorium, Central Pyrenees, Spain: Stratigraphical and Paleontological data. Acta Geol Hisp 26 (1):55–66.

García-López, S, Rodríguez-Cañero R, Sanz-López J, Sarmiento GN, Valenzuela-Ríos JI (1996) Conodontos y episodios carbonatados en el Silúrico de la Cadena hercínica meridional y el Dominio Sahariano. Rev Esp Paleontol, num extr: 33–57.

García-Sansegundo J, Alonso JL (1989) Stratigraphy and structure of the southeastern Garona Dome. Geodin Acta 3:127–134.

García-Sansegundo J, Gavaldà J, Alonso JL (2004) Preuves de la discordance de l'Ordovicien supérieur dans la zone axiale des Pyrénées: exemple de dôme de la Garonne (Espagne, France). C R Géosci 336:1035–1040.

Gil-Peña I, Sanz-López J, Barnolas A, Clariana P (2000) Secuencia sedimentaria del Ordovícico superior en el margen occidental del domo del Orri (Pirineos Centrales). Geotemas 1:187–190.

Gil-Peña I, Barnolas A, Villas E, Sanz-López J (2004) El Ordovícico Superior de la Zona Axial. In Vera JA (ed) Geología de España. SGE-IGME, Madrid, p 247–249.

Goumerlon F (1987) Les radiolaires tournaisiens des nodules phosphatés de la Montagne Noire et des Pyrénées Centrales. Systematique-Biostratigraphie-Paleobiogeographie. Biostratigraphie du Paléozoïque 6:1–172.

Guitard G (1970) Le métamorphisme hercynien mésozonal et les gneiss œillés du massif du Canigou (Pyrénées orientales). Mém BRGM 63:1–353.

Hartevelt JJA (1970) Geology of the upper Segre and Valira valleys, central Pyrenees, Andorra/Spain. Leid Geol Meded 45:167–236.

Heddebaut C (1975) Etudes géologiques dans les Massifs paléozoïques basques (résumé de thèse). Bull BRGM 4 (2):5–30.

Johnson JG, Klapper G, Sandberg CA (1985) Devonian eustatic fluctuations in Euramerica. Geol Soc Am Bull 96:567–587.

Joseph, J, Brice D, Mouravieff N (1980) Données paléontologiques nouvelles sur le Frasnien des Pyrénées centrales et occidentales: implications paléogéographiques. Bull Soc Hist Nat Toulouse 116:16–41.

Joseph J, Mirouse R, Perret MF (1984) Calcaires dévoniens et carbonifères du Monte Tobazo (Pyrénées aragonaises, Huesca, Espagne). Acta Geol Hisp 19:149–166.

Joseph J, Tsien HH (1975) Calcaires mésodévoniens et leurs faunes de tétracoralliaires en haute vallée d'Ossau (Pyrénées Atlantiques). Bull Soc Hist Nat Toulouse 111:179–202.

Juch D, Schafer D (1974) L'Hercynien de Maya et de la vallée d'Arizakum dans la partie orientale du massif de Cinco-Villas (Pyrénées Occidentales de Espagne). Pirineos 111:41–58.

Kaiser S I, Steuber T, Becker RT (2008) Environmental change during the Late Famennian and Early Tournaisian (Late Devonian–Early Carboniferous) implications from stable isotopes and conodont biofacies in southern Europe. In: Aretz M, Herbig H-G, Somerville ID (eds) Carboniferous Platforms and Basins. Geol J 43:241–260.

Klarr K (1974) La structure géologique de la partie sud-est du Massif des Aldudes-Quinto Real (Pyrénées Occidentales). Pirineos 111:59–67.

Kleinsmiede WJF (1960) Geology of the valle d'Aran (Central Pyrenees). Leidse Geol Meded 25:129–245.

Korn D, Feist R (2007) Early Carboniferous ammonoid faunas and stratigraphy of the Montagne Noire (France). Fossil Record 10:99–124.

Kriegsman LM, Aerden DGAM, Bakker RJ, den Brok SWJ, Schutjens PMTM (1989) Variscan tectonometamorphic evolution of the eastern Lys-Caillaouas massif, Central Pyrenees-evidence for late orogenic extension prior to peak metamorphism. Geol Mijnbouw 68:323–333.

Krylatov S (1963) Note préliminaire sur les jaspes dinantiens des Pyrénées et leur cortège). Bull Soc géol Fr (sér 7) 5:393–400.

Laumonier B (1988) Les groupes de Canaveilles et de Jujols (''Paléozoïque inférieur'') des Pyrénées orientales – arguments en faveur de l'âge essentiellement Cambrien de ces séries. Hercynica 4:25–38.

Laumonier B, Guitard G (1986) Le Paléozoïque inférieur de la moitié orientale de la Zone Axiale des Pyrénées. Essai de synthèse. C R Acad Sci Paris 302:473–478.

Laumonier B, Abad A, Alonso JL, Baudelot S, Bessière G, Besson M, Bouquet C, Bourrouilh R, Brula P, Carreras J, Centène A, Courjault-Radé R, Courtessole R, Fauconnier D, García-Sansegundo J, Guitard G, Moreno-Eiris E, Perejón A, Vizcaïno D (1996) In: Barnolas A, Chiron JC (eds) Synthèse géologique et géophysique des Pyrénées. Tome 1: Cycle hercynien. Cambro-Ordovicien. BRGM-ITGE, Orléans-Madrid. p 157–209.

Laumonier B, Autran A, Barbey P, Cheilletz A, Baudin T, Cocherie A, Guerrot C (2004) Conséquences de l'absence de socle cadomien sur l'âge et la signification des séries pré-varisques (anté-Ordovicien supérieur) du sud de la France (Pyrénées, Montagne Noire). Bull Soc géol Fr 175:105–117.

Laumonier B, Calvet M, Wiazemsky M, Barbey P, Marignac C, Lambert J, Lenoble JL (2015) Notice explicative de la Carte géologique de la France (1/50.000), feuille Céret (1096). BRGM, Orléans.

Liesa M, Carreras J (1989) On the structure and metamorphism of the Roc de Frausa Massif (Eastern Pyrenees). Geodin Acta 3:149–161.

Liesa M, Carreras J, Castiñeiras P, Casas JM, Navidad M, Vilà M (2011) U-Pb zircon age of Ordovician magmatism in the Albera Massif (Eastern Pyrenees). Geol Acta 9:1–9.

Loi A, Pillola GL, Leone F (1995) The Cambrian and Early Ordovician of south-western Sardinia. In: 6th Paleobenthos International Symposium, October, 25–31 1995. Rendiconti del Seminario della Facoltà di Scienze dell'Università di Cagliari (suppl. vol. 65): 63–81.

Llopis Lladó N (1965) Sur le Paléozoïque inférieur de l'Andorre. Bull Soc géol Fr 7:652–659.

Llopis Lladó N (1969) Estratigrafía del Devónico de los valles de Andorra. Mem R Acad Cien Art Barcelona 39:219–290.

Llopis Lladó N, de Villalta JF, Cabanas R, Pelaez Pruneda JR, Vilas L (1968) Le Dévonien de l'Espagne. Int Symp Devonian System, Calgary (1967) 1, pp 171–187.

Majesté-Menjoulas C, Debat C, Mercier A (1991) Les massifs anciens des Pyrénées. Sci Geol Bull 44:337–369.

Majesté-Menjoulas C, Ríos LM (coord) et al (1996) Dévonien-Carbonifère inférieur. In: Barnolas A, Chiron JC, Guérangué B (eds) Synthèse géologique et géophysique des Pyrénées vol 1. Editons BRGM-ITGE, Orléans, Madrid, pp 235–301.

Margalef A (2015) Estudi estructural i estratigràfic del sud d'Andorra. PhD, Univ. Barcelona.

Margalef A, Castiñeiras P, Casas JM, Navidad M, Liesa M, Linnemann U, Hofmann M, Gärtner A (2016) Detrital zircons from the Ordovician rocks of the Pyrenees: Geochronological constraints and provenance. Tectonophysics 681:124–134.

Martí J, Muñoz JA, Vaquer R (1986) Les roches volcaniques de l'Ordovicien supérieur de la région de Ribes de Freser-Rocabruna (Pyrénées catalanes): caractères et signification. C R Acad Sci Paris 302:1237–1242.

Martí J, Casas JM, Guillén N, Muñoz JA, Aguirre G (2014) Structural and geodynamic constraints of Upper Ordovician volcanism of the Catalan Pyrenees. Gondwana 15 Abstracts book, 104.

Martínez F, Iriondo A, Dietsch C, Aleinikoff JN, Peucat JJ, Cirès J, Reche J, Capdevila R (2011) U-Pb SHRIMP-RG zircon ages and Nd signature of lower Paleozoic rifting-related magmatism in the Variscan basement of the Eastern Pyrenees. Lithos 127:10–23.

Martínez Catalán JR (2012) The Central Iberian arc, an orocline centered in the Iberian Massif and some implications for the Variscan belt. Int J Earth Sci 101:1299–1314.

Martínez Chacón ML, Winkler Prins CF, Sanz-López J, Ferrer E, Magrans J (2003) Braquiópodos misisípicos de los alrededores de Barcelona (Cadenas Costeras Catalanas, NE España). Rev Esp Paleontol 18:189–204.

Martínez-Pérez C, Valenzuela-Ríos JI (2014) New Lower Devonian polygnathids (Conodonta) from the Spanish Central Pyrenees, with comments on the early radiation of the group. J Iber Geol 40:141–155.

Melgarejo JC (1992) Estudio geológico y metalogenético del Paleozoico del sur de las Cordilleras Costeras Catalanas. Mem ITGE 103.

Melgarejo JC, Martí J (1989) El vulcanisme bàsic del Carbonífer inferior de la serra de Miramar. Acta Geol Hisp 24:131–138.

Mey PHW (1967) The Geology of the upper Ribagorzana and Baliera valleys, Central Pyrenees, Spain. Leidse Geol Meded 41:153–220.

Mey PHW (1968) Evolution of the Pyrenean Basins during the Late Paleozoic. Internat Symp Devonian System, Calgary (1967) 1, pp 1157–1166.

Mezger J, Gerdes A (2016) Early Variscan (Visean) granites in the core of central Pyrenean gneiss domes: implications from laser ablation U-Pb and Th-Pb studies. Gondwana Res 29:181–198.

Mirouse R (1966) Recherches géologiques dans la partie occidentale de la zone primaire axiale des Pyrénées. Mém Carte géol Fr, Paris.

Montesinos JR, Sanz López J (1999) Ammonoideos del Devónico Inferior y Medio en el Pirineo Oriental y Central. Antecedentes históricos y nuevos hallazgos. Rev Esp Paleontol, num extr: 97–108.

Muñoz JA (1985) Estructura alpina i herciniana a la vora sud de la zona axial del Pirineu oriental. PhD, Univ. Barcelona.

Muñoz JA (1992) Evolution of a continental colision belt: ECORS-Pyrenees crustal balanced cross-section. In: Mc Clay KR (ed) Thrust Tectonics, Chapman & Hall, London, p 235–246.

Muñoz JA, Casas JM (1996) Tectonique préhercynienne. In: Barnolas A, Chiron JC (eds) Synthèse géologique et géophysique des Pyrénées, BRGM-ITGE, Orléans-Madrid, p 587–1589.

Navidad M, Castiñeiras P, Casas JM, Liesa M, Fernández-Suárez J, Barnolas A, Carreras J, Gil-Peña I (2010) Geochemical characterization and isotopic ages of Caradocian magmatism in the northeastern Iberia: insights into the Late Ordovician evolution of the northern Gondwana margin. Gondwana Res 17:325–337.

Navidad M, Casas J M, Castiñeiras P, Liesa M, Belousova E, Proenza J, Aiglsperger Th (2018) Ordovician magmatism in northern Gondwana: Evolution based on new U-Pb geochronology, whole-rock geochemistry, and Nd isotopes in orthogneisses and metabasic rocks from the Eastern Pyrenees. Lithos 314–315, 479–496.

Padel M (2016) Influence cadomienne dans les séries pré-sardes des Pyrénées Orientales: approche géochimique, stratigraphique et géochronologique. PhD Thesis. University of Lille I.

Padel M, Álvaro JJ, Clausen S, Guillot F, Poujol M, Chichorro M, Monceret E, Pereira MF, Vizcaïno D (2017) U-Pb laser ablation ICP-MS zircon dating across the Ediacaran-Cambrian transition of the Montagne Noire, southern France. Comptes Rendus Geoscience 349:380–390.

Padel M, Clausen S, Álvaro JJ, Casas JM (2018) Review of the Ediacaran-Lower Ordovician (pre-Sardic) stratigraphic framework of the Eastern Pyrenees, southwestern Europe. Geol Acta 16, 339–355.

Palau J, Sanz J (1989) The Devonian units of the Marimanya Massif and their relationship with the Pyrenean Devonian facies areas. Geodin Acta 3:171–182.

Palme H, O'Neill HSC (2004) Cosmochemical estimates of mantle composition. In: RW Carlson (ed) The mantle and core. Treatise on Geochemistry. HD Holland, HD, Turekian KK (eds), Elsevier-Pergamon, Oxford, 2:1–38.

Pearce JA (1996) Sources and setting of granitic rocks. Episodes 19 (4):120–125.

Pearce JA (2008) Geochemical fingerprinting of oceanic basalts with applications to ophiolite classification and the search for Archean oceanic crust. Lithos 100:14–48.

Pearce JA, Harris NBW, Tindle AG (1984) Trace element discrimination diagrams for the tectonic interpretation of granitic rocks. J Petrol 25:956–983.

Perejón A, Moreno Eiris E, Abad A (1994) Montículos de arqueociatos y calcimicrobios del Cámbrico Inferior de Terraldes, Gerona (Pirineo Oriental, España). Bol R Soc Esp Hist Nat (Sec Geol) 89:55–95.

Perret MF (1976) Une transgression dinantienne dans les Pyrénées occidentales: datation micropaléontologique et analogies. C R somm Soc géol Fr 6:257–259.

Perret MF (1993) Recherches micropaléontologiques et biostratigraphiques (Conodontes – Foraminifères) dans le Carbonifère pyrénéen. Strata 21, Toulouse.

Perret MF, Weyant M (1994) Les biozones à conodontes du Carbonifère des Pyrénées. Comparaisons avec d'autres régions du globe. Geobios 27:689–715.

Perret MF, Joseph J, Mirouse R, Mouravieff A (1972) Un précieux jalon chronostratigraphique dans le Paléozoïque pyrénéen: la datation des "Calcaires rubanés" du Pic Larrue (Hautes Pyrénées). C R Acad Sci Paris D 274:2439–2442.

Pillola GL (1989) Données lithologiques et stratigraphiques sur le Cambrien et le Trémadoc de l'Iglesiente (SE de la Sardaigne). In : Sassi FP, Bourrouilh R (eds) IGCP Project no. 5, Correlation of Prevariscan and Variscan events of the Alpine-Mediterranean Mountain Belt. Newsletter 7, 228–239.

Pillola GL (1990) Lithologie et Trilobites du Cambrien inférieur du SW de la Sardaigne (Italie): implications paléobiogéographiques. C R Acad Sci Paris 310:321–328.

Pillola GL, Piras S, Serpagli E (2008) Upper Tremadoc-Lower Arenig? Anisograptid-Dichograptid fauna from the Cabitza Formation (Lower Ordovician, SW Sardinia, Italy). Rev Micropal 51:167–181.

Pitra P, Poujol M, Den Driessche JV, Poilvet JC, Paquette JL (2012) Early Permian extensional shearing of an Ordovician granite: The Saint-Eutrope "C/S-like" orthogneiss (Montagne Noire, French Massif Central). C R Géosci 344:377–384.

Plusquellec Y, Fernández-Martínez E, Sanz-López J, Soto F, Magrans J, Ferrer E (2007) Tabulate corals and stratigraphy of Lower Devonian and Mississippian rocks near Barcelona (Catalonian Coastal Ranges, Northeast Spain). Rev Esp Paleontol 22:175–192.

Poblet J (1991) Estructura herciniana i alpina del versant sud de la zona axial del Pirineu central. PhD thesis, Univ. Barcelona.

Poty E (2007) The Avins event: a remarkable worldwide spread of corals at the end of the Tournaisian (Lower Carboniferous). In Hubmann B, Piller WE (eds) Fossil corals and sponges. Graz 2003. Schriften erdwiss Komm (Oesterreichische Akad Wiss) 17, Wien, pp 231–250.

Puddu C, Casas JM (2011) New insights into the stratigraphy and structure of the Upper Ordovician rocks of the la Cerdanya area (Pyrenees). In: Gutiérrez-Marco JC, Rábano I, García-Bellido D (eds) Ordovician of the World. Cuad. Museo Geomin 14:441–445.

Pujadas J, Casas JM, Muñoz JA, Sàbat F (1989) Thrust tectonics and Paleogene syntectonic sedimentation in the Empordà area (southeastern Pyrenees). Geodin Acta 3:195–206.

Raymond D (1987) Le Dévonien et le Carbonifère inférieur du sud-ouest de la France (Pyrénées, Massif de Mouthoumet, Montagne Noire): sédimentation dans un bassin flexural en bordure sud de la Chaîne de collision varisque. Geol Rundsch 76:795–803.

Raymond D, Lethiers F (1990) Signification géodynamique de l'événement radiolaritique dinantien dans les zones externes sud-varisques (Sud de la France et Nord de l'Espagne). C R Acad Sci Paris 310:1263–1269.

Requadt H (1974) Aperçu sur la stratigraphie et le facies du Devonien inferieur et le moyen dans les Pyrénées Occidentales d'Espagne. Pirineos 111:109–127.

Robert JF (1980) Etude géologique et métallogénique du Val de Ribas sur le versant espagnol des Pyrénées Catalanes. PhD, Univ. Besançon.

Robert JF, Thiébaut J (1976) Découverte d'un volcanisme acide dans le Caradoc de la région de Ribes de Freser (Prov. de Gérone). C R Acad Sci, Paris 282:2050–2079.

Roger F, Respaut JP, Brunel M, Matte Ph, Paquette JL (2004) Première datation U-Pb des orthogneiss œillés de la zone axiale de la Montagne Noire (Sud du Massif central): nouveaux témoins du magmatisme ordovicien dans la chaîne varisque. C R Géosci 336:19–28.

Roqué Bernal J, Štorch P, Gutiérrez-Marco JC (2017) Bioestratigrafía (graptolitos) del límite Ordovícico-Silúrico en los Pirineos orientales (curso alto del río Segre, Lleida). Geogaceta 61:27–30.

Rudnick RL, Gao S (2004) Composition of the Continental Crust. In: Rudnick, RL (ed) The Crust. Treatise on Geochemistry. Holland HD, Turekian KK (eds), Elsevier-Pergamon, Oxford, 3:1–64.

Sánchez de Posada LC, Sanz-López J, Gozalo R (2008) Ostracod and conodont faunal changes across the Frasnian-Famennian boundary at Els Castells, Spanish central Pyrenees. Rev Micropal 51: 205–219.

Santanach PF (1972a) Sobre una discordancia en el Paleozoico inferior de los Pirineos orientales. Acta Geol Hisp 7:129–132.

Santanach PF (1972b) Estudio tectónico del Paleozoico inferior del Pirineo entre la Cerdaña y el río Ter. Acta Geol Hisp 7:44–49.

Sanz-López J (1995) Estratigrafía y bioestratigrafía (Conodontos) del Silúrico superior–Carbonífero inferior del Pirineo Oriental y Central. Dissertation, University of Barcelona.

Sanz-López J (2002a) Devonian and Carboniferous pre-Stephanian rocks from the Pyrenees. In: García-López S, Bastida F (eds) Palaeozoic conodonts from northern Spain. Eight International Conodont Symposium held in Europe. Publ IGME, Cuad Mus Geomine 1, Madrid, pp 367–389.

Sanz-López J (2002b) Devonian and Lower Carboniferous rocks from the Cadí nappe (eastern Pyrenees). In: García-López S, Bastida F (eds) Palaeozoic conodonts from northern Spain. Eight International Conodont Symposium held in Europe. Publ IGME, Cuad Mus Geomin, Madrid 1:419–438.

Sanz-López, J, Gil-Peña I, Rodríguez-Cañero R (2002c) Conodont content and stratigraphy of the Llessui Formation from the south central Pyrenees. In: García-López S, Bastida F (eds) Palaeozoic conodonts from northern Spain. Eight International Conodont Symposium held in Europe. Publ IGME, Cuad Mus Geomin 1, Madrid, pp 391–401.

Sanz-López J (2004) Silúrico, Devónico y Carbonífero pre- y sin-varisco en Geología de los Pirineos. In: Vera JA (ed.) Geología de España. SGE-IGME, Madrid, pp 250–254.

Sanz-López J, Blanco-Ferrera S (2012) Revisión estratigráfica del Misisipiense al Pensilvaniense más bajo de la zona Cantábrica y la posición de los límites entre los pisos. Geo-Temas 13:90 (annexed CD: 163–166).

Sanz-López J, Palau J (2000) Conodontos del Wenlock del macizo del Marimanya, Pirineo central. 1st Congr Iber Paleontol, 16th J Soc Esp Paleontol, Évora, pp 278–279.

Sanz-López J, Sarmiento GN (1995) Asociaciones de conodontos del Ashgill y del Llandovery en horizontes carbonatados del valle del Freser (Girona). 11th J Paleontol, Tremp, pp 157–160.

Sanz-López J, Valenzuela-Ríos JI, García-López S, Gil Peña I, Robador A (1999) Nota preliminar sobre la estratigrafía y el contenido en conodontos del Prídolí-Lochkoviense inferior en la unidad de els Castells (Pirineo central). Temas Geol-Min ITGE 26 (2), pp 638–642.

Schmidt H (1931) Das Paläozoikum der spanischen Pyrenäen. Abh Ges Wiss K 3 5, Göttingen.

Shervais J (1982) Ti-V plots and the petrogenesis of modern and ophiolitic lavas. Earth and Planetary Sci Letters 59:101–118.

Slavík L, Valenzuela-Ríos JI, Hladil J, Chadimová L, Liao J-C, Hušková A, Calvo H, Hrstka T (2016) Warming or cooling in the Pragian? Sedimentary record and petrophysical logs across the Lochkovian-Pragian boundary in the Spanish central Pyrenees: Palaeogeogr Palaeoclim Palaeocol 449, 300–320.

Speksnijder A (1986) Geological analysis of Paleozoic large-scale faulting in the south-central Pyrenees. Geol Ultraiectina 43.

Stampfli GM, von Raumer JF, Borel GD (2002) Paleozoic evolution of pre–Variscan terranes: from Gondwana to the Variscan collision. In: Martínez Catalán JR, Hatcher RD, Arenas R, Díaz García F

(eds) Variscan–Appalachian Dynamics: the Building of the Late Paleozoic Basement. Geol Soc Am, Spec Pap 364:263–280. Boulder, Colorado.

Sun SS, McDonough WF (1989) Chemical and isotopic systematics of oceanic basalts; implications for mantle composition and processes. In: Saunders AD, Norry MJ (eds) Magmatism in the Ocean Basins. Geol Soc London, Spec Vol 42: 429–448.

Syme EC (1998) Ore-associated and barren rhyolites in the central Flin Flon Belt: Case study of the Flin Flon mine sequence. Manitoba Energy and Mines, Open File Rep OF98-9:1–32.

Vachard D, Cózar P, Aretz M, Izart A (2016) Late Viséan–Serpukhovian foraminifers in the Montagne Noire (France): Biostratigraphic revision and correlation with the Russian substages. Geobios 49:469–498.

Valenzuela-Ríos JI, Slavík L, Liao J-C, Calvo H, Hušková A, Chadimová L (2015) The middle and upper Lochkovian (Lower Devonian) conodont successions in key peri-Gondwana localities (Spanish Central Pyrenees and Prague Synform) and their relevance for global correlations. Terra Nova 27:409–415.

Walliser OH (1996) Global events in the Devonian and Carboniferous, In: Walliser OH (ed) Global events and event stratigraphy in the Phanerozoic. Springer-Verlag, Berlin, pp 225–250.

Wirth M (1967) Zur Gliederung des höheren Paläozoikums (Givet-Namur) im Gebiet des Quinto Real (West pyrenäen) mit Hilfe von Conodonten). N J Geol Palaeont Abh 127:179–244.

Wood D (1980) The application of a Th-Hf-Ta diagram to problems of tectonomagmatic classification and to establishing the nature of crustal contamination of basaltic lavas of the British Tertiary volcanic province. Earth Planet Sci Lett 50:11–30.

Zwart HJ (1979) The Geology of the Central Pyrenees. Leidse Geol Meded 50:1–74.

5.8 Remarks and discussion on the Sardic unconformity and related tectonics in Pyrenees and Sardinia

From the analysis of the regional geologic data described in the Pyrenees: (i) the occurrence of an Upper Ordovician unconformity, (ii) the occurrence of pre-unconformity deformations, and Upper Ordovician fracture event; and (iii) the emplacement of volcanic and magmatic byproducts with a calc-alkaline affinity between 477-446 Ma, with two peaks (473-470 Ma, and 457 Ma).

According to previous authors (see ***Chapter 1***), the Upper Ordovician unconformity analyzed in the Eastern Pyrenees (Talltendre area - Canigò unit; Bruguera unit - Ribes de Freser area) is comparable to the Sardic one.

The new data obtained by Martí et al. (2019), stating the Ordovician age (460 Ma) of the ignimbrites overlaying the Campelles Series cropping out in the Bruguera unit (Ribes de Freser antiformal stack, Eastern Pyrenees), suggests that the contact between the Cambrian-Ordovician Campelles Series and the former ignimbrites corresponds to the Sardic unconformity.

In both the zones, Talltendre area and Bruguera unit, it range from angular unconformity to para-conformity, and separates two successions with different structural features, highlighting a stratigraphic gap which include part of the Floian and the whole Middle Ordovician (Talltendre; Casas & Palacios, 2012).

The Sardic unconformity originated by the emersion/emergence of the Cambrian-Lower Ordovician deposits in response to uplifting. The former uplift caused emersion and erosion of the Cambrian-Lower Ordovician deposits in both the pre-Sardic successions of the Talltendre and Ribes de Freser zones (Bruguera unit), but with some differences. In the Talltendre zone, the emersion and erosion occurred, and led to palaeorelief formation, together to the occurrence of pre-Sardic deformations. The monotonous character of the pre-Sardic succession and its thickness does not allow us to estimate a plausible erosion. In the Ribes de Freser zone too, the Variscan and the Alpine structure superimposed (nappe stacking), do not allow to estimate the real erosion.

The deformations (folding) affecting the pre-unconformity successions cropping out in the Talltendre and Ribes de Freser area (Bruguera unit) could be responsible for the different bedding attitudes of the former series, too. The age of the Sardic deformations is included between Early (Floian) and Middle Ordovician (Darriwilian). These folding, albeit all sealed by the Sardic unconformity and foliation-free, differs in size and orientation (e.g., N-S trending folds in the Bruguera unit vs. WNW-ESE or NE-SW trending folds in the Talltendre area), making difficult to assign an univocal trend to the former deformations, or understand how the original compression developed.

Furthermore, normal faulting affected the pre-Sardic succession, the unconformity, and the base of the Upper Ordovician sequence. The deposition of the post-unconformity succession (Rabassa and Cava Formations) is contemporaneous to extensional tectonics which caused faulting and the fragmentation of the “basin”. The former faults appears in La Molina (La Cerdanya Unit) and in the Conflent areas (Casas, 2010), too.

The extensional tectonics could be responsible for the accomodation space variations, and, although the faults peter out in the Katian deposit (Cava Formation), they could be related to the creation of local different contexts (e.g., El Baell Formation).

Considering the post-Sardic successions cropping out in the Talltendre and Ribes de Freser areas, it is possible to distinguish between a domain characterized by scarce volcaniclastic/volcanic deposits (Talltendre area), and a rich-volcanic one (Ribes de Freser area). The former domains share few analogies, but exhibit distinctive features. Both the domains share a pre-Sardic (Upper Cambrian-Lower Ordovician) siliciclastic deposits (Jujols Group) related to shallow marine platform, which represent the latter deposit below the Sardic unconformity.

Besides, the domains share similar successions above the Sandbian transgression (former "Caradocian"), which reflect the establishment of siliciclastic continental to marine shelf deposits, punctuated by carbonate key levels (Estana and El Baell Formations) of Katian age.

Considering the pre- and the post- Sardic sequences (**Fig. 8.2**), Casas et al. (2019) illustrated a stratigraphic comparison between the former series cropping out in Sardinia and Eastern Pyrenees, in which the unconformity and the limestone beds represent the key levels. Comparing the stratigraphic characters of the post-Sardic sequences cropping out in Sardinia and the pyreneean ones, it is possible to highlight the similarity between the Foreland (External Zone, Sardinia) and the Talltendre series, and between the Nappe Zone (Sarrabus and Gerrei units, Sardinia) and the Ribes de Freser/Bruguera units.

The last discoveries on the Ordovician age of the magmatic products encased in the pre- and post- Sardic successions in both the Nappe and Inner Zones of Sardinia, in the Eastern and Central Pyrenees, In Montagne Noire and Mouthoumet Massif, highlighted the importance of the magmatic activity related to the Sardic unconformity (**Fig. 8.2**). Casas et al. (2019) show clearly the occurrence of an important magmatic and volcanic Ordovician activity, which developed diachronically. Furthermore, in Sardinia three cycles could be distinguished, and in the Eastern Pyrenees, two cycles: the Sandbian/Katian one is coincident for the two areas, while the previous cycle is Floian (Lower Ordovician) in the Pyrenees, and Middle Ordovician in Sardinia.

As stated in the Cambrian-Ordovician successions of Sardinia and Pyrenees, Sardic deformations in both the areas do not show the same orientation. Taking into account the rotation of the Sardinia-Corsica batholith, the direction of the Sardic deformations (folding and faulting) differs from Sardinia to Pyrenees. Sardic deformations (folding) show different trending attitude for the Talltendre and Bruguera areas, taking into account the comparison with the former and other areas in the same tectonic unit (La Molina, Casas, 2010). This could be due on the fact that the Sardic deformations generated in response to other structures (extensional faults, Talltendre area - Puddu et al., 2019), or that they generated after a compressive stress (Su Scoffoni area, Sarrabus Unit, External Nappe Zone; Cocco & Funedda, 2019).

Faulting affecting the pre-unconformity succession in the Foreland of Sardinia (Pasci et al., 2008), although probably linked to an half-grabens environment in which the

post-unconformity deposit (Monte Argentu Formation) developed (Brusca & Dessau, 1968; Martini et al., 1991), is lacking in the pre-Sardic deposit of the Nappe zone, and differs from the faulting developed in the investigated pyrenean areas. There, the former faulting affects only the Cambro-Ordovician deposit, are often thrusts fault, and are sealed by the unconformity and the Upper Ordovician deposit. No pyrenean-like faults have been individuated in Sardinia

.

CHAPTER 6

CHAPTER 6

A COMPARISON OF THE TOLEDANIAN AND SARDIC VOLCANISM IN SOUTH-WESTERN EUROPE

6.1 Comparative geochemical study on Furongian-earliest Ordovician (Toledanian) and Ordovician (Sardic) felsic magmatic events in southwestern Europe: underplating of hot mafic magmas linked to the opening of the Rheic Ocean.
(*paper 4*)

Comparative geochemical study on Furongian-earliest Ordovician (Toledanian) and Ordovician (Sardic) felsic magmatic events in south-western Europe: underplating of hot mafic magmas linked to the opening of the Rheic Ocean

J. Javier Álvaro[a]*, Teresa Sánchez-García[b], Claudia Puddu[c], Josep Maria Casas[d], Alejandro Díez-Montes[e], Montserrat Liesa[f] & Giacomo Oggiano[g]

[a] *Instituto de Geociencias (CSIC-UCM), Dr. Severo Ochoa 7, 28040 Madrid, Spain, jj.alvaro@csic.es*
[b] *Instituto Geológico y Minero de España, Ríos Rosas 23, 28003 Madrid, Spain, t.sanchez@igme.es*
[c] *Dpto. Ciencias de la Tierra, Universidad de Zaragoza, 50009 Zaragoza, Spain, claudiapuddugeo@gmail.com*
[d] *Dpt. de Dinàmica de la Terra i de l'Oceà, Universitat de Barcelona, Martí Franquès s/n, 08028 Barcelona, Spain, casas@ub.edu*
[e] *Instituto Geológico y Minero de España, Plaza de la Constitución 1, 37001 Salamanca, Spain, al.diez@igme.es*
[f] *Dept. de Mineralogia, Petrologia i Geologia aplicada, Universitat de Barcelona, Martí Franquès s/n, 08028 Barcelona, Spain, mliesa@ub.edu*
[g] *Dipartimento di Scienze della Natura e del Territorio, 07100 Sassari, Italy, giacoggi@uniss.it*

* Corresponding author

ABSTRACT

A geochemical comparison of Early Palaeozoic felsic magmatic episodes throughout the south-western European margin of Gondwana is made, and includes (i) Furongian-Early Ordovician (Toledanian) activies recorded in the Central Iberian and Galicia-Trás-os-Montes Zones of the Iberian Massif, and (ii) Early-Late Ordovician (Sardic) activities in the eastern Pyrenees, Occitan Domain (Albigeois, Montagne Noire and Mouthoumet massifs) and Sardinia. Both phases are related to uplift and denudation of an inherited palaeorelief, and stratigraphically preserved as distinct angular discordances and paraconformities involving gaps of up to 22 m.y. The geochemical features of the Toledanian and Sardic, felsic-dominant activies point to a predominance of magmatic byproducts derived from the melting of metasedimentary rocks, rich in SiO_2 and K_2O and with peraluminous character. Zr/TiO_2, Zr/Nb, Nb/Y and Zr vs. Ga/Al ratios, and REE and $\varepsilon Nd_{(t)}$ values suggest the contemporaneity, for both phases, of two geochemical scenarios characterized by arc and extensional features evolving to distinct extensional and rifting conditions associated with the final outpouring of mafic tholeiitic-dominant lava flows. The Toledanian and Sardic magmatic phases are linked to neither metamorphism nor penetrative deformation; on the contrary, their unconformities are associated with foliation-free open folds subsequently affected by the Variscan deformation. The geochemical and structural framework precludes subduction generated melts reaching the crust in a magmatic arc to back-arc setting, but favours partial melting of sediments and/or granitoids in a continental lower crust

triggered by the underplating of hot mafic magmas related to the opening of the Rheic Ocean.

Keywords: granite, orthogneiss, geochemistry, Cambrian, Ordovician, Gondwana.

1. Introduction

A succession of Early-Palaeozoic magmatic episodes, ranging in age from Furongian (former "late Cambrian") to Late Ordovician, is widespread along the south-western European margin of Gondwana. Magmatic pulses are characterized by preferential development in different palaeogeographic areas and linked to the development of stratigraphic unconformities, but they are related to neither metamorphism nor penetrative deformation (Gutiérrez Marco et al., 2002; Montero et al., 2007). In the Central Iberian Zone of the Iberian Massif (representing the western branch of the Ibero-Armorican Arc; **Fig. 1A-B**), this magmatism is mainly represented by the Ollo de Sapo Formation, which has long been recognized as a Furongian-Early Ordovician (495-470 Ma) assemblage of felsic-dominant volcanic, subvolcanic and plutonic igneous rocks. This magmatic activity is contemporaneous with the development of the Toledanian Phase, which places Lower Ordovician (upper Tremadocian-Floian) rocks onlapping an inherited palaeorelief formed by Ediacaran-Cambrian rocks and involving a sedimentary gap of ca. 22 m.y. This unconformity can be correlated with the "Furongian gap" identified in the Ossa-Morena Zone of the Iberian Massif and the Anti-Atlas Ranges of Morocco (Álvaro et al., 2007, 2018; Álvaro & Vizcaïno, 2018; Sánchez-García et al., 2019), and with the "lacaune normande" in the central and North-Armorican Domains (Le Corre et al., 1991).

Another felsic-dominant magmatic event, although younger (Early-Late Ordovician) in age, has been recognized in some massifs situated along the eastern branch of the Variscan Ibero-Armorican Arc, such as the Pyrenees, the Occitan Domain and Sardinia (**Fig. 1A, C-E**). This magmatism is related to the Sardic unconformity, where Furongian-Lower Ordovician rocks are unconformably overlain by those attributed to the Sandbian-lower Katian (former Caradoc). The Sardic Phase is related to both: (i) a sedimentary gap of ca. 16-20 m.y., and an unconformity that geometrically ranges from 90° (angular discordance) to 0° (paraconformity) (Barca & Cherchi, 2004; Funneda & Oggiano, 2009; Álvaro et al., 2016, 2018; Casas et al., 2019); and (ii) a Mid Ordovician development of cleavage-free folds lacking any contemporaneous metamorphism (for an updated revision, see Casas et al., 2019). The gap is 16-20 m.y. and the magmatic activity took place during a time span of about 25-30 m.y. (from 475 to 445 Ma) so, both ranges can be considered as broadly contemporaneous.

Although a general consensus exists to associate this Furongian-Ordovician magmatism with the opening of the Rheic Ocean and the drift of Avalonia from northwestern Gondwana (Díez Montes et al., 2010; Nance et al., 2010; Thomson et al., 2010; Álvaro et al., 2014*a*), the origin of this magmatism has received different interpretations. In the Central Iberian Zone, for instance, several geodynamic models have been proposed, such as: (i) subduction-related melts reaching the crust in a

magmatic arc to back-arc setting (Valverde-Vaquero & Dunning, 2000; Castro et al., 2009); (ii) partial melting of sediments or granitoids in a continental lower crust affected by the underplating of hot mafic magmas during an extensional regime (Bea et al., 2007; Montero et al., 2009; Díez Montes et al., 2010); and (iii) post-collisional decompression melting of an earlier thickened continental crust, and without significant mantle involvement (Villaseca et al., 2016). In the Occitan Domain (southern French Massif Central and Mouthoumet massifs) and the Pyrenees, Marini (1988), Pouclet et al. (2017) and Puddu et al. (2019) have suggested a link to mantle thermal anomalies. Navidad et al. (2018) proposed that the Pyrenean magmatism was induced by progressive crustal thinning and uplift of lithospheric mantle isoterms. In Sardinia, Oggiano et al. (2010), Carmignani et al. (2001), Gaggero et al. (2012) and Cruciani et al. (2018) have suggested that a subduction scenario, mirroring an Andean-type active margin, caused the main Mid-Ordovician magmatic activity. In the Alps, the Sardic counterpart is also interpreted as a result of the collision of the so-called Qaidam Arc with the Gondwanan margin, subsequently followed by the accretion of the Qilian Block (Von Raumer & Stampfli, 2008; Von Raumer et al., 2013, 2015). This geodynamic interpretation is mainly suggested for the Alpine Briançonnais-Austroalpine basement, where the volcanosedimentary complexes postdating the Sardic tectonic inversion and folding stage portray a younger arc-arc oblique collision (450 Ma) of the eastern tail of the internal Alpine margin with the Hun terrane, succeeded by conspicuous exhumation in a transform margin setting (430 Ma) (Zurbriggen et al., 1997; Schaltegger et al., 2003; Franz & Romer, 2007; Von Raumer & Stampfli, 2008; Von Raumer et al., 2013; Zurbriggen, 2015, 2017).

Until now the Toledanian and Sardic magmatic events had been studied on different areas and interpreted separately, without taking into account their similarities and differences. In this work, the geochemical affinities of the Furongian-Early Ordovician (Toledanian) and Early-Late Ordovician (Sardic) felsic magmatic activities recorded in the Central Iberian and Galicia-Trás-os-Montes Zones, Pyrenees, Occitan Domain and Sardinia are compared. The re-appraisal is based on 17 new samples from the Pyrenees, Montagne Noire and Sardinia, completing the absence of analysis in these areas and wide-ranging a dataset of 93 previously published geochemical analyses throughout the study region in south-western Europe. This comparison may contribute to a better understanding of the meaning and origin of this felsic magmatism, and thus, to discuss the geodynamic scenario of this Gondwana margin (**Fig. 1A**) during Cambrian-Ordovician times, bracketed between the Cadomian and Variscan orogenies.

2. Emplacement and age of magmatic events

This section documents the emplacement (summarized in **Fig. 2**) and age (**Fig. 3**) of the Toledanian and Sardic magmatic events throughout the south-western basement European Variscan Belt, in the northwestern margin of Gondwana during Cambro–Ordovician times.

2.1. Iberian Massif

In the Ossa Morena and southern Central Iberian Zones of the Iberian Massif (**Fig. 1A-B**), the so-called Toledanian Phase is recognized as an angular discordance that separates variably tilted Ediacaran-Cambrian Series 2 rifting volcanosedimentary packages from overlying passive-margin successions. The Toledanian gap comprises, at least, most of the Furongian and basal Ordovician, but the involved erosion can incise into the entire Cambrian and the upper Ediacaran Cadomian basement (Gutiérrez-Marco et al., 2019; Álvaro et al., 2019; Sánchez-García et al., 2019). Recently, Sánchez-García et al. (2019) have interpreted the Toledanian Phase as a break-up (or rift/drift) unconformity with the Armorican Quartzite (including the Purple Series and Los Montes Beds; McDougall et al., 1987; Gutiérrez-Alonso et al., 2007; Shaw et al., 2012, 2014) sealing an inherited Toledanian palaeorelief (**Fig. 2**).

The phase of uplift and denudation of an inherited palaeorelief composed of upper Ediacaran-Cambrian rocks is associated with the massive outpouring of felsic-dominant calc-alkaline magmatic episodes related to neither metamorphic nor cleavage features. This magmatic activity is widely distributed throughout several areas of the Iberian Massif, such as the Cantabrian Zone and the easternmost flank of the West Asturian-Leonese Zone, where sills and rhyolitic lava flows and volcaniclastics mark the base of the Armorican Quartzite (dated at ca. 477.5 Ma; Gutiérrez-Alonso et al., 2007, 2016), and the lower Tremadocian Borrachón Formation of the Iberian Chains (Álvaro et al., 2008). Similar ages have been reported from igneous rocks of the Basal Allochthonous Units and the Schistose Domain in the Galicia-Trás-os-Montes Zone (500-462 Ma; Valverde-Vaquero et al., 2005, 2007; Montero et al., 2009; Talavera et al., 2008, 2013; Dias da Silva et al., 2012, 2014; Díez Fernández et al., 2012; Farias et al., 2014) and different areas of the Central Iberian Zone, including the contact between the Central Iberian and Ossa-Morena Zones, where the Carrascal and Portalegre batoliths are intruded and the felsic volcanosedimentary Urra Formation marks the unconformity that separates Cambrian and Ordovician strata (494-470 Ma, Solá et al., 2008; Antunes et al., 2009; Neiva et al., 2009; Romaõ et al., 2010; Rubio-Ordóñez et al., 2012; Villaseca et al., 2013) (**Fig. 1B**).

Figure 1. A. Reconstruction of the south-western European margin of Gondwana in Late Carboniferous-Early Permian times; modified from Pouclet et al. (2017). B. Setting of samples in the Central Iberian and Galicia-Trás-os-Montes zones; *59* Carrascal, *68* Guadarrama, *70* Sanabria, *74* Miranda do Douro, *77* Ollo de Sapo, *79* Portalegre, *82* Saldanha, *84* San Sebastián, *90* Urra, *Bc* Bragança Complex, *BCSZ* Badajoz-Córdoba Shear Zone, *Br* Brévenne, *Ce* Cévennes massif, *CIZ* Central Iberian Zone, *COC* Cabo Ordenes Complex, *CZ* Cantabrian Zone, *GAPL* Grimaud-Asinara-Posada Line, *Gu* Guéret, *GTMZ* Galicia-Trás-os-Montes Zone, *IZ* Inner Zone, *Ma* Margueride, *MC* Morais Complex *ME* Maures-Estérel massif, *Mo* Mouthoumet massif, *Mv* Morvan, *NPFT* North Pyrenean Fault Thrust, *OC* Ordenes Complex, *OD* Occitan Domain, *OMZ* Ossa-Morena Zone, *PTFSZ* PYR Porto-Tomar-Ferreira do Alentejo Shear Zone, Pyrenean Domain, *Sa* Sanabria, *SAD* South Armorican Domain, *SASZs* South-Armorican Shear-Zone southern branch, *SHF* Sillon Houiller Fault, *SISZ* South-Iberian Shear Zone, *SPFT* South Pyrenean Fault Thrust, *Vc* Variscan Corsica, *Ve* Velay, *VBS* Verin-Bragança Synform and *WALZ* West Asturian-Leonese Zone; modified from Sánchez-García et al. (2019). C. Setting of samples in the Montagne Noire and Mouthoumet massifs; *Am1-2* Larroque hamlet (Ambialet), *Stg* St.Géraud, *Sta* St. André, *Mj* Montjoi, *Qu*

Quintillan, *GL* Roque de Bandies, *VLR* Villerouge-Termenès, *VIN* Le Vintrou, *HER* Gorges d'Héric (Caroux massif), *Ax1* S Mazamet (Nore massif), *Ax2* (Rou) S Rouayroux (Agout massif); modified from Álvaro et al. (2016). D. Setting of Pyrenean samples; *AB-08-01, 02, 03* Albera metavolcanics, *AB-08-05* Albera orthogneisses, *BN-1* Andorra rhyolites, *fc-1803* Pallaresa rhyolites; modified from Casas et al. (2019). E. Setting of Sardinian samples; *CS 2,3,4,8* Spartivento Cap, *T2* Tuerreda, *CC5* Cuile Culurgioni, *MF1* Monte Filau, *MFS1* Monte Settiballas, *PB* Punta Bianca; modified from Oggiano et al. (2010).

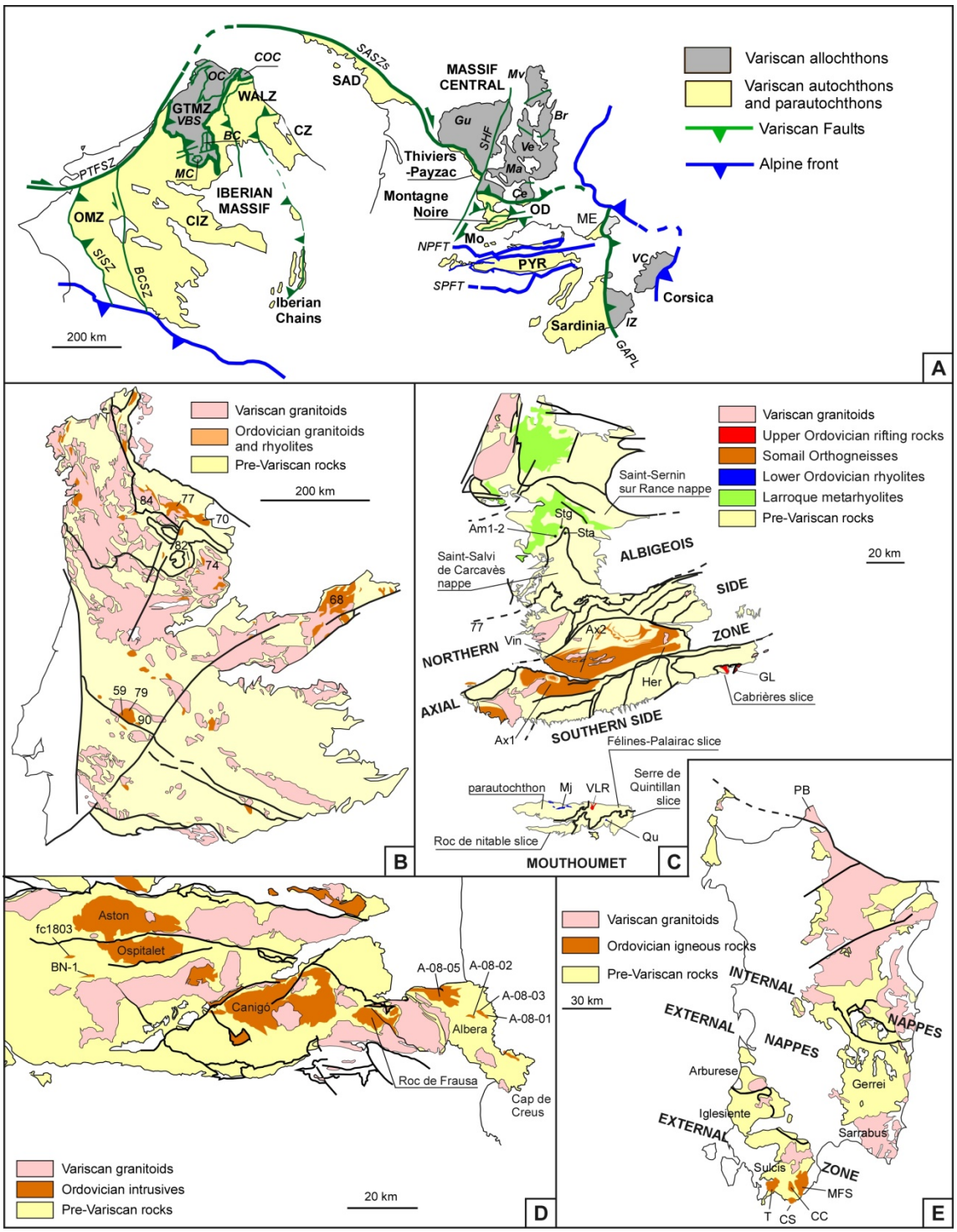

The most voluminous Toledanian-related volcanic episode is represented by the Ollo de Sapo Formation, which crops out throughout the northeastern Central Iberian Zone. It mainly consists of felsic volcanosedimentary and volcanic rocks, interbedded at the base of the Lower Ordovician strata and plutonic bodies. The Ollo de Sapo volcanosedimentary Formation has long been recognized as an enigmatic Furongian-Early Ordovician (495-470 Ma) magmatic event exposed along the core of a 600 km-long antiform (labelled as *77* in **Fig. 1B**) (Valverde-Vaquero & Dunning, 2000; Bea et al., 2006; Montero et al., 2007, 2009; Zeck et al., 2007; Castiñeiras et al., 2008*a*; Díez Montes et al., 2010; Navidad & Castiñeiras, 2011; Talavera et al., 2013; López-Sánchez et al., 2015; Díaz-Alvarado el al., 2016; Villaseca et al., 2016; García-Arias et al., 2018). The peak of magmatic activity was reached at ca. 490-485 Ma and its most recognizable characteristic is the presence of abundant megacrysts of K-feldspar, plagioclase and blue quartz. There is no evident space-time relationship in its distribution (for a discussion, see López-Sánchez et al., 2015) and, collectively, the Ollo de Sapo Formation rocks record a major tectonothermal event whose expression can be found in most of the Variscan massifs of continental Europe including the Armorican and Bohemian massifs (e.g., von Quadt, 1997; Kröner & Willmer, 1998; Linnemann et al., 2000; Tichomirowa et al., 2001; Friedl et al., 2004; Mingram et al., 2004; Teipel et al., 2004; Ballèvre et al., 2012; El Korh et al., 2012; Tichomirowa et al., 2012; for a summary, see Casas and Murphy, 2018). The large volume of magmatic rocks located in the European Variscan Belt led some authors to propose the existence of a siliceous Large Igneous Province (LIP) (Díez Montes et al., 2010; Gutiérrez-Alonso et al., 2016), named Ibero-Armorican LIP by García-Arias et al. (2018).

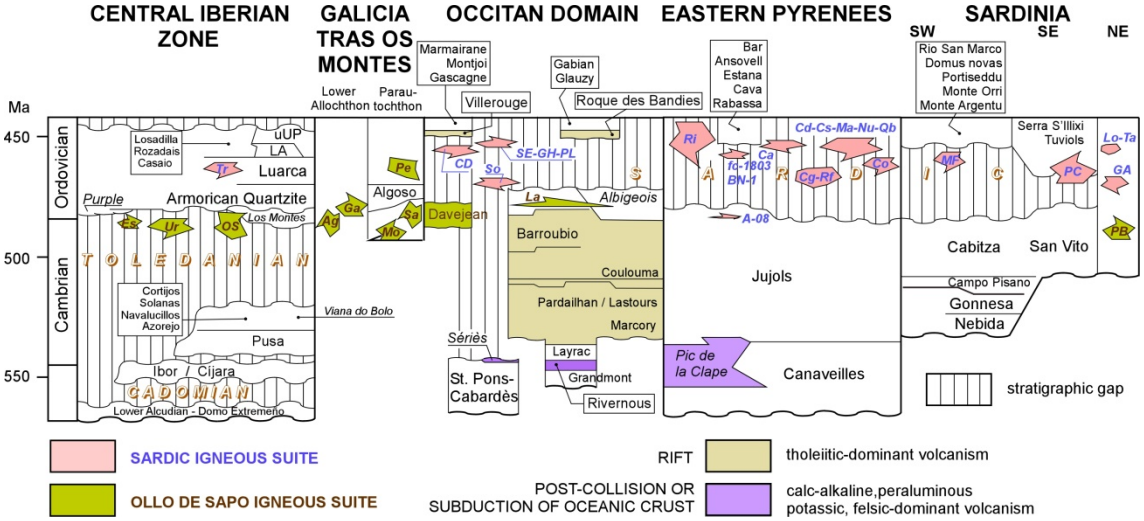

Figure 2. Stratigraphic comparison of the Cambro-Ordovician successions from the Central Iberian Zone, Galicia Trás-os-Montes Zone, Occitan Domain, Eastern Pyrenees and Sardinia; modified from Álvaro et al. (2014b, 2016, 2018), Pouclet et al. (2017) and Sánchez-García et al. (2019); the northern Central Iberian Zone, in the vicinity of Salamanca, is not included here (Díez Balda et al., 1990); abbreviations: *A-08* Albera orthogneisses and metavolcanics (ca. 465–472 Ma; Liesa et al., 2011), *Ag* Agualada, *BN-1* Andorra rhyolites, *Ca* Campelles ignimbrites (ca. 455 Ma, Martí et al., 2014), *CD* Cadí gneiss (456 ± 5 Ma, Casas et al., 2010), *Cg* Canigó gneiss (472-462 Ma, Cocherie et al., 2005; Navidad et al., 2018), *Co* Cortalets metabasite (460 ± 3 Ma, Navidad et al., 2018), *Cs* Casemí gneiss (446 ± 5 and 452 ± 5 Ma,

Casas et al., 2010), *Es* Estremoz rhyolites (499 Ma, Pereira et al., 2012), *fc-1803* Pallaresa rhyolites (ca. 453 Ma; Clariana et al., 2018), *Ga* Galiñero, *GA* Golfo Aranci orthogneiss (469 ± 3.7 Ma, Giacomini et al., 2006), *GH* Gorges d'Heric orthogneiss (450 ± 6 Ma, Roger et al., 2004), *La* Larroque Volcanic Complex, *LA* La Aquiana Limestone, *Ma* Marialles microdiorite (453 ± 4 Ma, Casas et al., 2010), *Lo* Lodè orthogneiss (456 ± 14 Ma, Helbing and Tiepolo, 2005), *MF* Monte Filau-Capo Spartivento orthogneiss (449 ± 6 Ma, Ludwing and Turi, 1989; 457.5 ± 0,3 and 458.2 ± 0.3 Ma, Pavanetto et al., 2012), *Mo* Mora (493.5 ± 2 Ma, Dias Da Silva et al., 2014), *Nu* Núria gneiss (457 ± 4 Ma, Martínez et al., 2011), *OS* Ollo de Sapo rhyolites and ash-fall tuff beds (ca. 477 Ma., Gutiérrez-Alonso et al., 2016), *Pe* Peso Volcanic Complex, *PL* Pont de Larn orthogneiss (456 ± 3 Ma, Roger et al., 2004), *Qb* Queralbs gneiss (457 ± 5 Ma, Martínez et al., 2011), *PB* Punta Bianca orthogneiss (broadly Furongian−Tremadocian in age), *PC* Porto Corallo dacites (465.4 ± 1.9 and 464 ± 1 Ma, Giacomini et al., 2006; Oggiano et al., 2010), *Ri* Ribes granophyre (458 ± 3 Ma, Martínez et al., 2011), *Rf* Roc de Frausa gneiss (477 ± 4, 476 ± 5 Ma, Cocherie et al., 2005; Castiñeiras et al., 2008), *So* Somail orthogneiss (471 ± 4 Ma, Cocherie et al. 2005), *Sa* Saldanha (483.7 ± 1.5; Dias da Silva, 2014), *SE* Saint Eutrope gneiss (455 ± 2 Ma, Pitra et al., 2012), *Ta* Tanaunella orthogneiss 458 ± 7 Ma (Helbing and Tiepolo, 2005), *Tr* Turchas, *Ur* Urra rhyolites and *uUP* undifferentiated Upper Ordovician.

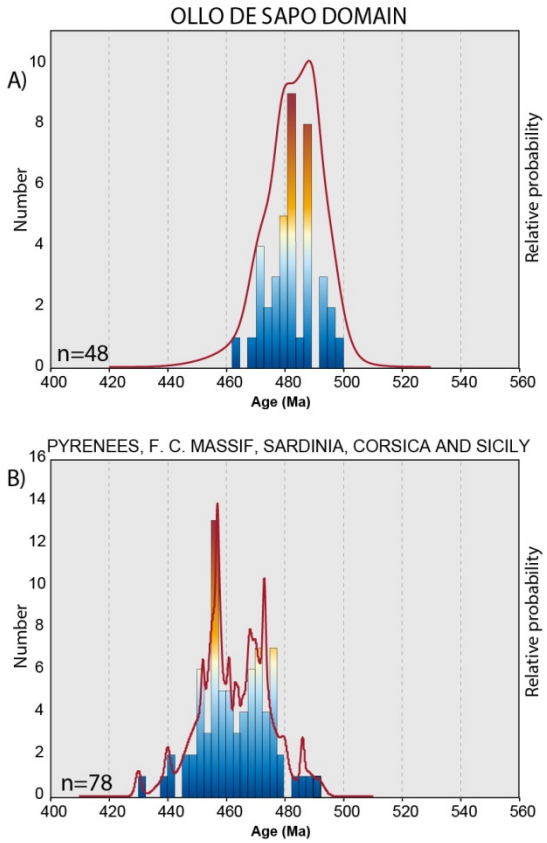

Figure 3. Relative probability plots of the age of the Cambrian–Ordovician magmatism for (A) the Ollo de Sapo domain from the Central Iberian Zone; and (B) Pyrenees (Guilleries and Gavarres massifs), French Central Massif (including Montagne Noire), Sardinia, Corsica and Sicily (*n* = number of analyses). Data obtained from references cited in the text.

The Sardic Phase has been proposed marking a stratigraphic discontinuity close to the Middle-Upper Ordovician boundary interval in some areas of the Central Iberian (e.g., Buçaco and the Truchas Syncline; Martínez Catalán et al., 1992; Días da Silva et al., 2016) and the Morais Allochthonous Complex of the Galicia-Trás-os-Montes Zones (Días da Silva, 2014; Días da Silva et al., 2014, 2016). In the Truchas Syncline, the significance of the discontinuity (or discontinuities) was questioned by a biostratigraphic study of conodonts and the re-interpretation of some of these scouring surfaces as the result of Hirnantian glaciogenic incisions (Sarmiento et al., 1999). The pre–Hirnantian discontinuities have been interpreted as linked to the development of "horsts and half-grabens of local extent" , as a result of which "tilting and gentle folding of the Lower-Middle Ordovician strata, due to the rotation of individual half-grabens and horsts, create the Sardic unconformity in Iberia" (Da Silva et al., 2016: pp. 1131 and 1143). However, the presence of synsedimentary listric faults associated with local outpouring of a basic volcanism, related to extensional pulses in the Ordovician passive-margin platform fringing Northwest Gondwana, cannot be associated with the Sardic Phase. As summarized in this work, the Sardic Phase is characterized by generalized cortical uplift, denudation of exposed uplifted areas under subaerial exposure, stratigraphic gaps of about 25-30 m.y., broad intrusion of felsic granitic plutons (now orthogneisses after Variscan deformation and metamorphism) with calc-alkaline affinity, and record of alluvial-to-fluvial deposits onlapping the unconformity. These are the features that characterize the Ordovician Sardic Phase, not the record of Ordovician volcanism and of local listric faults (e.g., Casas et al., 2010, 2019; Álvaro et al., 2016).

In contrast, the Sardic aftermath is represented by a basic-dominant volcanic activity, mainly of tholeiitic affinity, and lining rifting branches highlighting the onset of listric-fault networks; this event could be geodynamically compared with some processes recorded in the Central Iberian and the Galician-Trás-os-Montes Zones, but not with the Sardic Phase. Therefore, the presence of the Sardic Phase in Iberia was already ruled out by the information published during the last two decades, and should not be maintained except if the above-reported tectonothermal events are really found in Iberia. The presence of an Ordovician volcanism associated with listric faults is not an argument to support the record of the Sardic Phase.

2.2. Central and Eastern Pyrenees

In the central and eastern Pyrenees (**Fig. 1D**), earliest Ordovician volcanic-free passive-margin conditions, represented by the Jujols Group (Padel et al., 2018), were succeeded by a late Early-Mid Ordovician phase of uplift and erosion that led to the onset of the Sardic unconformity (**Fig. 2**). Uplift was associated with magmatic activity, which continued until Late Ordovician times. An extensional interval took place then developing normal faults that controlled the sedimentation of post-Sardic siliciclastic deposits infilling palaeorelief depressions. Acritarchs recovered in the uppermost part of the Jujols Group suggest a broad Furongian-earliest Ordovician age (Casas & Palacios, 2012), conterminous with a maximum depositional age of ca. 475 Ma, based on the age of the youngest detrital zircon populations (Margalef et al., 2016). On the other hand, a

ca. 459 Ma U-Pb age for the Upper Ordovician volcanic rocks overlying the Sardic Unconformity has been proposed in the eastern Pyrenees (Martí et al., 2019), and ca. 452-455 Ma in the neighbouring Catalan Coastal Ranges, which represent the southern prolongation of the Pyrenees (Navidad et al., 2010; Martínez et al., 2011). Thus, a time gap of about 16-23 m.y. can be related to the Sardic Phase in the eastern Pyrenees and the neighbouring Catalan Coastal Ranges.

Coeval with the late Early-Mid Ordovician phase of generalized uplift and denudation, a key magmatic activity led to the intrusion of voluminous granitoids, about 500 to 3000 m thick and encased in strata of the Ediacaran-Lower Cambrian Canaveilles Group (**Fig. 2**). These granitoids constitute the protoliths of the large orthogneissic laccoliths that punctuate the backbone of the central and eastern Pyrenees. These are, from west to east (**Fig. 1D**), the Aston (467–470 Ma; Denèle et al., 2009; Mezger & Gerdes, 2016), Hospitalet (about 472 Ma, Denèle et al., 2009), Canigó (472-462 Ma, Cocherie et al., 2005; Navidad et al., 2018), Roc de Frausa (477-476 Ma; Cocherie et al., 2005; Castiñeiras et al., 2008b) and Albera (about 470 Ma; Liesa et al., 2011) massifs, which comprise a dominant Floian-Dapingian age. It is noticeable the fact that only a minor representation of coeval basic magmatic rocks are outcropped. The acidic volcanic equivalents have been documented in the Albera massif, where subvolcanic rhyolitic porphyroid rocks have yielded similar ages to those of the main gneissic bodies at about 474-465 Ma (Liesa et al., 2011). Similar acidic byproducts are represented by the rhyolitic sills of Pierrefite (Calvet et al., 1988).

The late Early-Mid Ordovician ("Sardic") phase of uplift was succeeded by a Late Ordovician extensional interval responsible for the opening of (half-)grabens infilled with the basal Upper Ordovician alluvial-to-fluvial conglomerates (La Rabassa Conglomerate Formation). At map scale, a set of NE-SW trending normal faults abruptly controlling the thickness of the basal Upper Ordovician formations can be recognized in the La Cerdanya area (Casas & Fernández, 2007; Casas, 2010). Sharp variations in the thickness of the Upper Ordovician strata have been documented by Hartevelt (1970) and Casas & Fernández (2007). Drastic variations in grain size and thickness can be attributed to the development of palaeotopographies controlled by faults and subsequent erosion of uplifted palaeoreliefs, with subsequent infill of depressed areas by alluvial fan and fluvial deposits, finally sealed by Silurian sediments (Puddu et al., 2019). A Late Ordovician magmatic pulse contemporaneously yielded a varied set of magmatic rocks. Small granitic bodies are encased in the Canaveilles strata of the Canigó massif. They constitute the protoliths of the Cadí (about 456 Ma; Casas et al., 2010), Casemí (446 to 452 Ma; Casas et al., 2010), Núria (ca. 457 Ma; Martínez et al., 2011) and Canigó G-1 type (ca. 457 Ma; Navidad et al., 2018) gneisses.

The lowermost part of the Canaveilles Group (the so-called Balaig Series) host metre-scale thick bodies of metadiorite sills related to an Upper Ordovician protolith, (ca. 453 Ma, SHRIMP U-Pb in zircon; Casas et al., 2010). Coeval calc-alkaline ignimbrites, andesites and volcaniclastic rocks are interbedded in the Upper Ordovician succession of the Bruguera and Ribes de Freser areas (Robert & Thiebaut, 1976; Ayora, 1980; Robert, 1980; Martí et al., 1986, 2019). In the Ribes area, a granitic body with granophyric texture, dated at ca. 458 Ma by Martínez et al. (2011), intruded at the base

of the Upper Ordovician succession. In the La Pallaresa dome, some metre-scale rhyodacitic to dacitic subvolcanic sills, Late Ordovician in age (ca. 453 Ma, Clariana et al., 2018), occur interbedded within the pre-unconformity strata and close to the base of the Upper Ordovician.

2.3. Occitan Domain: Albigeois, Montagne Noire and Mouthoumet massifs

The parautochthonous framework of the southern French Massif Central, named Occitan Domain by Pouclet et al. (2017), includes among others, from south to north, the Mouthoumet, Montagne Noire and Albigeois massifs. The domain represents the southeastern prolongation of the Variscan South Armorican Zone (including southwestern Bretagne and Vendée). Since Gèze (1949) and Arthaud (1970), the southern edge of the French Massif Central has been traditionally subdivided, from north to south, into the northern, axial and southern Montagne Noire (**Fig. 1C**). The Palaeozoic succession of the northern and southern sides includes sediments ranging from late Ediacaran to Silurian and from Terreneuvian (Cambrian) to Visean in age, respectively. These successions are affected by large scale, south-verging recumbent folds that display a low to moderate metamorphic grade. Their emplacement took place in Late Visean to Namurian times (Engel et al., 1980; Feist & Galtier, 1985; Echtler & Malavieille, 1990). The Axial Zone consists of plutonic, migmatitic and metamorphic rocks forming a regional ENE-WSW oriented dome (**Fig. 1C**), where four principal lithological units can be recognized (i) schists and micaschists, (ii) migmatitic orthogneisses, (iii) metapelitic metatexites, and (iv) diatexites and granites (Cocherie, 2003; Faure et al., 2004; Roger et al., 2004, 2015; Bé Mézème, 2005; Charles et al., 2009; Rabin et al., 2015). The Rosis micaschist synform subdivides the eastern Axial Zone into the Espinouse and Caroux sub-domes, whereas the southwestern edge of the Axial Zone comprises the Nore massif.

In the Occitan Domain, two main Cambro-Ordovician felsic events can be identified giving rise to the protoliths of (i) the Larroque metarhyolites in the northern Montagne Noire and Albigeois, thrusted southward from Rouergue; and (ii) the migmatitic ortogneisses that form the Axial Zone of the Montagne Noire (Fig. 2).

(i) The Larroque volcanosedimentary Complex is a thick (500-1000 m) package of porphyroclastic metarhyolites located on the northern Montagne Noire (Lacaune Mountains), Albigeois (St-Salvi-de-Carcavès and St-Sernin-sur-Rance nappes) and Rouergue; the Variscan setting of the formation is allochthonous in the Albigeois and parautochthonous in the rest. This volcanism is encased in the so-called “Série schisto-gréseuse verte” (see Guérangé-Lozes et al., 1996; Guérangé-Lozes and Alabouvette, 1999; Pouclet et al., 2017) (**Fig. 2**). The Larroque volcanic rocks consist of deformed porphyroclastic rhyolites rich in largely fragmented, lacunous (rhyolitic) quartz and alkali feldspar phenocrysts. The metarhyolites occur as porphyritic lava flows, sills and other associated facies, such as aphyric lava flows, porphyritic and aphyric pyroclastic flows of welded or unwelded ignimbritic types, fine to coarse tephra deposits, and epiclastic and volcaniclastic deposits. These rocks are named “augen gneiss” or augengneiss and do not display a high-grade gneiss paragenesis but a general lower

grade metamorphic mineralogy. The Occitan augengneisses mimic the Ollo de Sapo facies from the Central Iberian Zone because of their large bluish quartz phenocrysts. Based on geochemical similarities and contemporaneous emplacement, Pouclet et al. (2017) suggested that this event also supplied the Davejean acidic volcanic rocks in the Mouthoumet Massif, which represent the southern prolongation of the Montagne Noire (**Fig. 2**), and the Génis rhyolitic unit of the western Limousin sector.

(ii) Some migmatitic orthogneisses make up the southern Axial Zone, from the western Cabardès to the eastern Caroux domes. The orthogneisses, derived from Ordovician metagranites bearing large K-feldspar phenocrysts, were emplaced at about 471 Ma (Somail Orthogneiss, Cocherie et al., 2005), 456 to 450 Ma (Pont de Larn and Gorges d'Héric gneisses, Roger et al., 2004) and ca. 455 Ma (Sain Eutrope gneiss, Pitra et al., 2012). They intruded a metasedimentary pile, traditionally known as "Schistes X" and formally named St. Pons-Cabardès Group (**Fig. 2**). The latter consists of schists, greywackes, quartzites and subsidiary volcanic tuffs and marbles (Demange et al., 1996; Demange, 1999; Alabouvette et al., 2003; Roger et al., 2004; Cocherie et al., 2005). The group is topped by the Sériès Tuff, dated at about 545 Ma (Lescuyer & Cocherie, 1992), which represents a contemporaneous equivalent of the Cadomian Rivernous rhyolitic tuff (542.5 to 537.1 Ma) from the Lodève inlier of the northern Montagne Noire (Álvaro et al., 2014b, 2018; Padel et al., 2017). Age of migmatization has been inferred from U–Pb dates on monacite from migmatites and anatectic granites at 333 to 327 Ma (Bé Mézème, 2005; Charles et al., 2008); as a result, the 330-325 Ma time interval can represent a Variscan crustal melting event in the Axial Zone.

As in the Pyrenees, the Middle Ordovician is absent in the Occitan Domain. Its gap allows distinction between a Lower Ordovician pre-unconformity sedimentary package para- to unconformably overlain by an Upper Ordovician-Silurian succession (Álvaro et al., 2016; Pouclet et al., 2017).

2.4. Sardinia

In Sardinia the Cambro-Ordovician magmatism is well represented in the external (southern) and internal (northern) nappe zones of the exposed Variscan Belt (**Fig. 1E**), and ranges in age from late Furongian to Late Ordovician. A Furongian-Tremadocian (ca. 491-480 Ma) magmatic activity, predating the Sardic phase, is mostly represented by felsic volcanic and subvolcanic rocks encased in the San Vito sandstone Formation. The Sardic-related volcanic products differ from one nappe to another: intermediate and basic (mostly metandesites and andesitic basalts) are common in the nappe stacking of the central part of the island (Barbagia and Goceano), whereas felsic metavolcanites prevail in the southeastern units. Their age is bracketed between 465 and 455 Ma (Giacomini et al., 2006; Oggiano et al., 2010; Pavanetto et al., 2012; Cruciani et al., 2018) and matches the Sardic gap based on biostratigraphy (Barca et al., 1988).

Teichmüller (1931) and Stille (1939) were the first to recognize in southwestern Sardinia an intra-Ordovician stratigraphic hiatus. Its linked erosive unconformity is supported by a correlatable strong angular discordance in the Palaeozoic basement of the Iglesiente-Sulcis area, External Zone (Carmignani et al., 2001). This major

discontinuity separates the Cambrian-Lower Ordovician Nebida, Gonnesa and Iglesias groups (Pillola et al., 1998) from the overlying coarse-grained ("Puddinga") Monte Argentu metasediments (Leone et al., 1991, 2002; Laske et al., 1994). The gap comprises a chronostratigraphically constrained minimum gap of about 18 m.y. that includes the Floian and Dapingian (Barca et al., 1987, 1988; Pillola et al., 1998; Barca & Cherchi, 2004) (**Fig. 2**). The hiatus is related to neither metamorphism nor cleavage, though some E-W folds have been documented in the Gonnesa Anticline and the Iglesias Syncline (Cocco et al., 2018), which are overstepped by the "Puddinga" metaconglomerates. Both the E-W folds and the overlying metaconglomerates were subsequently affected by Variscan N-S folds (Cocco & Funneda, 2011, 2017). Sardic-related volcanic rocks are not involved in this area, but Sardic-inherited palaeoreliefs are lined with breccia slides that include metre- to decametre-scale carbonate boulders ("Olistoliti"), some of them hosting synsedimentary faults contemporaneously mineralized with ore bodies (Boni & Koeppel, 1985; Boni, 1986; Barca, 1991; Caron et al., 1997). The lower part of the unconformably overlying Monte Argentu Formation deposited in alluvial to fluvial environments (Martini et al., 1991; Loi et al., 1992; Loi & Dabard, 1997).

A similar gap was reported by Calvino (1972) in the Sarrabus-Gerrei units of the External Nappe Zone. The so-called "Sarrabese Phase" is related to the onset of thick, up to 500 m thick, volcanosedimentary complexes and volcanites (Barca et al., 1986; Di Pisa et al., 1992) with a Darriwilian age for the protoliths of the metavolcanic rocks (465.4 to 464 Ma; Giacomini et al., 2006; Oggiano et al., 2010). In the Iglesiente-Sulcis region (**Fig. 1E**), Carmignani et al. (1986, 1992, 1994, 2001) suggested that the "Sardic-Sarrabese phase" should be associated with the compression of a Cambro-Ordovician back-arc basin that originated the migration of the Ordovician volcanic arc toward the Gondwanan margin.

Some gneissic bodies, interpreted as the plutonic counterpart of metavolcanic rocks, are located in the Bithia unit (e.g., the Monte Filau area, 458 to 457 Ma, surrounded by a Mid-Ordovician andalusite thermal aureole; Pavanetto et al., 2012; Costamagna et al., 2016) and in the internal units (Lodè orthogneiss, ca. 456 Ma; Tanaunella orthogneiss, ca. 458 Ma, Helbing & Tiepolo, 2005; Golfo Aranci orthogneiss, ca. 469 Ma, Giacomini et al., 2006).

The Sardic palaeorelief is sealed by Upper Ordovician trangressive deposits. The sedimentary facies show high variability, but the -mostly terrigenous- sediments vary from grey fine- to medium-sized sandstones, to muddy sandstones and mudstones. They are referred to the Katian Punta Serpeddì and Orroeledu formations (Pistis et al., 2016). This post-Sardic sedimentary succession is coeval with a new magmatic pulsation represented by alkaline to tholeiitic within-plate basalts (Di Pisa et al., 1992; Gaggero et al., 2012).

	PYRENEES			MONTAGNE NOIRE				SARDINIA									
	Albera	Pallaresa	Andorra		Axial	Zone					External	Zone				Inner	Zone
Sample	**A-08-03**	**fC1803**	**BN 1**	**Ax - 1**	**Ax - 2**	**HER**	**VIN**	**CC 5**	**CS 2**	**CS 3**	**CS 5**	**CS 8**	**MF 1**	**MFS 1**	**T 2**	**PB50**	**PB100**
Long. (E)	3º7'39''	1º27'43''	1º33'29''	2º13'50''	2º33'58''	2º57'58''	2º13'50''	8º50'37''	8º50'35''	8º50'35''	8º50'40''	8º50'35''	8º50'47''	8º52'02''	8º48'54''	9°09'32''	9°09'32''
Lat. (N)	42º25'2''	42º36'1''	42º32'30''	43º34'32''	43º29'3''	43º34'32''	43º17'45''	38º54'16''	38º52'38''	38º52'38''	38º52'36''	38º52'39''	38º54'58''	38º53'57''	38º53'57''	41°11''	41°11'04''
SiO_2	68.38	71.67	69.18	70.38	67.43	68.31	73.97	76.43	75.14	76.52	76.61	76.36	72.13	75.94	75.55	68.93	67.24
TiO_2	0.57	0.63	0.61	0.36	0.64	0.61	0.20	0.08	0.08	0.09	0.04	0.06	0.31	0.13	0.18	0.41	0.46
Al_2O_3	15.68	14.24	15.05	14.90	15.76	15.39	13.82	13.28	12.81	11.80	12.71	12.63	13.80	13.16	12.94	16.32	15.79
Fe_2O_3	4.09	4.54	4.20	3.04	4.11	4.19	2.05	0.69	1.39	1.44	1.28	1.35	2.96	1.55	1.62	3.19	4.78
MnO	0.07	0.06	0.05	0.04	0.04	0.04	0.04	0.01	0.01	0.01	0.01	0.01	0.02	0.03	0.04	0.08	0.08
MgO	1.35	0.78	1.16	0.78	1.33	1.34	0.43	0.08	0.15	0.16	0.06	0.05	0.36	0.19	0.08	1.15	1.58
CaO	0.21	0.53	1.78	1.22	1.44	1.58	0.62	0.32	0.25	0.15	0.20	0.35	0.61	0.38	0.17	3.05	2.70
Na_2O	4.07	1.67	3.40	3.33	2.78	2.93	2.87	3.04	1.71	1.58	2.91	3.35	2.89	2.57	2.53	3.85	3.43
K_2O	2.84	2.91	2.71	4.35	4.68	4.03	4.55	4.79	7.84	7.43	5.16	4.91	5.47	4.94	5.36	2.26	2.96
P_2O_5	0.17	0.24	0.20	0.21	0.2	0.19	0.18	0.15	0.05	0.05	0.03	0.04	0.12	0.11	0.07	0.15	0.14
L.O.I.	2.03	2.60	1.50	1.2	1.3	1.2	1.2	1.1	0.4	0.7	0.9	0.8	1.1	0.9	1.4	0.90	0.70
Total	99.05	99.42	99.42	99.51	99.30	99.39	99.73	99.90	99.69	99.79	99.78	99.78	99.47	99.75	99.78	99.97	99.37
As	77.20	1.70	6.80	2.50	6.00	1.80	1.90	0.70	1.00	0.50	2.80	1.10	1.80	101.10	4.00	5.00	5.00
Ba	742.50	388.00	398.00	499	1050	767	256	60	467	109	21	27	784	194	192	689.00	600.00
Be	2.44	3.00	2.00	4.00	2.00	5.00	3.00	6.00	3.00	1.00	9.00	2.00	7.00	3.00	7.00	3.00	5.00
Bi	0.30	0.20	0.10	0.20	0.20	0.20	0.40	0.30	0.10	0.10	0.10	0.10	0.10	0.70	0.40	4.00	4.00
Cd	0.18	0.10	0.10	0.10	0.10	0.10	0.10	0.10	0.10	0.10	0.10	0.10	0.10	0.10	0.10		
Co	5.84	4.60	6.20	5.20	5.20	5.40	2.70	0.50	1.60	1.00	0.80	0.60	2.30	1.50	1.20	5.00	14.00
Cs	9.79	5.60	4.90	14.30	7.10	6.80	7.30	4.20	3.40	1.60	4.50	4.60	6.40	3.90	4.10	4.20	9.40
Cu	16.34	13.20	10.30	7.20	7.40	10.10	8.70	4.70	4.60	8.20	26.80	2.50	5.00	5.50	5.00	10.00	60.00
Ga	21.03	19.80	18.80	19.10	19.20	18.90	16.70	19.30	14.90	15.30	19.40	19.20	20.70	19.00	19.90	17.00	18.00
Hf	6.40	7.30	6.40	5.00	6.90	5.70	3.10	3.10	4.10	4.30	3.50	3.80	8.80	3.70	5.80	5.90	5.30
Mo	1.20	0.90	1.00	0.60	0.90	0.60	0.30	0.70	0.70	0.70	0.80	0.50	1.70	0.80	1.60	2.00	2.00
Nb	10.49	11.30	11.30	9.60	12.40	11.90	7.90	10.30	7.70	12.10	13.20	13.30	20.20	9.10	20.60	9.00	11.00
Ni	16.56	8.00	7.70	20.00	20.00	20.00	20.00	20.00	20.00	20.00	20.00	20.00	20.00	20.00	20.00	20.00	80.00
Pb	7.94	9.80	22.90	3.50	4.60	5.10	3.60	2.90	7.40	8.60	4.50	5.50	5.10	6.30	5.50	21.00	24.00
Rb	124.40	123.70	137.20	204.6	161.6	142.2	188.2	289.9	206.1	187.4	294.1	275.1	208.7	256.4	227.1	85.00	118.00
Sb	2.27	0.10	0.30	0.10	0.10	0.10	0.10	0.10	0.10	0.10	0.10	0.10	0.10	0.10	0.10	5.00	5.00
Sc		10.00	10.00	6.00	9.00	9.00	4.00	3.00	3.00	4.00	4.00	4.00	15.00	4.00	8.00	9.00	12.00
Sn	2.11	5.00	5.00	9.00	3.00	3.00	7.00	9.00	4.00	3.00	13.00	15.00	7.00	15.00	12.00	3.00	3.00
Sr	158.00	201.80	83.70	91.20	160.30	150.10	68.70	30.70	73.90	25.20	7.90	8.10	59.90	45.60	25.00	217.00	167.00
Ta	1.07	1.10	1.10	0.80	1.00	0.80	0.70	2.10	0.90	1.10	3.40	1.70	1.60	1.70	2.30	1.00	1.20
Th	11.90	15.70	13.50	11.10	14.40	14.30	5.90	9.10	14.10	17.00	13.50	13.10	22.80	10.20	26.90	13.30	11.50
U	3.70	5.10	4.60	4.10	3.60	3.20	4.80	3.30	2.90	3.20	3.50	3.50	4.60	8.10	4.90	4.50	2.20
V	44.49	49.00	36.00	36.00	63.00	68.00	22.00	8.00	8.00	8.00	8.00	8.00	15.00	8.00	10.00	62.00	53.00
W	1.80	1.90	2.50	3.20	2.60	1.60	3.00	5.60	0.90	2.10	5.20	3.00	2.40	4.40	3.50	1.00	20.00
Y	29.29	43.90	50.60	28.30	38.40	36.20	27.80	28.00	60.10	53.60	44.40	46.00	61.60	31.80	55.80	29.00	24.00
Zn	63.71	52.00	70.00	55.00	71.00	78.00	46.00	7.00	35.00	39.00	15.00	24.00	37.00	30.00	22.00	70.00	70.00
Zr	233.30	263.20	237.10	174.40	249.20	219.10	93.70	73.50	93.80	105.10	62.20	74.50	311.80	108.10	161.90	245.00	214.00
La	27.90	45.30	38.00	29.60	39.50	38.70	13.60	10.50	22.70	19.50	12.10	13.40	54.20	17.90	31.30	26.90	34.30
Ce	59.00	86.90	75.50	58.10	77.00	78.20	26.70	21.60	42.10	39.70	26.20	29.90	109.80	37.40	97.60	53.20	70.50
Pr	7.26	9.80	8.47	6.99	9.41	9.55	3.36	2.36	4.73	4.85	3.00	3.24	11.94	4.07	6.86	5.88	8.20
Nd	27.83	35.60	31.20	26.00	36.40	36.40	12.60	8.40	16.60	17.10	10.50	10.90	44.70	15.00	24.00	21.60	29.40
Sm	5.80	7.69	7.16	5.70	7.55	7.63	3.15	2.43	4.10	4.41	3.28	3.44	9.37	3.88	4.93	4.70	6.00
Eu	0.98	1.05	1.03	0.87	1.27	1.15	0.41	0.14	0.43	0.13	0.06	0.09	1.17	0.30	0.19	0.95	0.93
Gd	5.22	8.32	7.89	5.59	7.28	7.05	3.38	3.20	5.60	5.50	4.42	4.69	10.60	4.50	6.34	4.00	5.10
Tb	0.87	1.26	1.27	0.89	1.17	1.10	0.67	0.69	1.13	1.18	1.03	1.07	1.70	0.82	1.27	0.70	0.80
Dy	5.30	6.68	8.00	5.09	6.89	6.39	4.59	4.30	7.69	8.23	7.31	7.66	10.28	5.24	9.00	3.70	4.30
Ho	1.06	1.52	1.73	0.99	1.42	1.30	0.98	0.91	1.91	1.91	1.59	1.65	2.13	1.12	2.01	0.70	0.80
Er	2.98	4.52	4.96	2.64	3.92	3.56	3.07	2.85	5.80	6.46	5.35	5.38	6.25	3.64	6.17	2.20	2.10
Tm	0.46	0.60	0.73	0.38	0.57	0.50	0.44	0.43	0.91	1.00	0.85	0.85	0.89	0.52	0.92	0.35	0.32
Yb	3.00	3.98	4.72	2.33	3.56	3.11	2.83	2.95	5.81	6.60	6.10	6.16	5.53	3.70	6.04	2.50	2.20
Lu	0.44	0.58	0.69	0.33	0.53	0.45	0.39	0.44	0.90	0.94	0.92	0.94	0.86	0.56	0.90	0.41	0.36

Table 1 - Chemical analyses of magmatic rocks. ICP and ICP–MS methods at ACME–LABS in Canada.

3. Geochemical data

3.1. Materials and methods

The rocks selected for geochemical analysis (231 samples; see tectonostratigraphic location in **Fig. 1** and stratigraphic emplacement in **Fig. 2**) have recorded different degrees of hydrothermalism and metamorphism, as a result of which only the most immobiles elements have been considered. The geochemical calculations, in which the major elements take part, have been made from values recalculated to 100 in volatile free compositions; Fe is reported as FeO_t.

The geochemical dataset of the Central Iberian Zone includes 152 published geochemical data, from which 85 are plutonic and 67 volcanic and volcaniclastic rocks from the Ollo de Sapo Formation (Galicia, Sanabria and Guadarrama areas), and the contact between the Central Iberian and Ossa Morena Zones (Urra Formation and Portalegre and Carrascal granites). Other data were yielded from six volcanic rocks of the Galicia-Trás-os-Montes Zone (Saldanha area) (**Fig. 1B**; **Repository Data**).

The dataset of the eastern Pyrenees consists of 38 samples, six of which are upper Lower Ordovician volcanic rocks, and seven upper Lower Ordovician plutonic rocks, together with nine Upper Ordovician volcanic and 14 Upper Ordovician plutonic rocks (**Repository Data**). New data reported below include two samples of subvolcanic sills intercalated in the pre–Sardic unconformity succession (Clariana et al., 2018; Margalef, unpubl.; **Table 1**).

The study samples from the Occitan Domain comprise six metavolcanic rocks, four from the Larroque volcanosedimentary Complex in the Albigeois and northern Montagne Noire and two from the Mouthoumet massif (Pouclet et al., 2017) (**Repository Data**), and four new samples for the Axial Zone gneisses (**Table 1).**

In the Sardinian dataset, 25 published analyses are selected: five correspond to the Golfo Aranci orthogneiss (Giacomini et al., 2006), six to metavolcanics from the central part of the island (Giacomini et al., 2006; Cruciani et al., 2013), and five to metavolcanics and one to gneisses from the Bithia unit (Cruciani et al., 2018) (Repository Data). Ten new analyses are added from the Monte Filau and Capo Spartivento gneisses of the Bithia unit, and from the Punta Bianca gneisses embedded within the migmatites of the High-grade Metamorphic complex of the Inner Zone (**Table 1**).

Whole-rock major and trace elements and rare earth element (REE) compositions were determined at ACME Laboratories, Vancouver, Canada. $LiBO_2$ fusion followed by X-ray fluorescence spectroscopy (XRF) analysis was used to determine major elements. Rare earth and refractory elements were measured by ICP-MS following a lithium metaborate/tetraborate fusion and nitric acid digestion on 0.2 g of sample. For base metals, 0.5 g of sample was digested in Aqua Regia at 95 ºC and analyzed by inductively coupled plasma - atomic emission spectrometry (ICP-AES). Analyses of standards and duplicate samples indicate precision to better than 1 % for major oxides, and 3-10 % for minor and trace elements.

Additional Sm-Nd isotopic analyses were performed at Centro de Geocronologia y Geoqulmica Isotopica from the Complutense University, Madrid. They were carried out in whole-rock powders using a ^{150}Nd-^{149}Sm tracer by isotope dilution-thermal ionization mass spectrometry (ID-TIMS). The samples were first dissolved through oven digestion in sealed Teflon bombs with ultrapure reagents to perform two-stage conventional cation-exchange chromatography for separation of Sm and Nd (Strelow, 1960; Winchester, 1963), and subsequently analysed using a Sector 54 VG-Micromass multicollector spectrometer. The measured $^{143}Nd/^{144}Nd$ isotopic ratios were corrected for possible isobaric interferences from ^{142}Ce and ^{144}Sm (only for samples with $^{147}Sm/^{144}Sm < 0.0001$) and normalized to $^{146}Nd/^{144}Nd = 0.7219$ to correct for mass fractionation. The Lajolla Nd international isotopic standard was analysed during

sample measurement, and gave an average value of $^{143}Nd/^{144}Nd$ = 0.5114840 for 9 replicas, with an internal precision of ± 0.000032 (2σ). These values were used to correct the measured ratios for possible sample drift. The estimated error for the $^{147}Sm/^{144}Nd$ ratio is 0.1%.

A general classification of the analyzed samples, following Winchester & Floyd (1977), can be seen in **Figure 4A-B**, and the geographical coordinates of the new samples in **Table 1**. For geochemical comparison (summarized in **Table 2**), two large groups or suites are differentiated in order to check the similarities and differences between the magmatic rocks, and to infer a possible geochemical trend following a palaeogeographic SW-NE transect. The description reported below follows the same palaeogeographic and chronological order.

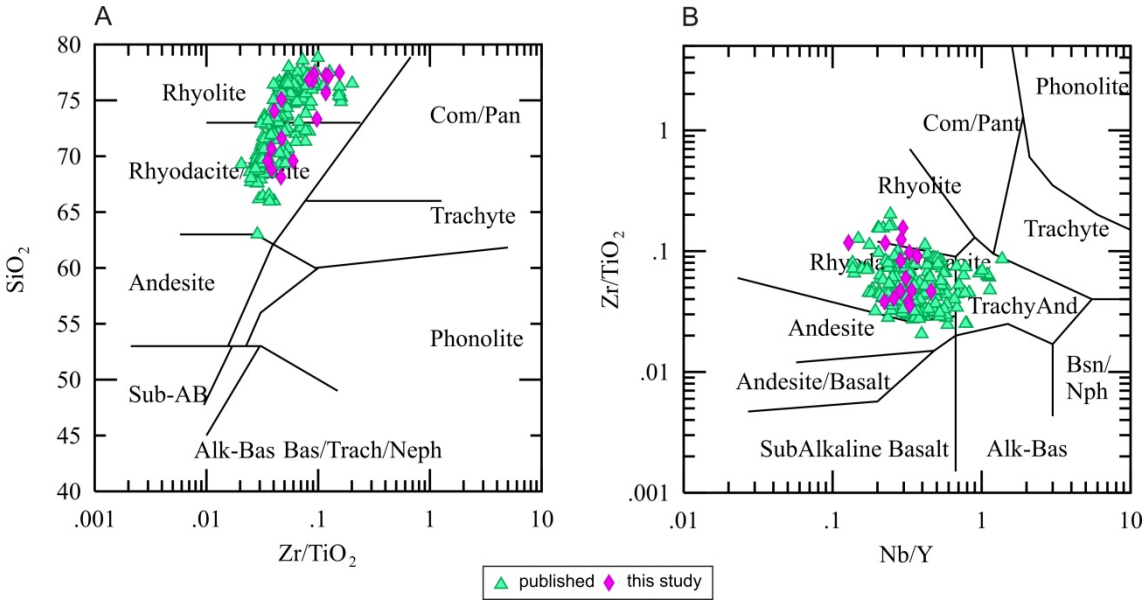

Figure 4 - SiO_2 vs. Zr/TiO_2 and Zr/TiO_2 vs. Nb/Y plots (Winchester and Floyd, 1977) showing the composition of new samples (purple diamonds) and those taken from the literature (green triangles).

ORTHOGNEISS FACIES	code	composition	SiO2 wt. %	Na2O wt. %	K2O wt. %	A/CNK ratio	εNd	TDM (Ga)	$^{147}Sm/^{144}Nd$	area
(1) Furongian-Mid Ordovician Suite										
CIZ - Ollo de Sapo orthogneiss	OG	K-rich dacite to rhyolite	75–60.3	3.9–0.1	5.9–3.4	3.1–1.0	–5.1 to –1.8	1.8–1.1	0.15-0.09	Sanabria (ca. 472 Ma) and Guadarrama (ca. 488-473 Ma)
CIZ - Leucogneiss	LG	K-rich dacite to rhyolite	75.9–73.6	3.1–2.7	5.3–4.2	1.3–1.1	–5.1 to –4.9	4.1	0.22-0.18	Guadarrama
CIZ - Metagranite	GRA	K-rich dacite to rhyolite	77–64.6	4.8–0.5	6.3–2.5	1.8–1.0	–5.2 to +2.6	3.6–0.9	0.19-.0.09	NE Central System, Sanabria, Miranda do Douro (ca. 496-473 Ma). CIZ (496-471 Ma for Carrascal, Fermoselle, Ledesma, Portalegre and Vitigudino granites)
CIZ/GTMZ - Volcanic rocks	VOL	andesite to rhyolite	79.3–64.6	3.2–0.1	6.3–2.2	2.7–1.1	–5.5 to –1.6	1.7–1.3	0.15-0.13	Saldanha Fm. in GTMZ, Ollo de Sapo Fm. in Sanabria, and Urra Fm.
CIZ - San Sebastián orthogneiss	OSS	rhyolite	75.4–73.8	3.1–2.5	5.4–4.9	1.2–1.1	–4.0 to 0	1.6–1.2	0.14-0.14	Sanabria (ca. 470-465 Ma)
PYR - augengneiss	G2*	dacite to rhyolite	73.6–68.3	3.9–3.2	4.4–2.5	1.2-1.1	–4.4 to –3.0	1.4–1.2	0.14-0.13	ca. 476-462 Ma
PYR - orthogneiss	G3*	K-rich dacite	73.5–68.4	2.9–2.4	4.4	1.2	–4.2	1.33	0.13	ca. 463 Ma
PYR - volcanic rocks	V1	Na-rich rhyolite	73.5–68.4	7.8–2.4	3.2–1.3	2.0–1.1	–5.1 to –2.6	1.7–1.6	0.19-0.13	Pierrefite Fm. and Albera massif (ca. 472-465 Ma)
OCC - volcanic rocks	VOL-OD	K-rich dacite to rhyolite	75.6–66.7	3.7–0.6	9.3–2.3	2.4–1.3				Saint-Sernin-sur-Rance and Saint-Salvi-de-Carcavès nappes
SAR - orthogneiss	OG-SMO	K-rich rhyolite	74–67.2	3.8–2.6	5.8–2.3	1.3–1.1				ca. 469 Ma
SAR - volcanic rocks	VOL-SMO	K-rich dacite to rhyolite	76.7–67.6	4.7–1.9	5.4–2.9	2.0–1.2			0.16	ca. 464-462 Ma
(2) Upper Ordovician Suite										
PYR - orthogneiss	G1*	K-rich dacite to rhyodacite	76.4–73.4	3.1–2.6	5.3–4.7	1.2–1.1	–5.3 to –3.1	2.7–1.5	0.17-0.12	ca. 457 Ma
PYR - orthogneiss	CADí	K-rich dacite to rhyodacite	69.4	3	4	1.2	-4.1	1.5	0.13	Cadí massif (ca. 456 Ma)
PYR - orthogneiss	CASEMí	K-rich dacite to rhyodacite	76–71.9	4–1.8	6.3–3.2	1.2–0.9	–3.6 to –1.3	2.6–1.3	0.17-0.13	Casemí massif (ca. 451-446)
PYR - volcanic rocks	V2	andesite to rhyodacite	86.1–63	6–0	4.3–0.6	3.6–1	–5.1 to –2.6	1.7–1.6	0.14-0.14	Ribes de Freser, Andorra (ca. 457 Ma), Pallaresa (ca. 453 Ma), Els Metges (ca. 455.2 Ma)
OCC - orthogneiss	OG-OD	K-rich dacite to rhyolite	73.9–67.4	3.3–2.8	4.7–4	1.3–1.2	–4 to –3.5	1.8–1.4	0.15-0.13	Gorges d'Héric (ca. 450 Ma; Caroux), S Mazamet (Nore), S Rouairoux (Agout), Le Vintrou
SAR - External Zone orthogneiss	OG-SUD	K-rich dacite to rhyolite	76.6–72.1	3.3–1.6	7.8–4.8	1.3–1.1	–3.3 to –1.6	4.2–1.2	0.19-0.12	Capo Spartivento, Cuile Culurgioni, Tuerredda, Monte Filau, Monte Settiballas (ca. 458-457 Ma)
SAR - Nappe Zone volcanic rocks	VOL-SUD	K-rich dacite to rhyodacite	76.7–70.7	3.3–1.6	7.8–4.8	1.3–1.1				Truzzulla Fm. at Monte Grighini

Table 2 -Summarized geochemical features of the Furongian and Ordovician felsic episodes described in the text; data from Lancelot et al. (1985), Calvet et al. (1988), Valverde-Vaquero and Dunning (2000), Roger et al. (2004), Vilà et al. (2005), Giacomini et al. (2006), Díez-Montes (2007), Montero et al. (2007, 2009), Solá (2007), Zeck et al. (2007), Castiñeiras et al. (2008b), Talavera (2009), Casas et al. (2010), Navidad et al. (2010, 2018), Liesa et al. (2011), Martínez et al. (2011, 2018), Navidad and Castiñeiras (2011), Gaggero et al. (2012), Talavera et al. (2013), Villaseca et al. (2016), Pouclet et al. (2017), Cruciani et al. (2018) and this work. Abbreviations: *CIZ* Central Iberian Zone, *GTOMZ* Galicia-Trás-os-Montes Zone, *OCC* Occitan Domain, *PYR* Pyrenees and *SAR* Sardinia; * *sensu* Guitard (1970); A/CNK ratio is always peraluminous.

3.2. Furongian–to–Mid Ordovician Suite

In the Central Iberian and Galicia-Trás-os-Montes Zones, the Furongian–to–Mid Ordovician magmatic activity is pervasive. Their main representative is the Ollo de Sapo Formation, which includes volcanic and subvolcanic rocks (67 samples) as well as plutonic rocks (85 samples) (data from Murphy et al., 2006; Díez-Montes, 2007; Montero et al., 2007, 2009; Solá, 2007; Solá et al., 2008; Talavera, 2009; Villaseca et al., 2016). From the Parautochthon Schistose Domain of the Galicia-Trás-os Montes Zone, six samples of rhyolite tuffs of the Saldanha Formation (Dias da Silva et al., 2014) are selected, which share geochemical features with the Ollo de Sapo Formation. In summary, five facies are differentiated in the Central Iberian and Galicia-Trás-os Montes Zones: the Ollo de Sapo orthogneisses, some leucogneisses, metagranites and volcanic rocks, and the San Sebastián orthogneiss (for a geochemical characterization, see **Table 2**).

In the central and eastern Pyrenees, an Early-Mid Ordovician magmatic activity gave rise to the intrusion of voluminous (about 500-3000 m in size) aluminous granitic bodies, encased into the Canaveilles beds (Álvaro et al., 2018; Casas et al., 2019). They constitute the protoliths of the large orthogneissic laccoliths that form the core of the domal massifs scattered throughout the backbone of the Pyrenees. Rocks of the Canigó, Roc de Frausa and Albera massifs have been taken into account in this work, in which volcanic rocks of the Pierrefite and Albera massifs, and the so-called *G2* and *G3* orthogneisses by Guitard (1970) are also included. All subgroups vary compositionally from subalkaline andesite to rhyolite, as illustrated in the Pearce's (1996) diagram of **Figure 5** (data compiled from Vilà et al., 2005; Castiñeiras et al., 2008*b*; Liesa et al., 2011; Navidad et al., 2018).

Although most rocks in this area are acidic, it is remarkable the presence of minor mafic bodies (Cortalet and Marialles metabasites, not studied in this work), which could indicate a mantle connection with parental magmas during the Mid and Late Ordovician. As well, it should be noted that there are no andesitic rocks in the area.

In the Occitan Domain, six samples of the Larroque volcanosedimentary Complex (Early Tremadocian in age) represent basin floors and subaerial explosive and effusive rhyolites (Pouclet et al., 2017). The porphyroclastic rocks of the Larroque metarhyolites were sampled in the Saint-Géraud and Larroque areas from the Saint-Sernin-sur-Rance nappe and the Saint-André klippe above the Saint-Salvi-de-Carcavès nappe (Pouclet et al., 2017).

In the Middle Ordovician rocks of Sardinia, 11 samples are selected, five of which correspond to orthogneisses of the Aranci Gulf, in the Inner Zone of the NE island (Giacomini et al., 2006), completed with six volcanic rocks of the External Zone (Giacomini et al., 2006; Cruciani et al., 2018) (**Table 2**).

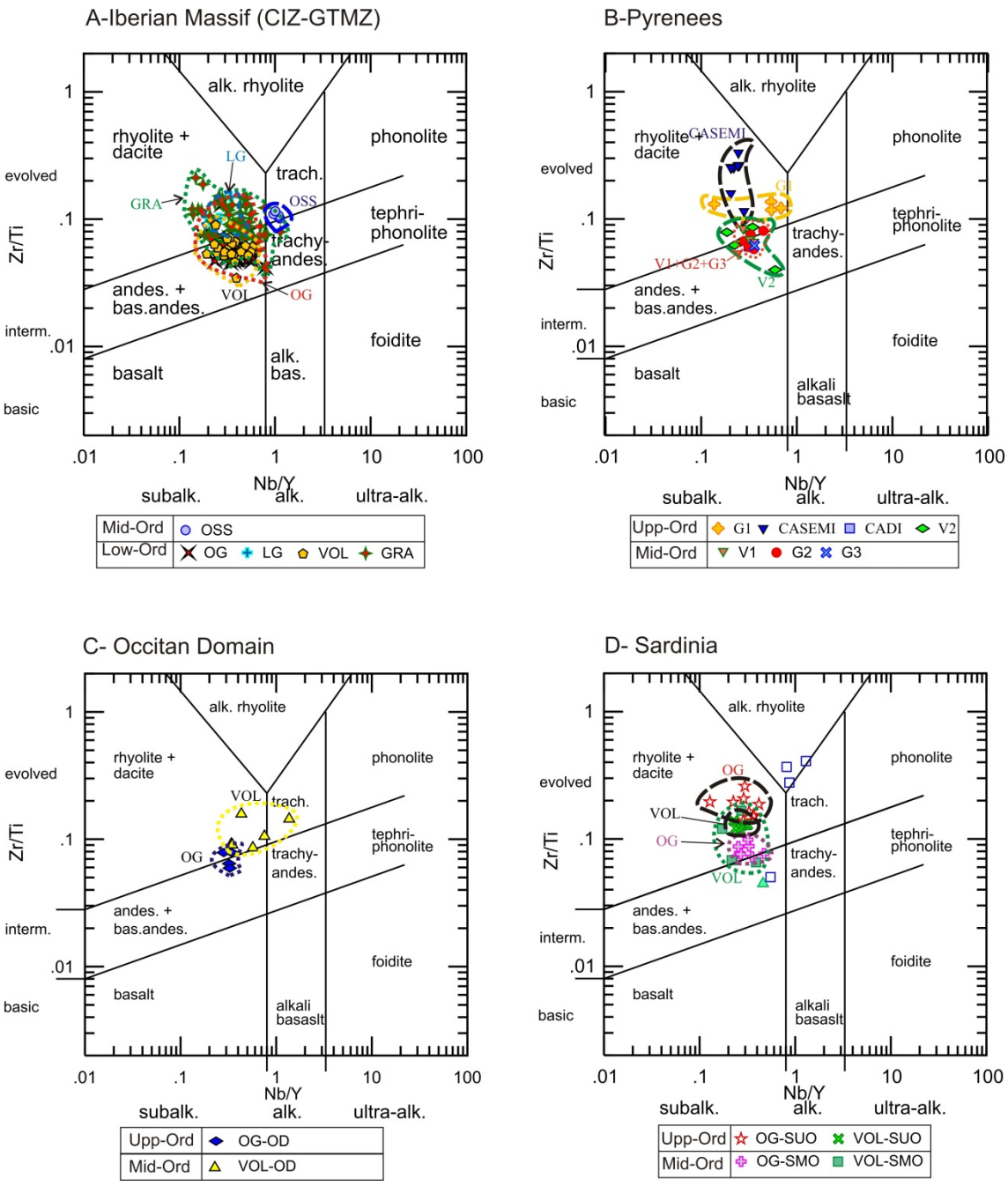

Figure 5 - Zr/Ti vs. Nb/Y discrimination diagram (after Winchester & Floyd, 1977; Pearce, 1996). A. Lower-Middle Ordovician rocks of Iberian Massif (Central Iberian and Galicia-Trás-os-Montes zones). B. Middle-Upper Ordovician rocks of the eastern Pyrenees. C) Middle Ordovician rocks of the Occitan Domain. C-D. Middle-Upper Ordovician rocks of Sardinia.

3.3 Upper Ordovician Suite

In the central and eastern Pyrenees, four Upper Ordovician subgroups are distinguished based on their field occurrence and geochemical and geochronological features: the *G1*-type orthogneisses *sensu* Guitard (1970); the Cadí and Casemí orthogneisses and the metavolcanic rocks that include the Ribes de Freser rhyolites; the Els Metges volcanic

tuffs; and the rhyolites from Andorra and Pallaresa areas (the latter dated at ca. 453 Ma; Clariana et al., 2018) (**Table 2**). The suite is completed with the Somail orthogneisses of the Axial Montagne Noire (dated at ca. 450 Ma at Gorges d'Héric; Roger et al., 2004) and the orthogneisses from the Sardinian External Zone (dated at ca. 458-457 Ma at Monte Filau; Pavanetto et al., 2012) and the volcanic roks from the Sardinian Nappe Zone (**Table 2**).

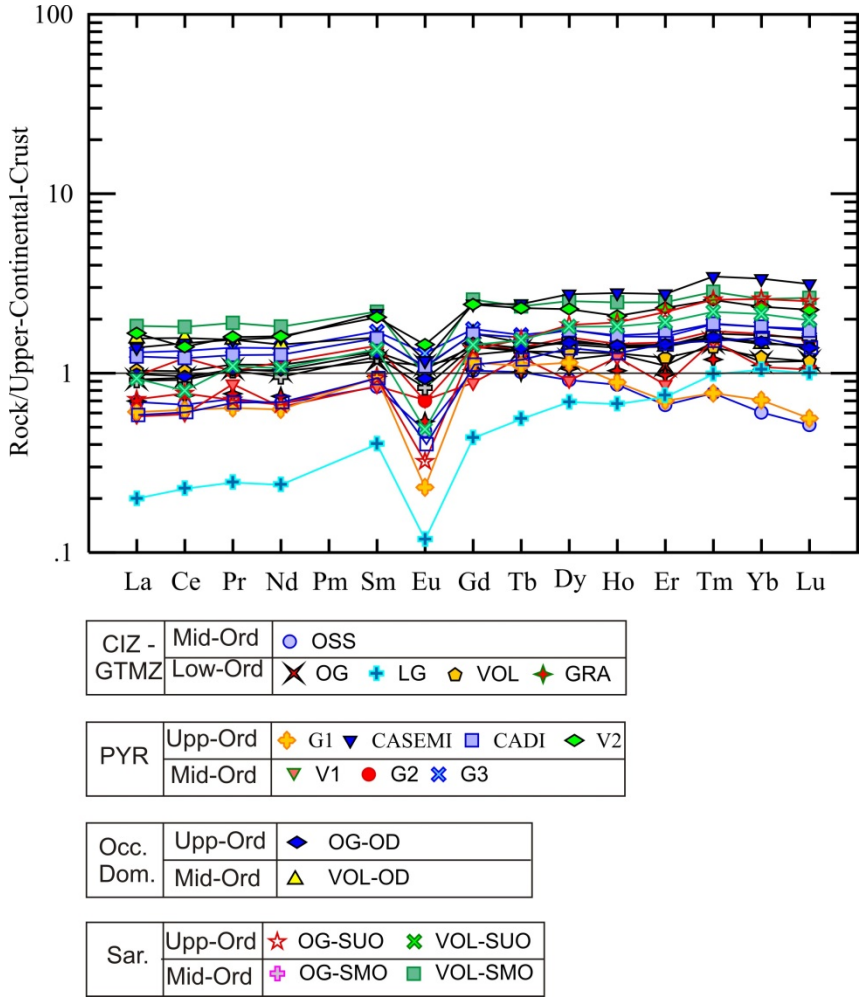

Figure 6 - Upper Crustal-normalized REE patterns (Rudnick & Gao, 2003) with average values for all distinguished groups; symbols as in Figure 4.

4. Geochemical framework

A geochemical comparison between the Furongian-Ordovician felsic rocks of all the above-reported groups offers the opportunity to characterize the successive sources of crustal-derived melts along the south-western European margin of Gondwana.

The geochemical features point to a predominance of materials derived from the melting of metasedimentary rocks, rich in SiO_2 and K_2O (average $K_2O/Na_2O = 2.25$) and peraluminous ($0.4 < C_{norm} < 4.5$ and $0.94 < A/CNK > 3.12$), with only three

samples with A/CNK <1 (samples 100786 of the Casemí subgroup, and T26 and T27 of the San Sebastián subgroup).

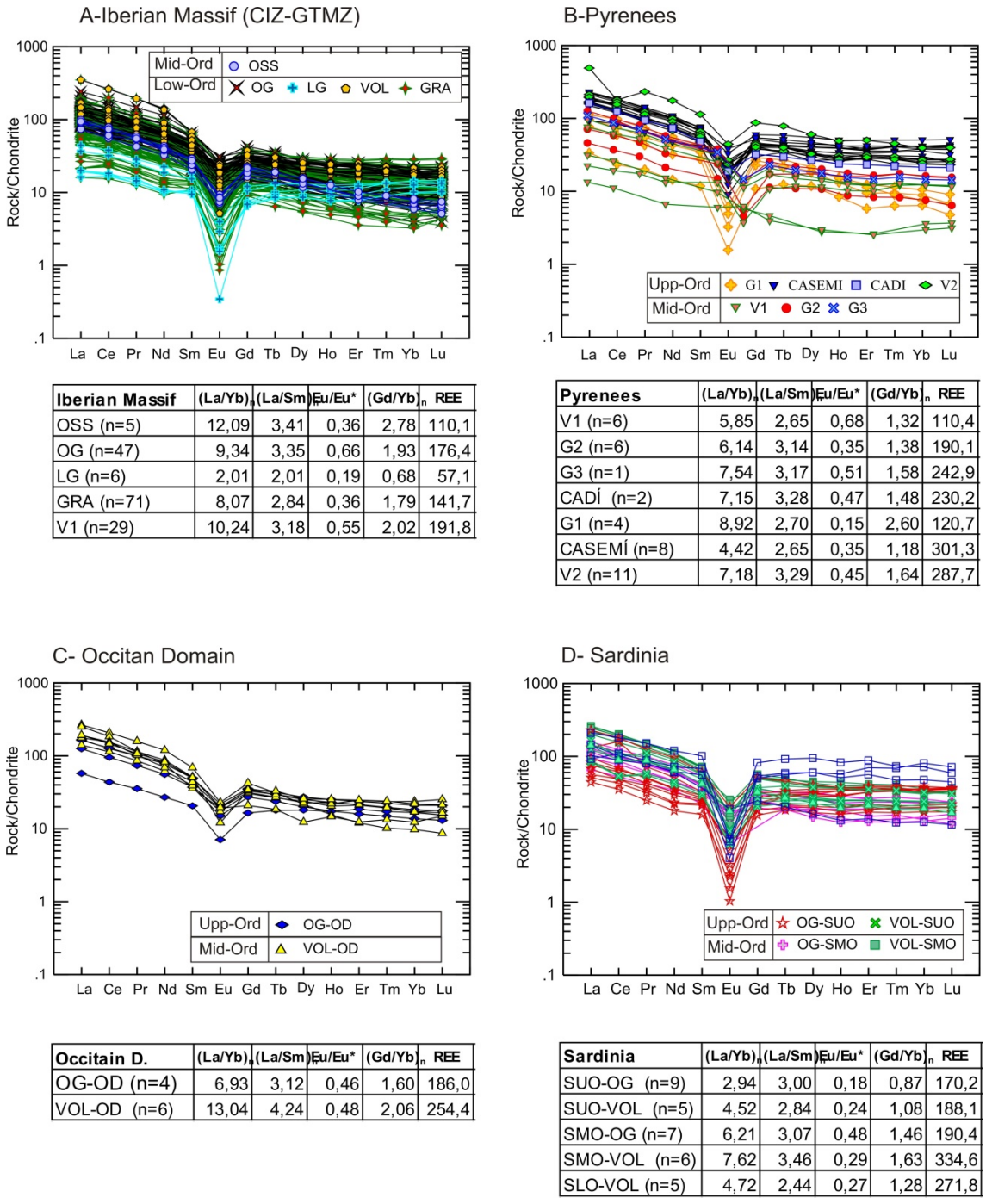

Iberian Massif	$(La/Yb)_n$	$(La/Sm)_n$	Eu/Eu*	$(Gd/Yb)_n$	REE
OSS (n=5)	12,09	3,41	0,36	2,78	110,1
OG (n=47)	9,34	3,35	0,66	1,93	176,4
LG (n=6)	2,01	2,01	0,19	0,68	57,1
GRA (n=71)	8,07	2,84	0,36	1,79	141,7
V1 (n=29)	10,24	3,18	0,55	2,02	191,8

Pyrenees	$(La/Yb)_n$	$(La/Sm)_n$	Eu/Eu*	$(Gd/Yb)_n$	REE
V1 (n=6)	5,85	2,65	0,68	1,32	110,4
G2 (n=6)	6,14	3,14	0,35	1,38	190,1
G3 (n=1)	7,54	3,17	0,51	1,58	242,9
CADÍ (n=2)	7,15	3,28	0,47	1,48	230,2
G1 (n=4)	8,92	2,70	0,15	2,60	120,7
CASEMÍ (n=8)	4,42	2,65	0,35	1,18	301,3
V2 (n=11)	7,18	3,29	0,45	1,64	287,7

Occitain D.	$(La/Yb)_n$	$(La/Sm)_n$	Eu/Eu*	$(Gd/Yb)_n$	REE
OG-OD (n=4)	6,93	3,12	0,46	1,60	186,0
VOL-OD (n=6)	13,04	4,24	0,48	2,06	254,4

Sardinia	$(La/Yb)_n$	$(La/Sm)_n$	Eu/Eu*	$(Gd/Yb)_n$	REE
SUO-OG (n=9)	2,94	3,00	0,18	0,87	170,2
SUO-VOL (n=5)	4,52	2,84	0,24	1,08	188,1
SMO-OG (n=7)	6,21	3,07	0,48	1,46	190,4
SMO-VOL (n=6)	7,62	3,46	0,29	1,63	334,6
SLO-VOL (n=5)	4,72	2,44	0,27	1,28	271,8

Figure 7 - Chondrite-normalized REE patterns (Sun & McDonough, 1989) for all study samples.

The result of plotting the REE content vs. average values of continental crust (Rudnick & Gao, 2004; **Fig. 6**) yields a flat spectra and a base level shared by most of the considered groups. The total content in REE is moderate to high (average REE = 176 ppm, ranging between 482.2 and 26.0 ppm; **Fig. 7**), with a maximum in the

subgroup of the Middle Ordovician volcanic rocks from Sardinia (average REE = 335 ppm, *VOL-SMO*), and with LREE values more fractionated than HREE ones, and negative anomalies of Eu, which would indicate a characteristic process of magmatic evolution with plagioclase fractionation. These features are common in peraluminous granitoids.

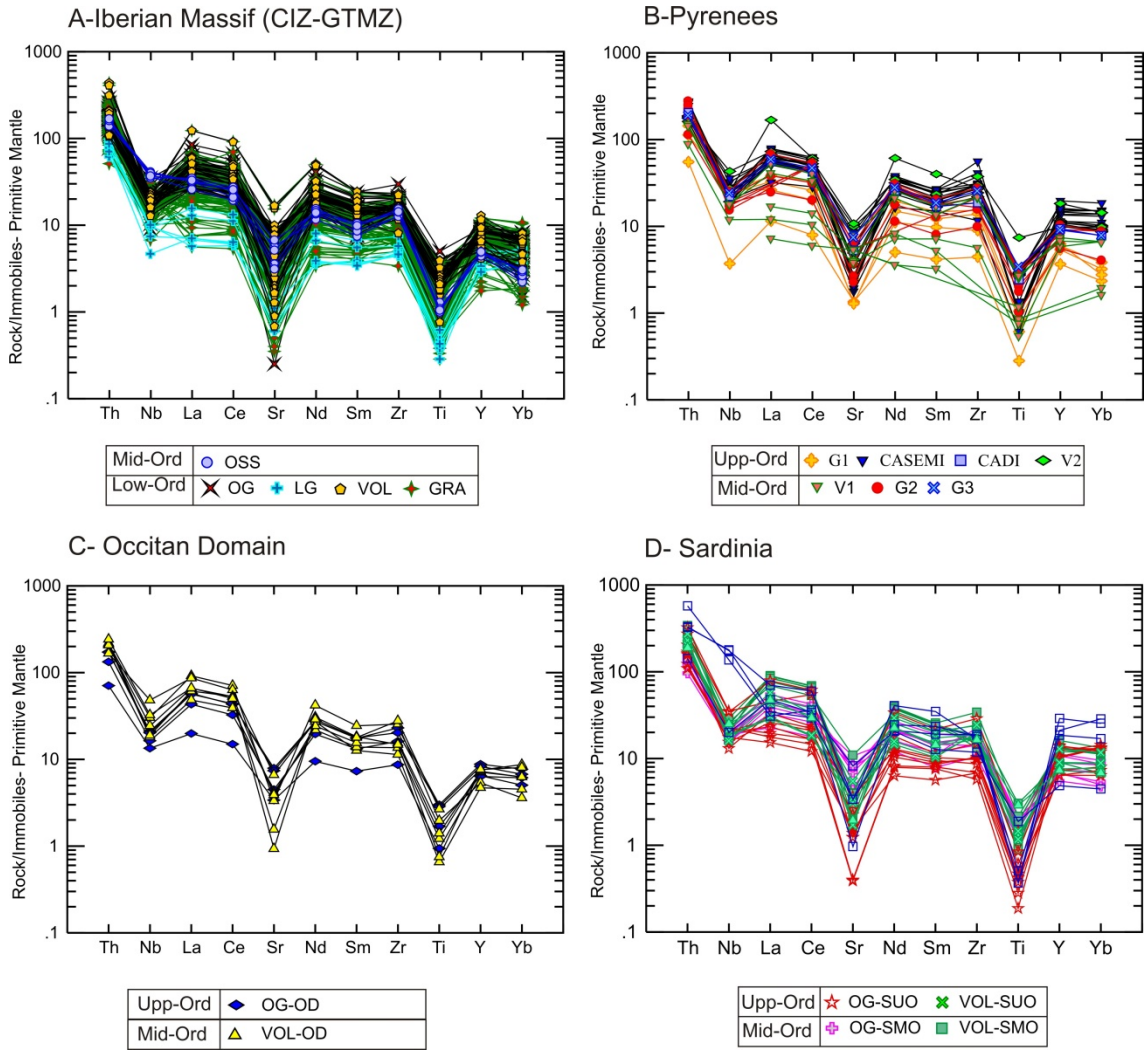

Figure 8 - Multi-element diagram normalised to Primitive Mantle of Palme & O'Neill (2004) for all study samples.

All subgroups display similar chondritic normalized REE patterns (**Fig. 7**), with an enrichment in LREE relative to HREE, which should indicate the involvement of crustal materials in their parental magmas. Nevertheless, some variations can be highlighted, such as the lesser fractionation in REE content of some subgroups. These are the leucogneisses from the Iberian massif (*LG*, La/Yb_n = 2.01), the Upper Ordovician orthogneisses from Sardinia (*OG-SUO*, La/Yb_n = 2.94), the Casemí orthogneisses (La/Yb_n = 4.42) and the Middle Ordovician volcanic rocks from Sardinia (*OG-SUO*,

La/Yb_n = 2.94). This may be interpreted as a greater degree of partial fusion in the origin of their parental magmas (Rollinson, 1993).

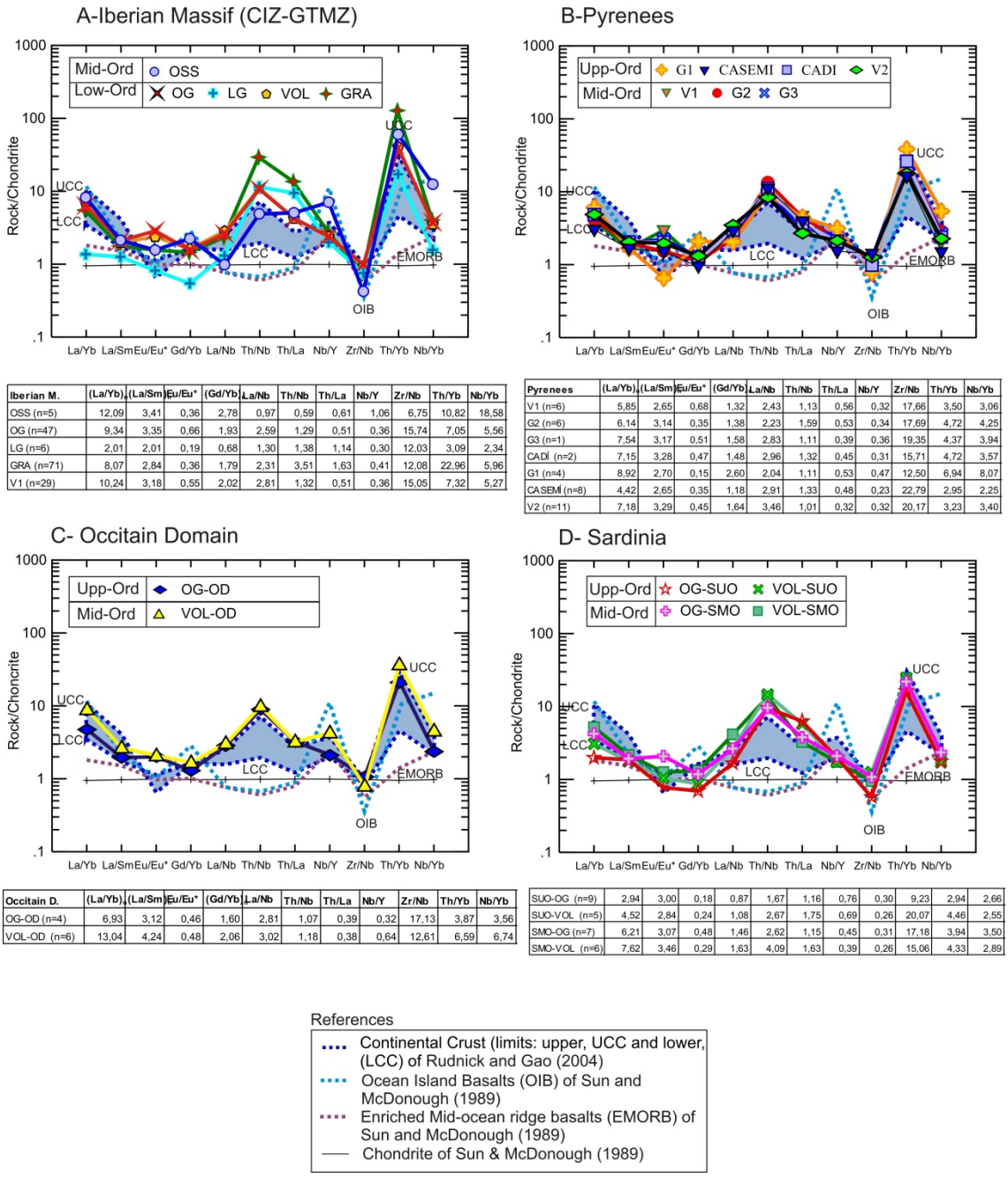

Iberian M.	$(La/Yb)_n$	$(La/Sm)_n$	Eu/Eu*	$(Gd/Yb)_n$	La/Nb	Th/Nb	Th/La	Nb/Y	Zr/Nb	Th/Yb	Nb/Yb
OSS (n=5)	12,09	3,41	0,36	2,78	0,97	0,59	0,61	1,06	6,75	10,82	18,58
OG (n=47)	9,34	3,35	0,66	1,93	2,59	1,29	0,51	0,36	15,74	7,05	5,56
LG (n=6)	2,01	2,01	0,19	0,68	1,30	1,38	1,14	0,30	12,03	3,09	2,34
GRA (n=71)	8,07	2,84	0,36	1,79	2,31	3,51	1,63	0,41	12,08	22,96	5,96
V1 (n=29)	10,24	3,18	0,55	2,02	2,81	1,32	0,51	0,36	15,05	7,32	5,27

Pyrenees	$(La/Yb)_n$	$(La/Sm)_n$	Eu/Eu*	$(Gd/Yb)_n$	La/Nb	Th/Nb	Th/La	Nb/Y	Zr/Nb	Th/Yb	Nb/Yb
V1 (n=6)	5,85	2,65	0,68	1,32	2,43	1,13	0,56	0,32	17,66	3,50	3,06
G2 (n=6)	6,14	3,14	0,35	1,38	2,23	1,59	0,53	0,34	17,69	4,72	4,25
G3 (n=1)	7,54	3,17	0,51	1,58	2,83	1,11	0,39	0,36	19,35	4,37	3,94
CADI (n=2)	7,15	3,28	0,47	1,48	2,96	1,32	0,45	0,31	15,71	4,72	3,57
G1 (n=4)	8,92	2,70	0,15	2,60	2,04	1,11	0,53	0,47	12,50	6,94	8,07
CASEMI (n=8)	4,42	2,65	0,35	1,18	2,91	1,33	0,48	0,23	22,79	2,95	2,25
V2 (n=11)	7,18	3,29	0,45	1,64	3,46	1,01	0,32	0,32	20,17	3,23	3,40

Occitain D.	$(La/Yb)_n$	$(La/Sm)_n$	Eu/Eu*	$(Gd/Yb)_n$	La/Nb	Th/Nb	Th/La	Nb/Y	Zr/Nb	Th/Yb	Nb/Yb
OG-OD (n=4)	6,93	3,12	0,46	1,60	2,81	1,07	0,39	0,32	17,13	3,87	3,56
VOL-OD (n=6)	13,04	4,24	0,48	2,06	3,02	1,18	0,38	0,64	12,61	6,59	6,74

SUO-OG (n=9)	2,94	3,00	0,18	0,87	1,67	1,16	0,76	0,30	9,23	2,94	2,66
SUO-VOL (n=5)	4,52	2,84	0,24	1,08	2,67	1,75	0,69	0,26	20,07	4,46	2,55
SMO-OG (n=7)	6,21	3,07	0,48	1,46	2,62	1,15	0,45	0,31	17,18	3,94	3,50
SMO-VOL (n=6)	7,62	3,46	0,29	1,63	4,09	1,63	0,39	0,26	15,06	4,33	2,89

References
- Continental Crust (limits: upper, UCC and lower, (LCC) of Rudnick and Gao (2004)
- Ocean Island Basalts (OIB) of Sun and McDonough (1989)
- Enriched Mid-ocean ridge basalts (EMORB) of Sun and McDonough (1989)
- Chondrite of Sun & McDonough (1989)

Figure 9 - Chondrite-normalised isotope ratio patterns (Sun & McDonough, 1989) for standard comparison for all study samples. Blue area: limits of continental crustal values (Lower and Upper) of Rudnick & Gao (2003).

There are three geochemical groups displaying $(Gd/Yb)_n$ values > 2, and $(La/Yb)_n$ values ≥ 9. These groups are *OSS* (Central Iberian Zone), *VOL-OD* (Occitan Domain) and *G1* (Pyrenees), and share higher alkalinity features.

Some *V1* rocks from the Pyrenees (Pierrefite Formation) show no negative anomalies in Eu. Their parental magmas could have been derived from deeper origins and related to residual materials of the lower continental crust, in areas of production of K-rich granites (Taylor & McLenan, 1989).

The spider diagrams (Fig. 8), however, exhibit strong negative anomalies in Nb, Sr and Ti, which indicate a distinct crustal affiliation (Díez-Montes, 2007). Only the San Sebastián orthogneisses (*OSS*) show distinct discrepancies in respect of the remaining samples from the Ollo de Sapo Formation. They display lower negative anomalies in Nb and a more alkaline character by comparison with the rest of the Ollo de Sapo rocks, which point to alkaline affinities and greater negative anomalies in Nb.

Despite some small differences in the chemical ranges of some major elements, most felsic Ordovician rocks from the Iberian massif (Central Iberian and Galicia-Trás-os Montes Zones), eastern Pyrenees, Occitan Domain and Sardinia share a common chemical pattern. The Lower-Middle Ordovician rocks of the eastern Pyrenees show less variation in the content of Zr and Nb (**Fig. 8B**). The volcanic rocks of these groups show a different REE behaviour, which would indicate different sources. Two groups are distinguished in Figure 7, one with greater enrichment in REE and negative anomaly of Eu, and another with lesser content of HREE and without Eu negative anomalies.

Figure 9 illustrates how the average of all the considered groups approximates the mean values of the Rudnick and Gao's (2003) upper continental crust (UCC). In this figure, small deviations can be observed, some of them toward lower continental crust (LCC) values and others toward bulk continental crust (BCC), indicating variations in their parental magmas but with quite similar spectra. Overall chondrite-normalized patterns are close to the values that represent the upper continental crust, with slight enrichments in the Th/Nb, Th/La and Th/Yb ratios.

Finally, in the Occitan volcanic rocks (*VOL-OD*) the rare earth elements are enriched and fractionated (33.2 ppm < La < 45.6 ppm; 11.2 < La/Yb < 14.5). The upper continental crust normalized diagram exhibits negative anomalies of Ti, V, Cr, Mn and Fe associated with oxide fractionation, of Zr and Hf linked to zircon fractionation, and of Eu related to plagioclase fractionation. The profiles are comparable to the Vendean Saint-Gilles rhyolitic ones. The Th vs. Rb/Ba features are also similar to those of the Saint-Gilles rhyolites, and the Iberian Ollo de Sapo and Urra rhyolites (Solá et al., 2008; Díez Montes et al., 2010).

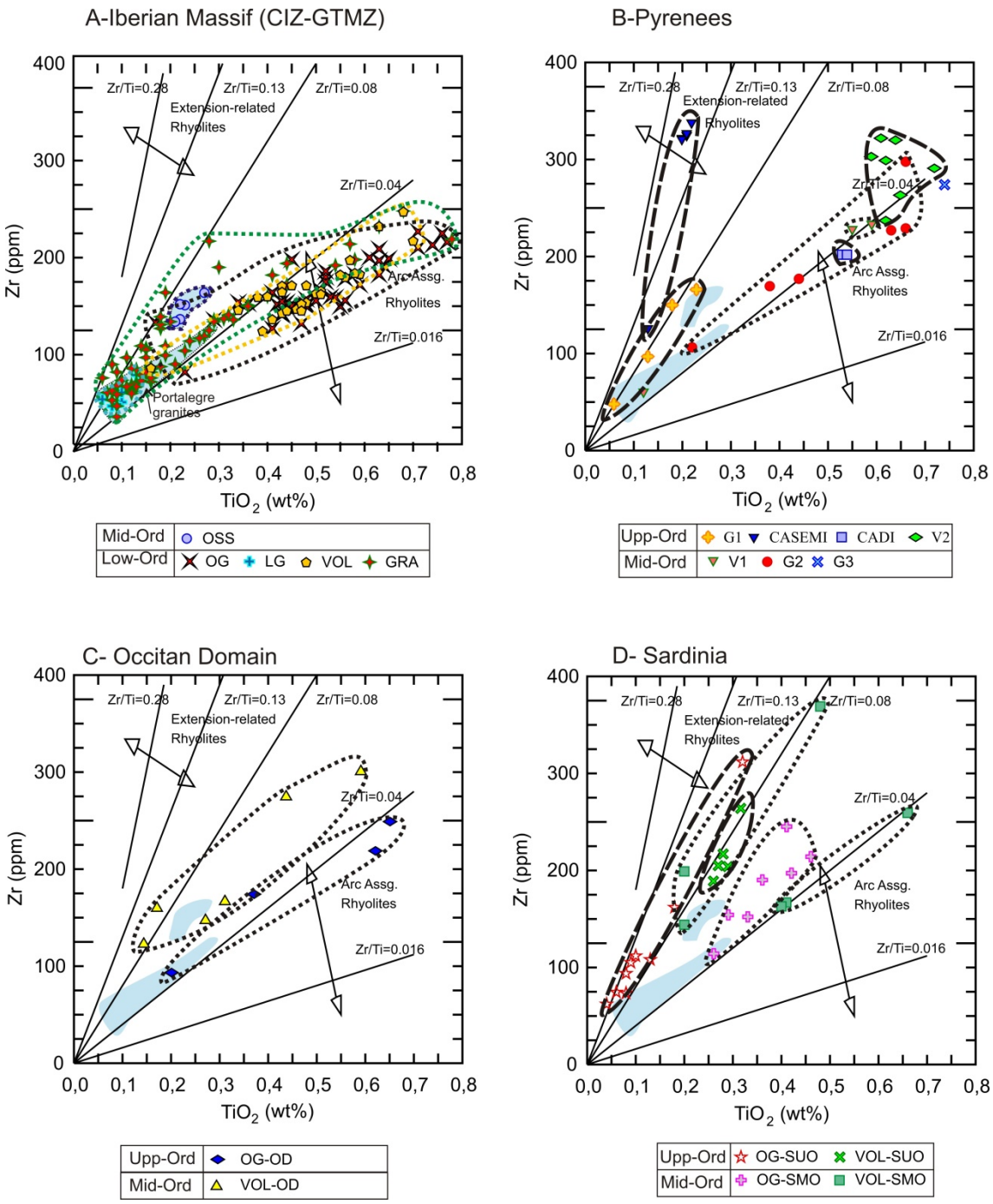

Figure 10 - Tectonic discriminating diagram of Zr vs. TiO_2 (Syme, 1998) for all study samples. Double-sided arrows indicate ranging of differents fields: rhyolites in tholeiitic and calc-alkaline arc suites have Zr/TiO_2 ratios ranging from about 0.016 to 0.04, and extension-related rhyolites from about 0.13 to 0.28 (Syme, 1989).

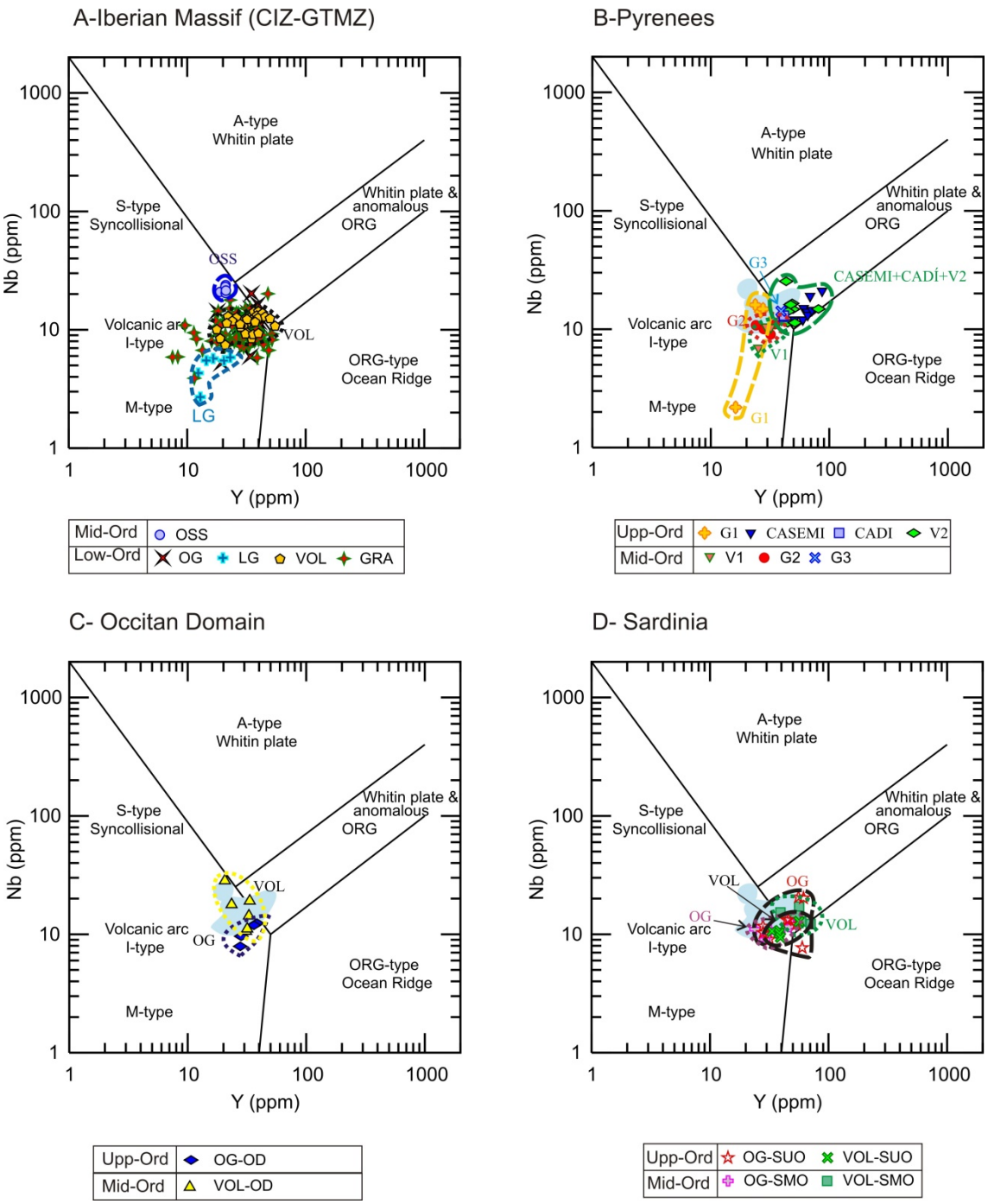

Figure 11 - Tectonic discriminating diagram of Y vs. Nb (Pearce et al., 1984) for all study samples.

4. Discussion

4.1 Inferred tectonic settings

In order to clarify the evolution of geotectonic environments, the data have been represented in different discrimination diagrams. The Zr/TiO_2 ratio (Lentz, 1996; Syme, 1998) is a key index of compositional evolution for intermediate and felsic rocks. In the

Syme diagram (**Fig. 10**), most rocks from the Central Iberian Zone represent a characteristic arc association, although there are some contemporaneous samples characterized by extensional-related values (Zr/Ti = 0.10, *LG*). The rocks of the Middle-Ordovician San Sebastián orthogneisses (*OSS*) show values of Zr/Ti = 0.08, intermediate between extensional and arc conditions. This could be interpreted as a sharp change in geotectonic conditions toward the Mid Ordovician (**Fig. 10A**). For a better comparison, the samples of the San Sebastián orthogneisses (*OSS*) and the granites (*GRA*) have been distinguished with a shaded area in all the diagrams, since they have slightly different characteristics to the rest of the samples from the Ollo de Sapo group. The samples *G1* (Pyrenees) and *VOL* (Central Iberian Zone) broadly share similar values, as a result of which, the three latter groups (*OSS*, *G1* and *VOL*) arrange following a good correlation line. The same trend seems to be inferred in the eastern Pyrenees (**Fig. 10B**), where the Middle Ordovician subgroups display arc features, but half of the Upper Ordovician subgroups show extensional affinities (*G1* and Casemí orthogneisses). In the case of the Occitan orthogneisses (**Fig. 10C**), they show arc characters, which contrast with the contemporaneous volcanic rocks displaying extensional values with Zr/Ti = 0.10. This disparity between plutonic and volcanic rocks could be interpreted as different conditions for the origin of these magmas. In Sardinia (**Fig. 10D**), the same evolution from arc to extensional conditions is highlighted for the Upper Ordovician samples, although some Middle Ordovician volcanic rocks already shared extensional patterns (Zr/Ti = 0.09). In summary, there seems to be a geochemical evolution in the Ordovician magmas grading from arc to extensional environments.

In the Nb-Y tectonic discriminating diagram of Pearce et al. (1984) (**Fig. 11**), most samples plot in the volcanic arc-type, though some subgroups project in the whitin-plate and anomalous ORG. The majority of samples display very similar Zr/Nb and Nb/Y ratios, typical of island arc or active continental margin rhyolites (Díez-Montes et al., 2010). Only some samples plot separately: *OSS* samples with highest Nb contents (>20 ppm), and some volcanic rocks of the Occitan Domain (average Nb =16.87 ppm). In the eastern Pyrenees, the Middle Ordovician rocks plot in the volcanic arc field, whereas the Upper Ordovician ones point in the ORG type, except the Casemí samples. This progress of magmatic sources agrees with the evolution seen in Figure 10. In the Ocitan Domain, *VOL-OD* samples share values with those of the San Sebastián orthogneiss, while *OG-OD* shares values with those of *OG* from the Central Iberian Zone.

The Zr vs. Nb diagram (Leat et al., 1986; modified by Piercey, 2011) (Fig. 12) illustrates how magmas evolved toward richer values in Zr and Nb, which is consistent with what it is observed in the Syme diagram (**Fig. 10**). Figure 12A documents how most samples show a general positive correlation. These different groups correspond to the *OSS* and Portalegre granites, highlighted in the figure. The two groups indicate a tendency toward alkaline magmas. Some samples, such as the Pyrenean *G1*, some Occitan *VOL-OD* samples and some Sardinian *OG-UOS* samples share the same affinity, clearly distinguished from the general geochemical trend exhibited by the Central Iberian Zone.

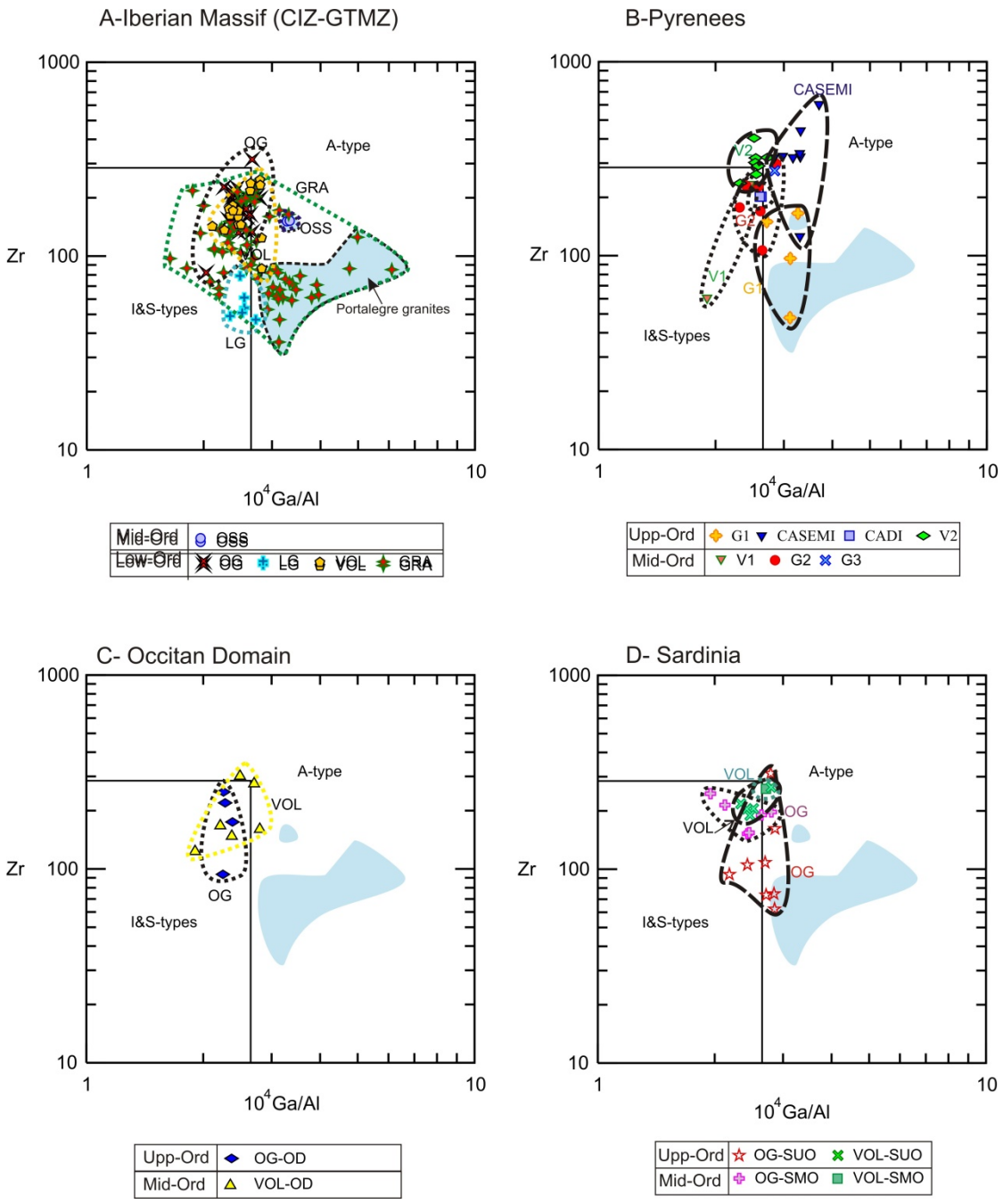

Figure 12 - Zr vs. 10^4 Ga/Al discrimination diagram (Whalen et al., 1987).

On a Zr vs. Ga/Al diagram (Whalen et al., 1987) (**Fig. 13**), the samples depict an intermediate character between anorogenic or alkaline (A-type) and orogenic (I&S-type). In the Central Iberian Zone, samples from the San Sebastián orthogneisses and Portalegre granites show characters of A-type granites, while the remaining samples display affinities of I&S-type granites. For the Central Iberian Zone, a clear magmatic shift toward more extensional geotectonic environments is characterized. For the eastern Pyrenees, we find the same situation as in the Central Iberian Zone, with a magmatic evolution toward A-granite type characteristics, indicating more extensional geotectonic

environments. In the Occitan Domain, the samples show a clear I&S character. In the Sardinian case, the same seems to happen as in the Central Iberian Zone: the Upper Ordovician orthogneisses suggest a more extensional character.

In summary, all the reported diagrams point to a magmatic evolution through time, grading from arc to extensional geotectonic environments (with increased Zr/Ti ratios) and to granite type-A characters. This geotectonic framework is consistent with that illustrated in Figure 10. The geochemical characters of these rocks show a rhyodacite to dacite composition, peraluminous and calc-alkaline K-rich character, and an arc-volcanic affinity for most of samples, but without intermediate rocks associated with andesitic types. Hence a change in time is documented toward more alkaline magmas.

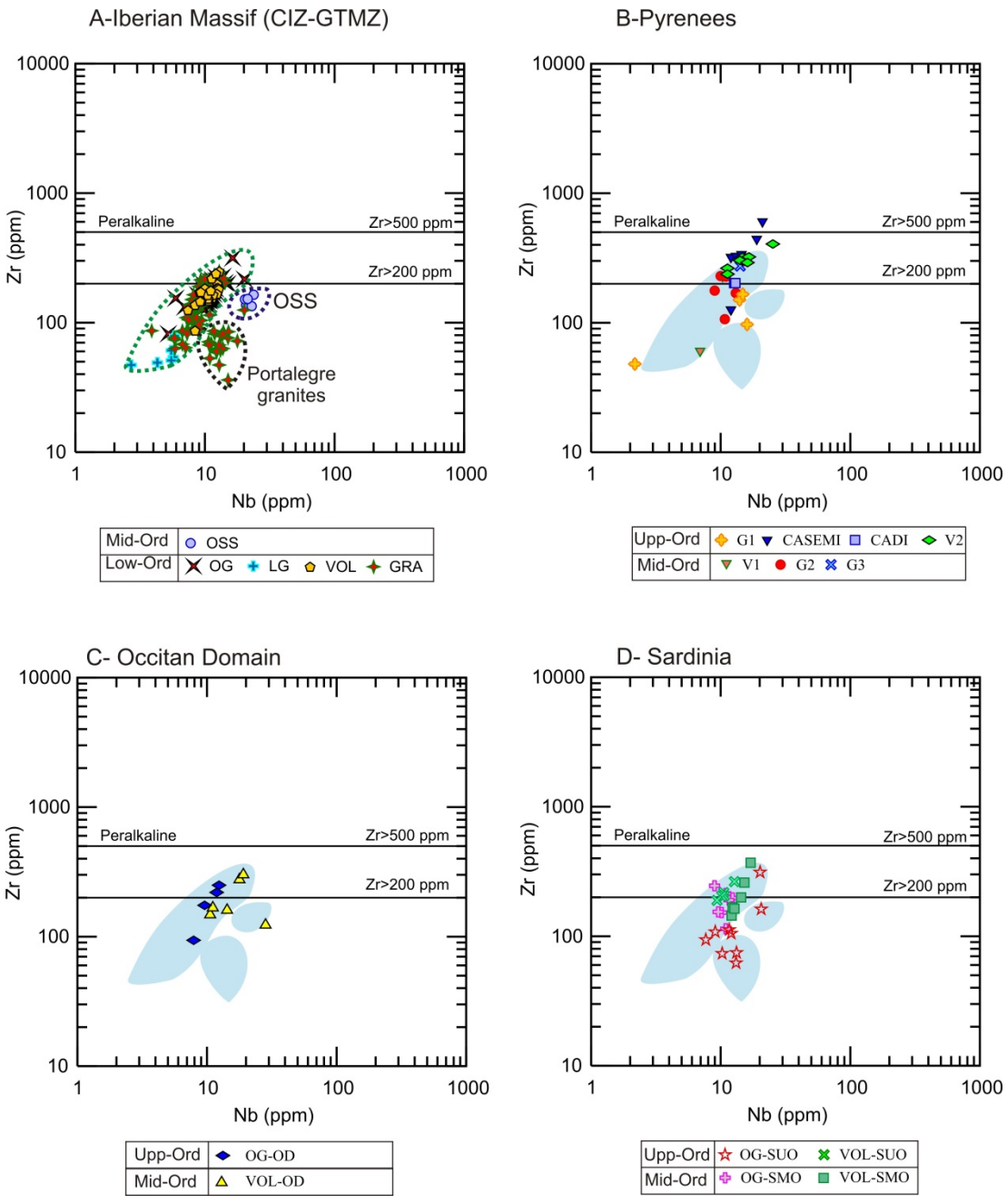

Figure 13 Zr-Nb plot diagram (Leat et al., 1986; modified by Piercey, 2011) for all study samples.

4.2 Interpretation of εNd values

$\varepsilon Nd_{(t)}$ values are useful to interpret the nature of magmatic sources. Most samples of the above-reported groups show no significant differences in isotopic $\varepsilon Nd_{(t)}$ values, and Nd_{CHUR} model ages (**Fig. 14**). Some exceptions are related to granites from the southern Central Iberian Zone, which display positive values (from +2.6 to -2.4) and T_{DM} values from 0.90 to 3.46 Ga. These granites, space-related with calcalkaline diorites and gabbros, were interpreted by Solá et al. (2008) as the result of underplating and temporal storage of mantle-derived magmas as a potential source for the intrusive "orogenic melts" during Early Palaeozoic extension.

Some samples from (i) the Central Iberian Zone, such as VI-3 (Leucogneiss subgroup) and PORT2 and PORT15 (Granite subgroup); (ii) the eastern Pyrenees, such as 99338 (G1 subgroup) and 100786 samples (Casemí subgroup); and (iii) the Sardinian CS5, CS8 and CC5 samples (Upper Ordovician Orthogneiss subgroup) display anomalous T_{DM} values and $^{147}Sm/^{144}Nd$ ratios > 0.17 (**Table 2**; **Fig. 14**), a character relatively common in some felsic rocks (DePaolo, 1988; Martínez et al., 2011). According to Stern et al. (2012), these values should not be considered, but a possible explanation for these high ratios may be related to the M-type tetrad effect (e.g., Irber, 1999; Monecke et al., 2007; Ibrahim et al., 2015), which affects REE fractionation in highly evolved felsic rocks due to the interaction with hydrothermal fluids. This process can be reflected as an enrichment of Sm related to Nd. Other authors, however, explain this enrichment as a result of both magmatic evolution (e.g., McLennan, 1994; Pan, 1997) and weathering processes after exhumation (e.g., Masuda & Akagi, 1989; Takahasi et al., 2002).

In the granites of the southern Central Iberian Zone and the volcanic rocks of Sardinia, positive values in $\varepsilon Nd_{(t)}$ could be interpreted as a more primitive nature of their parental magmas, even though the samples with highest T_{DM} values are those that display higher $^{147}Sm/^{144}Nd$ ratios (> 0.17; **Table 2**).

The volcanic rocks of the Central Iberian Zone display some differences following a N-S transect, being $\varepsilon Nd_{(t)}$ values less variable in the north ($\varepsilon Nd_{(t)}$: -4.0 to -5.0) than in the south ($\varepsilon Nd_{(t)}$: -1.6 to -5.5). The isotopic signature of the Urra volcaniclastic rocks is compatible with magmas derived from young crustal rocks, with intermediate to felsic igneous compositions (Solá et al., 2008). The volcanic rocks of the northern Central Iberian Zone could be derived from old crustal rocks (Montero et al., 2007). The isotopic composition of the granitoids from the southern Central Iberian Zone has more primitive characters than those of the northern Central Iberian Zone, suggesting different sources for both sides (Talavera et al., 2013). *OSS* shows lower inheritance patterns, more primitive Sr-Nd isotopic composition than other rocks of the Ollo de Sapo suite, and an age some 15 m.y. younger than most meta-igneous rocks of the Sanabria region (Montero et al., 2009), likely reflecting a greater mantle involvement in its genesis (Díez-Montes et al., 2008).

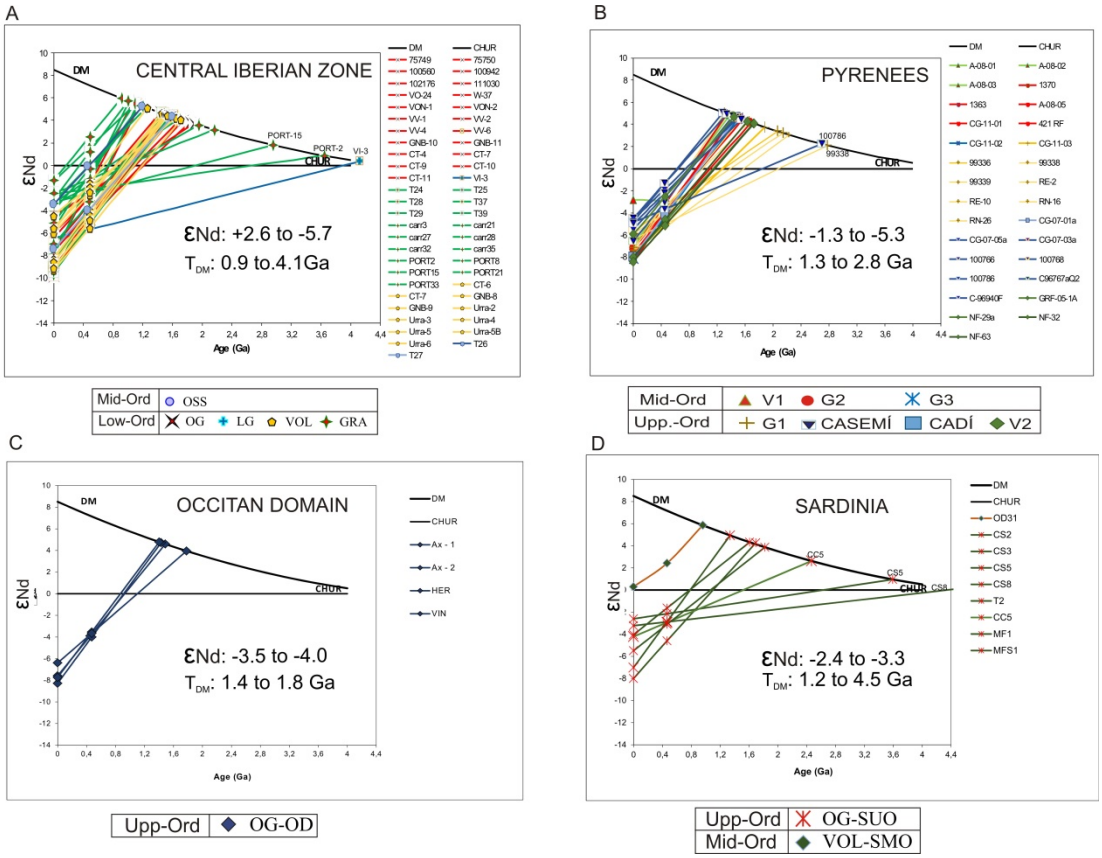

Figure 14 - $\varepsilon Nd_{(t)}$ vs. age diagram (DePaolo & Wasserburg, 1976; DePaolo, 1981) for study sampled. A. Central Iberian and Galicia-Trás-os-Montes Zones. B. Eastern Pyrenees. C. Occitan Domain. D. Sardinia; see references in the text.

According to Talavera et al. (2013), the Cambro-Ordovician rocks of the Galicia-Trás-os-Montes Zone schistose area and the magmatic rocks of the northern Central Iberian Zone are contemporary. Both metavolcanic and metagranitic rocks almost share the same isotopic compositions.

The Upper Ordovician orthogneisses from the Occitan Domain show very little variation in $\varepsilon Nd_{(t)}$ values (-3.5 to -4.0), typical of magmas derived from young crustal rocks. The variation in TDM values is also small (1.4 to 1.8 Ga) indicating similar crustal residence times to other rock groups.

In Sardinia, $\varepsilon Nd_{(t)}$ values present a greater variation (-1.6 to -3.3), but they are also included in the typical continental crustal range. As noted above, unusual TDM values (between 1.2 to 4.5 Ga) may be due to post-magmatic hydrothermal alteration processes.

5. Geodynamic setting

In the Iberian Massif, the Ediacaran-Cambrian transition was marked by paraconformities and angular discordances indicating the passage from Cadomian volcanic arc to rifting conditions. The axis of the so-called Ossa-Morena Rift lies along

the homonymous Zone (Quesada, 1991; Sánchez-García et al., 2003, 2008, 2010) close to the remains of the Cadomian suture (Murphy et al., 2006). Rifting conditions were accompanied by a voluminous magmatism that changed from peraluminous acid to bimodal (Sánchez-García et al., 2003, 2008, 2016, 2019). Some authors (Álvaro et al., 2014; Sánchez-García et al., 2019) propose that this rift resulted from a SW-to-NE inward migration, toward innermost parts of Gondwana, of rifting axes from the Anti-Atlas in Morocco to the Ossa-Morena Zone in the Iberian Massif. According to this proposal the rifting developed later (in Cambro-Ordovician times) in the Iberian, Armorican and Bohemian massifs.

The Furongian-Ordovician transition to drifting conditions is associated, in the Iberian Massif, Occitan Domain, Pyrenees and Sardinia, with a stepwise magmatic activity contemporaneous with the record of the Toledanian and Sardic unconformities. These, related to neither metamorphism nor penetrative deformations, are linked to uplift, erosion and irregularly distributed mesoscale deformation that gave rise to angular unconformities up to 90º. The time span involved in these gaps is similar (22 m.y. in the Iberian Massif, 16-23 m.y. in the Pyrenees and 18 m.y. in Sardinia). This contrasts with the greater time span displayed by the magmatic activity (30-45 m.y.), which started before the unconformity formation (early Furongian in the Central Iberian Zone vs. Floian in the Pyrenees, Occitan Domain and Sardinia), continued during the unconformity formation (Furongian and early Tremadocian in the Central Iberian Zone vs. Floian-Darriwilian in the Pyrenees, Occitan Domain and Sardinia), and ended during the sealing of the uplifted and eroded palaeorelief (Tremadocian-Floian volcaniclastic rocks at the base of the Armorican Quartzite in the Central Iberian Zone vs. Sandbian-Katian volcanic rocks at the lowermost part of the Upper Ordovician successions in the Pyrenees, Occitan Domain and Sardinia; Gutiérrez-Alonso et al., 2007, 2016; Navidad et al., 2010; Martínez et al., 2011; Álvaro et al., 2016; Martí et al., 2019). In the Pyrenees, Upper Ordovician magmatism and sedimentation coexist with normal faults controlling marked thickness changes of the basal Upper Ordovician succession and cutting the lower part of this succession, the Sardic unconformity and the underlying Cambro-Ordovician sequence (Puddu et al., 2018, 2019).

Although the Toledanian and Sardic Phases reflect similar geodynamic conditions in two distinct palaeogeographic areas, at present forming the western and eastern branches of the Variscan Ibero-Armorican Arc, they display different peaks in magmatic activity with a minor chronological overlapping (**Fig. 3**). This may reflect a SW-to-NE “zip-like” propagation of the latest Ediacaran-Terreneuvian rifting axes in the so-called Atlas-Ossa Morena Rift.

Toledanian Phase

The Early Ordovician (Toledanian) magmatism of the Central Iberian Zone evolved to a typical passive-margin setting, with geochemical features dominated by acidic rocks, peraluminous and rich in K, and lacking any association with basic or intermediate rocks. Some of the orthogneisses of the Galicia-Trás-os-Montes Zone basal and allochthonous complex units share these same patterns. This fact has been interpreted

by some authors as a basin environment subject to important episodes of crustal extension (Martínez-Catalán et al., 2007; Díez-Montes et al., 2010). In contrast, Villaseca et al. (2016) interpreted this absence as evidence against rifting conditions, though the absence of contemporary basic magmatism may be explained by the partial fusion of a thickened crust, through recycling of Neoproterozoic crustal materials. The thrust of a large metasedimentary sequence could generate dehydration and metasomatism of the rocks above this sequence, triggering partial fusion at different levels, although the increase in peraluminosity with the basicity of the orthogneisses is against any AFC process involving mantle materials. However, this increase in peraluminosity with the basicity has not been revealed in the samples studied above. Following Villaseca et al.'s (2016) model, a flat subduction of the southern part of the Central Iberian Zone would have taken place under its northern prolongation, whereas the reflection of such a subduction is not evident in the field. The calc-alkaline signature of this magmatism has also been taken into account as proof of its relationship with volcanic-arc environments (Valverde-Vaquero & Dunning, 2000). However, calc-alkaline features may be also interpreted as a result of a variable degree of continental crustal contamination and/or previously enriched mantle source (Sánchez-García et al., 2003, 2008, 2016, 2019; Díez-Montes et al., 2010). Finally, other granites not considered here of Tremadocian age have been reported in the southern Central Iberian Zone, such as the Oledo massif and the Beira Baixa-Central Extremadura, which display a I-type affinity (Antunes et al., 2009; Rubio Ordóñez et al., 2012). These granites could represent different sources for the Ordovician magmatism in the Central Iberian Zone.

Sánchez-García et al. (2019) have proposed that the anomaly that produced the large magmatism throughout the Iberian Massif could have migrated from the rifting axis to inwards zones and the acid, peraluminous, K-rich rocks of Mid Ordovician in age should represent the initial stages of a new rifting pulse, resembling the peraluminous rocks of the Early Rift Event *sensu* Sánchez-García et al. (2003) from the Cambrian Epoch 2 of the Ossa-Morena Rift.

In the parautochthon of the Galicia-Trás-os-Montes Zone, the appearance of tholeiitic and alkaline-peralkaline magmatism in the Mid Ordovician would signal the first steps toward extensional conditions (Díez Fernández et al., 2012; Dias da Silva et al., 2016). In the Montagne Noire and the Mouthoumet massifs contemporaneous tholeiitic lavas indicate a similar change in the tectonic regimen (Álvaro et al., 2016). This gradual change in geodynamic conditions is also marked by the appearance of rocks with extensional characteristics in some of subgroups considered here, such as the Central Iberian Zone (San Sebastián orthogneisses), eastern Pyrenees (Casemí orthoneisses, and G1), volcanic rocks of the Occitan Domain, and the orthogneises and volcanic rocks from Sardinia.

Sardic Phase

In the eastern Pyrenees, two peaks of Ordovician magmatic activity are observed (Casas et al., 2019). Large Lower-Middle Ordovician peraluminous granite bodies are known

representing the protoliths of numerous gneissic bodies with laccolithic morphologies. In the Canigó massif, the Upper Ordovician granite bodies (protholits of Cadí, Casemí, *G1*) are encased in sediments of the Canaveilles and Jujols groups. During this time span, there was generalized uplift and erosion that culminated with the onset of the Sardic unconformity. The Sardic Phase was succeeded by an extensional interval related to the formation of normal faults affecting the pre–unconformity strata (Puddu et al., 2018, 2019). The volcanic arc signature can be explain by crustal recycling (Navidad et al., 2010; Casas et al., 2010; Martínez et al., 2011), as in the case of the Toledanian Phase in the Central Iberian Zone, although, according to Casas et al. (2019), the Pyrenees and the Catalan Coastal Ranges were probably fringing the Gondwana margin in a different position than that occupied by the Iberian Massif. As a whole, the Ordovician magmatism in the Pyrenees lasted about 30 m.y., from ca 477 to 446 Ma, in a time span contemporaneous with the formation of the Sardic unconformity (**Fig. 2**). Recently, Puddu et al. (2019) proposed that a thermal doming, bracketted between 475 and 450 Ma, could have stretched the Ordovician lithosphere. The emersion and denudation of the inherited Cambrian-Ordovician palaeorelief would have given rise to the onset of the Sardic unconformity. According to these authors, thermal doming triggered by hot mafic magma underplating may also be responsible for the late Early-Late Ordovician coeval magmatic activity.

In the Occitan Domain, there was a dramatic volcanic event in early Tremadocian times, with the uprising of basin floors and the subsequent effusion of abundant rhyolitic activities under subaerial explosive conditions (Larroque volcanosedimentary Complex in the Montagne Noire, and Davejean acidic volcanic counterpart in the Mouthoumet Massif). Pouclet el al., (2017) interpreted this as a delayed Ollo de Sapo-style outpouring where a massive crustal melting required a rather significant heat supply. Asthenospheric upwelling leading to the interplay of lithospheric doming, continental break-up, and a decompressionally driven mantle melting can explain such a great thermal anomaly. The magmatic products accumulated on the mantle-crust contact would provide enough heat transfer for crustal melting (Huppert & Sparks, 1988). Subsequently, a post-Sardic reactivation of rifting conditions is documented in the Cabrières klippes (southern Montagne Noire) and the Mouthoumet massif. There, a Late Ordovician fault-controlled subsidence linked to the record of rift-related tholeiites (Roque de Bandies and Villerouge formations) were contemporaneous with the record of the Hirnantian glaciation (Álvaro et al., 2016). Re-opening of rifting branches (Montagne Noire and Mouthoumet massifs) was geometrically recorded as onlapping patterns and final sealing of Sardic palaeoreliefs by Silurian and Lower Devonian strata.

Sardinia illustrates an almost complete record of the Variscan Belt (Carmignani et al., 1994; Rossi et al., 2009). Some plutonic orthogneises of the Inner Zone belong to this cycle, such as the orthogneises of Golfo Aranci (Giacomini et al., 2006). Gaggero et al. (2012) described three magmatic cycles. The first cycle is well represented in the Sarrabus unit by Furongian-Tremadocian volcanic and subvolcanic interbeds within a terrigenous sucession (San Vito Formation) which is topped by the Sardic uncomformity. Some plutonic orthogneises of the Inner Zone belong to this cycle, such as the orthogneises of Golfo Aranci (Giacomini et al., 2006) and the PB orthogneiss of

Punta Bianca). The second Mid-Ordovician cycle, about 50 m.y. postdating the previous cycle, is of an arc-volcanic type with calc-alkaline affinity and acidic-to-intermediate composition. The acidic metavolcanites are referred in the literature as “porphyroids”, which crop out in the External Nappe Zone and some localities of the Inner Zone. The intermediate to basic derivates are widespread in Central Sardinia (Serra Tonnai Formation). Some plutonic rocks (Mt. Filau orthogneisses and Capo Spartivento) of the second cycle are discussed above. The third cycle consists of alkalic meta-epiclastites interbedded in post-Sandbian strata and metabasites marking the Ordovician/Silurian contact and reflecting rifting conditions. In this work only the first two cycles are considered. Giacomini et al. (2006) cite coeval mafic rocks of felsic magmatism of Mid Ordovician age (Cortesogno et al., 2004; Palmeri et al., 2004; Giacomini et al., 2005), although they interpret a subduction scenario of the Hun terrain below Corsica and Sardinia in the Mid Ordovician.

Origin of intracrustal siliceous melts

In this scenario, the key to generate large volumes of acidic rocks in an intraplate context would be the existence of a lower-middle crust, highly hydrated, in addition to a high heat flow, possibly caused by mafic melts (Bryan et al., 2002; Díez-Montes, 2007). This could be the scenario initiated by the arrival of a thermal anomaly in a subduction-free area (Sánchez-García et al., 2003, 2008, 2019; Álvaro et al., 2016). The formation of large volumes of intracrustal siliceous melts could act as a viscous barrier, preventing the rise of mafic magmas within volcanic environments, and causing the underplating of these magmas at the contact between the lower crust and the mantle (Huppert & Sparks, 1988; Pankhurst et al., 1998; Bindeman & Valley, 2003). The cooling of these magmas could lead to crustal thickening and in this case, the volcanic arc signature can be explained by crustal recycling (Navidad et al., 2010; Díez-Montes et al., 2010; Martínez et al., 2011).

Sánchez-García et al. (2019) have proposed that the anomaly that produced the large magmatism throughout the Iberian Massif could have migrated from the rifting axis to inwards zones and the acid, peraluminous, K-rich rocks of Mid Ordovician in age should represent the initial stages of a new rifting pulse, resembling the peraluminous rocks of the Early Rift Event *sensu* Sánchez-García et al. (2003) from the Cambrian Epoch 2 of the Ossa-Morena Rift. In the parautochthon of the Galicia-Trás-os-Montes Zone, the appearance of tholeiitic and alkaline-peralkaline magmatism in the Mid Ordovician would signal the first steps toward extensional conditions (Díez Fernández et al., 2012; Dias da Silva et al., 2016). In the Montagne Noire and the Mouthoumet massifs contemporaneous tholeiitic lavas indicate a similar change in the tectonic regimen (Álvaro et al., 2016). This change in geodynamic conditions is also marked by the appearance of rocks with extensional characteristics in some of subgroups considered here, such as the Central Iberian Zone (San Sebastián orthogneisses), eastern Pyrenees (Casemí orthogneisses, and G1), volcanic rocks of the Occitan Domain, and the orthogneises and volcanic rocks from Sardinia. In the Pyrenees, Puddu et al. (2019) proposed that a thermal doming, between 475 and 450 Ma, should have stretched the

Ordovician lithosphere leading to emersion and denudation of a Cambrian-Ordovician palaeorelief, and giving rise to the onset of the Sardic unconformity. According to these authors, thermal doming triggered by hot mafic magma underplating may also be responsible for the late Early-Late Ordovician coeval magmatic activity

A major continental break-up, leading to the so-called Tremadocian Tectonic Belt, was suggested by Pouclet et al. (2017), which initiated by upwelling of the asthenosphere and tectonic thinning of the lithosphere. Mantle-derived mafic magmas were underplated at the mantle-crust transition zone and intruded the crust. These magmas provided heat for crustal melting, which supplied the rhyolitic volcanism. After emptying the rhyolitic crustal reservoirs, the underlying mafic magmas finally rose and reached the surface. According to Pouclet et al. (2017), the acidic magmatic output associated with the onset of the Larroque metarhyolites resulted in massive crustal melting requiring a rather important heat supply. Asthenospheric upwelling leading to lithospheric doming, continental break-up, and a decompressionally driven mantle melting can explain such a great thermal anomaly. Magmatic products accumulated on the mantle-crust contact providing enough heat transfer for crustal melting.

6. Conclusions

A geochemical comparison of 231 plutonic and volcanic samples of two major suites, Furongian-Mid Ordovician and Late Ordovician in age, from the Central Iberian and Galicia-Trás-os-Montes Zones of the Iberian Massif and in the eastern Pyrenees, Occitan Domain (Albigeois, Montagne Noire and Mouthoumet massifs) and Sardinia points to a predominance of materials derived from the melting of metasedimentary rocks, peraluminous and rich in SiO_2 and K_2O. The total content in REE is moderate to high. Most felsic rocks display similar chondritic normalized REE patterns, with an enrichment of LREE relative to HREE, which should indicate the involvement of crustal materials in their parental magmas.

Zr/TiO_2, Zr/Nb, Nb/Y and Zr vs. Ga/Al ratios, and REE and εNd values reflect contemporaneous arc and extensional scenarios, which progressed to distinct extensional conditions finally associated with outpouring of mafic tholeiitic-dominant rifting lava flows. Magmatic events are contemporaneous with the formation of the Toledanian (Furongian-Early Ordovician) and Sardic (Early-Late Ordovician) unconformities, related to neither metamorphism nor penetrative deformation. The geochemical and structural framework precludes subduction generated melts reaching the crust in a magmatic arc to back-arc setting. On the contrary, it favours partial melting of sediments and/or granitoids in a continental lower crust triggered by the underplating of hot mafic magmas related to the opening of the Rheic Ocean as a result of asthenospheric upwelling.

7. Acknowledgements

The authors thank the constructive and useful revisions made by Laura Gaggero (Genoa, Italy) and Jochen Mezger (Fairbanks, USA). This paper is a contribution to

projects CGL2017-87631-P and PGC2018-093903-B-C22 from Spanish Ministry of Science and Innovation. We acknowledge support of the publication fee by the CSIC Open Access Publication Support Initiative through its Unit of Information Resources for Research (URICI).

Data availability - All data included in the paper and the Repository Data.

Author contributions - JJA, TSG and JMC: Methodology (Lead), Supervision (Lead), Writing - Original Draft (Lead), Writing - Review & Editing (Lead); CP, ADM, ML & GO: Methodology (Supporting), Supervision (Supporting), Writing - Original Draft (Supporting), Writing - Review & Editing (Supporting).

Competing interests - No competing interests

Repository Data

SUBGROUP	Sample	Unit Rock	Litology	Sm	Nd	$^{147}Sm/^{144}Nd$	$^{143}Nd/^{144}Nd_0$	eNd_{age}	Age (Ma)	Tdm Ga)	(87Sr/86Sr)measured	$(^{87}Sr/^{86}Sr)_{age}$	Author	Error*10^{-6}
PYR-V1	A-08-01	Albera (V1)	Rhyolitic porphyry	7,28	33,9	0,1298	0,512281	-3,0	470	1,38			1	
PYR-V1	A-08-02	Albera (V1)	Rhyolitic porphyry	3,06	9,4	0,1968	0,512492	-2,9	470				1	
PYR-V1	A-08-03	Albera (V1)	Orthogneiss	5,8	27,8	0,1261	0,512269	-3,0	470	1,34			2	
PYR-G2	1370	ALBERA	Orthogneiss	8,02	38,88	0,1247	0,512206	-4,1	470	1,43			11	
PYR-G2	1363	ALBERA	Orthogneiss	7,49	36,27	0,1248	0,512261	-3,0	470	1,34			11	
PYR-G2	A-08-05	ALBERA	Augen gneiss	5,48	23,5	0,1410	0,51224	-4,4	470	1,68			1	
PYR-G2	CG-11-01	ROC FRAUSA	Orthogneiss	8,73	40,87	0,1291	0,512239	-3,7	470	1,45			7	
PYR-G2	421 RF	ROC FRAUSA	Orthogneiss	3,45	15,1	0,1381	0,512269	-3,7	470	1,56			7	
PYR-G3	CG-11-02	Canigó-G3	Orthogneiss	7,96	36,9	0,1304	0,51222	-4,2	470	1,50			7	
PYR-G1	CG-11-03	NURIA	Orthogneiss	6,36	25,9	0,1484	0,512237	-5,0	455	1,88			7	
PYR-G1	99336	NURIA	Orthogneiss	1,79	6,67	0,1622	0,512347	-3,7	455	2,06			7	
PYR-G1	99338	NURIA	Orthogneiss	4,2	14,7	0,1727	0,512311	-5,0	455	2,78			7	
PYR-G1	99339	NURIA	Orthogneiss	5,25	19,9	0,1595	0,512255	-5,3	455	2,22			7	
PYR-G1	RE-2	NURIA	Augen gneiss	7,07	35,1	0,1218	0,51226	-3,0	450	1,30			3	5
PYR-G1	RE-10	NURIA	Augen gneiss	2,4	9,9	0,1465	0,512313	-3,4	450	1,65			3	10
PYR-G1	RN-16	NURIA	Two-mica gneiss	2,74	10,14	0,1634	0,512337	-3,9	450	2,14			3	6
PYR-G1	RN-26	NURIA	Two-mica gneiss	6,18	27,13	0,1377	0,512271	-3,7	450	1,54			3	5
PYR-G1	RN-27	NURIA	Two-mica gneiss	0,86	1,88	0,2766	0,51264	-4,7	450				3	4
PYR-CADÍ	CG-07-01a	CADÍ	Orthogneiss	7,3	34	0,1298	0,512227	-4,1	456,1	1,48	0,736385	0,708542	6	
PYR-Casemí	CG-07-05a	Casemí	Bt orthogneiss	11,29	50	0,1365	0,512393	-1,3	451,6	1,28	0,745438	0,696910	6	
PYR-Casemí	CG-07-03a	Casemí	Bt orthogneiss	8,36	34	0,1486	0,512401	-1,8	445,9	1,50	0,742716	0,702258	6	
PYR-Casemí	100766	Casemí	Bt orthogneiss	10,3	44	0,1415	0,512409	-1,3	445,9	1,34	0,754248	0,706702	6	
PYR-Casemí	100768	Casemí	Amp orthogneiss	11,3	48	0,1423	0,512355	-2,4	445,9	1,46	0,720992	0,707661	6	
PYR-Casemí	100786	Casemí	Bt orthogneiss	6,41	22	0,1761	0,51239	-3,7	445,9	2,70	0,817270	0,690857	6	
PYR-Casemí	C96767aQ2	Casemí	Bt orthogneiss	10,45	47	0,1344	0,5123	-3,0	445,9	1,42	0,770513	0,660161	6	
PYR-Casemí	C-96940F	Casemí	Amp orthogneiss	11,57	47	0,1488	0,512383	-2,2	445,9	1,54	0,720939	0,708524	6	
PYR-V2	GRF-05-1A	VOL2	Granophyre	8,51	37,09	0,1387	0,512334	-2,6	458	1,44			3	5
PYR-V2	NF-29a	VOL2	Volcanic tuff	8,67	37	0,1416	0,512227	-4,8	455,2	1,72	0,733067	0,703181	6	
PYR-V2	NF-32	VOL2	Volcanic tuff	7,75	34	0,1378	0,512227	-4,6	455,2	1,63	0,726113	0,707025	6	
PYR-V2	NF-63	VOL2	Volcanic tuff	8,57	37	0,1400	0,512205	-5,2	455,2	1,73	0,729263	0,705315	6	
OG-USO	CS 2	OG-SUO	granite	4,1	16,6	0,1493	0,512324823	-3,3	455	1,69			13	
OG-USO	CS 3	OG-SUO	orthogneiss	4,41	17,1	0,1559	0,512430393	-1,6	455	1,61			13	
OG-USO	CS 5	OG-SUO	orthogneiss	3,28	10,5	0,1888	0,512504267	-2,2	455	3,59			13	
OG-USO	CS 8	OG-SUO	orthogneiss	3,44	10,9	0,1908	0,512472405	-2,9	455	4,47			13	
OG-USO	CC 5	OG-SUO	orthogneiss	2,43	8,4	0,1749	0,512421502	-2,9	455	2,47			13	
OG-USO	T 2	OG-SUO	orthogneiss	4,93	24	0,1242	0,512333587	-1,6	455	1,21			13	
OG-USO	MF 1	OG-SUO	Bt orthogneiss	9,37	44,7	0,1267	0,512278098	-2,9	455	1,34			13	
OG-USO	MFS 1	OG-SUO	orthogneiss	3,88	15	0,1564	0,51235625	-3,1	455	1,82			13	
OG-OD	Ax - 1	OG_OD	orthogneiss	5,7	26	0,1325	0,512249	-3,9	471	1,49			13	
OG-OD	Ax - 2	OG_OD	orthogneiss	7,55	36,4	0,1254	0,512213	-4,2	471	1,43			13	
OG-OD	HER	OG_OD	orthogneiss	7,63	36,4	0,1267	0,512241	-3,7	471	1,40			13	
OG-OD	VIN	OG_OD	orthogneiss	3,15	12,6	0,1511	0,51231	-3,8	471	1,78			13	
CIZ-OSS	T26	O.San Sebastián	Ortoneis	4,45	19,2	0,1401	0,512463	-0,1	470	1,20	0,732730	0,703710	10	
CIZ-OSS	T27	O.San Sebastián	Ortoneis	4,19	18,2	0,1392	0,512258	-4,0	470	1,60	0,799900	0,717300	10	
CIZ-OG	75749	Guadarrama	Augengneis	6,75	31,48	0,1296	0,512177	-4,8	485	1,57	0,733216	0,709321	12	
CIZ-OG	75750	Guadarrama	Augengneis	6,34	30,42	0,1260	0,512199	-4,2	485	1,46	0,735218	0,707745	12	
CIZ-OG	100560	Guadarrama	Augengneis	6,15	25,81	0,1440	0,512262	-4,1	485	1,70	0,734722	0,709660	12	
CIZ-OG	100942	Guadarrama	Augengneis	7,66	32,67	0,1417	0,512217	-4,8	485	1,75	0,735847	0,705654	12	
CIZ-OG	102176	Guadarrama	Augengneis	6,9	32,3	0,1291	0,512216	-4,1	485	1,49	0,731965	0,710569	12	
CIZ-OG	111030	Guadarrama	Augengneis	4,72	19,5	0,1463	0,512331	-2,9	485	1,61	0,864523	0,705061	12	
CIZ-OG	VO-24	Guadarrama	Augengneis	9,13	45,1	0,1224	0,512167	-4,6	485	1,46	0,724878	0,711671	12	
CIZ-OG	W-37	Guadarrama	Augengneis	8,62	40,5	0,1287	0,512164	-5,0	485	1,57	0,733067	0,710913	12	
CIZ-OG	VON-1	Ollo	Gneiss	4,8	19,5	0,1488	0,512258	-4,5	485	1,84			5	
CIZ-OG	VON-2	Ollo	Gneiss	7	33,5	0,1263	0,512209	-4,0	485	1,45			5	
CIZ-OG	VV-1	Ollo	Gneiss	6,5	30,2	0,1301	0,512203	-4,4	485	1,53			5	
CIZ-OG	VV-2	Ollo	Gneiss	5,9	27,4	0,1302	0,512208	-4,3	485	1,52			5	
CIZ-OG	VV-4	Ollo	Gneiss	8,6	40,9	0,1271	0,512172	-4,8	485	1,53			5	
CIZ-OG	VV-6	Ollo	Gneiss	6,6	30,5	0,1308	0,51217	-5,1	485	1,60			5	
CIZ-LG	LV-1	Guadarrama	Leucogneiss	1,56	4,84	0,1948	0,512383	-4,9	485	-	1,043893	0,569762	12	
CIZ-LG	MJ-6	Guadarrama	Leucogneiss	1,66	4,64	0,2163	0,512412	-5,6	485	-	1,040461	0,705756	12	
CIZ-LG	VI-3	Guadarrama	Leucogneiss	1,47	4,84	0,1836	0,512306	-5,7	485	4,13	1,290630	0,716919	12	
CIZ-GRA	GNB-10	Ollo	Villadepera Gneiss	10,3	66,1	0,0942	0,512136	-3,5	485	1,16	0,718920	0,705210	4	
CIZ-GRA	GNB-11	Ollo	Villadepera Gneiss	10,3	63,7	0,0977	0,512232	-1,8	485	1,07	0,717930	0,704420	4	
CIZ-GRA	CT-4	Antoñita gneisses	Metagranite	2,29	8,52	0,1625	0,512407	-2,4	485	1,89	0,860980	0,711500	4	
CIZ-GRA	CT-6	Antoñita gneisses	Metagranite	6,17	28,6	0,1304	0,512219	-4,1	485	1,50	0,732710	0,710390	4	
CIZ-GRA	CT-7	Antoñita gneisses	Metagranite	5,86	27,9	0,1270	0,512214	-4,0	485	1,45	0,724290	0,709850	4	
CIZ-GRA	CT-9	Antoñita gneisses	Metagranite	6,13	27,8	0,1333	0,512268	-3,3	485	1,47	0,743290	0,710540	4	
CIZ-GRA	CT-10	Antoñita gneisses	Metagranite	4,73	20,9	0,1368	0,512244	-4,0	485	1,58	0,747940	0,711050	4	
CIZ-GRA	CT-11	Antoñita gneisses	Metagranite	4,92	21,9	0,1358	0,512307	-2,7	485	1,44	0,753280	0,711680	4	
CIZ-GRA	T24	Covelo ortoneis	Ortoneis	7,03	33,5	0,1269	0,512209	-4,1	485	1,46	0,725350	0,708760	10	
CIZ-GRA	T25	Covelo ortoneis	Ortoneis	4,76	19,5	0,1476	0,512565	1,6	485	1,10	0,740580	0,703530	10	
CIZ-GRA	carr3	Carrascal	granodiorite	5,238	23,584	0,1343	0,512572	2,6	485	0,91	0,722148	0,704966	8	
CIZ-GRA	carr21	Carrascal	sienogranite	3,165	16,387	0,1168	0,512349	-0,7	485	1,09	0,738584	0,703646	8	
CIZ-GRA	carr27	Carrascal	monzogranite	5,989	28,198	0,1284	0,512484	1,2	485	1,00	0,731355	0,705701	8	
CIZ-GRA	carr28	Carrascal	sienogranite	5,728	23,977	0,1444	0,512475	0,1	485	1,25	0,815668	0,704489	8	
CIZ-GRA	carr32	Carrascal	sienogranite	5,855	27,881	0,1269	0,512378	-0,8	485	1,17	0,761622	0,706539	8	
CIZ-GRA	carr35	Carrascal	sienogranite	4,804	21,317	0,1362	0,512433	-0,3	485	1,20	0,758740	0,703364	8	
CIZ-GRA	PORT2	Portalegre	GP2	2,174	6,943	0,1893	0,512509	-2,1	485	3,64	1,319068	0,579433	8	
CIZ-GRA	PORT4	Portalegre	GP1	3,064	11,173	0,1658	0,51249	-1,0	485	1,75	0,837065	0,704971	8	

CIZ-GRA	PORT8	Portalegre	GP3	3,513	12,059	0,1761	0,512511	-1,2	485	2,16	1,034521	0,697382	8	
CIZ-GRA	PORT15	Portalegre	GP3	2,203	7,272	0,1831	0,512471	-2,4	485	2,95	1,130756	0,651033	8	
CIZ-GRA	PORT21	Portalegre	GP1	3,013	10,826	0,1682	0,512459	-1,7	485	1,95	0,813227	0,700513	8	
CIZ-GRA	PORT33	Portalegre	GP1a	3,4	12,68	0,1621	0,512467	-1,2	485	1,69	0,866600	0,706504	8	
CIZ-VOL	CT-6	Ollo	Metavolcanic	6,17	28,6	0,1304	0,512219	-4,1	495	1,50	0,732710	0,710390	4	
CIZ-VOL	CT-7	Ollo	Metavolcanic	5,86	27,9	0,1270	0,512214	-4,0	485	1,45	0,724290	0,709850	4	
CIZ-VOL	GNB-8	Ollo	Metavolcanic	6,46	30,3	0,1289	0,512199	-4,4	485	1,51	0,738570	0,707550	4	
CIZ-VOL	GNB-9	Ollo	Metavolcanic	7,53	34,8	0,1308	0,512174	-5,0	485	1,59	0,733020	0,707000	4	
CIZ-VOL	Urra-2	URRA	Porphyroid	8,94	41,8	0,1293	0,512344	-1,6	485	1,26	0,708504	0,717378	9	
CIZ-VOL	Urra-3	URRA	Porphyroid	4,68	18,2	0,1555	0,512411	-1,9	488	1,65	0,700342	0,791190	9	
CIZ-VOL	Urra-4	URRA	Porphyroid	6,08	26	0,1414	0,512331	-2,6	485	1,50	0,790830	0,738052	9	
CIZ-VOL	Urra-5	URRA	Porphyroid	5,57	23,2	0,1451	0,512356	-2,3	485	1,52	0,682599	0,731206	9	
CIZ-VOL	Urra-5B	URRA	Porphyroid	3,77	16,8	0,1357	0,512163	-5,5	485	1,71	0,703259	0,747854	9	
CIZ-VOL	Urra-6	URRA	Porphyroid	6,23	29,5	0,1277	0,512174	-4,8	485	1,54	0,708103	0,756229	9	

CHAPTER 7

CHAPTER 7

DISCUSSION

Based on the geological characters described above in southern Sardinia, a critical re-appraisal of other intra-Ordovician gaps from neighbouring areas of peri-Gondwana associated with the Sardic Phase can be updated.

1. Eastern Pyrenees

In the eastern Pyrenees, the aftermath of the late Ediacaran-early Terreneuvian magmatism, related to the Cadomian subduction (Pic de la Clape Formation; Casas et al., 2015; Padel et al., 2018*b*), records the transition to quiescent Cambrian–Lower Ordovician conditions (**Fig. 21**). The latter time span (Jujols Group) represents an interval with no remarkable tectonic activity, followed by a late Early-Mid Ordovician episode of uplift and erosion that led to the formation of the Sardic unconformity *s.s.* Uplift was accompanied by magmatic activity that pursuits until the Late Ordovician, the latter coinciding with an extensional pulse that developed normal faults and controlled the record of post-Sardic sediments inflling palaeorelief depressions, although the significance of this magmatism and tectonic activity is still under debate (see discussion in Casas et al., 2019). Based on the maximum depositional age of the Cambrian-Lower Ordovician succession (Jujols Group, ca. 475 Ma, minimum age of the detrital zircon population, Margalef et al.. 2016) and the ca. 455 Ma U-Pb age for the Upper Ordovician volcanic rocks directly overlying the Sardic unconformity in the Bruguera tectonostratigraphic unit (Martí et al., 2019), a time gap of about 20 m.y. can be associated with the Sardic Phase. Contemporaneous to the Early-Mid Ordovician episode of generalized uplift, an important magmatic activity gave rise to the intrusion of voluminous aluminous granites, about 500 to 3000 m thick and emplaced into the Canaveilles and Jujols metasedimentary strata. They constitute the protoliths of the large laccolith-shaped, orthogneissic bodies that crop out at the core of the domal massifs that punctuate the backbone of the Pyrenees. These are, from west to east, the Aston (470 ± 6 Ma, Denèle et al.. 2009; 467±2 Ma, Mezger & Gerdes, 2016), Hospitalet (472 ± 2 Ma, Denèle et al., 2009), Canigó (472 ± 6 to 467 ± 7 Ma, Cocherie et al., 2005), Roc de Frausa (477 ± 4 Ma, Cocherie et al., 2005; 476±5 Ma, Castiñeiras et al., 2008) and Albera (470 ± 3 Ma, Liesa et al., 2011) massifs, which exhibit a dominant Floian-Dapingian age. It should be noted that only a minor representation of coeval basic magmatic rocks are exposed (e.g., Cortalet metabasite). The acidic volcanic equivalents have been reported in the Albera massif, where subvolcanic rhyolitic porphyroid rocks yielded similar ages than those of the main gneissic bodies: 465 ± 4, 472 ± 3, 473 ± 2 and 474 ± 3 Ma (Liesa et al., 2011). Other acidic products are represented by the rhyolitic sills of Pierrefte (Calvet et al., 1988). This late Early-Mid Ordovician (“Sardic”) episode of uplift was followed by a stepwise succession of Late Ordovician extensional pulsations, which preceded and were contemporaneous with the

opening of grabens and half-grabens inflled with the alluvial-to-fuvial Rabassa Conglomerate Formation. At outcrop scale, a synsedimentary hydrothermal activity is associated with the development of decametre-sized normal faults lined with quartz veins and dykes, which subsequently fed the Rabassa conglomerates as vein quartz pebbles. At cartographic scale, a detailed geological map of the La Cerdanya area reveals a set of normal faults sharply affecting the thickness of the Rabassa and Cava formations (Casas & Fernández, 2007; Casas, 2010). In addition, sharp variations in the thickness of the Upper Ordovician succession have been reported by several authors (Hartevelt, 1970; Casas & Fernández, 2007). Drastic variations in thickness and grain size can be attributed to palaeorelief development controlled by fault activity and subsequent erosion of uplifted palaeotopographies, with subsequent infill controlled by alluvial fan and fuvial deposition, finally sealed during Silurian times (see some Silurian biostratigraphic precisions in Sánz-López et al., 2002). Simultaneously, a Late Ordovician magmatic pulse yielded a varied suite of magmatic rocks. Small granitic bodies are emplaced in the Canaveilles and Jujols strata of the Canigó massif and constitute the protoliths of the Cadí, Casemí and Núria gneisses (**Fig. 21**). The Cadí gneiss, dated at 456±5 Ma by Casas et al. (2010), is an aluminous metagranitic body with petrographic characteristics similar to those of the Canigó gneiss; it represents the lowest structural unit recognized in the Canigó massif. The Casemí gneiss is a tabular body up to 1000 m thick mainly made up of fne-grained biotitic and amphibolic granitic gneisses. Geochronological data indicate a Late Ordovician age for the protolith of this orthogneiss (446 ± 5 and 452 ± 5 Ma, SHRIMP U-Pb in zircon, Casas et al., 2010).

Figure 21 - Stratigraphic chart of the Ediacaran-Ordovician outcrops from the West Mediterranean margin of Gondwana with setting of the Pan-African, Cadomian, Toledanian and Sardic gaps; based on Robardet et al. (1994), Álvaro *et al.* (2007, 2014*a*, *b*, *c*, 2016*a*, 2018, in press *a*), Padel *et al*. (2016, 2018*a*, *b*), Pouclet et al. (2017), Casas et al. (2019) and Sánchez-García *et al*. (2019). Abbreviations: *A-A* Aceuchal-Alter do Chao Complex, *Ag* Agualada Complex, *Ca* Campelles ignimbrites (ca. 455 Ma, Martí *et al*., 2019), *Cd* Cadí gneiss (456 ± 5 Ma, Casas et al., 2010), *Cg* Canigó gneiss (472-462 Ma, Cocherie et al., 2005; Navidad et al., 2018), *CM* Campelles-Bruguera ignimbrites (460 Ma, Martí et al., 2019), *Co* Cortalets metabasite (460 ± 3 Ma, Navidad et al., 2018), *Cs* Casemí gneiss (446 ± 5 and 452 ± 5 Ma, Casas et al., 2010), *DCG* Detrital-Carbonate Group, *Es* Estremoz rhyolites (499 Ma, Pereira et al., 2012), *Ga* Galineiro Complex, *GH* Gorges d'Héric orthogneiss (450 ± 6 Ma, Roger et al., 2004), *JL* Jbel Lmgaysmat Formation (Tabanite Group), *La* Larroque Volcanic Complex, *LDG* Lower Detrital Group, *Ma* Marialles microdiorite (453 ± 4 Ma, Casas et al., 2010), *Mo* Mora Complex (493.5 ± 2 Ma, Dias Da Silva et al., 2014), *Nu* Núria gneiss (457 ± 4 Ma, Martínez et al., 2011), *Os* Ollo de Sapo rhyolites and ash-fall tuff beds (ca. 477 Ma., Gutiérrez-Alonso et al., 2016), *Pe* Peso Volcanic Complex, *PL* Pont de Larn orthogneiss (456 ± 3 Ma, Roger et al., 2004), *Qb* Queralbs gneiss (457 ± 5 Ma, Martínez et al., 2011), *PS* Punta Serpedi (465.4 ± 1.9 and 464 ± 1 Ma, Giacomini et al., 2006; Oggiano et al., 2010), *Ri* Ribes granophyre (458 ± 3 Ma, Martínez et al., 2011), *Rf* Roc de Frausa gneiss (477 ± 4, 476 ± 5 Ma, Cocherie et al., 2005; Castiñeiras et al., 2008), *Sa* Saldanha Complex (483.7 ± 1.5; Dias da Silva, 2014), *So* Somail orthogneiss (471 ± 4 Ma, Cocherie et al., 2005), *SE* Saint Eutrope gneiss (455 ± 2 Ma, Pitra et al., 2012), *Ur* Urra rhyolites (494.6 ± 6.8 and 488.3 ± 5.2 Ma, Solá et al., 2008) and *UDG* Upper Detrital Group.

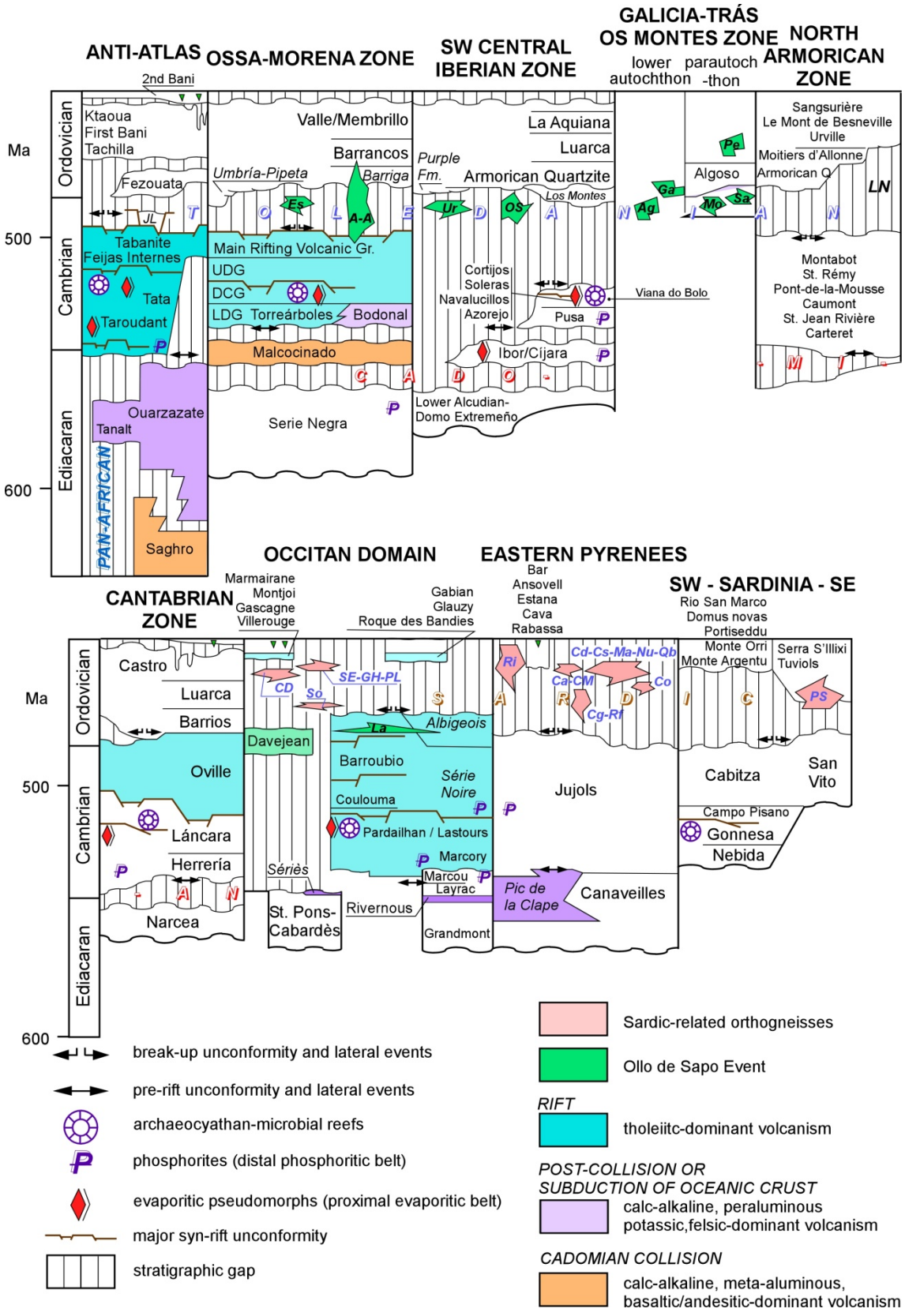
ANTI-ATLAS
OSSA-MORENA ZONE
SW CENTRAL IBERIAN ZONE
GALICIA-TRÁS OS MONTES ZONE
NORTH ARMORICAN ZONE
lower autochthon
parautoch -thon
2nd Bani
Ma
Ordovician
Cambrian
Ediacaran
500
600
Ktaoua
First Bani
Tachilla
Fezouata
Tabanite
Feijas Internes
Tata
Taroudant
Ouarzazate
Tanalt
PAN-AFRICAN
Saghro
Valle/Membrillo
Barrancos
Umbría-Pipeta
Barriga
Main Rifting Volcanic Gr.
UDG
DCG
LDG Torreárboles
Bodonal
Malcocinado
Serie Negra
Purple Fm.
La Aquiana
Luarca
Armorican Quartzite
Los Montes
Cortijos
Soleras
Navalucillos
Azorejo
Pusa
Ibor/Cijara
Lower Alcudian-Domo Extremeño
Viana do Bolo
Algoso
Sangsurière
Le Mont de Besneville
Urville
Moitiers d'Allonne
Armorican Q.
Montabot
St. Rémy
Pont-de-la-Mousse
Caumont
St. Jean Rivière
Carteret
OCCITAN DOMAIN
EASTERN PYRENEES
SW - SARDINIA - SE
CANTABRIAN ZONE
Marmairane
Montjoi
Gascagne
Villerouge
Gabian
Glauzy
Roque des Bandies
Bar
Ansovell
Estana
Cava
Rabassa
Rio San Marco
Domus novas
Portiseddu
Monte Orri
Monte Argentu
Serra S'Illixi
Tuviols
Castro
Luarca
Barrios
Oville
Láncara
Herrería
Narcea
Davejean
Barroubio
Coulouma
Pardailhan / Lastours
Marcory
Marcou
Layrac
Albigeois
Série Noire
Séríès
St. Pons-Cabardès
Rivernous
Grandmont
Jujols
Pic de la Clape
Canaveilles
Cabitza
San Vito
Campo Pisano
Gonnesa
Nebida
break-up unconformity and lateral events
pre-rift unconformity and lateral events
archaeocyathan-microbial reefs
phosphorites (distal phosphoritic belt)
evaporitic pseudomorphs (proximal evaporitic belt)
major syn-rift unconformity
stratigraphic gap
Sardic-related orthogneisses
Ollo de Sapo Event
RIFT
tholeiitc-dominant volcanism
POST-COLLISION OR SUBDUCTION OF OCEANIC CRUST
calc-alkaline, peraluminous potassic,felsic-dominant volcanism
CADOMIAN COLLISION
calc-alkaline, meta-aluminous, basaltic/andesitic-dominant volcanism

In the southern Canigó massif, the protoliths of the Núria granitic gneiss and the homonymous augen gneiss also yield Late Ordovician ages (457±4 and 457±5 Ma, respectively, Martínez et al., 2011). Moreover, metre-scale thick bodies of metadiorite are interlayered in the micaschists of the Balaig Series, which has also yielded a Late Ordovician age for the formation of its protolith (453±4 Ma, SHRIMP U–Pb in zircon, Casas et al., 2010). Coeval calc-alkaline volcanic rocks (ignimbrites, andesites and volcaniclastic rocks) are interbedded in the Upper Ordovician of the Ribes de Freser and Bruguera tectonostratigraphic units (Robert and Thiebaut, 1976; Ayora, 1980; Robert, 1980; Martí et al., 1986; see and updated structural and stratigraphic analysis in Puddu et al., 2018). The lower part of the Ribes de Freser unit is made up of dioritic bodies and volcaniclastic rocks, whereas rhyolitic lava flows and ignimbrites predominate in the central part, and ash levels, ignimbrites and volcaniclastic rocks constitute its upper part. The Ribes granitic body with granophyric texture, dated at 458±3 Ma by Martínez et al. (2011), intrudes at the base of the Upper Ordovician. On the other hand, the rhyolitic ignimbrites and andesitic lavas of the Bruguera unit have been recently dated at ca. 455 Ma by Martí et al. (2014). This volcanism was mainly explosive and displays calc-alkaline affinities (Martí et al., 1986).

3. Alps

In the Strona-Ceneri area of the Southern Alps, Zurbriggen et al. (1997) and Zurbriggen (2015) interpreted the pre-Mesozoic basement as a result of Ordovician orogenic processes, involving the so-called Cenerian Belt (Von Raumer et al., 2015). This is proposed as a composite overprint of subduction-accretion and cratonization phases characterized by a fore-arc volcanism hosted by an Alaskan-type orogeny involving HT-metamorphism (480–445 Ma), subsequently followed by anatexis (456-450 Ma; Schaltegger et al., 2003). The presence of a previously cleaved orthogneiss afected by km-scaled Variscan folds with steep axial planes and axes has been interpreted as a result of Ordovician compression (Stampfi et al., 2002; Franz & Romer, 2007; Stampfi et al., 2013; Von Raumer et al., 2013).

4. Sicily

U-Pb analyses in a metavolcanic suite interbedded in the metapelitic basement of the Peloritan Mountains (Sicily) have yielded ages of about 461–452 Ma (Trombetta et al., 2004). Based on geochemical evidence, these authors have interpreted the formation of a Mid-Ordovician volcanic arc that was affected by an early Katian (former Caradoc) tectono-thermal event.

5. Anti-Atlas

Although the Ordovician history of the Anti-Atlas is characterized by relative tectonic quiescence, by comparison with the Cambrian rifting history, the Ordovician succession is punctuated by a major, laterally extensive gap, marking a Dapingian hiatus. The

Ordovician represents over 41.2 myr of continuous sedimentation: (i) regionally preceded by major episodes of tilting and shoulder uplift of a graben–half-graben framework recording the dynamic geological history from the initial (rift to drift) break-up unconformity; (ii) punctuated by the Dapingian hiatus related to non-deposition and/or erosion; and (iii) the final post-glacial Silurian sealing of an inherited glaciogenic palaeorelief (Álvaro et al., in press *b*).

The Dapingian gap is marked by the absence of representative fossils in the Anti-Atlas (**Fig. 21**). This paraconformity is sealed by the Darriwilian-Sandbian-Katian First Bani and Ktaoua groups. In some areas of the Anti-Atlas, such as in the Tachilla and Ouarzemine jbels of the western Anti-Atlas, the Darriwilian sedimentation occurs directly sealing an inherited palaeorelief formed by Miaolingian strata; the corresponding Miaolingian-Dapingian gap should be associated with a Dapingian event responsible of uplift, tilting and erosion. Although no geodynamic explanation has yet been advanced for this gap, a possible distal influence of the Mid-Late Ordovician Sardic Phase may be recorded in this margin of Gondwana.

6. Central Iberian and Galicia-Trás-os-Montes Zones

In some areas of the Central Iberian Zone (e.g., Buçaco and the Truchas Syncline; Martínez Catalán et al., 1992; Días da Silva et al., 2016) and the Morais Allochthonous Complex of the Galicia-Trás-os-Montes Zone (Días da Silva, 2014; Días da Silva et al., 2014, 2016), a counterpart of the Sardic Phase has been proposed marking a stratigraphic discontinuity close to the Middle-Upper Ordovician boundary interval (**Fig. 21**). However, in the Truchas Syncline, the significance of the discontinuity (or discontinuities) was questioned by a biostratigraphic study of conodonts and the re-interpretation of some of these scouring surfaces as the result of Hirnantian glaciogenic incisions (Sarmiento et al., 1999). The pre-Hirnantian discontinuities have been interpreted as linked to the development of “horsts and half-grabens of local extent”, as a result of which “tilting and gentle folding of the Lower-Middle Ordovician strata, due to the rotation of individual half-grabens and horsts, create the Sardic unconformity in Iberia” (Da Silva et al., 2016: pp. 1131, 1143). However, the presence of synsedimentary listric faults associated with local outpouring of a basic volcanism related to extensional pulses in the Ordovician passive-margin platform fringing Northwest Gondwana should not be associated with the Sardic Phase. The Sardic Phase is characterized by generalized crustal uplift, denudation of exposed uplifted areas under subaerial exposure, stratigraphic gaps of about 25-30 m.y., broad intrusion of felsic granitic plutons (now orthogneisses after Variscan deformation and metamorphism) with calc-alkaline affinity, and record of alluvial-to-fluvial deposits sealing the unconformity. These are the features that characterize the Ordovician Sardic Phase, not the record of Ordovician volcanism and of local listric faults (e.g., Casas et al., 2010, 2019; Álvaro et al., 2016). In contrast, the Sardic aftermath is represented by a basic-dominant volcanic activity, mainly of tholeiitic affinity and lining rifting branches highlighting the onset of listric-fault networks; this event could be geodynamically compared with some processes recorded in the Central Iberian and the Galician-Trás-os-

Montes Zones, but not with the Sardic Phase. Therefore, the presence of the Sardic Phase in the Central Iberian and Galicia-Trás-os-Montes Zones should not be maintained except if the key Sardic tectono-thermal events described above are distinctly recognized.

7. Meguma terrane, Nova Scotia

In the Meguma terrane, another Mid-Late Ordovician gap has been suggested as coeval with the Sardic gap (White et al., 2018). The gap separates the Lower Ordovician Hellgate Formation (Halifax Group) from the unconformably overlying White Rock Formation (Silurian-Devonian Rockville Notch Group). The White Rock Formation consists of mafic and felsic metavolcanic rocks, interlayered and overlain by marine sedimentary strata, dated at about 446-434 Ma. The authors have suggested that the onset of the Sardic gap (not "phase") in the Meguma terrane would reflect the influence of the Ordovician geodynamic conditions preserved in the eastern branch of the Ibero-Armorican Arc, i.e. Occitan Domain, Eastern Pyrenees and Sardinia.

8. Turkey

In the Turkish Taurides, a Middle Ordovician tectonic activity on the so-called "Turkish platform" has been interpreted as a result of the onset of: (1) an unconformity separating Depositional Sequences 3 (late Furongian to early Mid Ordovician in age) and 4 (late Mid to Late Ordovician in age); (2) regressive events in the Taurides associated with gravity-driven facies (turbidites, mass-flow deposits); and (3) resultant reworking of palynomorph assemblages (Ghienne et al. 2010). The most significant tectonic instability is therefore suspected during the Darriwilian. However, these instable events associated with basic volcanism seem related to rifting pulses and the ensuing initiation of a major sag basin (the so-called Bedinan-Qasim trough). In Turkey, coeval granitic intrusions (Okay et al., 2008a) are probably linked to this Mid Ordovician continental rifting stage, thus extensional phase generated inland deformations throughout the Mediterranean-Turkish margin of Gondwana.

CHAPTER 8

CHAPTER 8

CONCLUSIONS

A revision of the stratigraphic, sedimentary and structural features that characterize the Sardic Phase in its type area has been envisaged in order to distinguish the key features of this phase outside SW Sardinia. The geological characters can be summarized as follows: (i) uplift and denudation of a subaerial palaeorelief; (ii) contemporaneous emplacement of a massive calc-alkaline magmatism everlastingly interpreted as representative of arc conditions; (iii) development of synsedimentary open folds lacking fold-related cleavage networks; (iv) absence of coeval metamorphic conditions; (v) development of a stratigraphic gap ranging from ca. 10 to 20 m.y.; and (vi) aftermaths characterized by sealing of an inherited palaeorelief by alluvial-to-fluvial deposits.

This PhD thesis has been mainly focused on the preservation of the Sardic Phase in Eastern Pyrenees, where the Sardic Unconformity separates two successions with different structural features. In the Ribes de Freser and La Cerdanya areas, the Cambro-Lower Ordovician and the Upper Ordovician successions share Late Ordovician extensional tectonics and two Variscan deformation events. The Cambro-Lower Ordovician succession is also affected by an Early-Mid Ordovician fold system associated with extensional faults. Upward propagation of some of them during Sandbian-Katian times caused the faults to affect the Sardic Unconformity and the lowermost part of the Upper Ordovician succession.

A new geological map at 1/5000 scale of the Ribes de Freser Alpine antiformal stack of the Eastern Pyrenees has provided a new stratigraphic, sedimentological and structural framework. The presence of shale/limestone alternations led the formal erection of the Katian El Baell Formation, proposed as a lateral equivalent of the monotonous (marlstone/limestone-dominant) Estana Formation. In its stratotype, the El Baell Formation displays three shallowing-upward sedimentary cycles, 200-230 m thick, related to changing conditions from clayey to carbonate substrates, controlled by episodes of shelly carbonate productivity derived from pelmatozoan-bryozoan meadows. A mud-mound is suggested forming the top of the formation as a result of plano-convex geometries, displaying preservation of ramose bryozoans in life position, capped by shelly bedded flanks. The thicker limestone levels, marking the top of the sedimentary cycles, contain fissure networks occluded with Pb-Zn-As ore mineralizations, whose clast counterparts occur forming lags of reworked extraclasts on the overlying beds, so pointing to synsedimentary conditions. The El Baell/Ansovell contact is marked by karstic clayey byproducts. Both the drastic changes in thickness and facies of the El Baell and Estana formations, and the presence of linked epithermal and fissuring episodes in the former, point to the onset of extensional tectonic pulsations, which may have controlled sharp modifications in accommodation space and development of (half-) grabens with hydrothermally mineralized bounding faults. In addition, a pre-Variscan (Mid Ordovician?) deformation event may have controlled the

wide dispersion of the folding axes of the main Variscan phase in the pre-Upper Ordovician succession preserved in the Bruguera unit.

We relate the extensional fault formation to a thermal doming that developed between 475 and 450 Ma. The doming should have produced stretching of the Ordovician lithosphere, together with emersion, uplift and erosion of the Cambro-Ordovician succession, giving rise to the formation of the Sardic Unconformity. Thermal doming may also be responsible for coeval magmatic activity that is well developed in the same area and caused by hot mafic magma underplating. We suggest a regional-scale thermal event ranging in age from Early-Mid- to Late Ordovician, which affected several areas of the Northern Gondwana margin. Its role in the geodynamic scenario that led to other significant Early Palaeozoic events, such as the opening of the Rheic Ocean and the drift of Avalonia *s.l.* from the western part of North Gondwana, requires investigation.

A comparison of the felsic magmatic activity recorded in the Furongian-Early Ordovician Toledanian Phase recorded in the Anti-Atlas, the Iberian Massif and the North and Central Armorican Massif, and the Sardic Phase recorded in southern Sardinia, Eastern Pyrenees and the Occitan Domain (Albigeois, Montagne Noire and Mouthoumet massifs) has yielded some interesting discussions. The geochemical comparison is based on 231 plutonic and volcanic samples of two major suites, from the Central Iberian and Galicia-Trás-os-Montes Zones of the Iberian Massif and in the eastern Pyrenees, Occitan Domain and Sardinia. This selection points to a predominance of materials derived from the melting of metasedimentary rocks, peraluminous and rich in SiO_2 and K_2O. The total content in REE is moderate to high. Most felsic rocks display similar chondritic normalized REE patterns, with an enrichment of LREE relative to HREE, which should indicate the involvement of crustal materials in their parental magmas. Zr/TiO_2, Zr/Nb, Nb/Y and Zr vs. Ga/Al ratios, and REE and εNd values reflect contemporaneous arc and extensional scenarios, which progressed to distinct extensional conditions finally associated with outpouring of mafic tholeiitic-dominant rifting lava flows. Magmatic events are contemporaneous with the formation of the Toledanian and Sardic unconformities, related to neither metamorphism nor penetrative deformation. The geochemical and structural framework precludes subduction generated melts reaching the crust in a magmatic arc to back-arc setting. On the contrary, it favours partial melting of sediments and/or granitoids in a continental lower crust triggered by the underplating of hot mafic magmas under extensional conditions, as a result of asthenospheric upwelling and related to the opening of the Rheic Ocean.

Finally, the Mid-Ordovician Sardic Unconformity recognized in southern Sardinia and the Eastern Pyrenees is compared with contemporaneous gaps recognized in the Occitan Domain, Sicily and the Alps. A critical re-appraisal of intra-Ordovician gaps related with the Sardic Phase has been made with reports referred to a Mid Ordovician gap from the Central Iberian and Galicia-Trás-os-Montes Zones of the Iberian Massif, the Dapingian gap of the Moroccan Anti-Atlas, and a Mid-Late Ordovician gap from the Meguma terrane in Nova Scotia (Canada).

CONCLUSIONES

Se presenta en esta tesis una descripción estratigráfica, sedimentológica y estructural de la Fase Sarda en su área tipo, con el objetivo de distinguir los caracteres clave que permitan reconocerla fuera del sudoeste de Cerdeña. Su caracterización geológica comprende: (1) un elevamiento cortical del zócalo generando su exposición subaérea y erosión superficial de un paleorelieve formado por rocas ediacáricas, cámbricas y del Ordovícico Inferior; (2) el emplazamiento coetáneo de un magmatismo de tipo calcoalcalino interpretado previamente como relacionado con un arco de subducción; (3) el desarrollo sinsedimentario de pliegues de gran longitud de onda carentes de esquistosidad; (4) la ausencia de condiciones metamórficas asociadas; (5) el registro de un hiato estratigráfico de 10 a 20 millones de años; y (6) un epílogo de la Fase Sárdica caracterizado por el sellado de un paleorelieve heredado mediante depósitos aluviales y fluviales del Ordovícico Superior.

Esta tesis doctoral se centra principalmente en la preservación de la Fase Sarda en el Pirineo Oriental, donde la discontinuidad separa dos sucesiones estratigráficas con diferentes estilos estructurales. En los sectores de Ribes de Freser y La Cerdanya, las sucesiones del Cámbrico-Ordovícico Inferior y del Ordovícico Superior comparten caracteres estructurales de tectónica distensiva datados del Ordovícico tardío, así como dos episodios de deformación varisca. Sin embargo, la sucesión del Cámbrico-Ordovícico Inferior aparece a su vez afectada por un sistema de pliegues de edad Ordovícico temprano-medio. La propagación de algunos de estos pliegues durante el Sandbiense-Katiense generó un sistema de fallas extensionales que afectan a la discontinuidad sarda y a la parte basal del Ordovícico Superior suprayacente.

Se ha realizado un mapa geológico a escala 1/5000 del apilamiento alpino de Ribes de Freser, en el Pirineo Oriental, donde se ha reconocido un nuevo estilo estratigráfico y sedimentológico de las rocas sedimentarias afectadas por la tectónica sarda. La presencia de alternacias de lutitas y calizas ha permitido la definición de una nueva formación katiense, la Formación de El Baell, que se propone como equivalente lateral de una sucesión monótona de calizas y margas, conocida como Formación de Estana. En su estratotipo, la Formación de El Baell comprende tres secuencias somerizantes, de 200 a 230 m de potencia, relacionadas con las condiciones fluctuantes de sustratos que de arcillosos cambian gradualmente a carbonatados, controlados por episodios de productividad carbonatada bioclástica derivada de praderas de briozoos y equinodermos. A techo de la formación se reconoce la nucleación y crecimiento de un montículo micrítico, como resultado del crecimiento de briozoos ramosos conservados en posición de vida y generando una geometría global de núcleo planoconvexo rodeado por flancos estratiformes. Los niveles carbonatados más potentes, que forman el techo de las secuencias de depósito, contienen redes de fisuras y venas rellenas con mineralizaciones polimetálicas, principalmente de Pb-Zn-As. La erosión de estas venas ha generado clastos polimetálicos que forman parte de brechas y conglomerados suprayacentes, reflejando su carácter sinsedimentario. El contacto entre las formaciones de El Baell y Ansovell está afectado por rellenos de arcillas cársticas sinsedimentarias.

Tanto los cambios bruscos de espesor y facies de las formaciones de El Baell y Estana, como la presencia de episodios de fisuración relacionados con hidrotermalismo epitermal registrados en la primera formación, apuntan el desarrollo de pulsos tectónicos distensivos responsables de la modificación del espacio de acomodación y el desarrollo de grábenes y semigrábenes limitados por fallas mineralizadas hidrotermalmente. Asimismo, un evento de deformación pre-varisco (probablemente Ordovícico medio) habría resultado responsable de la gran dispersión de los ejes de pliegues de la fase principal varisca, tal y como se conserva en la sucesión pre-sarda de la unidad tectonoestratigráfica de Bruguera.

Desde un punto de vista geodinámico, se relaciona el registro de fallas distensivas con el desarrollo de un domo térmico desarrollado entre 475 y 450 Ma. El domo habría generado el recurvamiento de la litosfera ordovícica responsable de la emersión y erosión superficial de la sucesión estratigráfica cambro-ordovícica, origen de la discontinuidad sarda. El domo térmico sería responsable a su vez de una actividad magmática coetánea registrada en el mismo sector, generada mediante fusión de magmas básicos en condiciones de infraplaca (*underplating*). Se sugiere que este evento térmico, de escala regional y edad ordovícica, habría afectado a parte del margen septentrional de Gondwana. Su influencia en la consecución de otros eventos geodinámicos del Paleozoico temprano, todos ellos derivados hacia la apertura del Océano Reico, require investigaciones adicionales.

Se ha realizado una comparación geoquímica de las actividades magmáticas asociadas a la Fase Toledánica (de edad Furongiense-Ordovícico temprano), registrada en el Anti-Atlas, el Macizo Ibérico y el Macizo Armoricano central y septentrional, y la Fase Sarda registrada en Cerdeña meridional, el Pirineo Oriental y el Dominio Occitano (macizos Albigenses, Montaña Negra y de Mouthoumet). La comparación se basa en 231 análisis de rocas plutónicas y volcánicas, agrupadas en dos asociaciones mayores; una comprende las Zonas Centroibérica y de Galicia-Trás-os-Montes Zones en el Macizo Ibérico, y otra el Pirineo Oriental, Dominio Occitano y Cerdeña. La selección de rocas ígneas incide en un predominio de rocas félsicas derivadas a partir de la fusión de rocas previas metasedimentarias, peraluminosas y ricas en SiO_2 y K_2O. El contenido total en REE varía entre moderado y alto. La mayoría de las rocas félsicas muestran patrones similares de REE normalizados a condrita, con un enriquecimiento en LREE con respect a HREE, que indicaría la participación de material crustal en los magmas originales. Las relaciones Zr/TiO_2, Zr/Nb, Nb/Y y Zr vs. Ga/Al, así como los valores en REE y εNd, reflejan condiciones de arco coincidentes con escenarios distensivos, progresando en el tiempo a condiciones claramente distensivas asociadas finalmente a la emanación de coladas de lava básica con afinidad predominante toleítica y bajo escenarios tipo *rift*. Estos eventos magmáticos son coetáneos con el registro de las discontinuidades toledánica y sarda, ambas carentes de metamorfismo o deformaciones penetrativas. Los datos estructurales y geoquímicos de las rocas ígneas impiden asociar dichos eventos a condiciones de subducción responsables de una fusión magmática afectando la corteza en escenarios de arco o tras-arco. Al contrario, los datos favorecen una fusion parcial de sedimentos y/o granitoides previos pertenecientes a una corteza continental inferior, desencadenada mediante el emplazamiento de magmas básicos

calientes en condiciones de infraplaca (*underplating*) mediante condiciones geodinámicas extensionales o distensivas, como resultado de un ascenso astenosférico relacionado con la apertura del Océano Reico.

Por último, se compara la disconinuidad sarda, de edad Ordovícico medio y reconocida en Cerdeña meridional y el Pirineo Oriental, con hiatos coetáneos del Dominio Occitano, Sicilia y los Alpes. Asimismo se realiza una revision crítica de la supuesta identificación de la Fase Sarda en otras áreas, que incluyen las Zonas Centroibérica y de Galicia-Trás-os-Montes Zones en el Macizo Ibérico, el hiato dapingiense del Anti-Atlas marroquí y el hiato del Ordovícico medio de la unidad tectonosestratigráfica de Meguma en Nueva Escocia (Canada).

CHAPTER 9

CHAPTER 9

REFERENCES

Abad, A. 1988. El Cámbrico inferior de Terrades (Gerona). Estratigrafía, facies y paleontología. *Batallería* 2, 47-56.

Alabouvette, B., Demange, M., Guérangé-Lozes, J. & Ambert, P., 2003. Notice explicative de la carte géologique de Montpellier au 1/250 000. BRGM, Orléans.

Albani, R., Di Milia, A., Minzoni, N & Togiorgi, M. 1985. Nuovi dati palinologici e considerazioni geologiche sulla età delle Arenarie di Solanas (Cambro-Ordoviciano – Sardegna centrale). *Atti Soc. Tosc. Sci. Nat. Mem.* (ser. A) 91, 1-20.

Álvaro, J.J. & Vizcaïno, D. 2018. The Furongian break-up (rift-drift) transition in the Anti-Atlas, Morocco. *J. Iber. Geol*. 44, 567-587.

Álvaro, J.J., Elicki, O., Geyer, G., Rushton, A.W.A. & Shergold, J.H. 2003. Palaeogeographical controls on the Cambrian trilobite immigration and evolutionary patterns reported in the western Gondwana margin. *Palaeogeogr., Palaeoclimat., Palaeoecol.* 195, 5-35.

Álvaro, J. J., Ferretti, F., González-Gómez, C., Serpagli, E., Tortello, M. F., Vecoli, M. & Vizcaïno, D. 2007. A review of the Late Cambrian (Furongian) palaeogeography in the western Mediterranean region, NW Gondwana. *Earth-Sci. Rev*. 85, 47-81.

Álvaro, J.J., Ezzouhairi, H., Ribeiro, M.L., Ramos, J.F. & Solá, A.R. 2008. Early Ordovician volcanism of the Iberian Chains (NE Spain) and its influence on preservation of shell concentrations. *Bull. Soc. géol. France* 179 (6), 569-581.

Álvaro, J. J., Monceret, E., Monceret, S., Verraes, G. & Vizcaïno, D. 2010. Stratigraphic record and palaeogeographic context of the Cambrian Epoch 2 subtropical carbonate platforms and their basinal counterparts in SW Europe, West Gondwana. *Bull. Geosci*. 85, 573-584.

Álvaro, J.J., Bauluz, B., Clausen, S., Devaere, L., Gil Imaz, A., Monceret, E. & Vizcaïno, D. 2014*a*. Stratigraphy of the Cambrian-Lower Ordovician volcanosedimentary complexes, northern Montagne Noire, France. *Stratigraphy* 11, 83-96.

Álvaro, J. J., Bellido, F., Gasquet, D., Pereira, F., Quesada, C. & Sánchez-García, T. 2014*b*. Diachronism of late Neoproterozoic-Cambrian arc-rift transition of North Gondwana: a comparison of Morocco and the Iberian Ossa-Morena Zone. *J. Afr. Earth Sci*. 98, 113-132.

Álvaro, J. J., Benziane, F., Thomas, R., Walsh, G. J. & Yazidi, A. 2014*c*. Neoproterozoic-Cambrian stratigraphic framework of the Anti-Atlas and Ouzellagh promontory (High Atlas), Morocco. *J. Afr. Earth Sci*. 98, 1-15

Álvaro, J.J., Colmenar, J., Monceret, E., Pouclet, A. & Vizcaïno, D. 2016. Late Ordovician (post-Sardic) rifting branches in the North-Gondwanan Montagne Noire and Mouthoumet massifs of southern France. *Tectonophysics* 681, 111-123.

Álvaro, J.J., Casas, J.M., Clausen, S. & Quesada, C. 2018. Early Palaeozoic geodynamics in NW Gondwana. *J. Iber. Geol*. 44, 551-565.

Álvaro, J.J., Casas, J.M. & Quesada, C. in press *a*. Reconstructing the pre-Variscan puzzle of Cambro-Ordovician basement rocks in the southwestern European margin of Gondwana. In: Pannotia to Pangaea: Neoproterozoic and Paleozoic Orogenic Cycles in the Circum-Atlantic Region (Murphy, J.B., Strachan, R.A. & Quesada, C., eds.). *Geol. Soc., London, Spec. Publ*. 503, https://doi.org/10.1144/SP503-2020-89.

Álvaro, J.J., Benharref, M., Destomes, J., Gutiérrez-Marco, J.C., Hunter, A.W., Lefebvre, B., Van Roy, P. & Zamora, S. in press *b*. Ordovician stratigraphy and benthic community replacements in the eastern Anti-Atlas, Morocco. In: The Great Ordovician Biodiversification Event: Insights from the Tafilalt Biota, Morocco (Hunter, A.A., Álvaro, J.J., Lefebvre, B., Val Roy, P. & Zamora, S., eds.). *Geol. Soc., London, Spec. Publ*. 485, https://doi.org/10.1144/SP485.20.

Álvaro, J.J., Cortijo, I., Jensen, S., Lorenzo, S., Palacios, T. & Pieren, A. 2019. Updated stratigraphic framework and biota of the Ediacaran and Terreneuvian in the Alcudia-Toledo Mountains of the Central Iberian Zone, Spain. *Est. Geol.* 75 (2), e093.

Amaral, A., Dias, R., Coke, C., Romão, J. & Ribeiro, A. 2014. Fase de deformação sarda na Zona Centro-Ibérica. *Comun. Geol.* 101, 239-242.

Annino, E. 1995. Gli eventi stratigrafici, tettonici e magmatici legati alla "Fase Sarda" (Ordoviciano medio) nella Sardegna centro-meridionale ed in alcuni settori paleozoici sud-europei. PhD, Cagliari Univ.

Annino, E., Barca, S. & Costamagna, L.G. 2000. Lineamenti stratigrafico-strutturali dell'Arburese (Sardegna sud-occidentale). *Rend. Semin. Fac. Sci. Univ. Cagliari, suppl.* 70, 403-426.

Antunes, I.M.H.R., Neiva, A.M.R., Silva, M.M.V.G. & Corfu, F. 2009. The genesis of I- and S-type granitoid rocks of the Early Ordovician Oledo pluton, Central Iberian Zone (central Portugal). *Lithos* 111, 168-185.

Aramburu, C. & García-Ramos, C. 1988. Presencia de la discontinuidad sárdica en la Zona Cantábrica. *Geogaceta* 5, 11-13.

Aramburu, C., Méndez-Bedia, I., Arbizu, M. & García-López, S. 2004. Zona Cantábrica. Estratigrafía. La secuencia preorogénica. In: Geología de España (Vera, J., ed.). Sociedad Geológica de España and Instituto Geológico y Minero de España, Madrid, pp. 27-34.

Arthaud, F. 1963. Un exemple de tectonique superposée dans le Paléozoïque de l'Iglesiente (Sardaigne). *C. R. Som. Soc. géol. France* 9, 303-304.

Arthaud, F. 1970. Etude tectonique et microtectonique comparée de deux domaines hercyniens: les nappes de la Montaigne Noire (France) et l'anticlinorium de l'Iglesiente (Sardaigne). *Publ. Univ. Sci. Tech. Languedoc, Série Géol. Struct.* 1, 1-175.

Arthaud, F., Burg, J.P. & Matte, P. 1976. L'évolution structurale hercynienne du massif de Mouthoumet (Sud de la France). *Bull. Soc. géol. France* (sér. 7) 18, 967-972.

Ayora, C. 1980. Les concentrationes metàl·liques de la Vall de Ribes. PhD, Barcelona Univ.

Ballèvre, M., Bosse, V., Ducassou, C. & Pitra, P. 2009. Palaeozoic history of the Armorican Massif: Models for the tectonic evolution of the suture zones. *C. R. Geosci.* 341, 174-201.

Ballèvre, M., Fourcade S., Capdevila, R., Peucat, J.J., Cocherie, A. & Mark Fanning, C. 2012. Geochronology and geochemistry of Ordovician felsic volcanism in the Southern Armorican Massif (Variscan belt, France): Implications for the breakup of Gondwana. *Gondwana Res*. 21, 1019-1036.

Barbey, P., Cheilletz, A. & Laumonier, B. 2001. The Canigou orthogneisses (Eastern Pyrenees, France, Spain): an Early Ordovician rapakivi granite laccolith and its contact aureole. *C. R. Acad. Sci, Paris* 332, 129-136.

Barca, S. 1991. Phénomènes de resédimentation et flysch hercynien à faciès Culm dans le "synclinal du Sarrabus" (SE de la Sardaigne, Italie). *C. R. Acad. Sci., Paris* 313 (2), 1051-1057.

Barca, S. & Cherchi, A. 2004. Regional geological setting. In: Barca, S., Cherchi, A. (eds.), Sardinian Palaeozoic Basement and its Meso-Cainozoic Cover (Italy). 32nd Int. Geol. Congress. Field Trip Guide Book-P39 (5), 3-8.

Barca, S. & Di Gregorio, F. 1979. La successione ordoviciano-siluriana inferiore nel Sarrabus (Sardegna sud-orientale). *Mem. Soc. Geol. It.* 20, 189-202.

Barca, S. & Maxia, M. 1982. Assetto stratigrafico e tettonico del Paleozoico del Sarrabus occidentale. In: Guida alla Geologia del Paleozoico sardo. Guide Geologiche Regionali, Soc. Geol. It. 87-93. Cagliari.

Barca, S., Cocozza, T., Del Rio, M. & Pittau Demelia, P. 1981a. Discovery of lower Ordovician acritarchs in the "Postgothlandiano" sequence of SW Sardinia (Italy): age and tectonic implications. *Boll. Soc. Geol. It.* 100, 377-392.

Barca, S., Del Rio. M. & Pittau Demelia. P. 1981b. Acritarchs in the "arenarie di San Vito" of south-east Sardinia: stratigraphical and geological implications. *Boll. Soc. Geol. It.* 100, 369-375.

Barca, S., Del Rio, M., Minzoni, N. & Pittau Demelia, P. 1985. Presenza di Tremadociano ad Acritarchi in Unità tettoniche Erciniche a Sud del Lago di Mulargia (Sardegna centrale). *Riv. It. Paleont. Strat.* 89 (3), 315-334.

Barca, S., Carmignani, L., Maxia, M., Oggiano, G. & Pertusati, P.C. 1986. The Geology of Sarrabus. In: Guide-Book to the Excursion on the Paleozoic Basement of Sardinia (Carmignani, L., Cocozza, T., Ghezzo, C., Pertusati, P.C. & Ricci, C.A., eds.). *IGCP Newsl., Spec. Iss.* 5, 51-60.

Barca, S., Carmignani, L., Cocozza, T., Franceschelli, M., Ghezzo, C., Memmi, I., Minzoni, N., Pertusati, P.C. & Ricci, C.A. 1987a. The Caledonian events in Sardinia. In: The Caledonian Orogen – Scandinavia and Related Areas [International Geological Correlation Programme, a contribution to Project No. 27 The Caledonide Orogen (IGCP-CO)] (Gee, D.G. & Sturt, B.A., eds.). John Wiley & Sons, Chichester, pp. 1195-1199.

Barca, S., Cocozza, T., Del Rio, M., Pillola, G.L. & Pittau Demelia, P. 1987b. Datation de l'Ordovicien inférieur par *Dictyonema flabelliforme* et Acritarches dans la partie supérieure de la formation "Cambrienne" de Cabitza (SW de la Sardaigne, Italie): Conséquences géodynamiques. *C. R. Acad. Sci., Paris* 305, 1109-1113.

Barca, S., Del Rio, M. & Pittau Demelia, P. 1988. New geological and stratigraphical data and discovery of lower Ordovician acritarchs in the San Vito sandstone of the Genn'Argiolas unit (Sarrabus, Southeastern Sardinia). *Riv. Ital. Paleont. Stratigr*. 94 (3), 339-360.

Barca, S., Ferretti, A., Massa, P. & Serpagli, E. 1992. Minor tectonic units within the Hercynian Arburese Nappe in Southwestern Sardinia. New structural and stratigraphic evidences. In: Contribution to the Geology of Italy with Special Regard to the Paleozoic Basement. A Volume Dedicated to Tommaso Cocozza (Carmignani, L. & Sassi, F.P., eds.). *IGCP Project no. 276, Newsl.* 5, 51-55.

Barnolas, A. & García-Sansegundo, J. 1992. Caracterización estratigráfica y estructural del Paleozoico de Les Gavarres (Cadenas Costero Catalanas, NE de España). *Bol. Geol. Min.* 10, 94-108.

Barnolas, A., Vélez, A.G. & Soubrier, J. 1980. Sobre la presencia del Caradoc en Les Gavarres. *Acta Geol. Hisp.* 25 (1), 9-13.

Barrouquère, G., Bessière, G., Majeste-Menjoulas, C. & Mirouse, R. 1983. Paleozoic stratigraphy and Variscan events in the Eastern Pyrenees In: Geotraverse A2: Stratigraphic Correlation Forms (Sassi & Szederkenyi, eds.). *I.G.C.P. no. 5, Newsl.* 5, 205-216.

Bea, F., Montero, P., Talavera, C. & Zinger, T., 2006. A revised Ordovician age for the Miranda do Douro orthogneiss, Portugal. Zircon U-Pb ion-microprobe and LA-ICPMS dating. *Geol. Acta* 4, 395-401.

Bea, F., Montero, P., González Lodeiro, F. & Talavera, C. 2007. Zircon inheritance reveals exceptionally fast crustal magma generation processes in Central Iberia during the Cambro-Ordovician. *J. Petrol*. 48, 2327-2339

Bé Mézème, E. 2005. Contribution de la géochronologie U-Th-Pb sur monazite à la compréhension de la fusion crustale dans la chaîne Hercynienne française et implication géodynamique. PhD, Univ. Orléans.

Beccaluva, L., Leone, F., Maccioni, L. & Macciotta, G. 1981. Petrology and tectonic setting of the Palaeozoic basic rocks from Iglesiente-Sulcis (Sardinia, Italy). *N. Jb. Miner., Abh.* 140 (2), 184-201.

Bechstädt, T. & Boni, M. (eds.) 1994. Sedimentological, stratigraphical and ore deposits field guide of the autochthonous Cambro-Ordovician of Southwestern Sardinia. *Serv. Geol. It. Mem. Desc. C. Geol. It.* 48, 1-434.

Bederke, E. 1939. Die kaledonische Gebirgsbildung in Mitteleuropa. *Z. dt. geol. Ges.* 91, 770-771.

Belaústegui, Z., Puddu, C. & Casas, J.M. 2016. New ichnological data from the lower Paleozoic of the Central Pyrenees: presence of *Arthrophycus brogniartii* (Harlan, 1832) in the Upper Ordovician Cava Formation. *Geo-Temas* 16, 271-274.

Berger, G. 1982. Notice explicative de la feuille de Leucate à 1/50 000, no. 1979. BRGM, Orléans.

Berger, G., Boyer, Débat, P., Demange, M., Freytet, P., Marchal, J. P. et al. (1993). Notice explicative de la feuille de Carcassonne à 1/50 000, no. 1037. BRGM, Orléans.

Berger, G., Boyer, F. & Rey, J. 1990. Notice explicative de la feuille de Lézignan-Corbières à 1/50 000, no. 1038. BRGM, Orléans.

Berger G., Boyer F., Débat P., Demange M., Freytet P., Marchal J.P., Mazéas H. & Vantrelle C. 1993. Notice explicative de la feuille de Carcassonne à 1/50 000, no. 1037. BRGM, Orléans.

Berger, G.M., Alabouvette, B., Bessière, G., Bilotte, M., Crochet, B., Dubar, M., Marchal, J.P., Tambareau, Y., Villatte, J. & Viallard, P. 1997. Notice explicative de la feuille de Tuchan à 1/50 000, no. 1078. BRGM, Orléans.

Bessière, G. & Baudelot, S. 1988. Le Paléozoïque inférieur du massif de Mouthoumet (Aude, France) replacé dans le cadre du domaine sud-Varisque: révision et conséquences. *C. R. Acad. Sci., Paris* (sér. 2) 307, 771-777.

Bessière, G. & Schulze, H. 1984. Le Massif de Mouthoumet (Aude, France): nouvelle définition des unités structurales et essai d'une reconstruction paléogéographique. *Bull. Soc. géol. France* 26, 885-894.

Bessière, G., Bilotte, M., Crochet, B., Peybernès, B., Tambereau, Y. & Villatte, J. 1989. Notice explicative de la feuille de Quillan à 1/50 000, no. 1077. BRGM, Orléans.

Bindeman, I.N. & Valley, J.W. 2003. Rapid generation of both high- and low-$\delta^{18}O$, large-volume silicic magmas at the Timber Mountain/Oasis Valley caldera complex, Nevada. *Geol. Soc. Am. Bull.* 115 (5), 581-595.

Boissevain, H. 1934. Etude géologique et morphologique de la vallée de la Haute Sègre. *Bull. Soc. Hist. Nat. Toulouse* 66, 33-170.

Boni, M. 1986. The Permo-Triassic vein and paleokarst ores in southwest Sardinia: contribution of fluid inclusion studies to their genesis and paleoenvironment. Mineral. Deposita 21, 53-62.

Boni, M. & Koeppel, V. 1985. Ore-lead isotope pattern from the Iglesiente-Sulcis area (SW Sardinia) and the problem of remobilization of metals. *Mineral. Deposita* 20, 185-193.

Boriani, A. 2008. Age and origins of the Italian continental crust: data and interpretations. *Rend. Soci. Geol. It., Abstracts* 3, 124.

Bornemann, J.G. 1881. Sur la classification des formations stratifiées anciennes de l'île de Sardaigne. *C. R. Congr. Géol. Int., Bologne*, pp. 221-232.

Bornemann, J.G. 1891. Die Versteinerungen des Cambrischen Schistensystems der Insel Sardinien nebst vergleichenden Untersuchungen über analoge Vorkommisse auns anderen Ländern. *Nova Acta Caes. Leop. Carol. Deut. Akad. Nat.* part 1, 51 (1), 1-148; part 2, 56 (3), 427-528.

Borrouilh, R., Cocozza, T., Demange, M., Durand-Delga, M., Gueirard, S., Julivert, M., Martínez, F.J., Massa, D., Mirouse, R. & Orsini, J.B. 1985. Essai sur l'évolution paléogéographique, structurale et métamorphique du Paléozoïque du Sud de la France et l'Ouest de la Méditerranée. *Mém. Soc. géol. France* 108, 159-188.

Bosellini, A. & Ogniben, G. 1968. Ricoprimenti ercinici nella Sardegna centrale. *Ann. Univ. Ferrara* 1, 1-15.

Boulange, M.F. & Boyer, F. 1964. Sur l'âge de la transgression post-Calédonienne dans le Sud de la Montagne Noire. *C. R. Acad. Sci., Paris* 259, 1309-1312.

Brouwer, H. 1965. Esiste la Fase Sarda in Sardegna? *Res. Ass. Min. Sarda* 70 (8), 86-89.

Brouwer, N. 1968. Verslag van een geologische kartering in de omgeving van de Cerdaña vallei, oostelijke Pyreneën, Spanje. PhD, Leiden Univ.

Brouwer, H. 1987. The Sardic tectonic phase in SW Sardinia: a concept rejected. In: Correlation of Prevariscan and Variscan events. Final Meeting, Cagliari, May 1986, *IGCP Project No. 5 Abstracts*, p. 25-31.

Brusca, C. & Dessau, G. 1968. I giacimenti piombo-zinciferi di S. Giovanni (Iglesias) nel quadro della geologia del Cambrico sardo. *L'Industria Mineraria* 19, 533-556.

Buzzi, L., Funedda, A., Gaggero, L. & Oggiano, G. 2007a. Sr-Nd isotope, trace and REE geochemistry of the Ordovician volcanism in the southern realms of the Variscan belt. EGU General Assembly 2007, Wien, 15-20 April 2007, Geophysical Research, Abstracts, p. 9.

Bryan, S.E., Riley, T.R., Jerram, D.A., Stephens, Ch.J. & Leat, Ph.T. 2002. Silicic volcanism: An undervalued component of large igneous provinces and volcanic rifted margins. In: Volcanic Rifted Margins (Menzies, M.A., Klemperer, S.L., Ebinger, C.J. & Baker, J., eds.). *Geol. Soc. Am., Spec. Pap.* 362, 99-120.

Buzzi, L., Funedda, A., Gaggero, L., Oggiano, G. & Tiepolo, M. 2007b. U-Pb zircon dating (LA-ICP-MS) of the Ordovician felsic volcanism through the Variscan Units in Sardinia (Italy). EGU General Assembly 2007, Wien, 15-20 April 2007, Geophysical Research Abstracts, p. 10.

Buzzi, L., Gaggero, L., Funedda, A., Oggiano, G. & Tiepolo, M. 2007c. Zircon geochronology and Sr/Nd study of the Ordovician magmatic events in the southern Variscides (Sardinia). *Géol. France* 2007 (2), 73.

Cadish, J. 1938. Zur Geologie des Insel Sardinien mit Beobachtung über ihre erzlagerstätten. *Geol. Rundsch.* 29, 52-71.

Calvet, P., Lapierre, E. & Charvet, J. 1988. Diversité du volcanisme ordovicien dans la région de Pierrefitte (Hautes Pyrénées): rhyolites calco-alcalines et basalts alcalins. *C. R. Acad. Sci., Paris* 3078, 805-812.

Calvino, F. 1956. Studio geologico petrografico sulla regione di Piano Lasina (Sardegna meridionale). *Ric. Sci*. 26, 114-130.

Calvino, F. 1959a. Primi risultati di uno studio stratigrafico e tettonico della Sardegna sud-orientale. *Mem. Acc. Patavina Sci. Lett. Arti* 41, 1-14.

Calvino, F. 1959b. Lineamenti strutturali del Sarrabus-Gerrei (Sardegna sud-orientale). *Boll. Serv. Geol. It.* 81 (4-5), 489-556.

Calvino, F. 1963. Note Illustrative della carta geologica d'Italia, Foglio 227-Muravera, 1:1.000.000. Serv. Geol. It., Roma.

Calvino, F. 1967. Note illustrative della Carta Geologica d'Italia. F 227 Muravera. Soc. Cooperativa Tipografica, 60 p.

Calvino, F. 1972. Note Illustrative della carta geologica d'Italia, Foglio 227-Muravera. Serv. Geol. It., 60 p. Roma.

Camerana, E, Ferraris, E., & Merlo, G. 1899. Intorno all'origine del calcare metallifero dell'Iglesiente. *Ass. Min. sarda* anno 1899

Cappelli, B., Carmignani, L., Castorina, F., Di Pisa, A., Oggiano, G. & Petrini, R. 1992. A Hercynian suture zone in Sardinia: geological and geochemical evidence. *Geodin. Acta* 5, 101-118.

Carmignani, L. & Pertusati, P.C. 1977. Analisi strutturale di un segmento della catena ercinica: il Gerrei (Sardegna sud- orientale). *Boll. Soc. Geol. It.* 96: 339-364.

Carmignani, L., Cocozza, T., Minzoni, N. & Pertusati, P.C. 1978. Falde di ricoprimento erciniche nella Sardegna a Nord-Est del Campidano. *Mem. Soc. Geol. It.* 19, 501-510.

Carmignani, L., Cocozza, T., Minzoni, N., Pertusati, P.C. & Ricci, C.A. 1979. E' la Corsica il retropaese della catena ercinica della Sardegna? *Mem. Soc. Geol. It*. 20, 47-55.

Carmignani, L., Cocozza, T., Minzoni, N. & Pertusati, P.C. 1981. Structural and palaeogeographic lineaments of the Variscan cycle in Sardinia. *Geol. Mijnbouw* 60, 171-181.

Carmignani, L., Cocozza, T., Gandin, A., & Pertusati, P.C. 1982. Lineamenti della geologia dell'Iglesiente-Sulcis - Guida alla Geologia del Paleozoico Sardo. *Guide Geologiche regionali Soc. Geol. It.*, 65-77.

Carmignani, L., Costagliola, C., Gattiglio, M., Leglise, H., Oggiano, G., Maxia, M. *et al*. 1982. Lineamenti geologici della Bassa Valle del Flumendosa (Sardegna Sud-Orientale). In: Paleozoico Sardo (Carmignani, L., Cocozza, T., Ghezzo, C., Pertusati, P.C. & Ricci, C.A., eds.). Guida alla geologia de Cagliari. Soc. Geol. It. – Guide Geologiche Regionali, pp. 95-107.

Carmignani, L., Cocozza, T., Ghezzo, C., Pertusati, P.C. & Ricci, C.A. 1986. Guide-book to the Excursion on the Palaeozoic Basement of Sardinia. *IGCP Project no. 5, Newsl. Spec. Iss*., 1-102.

Carmignani, L., Pertusati, P.C., Barca, S., Carosi, R., Di Pisa, A., Gattiglio, M., Musumeci, G. & Oggiano, G. 1992. Struttura della catena ercinica in Sardegna. Guida all'Escursione – Gruppo Informale di Geologia strutturale, 177 p.

Carmignani, L., Carosi, R., Di Pisa, A., Gattiglio, M., Musumeci, G., Oggiano, G. & Pertusati, P.C. 1994. The Hercynian Chain in Sardinia (Italy). *Geodin. Acta* 7, 31-47.

Carmignani, L., Conti, P., Barca, S., Cerbai, N., Eltrudis, A., Funedda, A. *et al.* 2001a. Foglio 549-Muravera. Note illustrative. Note illustrative della Carta Geologica d'Italia in scala 1:50.000, Serv. Geol. It., 140 p. Roma.

Carmignani, L., Oggiano, G., Barca, S., Conti, P., Salvadori, I., Eltrudis, A. *et al*. 2001b. Geologia della Sardegna. Note illustrative della Carta Geologica in scala 1:200.000 . *Mem. Descr. Carta Geol. It.* 60, 283.

Caron, C., Lancelot, J., Omenetto, P. & Orgeval, J.J., 1997. Role of the Sardic tectonic phase in the metallogenesis of SW Sardinia (Iglesiente): lead isotope evidence. *Eur. J. Miner*. 9, 1005-1016.

Carosi, R. & Palmeri, R. 2002. Orogen-parallel tectonic transport in the Variscan belt of north-eastern Sardinia (Italy): implications for the exhumation of medium-pressure metamorphic rocks. *Geol. Mag.* 139, 95-102.

Carreras, J. & Cappellà, I. 1994. Tectonic levels in the Palaeozoic basement of the Pyrenees: a review and a new interpretation. *J. Struct. Geol.* 16, 1509-1524.

Casas, J.M. 2010. Ordovician deformations in the Pyrenees: new insights into the significance of pre-Variscan ("sardic") tectonics. *Geol. Mag.* 147, 647-689.

Casas, J.M. & Fernández, O. 2007 On the Upper Ordovician unconformity in the Pyrenees: New evidence from the La Cerdanya area. *Geol. Acta* 5 (2), 193-198.

Casas, J.M. & Palacios, T. 2012. First biostratigraphical constraints on the pre-Upper Ordovician sequences of the Pyrenees based on organic-walled microfossils. *C. R. Geosci*. 344, 50-56.

Casas, J.M. & Puddu, C. 2010. Insights into the significance of Pre-Variscan ("Sardic") tectonics. R. S. T. 25-29/10/2020 Bordeaux, p. 48.

Casas, J.M., Martí, J & Ayora, C. 1986. Importance du volcanisme dans la composition lithostratigraphique du Paleozoique inferieur des Pyrénées Catalanes. *C. R. Acad. Sci., Paris* (sér. 2) 302 (19), 1193-1198.

Casas, J.M., Domingo, F., Poblet, J. & Soler, A. 1989. On the role of the Hercynian and Alpine thrusts in the Upper Paleozoic rocks of the Central and Eastern Pyrenees. *Geodin. Acta* 3, 135-147.

Casas, J.M., Parés, J.M. & Megías, L. 1998. La fábrica magnética de los materiales cambro-ordovícicos del Anticlinal de la Massana (Andorra, Pirineo Central). *Rev. Soc. Geol. España* 11, 317-329.

Casas, J.M., Castiñeiras, P., Navidad, M., Liesa, M. & Carreras, J. 2010. New insights into the Late Ordovician magmatism in the Eastern Pyrenees: U-Pb SHRIMP zircon data from the Canigó massif. *Gondwana Res.* 17, 317-324.

Casas, J.M., Castiñeiras, P., Navidad, M., Liesa, M., Martínez, M.F., Carreras, J., Reche, J., Iriondo, A., Aleinikoff, J., Cires, J. & Dietsch, C. 2011. Ordovician magmatism in NE Iberia. *Cuad. Mus. Geomin., IGME* 14, 95-100.

Casas, J.M., Queralt, P., Mencos, J. & Gratacós, O. 2012. Distribution of linear mesostructures in oblique folded surfaces: Unravelling superposed Ordovician and Variscan folds in the Pyrenees. *J. Struct. Geol.* 44, 141-150.

Casas, J.M., Navidad, M, Castiñeiras, P., Liesa, M., Aguilar, C., Carreras, J., Hofmann, M., Gärtner, A. & Linnemann, U. 2015. The Late Neoproterozoic magmatism in the Ediacaran series of the Eastern Pyrenees: new ages and isotope geochemistry. *Int. J. Earth Sci.* 104, 909-925.

Casas J.M., Sánchez-García T., Álvaro J.J., Puddu C. & Liesa M. 2017a. Ordovician magmatism in the Pyrenees. In: Ordovician Geodynamics: The Sardic Phase in the Pyrenees, Mouthoumet and Montaigne Noire massifs (Álvaro J.J., Casas J.M. & Clausen S., eds.).). 4-9 September 2017, Figueres, Catalonia. Abstract volume, p. 12.

Casas J.M., Sánchez-García T., Álvaro J.J., Puddu C. & Liesa M. 2017b. Ordovician magmatism in the Pyrenees. In: Ordovician Geodynamics: The Sardic Phase in the Pyrenees, Mouthoumet and Montaigne Noire massifs (Álvaro J.J., Casas J.M. & Clausen S., eds.).). 4-9 September 2017, Figueres, Catalonia. Abstract volume, p. 12.

Casas, J.M., Álvaro, J.J., Clausen, S., Padel, M., Puddu, C., Sanz-López, J., Sánchez-García, T., Navidad, M., Castiñeiras, P. & Liesa, M., 2019. Palaeozoic basement of the Pyrenees. In: The Geology of Iberia: A Geodynamic Approach (Quesada, C., Oliveira, J.T., eds.). Regional Geology Reviews, vol. 2, 229-259. Springer, Heidelberg.

Casini, L. & Oggiano, G. 2008. Late orogenic collapse and thermal doming in the northern Gondwana margin incorporated in the Variscan Chain: a case study from the Ozieri Metamorphic Complex, northern Sardinia, Italy. *Gondwana Res.* 13, 396-406.

Casini, L., Funedda, A. & Oggiano, G. 2010. A balanced foreland-hinterland deformation model for the Southern Variscan belt of Sardinia, Italy. *Geol. J.* 45 (5-6), 634-649.

Casini, L., Cuccuru. S., Maino. M., Oggiano. G. & Tiepolo. M. 2012. Emplacement of the Arzachena Pluton (Corsica-Sardinia Batholith) and the geodynamics of incoming Pangaea. *Tectonophysics* 544-545, 31-49.

Casini, L., Cuccuru, S., Puccini, A., Oggiano, G. & Rossi, P. 2015. Evolution of the Corsica-Sardinia Batholith and late-orogenic shearing of the Variscides. *Tectonophysics* 646, 65-78.

Castiñeiras, P., Navidad, M., Liesa, M., Carreras, J. & Casas, J.M. 2008a. U-Pb zircon ages (SHRIMP) for Cadomian and Lower Ordovician magmatism in the Eastern Pyrenees: new insights in the pre-Variscan evolution of the northern Gondwana margin. *Tectonophysics* 46, 228-239.

Castiñeiras, P., Villaseca, C., Barbero, L., Martín Romera, C., 2008b. SHRIMP U-Pb zircon dating of anatexis in high-grade migmatite complexes of Central Spain: implications in the Hercynian evolution of Central Iberia. International Journal of Earth Sciences, 97, 35-50.

Castiñeiras, P., Navidad, M., Casas, J.M., Liesa, M. & Carreras, J. 2011. Petrogenesis of Ordovician magmatism in the Pyrenees (Albera and Canigó Massifs) determined on the basis of Zircon minor and trace elements composition. *J. Geol.* 119 (5), 521-534.

Castro, A., García-Casco, A., Fernández, C., Corretgé, L.G., Moreno-Ventas, I., Gerya, T. & Löw, I. 2009. Ordovician ferrosilicic magmas: experimental evidence for ultrahigh temperaturas affecting a metagreywacke source. *Gondwana R*es. 16, 622-632

Castro, A., Corretgé, G., de la Rosa, J., Enrique, P., Martínez, F. J. Pascual, E. *et al.* 2002. Palaeozoic magmatism. In: The Geology of Spain (Gibbons, W. & Moreno, T., eds.). The Geological Society, London, pp. 117-153.

Cavet, P. 1957. Le Paléozoïque de la zone axiale des Pyrénées orientales françaises entre le Roussillon et l'Andorre. *Bull. Serv. Carte géol. France* 55, 303-518.

Cavet, P. 1969. L'Ordovicien supérieur et la série paléozoïque au Nord du granite de Querigut (Pyrénées de l'Aude). *Bull. Soc. géol. France* 7 (2), 847.

Charles, N., Faure, M. & Chen, Y. 2008. The emplacement of the Montagne Noire axial zone (French Massif Central): New insights from petro-textural, geochronological and AMS studies. 22ème Réunion des Sciences de la Terre, Nancy, 155.

Charles, N., Faure, M. & Chen, Y. 2009. The Montagne Noire migmatitic dome emplacement (French Massif Central): New insights from petrofabric and AMS studies. *J. Struct. Geol*. 31, 1423-1440.

Cherchi, A. & Montadert, L. 1982. The Oligo-Miocene rift of Sardinia and the early history of the western Mediterranean basin. *Nature* 298, 736-739.

Cherchi, A. & Trémolières, P. 1984. Nouvelles données sur l'évolution structurale au Mésozoïque et au Cénozoïque de la Sardaigne et leurs implications géodynamiques dans le cadre méditerranéen. *C. R. Acad. Sci., Paris* 298, 889-894.

Clariana, P. & García-Sansegundo, J. 2009. Variscan structure in the eastern part of the Pallaresa massif, Axial Zone of the Pyrenees (NW Andorra). Tectonic implications. *Bull. Soc. géol. France* 180, 501-511.

Clariana, P., García-Sansegundo, J. & Gavaldà, J. 2009. The structure in the Bagneres de Luchon and Andorra cross sections (Axial Zone of the central Pyrenees). *Trabajos de Geología, Universidad de Oviedo* 29, 175-181.

Clariana, P., Valverde-Vaquero, P., Rubio-Ordóñez, A., Beranoaguirre, A. & García-Sansegundo, J. 2018. Pre-Variscan tectonic events and Late Ordovician magmatism in the Central Pyrenees: U-Pb age and Hf zircon isotopic signature. *J. Iber. Geol*. 44 (4), 589-601.

Clin, M. 1959. Etude géologique de la haute chaîne des Pyrénées Centrales entre le cirque de Troumouse et le cirque du Lys. PhD, Univ. Nancy.

Cocchio, A.M. 1981. Microflores des séries du Paléozoïque inférieur du massif de Mouthoumet. Etude systématique et comparaison avec les séries des Pyrénées orientales et de la Montagne Noire. PhD, Univ.Toulouse.

Cocchio, A.M. 1982. Donnés nouvelles sur les acritarches du Trémadoc et de l'Arénig dans le Massif de Mouthoumet (Corbières, France). *Rev. Micropaléont.* 25, 26-39.

Cocco, F. & Funedda, A. 2011. New data on the pre-Middle Ordovician deformation in SE Sardinia: a preliminary note. *Rend. online Soc. Geol. It.* 15, 34-36.

Cocco, F. & Funedda, A. 2012. The Variscan basement of the Riu Ollastu area (Sarrabus, SE Sardinia, Italy). *Géol. France* 1, 89-90

Cocco, F. & Funneda, A. 2017. The Sardic Phase: field evidence of Ordovician tectonics in SE Sardinia. Italy. *Geol. Mag*. 156, 25-38.

Cocco, F. & Funedda, A. 2019. The Sardic phase: field evidence of Ordovician tectonics in SE Sardinia, Italy. *Geol. Mag.* 156, 25-38.

Cocco, F., Oggiano, G., Funedda, A., Loi, A. & Casini, L. 2018. Stratigraphic, magmatic and structural features of Ordovician tectonics in Sardinia (Italy): a review. *J. Iber. Geol*. 44, 619-639.

Cocherie, A. 2003. Datation avec le SHRIMP II du métagranite oeillé du Somail-Montagne Noire. *C. R. Tech.* ANA-ISO/NT. BRGM, Orléans.

Cocherie, A., Baudin, T., Guerrot, C., Autran, A., Fanning, M.C. & Laumonier, B. 2005. U-Pb zircon (ID-TIMS and SHRIMP) evidence for the early Ordovician intrusion of metagranites in the late Proterozoic Canaveilles Group of the Pyrenees and the Montagne Noire (France). *Bull. Soc. géol. France* 176, 269-282.

Cocozza, T. 1967a. I rapporti cambro-ordoviciani nella zona di Acquaresi (Iglesiente, Sardegna sud-occidentale). *Res. Ass. Min. Sarda* 72 (7), 3-37.

Cocozza, T. 1967b. Il Permo-Carbonifero del Bacino di San Giorgio (Iglesiente, Sardegna sud-occidentale). *Res. Ass. Min. Sarda* 72, 3-37.

Cocozza, T. 1979. The Cambrian of Sardinia. *Mem. Soc. Geol. It.* 20, 163-187.

Cocozza, T. & Gandin, A. 1990. Carbonate deposition during early rifting: the Cambrian of Sardinia and the Triassic-Jurassic of Tuscany, Italy. *Spec. Publs. int. Ass. Sediment.* 9, 9-37.

Cocozza, T. & Leone, F. 1977. Sintesi della successione stratigrafica paleozoica della Sardegna sud-occidentale. In: Escursione in Sardegna 1977: risultati e commenti. *GLP* 1977 (suppl. 2), 75-23. Parma.

Cocozza, T. & Minzoni, N. 1977. Osservazioni sul vulcanismo paleozoico sardo. In: Escursione in Sardegna: risultati e commenti (Vai, G.B. Ed.). *Boll. Gruppo di Lavoro sul Paleozoico, Suppl*. 2, 25-29.

Cocozza, T. & Valera, R. 1966. Nuove osservazioni sulla discordanza Cambro-Ordoviciana nella zona di Nebida (Sardegna sud-occidentale). *Res. Ass. Min. Sarda* 71 (7), 58-71.

Cocozza, T., Jacobacci, A., Nardi, R & Salvadori, I. 1974. Schema stratigrafico-strutturale del Massiccio Sardo-Corso e minerogenesi della Sardegna. *Mem. Soc. Geol. It.* 13, 85-186.

Cocozza, T., Conti, L., Cozzupoli, D., Lombardi, G., Scharbert, S. & Traversa, G. 1977. Rb/Sr age and geopetrologic evolution of crystalline rocks in southern Sulcis (Sardinia). *N. Jb. Geol. Paläont., Mh.* 1977 (2), 95-102.

Conti, P. & Patta, E.D. 1998. Large scale W-directed tectonics in southeastern Sardinia. *Geodin. Acta* 11, 217-231.

Conti, P., Di Sabatino, B., Negretti, G. & Tucci, P. 1978. Aspetti petrologici comparativi fra gli “Scisti di Cabitza” (Cambrico medio) e le sequenze dell’Ordoviciano inferiore (Sardegna meridionale). *Per. Miner.* 47 (1-3), 73-81.

Conti, P., Funedda, A. & Cerbai, N. 1998. Mylonite development in the Hercynian basement of Sardinia (Italy). *J. Struct. Geol.* 20 (2-3), 121-133.

Conti, P., Carmignani, L., Oggiano, G., Funedda, A. & Eltrudis, A. 1999. From thickening to extension in the Variscan belt – kinematic evidence from Sardinia (Italy). *Terra Nova* 11 (2-3), 93-99.

Conti, P., Carmignani, L. & Funedda, A. 2001. Change of nappe transport direction during the Variscan collisional evolution of central-southern Sardinia (Italy). *Tectonophysics* 332 (1-2), 255-273.

Cornet, C. 1980. Genèse structurale des Corbières. *Bull. Soc. géol. France* (sér. 7) 22, 179-184.

Correira Romão, J.M., Coke, C., Dias, R. & Ribeiro, A. 2005. Transient inversion during the opening of the Wilson cycle “Sardic phase” in the Iberian Variscides – Stratigraphic and tectonic record. *Geodin. Acta* 18 (2), 115-129.

Cortesogno, L., Gaggero, L., Oggiano, G. & Paquette, J.L. 2004. Different tectono-thermal evolutionary paths in eclogitic rocks from the axial zone of the Variscan Chain in Sardinia (Italy) compared with the Ligurian Alps. *Ofioliti* 29, 125-144.

Costamagna, L.G., Elter, F.M., Gaggero, L. & Mantovani, F. 2016. Contact metamorphism in Middle Ordovician arc rocks (SW Sardinia, Italy): New paleogeographic constraints. *Lithos* 264, 577-593.

Cruciani. G., Franceschelli. M., Elter. F.M., Puxeddu. M. & Utzeri. D. 2008. Petrogenesis of Al-silicate-bearing trondhjemitic migmatites from NE Sardinia, Italy. *Lithos* 102, 554-574.

Cruciani. G., Franceschelli. M., Musumeci. G., Spano. M. E. & Tiepolo. M. 2013. U-Pb zircon dating and nature of metavolcanics and metarkoses from the Monte Grighini Unit: new insights on late Ordovician magmatism in the Variscan belt in Sardinia, Italy. *Int. J. Earth Sci.* 102 (8), 2077-2096.

Cruciani, G., Franceschelli, M., Puxeddu, M. & Tiepolo, M. 2018. Metavolcanics from Capo Malfatano, SW Sardinia, Italy: New insight on the age and nature of Ordovician volcanism in the Variscan foreland zone. *Geol. J.* 53 (4), 1573-1585.

Cruciani, G., Fancello, D., Franceschelli, M. & Musumeci, G. 2019. Geochemistry of the Monte Filau orthogneiss (SW Sardinia, Italy): insight into the geodynamic setting of Ordovician felsic magmatism in the N/NE Gondwana margin. *It. J. Geosci.* 138, 136-152.

Dack. A.V. 2009. Internal Structure and geochronology of the Gerrei Unit in the Flumendosa area, Variscan External Nappe Zone, Sardinia, Italy. PhD, Boise State Univ.

Dalloni, M. 1930. Etude géologique des Pyrénées Catalanes. *Ann. Fac. Sci. Marseille* 26 (3), 1-373.

Dean, W.T., Monod, O., Rickards, R.B., Demir, O. & Bultynck, P. 2000. Lower Palaeozoic stratigraphy and palaeontology, Karadere-Zirze area, Pontus Mountains, northern Turkey. *Geol. Mag.* 137 (5), 555-582.

Debrenne, F., & Gandin, A. 1985. La Formation de Gonnesa (Cambrien, SW Sardaigne): biostratigraphie, paléogéographie, paléoécologie des Archéocyathes. *Bull. Soc. géol. France* 8, 531-540.

Debrenne, F., Gandin, A. & Pillola, G.L. 1989. Biostratigraphy and depositional setting of the Punta Manna type section (Nebida Formation, Lower Cambrian, SW Sardinia). *Riv. It. Paleont. Strat.* 94 (4), 483-514.

Dégardin, J.M. (coord.) *et al*. 1996. Ordovicien supérieur-Silurien. In: Synthèse géologique et géophysique des Pyrénées, vol. 1 (Barnolas, A., Chiron, J.C. & Guérangué, B, eds.). BRGM-ITGE, Orléans & Madrid, pp. 211-233.

Del Bono, G.L. 1965. Relazione generale su una nuova interpretazione della serie Cambrico-Ordoviciana dell'Iglesiente. *Res. Ass. Min. Sarda* 70 (8), 5-63.

Del Greco, K., Johnston, S. T. & Shaw, J. 2016. Tectonic setting of the North Gondwana margin during the Early Ordovician: a comparison of the Ollo de Sapo and Famatina magmatic events. *Tectonophysics* 681, 73-84.

Del Rio, M. 1973. Palinologia di un livello “Permo-Carbonifero” del bacino di San Giorgio (Iglesiente, Sardegna sud-occidentale). *Boll. Soc. Geol. It.* 92, 485-494.

Delaperrière, E. & Lancelot, J. 1989. Datation U-Pb sur zircons de l'orthogneiss du Capo Spartivento (Sardaigne, Italie), nouveau témoin d'un magmatisme alcalin ordovicien dans le sud de l'Europe. *C. R. Acad. Sci., Paris* 309, 835-842.

Delaperrière, E. & Respaut, J.P. 1995. Un âge ordovicien de l'orthogneiss de la Preste par la méthode d'évaporation directe du plomb sur monozircon remet en question l'existence d'un socle précambrien dans le Massif du Canigou (Pyrenées Orientales, France). *C. R. Acad. Sci., Paris* 320, 1179-1185.

Delaperrière, E. & Soliva, J. 1992. Détermination d'un âge Ordovicien supérieur-Silurien du gneiss de Casemi (Massif du Canigou, Pyrénées Orientales) par la méthode d'évaporation du plomb sur monozircon. *C. R. Acad. Sci., Paris* 314, 345-350.

Deloule, E., Alexandrov, P., Cheilletz, A., Laumonier, B. & Barbey, P. 2002. In-situ U-Pb zircon ages for Early Ordovician magmatism in the eastern Pyrenees, France: the Canigou orthogneisses. *Int. J. Earth Sci*. 91, 398-405.

Demange, M. 1999. Evolution tectonique de la Montagne noire: un modèle en transpression. *C. R. Acad. Sci., Paris* 329, 823-829.

Demange, M., Guérangé-Lozes, J. & Guérangé, B. 1996. Notice explicative de la feuille de Lacaune (987) au 1:50 000. BRGM, Orléans.

Den Brok, S.W.J. 1989. Evidence for pre-Variscan deformation in the Lys Caillaouas area, Central Pyrenees, France. *Geol. Mijnbouw* 68, 377-380.

Denèle, Y., Barbey, P., Deloule, E., Pelleter, E., Olivier, P. & Gleizes, G. 2009. Middle Ordovician U-Pb age of the Aston and Hospitalet orthogneissic laccoliths: their role in the Variscan evolution of the Pyrenees. *Bull. Soc. géol. France* 180, 209-221.

DePaolo, D.J. 1981. Neodymiun isotopes in the Colorado Front Range and crust-mantle evolution in the Proterozoic. *Nature* 291,193-196.

DePaolo, D.J. 1988. Neodymium isotope geochemistry. An introduction. *Minerals and Rocks Series* 20, 1-187. Springer-Verlag, Berlin.

DePaolo, D.J. & Wasserburg, G.J. 1976. Nd isotopic variations and petrogenetic models. *Geophys. Res. Lett.* 3 (5), 249-252.

Dias da Silva, Í. 2014. Geología de las Zonas Centro Ibérica y Galicia-Tras-os-Montes en la parte oriental del Complejo de Morais, Portugal/España. *Serie Nova Terra* 45, 1-424.

Dias da Silva, I., Valverde-Vaquero, P., González-Clavijo, E., Díez-Montes, A. & Martínez-Catalán, J.R. 2012. Structural and stratigraphical significance of U-Pb ages from the Saldanha and Mora volcanic complexes (NE Portugal, Iberian Variscides). *Géol. France* 1, 105-106.

Dias da Silva, Í., Valverde-Vaquero, P., González Clavijo, E., Díez-Montes, A. & Martínez Catalán, J.R., 2014. Structural and stratigraphical significance of U-Pb ages from the Mora and Saldanha volcanic complexes (NE Portugal, Iberian Variscides). In: The Variscan Orogeny: Extent, Timescale and the Formation of the European Crust. (Schulmann, K., Martínez Catalán, J.R., Lardeaux, J.M., Kanoušek, V. & Oggiano, G., eds.). *Geol. Soc., London, Spec. Publ.* 405, 115-135.

Dias da Silva, I., Díez Fernández, R., Díez Montes, A., González Clavijo, E. & Foster, D.A. 2016. Magmatic evolution in the N-Gondwana margin related to the opening of the Rheic Ocean - evidence from the Upper Parautochthon of the Galicia-Trás-os-Montes Zone and from the Central Iberian Zone (NW Iberian Massif). *Int. J. Earth Sci.* 105, 1127-1151.

Díaz-Alvarado, J., Fernández, C., Chichorro, M., Castro, A. & Pereira, M.F. 2016. Tracing the Cambro-Ordovician ferrosilicic to calc-alkaline magmatic association in Iberia by *in situ* U-Pb SHRIMP zircon geochronology (Gredos massif, Spanish Central System batholith). *Tectonophysics* 681, 95-110.

Díez Balda, M.A., Vegas, R. & González Lodeiro, F. 1990. Part IV. Central Iberian Zone. Structures. In: Pre-Mesozoic Geology of Iberia (Dallmeyer, R.D. & Martínez García, E., eds.),. Springer-Verlag, Berlin, pp. 172-188.

Díez Fernández, R., Castiñeiras, P. & Gómez Barreiro, J. 2012. Age constraints on Lower Paleozoic convection system: Magmatic events in the NW Iberian Gondwana margin. Gondwana Res. 21, 1066-1079.

Díez-Montes, A. 2007. La Geología del Dominio "Ollo de Sapo" en las Comarcas de Sanabria y Terra do Bolo. PhD, Univ. Salamanca. *Laboratorio Xelóxico de Laxe, Serie Nova Terra* no. 34, A Coruña.

Díez Montes, A., Martínez Catalán, J.R. & Bellido Mulas, F. 2010. Role of the Ollo de Sapo massive felsic volcanism of NW Iberia in the Early Ordovician dynamics of northern Gondwana. *Gondwana Res.* 17, 363-376.

Di Pisa, A., Gattiglio, M & Oggiano, G. 1992. Pre-Hercynian magmatic activity in the Nappe Zone (internal and external) of Sardinia: evidence of two within-plate basaltic cycles. In: Contribution to the Geology of Italy with Special Regard to the Paleozoic basement. A Volume Dedicated to Tommaso Cocozza (Carmignani, L. & Sassi, F.P., eds.). *IGCP Project no. 276, Newslett.* 5, 33-44.

Di Simplicio, P., Ferrara, G., Ghezzo, C., Guasparri, G., Pellizzer, R., Ricci, C.A., Rita, F. & Sabatini, G. 1974. Il metamorfismo e il magmatismo paleozoico della Sardegna. *Rend. Soc. It. Min. Petr.* 30, 979-1068.

Donzeau, M. & Laumonier, B. 2008. Sur l'importance des événements sardes (médio-ordoviciens) dans les Pyrénées. 23ème Réun. Ann. Sci. Terre, Nancy. Abstract volume, p. 163.

Dunnet, D. 1969. Deformation in the Palaeozoic rocks of the Iglesiente, SW Sardinia. PhD, London Univ.

Duran, M., Gil Ibarguchi, J.I., Julivert, M. & Ubach, S. 1984. Early Palaeozoic and volcanism in the Catalonian Coastal ranges (North Western Mediterranean). PICG n5. *Newsletter* (Sassi F.P. & Julivert M. eds) 6, 33-43.

Durand-Delga, M. & Gèze, B. 1956. Les venues éruptives ordoviciennes de la Camp, près de Félines-Termenès (massif de Mouthoumet, Aude). *C. R. somm. Soc. géol. France*, 268-272.

Echtler, H. & Malavieille, J. 1990. Extensional tectonics, basement uplift and Stephano-Permian collapse basin in a late Variscan metamorphic core complex (Montagne Noire, southern Massif Central). *Tectonophysics* 177, 125-138.

Edel, J.B., Montigny, R. & Thuizat, R. 1981. Late Paleozoic rotations of Corsica and Sardinia: new evidence from paleomagnetic and K-Ar studies. *Tectonophysics* 79, 201-233.

El Korh, A., Schmidt , S.Th., Ballèvre, M., Ulianov, A. & Bruguier, O. 2012. Discovery of an albite gneiss from the Ile de Groix (Armorican Massif, France): geochemistry and LA-ICP-MS U-Pb geochronology of its Ordovician protolith. *Int. J. Earth Sci. 101*, 1169-1190.

Elter, F.M., Musumeci, G. & Pertusati, P.C. 1990. Late Hercynian shear zones in Sardinia. *Tectonophysics* 176, 387-404.

Eltrudis, A., Franceschelli, M., Gattiglio, M. & Porcu, R. 1995. Discontinuous metamorphic zonation in the Palaeozoic units of the Hercynian chain of SW Sardinia, Italy: evidence from structural and illite crystallinity data. *Schwez. Mineral. Petrogr. Mitt.* 75, 201-211.

Engel, W., Feist, R. & Franke, W. 1980-81. Le Carbonifère anté-stéphanien de la Montagne Noire: rapport entre mise en place des nappes et sédimentation. *Bull. BRGM* (sér. 2) 1 (4), 341-389.

Farias, P., Ordoñez-Casado, B., Marcos, A., Rubio-Ordóñez, A. & Fanning, C.M. 2014. U-Pb zircon SHRIMP evidence for Cambrian volcanism in the Schistose Domain within the Galicia-Trás-os-Montes Zone (Variscan Orogen, NW Iberian Peninsula). *Geol. Acta* 12 (3), 209-218.

Faura i Sans, M. 1913. Sintesis estratigrafica de los terranes primarios de Cataluña. *Mem. R. Soc. Esp. Hist. Nat.* 9 (1), 1-202.

Faure, M., Ledru, P., Lardeaux, J.M. & Matte, P., 2004. Paleozoic orogenies in the French Massif Central. A cross section from Béziers to Lyon. 32nd Int. Geol. Congress Florence (Italy), Field-trip guide book, 40 p.

Feist, R. & Etchler, H. 1994. The Massif Central: external zones. In: Pre-Mesozoic Geology of France and Related Areas (Keppie, J., ed.), pp. 291-297. Springer, Berlin.

Feist, R. & Galtier, J. 1985. Découverte de flores d'âge namurien probable dans le flysch à olistolithes de Cabrières (Hérault). Implications sur la durée de la sédimentation synorogénique dans la Montagne Noire (France Méridionale). *C. R. Acad. Sci., Paris* 300, 207-212.

Ferrara, G., Ricci, C.A. & Rita, F. 1978. Isotopic ages and tectono-metamorphic history of the metamorphic basement of north-eastern Sardinia. *Contr. Min. Petr.* 68, 99-106.

Ferretti, A. 1992. Biostratigrafia a conodonti del margine settentrionale del Gondwana (Ordoviciano sup., Ashgill). PhD, Univ. Modena.

Ferretti, A. & Serpagli, E. 1991. First record of Ordovician conodonts from Southwestern Sardinia. *Riv. It. Paleont. Strat.* 91, 27-34.

Fondi, R. 1979. Orme di microsauri nel Carbonifero superiore della Sardegna. *Mem. Soc. Geol. It.* 20, 347-356.

Fontboté, J.M. 1949. Nuevos datos geológicos sobre la cuenca alta del Ter. *An. Inst. Est. Gerund.* 4, 1-57.

Fraas, E. 1904. Contributo allo studio delle anageniti. *Res. Ass. Min. sarda* 9 (6), 6-7.

Franceschelli, M., Puxeddu, M. & Cruciani, G. 2005. Variscan metamorphism in Sardinia, Italy: review and discussion. In: The Southern Variscan Belt (Carosi, R., Dias, R., Iacopini, D. & Rosenbaum, G., eds.). *J. Virtual Explorer* 19 (2).

Franceschelli, M., Battaglia, S., Cruciani, G., Pasci, S. & Puxeddu, M. 2017. Very low-temperature metamorphism in Ordovician metasedimentary rocks above and below the Sardic unconformity, SW Sardinia, Italy. *Int. J. Earth Sci.* 106 (2), 531-548.

Franz, L. & Romer, R.L. 2007. Caledonian high-pressure metamorphism in the Strona-Ceneri-Zone (Southern Alps of southern Switzerland and northern Italy). *Swiss J. Geosci*. 100, 457-467.

Friedl, G., Finger, F., Paquette, J.L., von Quadt, A., McNaughton, N.J. & Fletcher, I.R. 2004. Pre-Variscan geological events in the Austrian part of the Bohemian Massif deduced from U-Pb zircon ages. *Int. J. Earth Sci.* 93, 802-823

Funedda, A. 2000. Note preliminari su un intervallo sedimentario all'interno del ciclo vulcanico calcalino dell'Ordoviciano medio della Sardegna SE: la formazione di Su Muzzioni. *Boll. Soc. Sarda Sci. Nat.* 32, 29-39.

Funedda, A. 2009. Foreland- and hinterland-verging structures in fold-and-thrust belt: an example from the Variscan foreland of Sardinia. *Int. J. Earth Sci*. 98 (7), 1625-1642.

Funedda, A. &, Oggiano, G. 2009. Outline of the Variscan basement of Sardinia. In: The Silurian of Sardinia. Volume in Honour of Enrico Serpagli (Corradini, C., Ferretti, A., Štorch, P., eds.). *Rend. Soc. Paleontol. It.* 3, 23-35.

Funedda, A., Naitza, S., Conti, P., Dini, A., Buttau, C., Tocco, S. & Carmignani, L. 2011. The geological and metallogenic map of the Baccu Locci mine area (Sardinia, Italy). *Journal of Maps* 7 (1), 103-114.

Funedda, A., Meloni, M. A. & Loi, A. 2015. Geology of the Variscan basement of the Laconi-Asuni area (central Sardinia, Italy): the core of a regional antiform refolding a tectonic nappe stack. *Journal of Maps* 11 (1), 146-156.

Gaggero, L., Oggiano, G., Funedda, A. & Buzzi, L. 2012. Rifting and arc-related early Paleozoic volcanism along the North Gondwana margin: geochemical and geological evidence from Sardinia (Italy). *J. Geol.* 120 (3), 273-292.

Galassi, R. & Gandin, A. 1992. New structural data and their bearing on the Cambrian stratigraphy of the Iglesiente region (SW Sardinia, Italy). *C. R. Acad. Sci., Paris* 314, 93-100.

Gámez, J.A., de Gibert, J.M. & Casas, J.M. 2012. First ichnological data from the pre-Upper Ordovician rocks of the Pyrenees. *Geo-Temas* 13.

Garbarino, C., Naitza, S., Rizzo, R., Tocco, S., Barca, S., Forci, A. & Serri, R. 2005. New evidence of pre-Hercynian volcanics from Southern Sulcis (Southwestern Sardinia). *Boll. Soc. Geol. It.* 124, 69-85.

García-Arias, M., Díez-Montes, A., Villaseca, C. & Blanco-Quintero, I.F. 2018. The Cambro-Ordovician Ollo de Sapo magmatism in the Iberian Massif and its Variscan evolution: A review. *Earth-Sci. Rev*. 176, 345-372.

García-Sansegundo, J. & Alonso, J.L. 1989. Stratigraphy and structure of the southeastern Garona Dome. *Geodin. Acta* 3, 127-134.

García-Sansegundo, J., Gavaldà, J. & Alonso, J.L. 2004. Preuves de la discordance de l'Ordovicien supérieur dans la zone axiale des Pyrénées: exemple de dôme de la Garonne (Espagne, France). *C. R. Géosci.* 336, 1035-1040.

García-Sansegundo, J., Poblet, J., Alonso, J.L. & Clariana, P. 2011. Hinterland- foreland zonation of the Variscan orogen in the Central Pyrenees: comparison with the northern part of the Iberian Variscan Massif. In: Kinematic Evolution and Structural Styles of Fold-and-Thrust Belts (Poblet, J. & Lisle, R.J., eds). *Geol. Soc., London, Spec. Publ*. 349, 169-184.

Gattiglio, M. & Oggiano, G. 1990. L'unità tettonica di Bruncu Nieddu e i suoi rapporti con le unità della Sardegna centrale. *Boll. Soc. Geol. It.* 109, 547-555.

Gèze, B. 1949. Etude géologique de la Montagne Noire et des Cévennes méridionales. *Mém. Soc. géol. France* (nouv. sér.) 62, 1-215.

Gèze, B. 1952. Sur les rapports géologiques entre Languedoc et Sardaigne. *Boll. Soc. Geol. It.* 81, 44-147.

Ghienne, J.F., Monod, O., Kozlu, H. & Dean, W.T. 2010. Cambrian-Ordovician depositional sequences in the Middle East : A perspective from Turkey. Earth-Sci. Rev. 101 (3-4), 101-146.

Giacomini, F., Bomparola, R. M. & Ghezzo, C. 2005. Petrology and geochronology of metabasites with eclogite facies relics from NE Sardinia: constraints for the Palaeozoic evolution of Southern Europe. *Lithos* 82, 221-248.

Giacomini, F., Bomparola, R.M., Ghezzo, C. & Gulbransen, H. 2006. The geodynamic evolution of the Southern European Variscides: constraints from the U/Pb geochronology and geochemistry of the lower Palaeozoic magmatic-sedimentary sequences of Sardinia (Italy). *Contr. Min. Petr.* 152, 19-42.

Gil-Peña, I., Sanz-López, J., Barnolas, A. & Clariana, P. 2000. Secuencia sedimentaria del Ordovícico Superior en el margen occidental del Domo del Orri (Pirineos Centrales). *Geotemas* 1 (2), 187-190.

Gil-Peña, I., Barnolas, A., Sanz-López, J., García-Sansegundo, J. & Palau, J. 2001. Discontinuidad sedimentaria del Ordovícico terminal en los Pirineos centrales. *Geogaceta* 29, 57-60.

Gil-Peña, I., Barnolas, A., Villas, E. & Sanz-López, J. 2004. El Ordovícico Superior de la Zona Axial. In: Geología de España (Vera, J.A., ed.). SGE-IGME, Madrid, p. 247-249.

Giovannoni, M.A. & Zanfrà, S. 1978. Studio di brachiopodi ordoviciani della Sardegna meridionale. *Boll. Soc. Geol. It.* 99, 85-232.

Gnoli, M. & Pillola, G.L. 2002. The oldest nautiloid cephalopod of Sardinia: *Cameroceras* cf. *vertebrale* (Eichvald, 1960) from the Arenig (Early Ordovician) of Tacconis (South East Sardinia) and remarks on the associated biota. *N. Jb. Paläont., Mh.* 1, 19-26.

Gonord, H., Ragot, J.P. & Saugy, L. 1964. Observations lithostratigraphiques nouvelles sur la série de base (Ordovicien inférieur) des nappes de Cabrières, région de Gabian-Glauzy (Montagne Noire, Hérault). *Bull. Soc. géol. France* 7, 419-427.

Gortani, M. 1923. Osservazioni sul Paleozoico della Sardegna. *Boll. Soc. Geol. It.* 41 (4), 362-371.

Gortani, M. 1927. La serie paleozoica nelle Alpi Carniche e nella Sardegna. XIV Congr. Geol. Inter.

Grawlich, J.M. 1953. Osservazioni sulla scistosità nei terreni paleozoici dell'Iglesiente (Sardegna): significato dell'anagenite. *Boll. Soc. Geol. It.* 72, 3-6.

Guérangé-Lozes, J. & Alabouvette, B. 1999. Notice explicative, Carte géol. France (1/50 000), feuille Saint-Sernin-sur-Rance (960). BRGM, Orléans, 84 p.

Guérangé-Lozes, J., Guérangé, B., Mouline, M.P. & Delsahut, B. 1996. Notice explicative, Carte géol. France (1/50 000), feuille Réalmont (959). BRGM, Orléans, 78 p.

Guillot, S., Di Paola, S., Ménot, R.P., Ledru, P., Spalla, M.I., Gosso, G., Schwartz, S. 2008. Two Variscan suture zones in the External Crystalline Massifs of Western Alps and the importance of the dextral ECMs shear zone for Palaeozoic reconstruction. *Intern. J. Earth Sci.*, (submitted).

Guitard, G. 1970. Le métamorphisme hercynien mésozonal et les gneiss œillés du massif du Canigou (Pyrénées orientales). *Mém. BRGM* 63,1-353.

Gutiérrez-Alonso, G., Fernández-Suárez, J., Gutiérrez-Marco, J.C., Corfu, F., Murphy, J.B. & Suárez Martínez, S. 2007. U-Pb depositional age for the upper Barrios Formation (Armorican Quartzite facies) in the Cantabrian zone of Iberia: implications for stratigraphic correlation and paleogeography. In: The Evolution of the Rheic Ocean: from Avalonian-Cadomian Active Margin to Alleghenian-Variscan Collision (Linnemann, R.D., Nance, P. & Kraft, G.Z., eds.). *Geol. Soc. Am., London*, 287-296.

Gutiérrez-Alonso, G., Gutiérrez-Marco, J.C., Fernández-Suárez, J., Bernárdez, E. & Corfu, F. 2016. Was there a super-eruption on the Gondwanan coast 477 Ma ago? *Tectonophysics* 681, 85-94.

Gutiérrez-Marco, J.C., Robardet, M., Rábano, I., Sarmiento, G.N., San JoséLancha, M.A., Herranz Araújo, P. & Pieren Pidal, A.P. 2002. Ordovician. In: The Geology of Spain (Gibbons, W. & Moreno, T., eds). Geol. Soc., London, pp. 31-49.

Gutiérrez-Marco, J.C., Piçarra, J.M., Meireles, C.A., Cózar, P., García-Bellido, D.C., Pereira, Z. *et al*. 2019. Early Ordovician-Devonian Passive margin stage in the Gondwanan units of the Iberian massif. In: The Geology of Iberia: A Geodynamic Approach (Quesada, C. & Oliveira, J.T., eds.). *Regional Geology Reviews* 2, 75-98. Springer, Heidelberg.

Hajná, J., Žák, J. & Dörr, W. 2017. Time scales and mechanisms of growth of active margins of Gondwana: A model based on detrital zircon ages from the Neoproterozoic to Cambrian Blovice accretionary complex, Bohemian Massif. *Gondwana Res.* 42, 63-83.

Hajná, J., Žák, J., Dörr, W., Kachlík, V. & Sláma, J. 2018. New constraints from detrital zircon ages on prolonged, multiphase transition from the Cadomian accretionary orogen to a passive margin of Gondwana. *Precambr. Res. 317*, 159-178.

Hammann, W. 1992. The Ordovician trilobites from the Iberian Chains in the province of Aragón, NE Spain. I. The trilobites of the Cystoid Limestone (Ashgill Series). *Beringeria* 6, 1-219.

Hammann, W. & Leone, F. 2007. Trilobites of the post-Sardic (Upper Ordovician) sequence of southern Sardinia. Part 2. *Beringeria* 38, 1-138.

Hammann, W., Laske, R. & Pillola, G.L. 1990. *Tariccoia arrusensis* n.g. n.sp., an unusual trilobite-like arthropod. Rediscovery of the “phyllocarids beds” of Taricco (1922) in the Ordovician “Puddinga” sequence of Sardinia. *Boll. Soc. Paleont. It.* 29, 163-178.

Hartevelt, J.J.A. 1970. Geology of the upper Segre and Valira valleys, central Pyrenees, Andorra/Spain. *Leidse Geol. Med.* 45, 167-236.

Havre, H. 1932. Esquisse geologique de l'Iglesiente - part I - II. *Ass. Min. sarda* 2, 7.
Helbing, H. & Tiepolo, M. 2005. Age determination of Ordovician magmatism in NE Sardinia and its bearing on Variscan basement evolution. *J. Geol. Soc. London* 162, 689-700.
Henrotin, L. 1902. Allegato E. *Res. Ass. Min. Sarda* 7 (6), 13-14.
Henrotin, L. 1904. Nota sul conglomerato di Nebida. *Res. Ass. Min. sarda* 5, 8-9.
Henrotin, L. 1912. Discussione sulla stratigrafia paleozoica. *Ass. Min. sarda*, 4.
Henrotin, L. 1913. Ancora sulla stratigrafia dei terreni paleozoici dell'Iglesiente. *Ass. Min. sarda*, 5.
Huppert, H.E. & Sparks, R.S.J. 1988. The generation of granitic magmas by intrusion of basalt into continental crust. *J. Petrol.* 29, 599-624.
Ibrahim, M.E., El-Kalioby, B.A., Aly, G.M., El-Tohamy, A.M. & Watanabe, K. 2015. Altered granitic rocks, Nusab El Balgum Area, Southwestern Desert, Egypt. Mineralogical and geochemical aspects of REEs. *Ore Geol. Rev*. 70, 252-261.
Irber, W. 1999. The lanthanide tetrad effect and its correlation with K/Rb, Eu/Eu*, Sr/Eu, Y/Ho, and Zr/Hf of evolving peraluminous granite suites. *Geochim. Cosmochim. Acta* 63, 489-508.
Jégouzo, P., Peucat, J.J. & Audren, C., 1986. Caractérisation et signification géodynamique des orthogneiss calco-alcalins d'âge ordovicien de Bretagne méridionale. *Bull. Soc. géol. France* 2, 839-848.
Julivert, M. & Durán, H. 1983. Stratigraphic chart of Paleozoic sequence in Catalonian Coastal ranges (Northeastern Mediterranean). In: Geotraverse A2, IGCP Project no. 5 (Sassi & Szederkényi, eds.) *I.G.C.P. no 5, Newsl.* 5, 54-57.
Julivert, M & Martínez, F.J. 1980. The Paleozoic of the Catalonian Coastal Ranges (Northwestern Mediterranean). *I.G.C.P. no. 5, Newsl.* 2, 124-128.
Julivert, M & Martínez, F.J. 1983. Estructura de conjunto y visión global de la Cordillera Herciniana. In: Comba, J.A. (ed.) Libro Jubilar J.M. Ríos. Geología de España, Tomo I. IGME, 612-631.
Junker, B. & Schneider, H.H. 1983. The infracambrian Bithia Formation – Its facies development in Southwest Sardinia. *N. Jb. Geol. Paläont., Mh.* 24, 369-384.
Kozlu, H., Göncüoğlu, C.M., Sarmiento, G. & Ali Gül, M. 2002. Mid-Ordovician (Late Darriwilian) conodonts from the Southern-Central Taurides, Turkey: Geological implications. *Turkish J. Earth Sci.* 11, 113-126.
Kriegsman, L.M., Aerden, D.G.A.M., Bakker, R.J., den Brok, S.W.J. & Schutjens, P.M.T.M. 1989. Variscan tectonometamorphic evolution of the eastern Lys-Caillaouas massif, Central Pyrenees – evidence for late orogenic extension prior to peak metamorphism. *Geol. Mijnbouw* 68, 323-333.
Kröner, A. & Willner, A.P. 1998. Time of formation and peak of Variscan HP-HT metamorphism of quartz-feldspar rocks in the central Erzgebirge, Saxony, Germany. *Contrib. Mineral. Petrol*. 132, 1-20
La Marmora, A. 1857. Voyage en Sardaigne: troisième partie. Description géologique et paléontologique. Torino, Bocca Impr. Royale, 1857, vol. 2 (20), 707-781.
Lancelot, J. Allegret, A. & Iglesias Ponce de León, M. 1985. Outline of Upper Precambrian and Lower Paleozoic evolution of the Iberian Peninsula according to U-Pb dating of zircons. *Earth Planet. Sci. Lett*. 74, 325-337.
Laske, R. & Bechstädt, T. 1987. Alluviale Fächer und flachmarine Sedimentabfolgen im Hangenden der Sardischen Diskordanz (Ordovizium SW-Sardiniens). *Heid. Geow, Abh*. 8, 141-143.
Laske, R. & Bechstädt, T. 1989. Grobklastische sedimentation im Hangenden der sardischen diskordanz (?Mittleres/Oberes Ordovizium, SW-Sardinien). *Geol. Paläont. Mitt. Innsbruck* 16, 69-72.
Laske, R., Bechstädt, T. & Boni, M. 1994. The post-Sardic Ordovician series. In: Sedimentological, Stratigraphical and Ore Deposits Field Guide of the Autochtonous Cambro-Ordovician of Southwestern Sardinia (Bechstädt, T. & Boni, M., eds.). *Mem. Descr. Carta Geol. It.* 48, 115-146.
Laumonier, B. 1987. Révision de la lithostratigraphie du Paléozoique inférieur des Aspres, à l'Est du Massif du Canigou: conséquences stratigraphiques et structurales. *C. R. Acad. Sci., Paris* (sér. 2) 305, 611-614.
Laumonier, B. 1988. Les groupes de Canaveilles et de Jujols ('Paléozoïque inférieur') des Pyrénées orientales – arguments en faveur de l'âge essentiellement Cambrien de ces séries. *Hercynica* 4, 25-38.
Laumonier, B. & Guitard, G. 1986. Le Paléozoïque inférieur de la moitié orientale de la Zone Axiale des Pyrénées. Essai de synthèse. *C. R. Acad. Sci., Paris* 302, 473-478.

Laumonier, B., Abad, A., Alonso, J., Baudelot, S., Bresière, G., Besson, M., Bouquet, C., Bourrouilh, R., Brula, P., Carreras *et al*. 1996. Cambro-Ordovicien. Synthèse géologique et géophysique des Pyrénées (Barnolas, A. & Chiron, J.C., eds.), vol. 1, 157-209. BRGM & IGME, Orléans & Madrid.

Laumonier, B., Autran, A., Barbey, P., Cheilletz, A., Baudin, T., Cocherie, A. & Guerrot, C. 2004. Conséquences de l'absence de socle cadomien sur l'âge et la signification des séries pré-varisques (ante-Ordovicien supérieur) du sud de la France (Pyrenees, Montagne Noire). *Bull. Soc. géol. France* 175 (6), 643-655.

Laumonier, B., Calvet, M., Wiazemsky, M., Barbey, P., Marignac, C., Lambert, J. & Lenoble, J.L. 2015. Notice explicative de la Carte géologique de la France (1/50.000), feuille Céret (1096). BRGM, Orléans.

Leat, P.T., Jackson, S.E., Thorpe, R.S. & Stillman, C.J. 1986. Geochemistry of bimodal basalt-subalkaline/peralkaline rhyolite provinces within the Southern British Caledonides. J. Geol. Soc. 143, 259-273.

Le Corre, C., Auvray, B., Ballèvre, M. & Robardet, M. 1991. Le Massif Armoricain. *Sci. Géol., Bull.* 44, 31-103.

Lefort, J. P., & Ribeiro, A. 1980. La faille Porto-Badajoz-Cordoue a-t-elle contrôlé l'évolution de l'océan paléozoïque sud-armoric- ain? *Bull. Soc. géol. Fr., 22*(3), 455-462.

Lentz, D. 1996. U, Mo and REE mineralization in late-tectonic granite pegmatites, south-west Grenville Province, Canada. *Ore Geol. Rev*. 11, 197-227.

Leone, F., Hammann, W., Laske, R., Serpagli, E. & Villas, E. 1991. Lithostratigraphic units and biostratigraphy of the post-sardic Ordovician sequence in south-west Sardinia. *Boll. Soc. Paleont. Ital.* 30 (2), 201-235.

Leone, F., Menghi, L., Serpagli, E. & Štorch, P. 1993. Late Ordovician graptolites from Sardinia: a preliminary record. *Boll. Soc. Paleont. It.* 32 (3), 411-414.

Leone, F., Ferretti, A., Hammann, W., Loi, A., Pillola, G.L. & Serpagli, E. 2002. A general view on the post-Sardic Ordovician sequence from SW Sardinia. *Rend. Soc. Paleont. Ital.* 1, 51-68.

Lescuyer, J.L. & Cocherie, A., 1992. Datation sur monozircons des métadacites de Sériès: arguments pour un âge protérozoïque terminal des **"**schistes X**"** de la Montagne Noire (Massif central français). *C. R. Acad. Sci., Paris* (sér. 2) 314, 1071-1077.

Levera, C.F. 1904. Contributo allo studio delle anageniti. *Res. Ass. Min. sarda*, 9 (6), 6-7.

Liesa, M., Carreras, J., Castiñeiras, P., Casas, J.M., Navidad, M. & Vilà, M. 2011. U-Pb zircon age of Ordovician magmatism in the Albera Massif (Eastern Pyrenees). *Geol. Acta* 9, 1-9.

Linnemann, U., Gehmlich, M., Tichomirowa, M., Buschmann, B., Nasdala, L., Jonas, P. et al. 2000. From Cadomian subduction to early Palaeozoic rifting: the evolution of Saxo-Thuringia at the margin of Gondwana in the light of single zircon geochronology and basin development (Central European Variscides, Germany). In: Orogenic Processes: Quantification and Modelling in the Variscan Belt (Franke, W., Haak, V., Oncken, O. & Tanner, D., eds.). *Geol. Soc., London, Spec. Publ*. 179, 131-153.

Llopis Lladó, N. 1965. Sur le Paléozoïque inférieur de l'Andorre. *Bull. Soc. géol. France* 7, 652-659.

Loi, A. & Dabard, M.P. 1997. Zircon typology and geochemistry in the palaeogeographic reconstruction of the late Ordovician of Sardinia (Italy). *Sediment. Geol.* 112, 263-279.

Loi, A., Barca, S., Chauvel, J.J., Dabard, M.P. & Leone, F. 1992. Analyse de la sédimentation post-phase sarde les dépôts initiaux à placers du SE de la Sardaigne. *C. R. Soc. géol. France* (sér. 2) 315, 1357-1364.

López-Sánchez, M.A., Iriondo, A., Marcos, A. & Martínez, F.J. 2015. A U-Pb zircon age (479 ± 5 Ma) from the uppermost layers of the Ollo de Sapo Formation near Viveiro (NW Spain): implications for the duration of rifting-related Cambro-Ordovician volcanism in Iberia. *Geol. Mag*. 152, 341-350.

Ludwig, K.R. & Turi, B. 1989. Paleozoic age of the Capo Spartivento Orthogneiss, Sardinia, Italy. *Chem. Geol*. 79, 147-153.

Lüneburg, C.M. & Lebit, H.D.W. 1998. The development of a single cleavage in an area of repeated folding. *J. Struct. Geol.* 20 (11), 1531-1548.

Margalef, A. & Casas, J.M. 2016. Corte geológico compensado del sur de Andorra: aportaciones a la estructura varisca del Pirineo central. *Geo-Temas* 16, 61-63.

Margalef, A., Castiñeiras, P., Casas, J.M., Navidad, M. & Liesa, M. 2014. Detrital zircons from the pre-Silurian rocks of the Pyrenees: Geochronological constraints and provenance. *RST* Pau 2014, p. 185.

Margalef, A., Castiñeiras, P., Casas, J.M., Navidad, M., Liesa, M., Linnemann, U., Hofmann, M. & Gärtner, A. 2016. Detrital zircons from the Ordovician rocks of the Pyrenees: Geochronological constraints and provenance. *Tectonophysics* 681, 124-134.

Marini, F. 1988. "Phase" sarde et distension ordovicienne du domaine sud-varisque, effets de point chaud? Une hypothèse fondée sur les données nouvelles du volcanisme albigeois. *C. R. Acad. Sci., Paris* (sér. 2) 306, 443-450.

Martí, J., Casas, J.M., Guillén, N., Muñoz, J.A. & Aguirre, G. 2014. Structural and geodynamic constraints of Upper Ordovician volcanism of the Catalan Pyrenees. In: *Gondwana 15 Abstracts Book*, 104, IGME.

Martí, J., Muñoz, J.A. & Vaquer, R. 1986. Les roches volcaniques de l'Ordovicien supérieur de la région de Ribes de Freser-Rocabruna (Pyrénées Catalanes): caractères et signification. *C. R. Acad. Sci., Paris* 302 (20), 1237-1242.

Martí, J., Solari, L., Casas, J.M. & Chichorro, M. 2019. New geochronological data on the Upper Ordovician volcanism in the Eastern Pyrenees (NE Iberia): Stratigraphic and geodynamic implications. *Geol. Mag*. 165 (10), 1783-1792.

Martínez, F.J., Iriondo, A., Dietsch, A., Aleinikoff, J.N., Peucat, J.J., Cirès, J., Reche, J. & Capdevila, R. 2011. U-Pb SHRIMP-RG zircon ages and Nd signature of lower Paleozoic rifting-related magmatism in the Variscan basement of the Eastern Pyrenees. *Lithos* 127 (1-2), 10-23.

Martínez, F.J., Dietsch, C., Aleinikoff, J., Cirés, J., Arboleya, M.L., Reche, J. & Gómez-Gras, D. 2016. Provenance, age, and tectonic evolution of Variscan flysch, southeastern France and northeastern Spain, based on zircon geochronology. *Geol. Soc. Am. Bull.* 128 (5-6), 842-859.

Martínez, F.J., Reche, J. & Arboleya, M.L. 2001. P-T modelling of the andalusite-kyanite séquence and related assemblages in the graphitic pelites. Prograde and retrograde paths in a late kyanite belt in the Variscan Iberia. Jour. Metam. Geol., 19, 661-677.

Martínez Catalán, J.R., Hacar Rodríguez, M.P., Villar Alonso, P., Peréz-Estaún, A. & González Lodeiro, F. 1992. Lower Paleozoic extensional tectonics in the limit between the West Asturian-Leonese and Central Iberian Zones of the Variscan Fold-Belt in NW Spain. *Geol. Runds*. 81 (2), 546-560.

Martínez Catalán, J.R., Arenas, R., Díaz García, F., González Cuadra, P., Gómez-Barreiro, J., Abati, J. *et al.* 2007, Space and time in the tectonic evolution of the northwestern Iberian Massif: Implications for the Variscan belt. In: 4-D Framework of Continental Crust (Hatcher, R.D., Jr., Carlson, M.P., McBride, J.H. & Martínez Catalán, J.R., eds). Geol. Soc. Am. Mem. 200, 403-423.

Martínez Catalán, J.R., Hacar Rodríguez, M.P., Villar Alonso, P., Peréz-Estaún, A. & González Lodeiro, F. 1992. Lower Paleozoic extensional tectonics in the limit between the West Asturian-Leonese and Central Iberian Zones of the Variscan Fold-Belt in NW Spain. *Geol. Runds.* 81, 546-560.

Martini, I.P., Tongiorgi, M., Oggiano, G. & Cocozza, T. 1991. Ordovician alluvial fan to marine shelf transition in SW Sardinia, Western Mediterranean Sea: tectonically ('Sardic phase') influenced clastic sedimentation. *Sediment. Geol.* 72, 97-115.

Masuda, A. & Akagi, T. 1989. Lanthanide tetrad effect observed in leucogranites from China. *Geochem. J*. 23, 245-253.

Mattauer, M. 2004. Orthogneisses in the deepest levels of the Variscan belt are not a Precambrian basement but Ordovician granites: tectonic consequences. *C. R. Geosci*. 336, 487-489.

McDougall, N., Brenchley, P.J., Rebelo, J.A. & Romano, M. 1987. Fans and fan deltas - precursors to the Armorican Quartzite (Ordovician) in western Iberia. *Geol. Mag*. 124, 347-359.

McLennan, S.M. 1994. Rare earth element geochemistry and the "tetrad" effect. *Geochim.Cosmochim. Acta* 58, 2025-2033.

Meloni, M.A., Oggiano, G., Funedda, A., Pistis, M., & Linnemann, U. 2017. Tectonics, ore bodies, and gamma-ray logging of the Variscan basement, southern Gennargentu massif (central Sardinia, Italy). *J. Maps* 13 (2), 196-206.

Memmi, I., Barca, S., Carmignani, L., Cocozza, T., Franceschelli, M., Gattiglio, M., Ghezzo, C., Minzoni, N., Naud, G., Pertusati, P.C. & Ricci, C.A. 1982. Il magmatismo pre-ercinico della

Sardegna. In: Guida alla Geologia del Paleozoico sardo. *Guide Geologiche Regionali, Soc. Geol. It.*, p. 157-164.

Memmi, I., Barca, S., Carmignani, L., Cocozza, T., Franceschelli, M., Gattiglio, M., Ghezzo, C., Minzoni, N., Naud, G., Pertusati, P.C. & Ricci, C.A. 1983. Further geochemical data on the Pre-Hercynian igneous activities of Sardinia and on their geodynamic significance. *I.G.C.P. no 5, Newsl.* 5, 87-91.

Meneghini, G. 1888. Paleontologia dell'Iglesiente, Fauna Cambriana: Trilobiti. *Mem. descr. Carta geol. It.* 3(2), 1-53.

Menéndez, S., Perejón, A. & Moreno-Eiris, E. 2015. Late Ovetian (Cambrian Series 2, Stage 3) archaeocyathan. Biostratigraphy of Spain. *Ann. Paléontol.* 101, 161-166.

Merlo, G. 1903. Lettera sui calcescisti e sugli scisti. *Ass. Min. sarda* 8, 6-7

Merlo, G. 1904. Circa alcune sezioni geologiche che possono servire allo studio della tettonica dell'Iglesiente. *Ass. Min. sarda* 5, 9-10.

Merlo, G. 1905. Ancora circa l'origine delle anageniti. *Ass. Min. sarda* 3, 11-13.

Mey, P.H.W. 1967. The geology of the Upper Ribagorzana and Baliera valleys, Central Pyrenees, Spain. *Leid. Geol. Meded*., 41, 153-220.

Mezger, J.E. 2009. Transpressional tectonic setting during the main Variscan deformation evidence from structural levels in the Bossòst and Aston-Hospitalet mantled gneiss domes, central Axial Zone, Pyrenees. *Bull. Soc. géol. France* 180, 199-207.

Mezger, J. & Gerdes, A. 2016. Early Variscan (Visean) granites in the core of central Pyrenean gneiss domes: implications from laser ablation U-Pb and Th-Pb studies. *Gondwana Res*. 29, 181-198.

Mezger, J.E., Rölke, C., & Schnapperelle, S. 2010. Structural and petrological map of the Mérens fault and shear zone, Aston-Hospitalet domes, Central Pyrenees. Conference 13 Symp. "Tektonik, Dtruktur und Kristallingeologie (TSK 13), Frankfurt.

Mingram, B., Kröner, A., Hegner, E. & Krentz, O. 2004. Zircon ages, geochemistry, and Nd isotopic systematics of pre-Variscan orthogneisses from the Erzgebirge, Saxony (Germany), and geodynamic interpretation. *Int. J. Earth Sci.* 93, 706-727.

Minzoni, N. 1975. La serie delle formazioni paleozoiche a Sud del Gennargentu. *Boll. Soc. Geol. It.* 94, 347-365.

Minzoni, N. 1980. Precambriano nel Sulcis meridionale (Sardegna). *Mineral. Petr. Acta* 24, 51-56.

Minzoni, N. 1985. Magmatismo paleozoico ed evoluzione geodinamica in Sardegna. In: Evoluzione Stratigrafica, Tettonica, Metamorfica e Magmatica del Paleozoico Italiano (Cocozza, T. & Ricci, C.A., eds.). *IGCP no 5, Note Brevi e Riassunti, Riunione Scientifica Siena*, p. 87-88.

Minucci, E. 1935. Le condizioni del Paleozoico nel Sulcis orientale (Sardegna). *Boll. Soc. Geol. It.* 54, 75-87.

Monecke, T., Dulski, P. & Kempe, U. 2007. Origin of convex tetrads in rare earth element patterns of hydrothermally altered siliceous igneous rocks from the Zinnwald Sn-W deposit, Germany. *Geochim. Cosmochim. Acta* 71, 335-353.

Monod, O., Kozlu, H., Ghienne, J.F., Dean, W.T., Günay, Y., Le Hérissé, A., Paris, F. & Robardet, M. 2003. Late Ordovician glaciation in southern Turkey. *Terra Nova* 15, 249-257.

Montero, P., Bea, F., González-Lodeiro, F., Talavera, C. & Whitehouse, M.J. 2007. Zircon ages of the metavolcanic rocks and metagranites of the Ollo de Sapo Domain in central Spain: implications for the Neoproterozoic to Early Palaeozoic evolution of Iberia. *Geol. Mag*. 144, 963-976.

Montero, P., Talavera, C., Bea, F., Lodeiro, F.G. & Whitehouse, M.J. 2009. Zircon geochronology of the Ollo de Sapo Formation and the age of the Cambro-Ordovician rifting in Iberia. *J. Geol*. 117, 174-191.

Moreira, N., Romão, J., Dias, R., Ribeiro, A. and Pedro, J. 2019. The Finisterra-Léon–Mid German crystalline rise domain; proposal of a new terrane in the Variscan Chain. In: Quesada, C. and Oliveira, J.T. (eds) The Geology of Iberia: A Geodynamic Approach. Volume 2: The Variscan Cycle. Regional Geology Reviews. Springer, Cham, Switzerland, 207-228.

Morre-Biot, N. & Robert, J.F. 1976. Sur la découverte d'un complexe ignimbritique stéphanien dans la région de Ribes de Freser (Province de Gérone, Espagne). *C. R. Acad. Sci., Paris* 282, 1933-1935.

Muñoz, J.A. 1985. Estructura alpina i herciniana a la vora sud de la Zona Axial del Pirineu oriental. PhD, Univ. Barcelona. *Monografies núm. 1. Publicació del Servei Geològic de Catalunya*. Generalitat de Catalunya, 227 pp.

Muñoz, J.A. 1992a. Estructura alpina i herciniana a la vora sud de la zona axial del Pirineu Oriental. *Serv. Geol. Cat.*, 227 pp.

Muñoz, J.A. 1992b. Evolution of a continental collision belt: ECORS-Pyrenees crustal balanced cross-section. In: Thrust Tectonics (McClay, K.R., ed.), p. 235-246. Chapman & Hall, London.

Muñoz, A. & Casas, J.M. 1996. Tectonique pré-Hercynienne. In: Synthèse géologique et géophysique des Pyrénées (Barnolas, E. & Chiron, J.C., eds.). Vol. 1 – Cycle Hercynien, pp. 585-589. BRGM, Orléans.

Muñoz, A., Sabat, F. & Santanach, P. 1983. Stratigraphic correlation form in the Eastern Pyrenees (Geotraverse A2). *IGCP Project no. 5*, pp. 102-107.

Murphy, J.B., Gutiérrez-Alonso, G., Nance, R.D., Fernández-Suárez, J., Keppie, J.D., Quesada, C. *et al*. 2006. Origin of the Rheic Ocean: rifting along a Neoproterozoic suture? *Geology* 34, 325-328.

Nance, R.D., Gutiérrez-Alonso, G., Keppie, J.D., Linnemann, U., Murphy, J.B., Quesada, C. *et al*., 2010. Evolution of the Rheic Ocean. *Gondwana Res.*17, 194-222.

Naud, G. 1979a. Les shales de Rio Canoni, formation-repère fossilifère dans l'Ordovicien supérieur de Sardaigne orientale. Conséquences stratigraphiques et structurales. *Bull. Soc. géol. France* 21 (2), 155-159.

Naud, G. 1979b. Tentative de synthèse sur l’évolution géodynamique de la Sardaigne anté-permienne. *Mem. Soc. Geol. It.* 20, 85-96.

Naud, G. 1981. Confirmation de l'existence de la discordance angulaire anté-ordovicienne dans le Sarrabus (Sardaigne sud-orientale): conséquences géodynamiques. *C. R. Acad. Sci., Paris* 292, 1153-1156.

Naud, G. & Pittau Demelia, P. 1985. Première découverte d'acritarches du Cambrien moyen à supérieur et du Trémadoc-Arénigien dans la basse vallée du Flumendosa: mise en évidence d'un nouveau témoin de la Phase Sarde en Sardaigne orientale. *I.G.C.P. no. 5, Newsl.* 7, 85-86.

Naud, G. & Tempier, C. 1977. Schème stratigraphique et tectonique des formations paléozoïques de la Sardaigne sud-orientale. *Réun. Ann. Sci. Terre* 19-22, 384.

Navidad, M. & Barnolas, A. 1991. El magmatismo (Ortoneises y volcanismo del Ordovícico superior) del Paleozoico de los Catalánides. *Bol. Geol. Min.* 102 (2), 187-202.

Navidad, M., & Castiñeiras, P. 2011. Early Ordovician magmatism in the northern Central Iberian zone (Iberian Massif): New U-Pb (SHRIMP) ages and isotopic Sr-Nd data. 11th ISOS - Ordovician of the World, *Cuadernos Museo Geominero*, 14, 391-398.

Navidad, M., Castiñeiras, P., Casas, J.M., Liesa, M., Fernández-Suárez, J., Barnolas, A., Carreras, J. & Gil-Peña, I. 2010. Geochemical characterization and isotopic ages of Caradocian magmatism in the northeastern Iberia: insights into the Late Ordovician evolution of the northern Gondwana margin. *Gondwana Res.* 17, 325-333.

Navidad, M., Castiñeiras, P., Casas, J.M., Liesa, M., Belousova, E., Proenza, J. & Aiglsperger, T. 2018. Ordovician magmatism in the Eastern Pyrenees: Implications for the geodynamic evolution of northern Gondwana. *Lithos* 314-315, 479-496.

Neiva, A.M.R., Williams, I.S., Ramos, J.M.F., Gomes, M.E.P., Silva, M.M.V.G. & Antunes, I.M.H.R. 2009. Geochemical and isotopic constraints on the petrogenesis of Early Ordovician granodiorite and Variscan two-mica granites from the Gouveia area, central Portugal. *Lithos* 111, 186-202.

Novarese. V. 1914. Il rilevamento geologico delle tavolette di Iglesias e Nebida. *Boll. R. Comm. Geol. It.* 44 (1913-1914), 29-59.

Novarese, V. 1922. Contributo alla geologia dell'Iglesiente: la serie paleozoica. *Boll. Regio Uff. geol. It.* 49 (10), 1-107.

Novarese, V. 1942. Sul Cambriano della Sardegna. *Boll. R. Uff. geol. It.* 47 (3), 1-28.

Novarese, V. & Taricco, M. 1923. Cenni sommari sul Paleozoico dell’Iglesiente. *Boll. Soc. Geol. It.* 4, 316-325.

Oggiano, G. 1994. Lineamenti stratigrafico-strutturali del basamento del Goceano (Sardegna centro-settentrionale). *Boll.Soc. Geol. It.* 113, 105-115.

Oggiano, G. & Mameli, P. 2006. Diamictite and oolitic ironstones, a sedimentary association at Ordovician-Silurian transition in the north Gondwana margin: new evidence from the inner nappe of Sardinian Variscides (Italy). *Gondwana Res.* 9, 500-511.

Oggiano, G., Martini, J.P. & Tongiorgi, M. 1986. Sedimentology of the Ordovician "puddinga" Formation (SW Sardinia). *IGCP Project no. 5: Correlation of Prevariscan and Variscan events*. Final meeting 25-31/05/1986. Abstracts, p. 61.

Oggiano, G., Cherchi, G.P., Aversano, A. & A. D. P. 2005. Note illustrative F 428 Arzachena, settore terrestre (Memorie Descrittive della Carta Geologica d'Italia). IPSZ, Rome.

Oggiano, G., Gaggero, L., Funedda, A., Buzzi, L. & Tiepolo, M. 2010. Multiple early Paleozoic volcanic events at the northern Gondwana margin: U-Pb age evidence from the Southern Variscan branch (Sardinia, Italy). *Gondwana Res.* 17, 44-58.

Okay, A., Satir, M., & Shang, K. 2008. Ordovician metagranitoid from the Anatolide-Tauride Block, northwest Turkey: geodynamic implications. *Terra Nova* 20 (4), 280-288.

Olivieri, R. 1970. Conodonti e zonatura del Devoniano superiore e riconoscimento di Carbonifero inferiore nei calcari di Corona Mizziu (Gerrei – Sardegna). *Boll. Soc. Paleont. It.* 8, 63-152.

Orsini, J.B. 1980. Le batholite Corso-Sarde: anatomie d'un batholite hercynien. Composition, structure, organisation d'ensemble. Sa place dans la chaîne Varisque française. PhD, Univ. Aix-Marseille.

Ovtracht, A. 1960. Palèogéographie du massif primaire du Mouthoumet (Aude, France). Rep. 21th Sess. Intern. geol. Congr. Norden, part XII, 55-64.

Ovtracht, A. 1967. Notice explicative de la feuille de Quillan à 1/80 000, no. 254. BRGM, Orléans.

Padel. M. 2016. Influence cadomienne dans les séries pré-sardes des Pyrénées Orientales: approche géochimique, stratigraphique et géochronologique. PhD, Univ. Lille I.

Padel, M., Álvaro, J.J., Clausen, S., Guillot, F., Poujol, M., Chichorro, M., Monceret, E., Pereira, M.F. & Vizcaïno, D. 2017. U-Pb laser ablation ICP-MS zircon dating across the Ediacaran-Cambrian transition of the Montagne Noire, southern France. *C. R. Geosci*. 349, 380-390.

Padel, M., Clausen, S., Álvaro, J.J. & Casas, J.M. 2018a. Review of the Ediacaran-Lower Ordovician (pre-Sardic) stratigraphic framework of the Eastern Pyrenees, southwestern Europe. *Geol. Acta* 16 (4), 339-355.

Padel, M., Álvaro, J.J., Clausen, S., Guillot, F., Poujol, M., Chichorro, M., Monceret, E., Pereira, M.F. & Vizcaïno, D. 2018b. U-Pb laser ablation ICP-MS zircon dating across the Ediacaran-Cambrian transition of the Montagne Noire, southern France. *C. R. Geosci.* 349, 380-390.

Palme, H. & O'Neill, H.S.C. 2004. Cosmochemical estimates of mantle composition. In: Treatise on Geochemistry 2 (Holland, H.D., Turekian, K.K., eds.), 1-38. Elsevier-Pergamon, Oxford.

Palmeri, R., Fanning, M., Franceschelli, M., Memmi, I. & Ricci, C.A. 2004. SHRIMP dating of zircons in eclogite from the Variscan basement in north-eastern Sardinia (Italy). *N. Jb. Min.* 6, 275-288.

Palmerini, V., Palmerini Sitzia, R. & Pilo, L. 1979. Le facies pelitiche degli "argilloscisti di Cabitza" (Cambriano medio della Sardegna). *Mem. Soc. Geol. It.* 20, 365-377.

Pan, Y.,1997. Controls on the fractionation of isovalent trace elements in magmatic and aqueous systems: evidence from Y/Ho, Zr/Hf, and lanthanide tetrad effect - a discussion of the article by M. Bau, 1996. *Contrib. Mineral. Petrol.* 128, 405-408.

Pankhurst, R.J., Rapela, C.W., Saavedra, J., Baldo, E., Dahlquist, J., Pascua, I. & Fanning, C.M. 1998. The Famatinian magmatic arc in the central Sierras Pampeanas, and Early to Middle Ordovician continental arc on the Gondwana margin. In: The Proto-Andean Margin of Gondwana (Pankhurst, R.J. & Rapela, C.E., eds.). *Geol. Soc., London, Spec. Publ*. 142, 343-367.

Pasci, S. Pertusati, P.C., Salvadori, I. & Murtas, A. 2008. I rilevamenti CARG del Foglio geologico 555 "Iglesias" e le nuove implicazioni strutturali sulla tettonica della "Fase Sarda". *Rend. online Soc. Geol. It., Abstracts* 3 (2), 614-615.

Pavanetto, P., Funedda, A., Northrup, C.J., Schmitz, M., Crowley, J. & Loi, A. 2012. Structure and U-Pb zircon geochronology in the Variscan foreland of SW Sardinia, Italy. *Geol. J.* 47, 426-445.

Pearce, J.A. 1996. Sources and settings of granitic rocks. *Episodes* 19,120-125.

Pearce, J.A., Harris, N.B.W. & Tindle A.G., 1984. Trace element discrimination diagrams for the tectonic interpretation of granitic rocks. *J. Petrol*. 25, 956-983.

Pereira, M.F., Solá, R., Chichorro, M. & Silva, J.B. 2012. North-Gondwana assembly, break-up and paleogeography: U-Pb isotope evidence from detrital and igneous zircons of Ediacaran and Cambrian rocks of SW Iberia. *Gondwana Rese.* 22, 866-881.

Pereira, M.F. Castro, A., Chichorro, M., Fernández, C., Díaz-Alvarado, J., Martí, J., Rodríguez, C. 2014. Chronological link between deep-seated processes in magma chambers and eruptions: Permo-Carboniferous magmatism in the core of Pangaea (Southern Pyrenees). Gondwana Research 25, 290-308

Perejón, A., Moreno-Eiris, E. & Abad, A. 1994. Montículos de arqueociatos y calcimicrobios del Cámbrico inferior de Terrades, Gerona (Pirineo oriental, España). *Bol. R. Soc. Esp. Hist. Nat. (Sec. Geol.)* 89, 55-95.

Pertusati, P.C. Sarria, E., Cherchi, G.P., Carmignani, L., Barca, S., Benedetti, M., Chighine, G., Cincotti, F., Oggiano, G., Ulzega, A. & Pintus, C. 2002. Note illustrative della Carta Geologica d'Italia alla scala 1:50000, Foglio Jerzu. *Serv. Geol. It.*, 27-80.

Piercey, S.J. 2011. The setting, style, and role of magmatism in the formation of volcanogenic massive sulphide deposits. *Miner. Deposita* 46, 449-471.

Pillola, G.L. (1991), Trilobites du Cambrien inférieur du SW de la Sardaigne, Italie. *Paleontogr. It.* 78, 1-173.

Pillola, G.L. & Gross, U. 1982. Stratigrafia del Membro di Matoppa della Formazione di Nebida (Cambrico inferiore) nell'area di M.te S. Giovanni-M.te Uda. In: Guida alla Geologia del Paleozoico Sardo. Guide Geologiche Regionali (Carmignani, L., Cocozza, T., Ghezzo, C., Pertusati, P.C. & Ricci, C.A., eds.). Soc. Geol. It., p. 79-82.

Pillola, G.L. & Gutiérrez-Marco, J.C. 1988. Graptolites du Trémadoc du sud-ouest de la Sardaigne. *Géobios* 21 (5), 553-565.

Pillola, G.L. & Leone, F. 1997. Arenig (Lower Ordovician) biota from SE Sardinia: biofacies and palaebiogeography. Geoitalia, 1 Forum FIST, 2: 72-73. C.L.E.U.P. Padova.

Pillola. G.L., Leone, F. & Loi, A. 1995. The Lower Cambrian Nebida Group of Sardinia. In: *6th Paleobenthos International Symposium*, Guide-Book. Cagliari, October 25-31, 1995 (Cherchi, A., ed.). *Rend. Sem. Fac. Sc. Univ. Cagliari*, suppl. vol. 65, 27-62.

Pillola, G.L., Leone, F. & Loi, A. 1998. The Cambrian and Early Ordovician of SW Sardinia. *Giorn. Geol.* ser. 3, 60 (spec. iss. ECOS VII Sardinia Guide book), p. 25-38.

Pillola, G.L., Leone, F. & Loi A. 2002. The Cambrian and Early Ordovician of SW Sardinia (Italy). *Rend. Soc. Paleont. Ital.* 1, 37-49.

Pillola G.L., Piras, S. & Serpagli, E. 2008. Upper Tremadoc-Lower Arenig? Anisograptid-Dichograptid fauna from the Cabitza Formation (Lower Ordovician, SW Sardinia, Italy). *Rev. Micropaleont.* 51, 167-181.

Pilotti, C. 1915. Carta Geologica Mineraria dell'Iglesiente. Scala 1: 25000. Tavoletta di Iglesias.

Pistis, M., Loi, A. & Dabard, M.P. 2016. Influence of relative sea-level variations on the genesis of palaeoplacers, the examples of Sarrabus (Sardinia, Italy) and the Armorican Massif (western France). *C. R. Geosci*. 348 (2), 150-157.

Pitra, P., Poujol, M., Den Driessche, J.V., Poilvet, J.C. & Paquette, J.L. 2012. Early Permian extensional shearing of an Ordovician granite: the Saint-Eutrope "C/S-like" orthogneiss (Montagne Noire, French Massif Central). *C.s R. Geosc.* 344, 377-384.

Pittau Demelia, P. 1985. Tremadocian (Early Ordovician) acritarchs of the Arburese unit, Southwest Sardinia (Italy). *Boll. Soc. Paleont. It.* 23 (2) (for 1984), 116-204.

Pittau Demelia, P. & Del Rio, M. 1982. Acritarchi e loro significato stratigrafico nelle successioni paleozoiche della Sardegna. Guida alla Geologia del Paleozoico sardo. Guide Geologiche Regionali Soc. Geol. It., pp. 33-35.

Poblet, J. 1991. Estructura herciniana i alpina del versant sud de la zona axial del Pirineu central. PhD, Barcelona Univ.

Poll, J.J.K. 1966. The geology of the Rosas-Terraseo area, Sulcis, South Sardinia. *Leidse Geol. Meded.* 35, 117-208.

Poll, J.J.K. & Zwart, H.J. 1964. On the tectonics of the Sulcis area, S. Sardinia. *Geol. Mijnbouw* 43 (4), 144-146.

Pompeckj, J.F. 1901. Verteineungen des Paradoxides Stufe von La Cabitza in Sardinia, und Bemerkungen zur Gliederung des Sardischen Cambrium. *Zeitschr. deutsch. geol. Gesell.* 53 (1), 1-23.

Pouclet, A., Álvaro, J.J., Bardintzeff, J.M., Gil Imaz, A., Monceret, E. & Vizcaïno D. 2017. Cambrian-Early Ordovician volcanism across the South Armorican and Occitan Domains of the Variscan Belt in France: Continental break-up and rifting of the northern Gondwana margin. *Geosci. Frontiers* 8, 25-64.

Puddu, C. & Casas, J.M. 2011. New insights into the stratigraphy and structure of the Upper Ordovician rocks of the la Cerdanya area (Pyrenees). *Cuad. Mus. Geomin.* 14, 441-445.

Puddu C., Casas J.M., & Álvaro J.J. 2017a. New knowledge on the Upper Ordovician rocks of El Baell, Ribes de Freser area, eastern Pyrenees. In: Ordovician Geodynamics: The Sardic Phase in the Pyrenees, Mouthoumet and Montaigne Noire massifs (Álvaro J.J., Casas J.M. & Clausen S., eds.).). 4-9 September 2017, Figueres, Catalonia. Abstract volume, pp. 24-27.

Puddu C., Casas J.M., & Álvaro J.J. 2017b. On the Upper Ordovician of the La Cerdanya area, Pyrenees. In: Ordovician Geodynamics: The Sardic Phase in the Pyrenees, Mouthoumet and Montaigne Noire massifs (Álvaro J.J., Casas J.M. & Clausen S., eds.).). 4-9 September 2017, Figueres, Catalonia. Abstract volume, pp. 27-29.

Puddu C., Casas J.M., & Álvaro J.J. 2017v. New knowledge on the Upper Ordovician rocks of El Baell, Ribes de Freser area, eastern Pyrenees. In: Ordovician Geodynamics: The Sardic Phase in the Pyrenees, Mouthoumet and Montaigne Noire massifs (Álvaro J.J., Casas J.M. & Clausen S., eds.).). 4-9 September 2017, Figueres, Catalonia. Abstract volume, pp. 24-27.

Puddu C., Casas J.M., & Álvaro J.J. 2017d. On the Upper Ordovician of the La Cerdanya area, Pyrenees. In: Ordovician Geodynamics: The Sardic Phase in the Pyrenees, Mouthoumet and Montaigne Noire massifs (Álvaro J.J., Casas J.M. & Clausen S., eds.).). 4-9 September 2017, Figueres, Catalonia. Abstract volume, pp. 27-29.

Puddu, C., Álvaro, J.J. & Casas, J.M. 2018. The Sardic unconformity and the Upper Ordovician successions of the Ribes de Freser area, Eastern Pyrenees. *J. Iber. Geol.* 44, 603-617.

Puddu, C., Álvaro, J.J., Carrera, N. & Casas, J.M. 2019. Deciphering the Sardic (Ordovician) and Variscan deformations in the Eastern Pyrenees, SW Europe. *J. Geol. Soc.* 176, 1191-1206.

Quesada, C. 1990. Ossa-Morena Zone. Introduction. In Pre-Mesozoic Geology of Iberia (Dallmeyer, R.D. & Martínez García, E., eds.). Springer, Berlin, pp. 249-251.

Quesada, C. 1991. Geological constraints on the Paleozoic tectonic evolution of tectonostratigraphic terranes in the Iberian Massif. *Tectonophysics* 185, 225-245.

Quesada, C. 2006. The Ossa-Morena Zone of the Iberian Massif: a tectonostratigraphic approach to its evolution. *Zeits. Deuts. Ges. Geowissens* 157 (4), 585-595.

Rabin, M., Trap, P., Carry, N. Fréville, K. Cenki-Tok, B. Lobjoie, C. Gonçalves, P. & Marquer, D. 2015. Strain partitioning along the anatectic front in the Variscan Montagne Noire massif (southern French Massif Central). *Tectonics* 34, 1709-1735.

Rasetti, F. 1972. Cambrian trilobite faunas of Sardinia. *Mem. Acc. Naz. Lincei* 11, 1-100.

Ravier, M. J., Thiébaut, J. & Chenevoy, M. 1975. Sur l'importance des événements calédoniens dans l'histoire de la chaîne pyrénéenne. *C. R. Acad. Sci., Paris* 280, 2521-2523.

Robardet, M., Verniers, J., Feist, R. & Paris, F. 1994. Le Paléozoïque anté–varisque de France, contexte paléogéographique et géodynamique. *Géol. France* 1994 (3), 3-31.

Robert, J.F. 1980. Étude géologique et métallogenique du val de Ribes sur le versant espagnol des Pyrénées catalanes. PhD, Univ. Franche-Compté.

Robert, J. F. & Thiebaut, J. 1976. Découverte d'un volcanisme acide dans le Caradoc de la région de Ribes de Freser (province de Gérone). *C. R. Acad. Sci., Paris* 282, 2049-2050.

Roger, F., Respaut, J.P., Brunel, M., Matte, P. & Paquette, J.L. 2004. Première datation U-Pb des orthogneiss oeillés de la zone axiale de la Montagne Noire (Sud du Massif central): nouveaux témoins du magmatisme ordovicien dans la chaîne Varisque. *C. R. Géosci.* 336, 19-28.

Roger, F., Teyssier, C., Respaut, J.P., Rey, P.F., Jolivet, M., Whitney, D.L., Paquette, J.L. & Brunel, M. 2015. Timing of formation and exhumation of the Montagne Noire double dome, French massif Central. *Tectonophysics* 640-641, 53-69.

Rollison, H.R. 1993. Using Geochemical Data: Evaluation, Presentation, Interpretation. Longman Group, London, 352 p.

Romão, J., Coke, C., Dias, R. & Ribeiro, A. 2005. Transient inversion during the opening stage of the Wilson cycle "sardic phase" in the Iberian variscides – stratigraphic and tectonic record. *Geodin. Acta* 18, 115-129.

Romão, J., Dunning, G., Marcos, A., Dias, R. & Ribeiro, A. 2010. O lacólito granítico de Mação-Penhascoso: idade e as suas implicações (SW da Zona Centro-Ibérica). *e-Terra* 16, 1-4.

Romão, J., Metodiev, D., Dias, R. & Ribeiro, A. 2013. Evolução geodinâmica dos sectores meridionais da Zona Centro-Ibérica. In: Geologia do Portugal 1, 206–257 (Dias, R., Araújo, A., Terrinha, P. & Kullberg, J.C, eds.). Escolar Editora, Lisbon.

Romão, J. & Ribeiro, A. 1993. Thrust tectonics of Sardic age in the Rosmaninhal area (Beira Baixa, Central Portugal). *Comun. Serv. Geol. Portugal* 78 (2), 87-95.

Roqué Bernal, J., Štorch, P. & Gutiérrez-Marco, J. C. 2017. Bioestratigrafía (graptolitos) del límite Ordovícico-Silúrico en los Pirineos orientales (curso alto del río Segre, Lleida). *Geogaceta* 61, 27-30.

Rossi, P., Oggiano, G. & Cocherie, A. 2009. A restored section of the "southern Variscan realm" across the Corsica-Sardinia micro- continent. *C. R. Geosci.* 341 (2-3), 224-238.

Rubio-Ordóñez, A., Valverde-Vaquero, P., Corretgé, L. G., Cuesta-Fernández, A., Gallastegui, G., Fernández-González, M. & Gerdes, A. 2012. An Early Ordovician tonalitic-granodioritic belt along the Schistose-Greywacke Domain of the Central Iberian Zone (Iberian Massif, Variscan Belt). *Geol. Mag*. 149, 927-939.

Rudnick, R.L. & Gao, S. 2003. Composition of the Continental Crust. In: Treatise on Geochemistry (Holland, H.D., Turekian, K.K., eds.), vol. 3, 1-64. Elsevier-Pergamon, Oxford.

Sánchez-García, T., Bellido, F. & Quesada, C. 2003. Geodynamic setting and geochemical signatures of Cambrian–Ordovician rift-related igneous rocks (Ossa-Morena Zone, SW Iberia). *Tectonophysics* 365, 233-255.

Sánchez-García, T., Quesada, C., Bellido, F., Dunning, G. & González de Tánago, J. 2008. Two-step magma flooding of the upper crust during rifting: the Early Paleozoic of the Ossa-Morena Zone (SW Iberia). *Tectonophysics* 461, 72-90.

Sánchez-García, T., Bellido, F., Pereira, M.F., Chichorro, M., Quesada, C., Pin, Ch. & Silva, J.B. 2010. Rift-related volcanism predating the birth of the Rheic Ocean (Ossa-Morena zone, SW Iberia). *Gondwana R*es. 17, 392-407.

Sánchez-García, T., Quesada, C., Bellido, F., Dunning, G.R., Pin, Ch., Moreno-Eiris, E. & Perejón, A. 2016. Age and characteristics of the Loma del Aire unit (SW Iberia): Implications for the regional correlation of the Ossa-Morena Zone. *Tectonophysics* 681, 58-72.

Sánchez-García, T., Chichorro, M., Solá, R., Álvaro, J.J., Díez Montes, A., Bellido, F. *et al*. 2019. The Cambrian–Early Ordovician Rift Stage in the Gondwanan Units of the Iberian Massif. In: The Geology of Iberia: A Geodynamic Approach (Quesada, C., Oliveira, J.T., eds.). *Regional Geol. Rev*. 1, 27–74.

Santanach Prat, P.F. 1972. Sobre una discordancia en el Paleozoico inferior de los Pirineos orientales. *Acta Geol. Hisp.* 7, 129-132.

Sánz-López, J. 2002. Devonian and Carboniferous pre- Stephanian rocks from the Pyrenees. *Cuad. Mus. Geomin.* (IGME) 1, 367-389.

Sánz-López, J., & Sarmiento, G.N. 1995. Asociaciones de conodontos del Ashgill y Llandovery en horizontes carbonatados del Valle del Freser (Girona), Tremp: XI Jornadas de Paleontología, p. 157-160.

Sanz-López, J., Gil-Peña, I. & Valenzuela-Ríos, J.I. 2002. Lower Palaeozoic rocks from the Pyrenees: A synthesis. In: Palaeozoic Conodonts from Northern Spain, 8th International Conodont Symposium held in Europe (García-López, S. & Bastida, F., eds.). *Ser. Cuad. Mus. Geomin.* (IGME) 1, 349-365.

Sarmiento, G.N., Gutiérrez-Marco, J.C. & Robardet, M. 1999. Conodontos ordovícicos del noroeste de España. Aplicación al modelo de sedimentación de la región limítrofe entre las zonas Asturoccidental-Leonesa y Centroibérica durante el Ordovícico Superior. *Rev. Soc. Geol. España* 12, 477-500.

Sartori, F. 1902. Sulla costituzione della formazione costiera di Nebida. *Ass. Min. sarda* 5, 9-11.

Sartori, F., & Testa, L. 1913. La stratigrafia del paleozoico d'Iglesias. *Ass. Min. sarda* 2, 3-4.

Schaltegger, U., Abrecht, J. & Corfu, F. 2003. The Ordovician orogeny in the Alpine basement: constraints from geochronology and geochemistry in the Aar Massif (Central Alps). *Schweiz. Miner. Petrogr. Mitteil.* 83, 183-195.

Schneider. H.H. 1974. Revision des Altpaläozoikums Sardiniens insbesondere des sardischen Konglomerates. *N. Jb. Geol. Paläont., Abh*. 146, 78-103.

Shaw, J., Johnston, S., Gutiérrez-Alonso, G. & Weil, A.B. 2012. Oroclines of the Variscan orogen of Iberia: paleocurrent analysis and paleogeographic implications. *Earth Planet. Sci. Lett*. 329-330, 60-70.

Shaw, J., Gutiérrez-Alonso, G., Johnston, S. & Pastor Galán, D. 2014. Provenance variability along the early Ordovician north Gondwana margin: paleogeographic and tectonic implications of U-Pb detrital zircon ages from the Armorican Quartzite of the Iberian Variscan belt. *Geol. Soc. Am. Bull*. 126 (5-6), 702-719.

Silva, A. & Ribeiro, A. 1985. Thrust tectonics of Sardic Age in the Alto Douro Region (Northeastern Portugal). *Com. Serv. Geol. Portugal* 71, 151-157.

Solá, A.R. 2007. Relações Petrogeoquímicas dos Maciços Graníticos do NE Alentejano. PhD, Univ. Coimbra.

Solá, A.R., Pereira, M.F., Williams, I.S., Ribeiro, M.L., Neiva, A.M.R., Montero, P., Bea, F. & Zinger, T. 2008. New insights from U-Pb zircon dating of Early Ordovician magmatism on the northern Gondwana margin: the Urra formation (SW Iberian Massif, Portugal). *Tectonophysics* 461, 114-129.

Speksnijder, A. 1987. The detection and significance of early deformation in the southern Variscan Pyrenees, Spain; implications for regional Paleozoic structural evolution. *Geol. Rund.* 76 (2), 451-476.

Stampfli, G.M. 1993. Le Briançonnais, terrain exotique dans les Alpes? *Eclog. Geol. Helv*. 86, 1-45.

Stampfli, G. M., Hochard, C., Vérard, C., Wilhem, C. & von Raumer, J.F. 2013. The geodynamics of Pangea formation. *Tectonophysics* 593, 1-19.

Stampfli, G.M., Von Raumer, J.F. & Borel, G.D. 2002. Paleozoic evolution of pre-Variscan terranes: from Gondwana to the Variscan collision. In: Variscan- Appalachian Dynamics: the Building of the Late Paleozoic Basement (Martínez Catalán, J.R., Hatcher, R.D., Arenas, R. & García, F.D., eds.). Geol. Soc. Am., 263–280. Boulder, USA.

Stern, R.J. 2002. Crustal evolution in the East African Orogen: a neodymium isotopic perspective. *J. Afr. Earth Sci*. 34, 109-117.

Stille, H. 1935. Der derzeitige tektoniske Erdzustand. *Sitz. Preuss Akad. Wiss*. Berlin, Phys.-Math. Kl., pp. 179-219.

Stille, H. 1939. Bemerkungen betreffend die ‘Sardische’ Faultung und den Ausdruck ‘Ophiolitisch’. *Zeits. Deuts. Gess. Geowiss* 91, 771-773.

Štorch, P. & Leone, F. 2003. Occurrence of the late Ordovician (Hirnantian) graptolite *Normalograptus ojsuensis* (Koren & Mikhaylova, 1980) in south-western Sardinia, Italy. *Boll. Soc. Paleont. Ital.* 42 (1-2), 31-38.

Štorch, P., Roque Bernal, J. & Gutiérrez-Marco, J.C. 2019. A graptolite-rich Ordovician-Silurian boundary section in the south-central Pyrenees, Spain: stratigraphical and palaeobiogeographical significance. *Geol. Mag*. 156 (6), 1069-1091.

Sun, S.S. & McDonough, W.F. 1989. Chemical and isotopic systematics of oceanic basalts: implications for mantle composition and processes. In: Magmatism in the Ocean Basins (Saunders, A.D. & Norry, M.J., eds.). *Geol. Soc., Spec. Publ*. 42, 13-345.

Syme, E.C. 1998. Ore-Associated and Barren Rhyolites in the central Flin Flon Belt: Case Study of the Flin Flon Mine Sequence. *Manitoba Energy and Mines, Open File Report* OF98-9, 1-32

Takahashi, Y., Yoshida, H., Sato, N., Hama, K., Yusa, Y. & Shimizu, H. 2002. W- and M-type tetrad effects in REE patterns for water-rock systems in the Tono uranium deposit, central Japan. *Chem. Geol*. 184, 311-335.

Talavera, C. 2009. Pre-Variscan magmatism of the Central Iberian Zone: chemical and isotope composition, geochronology and geodynamic significance. PhD, Univ. Granada.

Talavera, C., Bea F, Montero P. & Whitehouse, M. 2008. A revised Ordovician age for the Sisargas orthogneiss, Galicia (Spain). Zircon U-Pb ion-microprobe and LA-ICPMS dating. *Geol. Acta* 8, 313-317.

Talavera, C., Montero, P., Bea, F., González Lodeiro, F. & Whitehouse, M. 2013. U-Pb Zircon geochronology of the Cambro-Ordovician metagranites and metavolcanic rocks of central and NW Iberia. *Int. J. Earth. Sci*. 102, 1-23.

Taricco. M. 1920. Rinvenimento di *Dictyonema* nel Cambriano della Sardegna. *Boll. Soc. Geol. It.* 39, 34-40.

Taricco, M. 1922. Sul Paleozoico del Fluminese (Sardegna). *Boll. Regio Comitato geologico It.* 48 (6), 11-21.

Taricco, M. 1928. Il Cambriano del Sulcis (Sardegna). *Res. Ass. Min. Sarda* 33, 10-29. Iglesias.

Taylor, S.R. & McLennan, S.M. 1985. The Continental Crust: Its Composition and Evolution. Blackwell, London, 312 pp.

Teichmüller, R. 1931. Zur Geologie des Thyrrhenisgebietes, Teil 1: Alte und junge Krustenbewegungen im südlinchen Sardinien. *Abh. Der. wissen. Gess. Göttingen (Math.-Phys. Kl)* 3, 857-950.

Teipel, U., Eichhorn, R., Loth, G., Rohrmüller, J., Höll, R. & Kennedy, A. 2004. U-Pb SHRIMP and Nd isotopic data from the western Bohemian Massif (Bayerischer Wald, Germany): Implications for Upper Vendian and Lower Ordovician magmatism. *Int. J. Earth Sci*. 93, 782-801.

Teixell, A. 1998. Crustal structure and orogenic material budget in the central Pyrenees. *Tectonics* 17, 395-406.

Theodoridis, G. 1989. Zur genese des sardischen konglomerates (Iglesiente, SW Sardinien): ein resedimentationsprodukt mit überregionaler bedeutung. *Geol. Paläont. Mitt.* 16, 122-125.

Thompsom, M.D., Grunow, A.M. & Ramezani, J. 2010. Cambro-Ordovician paleogeography of the Southeastern New England Avalon Zone: Implications for Gondwana breakup. *Geol. Soc. Am. Bull*. 122, 76-88.

Tichomirowa, M., Berger, H.J., Koch, E.A,, Belyatski, B., Götze, J., Kempe, U., Nasdala, L. & Schaltegger, U. 2001. Zircon ages of high-grade gneisses in the Eastern Erzgebirge (Central European Variscides) - constraints on origin of the rocks and Precambrian to Ordovician magmatic events in the Variscan foldbelt. *Lithos* 56, 303-332.

Tichomirowa, M., Sergeev, S., Berger, H.J. & Leonhardt, D. 2012. Inferring protoliths of high-grade metamorphic gneisses of the Erzgebirge using zirconology, geochemistry and comparison with lower-grade rocks from Lusatia (Saxothuringia, Germany). *Contrib. Mineral. Petrol*. 164, 375-396.

Tommasini, S., Poli, G. & Halliday, A.N. 1995. The role of sediment subduction and crustal growth in Hercynian plutonism: isotopic and trace element evidence from the Sardinia-Corsica batholith. *J. Petrol.* 36, 1305-1332.

Tongiorgi, M., Bellagotti, E., Di Milia, A. & Trasciatti, M. 1982. Prima datazione su basi paleontologiche (Acritarchi) della Formazione di Solanas (Tremadociano-Arenigiano) (Meana Sardo, Sardegna Centrale). In: Guida alla Geologia del Paleozoico Sardo. Guide Geologiche Regionali (Carmignani, L., ed.). Soc. Geol. It., pp. 127-128. Cagliari.

Tongiorgi, M., Albani, R. & Di Milia, A. 1984. The Solanas sandstones of Central Sardinia: New paleontological data (Acritarchs) and an attempt of geological interpretation (a "post-sardinian" molasse?). *Bull. Soc. géol. France* 26, 665- 680.

Torsvik, T.H. & Cocks, R.M. 2004. Earth geography from 400 to 250 Ma: a palaeomagnetic, faunal and facies review. *J. Geol. Soc.* 161, 555-572.

Torsvik, T.H. & Cocks, R.M. 2009. The Lower Palaeozoic palaeogeographical evolution of the northeastern and eastern peri-Gondwanan margin from Turkey to New Zealand. *Geol. Soc. London Sp. Publ.* 325(1), 3-21.

Trombetta, A., Cirrincione, R., Corfu, F., Mazzoleni, P. & Pezzino, A. 2004. Mid-Ordovician U-Pb ages of porphyroids in the Peloritan Mountains (NE Sicily): palaeogeographical implications for the evolution of the Alboran microplate. *J. Geol. Soc*. 161, 265-276.

Tucci, P. 1983. Le metamorfiti dinamometamorfiche di Capo Malfatano (Sulcis, Sardegna). *Period. Min.* 52, 149-176.

Vai, G.B. 1982. Fasi di "rifting", nuovi dati stratigrafici e conse- guenze paleogeografiche nel Paleozoico inferiore. In: Guida alla Geologia del Paleozoico Sardo (Carmignani, L., Cocozza, T., Ghezzo, C., Pertusati, P.C. & Ricci, C.A., eds.). Soc. Geol. It. Guide Geologiche Regionali, pp. 193-195. Cagliari.

Vai, G.B. 1991. Palaeozoic strike-slip rift pulses and palaeogeo- graphy in the circum-Mediterranean Tethyan realm. *Palaeogeogr. Palaeoclimat. Palaeoecol.* 87, 223-252.

Vai, G.B. & Cocozza, T. 1974. Il "Postgotlandiano" sardo, Unità sinorogenetica ercinica. *Boll. Soc. Geol. It.* 92. 61-72.

Vai, G.B. & Cocozza, T. 1986. Tentative schematic zonation of the Hercynian chain in Italy. *Bull. Soc. géol. France* (sér. 8) 2 (1), 95-114.

Valera, R. 1964. Nuove osservazioni sui rapporti tra le orogenesi Caledonica ed Ercinica nel settore di M.te Murvonis a NE di Domusnovas (Iglesias). *Rend. Ass. Min. sarda* (anno 68) 6, 8-9.

Valera, R. 1967. Contributo alla conoscenza dell'evoluzione tettonica della Sardegna. *Res. Ass. Min. Sarda* 72, 3-95. Iglesias.

Valverde-Vaquero, P. & Dunning, G.R. 2000. New U-Pb ages for Early Ordovician magmatism in Central Spain. *J. Geol. Soc. London* 157, 15-26.

Valverde-Vaquero, P., Marcos, A., Farias, P. & Gallastegui, G. 2005. U-Pb dating of Ordovician felsic volcanism in the Schistose Domain of the Galicia-Trás-os-Montes Zone near Cabo Ortegal (NW Spain). *Geol. Acta* 3, 27-37.

Valverde-Vaquero, P., Farias, P., Marcos, A. & Gallastegui, G. 2007. U-Pb dating of Siluro-Ordovician volcanism in the Verín synform (Orense, Schistose Domain, Galicia-Trás-os-montes Zone). *Geogaceta* 41, 247-250.

Vardabasso, S. 1940. Qual'è il profilo normale del Cambrico sardo? *Res. Ass. Min. Sarda* 45, 100-110. Iglesias.

Vardabasso, S. 1950. Il problema stratigrafico del Cambrico sardo. *Rend. Acc. Naz. Lincei, Cl. Sci. FF. Mm., Nn*. (ser. 8) 9 (6), 312-319.

Vardabasso, S. 1956. La fase sarda dell'orogenesi caledonica in Sardegna. *Geotektoniske Symposium Hans Stille, Abstract book*, p. 121-127.

Vardabasso, S. 1966. Il Verrucano Sardo. Atti Symposium sul Verrucano. Pisa Settembre 1965. *Società Toscana Scienze Naturali*, p. 293-310. Pisa.

Vigliotti, L. & Langenheim, V.E. 1995. When did Sardinia stop rotating? New paleomagnetic results. *Terra Nova* 7, 424-435.

Vila, J.M. 1965. Relations entre la nappe des Corbières orientales et son substratum dans 1002 la région de Durban-Corbières (Aude). *C. R. Acad. Sci., Paris* 260, 1700–1703.

Vilà, M., Pin, C., Enrique, P. & Liesa, M. 2005. Telescoping of three distinct magmatic suites in an orogenic setting: Generation of Hercynian igneous rocks of the Albera Massif (Eastern Pyrenees). *Lithos* 83, 97-127.

Villaseca, C., Castiñeiras, P. & Orejana, D. 2013. Early Ordovician metabasites from the Spanish Central System: A remnant of intraplate HP rocks in the Central Iberian Zone. *Gondwana Res.* 27, 392-409.

Villaseca, C., Merino Martínez, E., Orejana, D., Andersen, T. & Belousova, E. 2016. Zircon Hf signatures from granitic orthogneisses of the Spanish Central System: Significance and sources of the Cambro-Ordovician magmatism in the Iberian Variscan Belt. *Gondwana Res.* 34, 60-83.

Vissers, R. 1992. Variscan extension in the Pyrenees. *Tectonics* 11, 1369-1384.

Von Gaertner, H. 1937. Montagne Noire und Mouthoumet als Teile des südwest europäischen Variskums. *Abh. D. Ges. D. Wiss. Zu Göttingen, Math.-Phys*. (K1, H17), 1-260.

Von Quadt, A. 1997. U-Pb zircon and Sr-Nd-Pb whole-rock investigations from the continental deep drilling (KTB). *Geol. Rundsch*. 86 (suppl.), S258-S271.

Von Raumer, J.F. & Stampfli, G.M. 2008. The birth of the Rheic Ocean – early Palaeozoic subsidence patterns and tectonic plate scenarios. *Tectonophysics* 461, 9-2.

Von Raumer, J.F., Stampfli, G.M., Borel, G. & Bussy, F. 2002. The organization of pre-Variscan basement areas at the Gondwana margin. *Int. J. Earth Sci*. 91, 35-52.

Von Raumer, J.F., Bussy, F., Schaltegger, U., Schulz, B. & Stampfli, G. 2013. Pre-Mesozoic Alpine basements: their place in the European Paleozoic framework. *Geol. Soc. Am. Bull.* 125, 89-108.

Von Raumer, J.F., Stampfli, G.M., Arenas, R. & Sánchez Martínez, S. 2015. Ediacaran to Cambrian oceanic rocks of the Gondwanan margin and their tectonic interpretation. *Int. J. Earth Sci.* 104, 1107-1121.

Westphal, M., Orsini, J.B. & Vellutini, P. 1986. Le micro-continent corso-sarde: sa position initiale, données paléomagnétiques et raccords géologiques. *Tectonophysics* 30, 141-157.

Whalen, J.B., Currie, K.L. & Chappell, B.W. 1987. A-type granites: Geochemical characteristics, discrimination and petrogenesis. *Contr. Miner. Petrol*. 95, 407-419.

White, C.E., Barr, S.M., Linnemann, U. 2018. U-Pb (zircon) ages and provenance of the White Rock Formation of the Rockville Notch Group, Meguma terrane, Nova Scotia, Canada: evidence for the "Sardian gap" and West African origin. *Can. J. Earth Sci.* 55 (6), 589-603.

Winchester, J.A. & Floyd, P.A. 1977. Geochemical discrimination of different magma series and their differentiation products using immobile elements. *Chem. Geol*. 20, 325-343.

Zeck, H.P., Whitehouse, M.J. & Ugidos, J.M. 2007. 496 ± 3 Ma zircon ion microprobe age for pre-Hercynian granite, Central Iberian Zone, NE Portugal (earlier claimed 618 ± 9 Ma). *Geol. Mag*. 144, 21-31.

Zoppi, G. 1888. Descrizione geologico-mineraria dell'Iglesiente (Sardegna). *Mem. Descr.Carta Geol It* 4 (1), 1-154. Roma.

Zurbriggen, R. 2015. Ordovician orogeny in the Alps – a reappraisal. *Int. J. Earth Sci*. 104, 335-350.

Zurbriggen, R. 2017. The Cenerian orogeny (early Paleozoic) from the perspective of the Alpine region. *Int. J. Earth Sci*. 106, 517-529.

Zurbriggen, R., Franz, L. & Handy, M.R. 1997. Pre-Variscan deformation, metamorphism and magmatism in the Strona-Ceneri Zone (southern Alps of northern Italy and southern Switzerland). *Schw. Miner. Petrogr. Mitteil*. 77, 361-380.

Zwart, H.J. 1979. The geology of the central Pyrenees. *Leidse Geol. Meded.* 50, 1-74.

Zwart, H.J. 1986. The Variscan geology of the Pyrenees. *Tectonophysics* 129, 9-27.

ANNEXES

ABSTRACTS AND PROCEEDINGS

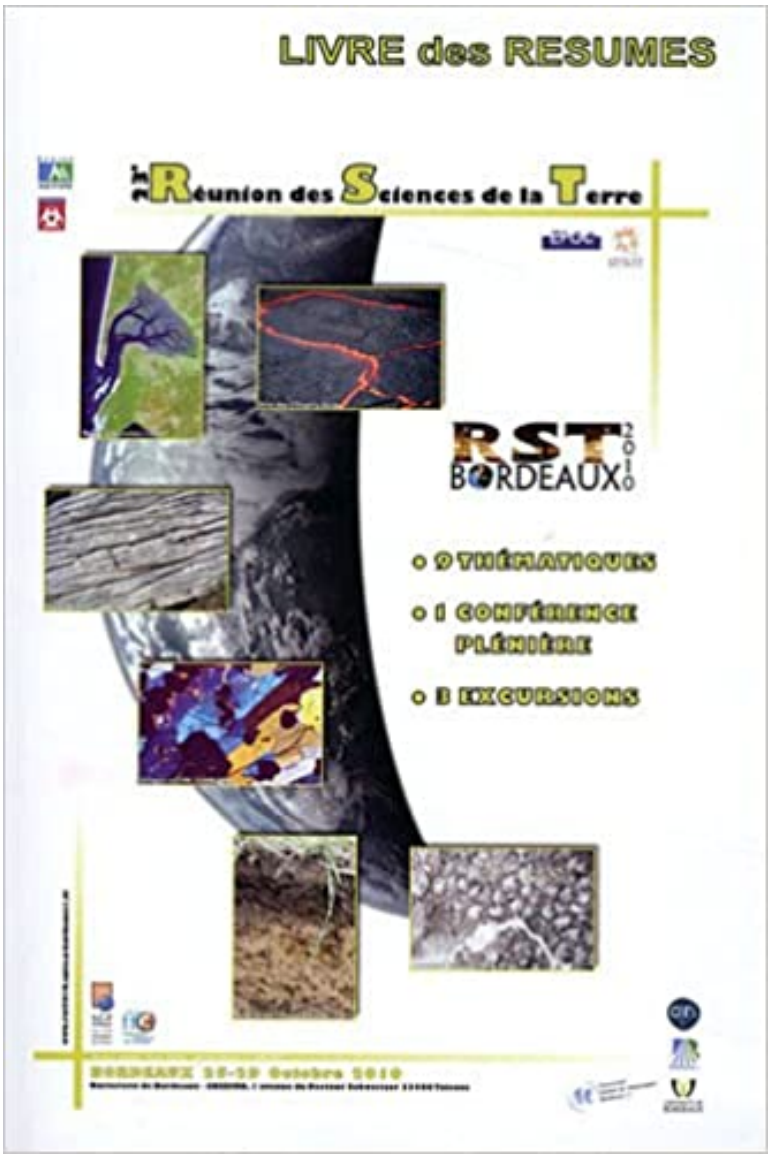
LIVRE des RESUMES
Réunion des Sciences de la Terre
RST 2010
BORDEAUX
• 9 THÉMATIQUES
• 1 CONFÉRENCE PLÉNIÈRE
• 3 EXCURSIONS

Ordovician deformations in the Pyrenees and Sardinia: new insights into the significance of pre-Variscan ("sardic") tectonics

Josep Maria Casas [1] and Claudia Puddu [2]

[1] Departament de Geodinàmica i Geofísica-Institut de recerca GEOMODELS, Universitat de Barcelona, Martí i Franquès s/n, Barcelona, 08028, Spain. e-mail: casas@ub.edu
[2] Department of Earth Sciences, University of Cagliari, Via Trentino 51, 09127 Cagliari, Italy.e-mail:cpuddu@unica.it

Several deformational events developed prior to the Variscan structures can be characterized in the Paleozoic rocks of the Pyrenees and Sardinia. In the Pyrenees a Middle (?) Ordovician folding event and a Late Ordovician fracture episode can be recognized. The Middle (?) Ordovician folding event gives rise to NW-SE to N-S oriented, metric to hectometric sized folds, without cleavage formation or related metamorphism. These folds can account for the deformation and uplift of the pre-Upper Ordovician (Cambro-Ordovician) sequence and for the formation of the Upper Ordovician unconformity. Ordovician folds control the orientation of the Variscan main-folding phase minor structures, fold axes and intersection lineation in the Cambro-Ordovician sediments. The Late Ordovician fracture episode gave rise to normal faults affecting the lower part of the Upper Ordovician series, the basal unconformity and the underlying Cambro-Ordovician metasediments. In Sardinia pre-Variscan tectonic is represented by a Middle Ordovician deformative event which affected the pre-Upper Ordovician sequence. This event ("Sardic Phase") gives rise to E-W oriented structures, as metric to hectometric folds without cleavage and thrusts, both structures sealed by the stratigraphic and angular unconformity located at the base of the Upper Ordovician sequence.
The aforementioned deformation episodes took place after the Early Ordovician magmatic event, which gave rise to a large volume of plutonic rocks in the Pyrenees and Sardinia as in other segments of the European variscides. The Middle Ordovician contractional event ("Sardic Phase") separated two extensional events from Early Ordovician to Silurian times. This event prevents us from assuming the existence of a continuous extensional regime through the Ordovician and Silurian times, and suggests a more complex evolution of this segment of the northern Gondwana margin during the Ordovician.

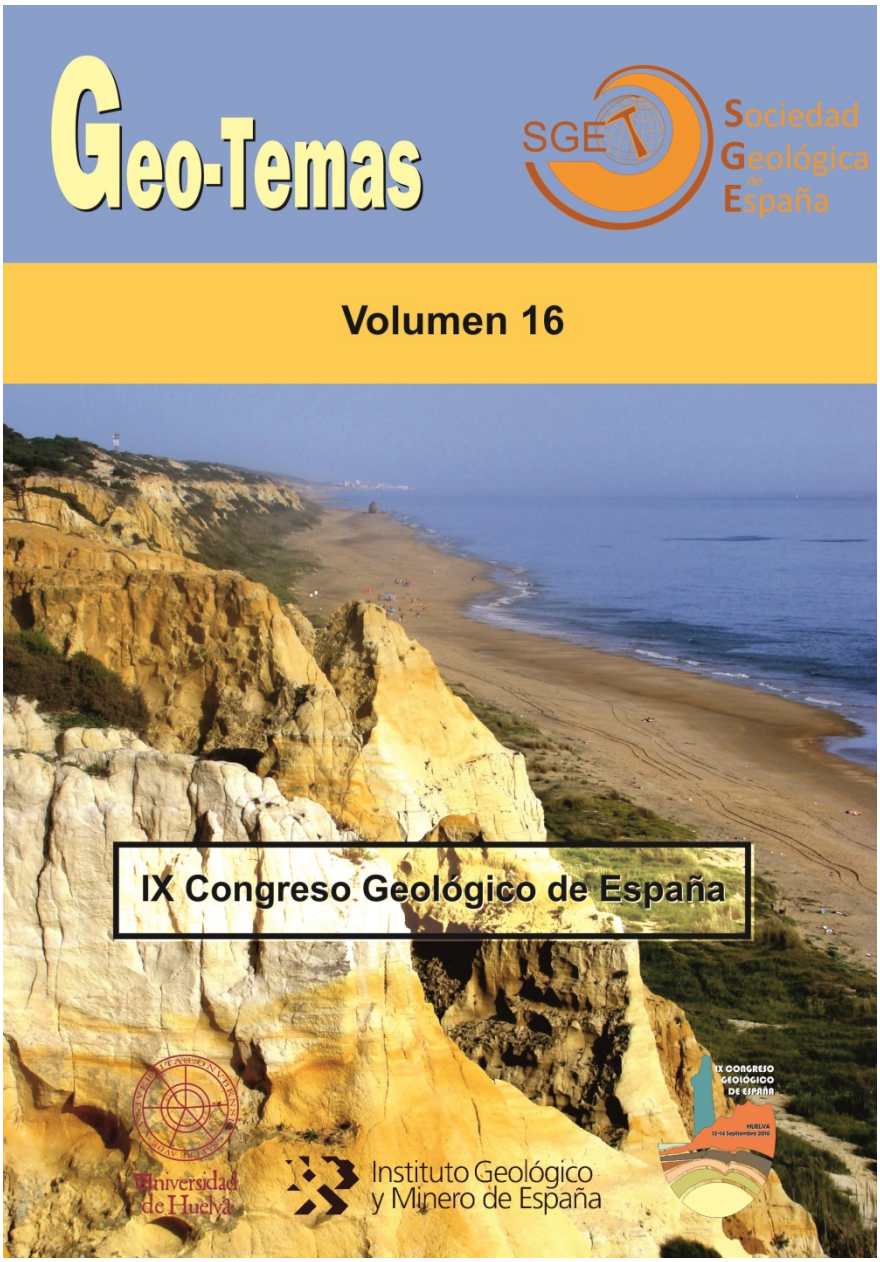
Geo-Temas
SGE
Sociedad Geológica de España
Volumen 16
IX Congreso Geológico de España
Universidad de Huelva
Instituto Geológico y Minero de España

New ichnological data from the lower Paleozoic of the Central Pyrenees: presence of *Arthrophycus brongniartii* (Harlan, 1832) in the Upper Ordovician Cava Formation

Nuevos datos icnológicos del Paleozoico inferior del Pirineo central: presencia de Arthrophycus brongniartii *(Harlan, 1832) en el Ordovícico Superior de la Formación Cava*

Z. Belaústegui[1], C. Puddu[2] and J.M. Casas[3]

1 IRBio (Biodiversity Research Institute) & Dpt. de Dinàmica de la Terra i de l'Oceà, Universitat de Barcelona (UB), Martí i Franquès s/n, 08028 Barcelona, Spain. zbelaustegui@ub.edu
2 Dpt. de Ciencias de la Tierra, Universidad de Zaragoza, Pedro Cerbuna 12, 50009 Zaragoza, Spain. 732168@unizar.es
3 Dpt. de de Dinàmica de la Terra i de l'Oceà & Institut de Recerca Geomodels, Universitat de Barcelona (UB), Martí i Franquès s/n, 08028 Barcelona. casas@ub.edu

Abstract: *The ichnogenus* Arthrophycus*, characteristic of Ordovician-Silurian sedimentary rocks, is described by the first time in the Pyrenees. This ichnogenus is located in fine-grained sandstones of the upper part of the Cava Formation, on the Upper Ordovician rocks of the southern slope of the la Rabassa Dome, close to the Andorra-Spain border. Studied samples exhibit characteristics* of the *ichnogenus* Arthrophycus *Hall, 1852, and in particular to the ichnospecies* A. brongniartii *(=*A. linearis*) (Harlan, 1832). Bioturbation structures are well preserved, and diagnostic features of the ichnosubspecies A. brongniartii protrusiva (Seilacher, 2000) can be observed. These data confirm the Ordovician age of the study section, otherwise well-established on the basis of its abundant fossil content.*

Key words: Arthrophycus*, Bioturbation, Ichnology, Ordovician, Pyrenees.*

Resumen: Se describe por primera vez el icnogénero *Arthrophycus* en rocas prevariscas del Pirineo. Este icnogénero, característico del Ordovícico-Silúrico, se ha localizado en areniscas de grano fino de la parte alta de la Formación Cava, en el Ordovícico superior del flanco sur del domo de la Rabassa, cerca de la frontera entre España y Andorra. El buen estado de conservación de las muestras permite precisar que se trata de la icnoespecie *A. brongniartii* (=*A. linearis*) (Harlan, 1832) y más concretamente de la icnosubespecie *A. brongniartii protrusiva* (Seilacher, 2000). Estos datos confirman la edad ordovícica de la serie, por otra parte bien establecida en base al abundante registro fósil que contiene.

Palabras clave: *Arthrophycus*, Bioturbación, Icnología, Ordovícico, Pirineo.

INTRODUCTION

In the Pyrenees a complete pre-Variscan succession, ranging in age from late Neoproterozoic to middle Carboniferous, can be recognized (Fig. 1). Late Neoproterozoic to Early Ordovician rocks constitutes a thick (3,000 m) succession of metasedimentary rocks with gneissic bodies and layers of marbles, quartzites and calc-silicates interbedded in its lower part. A well-dated Upper Ordovician succession (based on brachiopods, bryozoans, cystoids, corals, and trilobites; see Cavet, 1957 and Hartevelt, 1970) lies unconformably over the former sequence (Casas and Fernández, 2007).

Although it is difficult to evaluate the magnitude of this unconformity, it can be assumed that there was considerable erosion before the Upper Ordovician deposition because Upper Ordovician rocks overlie different sections of the pre-Upper Ordovician succession in the Central and Eastern Pyrenees. Although the age of the Upper Ordovician succession is well known, little attention has been paid to ichnofossils. In this work we present new data about the presence of trace fossils on the Upper Ordovician rocks of the Central Pyrenees.

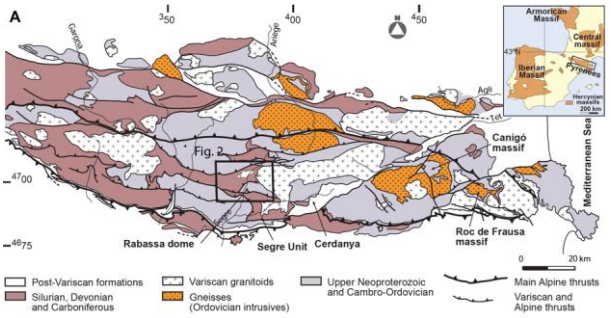

FIGURE 1. *Simplified geological map of the Central and Eastern Pyrenees with the location of the study area (After Casas y Fernández, 2007).*

GEOLOGICAL SETTING AND SAMPLES

Samples were collected near the Andorra-Spain border, on the southern slope of the La Rabassa Dome

(Fig. 2). In this area, the Upper Ordovician rocks constitute a low grade metamorphosed fining-upwards sequence with marked variations in thickness (100–1000 m).

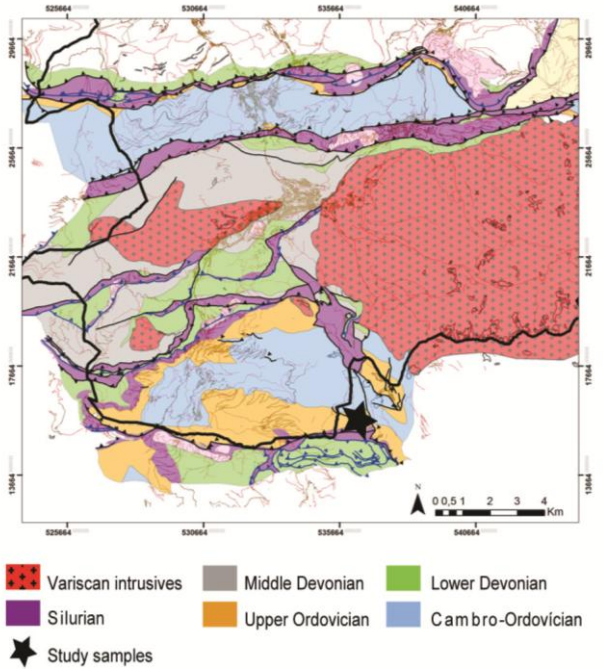

FIGURE 2. *Geological map of southern Andorra with the location of the studied samples (After Margalef, 2015).*

Hartevelt (1970) defined five main siliciclastic formations (Fig. 3) in this area. From base to top: A) The Rabassa Conglomerate Formation is made up of red–purple, unfossiliferous conglomerates and sandstones that form discontinuous lenses ranging in thickness from a few metres to 200 m. Subrounded to well-rounded clasts of slate, quartzite and quartz-veins reach up to 50 cm in diameter. The Rabassa conglomerates, attributed by Hartevelt (1970) to a Sandbian age, are conformably overlain by the Cava Formation. B) The Cava Formation, ranging in thickness from 100 to 800 m, consists of feldspathic sandstones (predominant in the lower part of this formation), overlain by shales, siltstones and fine-grained sandstones, typically green or purple in color in their upper parts. Brachiopods and bryozoans are locally abundant and allow attributing a Caradoc-Ashgill transition age (Katian) to this formation. C) The Estana Formation lies above the Cava Formation and consists of limestones and marly limestones, up to 10 meters in thickness, which constitutes a good stratigraphic key level, the "schistes troués" or "Grauwacke à Orthis" and the "Caradoc limestones" of French and Dutch geologists. Conodonts and brachiopoda are abundants, yielding a Middle Ashgillian (Katian) age. D) The Ansovell Formation consists of monotonous, black and grey slates, with very few sandstone lenses, that reach a thickness of 40–50 meters in the Rabassa Dome. This formation is overlain by the Bar Quartzite Formation. E) The Bar Quartzite Formation consists of dark-grey, medium-rounded grained quartzites with ripples in its upper part. Although Hartevelt (1970) proposed an Ashgillian age for the Ansovell and Bar formations, some authors suggest that the Ordovician-Silurian boundary can be located within the Bar quartzite. Samples were collected in the upper part of the Cava Formation, in purple fine-grained sandstones (Fig. 3).

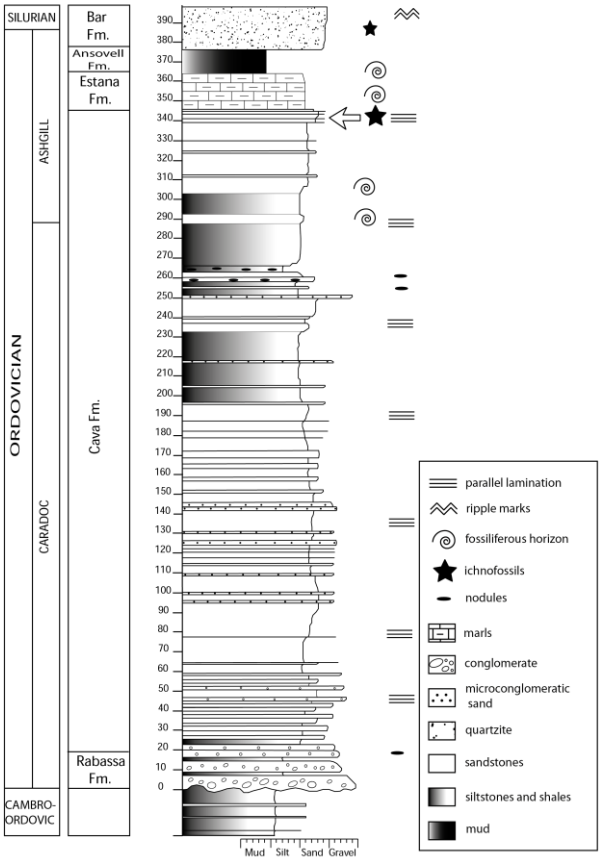

FIGURE 3. *Synthetic stratigraphic column of the pre-Silurian rocks of the Rabassa dome with the location of the studied samples.*

DESCRIPTIVE ICHNOLOGY

Ordovician trace fossils aims of this study have been identified as arthrophycid burrows (Fig. 4). Ichnofamily Arthrophycidae (or 'Arthrophycids') was erected by Seilacher (2000) to designate "Paleozoic worm burrows characterized: a) by regular transverse ridges, which are often discontinuous, giving the casts a squarish cross section; and b) by teichichnoid backfill structures (*spreiten*) resulting from transverse or oblique dislocation of a J-shaped tunnel through the sediment. Depending on the behavioral programs, the backfill structures may have linear, palmate, fan-shaped, spiral, or multi-winged geometries. Also, their internal structures may be either protrusive or retrusive.", and included the ichnogenera *Arthrophycus*, *Daedalus* and *Phycodes* within this new ichnofamily; with *Arthropycus* as typical ichnogenus.

Thereafter, Rindsberg and Martin (2003) emended the diagnosis of this ichnofamily as "burrows with vertical to horizontal *spreite* resulting from regular, oblique backfill

generally having a flattish floor and transverse sculpture; striae common; burrows of limited to indefinite length, simple or branched, straight or curved, in some cases composed of segments arranged angularly."

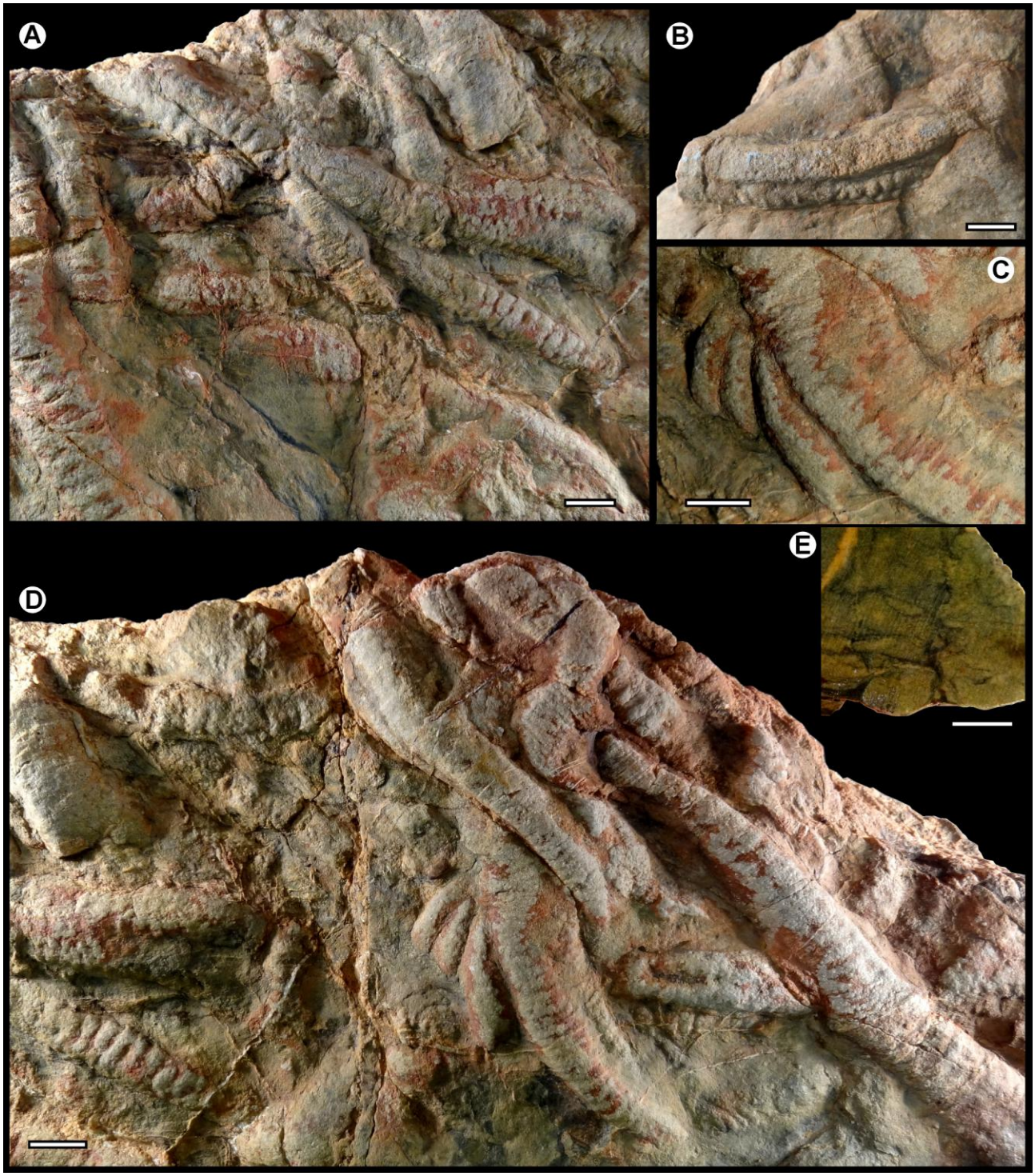

FIGURE 4. Arthrophycus brongniartii. *A & D) Several specimens showing the typical annulated ornamentation and different crosscutting relationships. B) Specimen exhibiting annulated arrangement and a longitudinal median groove. C) Detail of a fan-like arrangement of burrows (possible transition to* A. alleghaniensis*). E) Cross-section showing a vertical protrusive* spreite *with the main tunnel in the lower part. (Scale bars=1 cm; all pictures correspond to parallel sections to the bedding (hyporeliefs), except Fig. 3E).*

In particular, the bioturbation structures from the study area are linear-to-slightly-curved, unbranched and horizontal-to-subhorizontal burrows, parallel to the bedding and preserved as hyporeliefs (Fig. 4A, D). They exhibit an annulated arrangement (Fig. 4A-D), a squarish cross-section (up to 14 mm in diameter; Fig. 4E) and a longitudinal median groove (Fig. 4B). Once, a fan-like pattern is also observable (Fig. 4C). Although the studied traces occur in an intensely burrowed horizon (40 mm thick), a protrusive *spreite* can be occasionally preserved

(Fig. 4E). The traces were studied in natural exposures, which are mostly parallel to bedding. In order to carry out a detailed analysis of burrow geometry and morphology, several cross cuts were obtained from one of the samples.

All these architectural features are characteristic of the ichnogenus *Arthrophycus* Hall, 1852, and in particular to the ichnospecies *A. brongniartii* (=*A. linearis*) (Harlan, 1832). In addition, the presence of the protrusive *spreite* allows being more accurate with its ichnotaxonomic assignation, since this is a diagnostic feature of the ichnosubspecies *A. brongniartii protrusiva* (Seilacher, 2000).

With respect to the *Arthrophycus* tracemaker, worms and arthropods have been proposed as possible candidates (e.g. Seilacher, 2000, 2007; Rindsberg and Martin, 2003; Mángano et al., 2005). The hypothesis of a 'worm' producer (vermiform organism) is mainly based on a) the length and continuity of the structure, b) the presence of delicate bioglyphs interpreted as produced by wrinkles of a flexible cuticle, and c) the regular annulation as a result of peristaltic or hydrostatic movements of a vermiform producer (e.g. Seilacher, 2000; Mángano et al., 2005 and references therein). By contrast, an arthropod authorship is defended by a) the presence of 'chevrons' or zipper-like annulations attributed to appendage marks (see Mángano et al., 2005 and references therein), b) Silurian specimens with uncommon features for classic *Arthrophycus* (Rindsberg and Martin, 2003), and c) the occurrence of a unique long-bodied arthropod (*Pleuralata spinosa*) in stratigraphic proximity with *A. alleghaniensis* (see McCoy et al., 2012). In any case, the assignation of *Arthrophycus* as a feeding trace (fodinichnion) seems to be clear.

In addition, the importance of ichnofamily Arthropycidae also lies in its ichnostratigraphic significance, since in absence of index fossils or '*Cruziana* stratigraphy', it can be useful as alternative to date lower Paleozoic sedimentary rocks. In particular, the ichnogenus *Arthrophycus* is characteristic of Ordovician-Silurian rocks. Five ichnospecies have been described: *A. minimus* (Upper Cambrian (Furongian)/Lower Ordovician); *A. brongniartii* (Lower Ordovicain/Lower Silurian); *A. alleghaniensis* (Lower Silurian), *A. lateralis* (Lower Silurian); and *A. parallelus* (Carboniferous) (see Buatois and Mángano, 2011). In our particular case, the presence of *A. brongniartii* in the Cava Formation confirms its Upper Ordovician age, previously obtained from the fossil content (brachiopods and bryozoans).

ACKNOWLEDGEMENTS

ZB is supported by a BDR post-doctoral fellowship of the Universitat de Barcelona (UB). JMC acknowledges the support of the projects CGL2010-21298 and Consolider-Ingenio 2010 under CSD2006-00041 (Topoiberia). The authors want to devote this work to J.M. de Gibert who began the study of the prsented trace fossils.

REFERENCES

Buatois, L.A. and Mángano, M.G. (2011): *Ichnology. Organism-Substrate Interactions in Space and Time.* Cambridge University Press, New York, 358 p.

Casas, J.M. y Fernández, O. (2007): On the Upper Ordovician unconformity in the Pyrenees: New evidence from the La Cerdanya area. *Geologica Acta*, 5.2: 193-198.

Cavet, P. (1957): Le Paléozoïque de la zone axiale des Pyrénées orientales françaises entre le Roussillon et l'Andorre. *Bulletin Service Carte Géologique France*, 55**:** 303-518.

Hartevelt, J.J.A. (1970): Geology of the upper Segre and Valira valleys, central Pyrenees, Andorra/Spain. *Leidse Geologische Mededelingen*, 45: 167-236.

Mángano, M.G., Carmona, N.B., Buatois, L.A. and Muñiz, F. (2005): A new ichnospecies of *Arthrophycus* from the Upper Cambrian-Lower Tremadocian of Northwest Argentina: Implications for the arthrophycid lineage and potential in ichnostratigraphy. *Ichnos: An International Journal for Plant and Animal Traces*, 12: 179-190.

Margalef (2015): *Estudi estructural i estratigràfic del sud d'Andorra*. Tesis Doctoral, Univ. de Barcelona, 172 p.

McCoy, V.E., Strother, P.K. and Briggs, D.E.G. (2012): A possible tracemaker for *Arthrophycus alleghaniensis*. *Journal of Paleontology*, 86: 996-1001.

Rindsberg, A.K. and Martin, A.J. (2003): *Arthrophycus* in the Silurian of Alabama (USA) and the problem of compound trace fossils. *Palaeogeography, Palaeoclimatology, Palaeoecology*, 192: 187-219

Seilacher, A. (2000): Ordovician and Silurian Arthrophycid lchnostratigraphy. In: *Geological exploration in Murzuk Basin* (M.A. Sola and D. Worsley, eds.). Elsevier, Amsterdam, 237-258.

Seilacher, A. (2007): *Trace Fossil Analysis.* Springer, Berlin, 226 p.

PUBLICACIONES DEL INSTITUTO GEOLÓGICO Y MINERO DE ESPAÑA
Serie: CUADERNOS DEL MUSEO GEOMINERO, Nº 14

ORDOVICIAN OF THE WORLD

11th ISOS SPAIN 2011

Editors: Juan Carlos Gutiérrez-Marco
Isabel Rábano
Diego García-Bellido

MINISTERIO DE CIENCIA E INNOVACIÓN

Instituto Geológico y Minero de España

J.C. Gutiérrez-Marco, I. Rábano and D. García-Bellido (eds.), *Ordovician of the World.*
Cuadernos del Museo Geominero, 14. Instituto Geológico y Minero de España, Madrid. ISBN 978-84-7840-857-3

NEW INSIGHTS INTO THE STRATIGRAPHY AND STRUCTURE OF THE UPPER ORDOVICIAN ROCKS OF THE LA CERDANYA AREA (PYRENEES)

C. Puddu[1] and J.M. Casas[2]

[1] Department of Earth Sciences, University of Cagliari, Via Trentino 51, 09127 Cagliari, Italy. cpuddu@unica.it
[2] Departament de Geodinàmica i Geofísica-Institut de recerca GEOMODELS, Universitat de Barcelona, Martí i Franquès s/n, 08028 Barcelona, Spain. casas@ub.edu

Keywords: Middle Ordovician folding event, brachiopods, Upper Ordovician fractures, Upper Ordovician stratigraphy.

INTRODUCTION

It used to be assumed that deformation mesostructures recognized in the Paleozoic pre-Variscan rocks of the Pyrenees mainly derive from Variscan deformation. Recently, the presence of pre-Variscan folds, Mid Ordovician in age, has been documented in the southern slope of the Canigó massif (Casas, 2010). This work seeks to provide new insight into the structure of the Upper Ordovician rocks in the La Cerdanya area. Moreover, new data on the stratigraphy of the Upper Ordovician succession is also provided. Data were collected north of Bellver de Cerdanya, between the towns of Cortás, Eller, Ordén and Talltendre (Fig. 1) during detailed geological mapping (1/5.000) and structural analysis.

GEOLOGICAL SETTING

In this area, the upper part of the pre-Upper Ordovician rocks crops out extensively. It is a rather monotonous succession, composed of an unfossiliferous succession of rhythmic alternation of sandstones, siltstones and argillites. Layers vary in thickness from 1 mm to several cm and range in colour from grey to light green or light brown. Owing to its monotonous character, it is not easy to determine its lower limit and thickness, although a thickness of about 1500 m has been proposed for this upper part of the succession. This succession is classically known as Cambro-Ordovician, and corresponds to the "schistes de Jujols" established by Cavet (1957). Recent acritarch data (Casas and Palacios, pers. comm.) indicate that the uppermost part of this succession has a Late Cambrian (Furongian)-Early Ordovician (Tremadocian) age. The well dated Upper Ordovician succession (Cavet, 1957; Hartevelt, 1970) lies unconformably over the former unit (Santanach, 1972; García-Sansegundo et al., 2004; Casas and Fernández, 2007). The Upper Ordovician rocks constitute a fining upwards sequence similar to that described by Hartevelt (1970) in the Segre valley, in which this author defined five main siliciclastic stratigraphic formations. The Rabassa Conglomerate Formation, which constitutes the lowest part of the

CONTENTS

succession, is made up of red-purple, largely unfossiliferous, conglomerates and microconglomerates that range in thickness from a few to 200 meters. Hartevelt (1970) attributed the Rabassa conglomerates to the Caradoc. The Rabassa conglomerates are overlain by the Cava Formation that varies in thickness from 100 to 800 m. Microconglomerates and feldspatic sandstones predominate in the lower part, followed upwards by shales, siltstones and fine grained sandstones, typically green or purple in colour. Brachiopods and bryozoans are locally abundant. Gil Peña et al. (2004) attributed a late Caradoc–early Asghill age to this formation, which is Mid Late Ordovician. The Estana Formation lies above the Cava Formation and consists of limestones and marly limestones up to 10 m in thickness. This formation constitutes a good stratigraphic key level, with abundant fossils, conodonts and brachiopods, yielding a mid Ashgill age (Gil Peña et al., 2004). The Ansovell Formation overlies the Estana limestone and is made up of dark shales and siltstones with minor interbedded quartzite layers in the uppermost part. The Bar Quartzite Formation, located at the top of the Upper Ordovician succession, consists of a 5 to 10 m thick quartzite layer that overlies the Ansovell Formation. An Ashgill age was proposed for the Ansovell and Bar formations by Hartevelt (1970) although Gil-Peña et al. (2004) suggest that the Ordovician-Silurian boundary can be located within the Bar quartzite.

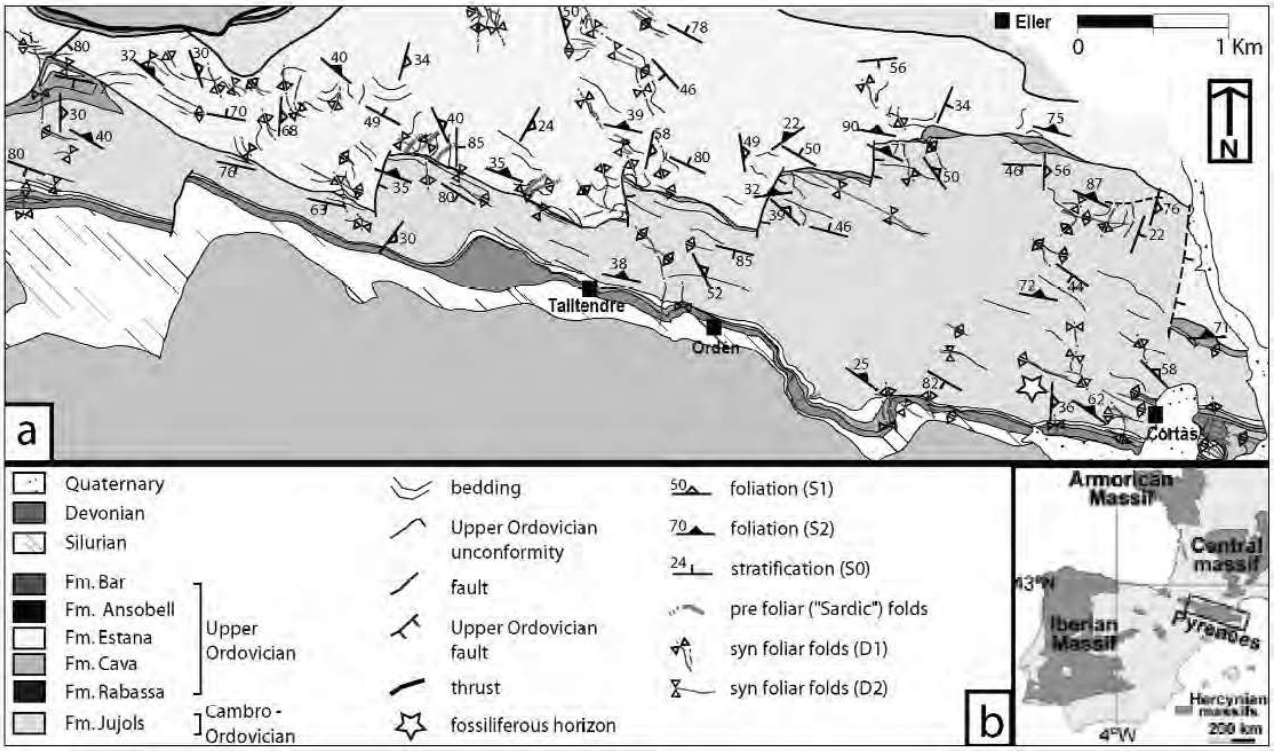

Figure 1. Geological map of the study area (a) with the location of the study area (b). The legend shows the main Variscan and pre-Variscan structures and the location of the fossiliferous horizon (W of Cortás) where the brachiopods were collected.

STRATIGRAPHY

In the stratigraphic section made near Ordén, the Upper Ordovician sequence exhibits a thickness of about 350 meters (Fig. 2). In this section the Cava Formation only presents three of the four members recognized by Hartevelt (1970): the basal member made of greenish to purple greywackes, sandstones, microcon-

CONTENTS

glomerates, siltstones and slates, with rock fragments in its lower part ("a" member); the red and greenish silty slates ("b" member), and the siltstone ("c" member), which contains in its upper part some fossiliferous level with brachiopods, bryozoans, cystoids and rugose corals. It should be noted that, in this section, three brachiopod genera (*Porambonites* sp., *Eoanastrophia* sp., and *Dolerorthis* sp.) were collected, which have not yet been described in the Cava Formation (Fig. 3).

The new brachiopod fauna comes from the uppermost part of the "c" member above the "coquina" horizon described by Hartevelt (1970). However, the state of preservation of the fossils only allowed a generic assignment, which represents an intermediate fauna between the late Caradoc - early Ashgill brachiopods collected in the "coquina" horizon located in the upper part of this member (*Svobodaina havliceki*, *Rostricellula* sp., *Rafinesquina* sp.; Gil Peña et al., 2004) and the mid Ashgill brachiopods of the Estana Fm. (*Dolerorthis* sp., *Eoanastrophia pentamera*, *Iberomena sardoa, Leangella anaclyta*, *Longvillia mediterranea*, *Nicolella actoniae*, *Porambonites* (*Porambonites*) *magnus*, *Ptychopleurella villasi*; Gil Peña et al., 2004).

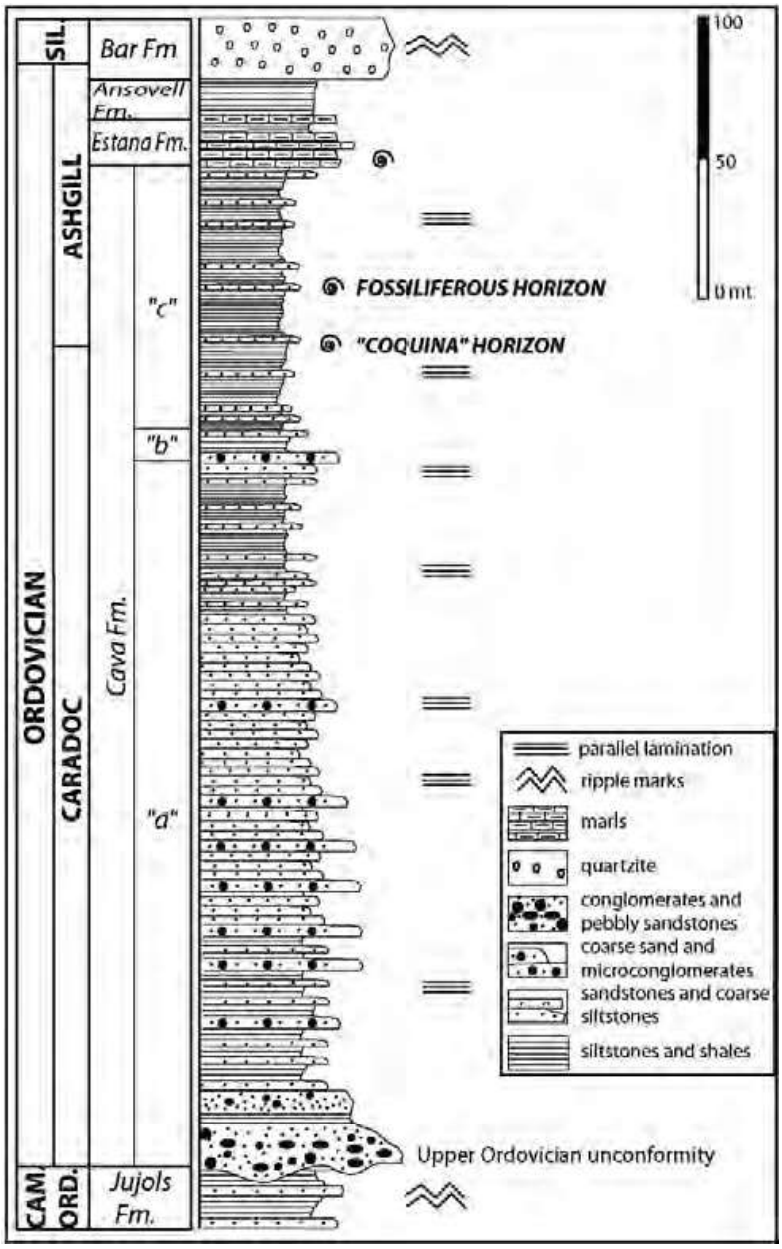

Figure 2. Stratigraphic section made near Ordén: the fossiliferous horizon with *Porambonites* sp., *Eoanastrophia* sp., and *Dolerorthis* sp. is located in the Cava Fm. between the "coquina" horizon of Hartevelt (1970) and the fossiliferous marls of the Estana Fm.

STRUCTURE

Different structures can be recognized in the study area: the Upper Ordovician unconformity, the Upper Ordovician normal faults, and three systems of folds: two of them of Variscan age and one of pre-Variscan age (Fig. 1a).

The Upper Ordovician unconformity, that separates the Upper Ordovician sediments from the underlying Cambro-Ordovician ones, can be identified from detailed mapping in several areas. The unconformity has a NW-SE trend and cuts the bedding of the pre-unconformity deposits at different angles ranging from a few to 90°.

CONTENTS

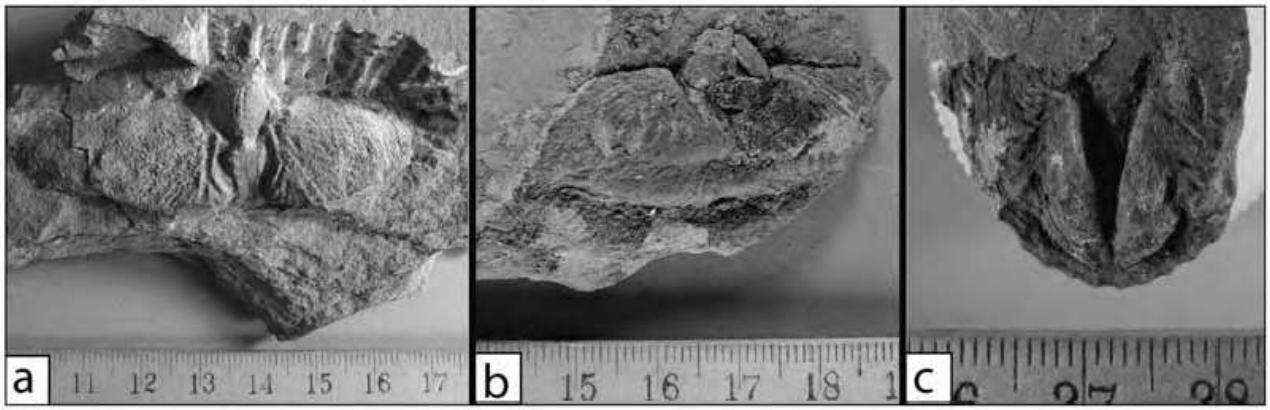

Figure 3. Brachiopods collected in the upper part of the "c" member of the Cava Fm.: a) *Porambonites* sp. (internal mould of ventral valve), b) *Dolerorthis* sp. (internal mould of ventral valve), c) *Eoanastrophia* sp. (internal mould of dorsal valve).

Several normal faults affect the Upper Ordovician succession, the Cambro-Ordovician sediments and the unconformity. The faults are steep and currently exhibit a broadly N-S to NNE-SSW cartographic trace. In most cases their hanging wall is the eastern block despite the presence of some antithetic faults. Displacement of some of these faults diminishes progressively upwards of the series and peters out in the upper part of the Upper Ordovician rocks, in the sediments of the Cava Formation, indicating that the faults became inactive during the Late Ordovician before deposition of the Ashgill metasediments (Fig. 1a).

Two systems of cleavage-related Variscan folds affect the pre- and the post-unconformity sediments, one with a N-S trend and the other with an E-W to NW-SE trend. Moreover, the pre-unconformity deposits are affected by another folding episode. This episode gave rise to metric to hectometric sized folds without foliation or metamorphism associated and oriented N-S to NE-SW. These folds were not recognized in the Upper Ordovician sediments and are sealed by the Upper Ordovician unconformity.

DISCUSSION

The brachiopods collected from the upper part of the Cava Formation represent an Ashgill fauna, intermediate between the late Caradoc–early Ashgill brachiopods of the "coquina" from the Cava Fm. and the mid Ashgill brachiopods of the Estana Fm. described by Hartevelt (1970) and revised by Gil Peña et al. (2004). This fauna marks a smooth transition between the *Svobodaina* fauna and the *Nicolella* one found in the Cava Fm. and in the Estana Fm. respectively, and represent a fauna similar to the one described in the Montagne Noire (France).

The similarities should be noted between the study area and the Iglesiente and Sarrabus regions in the south of Sardinia, classic zones where an Upper Ordovician ("Sardic") unconformity has been described. In Sardinia, a regional stratigraphic and angular unconformity separates the Cambro-Ordovician sequence from the underlying Upper Ordovician ones, as the stratigraphic gap marked by the "Sardic unconformity" is located between the Arenig?, dated by the youngest fossiliferous deposit under the unconformity (Pillola et al., 2007), and the late Caradoc, which is the age of the oldest fossiliferous horizon of the post-unconformity beds (Hammann, 1992; Leone et al., 2002). In Sardinia the pre-unconformity sequence is deformed by different E-W structures sealed by the unconformity and related to the "Sardic Phase" (Stille, 1939), in the form of metric to hectometric sized folds without cleavage, thrusts and thrust faults (Pasci et al., 2008).

CONTENTS →

The Upper Ordovician unconformity of the Pyrenees may be interpreted as equivalent to the "Sardic unconformity" and the pre-Variscan folds described in the Pyrenees may be equivalent to the "Sardic" folds of Middle Ordovician age. These folds were responsible for the deformation, uplift and erosion of the Cambro-Ordovician sediments and for the Upper Ordovician unconformity. Thus, the Pyrenees closely resemble the most external part of the Sardinian fragment of the Variscan orogen and exhibit marked differences with the rest of the Iberian Massif, where evidence of Ordovician deformation is limited.

Acknowledgements

This work has been partially funded by project CGL2007-66857-CO2-02. E. Villas is thanked for the identification of the brachiopods and J.C. Gutiérrez-Marco for the revision of a previous version of the manuscript.

REFERENCES

Casas, J.M. 2010. Ordovician deformations in the Pyrenees: new insights into the significance of pre-Variscan ("sardic") tectonics. *Geological Magazine*, 147, 674-689.

Casas, J.M. and Fernández, O. 2007. On the Upper Ordovician unconformity in the Pyrenees: New evidence from La Cerdanya area. *Geologica Acta*, 5, 193-198.

Cavet, P. 1957. Le Paléozoïque de la zone axiale des Pyrénées orientales françaises entre le Roussillon et l'Andorre. *Bulletin du Service de la Carte Géologique de France,* 55, 303-518.

Donzeau, M. and Laumonier, B., 2008, Sur l'importance des événements sardes (médio-ordoviciens) dans les Pyrénées. *23ème Réunion annuel des Sciences de la Terre*, Nancy, 163.

García-Sansegundo, J., Gavaldá, J. and Alonso, J.L. 2004. Preuves de la discordance de l'Ordovicien supérieur dans la zone axiale des Pyrénées : exemple du dôme de la Garonne (Espagne, France). *Comptes Rendus Geoscience*, 336, 1035-1040.

Gil-Peña, I., Barnolas, A., Villas, E. and Sanz-López, J. 2004. El Ordovícico Superior de la Zona Axial. In Vera, J.A. (ed), *Geología de España.* Sociedad Geológica de España-Instituto Geológico y Minero de España, Madrid, 247-249.

Hammann, W. 1992. The Ordovician trilobites from the Iberian Chains in the province of Aragon, NE Spain - I. The trilobites of the Cystoid Limestone (Ashgill series). *Beringeria*, 6, 1-219.

Hartevelt, J.J.A. 1970. Geology of the Upper Segre and Valira valleys, Central Pyrenees, Andorra/Spain. *Leidse Geologische Mededelingen*, 45, 167-236.

Leone, F., Ferretti, A, Hammann, W., Loi, A., Pillola, G.L. and Serpagli, E. 2002. A general view on the post-Sardic Ordovician sequence from SW Sardinia. *Rendiconti della Società Paleontologica Italiana*, 41 (1), 51-68.

Pasci, S., Pertusati, P.C., Salvadori, I. and Murtas, A. 2008. I rilevamenti CARG del Foglio geologico 555 "Iglesias" e le nuove implicazioni strutturali sulla tettonica della "Fase Sarda". *Rendiconti online della Società Geologica Italiana*, 3, 614-615.

Pillola, G.L., Piras, S. and Serpagli, E. 2007. Upper-Tremadoc-Lower Arenig? Anisograptid-Dichograptid fauna from the Cabitza Formation (Lower Ordovician, SW Sardinia, Italy). *Revue de Micropaléontologie*, 51, 167-181.

Santanach, P. 1972. Sobre una discordancia en el Paleozoico inferior de los Pirineos orientales. *Acta Geologica Hispanica*, 5, 129–132.

Stille, H. 1939. Bemerkungen betreffend die "sardische" Faltung und den Ausdruck "Ophiolithisch". *Zeitschrift der deutschen geologischen Gesselschaft,* 91, 771-773.

International Meeting

September 4-9th 2017, Figueres, Catalonia

ORDOVICIAN GEODYNAMICS:

The Sardic Phase in the Pyrenees, Mouthoumet and Montagne Noire massifs

J. Javier Álvaro, Josep Maria Casas and Sébastien Clausen (eds.)

(cover photo: panorama of the Canigó massif from the south)

Álvaro, J.J., Casas, J.M. and Clausen, S. 2017. Ordovician Geodynamics: the Sardic Phase in the Pyrenees, Mouthoumet and Montagne Noire massifs. *Géologie de la France* 1 (4), 1-83.

http://geolfrance.brgm.fr/ordovician-geodynamics-sardic-phase-pyrenees-mouthoumet-and-montagne-noire-massifs-international

Please, to cite any part of the content, follow this example:
Laumonier, B. 2017. Graus de Canaveilles along Conflent valley. In: Ordovician Geodynamics: the Sardic Phase in the Pyrenees, Mouthoumet and Montagne Noire massifs (Álvaro, J.J., Casas, J.M., Clausen, S., eds.), *Géologie de la France* 1 (4), 47-49.

Ordovician magmatism in the Pyrenees

Josep Maria Casas[1], Teresa Sánchez-García[2], J. Javier Álvaro[3], Claudia Puddu[4] & Monserrat Liesa[5]

[1] Dpt. de Dinàmica de la Terra i de l'Oceà-Institut de Recerca Geomodels, Universitat de Barcelona, Martí Franquès s/n, 08028 Barcelona, Spain, casas@ub.edu
[2] Dpto. Investigación Recursos Geológicos, Área Recursos Minerales y Geoquímica, Instituto Geológico y Minero de España, Ríos Rosas 23, 28003 Madrid, Spain, t.sanchez@igme.es
[3] Instituto de Geociencias (CSIC-UCM), Novais 12, 28040 Madrid, Spain, jj.alvaro@csic.es
[4] Dpto de Ciencias de la Tierra, Universidad de Zaragoza, Pedro Cerbuna 12, 50009 Zaragoza, Spain, claudiapuddugeo@gmail.com
[5] Dpt. de Mineralogia, Petrologia i Geologia aplicada, Universitat de Barcelona, Martí Franquès s/n, 08028 Barcelona, Spain, mliesa@ub.edu

Successive Ordovician magmatic pulsations are well documented in the pre-Variscan basement of the Pyrenees. According to radiometric data, magmatism lasted about 30 m.y., from ca. 477 to 446 Ma, and although the magmatic activity seems to be continuous, two peaks can be distinguished at 473-472 Ma and 457 Ma. Based on geochronological and geochemical data, two different magmatic complexes can be distinguished: latest Early-Mid Ordovician and Late Ordovician magmatism.

(a) During Early to Mid Ordovician times, the magmatic activity gave rise to the intrusion of voluminous aluminous granites, about 500 to 3000 m in size, that constitute the protoliths of the large laccolithe-shaped, orthogneissic bodies that crop out at the core of the Aston, Hospitalet, Canigó, Roc de Frausa and Albera massifs that punctuate the backbone of the Pyrenees. Only a minor representation of basic coeval magmatic rocks is exposed and acidic volcanic equivalents have been only reported in the Albera massif. Granites are medium to coarse grained and exhibit porphyritic textures with rapakivi K-feldspars, they are peraluminous and subalkaline and the geochemical characteristics indicate that these rocks were mainly derived from a continental crustal source.

(b) A Late Ordovician magmatic pulse yielded a varied suite of magmatic rocks. Small granitic bodies are emplaced in the lowermost part of the successions of the Canigó massif and constitute the protoliths of the Cadí, Casemí and Núria gneisses. Moreover, metre-scale thick bodies of metadiorite are interlayered in the same area. Coeval calc-alkaline and explosive volcanic rocks (ignimbrites, andesites and volcaniclastic rocks) are interbedded in the Upper Ordovician of the Ribes de Freser and Bruguera units, together with a granophyre body that crops out at the base of the Upper Ordovician succession. Metadiorites are metaluminous with slightly negative εNd values (-0.8) and a TDM age of 1.18 Ga. Their protoliths were derived from mantle melts with heterogeneous crustal contamination. Acidic volcanic rocks are peraluminous and subalkaline and εNd values between -5.1 to -4.8 indicate a crustal origin. Similar isotopic values have been obtained for the Ribes granophyre (εNd -2.6) and similar geochemical characteristics and εNd negative values (-3.2 to -5.2), from the Cadí and Núria gneiss, indicate that this assemblage was also derived from different magmas of continental crustal source. Finally, the εNd values of the Casemí gneiss (-1.9 to -1.3) suggests that their protoliths were derived from mantle melts with heterogeneous crustal contamination.

It should be noted that the latest Early-Mid Ordovician magmatism is coincident with the episode of uplift and erosion that led to the formation of the Sardic unconformity. This uplift was followed by an extensional pulse that developed normal faults, directly affecting the onset of the basal unconformity and controlling deposition of the (post-Sardic) Upper Ordovician strata, which were coeval with the Late Ordovician magmatic activity.

Figure 1. Sketch displaying the main Ordovician units at the central and NW Iberia.

Comparison between detrital zircon populations from the Ordovician rocks of the Pyrenees and other Perigondwanan terrains: palaeogeographic implications.

Aina Margalef[1], Pedro Castiñeiras[2], Josep Maria Casas[3], Marina Navidad[2] & Montserrat Liesa[4]

[1] Centre d'Estudis de la Neu i de la Muntanya d'Andorra, Institut d'Estudis Andorrans, Andorra, amargalef.cenma@iea.ad
[2] Departamento de Petrología y Geoquímica, Universidad Complutense de Madrid. 28040 Madrid, Spain
[3] Departament de Dinàmica de la Terra I de l'Oceà – Institut de Recerca GEOMODELS, Universitat de Barcelona (UB), Martí i Franquès s/n, Barcelona, 08028, Spain, casas@b.edu
[4] Dpt. de Mineralogia, Petrologia i Geologia aplicada, Universitat de Barcelona, Martí Franquès s/n, 08028 Barcelona, Spain, mliesa@ub.edu

The first LA-ICP-MS U-Pb detrital zircon ages from quartzites located below (three samples) and above (one sample) the Upper Ordovician unconformity of the Central Pyrenees (the Rabassa Dome, Andorra) are investigated. The maximum depositional age for the Jujols Group, below the unconformity, based on the youngest detrital zircon population, is around 475 Ma (Early Ordovician), whereas for the Bar Quartzite Formation, above the unconformity, the presence of only two zircons of 442 and 443 Ma precludes obtaining a precise maximum sedimentation age. A time gap of ~20 million years for the Upper Ordovician unconformity in the Pyrenees can be proposed, similar to that of the Sardic unconformity in Sardinia. The similar age patterns obtained on both sides of the Upper Ordovician unconformity suggest that there was no change in the source area of these series, while the absence of a Mid Ordovician age population may be due to a lack of sedimentation at that time. The four study samples present very similar U-Pb age patterns: the main age populations correspond to Neoproterozoic (Ediacarian-Cryogenian, ca. 550-750 Ma); Grenvillian (Tonian-Stenian, ca. 850-1100 Ma); Palaeoproterozoic (Orosirian, ca.1900-2100 Ma) and Neoarchean (ca. 2500-2650 Ma). The similarity with the Sardinian age distribution suggests that these two terranes could share the same source area and that they were paleogeographically close in Ordovician times in front of the Arabian-Nubian Shield.

New knowledge on the Upper Ordovician rocks of El Baell, Ribes de Freser area, eastern Pyrenees

Claudia Puddu[1], Josep Maria Casas[2] & J. Javier Álvaro[3]

[1] Dpto. Ciencias de la Tierra, Universidad de Zaragoza, Pedro Cerbuna 12, E-50009, Zaragoza, Spain, 732168@unizar.es
[2] Dpto de Dinàmica de la Terra i de l'Oceà, Universitat de Barcelona, Institut de recerca GEOMODELS, Martí Franquès s/n, 08028 Barcelona, Spain, casas@ub.edu
[3] Instituto de Geociencias (CSIC-UCM), José Antonio Novais 12, 28040, Madrid, Spain, *jj.alvaro@csic.es*

The Ribes de Freser area (Eastern Pyrenees), investigated by Robert (1980) and Muñoz (1985), is characterized by an Alpine antiformal stack, where several structural units are recognized. The stratigraphic succession exposed in these units and its thickness change considerably throughout the tectonic units. From bottom to top, three structural units can be

distinguished: Ribes de Freser, El Baell, and Bruguera units. The aim of this work is to provide new structural and stratigraphic data about the rocks cropping out in Bruguera and El Baell units.

The Ribes de Freser unit is made up of a 200-600 m-thick succession composed of Upper Ordovician volcanic and volcanosedimentary rocks interbedded in Katian sediments (Muñoz, 1985; Martí *et al*., 1986), affected by two Variscan fold systems: a NW-SE and a E-W one.

The El Baell unit shows a fossiliferous carbonate succession referred to Upper Ordovician (Robert, 1980; Muñoz, 1985) that differs considerably from the classic one described by Hartevelt (1970), and used as reference for the main part of the Pyrenees. It lies on the Paleocene-Upper Cretaceous series of the Ribes de Freser unit, which crops out in a tectonic window, and it is topped by the Bruguera unit. The Upper Ordovician succession is made up of about 500 m of shales bearing centimetre-thick carbonate nodules ("*schistes troués*"), limestones, marlstones and siltstones, with three metre-thick levels of limestone rich in crinoids, brachiopods, echinoderms and conodonts, referred to a Katian age, and unconformably overlain by the Hirnantian Ansovell blackish shales (Fig. 1). From bottom to top, the succession consists of siltstone/marlstone alternations, followed by the first limestone bar, which exhibits quartz veins and a synsedimentary breccia. Then, a thick pack of *schistes troués* and the second fossiliferous (echinoderm-rich) limestone bed are followed by *schistes troués*, siltstones and dark shales alternations, often intercalated with centimetre-thick carbonate levels, and marlstones. The last limestone bar shows fossiliferous and massive limestone, often recrystallized, and a *karst* on the top contact, which is capped by the Hirnantian black slates that contain scattered limestone dropstones, quartz veins and slumps.

Unfortunately, the base of the Upper Ordovician succession and the contact with Silurian beds is never exposed in this tectonic unit. The rocks of this unit are affected by a Variscan ENE-WSW-trending fold system, with tight folds, and N-plunging faults (Fig. 2).

The Bruguera unit is composed of a slate-dominated succession of pre-Variscan age (Muñoz, 1985) overlain by rhyolitic ignimbrites and andesitic lavas, recently dated at ~455 Ma (Martí *et al*., 2014). Two Variscan fold systems, with E-W- and NW-SE oriented open folds and no penetrative foliation (Fig. *2*) affect the Palaeozoic rocks of this unit (Muñoz, 1985). A Pre-Sardic fold system N-S oriented affects only the rocks of this unit.

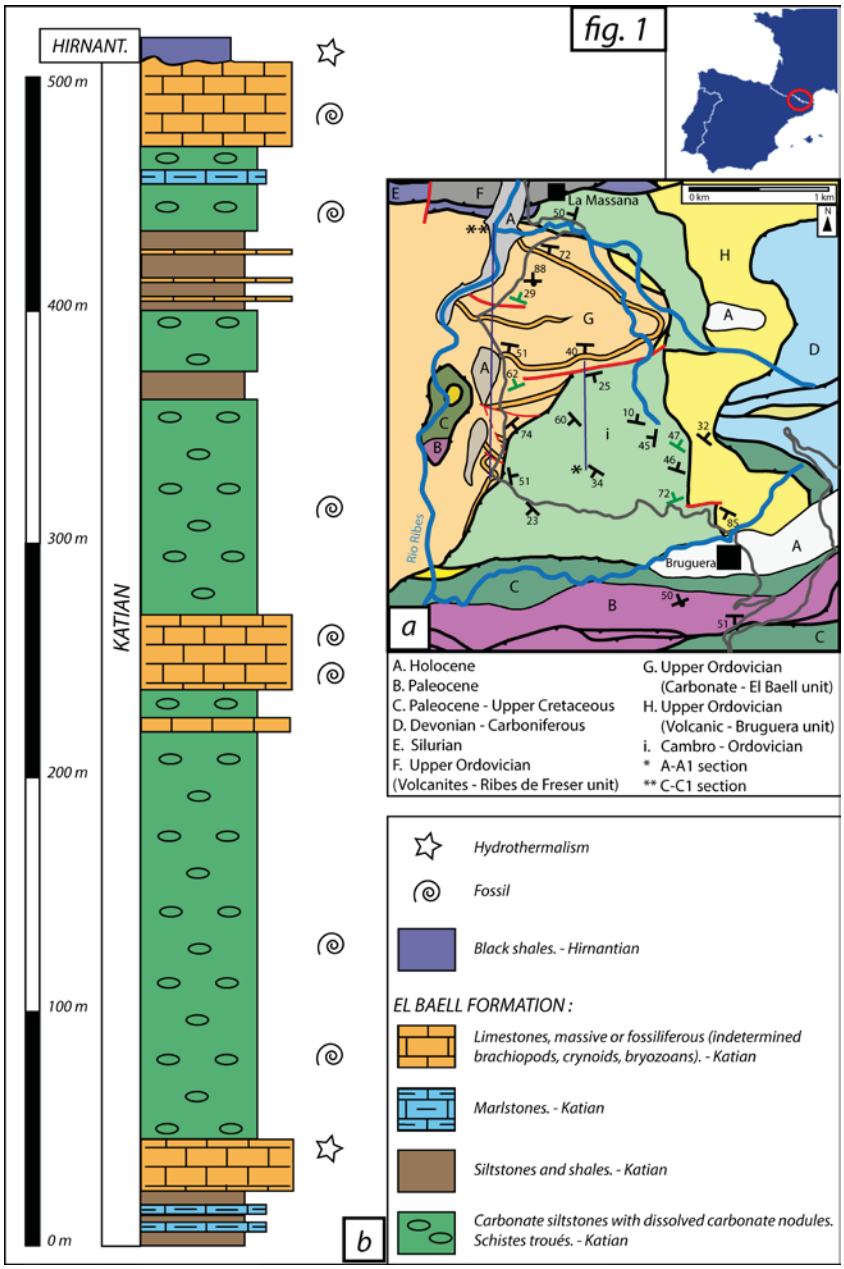

Figure 1. A. Geological sketch of the La Massana-Bruguera area in the eastern Pyrenees. B. Stratigraphic log of the sEl Baell unit in the study area.

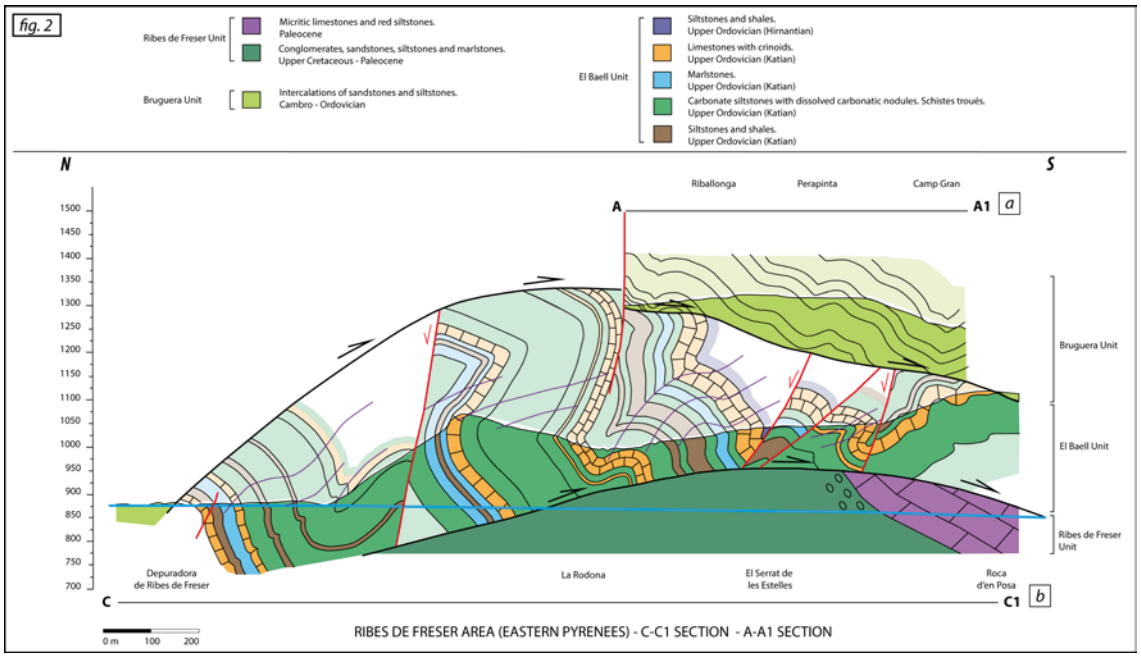

Figure 2. Cross-section of the El Baell unit.

On the Upper Ordovician of the La Cerdanya area, Pyrenees

Claudia Puddu[1], Josep Maria Casas[2] & J. Javier Álvaro[3]

[1] Dpto. Ciencias de la Tierra, Universidad de Zaragoza, Pedro Cerbuna 12, E-50009, Zaragoza, Spain, 732168@unizar.es
[2] Dpto de Dinàmica de la Terra i de l'Oceà, Universitat de Barcelona, Institut de recerca GEOMODELS, Martí Franquès s/n, 08028 Barcelona, Spain, casas@ub.edu
[3] Instituto de Geociencias (CSIC-UCM), José Antonio Novais 12, 28040, Madrid, Spain, jj.alvaro@csic.es

The aim of this work is to provide stratigraphic and structural features of the Upper Ordovician from the La Cerdanya area (Canigó unit), which exhibits a succession similar to that described by Hartevelt (1970) in the Central and Eastern Pyrenees. In the latter areas, the Upper Ordovician is represented mainly by a broad fining-upward package with some limestone key levels that ranges from 100 to 1000 m (Hartevelt, 1970).

The Upper Ordovician succession lies on the Cambrian and Lower Ordovician Jujols Group (Laumonier *et al*., 2004; Casas & Palacios, 2012) by the angular Sardic unconformity, which marks the base of the post-Sardic succession.

In the study area (Fig. 1), the lowest part of the Upper Ordovician succession is made up of 0-100 m thick of reddish-purple polygenic and heterometric conglomerates (Rabassa Conglomerate Formation), with clasts composed of vein quartz, quartzite and slate derived from underlying rocks. Locally, the Cambro-Ordovician is directly overlain by the Cava Formation (0-850 m thick), made up of conglomerates, sandstones and shales with volcanic intercalations, with fossiliferous levels of Katian age (Hartevelt, 1970). This formation is overlain by a 5-200 m-thick limestone and marly limestone, the fossiliferous Estana Formation of late Katian age (Gil-Peña *et al*., 2004). The top of the carbonate succession is capped by the black-grey shales of the Ansovell Formation, 20-320 m thick, and the Bar Quartzite, 2-20 m thick, referred to Hirnantian-Silurian age.

Both successions are affected by two Variscan fold systems with a penetrative foliation, while the Cambrian-Lower Ordovician succession is affected by a pre-Variscan fold system that

produced open folds without related foliation sealed by the conglomerates of the Rabassa Formation (Casas, 2010; Casas *et al*., 2012).

The pre-Sardic succession, the Sardic Unconformity and the lower part of the post-Sardic succession are cut and offset by some N-S-trending syn-sedimentary faults, which sharply affect the thickness of the Rabassa and Cava formations (Casas & Fernández, 2007; Casas, 2010). The displacement of the faults, which show a throws of about 0.2 to 0.9 km, progressively decreases upward and peters out in the upper part of the Cava Formation (Fig. 1). A synsedimentary hydrotermal activity is associated with these faults lined with quartz veins, which is present in the contact of Cambro-Ordovician sediments with synsedimentary faults (Figs. 3-4), and as their clast counterparts in the Rabassa conglomerate (Figs. 2-3).

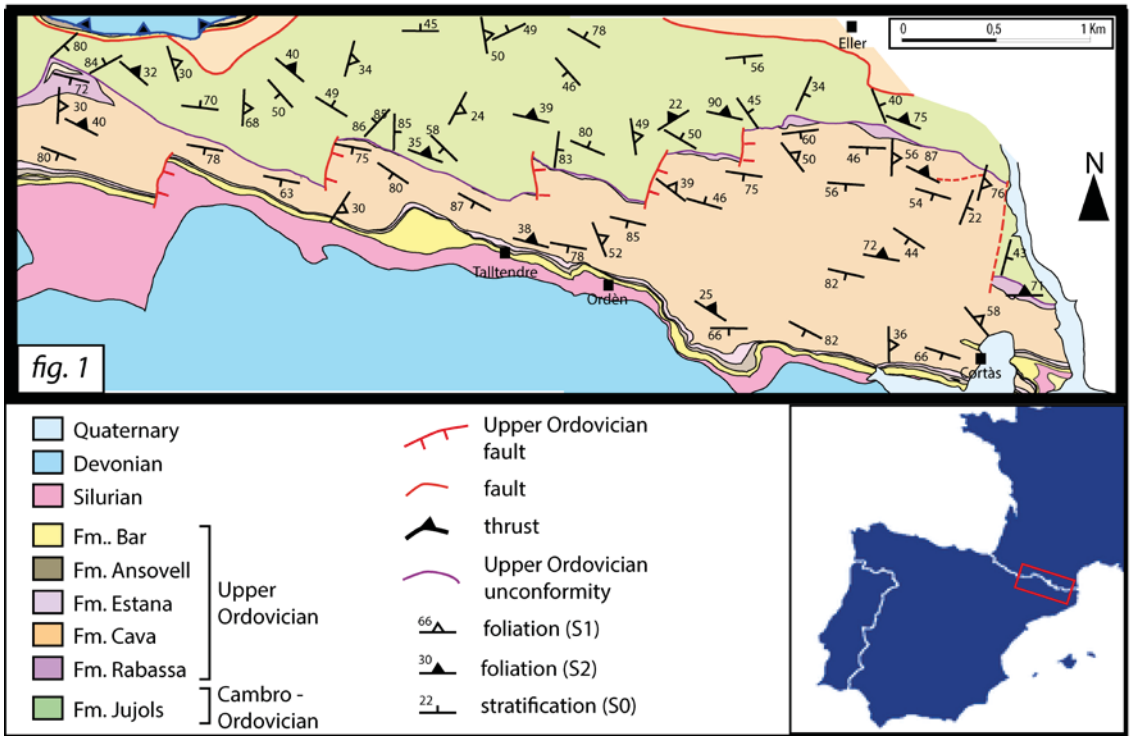

Figure 1. Geological map of the surroundings of Talltendre in the eastern Pyrenees.

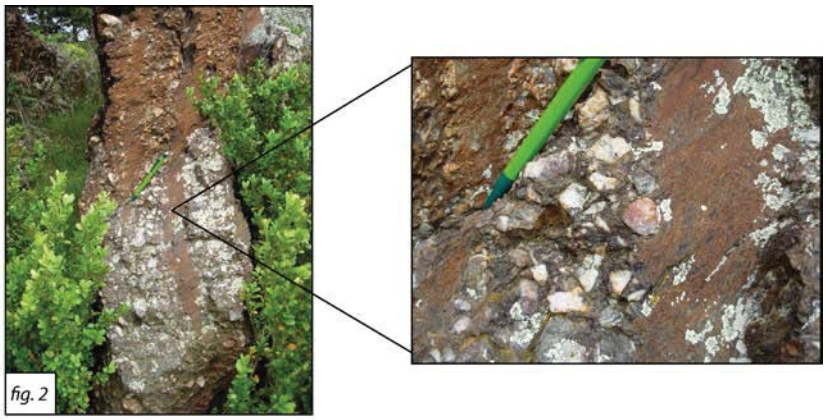

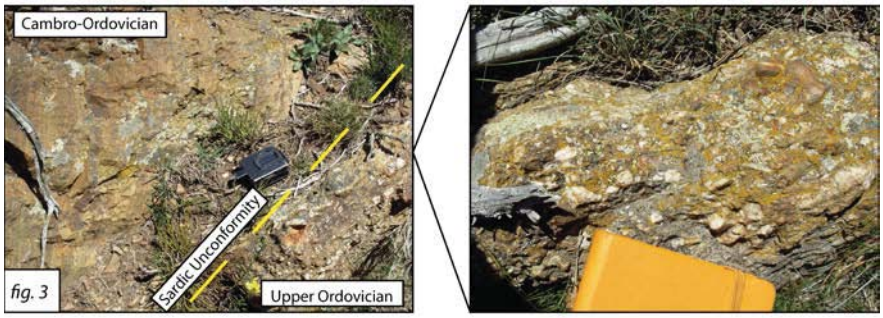

Figures 2-4. Macroscopic aspect of the Jujols/Rabassa contact close to Talltendre, showing common incorporation of hydrothermal quartz clasts derived from synsedimentary-related faults fringed by hydrothermal dykes.

Early Palaeozoic evolution of Gondwanan units in the Iberian Massif: from subduction through rifting and drift on the southern passive margin of the Rheic Ocean

Cecilio Quesada

Instituto Geológico y Minero de España (IGME); and Dept. Mineralogía, Univ. Complutense de Madrid, José Antonio Novais 2, 28040 Madrid, Spain, quesada.cecilio@gmail.com

STOP 6c

Upper Ordovician limestones along Ribes-Bruguera road

Josep Maria Casas, Claudia Puddu and J. Javier Álvaro

In the GIV-5263 road from Ribes de Freser to Bruguera (stop 6c, Fig. 4), we can examine a 500 m-thick succession entirely composed of limestones, marly limestones ("schistes troués") and shales (Figs. 8a-b). Its age is constrained by conodonts and crinoids that allowed Robert (1980) to propose an early Katian (former Caradoc) age. In this stop we can examine the uppermost part of this succession that exhibit an erosive contact with the overlying dark shales attributed to the Hirnantian. The succession is affected by Variscan south verging E-W oriented folds related to the formation of a cleavage, especially well developed in the marly limestones ("schistes troués"). Several normal faults cut the folds (Fig. 8c).

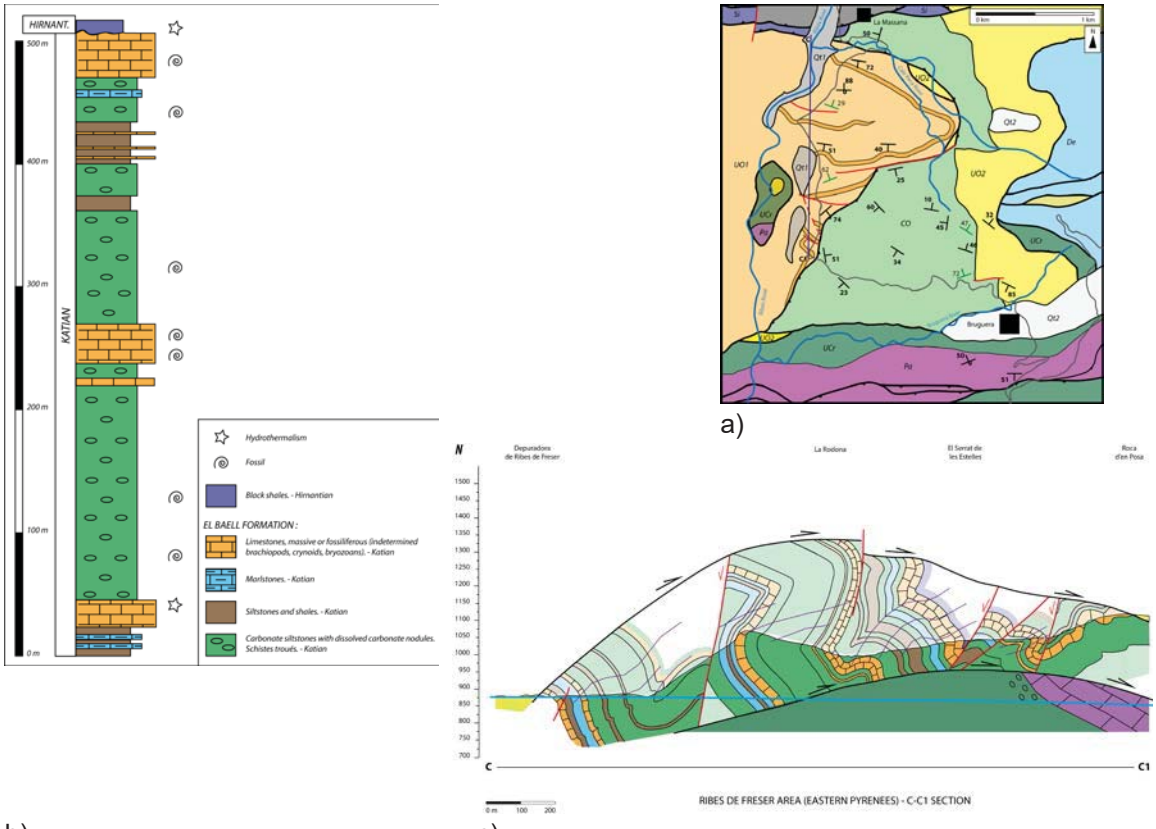

Figure 8. Geological map (a), stratigraphic log (b) and cross-section of the El Baell unit along the Ribes de Freser-Bruguera road, after Puddu *et al*. (this vol.).

The initial position of this unit cannot be pinpointed because, until now, similar successions have not been described in the Pyrenees. A preliminary restoration allows us to situate this unit in a pre-Alpine northernmost position, between the Ribes-Camprodon thrust and

the Tet valley, where Upper Ordovician rocks crop out at the southern limb slope of the Vilafranca del Conflent syncline.

STOP 6d

Sardic unconformity at La Molina station

Josep Maria Casas

In this stop we will visit the la Molina area, where Santanach (1972b) described the Upper Ordovician unconformity in the Pyrenees (Fig. 9). After his work, it is widely accepted that the Upper Ordovician succession unconformably overlies either the Jujols or Canaveilles groups (García-Sansegundo & Alonso, 1989; Den Brok, 1989; Kriegsman *et al*., 1989; García-Sansegundo *et al*., 2004; Casas & Fernández, 2007). However, the origin of this unconformity has been object of several interpretations. Santanach (1972b) in this zone and García-Sansegundo *et al*. (2004) in the Garona dome, attributed the Sardic unconformity to basement tilting, related to of a Late Ordovician faulting episode and subsequent erosion. To the west, in the Lys-Caillaouas massif, Den Brok (1989) and Kriegsman *et al*. (1989) proposed the existence of a pre-Variscan deformation event. A pre-Late Ordovician folding episode has been also suggested as related to the unconformity in this area (Casas, 2010; Casas *et al*., 2012). However, the meaning of this deformation episode is unclear: it is related neither to metamorphism nor cleavage development, although it seems related to uplift, widespread emersion and considerable erosion before the onset of Upper Ordovician deposition. As a result, the Upper Ordovician rocks directly onlap different formations of the pre-Sardic succession in the Central and Eastern Pyrenees.

Acritarchs recovered from the uppermost part of the Jujols Group near this stop point to a broad Furongian-Early Ordovician microphytoplancton assemblage (Casas & Palacios, 2012), which is coincident with a maximum depositional age of ca. 475 Ma for the uppermost part of the Jujols Group in the La Rabassa dome, on the basis on the youngest detrital zircon population (Margalef, 2015; Margalef *et al*., 2016). To the east, in the Albera massif, metapelites and metapsammites from the uppermost part of a metasedimentary succession that can be correlated with the Jujols Group are crosscut by acidic subvolcanic dykes, which constrain its minimum depositional age to 465-472 Ma (Liesa *et al*., 2011). All these data suggest a depositional age for the uppermost part of the Jujols Group at ca. 475 Ma. On the other hand, a ca. 455 Ma U-Pb age for the Upper Ordovician volcanic rocks directly overlying the Sardic unconformity has been proposed in the Bruguera unit (Martí *et al*., 2014) and in the Les Gavarres area (455±1.8 Ma, Navidad *et al*., 2010). Thus, a time gap of about 20 m.y. can be estimated for the Sardic Phase in the Pyrenees. Similar gaps are found in SW Sardinia (ca. 18 m.y.), the type area where the original unconformity was described, where the discontinuity is constrained by well-dated Upper Ordovician metasediments overlying upper Tremadoc-lower Floian(?) strata (Barca *et al*., 1987; Pillola *et al*., 2008).

3.2 – 7th September – Fieldtrip to eastern Pyrenees, Catalonia and Occitanie

STOP 7a

Upper Ordovician succession in Talltendre

Josep Maria Casas, Claudia Puddu and J. Javier Álvaro

The aim of this stop is to recognize stratigraphic and structural data from the Upper Ordovician rocks of the La Cerdanya area (Canigó unit). This area exhibits an Upper Ordovician succession similar to that described by Hartevelt (1970) in the Central and Eastern Pyrenees, which constitutes a broad fining-upward megasequence bearing a key limestone-marlstone interbed and marked thickness variations, ranging between 100 and 1000 m. Hartevelt (1970) defined five formations, which can be recognized with some lithologic variations all across most part of the cordillera (Fig. 12). Furthermore, as can be seen in the Ribes de Freres area (stops 6a and 6b), various volcanic and volcanosedimentary complexes crop out in different areas.

Unconformably overlying the Sardic-related palaeotopography (see stop 6d), the Rabassa Conglomerate Formation is made up of reddish-purple, unfossiliferous conglomerates with sharp lateral variations in thickness, from zero to 200 m. Conglomerates are composed of subrounded to well-rounded clasts rich in slates, quartzites and vein quartz, up to 50 cm in diameter, embedded in a green-purple granule-sized matrix. Their massive-to-channelized sets are interpreted as alluvial-to-fluvial deposits (Hartevelt, 1970). Due to its stratigraphic position, this author attributed the Rabassa conglomerates to the Sandbian-Early Katian (former Caradoc).

The overlying Cava Formation, 100-800 m thick, which either cover the Sardic unconformity or the Rabassa Conglomerate Formation, consists of feldspathic conglomerates and sandstones in the lower part, grading upward into variegated shales and fine-grained sandstones, with strongly burrowed quartzites in the uppermost part (Belaustegui *et al*., 2016). A contemporaneous volcanic influence is distinct in the southwestern part of the Canigó massif, where ash levels, andesites and metavolcanic rocks are embedded (e.g., in Ribes de Freser). Brachiopods, bryozoans and echinoderms are locally abundant, concentrated in fine-grained sandstones of the middle part of the formation, based on which, Gil Peña *et al*. (2004) attributed a Katian (former late Caradoc-early Asghill) age to this formation.

The Estana Formation, which lies above the Cava Formation, consists of limestones and marly limestones, up to 10 m thick. The unit constitutes a good stratigraphic marker bed, the so-called “schistes troués”, “Grauwacke à *Orthis*” and “Caradoc limestones” of French and Dutch geologists. Conodonts, brachiopods, bryozoans and echinoderms are abundant, yielding a Katian (former mid Ashgill; Gil Peña *et al*., 2004) age for the development of echinoderm-bryozoan meadows on shelly, offshore-dominated substrates.

The “Ansovell” Formation (Ansobell *sensu* Hartevelt, 1970) unconformably overlies the Estana limestone and consists of blackish shales with common slumping and convoluted layers, close to the base, and minor quartzite interlayers in the uppermost part. Where the Estana Formation tapers off, the Ansovell shales directly overlie the Cava sandstones. Finally, the Bar Quartzite Formation marks the top of the Upper Ordovician as a quartzitic layer, 5-10 m thick. An Hirnantian age (former late Ashgill) was proposed for the Ansovell and Bar formations by Hartevelt (1970), and confirmed by Roqué *et al*. (2017). Westward, in the Orri, Pallaresa and Garona domes, Gil-Peña *et al*. (2000, 2004) reported a calcareous conglomerate, up to 8 m thick, directly capping the erosive unconformity that marks the Estana/Ansovell contact, and attributed it to a Hirnantian glacial event.

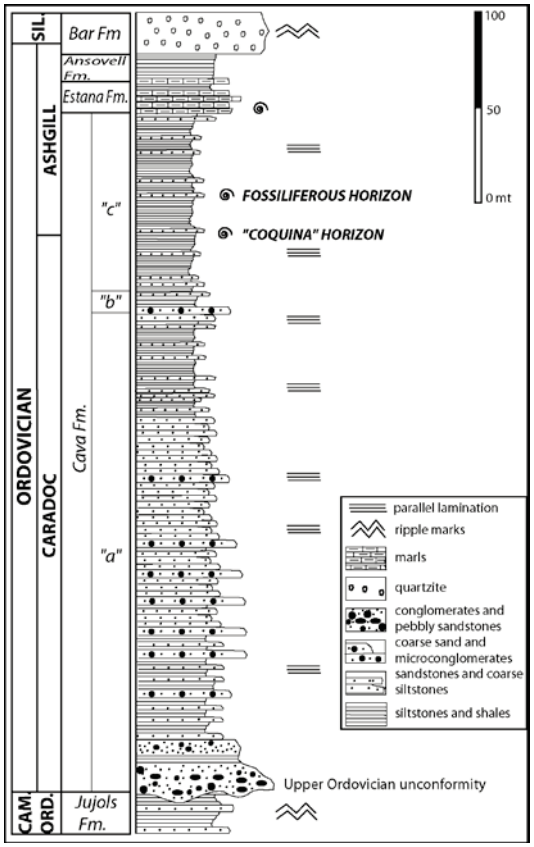

Figure 12. Synthetic stratigraphic column of the Upper Ordovician succession in the Ordèn-Talltendre area, after Puddu & Casas (2011).

In the Talltendre area, we can recognize the Upper Ordovician succession, the basal unconformity and several normal faults affecting the Upper Ordovician succession, the Cambro-Ordovician sediments and the basal unconformity (Fig. 13). Talltendre town is located on the quartzite of the Bar Quartzite Fm and, following the path from Talltendre to stop 7a, we can recognize, from top to bottom, all the Upper Ordovician succession (Fig. 13).

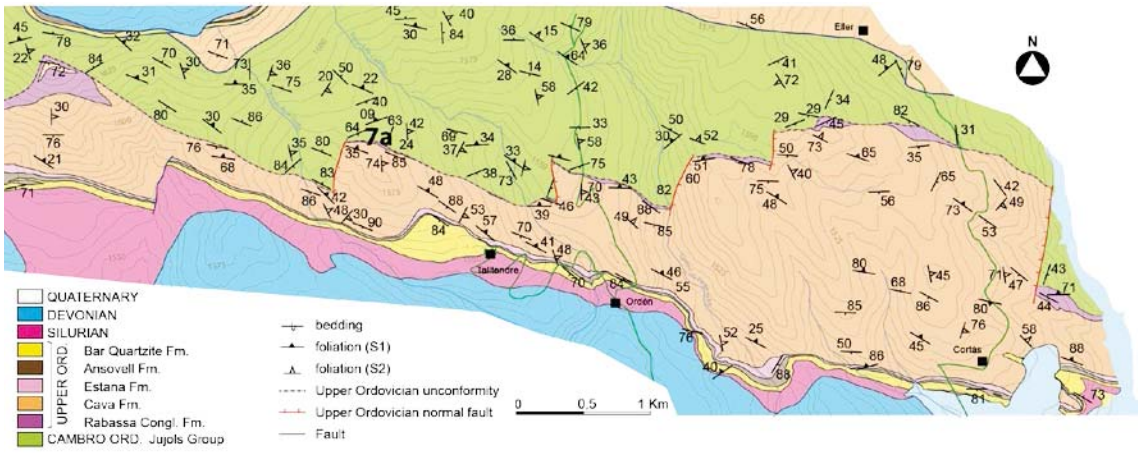

Figure 13. Geological map of the Talltendre area, north of Bellver de Cerdanya; modified from Puddu & Casas (2011).

It should be noted that near this area three brachiopod genera (*Porambonites* sp., *Eoanastrophia* sp., and *Dolerorthis* sp.) were collected, which have not yet been described in the Cava Formation (Fig. 14). The new brachiopod fauna comes from the uppermost part of the "c" member of the Cava Formation, above the “coquina” horizon described by Hartevelt (1970). Unfortunately, the state of preservation of the fossils only allowed a generic assignment, which represents an intermediate fauna between the “late Caradoc-early Ashgill” brachiopods collected in the “coquina” horizon located in the upper part of this member (*Svobodaina havliceki*, *Rostricellula* sp., *Rafinesquina* sp.; Gil Peña *et al*., 2004) and the “mid Ashgill” brachiopods of the Estana Formation (*Dolerorthis* sp., *Eoanastrophia pentamera*, *Iberomena sardoa, Leangella anaclyta*, *Longvillia mediterranea*, *Nicolella actoniae*, *Porambonites* (*Porambonites*) *magnus*, *Ptychopleurella villasi*; Gil Peña *et al*., 2004).

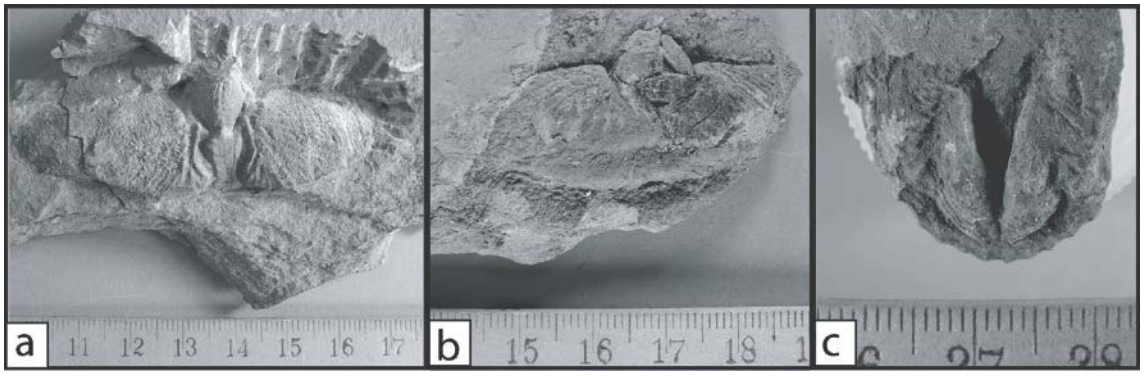

Figure 14. Brachiopods collected in the upper part of the “c” member from the Cava Formation: (a) *Porambonites* sp. (internal mould of ventral valve),)b) *Dolerorthis* sp. (internal mould of ventral valve), and (c) *Eoanastrophia* sp. (internal mould of dorsal valve).

Moreover, in this area, several normal faults affect the Upper Ordovician succession, the Cambro-Ordovician sediments and the unconformity. The faults are steep and currently exhibit broad N-S to NNE-SSW trending. In most cases, their hangingwall is the eastern block despite the presence of some antithetic faults; maximum throws of about 0.2 to 0.9 km can be recognized. Displacement progressively diminishes upward and peters out in the Cava rocks (Fig. 13). Based on these orientations, an E-W extension (in present day coordinates) can be proposed. The original orientation of the faults cannot be pinpointed owing to subsequent deformation events, although an original N-S orientation can be proposed. This orientation probably prevented the faults from being inverted during subsequent Variscan and Alpine deformation events, although the faults probably suffered rotations on horizontal E-W axes during these deformation episodes. On the other hand, sharp variations in the thickness of the Upper Ordovician succession have been reported by several authors; Llopis Lladó, 1965; Hartevelt, 1970; Speksnijder, 1986). Hartevelt (1970) documented variations from 200 to more than 850 m in the thickness of the Cava Formation: e.g., eastward from La Seu d’Urgell, the thickness of the Rabassa and Cava formations attain more than 800 m before sharply diminishing to some tens of metres within a few kilometres (Casas & Fernández, 2007). There, the maximum observed thickness occurs associated with the maximum grain size of the conglomerates (pebbles exceeding 50 cm in diameter are common). Sharp variations in thickness and grain size can be attributed to palaeorelief formation controlled by fault activity and subsequent erosion of uplifted palaeotopographies, with subsequent infill controlled by alluvial-fan and fluvial deposition.

In stop 7a, we can recognize the basal Upper Ordovician unconformity that separates the Upper Ordovician sediments from the underlying Cambro-Ordovician ones. This unconformity can be identified from detailed mapping in several neighbouring areas. In stop 7a, the unconformity has a NW-SE trend and cuts the bedding of the pre-unconformity deposits at

different angles, ranging from a few to 90º (Fig. 15). As in the La Molina area, a synsedimentary hydrotermal activity gave rise to quartz veins and dykes, which subsequently feed the Rabassa conglomerates as vein quartz pebbles (Fig. 15).

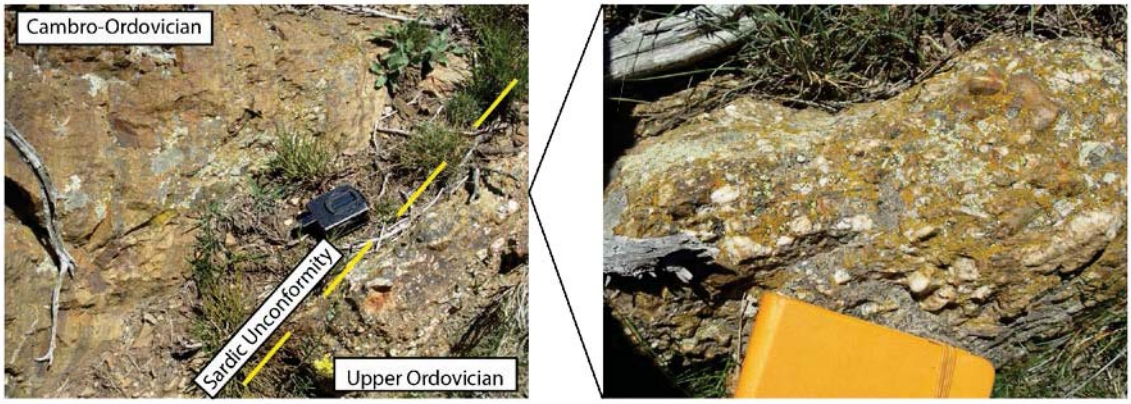

Figure 15. Sardic unconformity at the Taltendre area (stop 7a)

STOP 7b

Graus de Canaveilles along Conflent valley

Bernard Laumonier

The so-called Relais de l'Infante (Bains de Canaveilles) cross-section is certainly the best place in the Pyrenees to present and discuss the long-lasting question about the significance of the Canigou gneisses and the relationships between these gneisses and the micaschists of the surincombant metasedimentary Canaveilles (Nyer) Formation.

In the 1950s, in accordance with the ideas prevaling then, the quartzo-feldspatic Canigou gneisses were thought to be metasomatic rocks ("migmatites") derived from grauwackes, and the gneiss/micaschist contact was considered as an upper metasomatic front (e.g. Raguin, 1938; Guitard, 1955). However, this metasomatic model ("feldspathisation régionale") was gradually and rapidly abandoned:

(i) In 1958, G. Guitard concluded that the upper part of the gneisses, especially the leptynitic ones and the La Preste gneisses of the southeast of the Canigou massif, were derived by simple *in situ* ("topochimique") recrystallisation of rhyolites of variable thickness, unlike the underlying metasomatic biotite augen gneisses.

(ii) A few years later (Guitard,1963a, b), the author suggested that most of the Canigou gneisses are in fact orthogneisses, either metavolcanic (leptynitic gneisses) or metagranitic (augen gneisses). As a result, their large K-feldspar grains ("eyes") should not be porphyroblasts but porphyroclasts derived from the deformation of K-feldspar phenocrysts of former porphyritic, rapakivi biotite granites. However, another question was under debate then: did these metagranites represent an old Precambrian basement or did they correspond to a younger laccolitic intrusion?

(iii) In the following years, Guitard (1958, 1970[1965], *in* Jaffrezo et al., 1977), Autran *et al.* (1966, 1977), Fonteilles & Guitard (1988), Guitard *et al.* (1996, 1998), Laumonier & Guitard (1986) and Laumonier (1988) definitely favoured the first option, suggesting a model involving a Cadomian granitic basement (the G2 augen gneisses), a major post-Cadomian unconformity, a discordant Cambrian sedimentary cover (the Canaveilles series *sensu* Cavet, 1957), the base of which (G1 gneisses) is rhyolitic, and a major recumbent fold resulting in the reappearence of the Canaveilles Series under the stratoid Canigou gneisses, forming the Balatg Series.